New Reactivity of Masked Isocyanates with Organometallic Reagents

By

Alshimaa Mohamed Ahmed Mohamed

Thesis submitted to the
University of Ottawa
In partial fulfillment of the requirements for the
Ph.D. degree in chemistry

Ottawa-Carleton Chemistry Institute
University of Ottawa

Candidate	Supervisor
_____	_____
Alshimaa M. A. Mohamed	Prof. André M. Beauchemin

Abstract

The chemistry of heteroatom-substituted isocyanates is less explored compared to their carbon-substituted counterparts due to their inherent instability and propensity to oligomerize even at low temperatures. This instability together with their amphoteric character have limited their applications. However, the N-N-C=O and O-N-C=O structural motifs found in these isocyanates are prevalent in pharmaceuticals and agrochemicals. Therefore, harnessing the chemistry of *N*- and *O*- substituted isocyanates could open new pathways for the synthesis of these motifs. The development of blocking group chemistry for these isocyanates, which would control their concentration and reduce homocoupling side reactions, is a promising strategy to circumvent these limitations and to broaden the synthetic applications of heteroatom-substituted isocyanates.

The research presented in this thesis centers around the stoichiometric addition of organometallic reagents, particularly Grignard reagents, to heteroatom-substituted isocyanates to provide access to hydroxamates and hydrazides via C-C bond forming reaction with masked *O*-isocyanates and *N*-isocyanates, respectively. It is demonstrated that Grignard reagents can effectively generate free *O*- and *N*- isocyanates *in situ* from blocked precursors, enabling high-yielding addition reactions, provided that diorganomagnesium reagents are used. The investigation explores the formation of a relatively stable five-membered chelate as a key aspect in the addition of Grignard reagents to masked heteroatom-substituted isocyanates. This chelate controls the release of the reactive isocyanate, hence mitigating uncontrolled reactivity including oligomerization of isocyanates and/or rearrangement. Heating at reflux in THF is required to overcome the stability of the chelate formed upon deprotonation. Precise adjustment of the nature and coordination environment of the isocyanate/metal complex controls the release of the reactive isocyanate *in situ*, minimizing side reactions and enhancing the desired activity.

The study of nitrogen-substituted isocyanate precursors with sp^2 nitrogen atoms (imino-isocyanates) unveiled unexpected reactivity with the masked sp^2 *N*-isocyanate precursors bearing α-hydrogens. This new reactivity was the intramolecular cyclization to form five-membered pyrazolone derivatives. These unexpected outcomes supported the two previously developed concepts, by highlighting the importance of fine-tuning the equilibrium between the blocked and free heteroatom-substituted isocyanates by manipulating the stability of the five-membered complex, and the necessity to control the concentration of the free isocyanate to mitigate oligomerization and allow the desired reactivity to occur. Additionally, these outcomes underscored that the five-membered chelate possibly allowed the coordination of a 2^{nd} equivalent of Grignard to the nitrogen atom, presumably, facilitating the deprotonation of the α-proton via a six-membered transition state (i.e., a directed metalation event). This is followed by generating the

free isocyanate intermediate and the subsequent intramolecular nucleophilic attack on the electrophilic *N*-isocyanate which enabled accessing cyclic five-membered pyrazolones from hydrazone precursors.

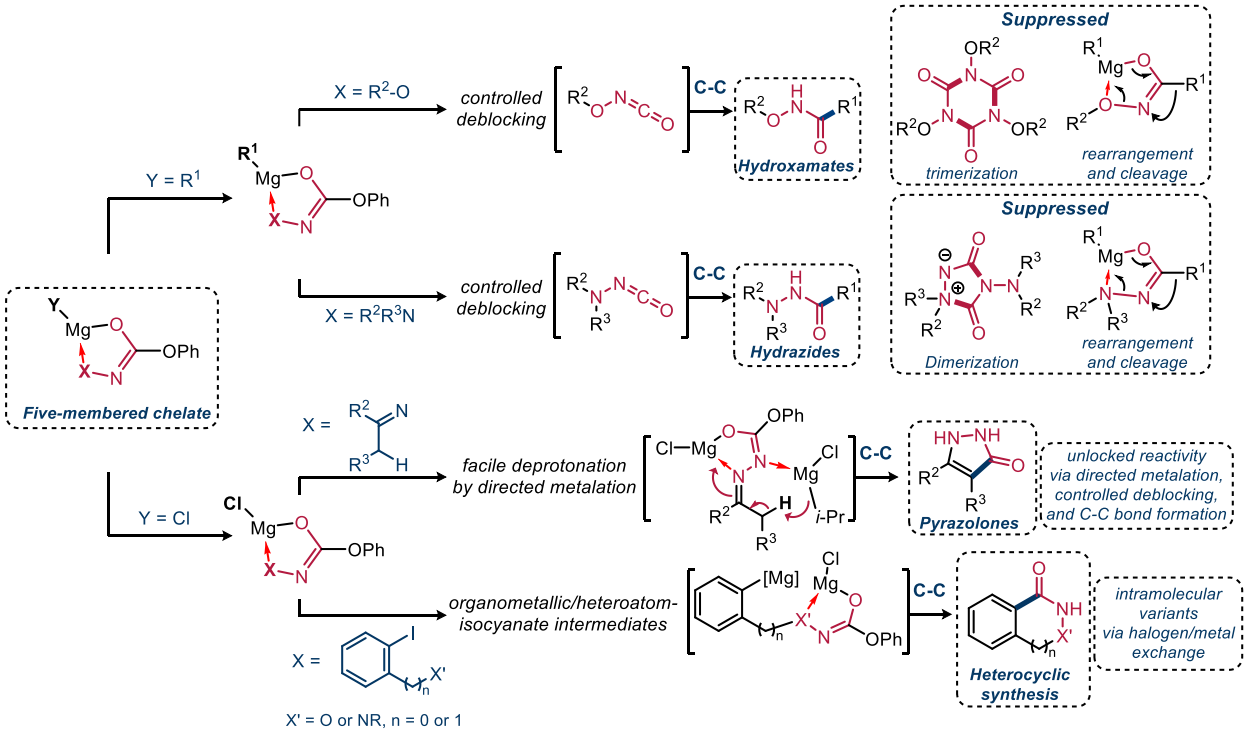

This reactivity was also explored using intramolecular variants of masked heteroatom-substituted isocyanates as potential precursors for the purpose of the synthesis of heterocyclic compounds. The productive reaction sequence involved deprotonation of the masked isocyanate to form a relatively stable chelate, followed by formation of organometallic reagent and cyclization onto the heteroatom-isocyanate intermediates. Preliminary findings demonstrated their ability to undergo intramolecular cyclization reactions to form heterocyclic compounds by C-C bond formation. This was confirmed by the successful formation of a six-membered heterocyclic benzoxazinone product. It was hypothesized that the formation of the relatively stable five-membered chelate made this approach feasible. Indeed, the Turbo Grignard reagent enables halogen-metal exchange under mild conditions to form the desired organomagnesium intermediate, which can then cyclize once *in situ* release of the free reactive isocyanate species is induced by heating the reaction conditions.

Overall, this work provides new approaches to conduct C-C bond forming reactions with masked *N*- and *O*-isocyanate reagents, both inter and intramolecularly. These reactions facilitate the synthesis of various N-N-C=O and O-N-C=O motifs, including protected hydroxamic acid derivatives, hydrazides, pyrazolones and other heterocyclic compounds.

Acknowledgements

First and foremost, my deepest and humble gratitude to the **Almighty Allah,** the source of all gifts in which we prosper.

I acknowledge my transformation from the person I was when I joined the Beauchemin group to the person I am as I depart graduate school. This transformation has resulted in a lengthy roster of individuals to whom I will always owe a debt of gratitude for their guidance and influence throughout these years. My deepest appreciation goes to André, who graciously welcomed me into the group and has been an outstandingly supportive supervisor. Academic research and lab work under his supervision has been immensely enjoyable and enlightening. His enthusiasm is contagious, and his support throughout my study has been instrumental. His consideration of my circumstances during the COVID-19 pandemic has been deeply appreciated. André: I have learned a lot from you.

I would like to express my deepest gratitude to Monica, the Beauchemin Lab manager. Since she joined the group in 2022, she has been a pillar of support. Her dedication, professional guidance, emotional support, and efforts to boost my self-confidence have been invaluable. Monica: Without your support, this thesis wouldn't have been possible.

I am grateful to my colleagues Fred, Bhavana, Josh, and Kwame, who have assisted me with the PhD project. Their help has been crucial in the successful completion of this work. Guys: Without your help, many of the developments made throughout my time in the Beauchemin lab would not have been possible.

I must extend my gratitude to several faculty members at the University of Ottawa. First and foremost, both Professor Fabien Gagosz and Stephen Newman have allotted me significant amounts of their time to discuss my research project. I would like to thank members of the University of Ottawa in NMR and MS spectroscopy facilities, especially Dr. Sharon Curtis, Dr. Peter Pallister, and Dr. Patrick Szell for their help over the years.

I am grateful to my colleagues Fred, Maxime, Daniel, and Braeden, who have revised my PhD thesis, providing valuable suggestions in the most critical time.

Finally, I would like to thank my lab mates Huy, Sherif, Braeden, Daniel, Max, William, Julia, Rosemary, Meredith, Binjie, Jasper, and David. Their camaraderie made the lab a pleasant place to work. Guys: I am lucky to have you as my lab mates.

Outside the lab: I would like to convey the gratitude to the persons who supported me during these long six years.

First and foremost, I dedicate this work to my beloved mother, whose memory has been a beacon of strength and resilience throughout my journey. Her passing during the first year of my PhD was a heartbreaking event that deeply affected me. Her love and lessons continue to guide me.

I am profoundly grateful to my father, whose unwavering support and encouragement have been invaluable. His strength and wisdom have been my pillars of support. Dad: You always stayed close.

To my husband, Ahmed, I owe a debt of gratitude. His companionship and shared endurance through the hurdles of this journey have been a source of immense strength. Ahmed: We have gone through all of this together. Thanks for everything.

My daughters, Nadeen and Leen, have shown remarkable endurance during the most challenging times. Their understanding and patience have been a source of motivation for me. Girls: I'm blessed to be the mother of two beautiful angels like you.

I am deeply thankful to my aunt, who provided emotional support when I needed it the most. Her kindness and empathy have been a source of comfort. Aunt Mona: You've always been there.

Alshimaa Mohamed

Ottawa, 2024

Statement of Contributions

Within the Beauchemin group, I have had the opportunity to work in collaboration with a number of graduate and undergraduate students on a variety of research initiatives. The contributing researchers are: Dr. Joshua Derasp **JD**: a senior PhD candidate who graduated in 2019; Mr. Kwame Agyei **KA**: an undergraduate (Honours) student during 2018-2019; Ms. Bhavana Uppalapati **BU**: a current PhD candidate; Mr. Frédéric Vuillermet **FV**: a current PhD candidate; myself, Alshimaa Mohamed **AM**: a PhD candidate. In each respective chapter, I provide a detailed account of my individual contributions to these projects, while also acknowledging the valuable input provided by my colleagues.

Chapter 2: **JD** initiated the project, conducted the control reaction with *C*-isocyanate precursor and developed the conditions that led to the formation of the first example of addition product using masked *O*-isocyanate precursor **2a**. **JD** performed the preliminary optimization using Turbo Grignard on compound **2a**. **KA** continued the optimization study on the precursor **2a**, by performing solvent screening and additive scan. **KA** successfully formed five addition products by reacting **2a** with five different organomagnesium halides. **JD** and **KA** helped addressing the limitations of employing organomagnesium halides on *O*-isocyanates, by observing the formation of the side product benzyl alcohol with precursor **2a** and isolating a symmetric anilide derivative, which resulted from rearrangement and N-O bond cleavage. **AM** performed extensive optimization on substrate **2a** using three different Grignard reagents and used dioxane to form diorganomagnesium species as nucleophiles. **AM** did the reaction scope employing different *O*-isocyanate as reaction partners as well as different Grignard reagents. **AM** optimized the reaction of precursor **2g** with Ph_2Mg and *i*-Pr_2Mg, for the products of this reaction to serve as potential amide linchpin reagents. **BU** tried different conditions on the product of the reaction of **2g** with Ph_2Mg (compound **3ge**) to serve as a potential amide linchpin reagent, but this approach was unsuccessful using this substrate **3ge**. **AM** explored reactivity using other organometallic reagents such as organolithium and organozinc. **AM** performed extensive optimizations on **2a** using diethylzinc. **JD** performed a preliminary reaction using *N*-isocyanate and got addition product in 21% NMR yield. **AM** explored the optimized reactivity of diorganomagnesium species on masked *N*-isocyanates, did the optimization and reaction scope.

Chapter 3: **FV** explored intramolecular cyclization of hydrazone carboxylates using several basic conditions combined with several Lewis acids, which were unsuccessful attempts to access pyrazolones from these precursors. **AM** achieved this kind of cyclization unexpectedly, employing Grignard conditions. **AM** and **FV** synthesized the hydrazone carboxylate precursors with almost equal contributions. **AM** performed the optimization of this pyrazolone forming intramolecular cyclizations using Grignard methodology, while **FV**

tried other conditions to eventually develop milder second-generation conditions. **AM** did the reaction scope using Grignard approach, while **FV** did the reaction scope using the second-generation conditions. It is important to note that the development and results obtained with the second-generation conditions will not be presented in this thesis.

Chapter 4: **AM** performed all the synthetic sequences to form the cyclization precursors and 3 out of 4 precursors were successfully synthesized. **AM** performed the cyclization of one precursor **10** to access the six-membered cyclic product **11** form *O*-isocyanate intramolecular variant. **BU** will be exploring the remaining cyclizations.

Contents

List of Figures

List of Schemes

List of Tables

Abbreviations and Units

°C	degree Celsius
δ	chemical shift in parts per million
Å	angstrom (10^{-10} metres)
Ac	acetyl
aq	aqueous
Ar	aryl
BG	blocking group
Bn	benzyl
Boc	*tert*-butoxycarbonyl
Bu	butyl
Bz	benzoyl
cat.	catalytic
Cbz	benzyloxycarbonyl
CDI	carbonyldiimidazole
CuCN	copper cyanide
Cy	cyclohexyl
Cys	cysteine
d	deuterium (in NMR solvents)
DBU	1,8-diazabicyclo[5.4.0]undec-7-ene
DCC	N,N'-dicyclohexylcarbodiimide
DCE	1,2-dichloroethane
DMA	dimethylacetamide
DMEDA	1,2-dimethylethylenediamine
DMF	dimethylformamide
DMSO	dimethyl sulfoxide
E	general electrophile
EDG	electron-donating group
EI	electron impact
equiv	equivalent
ESI	electrospray ionization
Et	ethyl
EWG	electron-withdrawing group
FTIR	fourier transform infrared
g	gram
h	hour
HOMO	highest occupied molecular orbital
HRMS	high-resolution mass spectrometry
Hz	Hertz
i	iso
i-Pr	isopropyl
IR	infrared
J	coupling constant
LDA	lithium diisopropylamide
LG	generic leaving group
LiHMDS	lithium bis(trimethylsilyl)amide
LiTMP	lithium 2,2,6,6-tetramethylpiperidide

LUMO	lowest unoccupied molecular orbital
Lys	lysine
µL	microlitre
m	meta
M	molar
[M]	metal
Me	methyl
Mg	magnesium
mg	milligram(s)
min	minute(s)
mL	millilitre(s)
mmol	millimole(s)
n-Bu	*n*-butyl
Ni	nickel
NMP	*N*-methyl-2-pyrrolidone
NMR	nuclear magnetic resonance
Nu	general nucleophile
o	ortho
OBz	*O*-benzoyl group
[Ox]	oxidation
p	para
PG	protecting group
Ph	phenyl
Pr	propyl
Py	pyridine
R	carbon-based substituent
RAMP	(*R*)-1-amino-2-methoxymethylpyrrolidine
RBF	round bottom flask
R_f	retention factor
rt	room temperature
SAMP	(*S*)-1-amino-2-methoxymethylpyrrolidine
sat.	saturated
sec	second
SI	Supporting information
t	tertiary
TBS	*tert*-butyldimethylsilyl
TBME	*tert*-butyl methyl ether
tert	tertiary
TFE	2,2,2-trifluoroethanol
TGA	Thermogravimetric analysis
THF	tetrahydrofuran
TIPS	triisopropylsilyl
TLC	thin layer chromatography
TMS	trimethylsilyl
TMEDA	*N,N,N',N'*-tetramethylethylenediamine
Ts	*para*-toluenesulfonyl
X	generic halide
µW	microwave

Chapter 1 Introduction

1.1 Organometallic Reagents with Isocyanates

1.1.1 Isocyanates: Their Synthesis and Reactivity

First identified by Wurtz in 1849,[1] isocyanates are a class of highly reactive heterocumulenes. Their potential to polymerize and create polyurethanes was not discovered until 1947 by Bayer,[2] which ignited a wave of research interest in these substances. Isocyanates have since become a fundamental organic component with a wide range of industrial uses, including but not limited to coatings, paints, and adhesives.[3] Diisocyanates, including methylene diphenyl diisocyanate (MDI) and toluene diisocyanate (TDI), are used in the polyurethane industry, particularly in foam production. Aliphatic diisocyanates like hexamethylene diisocyanates (HDI) are typically employed in polymer coatings. Methyl isocyanate (MIC) is frequently used in the production of pesticides and polymers (Figure 1.1).[4] The pivotal role of isocyanates in the synthesis of amides, urea, carbamate, and heterocyclic compounds underscores their importance in the manufacture of fine chemicals, such as those used in agrochemical and pharmaceutical development.[5]

Figure 1.1. Structures of common isocyanates.

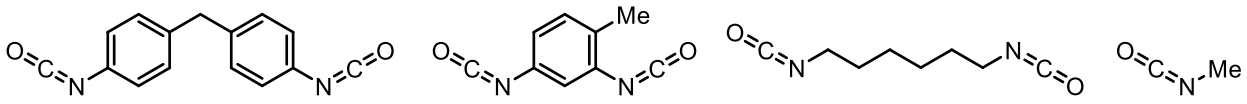

Isocyanates are predominantly synthesized via the phosgene process, which remains the cornerstone of industrial isocyanate production together with non-phosgene synthetic routes. The phosgene method encompasses both liquid and gas phase approaches, determined by the reaction conditions and the phase of the organic amine (Scheme 1.1, a). The liquid phase phosgene method facilitates isocyanate production under mild conditions, including room temperature, but it requires longer reaction times, includes higher solvent usage, and generates significant byproducts.[6,7] Conversely, the gas phase phosgene process involves vaporizing amine compounds at elevated temperatures (200-600 °C) and reacting them directly with gaseous phosgene to produce isocyanate. Initially used for aliphatic isocyanate production, this method has been adapted for aromatic isocyanates through reactor improvements.[8] Its advantages include short reaction residence times (less than 1 minute), fewer byproducts and high space-time yields. Preliminary pilot tests indicate that this process can reduce solvent consumption by 80% and energy consumption by 60%.[7,9] Currently, the phosgene process is the most critical technological approach for industrial organic isocyanate production, offering benefits such as a well-established process, high yields,

rapid reactions, and cost-effectiveness. However, the inherent toxicity of phosgene and the corrosive nature of hydrogen chloride byproduct present significant safety hazards and their use and production during the synthetic process contradicts the principles of green chemistry and intrinsic safety. Consequently, the development of non-phosgene synthetic routes for isocyanate production is emerging as a promising area for future advancements in the field.[7] These non-phosgene methods include reductive carbonylation of nitro compounds,[10–12] oxidative carbonylation of primary amines,[13] dimethyl carbonate approach,[14] and urea method (Scheme 1.1, b).[15]

Scheme 1.1. Synthetic approaches of isocyanates.

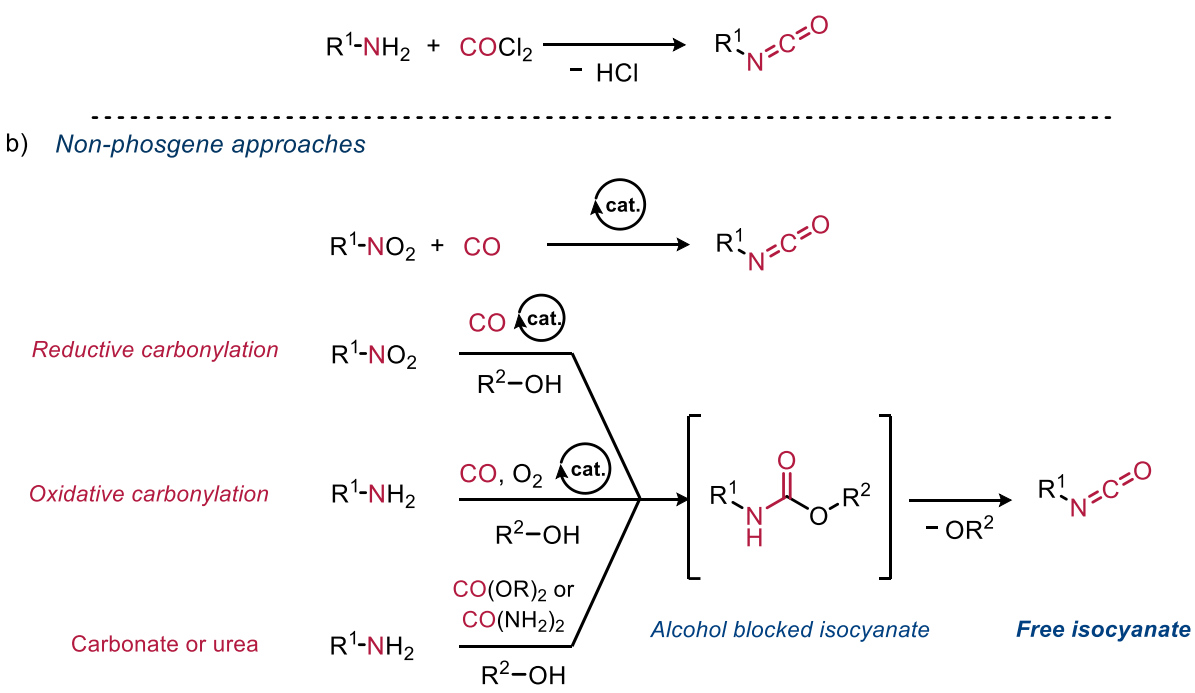

Isocyanates are highly reactive electrophiles. The high reactivity of these compounds towards different nucleophiles can be justified considering their allenic nature together with the major resonance contributor (Figure 1.2). The highly electronegative oxygen and nitrogen surrounding the carbon leads to a highly polarized heterocumulene where most of the electron density shifted toward the heteroatoms, leaving a carbon atom with a significant partial positive charge.[16]

Figure 1.2. Major resonance contributors of isocyanates.

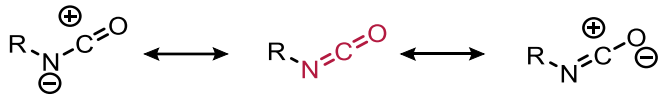

The reactivity of various protic nucleophiles toward isocyanates to generate carbamates, ureas, etc., is the most common application of isocyanates, which has been extensively researched.[5] However, due to their affordability and widespread availability in the market, isocyanates have garnered attention as potential building blocks for amide synthesis, which involves the addition of various carbon-based nucleophiles. Several methodologies have been reported describing stoichiometric carbon centered nucleophilic addition to isocyanates, including the amide bond formation reaction of isocyanates with carboxylic acids,[17,18] C-C bond forming electrophilic aromatic substitution with isocyanates,[19] and C-C bond formation through radical addition to isocyanates.[20]

1.1.2 Stoichiometric Organometallic Addition to Isocyanates

The process of introducing various stoichiometric organometallic reagents to isocyanates, leading to the synthesis of amide products, has its roots in the early 1900s.[21] Despite its potential, this synthetic technique has not been widely adopted due to limited substrate compatibility and the need for more optimal reaction conditions. Intermittent reports of this chemical reactivity can be found in scientific literature throughout the 20th century, with a marked increase in the 21st century. The scope of these studies encompasses the use of diverse organometallics, including organolithium, organomagnesium, organozinc, organoaluminium, organoboron, and organocuprates.[22–33] The recent advancements in the stoichiometric organometallic addition to isocyanates have resulted in their employment as powerful alternative amide bond syntheses.[34] The mechanism of stoichiometric addition of Grignard reagents to isocyanates was described by Gilman *et al.* in 1924.[23] Shortly after, the Gillman group also described a titration method for organomagnesium reagents using the reaction of Grignard reagents with isocyanates.[22] In 2012, a C-C bond forming addition of Grignard reagents to isocyanates to access sterically hindered/electronically deactivated amides was disclosed by Bode and coworkers.[35] These amides are typically difficult to access via standard condensation methods. The addition of equimolar amounts of Grignard reagent to isocyanates was facile at room temperature, and the reaction tolerated various conditions and functional groups on both reaction partners (Scheme 1.2, a). In the same year, through their attempts to develop a more selective coupling to synthesize isoquinolones, Ready and coworkers reported a one-pot, four-component coupling method that involved the addition of Grignard reagents to the isocyanate, resulting in an amide anion.[36] This amide anion then guides an ortho metalation event, which is later utilized for additional modifications to access isoquinolones (Scheme 1.2, b).

Scheme 1.2. Synthesis of sterically hindered amides from Grignard addition to isocyanates (Bode et al.). b) Four component one-pot synthesis of isoquinolones (Ready et al.).

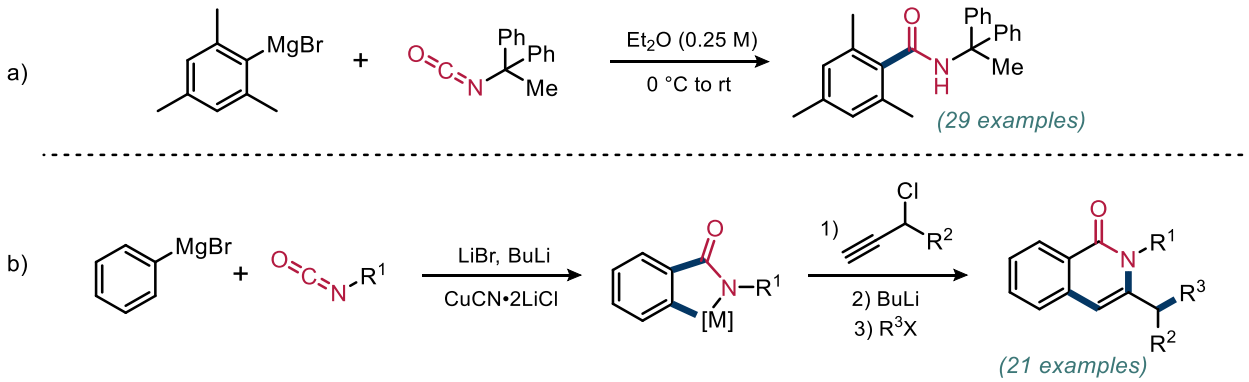

Pace and his team have made significant advancements in the field of organometallic reagents reacting with isocyanates and isothiocyanates.[34] They were the first to document the addition of lithium carbenoids to isocyanates, which give access to α-halogenated and dihalogenated amides (Scheme 1.3, a).[37,38] The use of Barbier-type conditions was particularly noteworthy, where LiTMP was used to selectively form lithium carbenoids from dihalomethane precursors, bypassing the direct addition to the isocyanate. The use of the lithium amide such as LDA or less hindered amide bases resulted in the unwanted formation of urea side product in large quantities.

Building on Bode's work, Pace then developed a facile method to produce various thioamides by reacting isothiocyanates with different organolithium reagents (Scheme 1.3, a).[39] Remarkably, their approach demonstrated the formation of enantioenriched products through the use chiral lithiated species with sparteine and *s*-BuLi, but they have not applied this to isocyanate substrates. Aggarwal and coworkers, however, have reported a stereoretentive process by adding chiral α-heteroatom (O or S) organolithium reagents to various electrophiles including isocyanates (Scheme 1.3, b).[40] In 2016, Pace reported a chemoselective reduction of isocyanates to the desired formamide using the Schwartz reagent,[41] to tolerate various sensitive function groups (ester, nitro, nitrile, alkene) and effectively avoiding overreduction (Scheme 1.3, a).

Scheme 1.3. a) Pace et al. contributions to the addition of organometallic reagents onto isocyanates and isothiocyanates. b) Aggarwal et al. stereoretentive addition of chiral organolithium reagents to isocyanates.

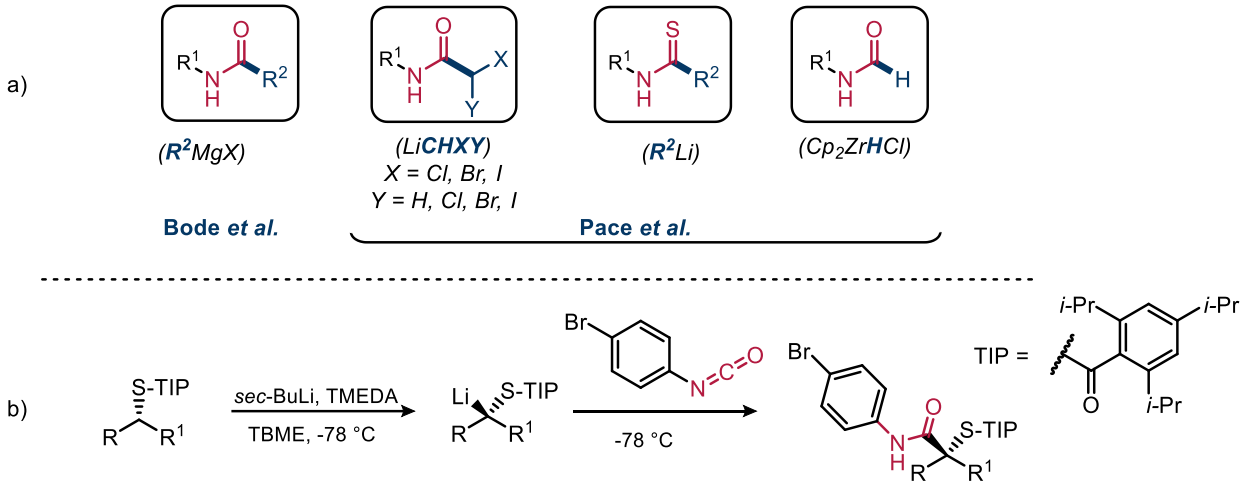

Flow chemistry has been employed to broaden the application of organometallic addition to isocyanates. There are a few examples involving Grignard reagents. Inspired by Bode's work, Kerr and coworkers have unveiled a high-yielding, atom-efficient, functional group tolerant, and scalable amide synthesis through isocyanate/Grignard addition performed by flow chemistry.[42] The application of flow chemistry and the use of sub-stoichiometric quantities of $CuBr_2$ have further enhanced this process, enabling it to accommodate a broad range of substrates (Scheme 1.4). Attempted additions to non-sterically hindered isocyanates were unsuccessful due to fast oligomerization, resulting in the formation of undesired acylurea side products. However, the use of flow chemistry effectively reduced the formation of this unwanted side products through tuning of reactivity via controlling the residence time, offering a more general amide synthetic method with a broader scope than previously reported under batch conditions.

Scheme 1.4. Flow synthesis of amide from isocyanates and Grignard reagents.

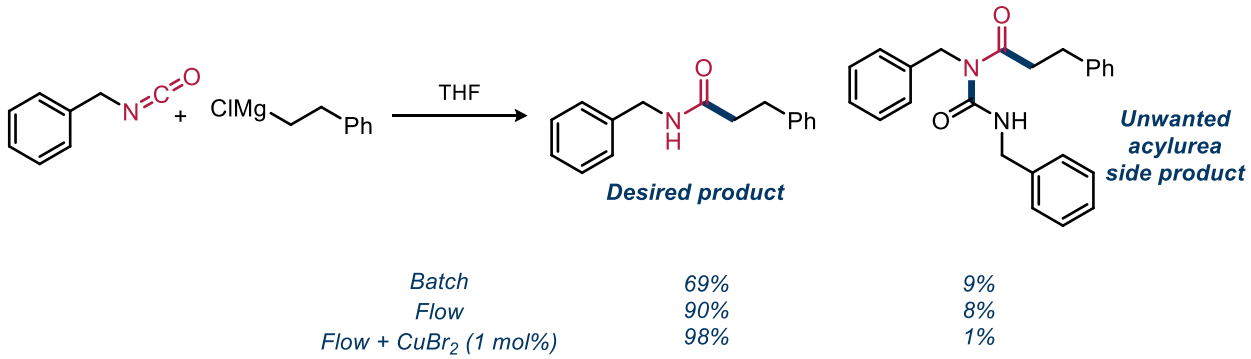

The implementation of flow chemistry for the addition of organolithium reagents to isocyanates has been studied by Kim and coworkers in the course of innovative methodology to produce thioquinazolinones.[43]

o-Bromophenylisothiocyanates selectively underwent lithium halogen exchange, followed by trapping with an isocyanate. This heterocycle can then undergo a substitution reaction to yield the desired thioquinazolinones (Scheme 1.5).

Scheme 1.5. Flow synthesis of thioquinazolinones using isothiocyanates.

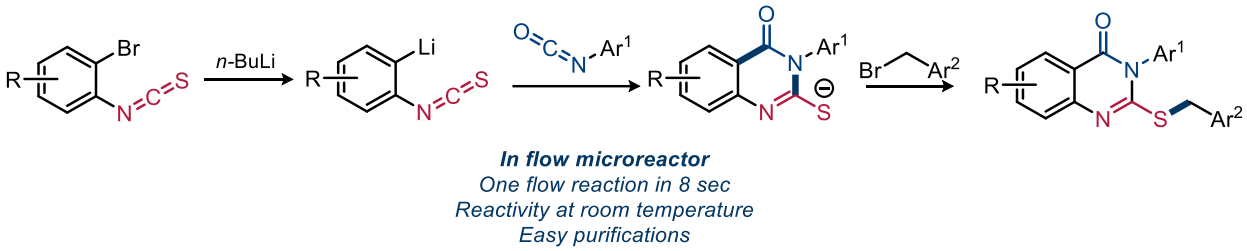

1.2 Masked (Blocked) Isocyanates

Isocyanates are known for their flammability, toxicity, and significant harm when inhaled. All isocyanates are moisture-sensitive, decomposing into amines and ureas upon contact with water. Due to their toxicity and sensitivity to moisture, together with difficulties in controlling their reactivity, the direct use of the free form of isocyanates has become less favored. Additionally, the storage of these isocyanates becomes increasingly challenging when dealing with large industrial quantities. To address problems related to the toxicity of isocyanates, their uncontrolled reactivities, and their sensitivity to moisture, the polyurethane industry has developed a range of masked or blocked isocyanates.

1.2.1 Blocking Group Strategy

The strategy of blocking isocyanates, as initially described by Wicks,[44] involves using "an isocyanate which has been reacted with material which will prevent its reaction at room temperature with compounds that conventionally react with isocyanates but will permit that reaction to occur at higher temperatures." This approach has largely diminished the exposure to the toxic free isocyanates, given access to shelf stable isocyanate precursors, hence, more convenient storage and handling.[45] Furthermore, it has provided better control over reactivity, by controlling the concentration of the free (reactive) form of isocyanate, which is released slowly in the reaction mixture, thereby cleaner reactions are secured. This strategy has expanded the range of applications achievable within isocyanate chemistry.[46] The process of deblocking isocyanates is a chemical equilibrium wherein the blocking group (BG) is cleaved, forming the free isocyanate (reactive form of isocyanate) *in situ*, that can subsequently interact with a nucleophile (Figure 1.3, a).[47] This remarkable development has urged significant focus on studying the kinetics of nucleophilic substitution reactions with various blocked isocyanates.[48] Control over the release of the free form of isocyanate in blocked systems is achieved by manipulating factors that affect not only the equilibrium

between the free and the blocked form of isocyanate but also the activity of the reaction partners as well as the minimum activation energy needed to access the products. These factors include temperature, nature of blocking group, isocyanate structure, and reaction medium (solvents, etc.). Common blocking groups include alcohols and phenols, amines and anilines, amides, oximes, and heterocycles, such as imidazoles or pyrazoles (Figure 1.3, b).

Figure 1.3. a) General reaction of a blocked isocyanate with a nucleophile. b) Blocking group categories with representative examples of blocking groups.

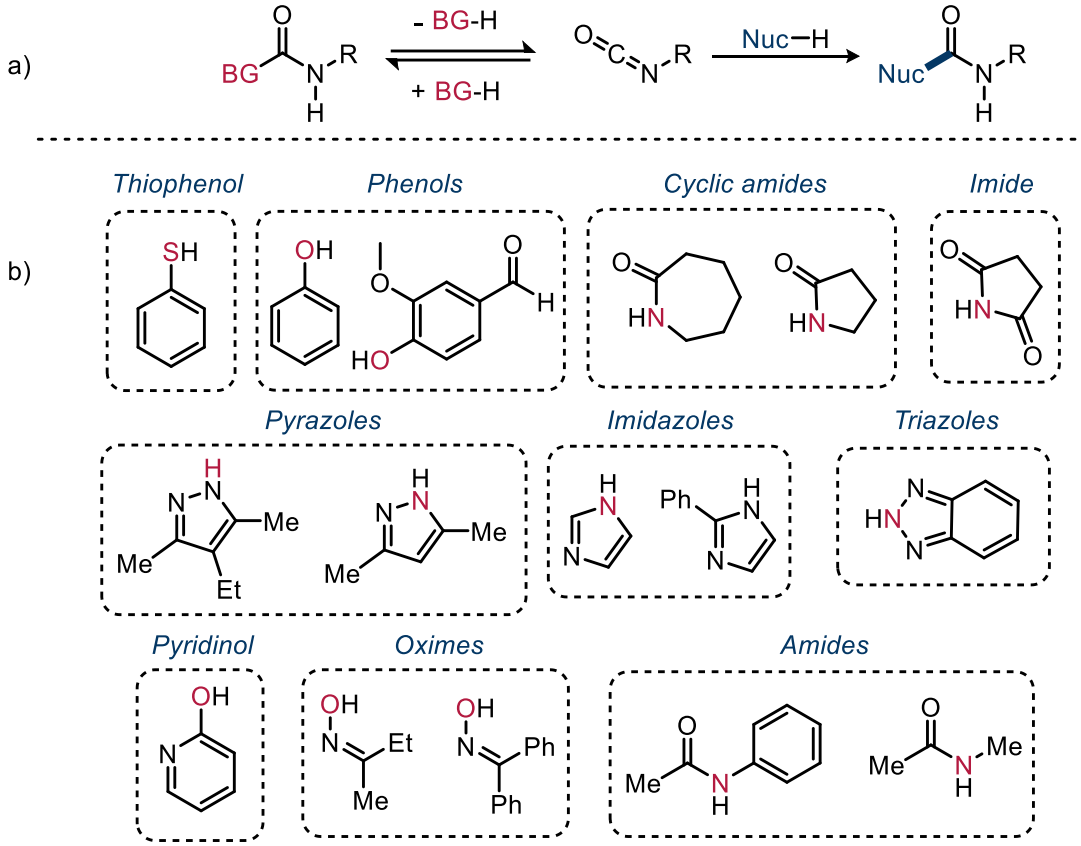

The nature of the blocking group can influence the deblocking equilibrium, therefore, the ideal conditions required for the deblocking processes vary according to the blocking group. Although "deblocking temperatures" are often mentioned in various studies of blocked isocyanates, closer observations of these reports reflect that variation of these temperature value does not accurately reflect the equilibrium in the deblocking process. Since deblocking temperatures are determined and reported using various methods (such as IR, FTIR, TGA, UV-VIS, etc.), where both reaction conditions and detection methods vary, therefore the temperature ranges typically provided in reviews cannot be considered as universally applicable values.[49] Furthermore, "deblocking temperatures" do not always correlate with reactivity. For instance, a primary amine blocked isocyanate might show high reactivity at a certain temperature, while

achieving similar reactivity using a primary alcohol as a blocking group would require a substantial temperature increase. Deblocking temperature does not always correlate with reactivity in solution; good reactivity can be obtained at a lower temperature than the measured deblocking temperature. Hence, it depends more on the nature of the blocking group and the isocyanate structure.

Certain temperature related trends, however, can be observed, when temperatures are examined in the same blocking group categories.[50] For instance, Kothandaraman and coworkers reported a correlation between the pKa values of phenols and the deblocking temperature of phenol-blocked TDI monomers, as determined by IR spectroscopy (Table 1.1).[51] Interestingly, these phenols likely share similar deblocking mechanisms that impact the deblocking equilibrium. The deblocking mechanism for the blocking groups, which uses intramolecular proton transfer can provide some general insights into relative reactivity, but so far, no precise predictive models have been reported (Figure 1.4).[46]

Table 1.1. Dissociation temperatures of phenol-blocked TDI.

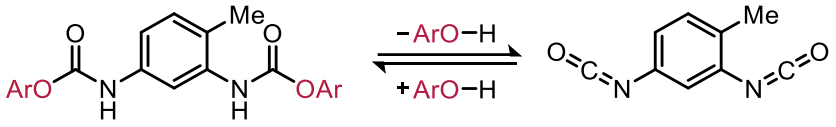

Phenol blocked TDI *TDI*

Phenol blocking group	pKa of ArOH	Minimum dissociation temperature (°C)	50% dissociation temperature (°C)
phenol	9.98	110	130
o-cresol	10.29	120	150
m-cresol	10.08	120	140
p-cresol	10.14	165	>180
guaiacol	9.98	70	130
2,6-dimethylphenol	10.6	125	155
o-chlorophenol	8.56	75	95

Figure 1.4. Proposed intramolecular interactions important for deblocking for several blocked carbon-substituted isocyanates.

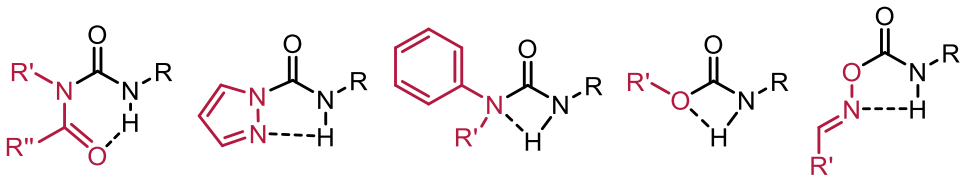

BG = *Amide* *Pyrazole* *Amine Aniline* *Alcohol Phenol* *Oxime*

The effectiveness of the blocking group approach is largely dependent on the nature of the blocking groups reported. The cleavage of the blocking groups is attributed to different steric and electronic factors related to the structure of the blocking group. Furthermore, the capacity to fine tune the equilibrium between blocked and free isocyanate through the manipulation of blocking groups is a fundamental part of the blocking group strategy. Phenol, for instance, is a frequently used blocking group because of its relatively low deblocking temperature. The electronic properties of the phenol can be easily adjusted with varying substitution on the ring, to play a vital role in isocyanate deblocking. Electron-donating substituents tend to favor the blocked form, while the opposite is true for electron-withdrawing substituents (Figure 1.5). This pattern is thought to be due to changes in the strength of the C-O bond in the resulting blocked isocyanate.[45,47] Furthermore, the stability of the resulting phenolate (after cleavage) justifies the previous pattern. Noteworthy, for the phenol system, electronic effects tend to dominate over steric effects, with blocking groups like *o*-cresol and 2,6-dimethylphenol showing higher deblocking temperatures than their phenol equivalent.

Figure 1.5. Electronics of different phenol blocking groups affecting the blocking equilibrium.

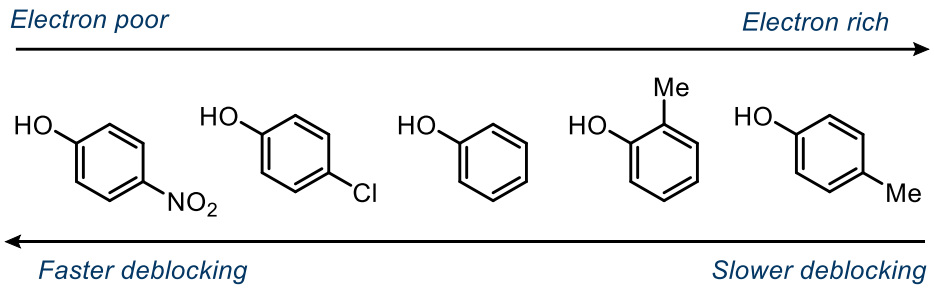

Different trends related to electronics have also been observed. Kothandaraman *et al.* demonstrated that, for the benzophenone oxime blocking group, the presence of electron donating groups lower the deblocking temperature, while it increases with electron-withdrawing groups.[51] The measurements were performed using thermogravimetric analysis. This trend was consistent with the proposed intramolecular interaction in oximes forming five-membered complexes, thereby augmenting the deblocking mechanism (Figure 1.4), where the oxime nitrogen lone pair assists in deprotonating the carbamate N-H, as such, the more basic the nitrogen, the more facile the deblocking. Similar trends are observed with anilines and pyrazoles.[51] Interestingly, this is contrary to the trend seen for phenols, wherein the electronic trend for deblocking seems to be more associated with the stability of the resulting phenolate than the oxygen basicity (Table 1.2). In general, predicting the effects of the identity of blocking groups on specific reactions and conditions can be challenging.

Table 1.2. Deblocking trends differences in oxime blocked TDI vs phenol blocked TDI reflecting different electronic contributions.

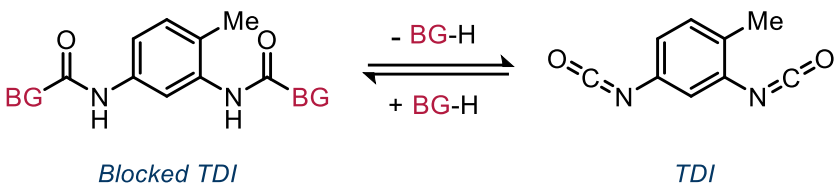

Blocked TDI *TDI*

Blocked TDI		Deblocking temperature
Oxime blocked TDI	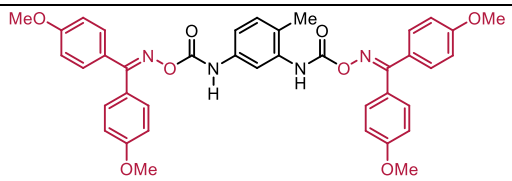	198 °C
	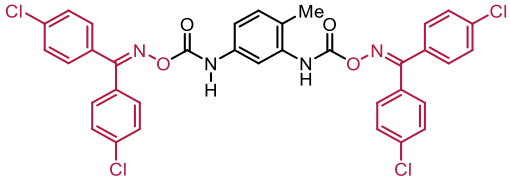	290 °C
Phenol blocked TDI	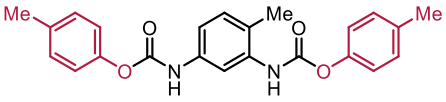	180 °C
	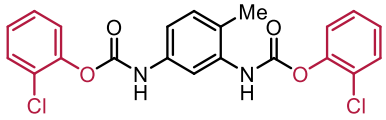	95 °C

The deblocking equilibrium is also dependant on the isocyanate structure (both electronic and steric environments). It is typically observed that alkyl isocyanates deblock at higher temperatures in comparison to aryl isocyanates. This is consistent with the greater thermodynamic stability of aromatic isocyanates, which results from the conjugation of the π-system. Similarly, aryl isocyanates with electron-donating substituents tend to shift the equilibrium towards the blocked form compared to their electron-deficient counterparts. Steric effects of the isocyanate also influence the deblocking equilibrium. This is more obvious when observing the trends using the same blocking group category. More sterically hindered isocyanates tend to deblock faster than less sterically hindered isocyanate (Scheme 1.6). However, this cannot be considered as a conclusive trend, because it is also largely dependent on the nature of the reacting nucleophile.[47]

Scheme 1.6. Effect of the steric hindrance on the deblocking equilibrium.

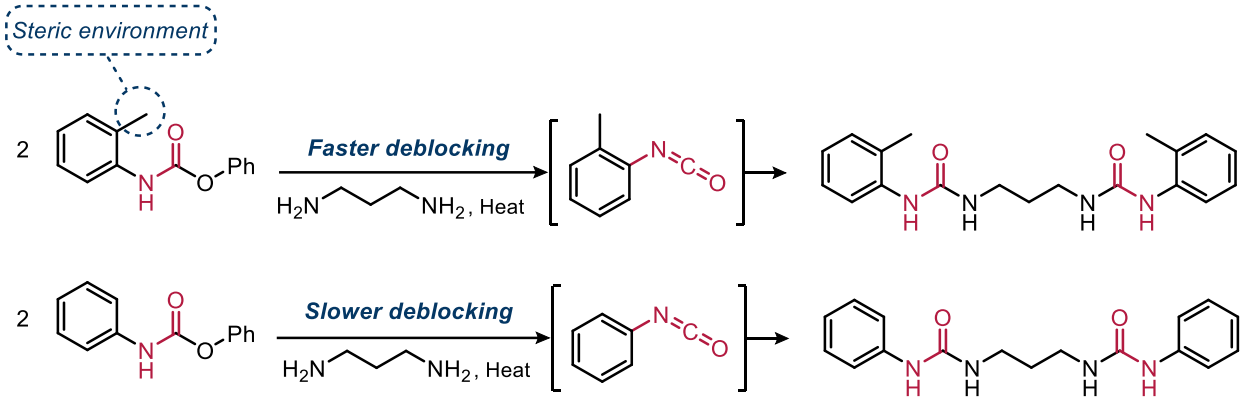

The reaction medium, including the nature of solvent, in blocked isocyanates reactions may also influence the position of the deblocking equilibrium. For the same blocking group category, non-polar solvents tend to shift the equilibrium in the direction of the blocked isocyanate, while polar aprotic solvents tend to do the opposite. This is likely due to the capacity of polar aprotic solvents to form stronger hydrogen bonds with the blocking group, which shifts the equilibrium toward the formation of the free isocyanate. It is important to note that in systems where the kinetics are primarily controlled by the subsequent addition of the nucleophile to the free isocyanate, non-polar solvents might be preferred as they promote the generation of nucleophile/isocyanate adducts.[47,48]

1.2.2 Uses of Blocked Isocyanates

Blocked isocyanates are commonly employed in the polyurethane industry. A recent study by Kim and coworkers reported the use of 3-(4-bromophenyl)-1*H*-pyrazole as an efficient blocking group for the widely used toluene diisocyanate (TDI) monomer (Scheme 1.7), enabling the generation of polyurethanes derived from glycols.[52]

Scheme 1.7. Example of a blocked TDI polymerization using a pyrazole-based blocking group.

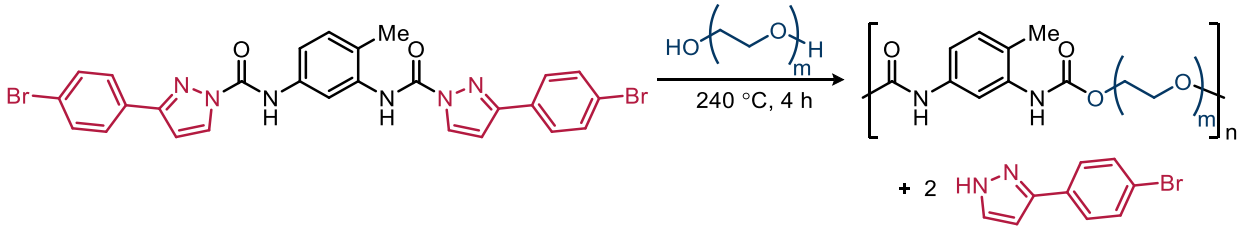

In a recently published study in polymerization chemistry, Dornbusch and coworkers introduced vanillin as an effective blocking agent that operates at moderate temperatures, for blocking of hexamethylene diisocyanate trimer (HDI trimer) to provide better water dispersion.[53] The relatively low temperature

required for deblocking with vanillin allows for *in situ* generation of HDI-trimer, which reacts with binders with terminal OH group, following the deblocking process (Scheme 1.8). As such, vanillin was deemed appropriate as a non-toxic blocking agent for isocyanates, facilitating the manufacture of crosslinkers for single-component, water-based coatings.

Scheme 1.8. Vanillin-blocked crosslinker (HDI-trimer) and its reaction with OH-binder.

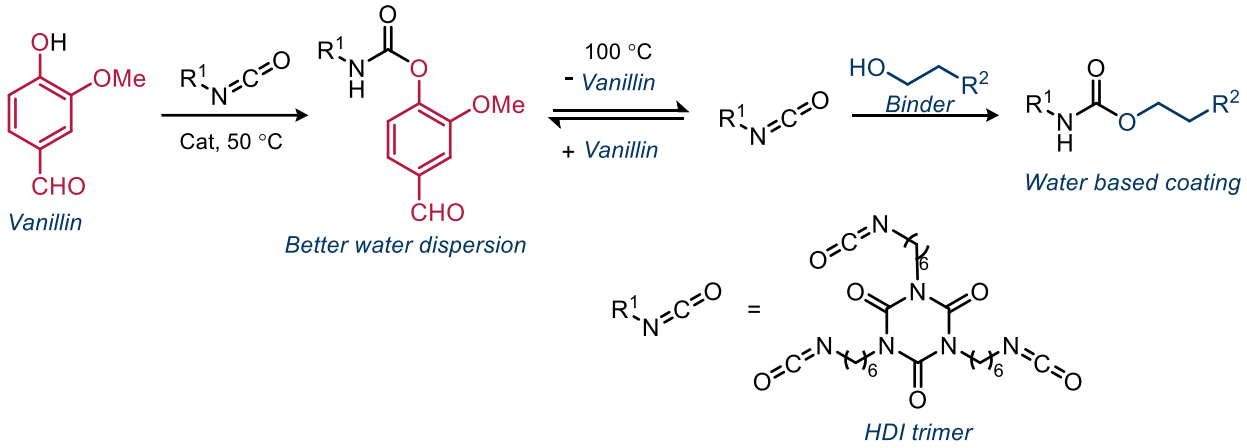

1.2.3 Non-Polyurethane Based Applications of Blocked Isocyanates

The strategy of using blocking groups has significantly advanced the field of fine chemical synthesis. The use of this approach extends beyond the realm of polymerizations and has been enthusiastically adopted by medicinal chemists for the production of ureas via blocked isocyanates.[54–57] While isocyanates serve as a predominant framework for urea synthesis, the requirement for highly functionalized derivatives, a common objective among medicinal chemists, has seemingly propelled the field towards the adoption of blocked isocyanate chemistry.

Buchwald *et al.* reported a palladium catalysed cross-coupling reaction to access both free and blocked isocyanates from sodium cyanate coupling with aryl chloride/triflates. This coupling was followed by a nucleophilic addition of amines to the *in situ* formed isocyanates to access ureas (Scheme 1.9).[58] The generation of blocked isocyanates instead of free isocyanates was achieved by the addition of phenol to the reaction mixture. They revealed that blocked isocyanates mitigated the unwanted competing degradation pathway and catalyst deactivation that were observed with free isocyanate counterparts. The same group then investigated a similar approach to access carbamates by switching to alcohol nucleophiles instead of amines (Scheme 1.9). This approach proved successful in case of free isocyanates, but the blocking group strategy was not compatible with the poorly nucleophilic alcohols.[59] This study demonstrated that using a blocking group strategy to regulate the release of free isocyanates can address

key synthetic challenges in some reactions. However, this approach may not be suitable for all types of reactions and requires careful optimization to achieve the intended reactivity and product formation.

Scheme 1.9. Palladium catalysed cross-coupling reaction to access blocked isocyanates and their reaction with various nucleophiles.

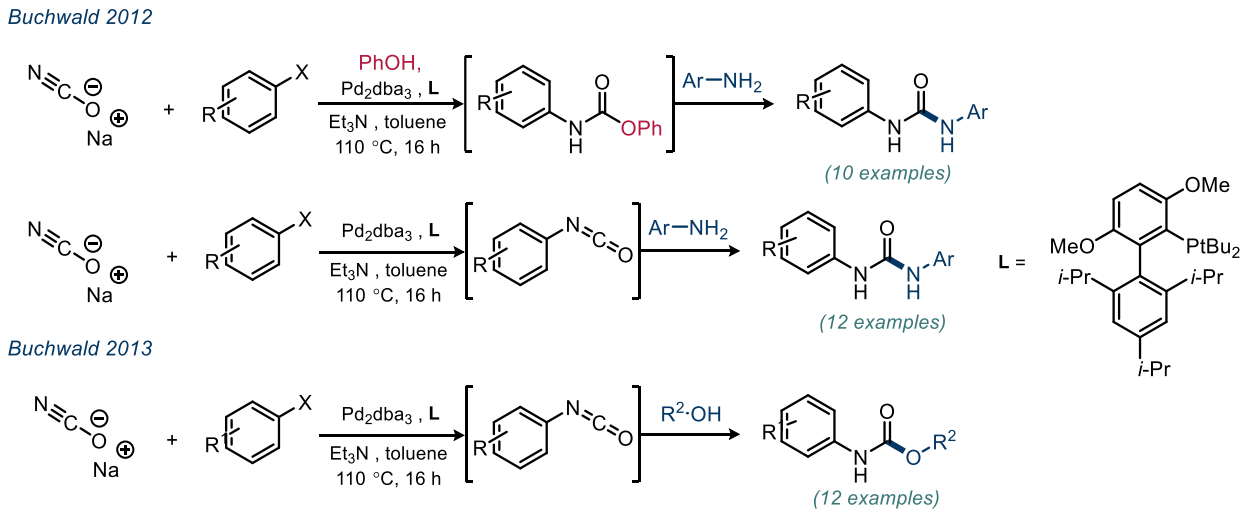

Buchwald and Pentelute have pioneered an inventive application of blocked isocyanates. They employed a bifunctional palladium oxidative addition complex as a cross-linking agent for peptides and proteins (Scheme 1.10).[60] This palladium coupled complex maintains stability over several months and undergoes arylation selectively at cysteine residues. The cross-linking process is initiated when peptides or proteins containing lysine are introduced, leading to a reaction between the primary amine of lysine residue and the blocked isocyanate motif. This approach proved to be effective for both intra- and intermolecular cross-linking reactions.

Scheme 1.10. The development of palladium coupled complex with a blocked isocyanate functional group as a cross-linking agent for proteins.

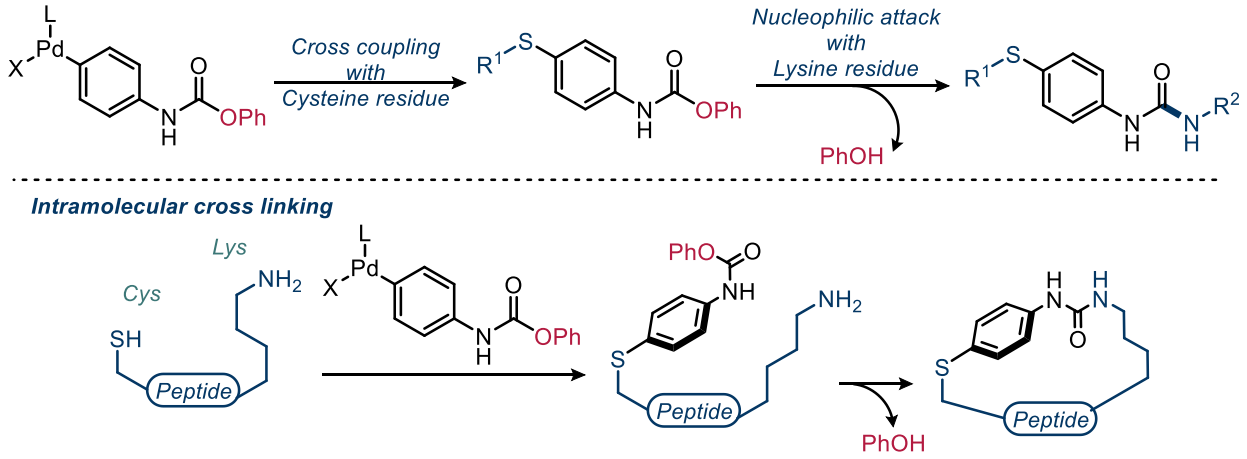

Imidazole blocked isocyanates have also been applied in substitution reactions involving a variety of protic nucleophiles. Imidazole blocking groups cleave under acidic reaction conditions in contrast to phenolic blocking groups which cleave under basic conditions.[61,62] Imidazole blocked isocyanates can be readily synthesized through the reaction of an amine with CDI. Batey and coworkers disclosed a straightforward synthesis of imidazole blocked methyl isocyanate, produced quantitatively using carbonyldiimidazole (CDI) and methyl amine. [63,64] This precursor exhibits a broad reactivity profile, readily engaging with a variety of amines to yield urea products. Additionally, reactivity was observed with diverse alcohols and thiols (Scheme 1.11). The ease with which this wide range of reactivities were accessed under mild conditions, circumvented the need to directly use the harmful free methyl isocyanate. However, similarly to phenol blocked isocyanates, the presence of sodium hydride (NaH) was crucial when dealing with weak nucleophiles such as deactivated amines or alcohols. This advancement was promptly employed by the same group in their total synthesis of agelastatin A.[64]

Scheme 1.11. Blocked methyl isocyanate synthesis and substitution.

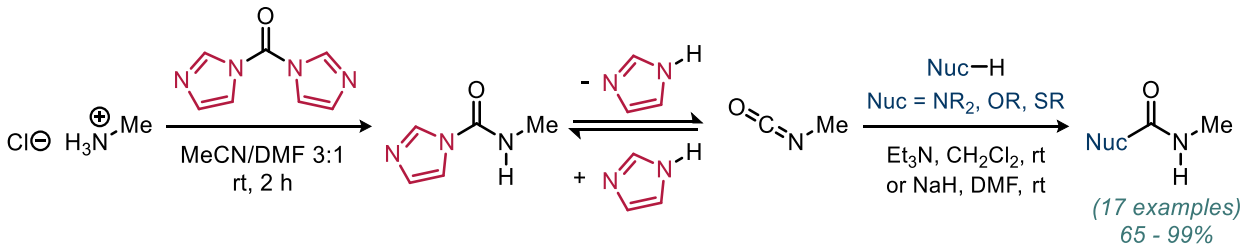

1.2.4 Amide Bond Formation Using Blocked Isocyanates

The exploration of blocked isocyanates as a platform for the synthesis of amide bonds has not been as thoroughly investigated as the synthesis of urea, carbamates and thiocarbamate derivatives. Early reports

introduced the formation of amide bond via the reaction of imidazole and pyrazole blocked isocyanates with carboxylic acids. Gante and coworkers employed both of these blocking groups for peptide coupling with amino acids, and observed that imidazole proved to be more efficient in yielding the desired product than pyrazole blocked derivatives.[65] Thereafter, Gertzmann and Gürtler successfully achieved amide bond formation with pyrazole blocked isocyanates, although a bidentate Lewis acid catalyst was required to ensure high yields.[66] Campagne and coworkers achieved amide bond formation by employing catalytic $CuBr_2$ and 1-hydroxybenzotriazole (HOBt), which facilitated room temperature reactivity. They used blocked isocyanate precursors with an ester substituent (protected carboxylic group) as the electrophile and a carboxylic acid with a protected amino substituent as the nucleophile to access peptides by performing sequential amide bond forming reactions (Scheme 1.12). Performing the reaction under basic conditions (i.e., Et_3N) did not yield the desired product, thereby emphasizing the critical role of acid activation with these imidazole blocked derivatives.[67]

Scheme 1.12. Amide bond formation using blocked isocyanate and carboxylic acids to access peptides.

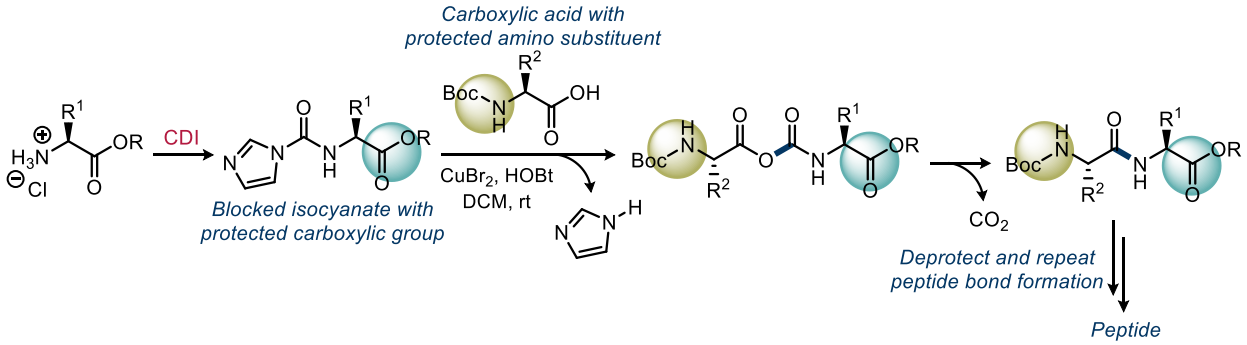

1.2.5 Carbon-Based Nucleophilic Addition to Blocked Isocyanates

Boroxines have been employed in C-C bond formation through the transition metal catalysed synthesis of amides from blocked isocyanate precursors. In 2015 Zhang and coworkers reported a novel synthetic method employing rhodium(I) as the transition metal for this approach.[68] They generated benzamides from the reaction of benzyl and *tert*-butyl carbamates with aryl boroxines (Scheme 1.13).

Scheme 1.13. Synthesis of amides through C-C bond formation using blocked isocyanates and boroxines in a rhodium(I) catalysed coupling.

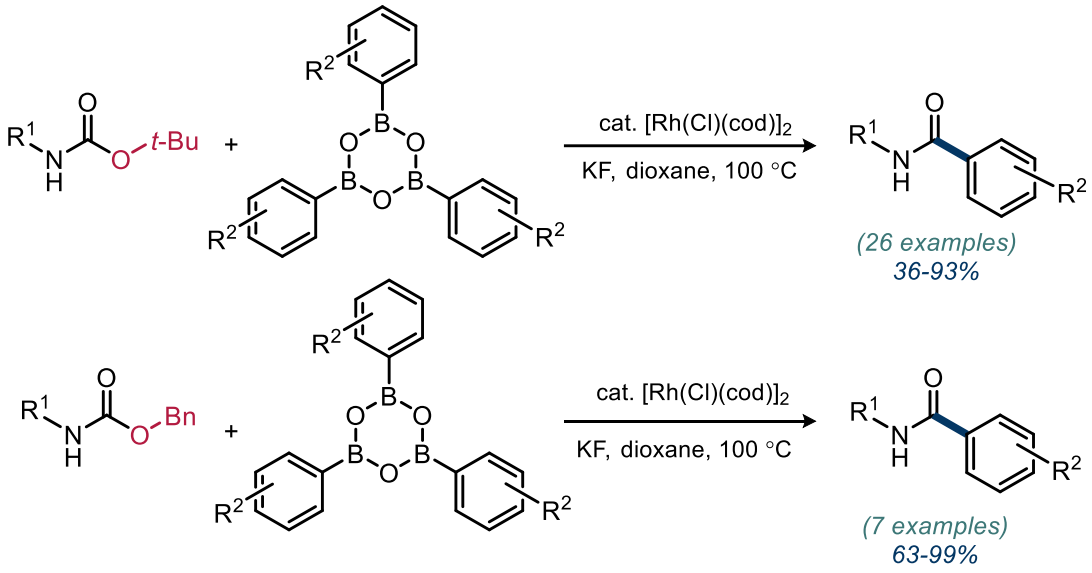

In the same context, Beauchemin and Derasp reported the use of phenol blocked isocyanates in rhodium catalyzed synthesis of amides (Scheme 1.14, a).[69] The conditions allowed wider scope and tolerated liable functionalities such as pendant nucleophiles. The *in situ* generation of both reactive species (organorhodium nucleophile and free isocyanate electrophile) mitigated the toxicity and provided a controlled release of the free reactive form of isocyanate which resulted in wider functional group tolerance and overcoming the unwanted oligomerization reactions. Furthermore, when blocked precursors are used, isocyanates with pendant nucleophiles can also be accommodated (Scheme 1.14, b).

Scheme 1.14. a) Blocked isocyanates and boroxines in a rhodium(I) catalysed amide synthesis through C-C bond formation. b) Example of successful reaction of isocyanates bearing protic nucleophilic groups with boroxine.

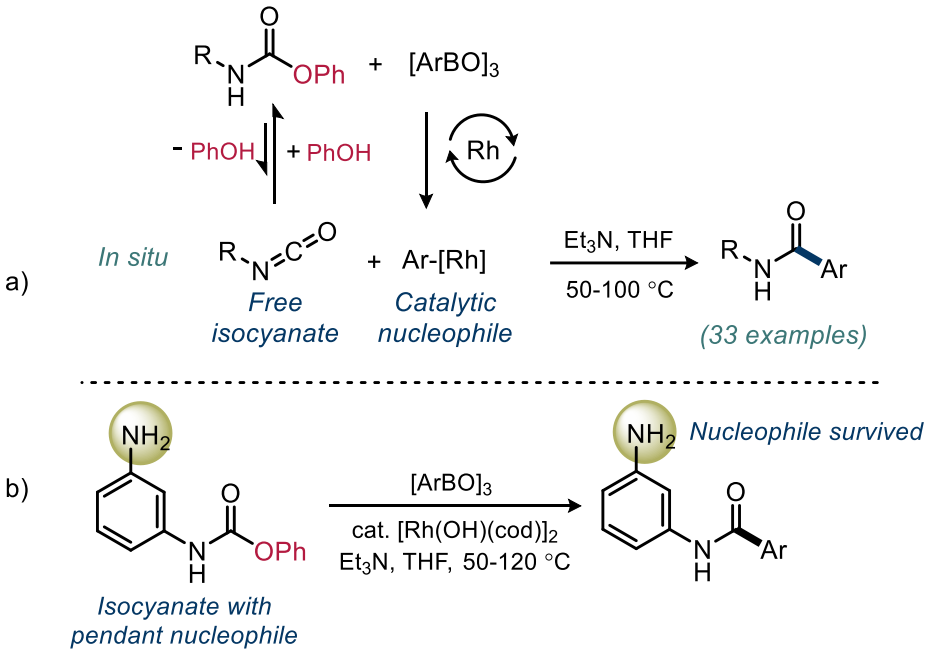

In 2009, González and coworkers first introduced the addition of Grignard reagent to blocked or masked isocyanates, and unexpectedly accessed amides from carbamate precursors via a C-C bond forming reaction.[70] In their attempt to prepare diphenyl-L-prolinol, excess phenyl magnesium bromide was employed as a reaction partner with *N*-Cbz-L-proline methyl ester starting material, where the Cbz group was used to protect the amine group. Instead of achieving C-N cleavage by the Grignard reagent, a C-O cleavage and a Grignard nucleophilic addition to the carbonyl carbon took place at room temperature to furnish the amide (Scheme 1.15, a). Consequently, through investigation on carbamates of primary amines and carbamates of secondary amines, it was revealed that while carbamates of secondary amines produced amies and ketones upon treatment with Grignard reagents, carbamates of primary amines gave rise to amides in high yield and that primary amines can be converted into amides in a one-pot reaction through carbamate protection and Grignard addition (Scheme 1.15, b). They postulated that the reaction proceeded through the formation of a four-membered *N,O*-magnesium chelate (Scheme 1.15, c).

Scheme 1.15. a) Unexpected amide formation from the reaction of carbamate starting material with Grignard. b) The reaction outcomes of Grignard reagent with carbamates of secondary amines vs carbamates of primary amines. c) Accessing amides via C-C bond forming reaction of Grignard reagents with benzyl alcohol blocked isocyanates showing the proposed four-membered N,O-magnesium chelate.

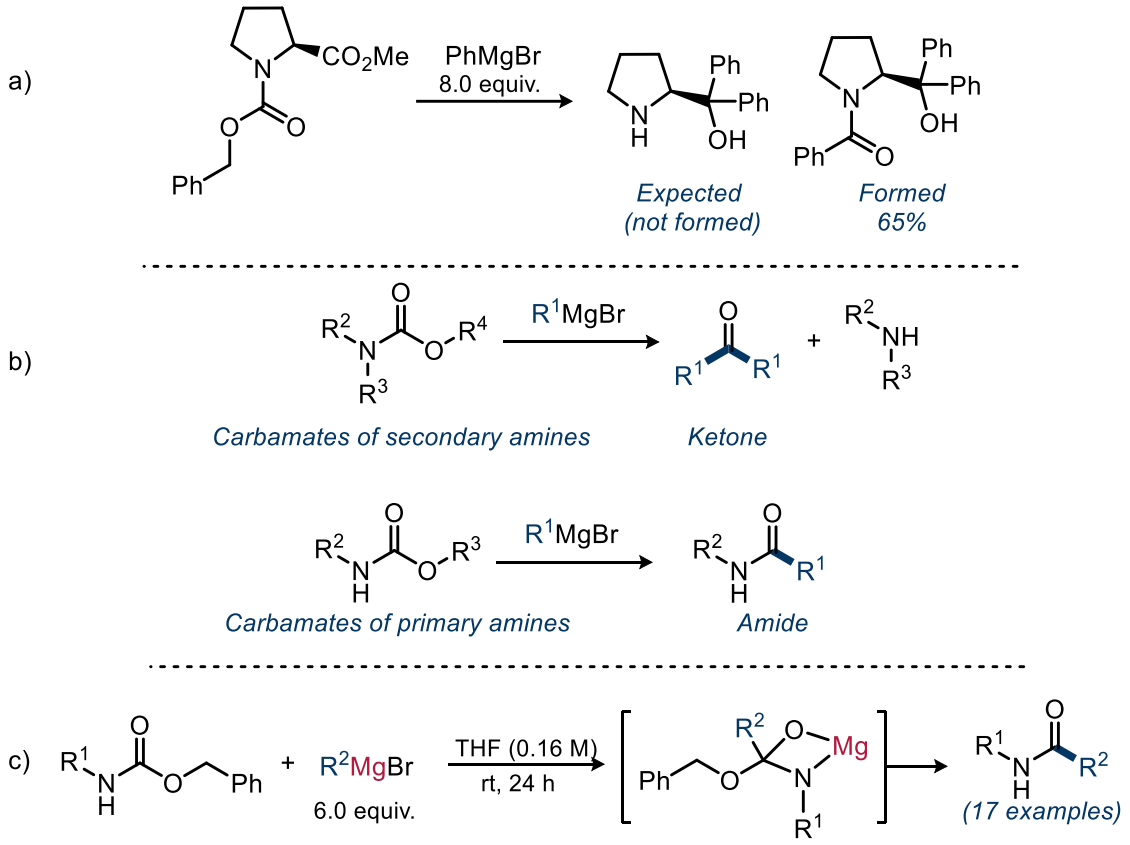

Bode and coworkers have expanded upon their previous research by demonstrating a notable application of Grignard addition to sterically hindered isocyanates (Scheme 1.2).[35] They postulated that in the presence of *N*-carboxyanhydrides (NCA), which can be considered blocked isocyanate precursors, an excess of Grignard reagent would first lead to deprotonation, subsequently releasing the isocyanate for a nucleophilic attack by the residual Grignard reagent (Scheme 1.16).[71] This method proved effective with various aryl Grignard reagents, though alkyl variants resulted in complex mixtures. The latter issue was addressed by introducing a sterically bulky sacrificial base. Additionally, the process was compatible with different organolithium reagents. Chiral NCA precursors were also employed without any detectable epimerization. The hypothesized isocyanate intermediacy was corroborated by React-IR studies. Notably, the isocyanate group remained intact within the reaction mixture alongside mesityl Grignard at -78 °C, with the addition reaction only occurring upon temperature elevation. Noteworthy, *N*-carboxyanhydrides (NCAs) were employed as a useful platform to access amides via the use of carboxylic acids nucleophilic substitution reactions followed by extrusion of carbon dioxide.[72]

Scheme 1.16. C-C Bond formation from the reaction of N-carboxyanhydrides with organometallic reagents (Grignard and organolithium).

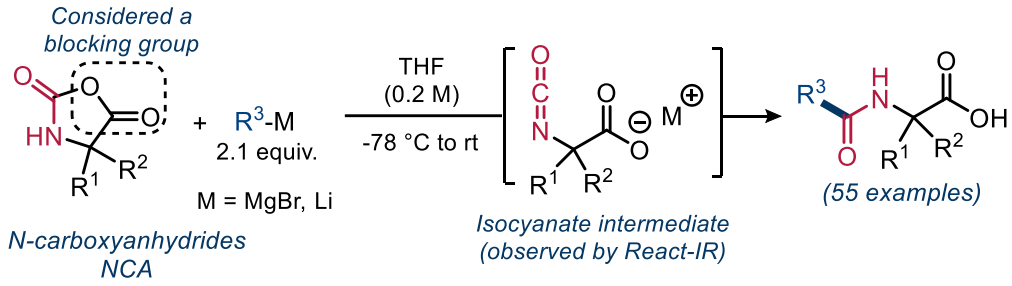

In the same context of C-C bond formation by employing Grignard reagents reacting with blocked isocyanates, Maes *et al*. described a relevant transformation that used thiophenol masked isocyanates.[73] A variety of sterically hindered Grignard reagents yielded the desired amide addition products in good yields (Scheme 1.17). Diphenyl disulfide by-product that resulted after the acidic workup was readily isolated and recycled in the process of the production of the thiophenol blocked isocyanate starting materials. Notably, the process did not result in the oligomeric side products, even when non-sterically hindered thiocarbamate partners were used as previously documented by Kerr *et al*.[42] However, the use of alkyl or less bulky aryl Grignard reagents led to the formation of urea side products, as a consequence of the aminolysis of the thiocarbamate precursor during the workup process. This complication was effectively circumvented using more reactive organolithium compounds.

Scheme 1.17. C-C Bond formation from the reaction of thiophenol masked isocyanates with Grignard reagents.

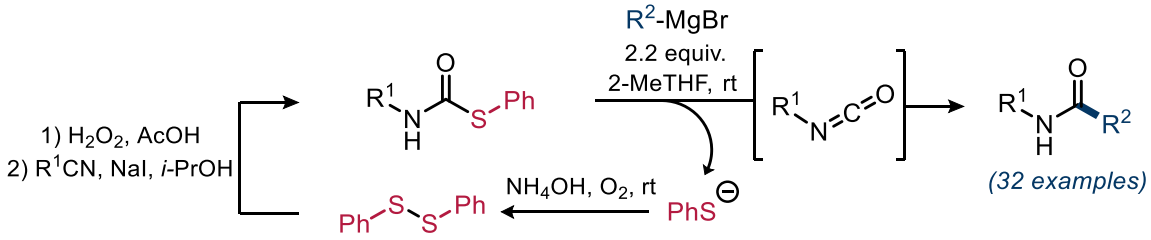

Finally, Kambe and coworkers employed trifluoromethyl blocked isocyanates as a platform to access amides via stoichiometric nucleophilic substitution reactions using Grignard reagents as carbon nucleophiles.[74] They introduced these bench stable, readily accessible trifluoroacetyl amides as versatile precursors for isocyanates (Scheme 1.18, a). This study suggested that the reaction pathway proceeded via the *in situ* formation of the free isocyanate intermediate at high temperatures, as supported by the control reactions outcomes (Scheme 1.18, b). Additionally, several proposed mechanisms of the productive and unproductive (degradation) pathways were described to justify the desired products

formation along with the side products that were observed with most of their reaction outcomes. The postulated mechanism started with N-H deprotonation by Grignard reagent to give intermediate X (Scheme 1.18, c), followed by a productive pathway A, which involved elimination/addition pathway to generate a free isocyanate intermediate then addition of the carbon nucleophile (Grignard). Another hypothesized pathway B was the addition/elimination sequence to form dual anionic intermediate followed by elimination of the blocking group (-CF_3) (a productive pathway). A competing degradation pathway involved the addition/elimination sequence to form dual anionic intermediate followed by elimination of amine moiety to access a trifluoroacetyl ketone product which is a common side product for this reaction (Scheme 1.18, c). A wide scope of functional groups including aryl, quinolin-8-yl, and (hetero)alkyl functional groups as well as F, Cl, and Br substituents were amenable to this reactivity.

Scheme 1.18. a) Accessing amides via C-C bond forming reaction of Grignard reagents with CF_3 blocked isocyanates. b) Selected control reactions performed by Kambe et al. c) The proposed reaction mechanism showing two productive pathways and an unproductive pathway for the formation of a commonly observed side product.

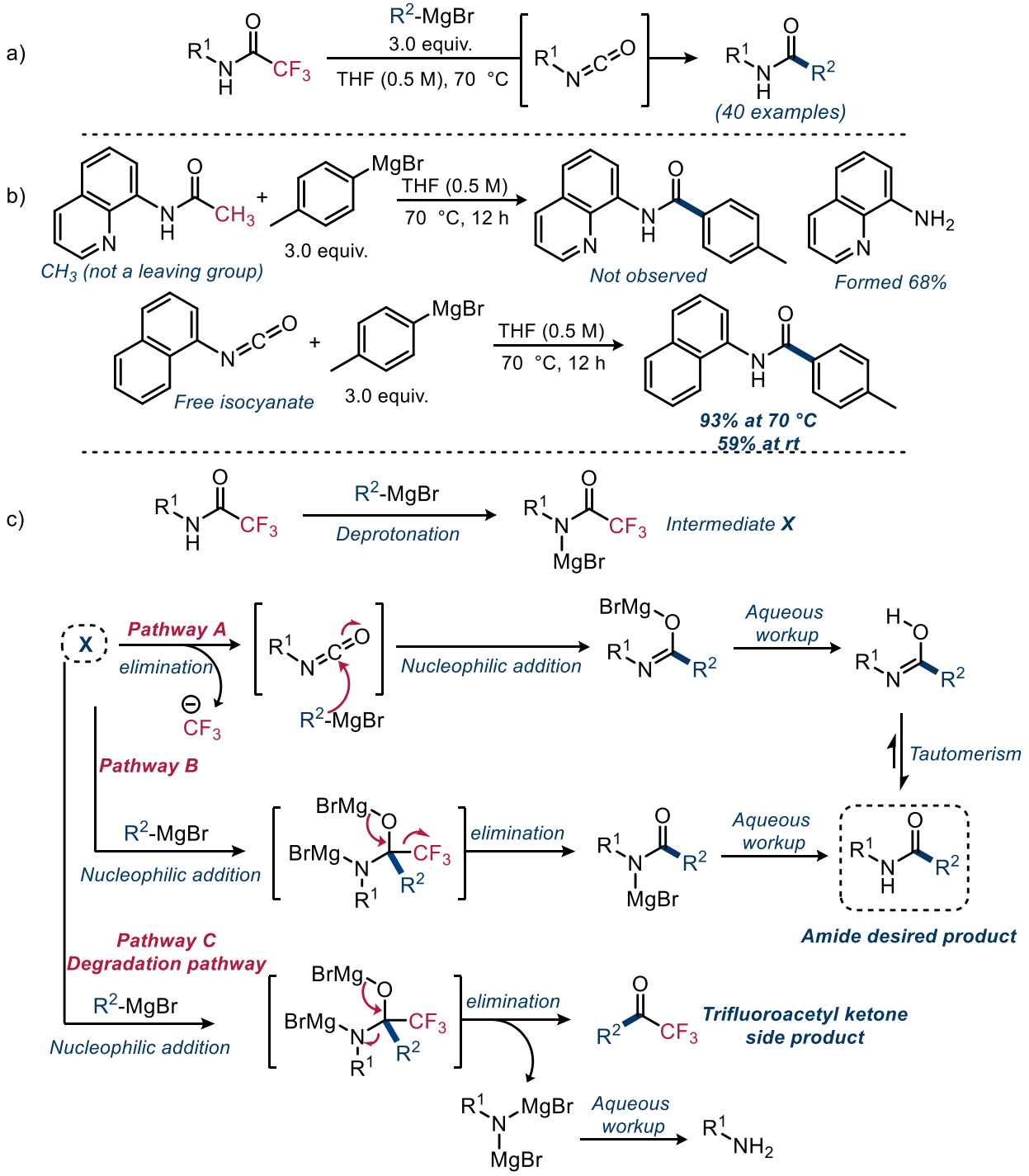

1.3 Heteroatom-Substituted Isocyanates and Their Masked (Blocked) Derivatives

In contrast to the well-established chemistry of carbon-substituted isocyanates, amphoteric heteroatom-substituted derivatives such as *N*- and *O*-isocyanates are still limited in synthetic reports. They are notoriously unstable and tend to oligomerize at low temperatures, typically forming dimerization products for *N*-isocyanates and trimeric isocyanurate products for *O*-isocyanates (Figure 1.6, b).[75,76] The effectiveness of these oligomerizations is such that it precludes the storage of heteroatom-substituted isocyanates in their free form. While the toxicity of *N*- and *O*- substituted isocyanates is a lower concern due to their transient existence, their dual character of being amphoteric (carrying both nucleophilic and electrophilic centers) have limited their applications for decades (Figure 1.6, a).

Figure 1.6. a) Heteroatom-substituted isocyanates (N- and O- isocyanates) showing their amphoteric nature. b) Oligomerization (homocoupling) reactions of N- and O- isocyanates.

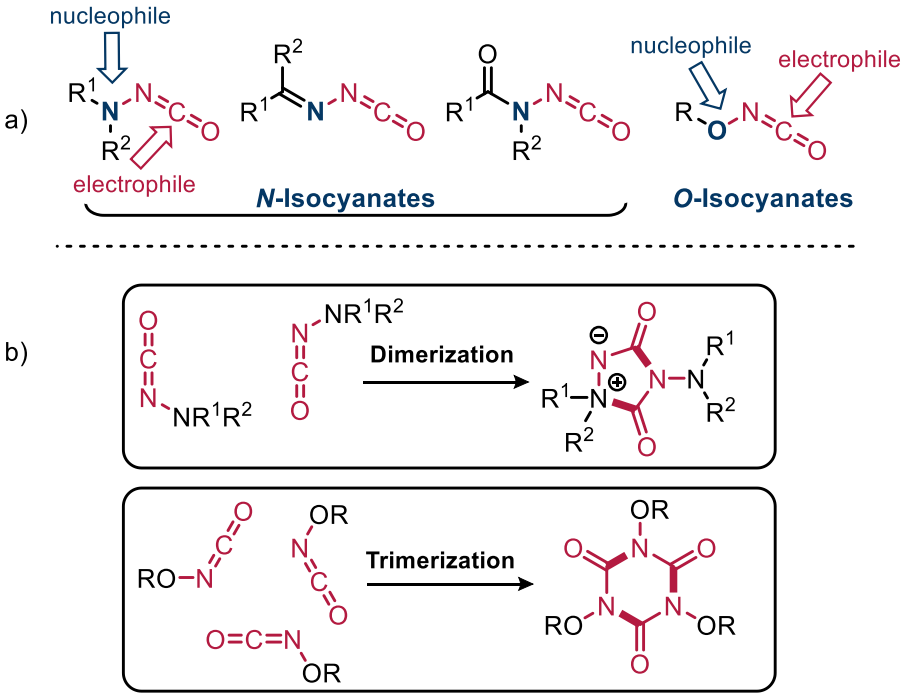

Nevertheless, N-N-C=O and O-N-C=O motifs are common subunits in pharmaceuticals and agrochemicals (Figure 1.7). Therefore, exploiting the chemistry of *N*- and *O*- substituted isocyanates could provide a promising avenue for the synthesis of such motifs. This reflects the importance of employing of *N*- and *O*-isocyanates as candidates for the development of their blocking group chemistry to overcome limitations by controlling their concentration (*in situ* release) to reduce homocoupling side reactions (Scheme 1.19).

Figure 1.7. a) Selected pharmaceuticals and agrochemicals containing the N-N-C=O motif. b) Selected bioactive molecules containing the O-N-C=O motif.

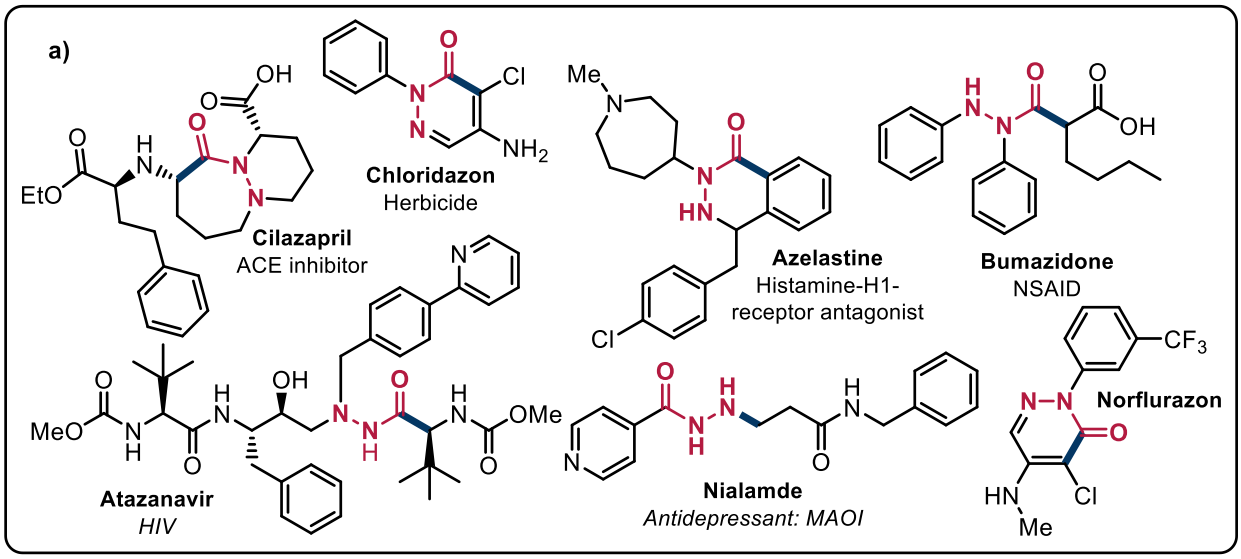

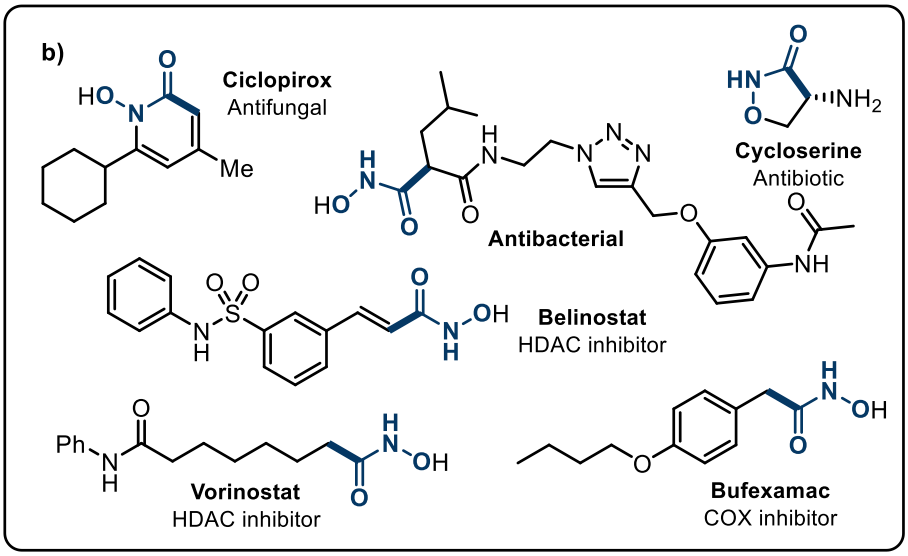

Scheme 1.19. Employing blocking group strategy on N- and O-isocyanates.

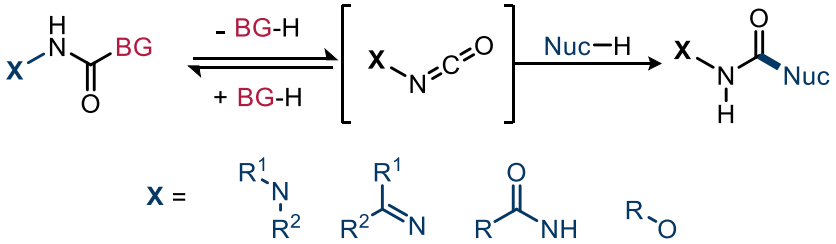

1.4 *N*-Isocyanates Synthesis and Reactivity

Throughout the 20th century, studies on *N*-substituted isocyanates have been intermittently reported. Most of these studies focused on reactivity based on solvolysis, with only a few reports on synthetic advancements using such species.[75,76] This can be attributed to the complex methods required to access such motifs, further complicated by their extreme instability, as they tend to undergo homocoupling even at temperatures as low as -40 °C to generate dimerization products.

Pioneering work for the *in situ* synthesis of *N*-isocyanates and their subsequent capture by other reagents to provide access to valuable compounds have been reported in the early 20th century. Stollé and Lwowski used carbamoyl azides as starting materials, allowing the *in situ* formation of the *N*-isocyanate via the Curtius rearrangement.[77,78] In the 1920's, Stollé disclosed the first examples of *aza*-Curtius (the nitrogen analogue of the Curtius rearrangement).[79] Under thermolysis conditions, carbamoyl azides underwent rearrangement and formation of N-N bonds via extrusion of N_2. The proposed intermediate was an *N*-isocyanate, which reacted intra- or inter-molecularly depending on the reaction conditions: indeed, when the *aza*-Curtius was performed in anhydrous solvent, an indazolone moiety was observed. On the other hand, when the reaction was performed in water, a carbazide was obtained via hydrolysis of the *N*-isocyanate intermediate. Finally, when the thermolysis was run in alcohol solvent, the corresponding carbazate was formed (Scheme 1.20).

Scheme 1.20. Stollé aza-Curtius rearrangement for N-isocyanate synthesis and subsequent functionalization.

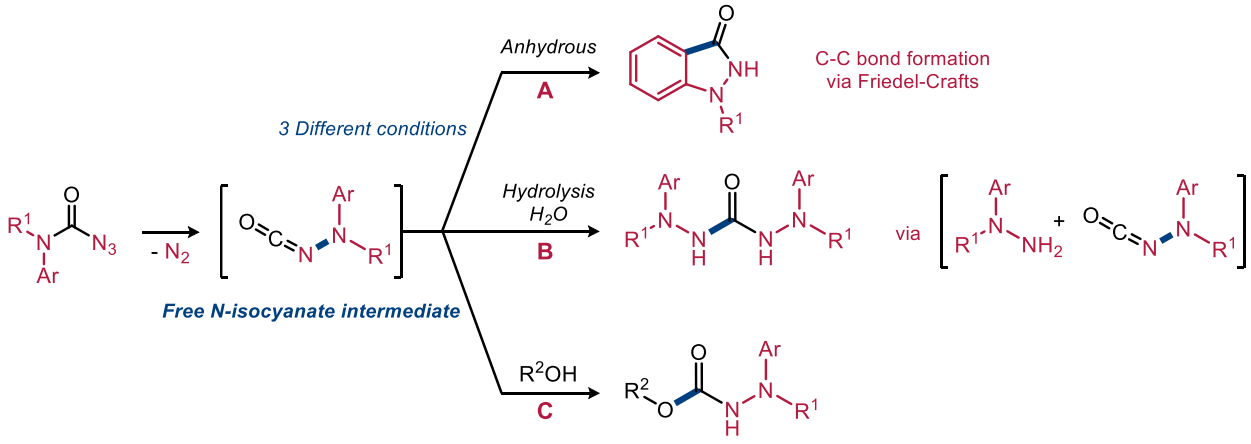

Moreover, cycloadditions of *in situ* generated *N*-isocyanates were reported by Lwowski and coworkers,[78] who were the first to report intermolecular cycloadditions of *N*-isocyanates with various π-systems including alkynes,[80] carbodiimides[81] and *C*-isocyanates[82] (Scheme 1.21, a). Fundamental insights on *N*-isocyanate reactivity were gained through these early efforts. Similar reactivity was observed by Jones

when imino-isocyanates were used as intermediates, and intermolecular aminocarbonylation was reported (Scheme 1.21, b).[83]

Scheme 1.21. a) Lwowski's aminocarbonylation with amino-isocyanates. b) First imino-isocyanate [3+2] cycloadditions on alkenes and alkynes by Jones.

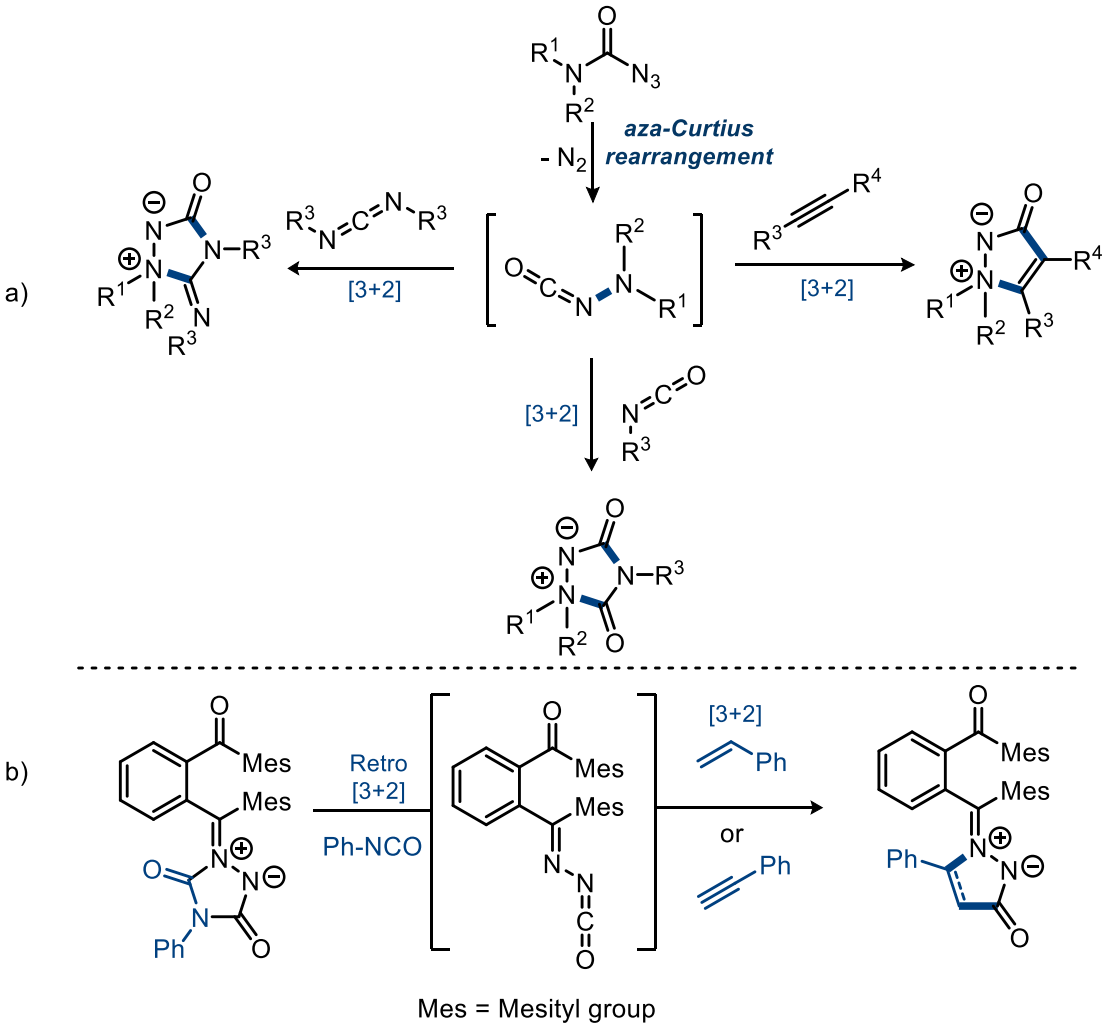

Mes = Mesityl group

1.4.1 Masked *N*-Isocyanates

Following the advancements of the blocking group approach with carbon-substituted isocyanates, there have been several successful endeavors to employ this strategy for nitrogen-substituted isocyanates over the last two decades. There is a necessity of implementation of a blocking group strategy with this species, for the purpose of exploiting their reactivity in a broader fashion for various synthetic applications, by allowing a high degree of control over the reactivity of these reactive intermediates. Of particular significance, the Beauchemin group has been engaged in studies on *N*-isocyanates over a prolonged period (≈14 years). They reported that amphoteric amino- and imino-isocyanates can be formed *in situ* (Scheme 1.22 and Scheme 1.23) under mild conditions and engage in high-yielding alkene cycloadditions[84–86] and

nucleophilic additions,[87,88] despite their known tendency to dimerize. In contrast to the pioneering work of Lwowski (intermolecular alkyne aminocarbonylation) and Jones (intermolecular alkene aminocarbonylation), the Beauchemin group successfully applied the blocking group strategy with *N*-isocyanates. This allowed for the easy access to *N*-isocyanates from their bench stable, readily available hydrazide and hydrazone precursors, thereby allowing the development of both intra and intermolecular variants of this reactivity (Scheme 1.22 and Scheme 1.23). In addition, this approach provided a fruitful platform for the synthesis of a variety of important compounds bearing the N-N-C=O motif. These derivatives are amenable to various substitution, cycloaddition and cascade reactions, leading to the formation of a range of semi-carbazides and heterocyclic compounds through reaction sequences. In their studies, the dual-reactive nature of *N*-isocyanates has been effectively utilized for various cyclization reactions. Additionally, several of these studies involved blocking group screening experiments to further optimize the blocking groups used to aid in controlled deblocking for each study depending on the mode of reactivity.[85,87,89]

Scheme 1.22. Selected previous Beauchemin group studies on amino-isocyanates.

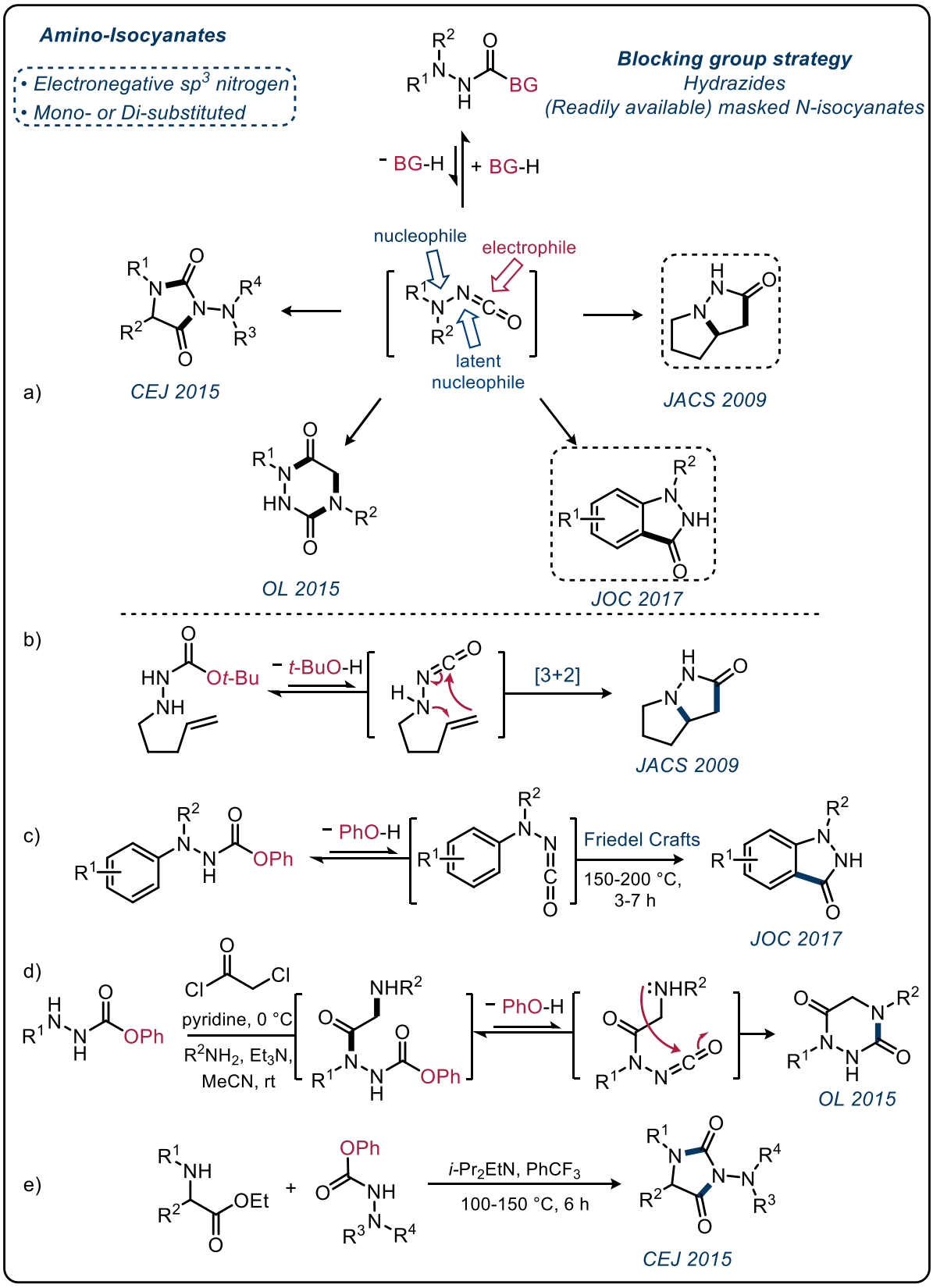

Scheme 1.23. Selected previous Beauchemin group studies on imino-isocyanates.

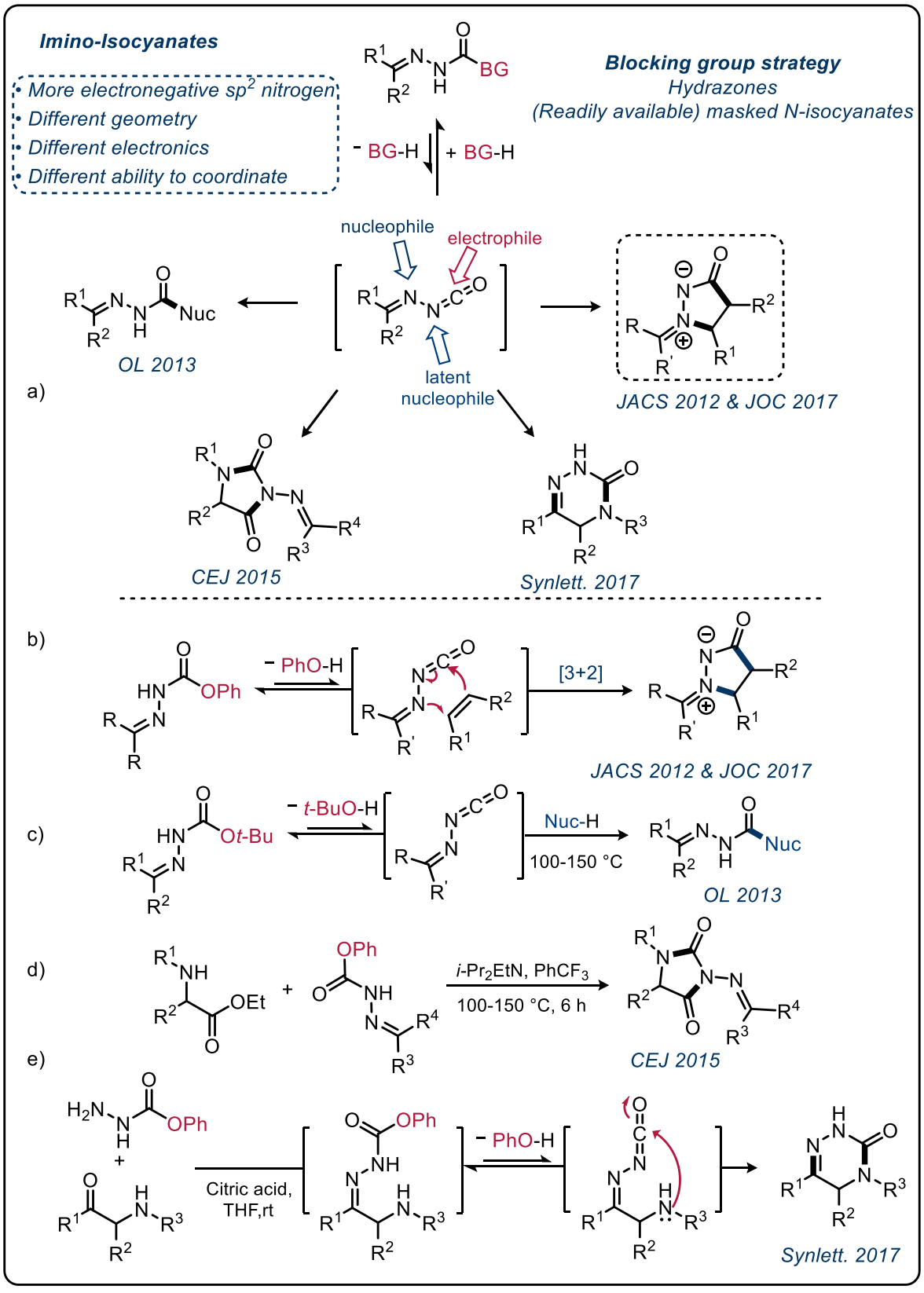

The group's efforts towards *N*-isocyanates were first reported in 2009, building on a hydroamination reactivity study of different hydrazine derivatives that initially led to the discovery of an intriguing side product in low yield. This side product was found to be the result of a [3+2] cycloaddition between an *N*-isocyanate intermediate and a pendant olefin (Scheme 1.22, b). This unexpected alkene aminocarbonylation reactivity promoted the exploration of alternative R groups to serve as blocking groups that would cleave under the reaction conditions to access the cycloaddition product. Manipulating the structure by changing R group (R = O*t*-Bu, NH_2) enabled the cyclization reaction to occur at high temperatures (150-200 °C, necessary given their poor leaving group ability), while using R = Ph group offered a platform to perform Cope-type hydroaminations (Scheme 1.24). Since this initial report, the Beauchemin lab has dedicated considerable effort to enhancing the reactivity of these blocked *N*-isocyanate precursors.

Scheme 1.24. Different reactivities by changing R group R = Ot-Bu gives aminocarbonylation, R = Ph allows Cope-type hydroaminations.

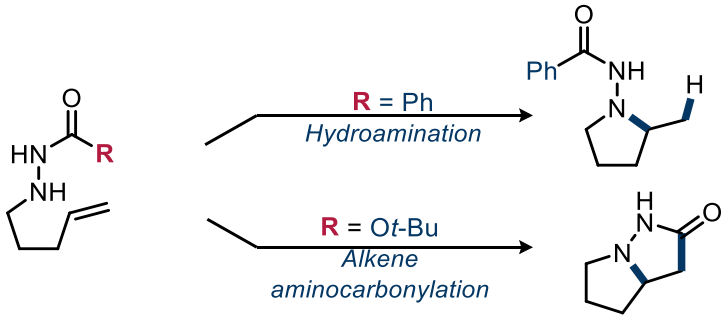

The same approach was probed using hydrazone starting materials to access bench-stable, readily isolable azomethine imines, which are crystalline cyclic dipole products (Scheme 1.23, b).[85,90] A concerted [3+2] cycloaddition aminocarbonylation event between an alkene and an *in situ* generated imino-isocyanate intermediate took place and was validated using computational chemistry. A thorough investigation provided support of their postulate about the intermediary of imino-isocyanate in free form in the concerted mechanism, by conducting a control experiment on an *N*-isocyanate substrate with a *N*-methyl substituent on the nitrogen atom required to form the isocyanate *in situ*. The failure of this reaction to generate the substitution product, in substitution and cascade reactions, provided evidence that the reaction pathway took place through the formation of the free isocyanate (Scheme 1.25, a). Additionally, the free *N*-isocyanate was observed for the first time by FTIR under closely related reaction conditions

(Scheme 1.25, b).[90] Furthermore, the study offered better information on the behavior of imino-isocyanate with the more electronegative sp^2 nitrogen atom (the lone pair on nitrogen are less available for donation). The results revealed that electron-rich alkene substrates were most reactive, and this supported that the LUMO of the imino-isocyanate was reacting with the HOMO of the alkene. Hydrazones precursors were also employed in substitution reactions with various heteroatomic nucleophiles. A range of semicarbazone and hydrazone derivatives were efficiently synthesized from hydrazone precursors and protic nucleophiles such as amines, alcohols, or thiols (Scheme 1.23, c). A blocking group screening suggested that phenol proved to be an effective blocking group which allowed room temperature reactivity, while *tert*-butanol allowed exchange at higher temperatures (80 - 120 °C). Strong nucleophiles as amines provided rapid access to the substitution products (20 minutes), while weaker phenols and thiols needed longer times.

Scheme 1.25. a) A control reaction to support the postulate of formation of free N-isocyanate in situ. b) Observation of the free N-isocyanate by FTIR, NCO stretching observed by in situ IR.

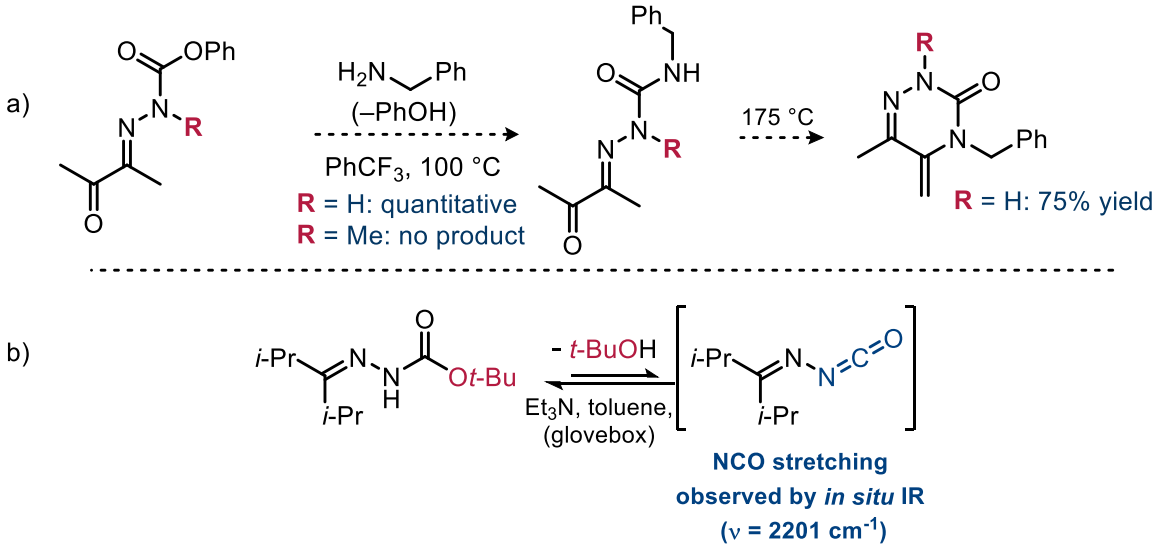

Guided by the study of the addition of α-amino esters on blocked amino isocyanates to access dipeptide analogues,[88] the reactivity of amino- vs imino- isocyanates was then explored for substitution cascade reactions using α-amino esters. The cascade proceeded through the addition of α-amino esters to isocyanate intermediates generated *in situ*, followed by cyclization to afford the hydantoin products (Scheme 1.22, e and Scheme 1.23, d).[91] Noteworthy, imino-isocyanates were observed to be more reactive than amino-isocyanates which required higher temperatures and gave lower yields. This shed light on the reactivity differences among similar heteroatom-substituted isocyanates with different hybridization. The

cyclization led to the selective formation of a five-membered hydantoin over the six-membered *aza*-diketopiperazine (Scheme 1.26).

Scheme 1.26. The selective formation of a five-membered hydantoins by the cascade reaction of N-isocyanates with α-amino esters.

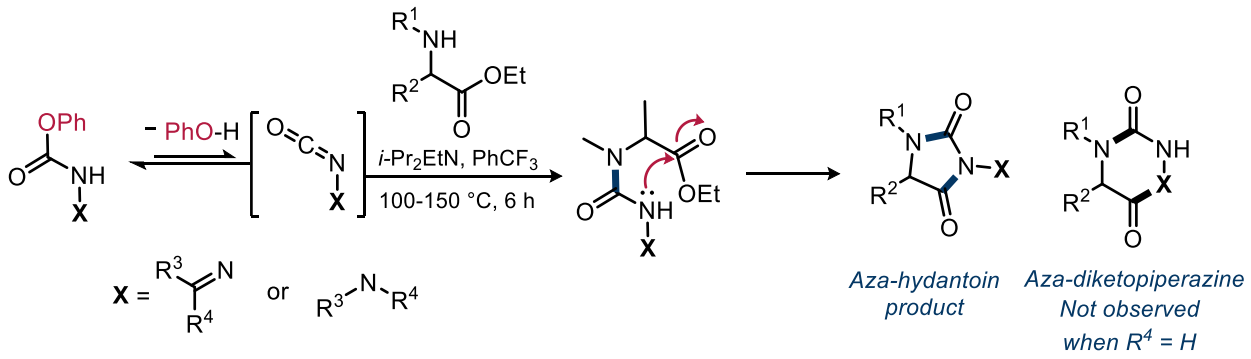

Aza-diketopiperazines, however were accessed from hydrazide precursors, through a one-pot reaction involving acylation of the hydrazide precursor with chloroacetyl chloride, nucleophilic substitution with a primary amine, followed by intramolecular cyclization by the attack of the amine nucleophile on the *in situ* generated free isocyanate (Scheme 1.22, d).[92] This reaction pathway was validated by conducting a separate control experiment to determine whether the product of amine substitution on isocyanate would undergo acylation reaction to form the cyclized product (Scheme 1.27, a). The result of this experiment clearly demonstrated that only the former pathway can lead to the desired product (Scheme 1.27, b).

Scheme 1.27. a) A control reaction to validate one pathway over the other. b) A productive and an unproductive pathway for the synthesis of aza-DKP from hydrazide precursor, chloroacetyl chloride, and primary amines.

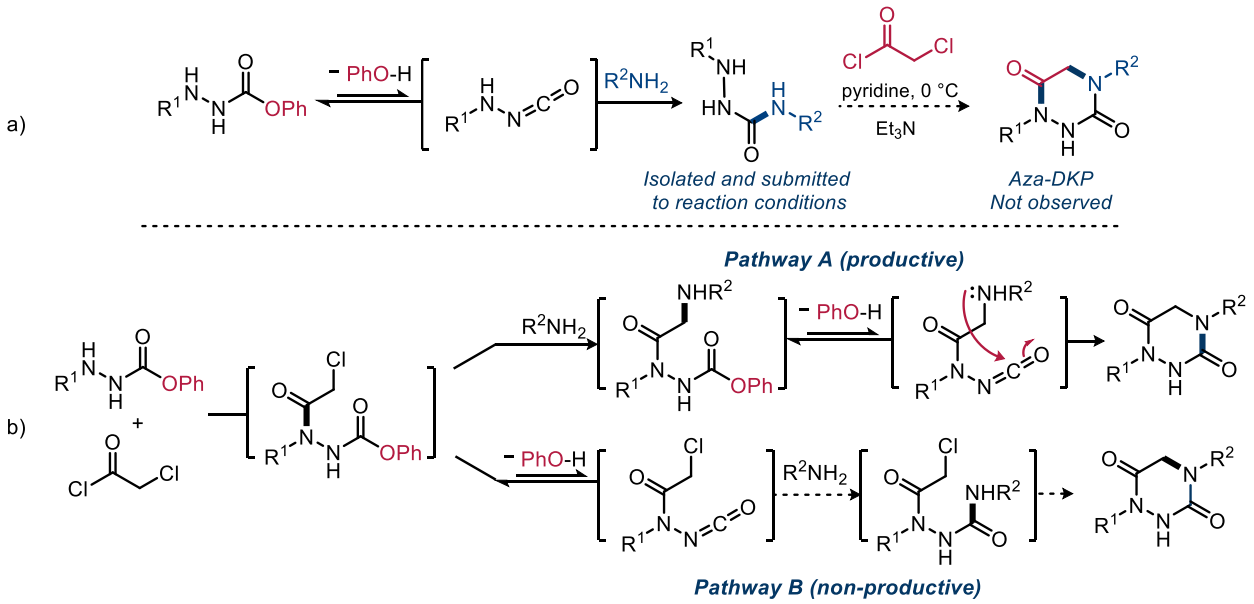

1.4.2 Previous Efforts on Carbon-Based Nucleophilic Addition to Masked *N*-Isocyanates

In all previous attempts, the reactivity of blocked *N*-isocyanates has had a major limitation: the addition of carbon nucleophiles to *N*-isocyanates remains poorly developed. The C-C bond forming reactions have been strictly confined to producing specific heterocycles, which result from cycloaddition reactions or the formation of 5-aminopyridazinone.[84,85,90] The synthesis of hydrazides from masked *N*-isocyanate precursors was investigated via carbon based nucleophilic addition to masked *N*-isocyanates. The previous successful endeavors of amide bond formation via addition of carboxylic acids to masked *C*-isocyanates (Section 1.2.3) motivated exploring this approach with masked *N*- and *O*- isocyanates. For *N*-isocyanates, both amino- and imino-substituted isocyanate derivatives with phenol blocking group were probed, and carboxylic acids were attempted as nucleophiles to achieve this goal. This strategy was met with failure with *N*-isocyanates (Scheme 1.28, a), presumably due to competing oligomerization reaction that predominates in the absence of strong nucleophiles. However, the generation of oxadiazolones and their use as a platform to access hydrazides instead of regular masked *N*-isocyanates was successful, resulting in the formation of the desired addition products (Scheme 1.28, b).[93] Such reactivity of oxadiazolones may be justified by the hypothesis that these precursors are actually heterocyclic precursors of blocked *N*-isocyanates. However, unlike their non-heterocyclic equivalents, these derivatives are highly resistant to oligomerization due to their aromatic nature.

Scheme 1.28. a) Initial attempts to amidate amino- and imino-substituted isocyanate derivatives. b) Successful application of oxadiazolone precursor in N-isocyanate amidation.

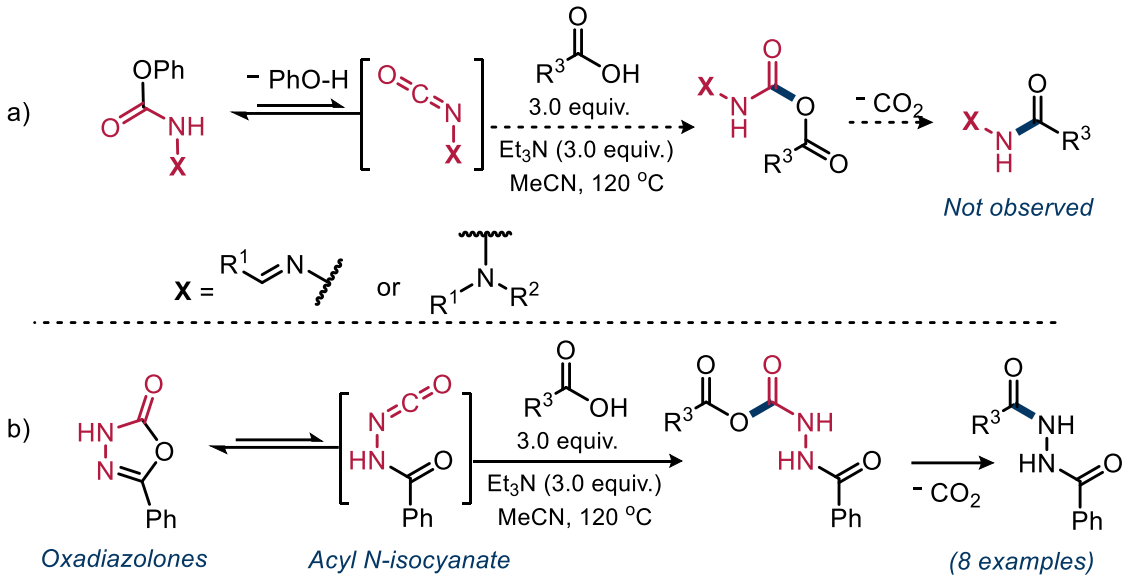

Furthermore, Friedel-Crafts cyclization was employed with blocked amino-isocyanates bearing *N*-aromatic substituents to afford C-C bond formation to access indazolones (Scheme 1.22, c).[89] Limitation of this methodology include that it was restricted to intramolecular cyclization of aromatic-substituted hydrazides, so a narrow scope of C-C bond formation was developed using this approach, combined with the harsh conditions employed. These limitations underscore an area of unexplored potential in the field. In summary, the Beauchemin group has exploited the amphoteric nature of *N*-isocyanates by applying a blocking group strategy which allowed a high degree of control over the reactivity of these reactive intermediates. This strategy led to facile synthesis of bench stable hydrazide and hydrazone precursors which demonstrated a clear potential for being a fruitful platform for the synthesis of various derivatives employing two major reaction manifolds, leveraging the amphoteric nature of *N*-isocyanates: 1) cycloaddition reactivity, which resulted in the formation of cyclic-azomethine imines and pyrazolones, and 2) substitution cascades, which led to the formation of *aza*-hydantoins, azauracil, *aza*-diketopiperazines, acyl-phtalazinones, acyl pyrazoles, and saturated heterocyclic derivatives.

1.5 *O*-Isocyanates Synthesis and Reactivity

O-Isocyanates are even scarcer than their nitrogen counterparts, despite the frequent occurrence of the O-N-C=O motif in widely used chelating pharmaceuticals, such as hydroxamic acid HDAC inhibitors, non-steroidal anti-inflammatory drugs, as well as in agrochemicals (Figure 1.7, b).[94–97] There are only a handful of reports about *O*-isocyanates in the literature prior to 2017. Similar to *N*-isocyanates, *O*-isocyanates are amphoteric and unstable, with high intrinsic propensity to oligomerize (homotrimerize) to form isocyanurates. However, their weak N-O bond adds complexity to the synthetic use of this species, which is not experienced in *N*-isocyanates. Their precursors and reaction products are more likely to undergo rearrangement reactions due to the weak N-O bond. Indeed, these unexpected rearrangements constitute a significant portion of the initial studies on *O*-isocyanates. Subsequently, the blocking group strategy has been applied to allow for the better use of this species as useful building blocks in organic synthesis. For an extended duration, masked *O*-isocyanate applications have been restricted to reactions that use strong protic nucleophiles, presumably due to competing trimerization reaction that predominates in the absence of strong nucleophiles. Nevertheless, the use of *O*-isocyanates in C-C bond forming reactions or amide bond forming reactions, wherein they serve as a platform for hydroxamate/hydroxamic acid synthesis, is very appealing. These functional groups exhibit strong biological activity and have applications ranging from synthetic intermediates to chiral ligand backbones. However, progress towards synthesizing these powerful functional groups is still lacking.

1.5.1 *O*-Isocyanates Synthesis by Lossen Rearrangement

The Lossen rearrangement is a chemical transformation characterized by the activation of an oxygen atom within a hydroxamic acid molecule, which subsequently behaves as a leaving group. This prompts the migration of a carbon group (R) following N-H proton abstraction by a base, resulting in the formation of an isocyanate product (Scheme 1.29).[98–100] This reaction, identified in the latter part of the 19th century, has been extensively utilized in conjunction with the Curtius and Hofmann rearrangements. Over the decades, these reactions have facilitated the synthesis of isocyanates and their derivatives, contributing significantly to advancements in the field of organic chemistry.

Scheme 1.29. General reaction mechanism for the Lossen rearrangement.

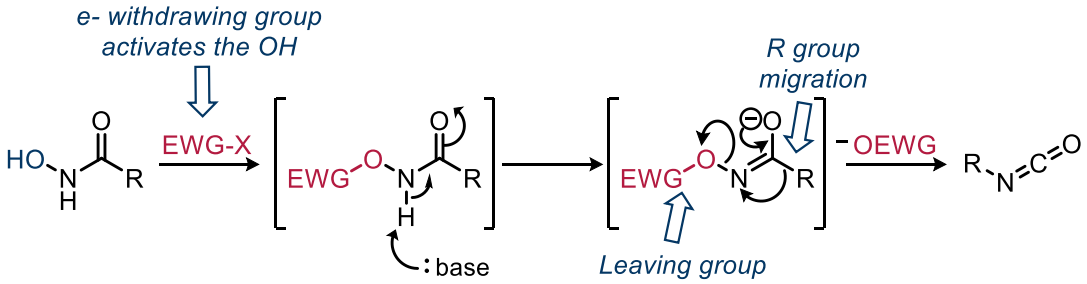

In the literature on Lossen rearrangement, the occurrence of heteroatom migration is quite rare, and in several cases, it has been reported as an unwanted side reaction. Indeed, unexpected formation of *oxa*-Lossen rearrangement products (oxygen-based migrating groups) has been observed by several groups in their attempts to perform electrophilic amination using bis-protected hydroxylamines (Scheme 1.30). Beauchemin and Polat have recently conducted an extensive study on the *aza*-Lossen rearrangement, employing *N*-hydroxyureas as precursors.[101]

Scheme 1.30. Unexpected O-isocyanate formation via oxa-Lossen rearrangement.

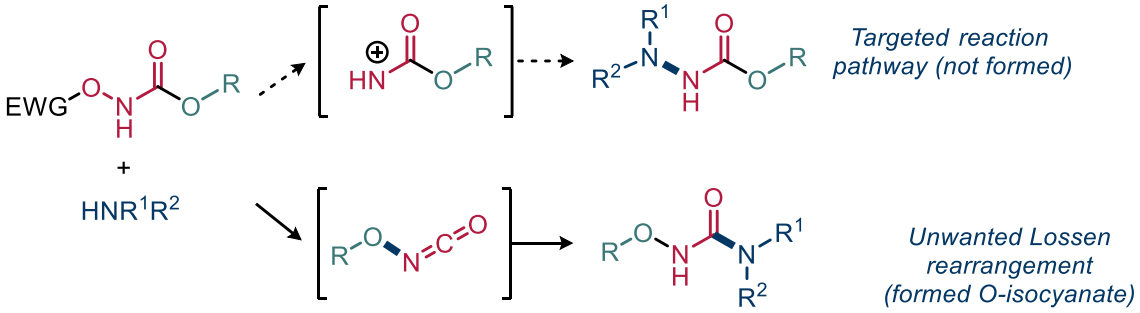

Hanessian and Johnstone were initially attempting to generate NH-Boc α-amino acids using the reaction of dicarbonyl nucleophiles with sulfonyl hydroxylamine derivatives ($PyrSO_2ONHBoc$).[102] However, instead of the expected result, they generated *O*-*t*-butoxy-carbonylamino derivatives through the addition of enolates to *t*-butoxy-isocyanate, as confirmed by X-ray spectroscopy (Scheme 1.31, a). Similar reactivity was also reported using TsONHBoc. Additionally, Pellacani *et al.* reported an unexpected Lossen rearrangement that resulted in the formation of imidazolidin-2-ones, with an *O*-isocyanate proposed as the intermediate (Scheme 1.31, b).[103]

Scheme 1.31. a) Hanessian oxa-Lossen mediated formation of O-t-butoxy-carbonylamino derivatives through the addition of enolates to t-butoxy-isocyanate. b) Pellacani synthesis of imidazolidin-2-ones via oxa-Lossen rearrangement.

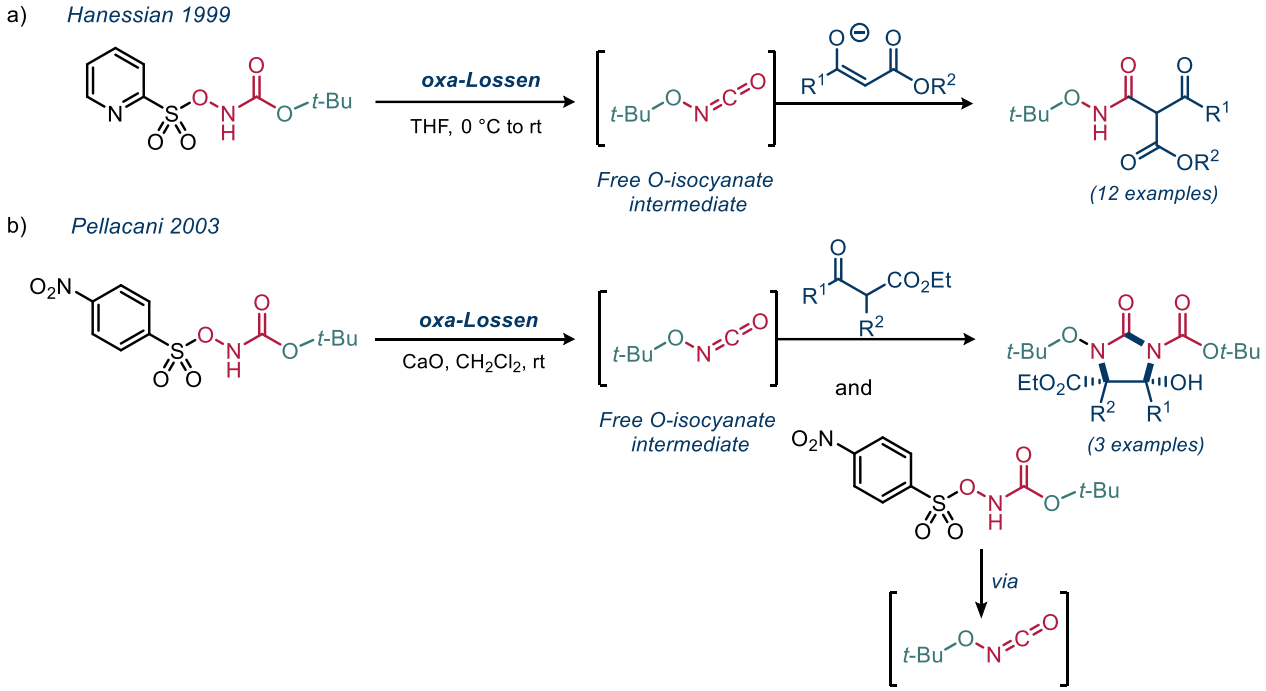

In the same context, Priefer and coworkers were trying to access protected hydrazines through the electrophilic amination of amines. However, they ended up observing *N*-*t*-butoxyurea products instead (Scheme 1.32, a).[104] The authors suggested an *oxa*-Lossen mechanism to explain this outcome, referring to the work of Hanessian and Pellacani as evidence that the reaction goes through the formation of the free *O*-isocyanate as an intermediate.

Furthermore, Thambidurai group were aiming to form hydrazines via N-N bond formation with amines using TsONHBoc. Although they reported in 2011 and 2012 that their reaction conditions led to the formation of the targeted hydrazine derivatives,[105,106] they issued corrections to both papers in 2014 and 2015, changing the structure of the products to *N*-oxyureas.[107,108] In these corrections, the authors suggested an *O*-isocyanate intermediate that was formed via an *oxa*-Lossen rearrangement and then captured with an amine nucleophile, similar to Priefer's work (Scheme 1.32, b).

These studies highlight not only the unpredictable reactivity of species containing hydroxylamine, but also demonstrate that substitution reactions on *O*-isocyanate can proceed successfully. However, these studies did not develop the scope of *O*-isocyanate oxygen substitution (their precursors were limited to *t*-Bu).

Scheme 1.32. a) Priefer's synthesis of N-t-butoxyurea products via oxa-Lossen mechanism. b) Thambidurai's synthesis of N-oxyureas via oxa-Lossen rearrangement.

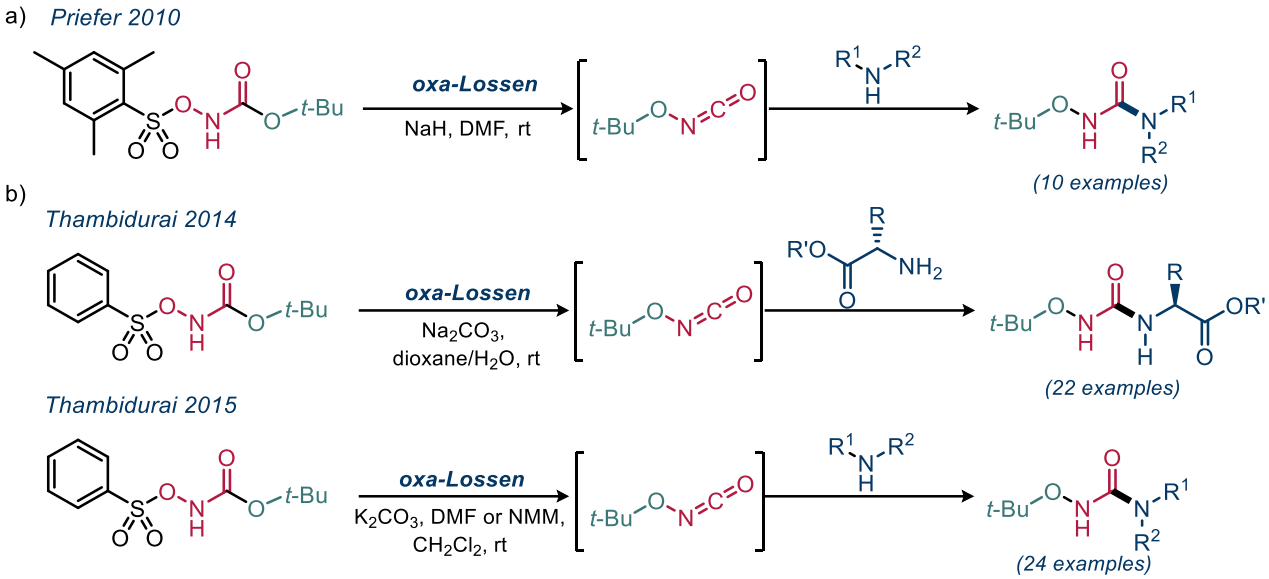

1.5.2 *O*-Isocyanates Reactivity by Application of Blocking Group Strategy

In 1994, a group of researchers from the BMS pharmaceutical research institute was first to disclose the synthesis and synthetic application of a masked *O*-isocyanate. This pioneering work demonstrated that homotrimerization of *O*-isocyanates can be avoided through *in situ* isocyanate formation, likely by controlling the concentration of *O*-isocyanate available.[109] Initially, the BMS scientists used equimolar *O*-benzylhydroxylamine and CDI to access an imidazole-blocked *O*-isocyanate, to be employed in substitution reactions with various amine and aniline nucleophiles (Scheme 1.33). Some products underwent a subsequent cyclization reaction through an intramolecular nucleophilic attack of isocyanate nitrogen on a carbonyl electrophile residue. Although no reactions have been reported to either confirm or refute the intermediacy of an *O*-isocyanate, there is a possibility that an elimination/addition mechanism took place, because even moderately nucleophilic anilines demonstrated acceptable reactivity using this approach. This approach by Romine and coworkers underscores the efficient reactivity of blocked *O*-isocyanates, but the conditions are not ideal for synthesis. Hydroxylamines are susceptible to degradation when stored as the free base, so it would be more suitable to store them as the blocked precursor. A comprehensive study of the effects of *O*-substitution is also needed because they only introduced *O*-benzyl isocyanate as precursor for this synthesis. A closely related study was conducted by Tsukamoto and colleagues during their attempt to synthesize novel D-amino acid oxidase inhibitors, using 4-nitrophenyl benzyloxycarbamate to access *N*-hydroxyureas via an amine substitution process.[110]

Scheme 1.33. First report of blocked O-isocyanate reactivity using in situ formation of an imidazole-blocked precursor.

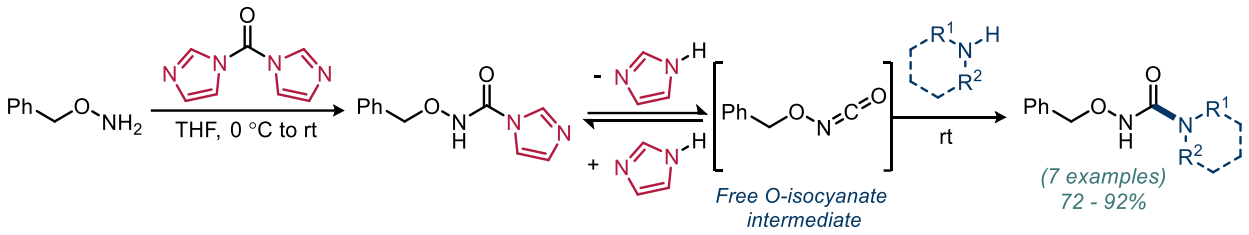

The Beauchemin group started research on *O*-isocyanates by studying the synthesis of their masked form and their use as a platform for cascade reactions. In an attempt to access hydroxylamine containing heterocyclic molecules, they reported the use of phenol blocked isocyanate as a precursor for this reaction wherein the deblocking conditions involved employment of a base catalyst and heat. This gave access to the five-membered *oxy*-hydantoins via the rection of phenol-blocked *O*-isocyanates with α-amino esters, and the six-membered *oxy*-dihydrouracils via the rection of phenol-blocked *O*-isocyanates with β-amino esters (Scheme 1.34, a).[111] Notably, an *N*-methoxy carbamate was employed as the *O*-isocyanate reaction partner under the optimized conditions and at elevated temperatures to investigate the likelihood of an *O*-isocyanate intermediate. The substitution reaction with sarcosine ethyl ester as the nucleophile was met with failure in all trials, where the presence of methyl substituent on the nitrogen completely shut down the reactivity, implying that an addition/elimination mechanism is not taking place. The complete recovery of both starting materials indicates an elimination/addition mechanism is happening instead, involving a free *O*-isocyanate intermediate as a part of the reaction pathway (Scheme 1.34, b). This was a significant discovery during the development of *O*-isocyanate reactivity in the Beauchemin lab, and this mechanistic test has been replicated for a range of new approaches with a proposed *O*-isocyanate intermediate.

Scheme 1.34. a) Accessing oxy-hydantoins and oxy-dihydrouracils via the rection of phenol-blocked O-isocyanates with amino esters. b) A control reaction to validate elimination/addition mechanism (generation of free O-isocyanate intermediate) over addition/elimination mechanism.

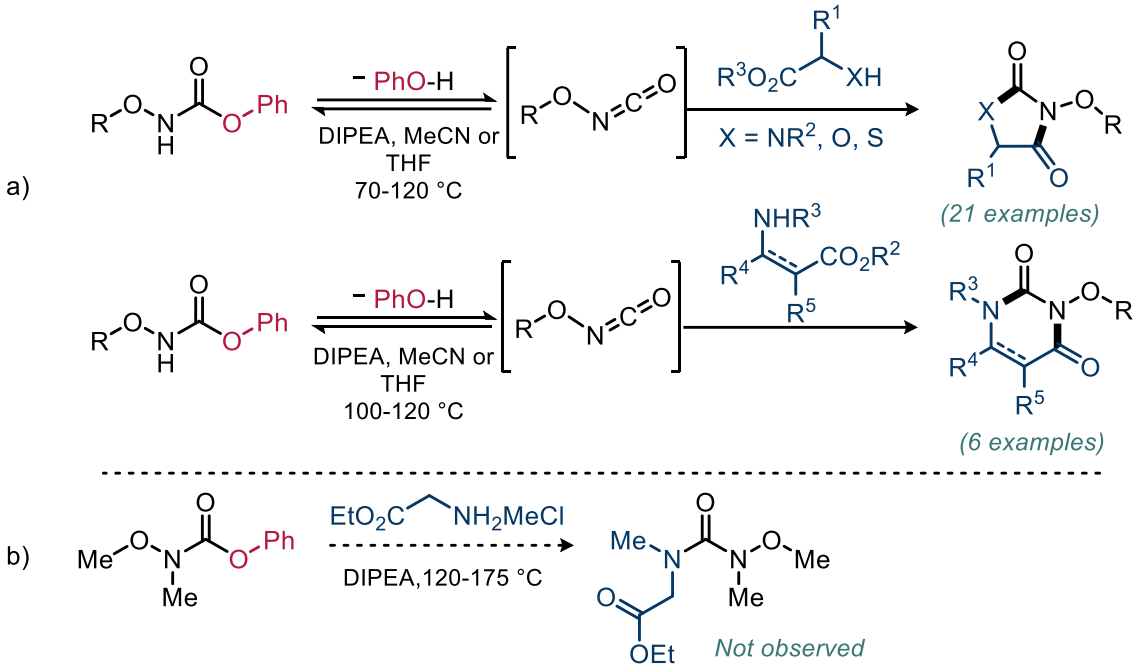

In a second publication from the Beauchemin lab, the five-membered *oxy*-benzimidazolones and the six-membered *oxy*-dihydroquinazolinones were produced through a substitution reaction and copper-catalyzed amination cascade (Scheme 1.35).[112] Phenol was employed as a blocking group once more, and a suitable deblocking equilibrium was achieved using high temperature and base catalysis. Notably, this process was carried out in a single pot, with reagents added sequentially instead of all at once. Neither of these previous studies probed the use of alternative blocking groups, nor did they investigate the optimization of the substitution reaction on the masked *O*-isocyanates separately. Consequently, a more comprehensive investigation of the substitution of blocked *O*-isocyanates was deemed necessary.

Scheme 1.35. Synthesis of oxy-benzimidazolones and oxy-dihydroquinazolinones via substitution reaction and amination cascade on masked O-isocyanates.

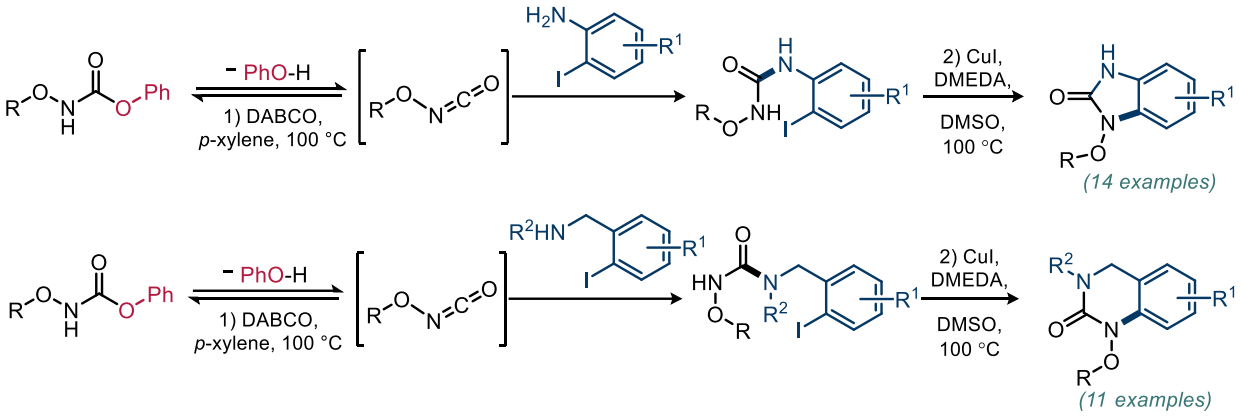

Subsequently, a comprehensive study was conducted by the Beauchemin group wherein the use of *oxy*-carbamate *O*-isocyanate precursors provided a pathway to the synthesis of the useful *N*-oxyureas, through the process of substitution with amine nucleophiles (Scheme 1.36).[113] The attempt to identify suitable *O*-isocyanate precursors shed light on the varying reactivity of isocyanate masking groups. This research has resulted in the development of bench stable *O*-isocyanate precursors, which enhance the versatility of *N*-oxyureas synthesis. It also showcases the controlled reactivity of masked *O*-isocyanates. Furthermore, the unsaturated hydroxyureas products of this reaction are of special interest as they gave access to the first example of Cope-type hydroamination on unsaturated hydroxyureas.

Scheme 1.36. The use of oxy-carbamate O-isocyanate precursors for the synthesis of the N-oxyureas through substitution with amines.

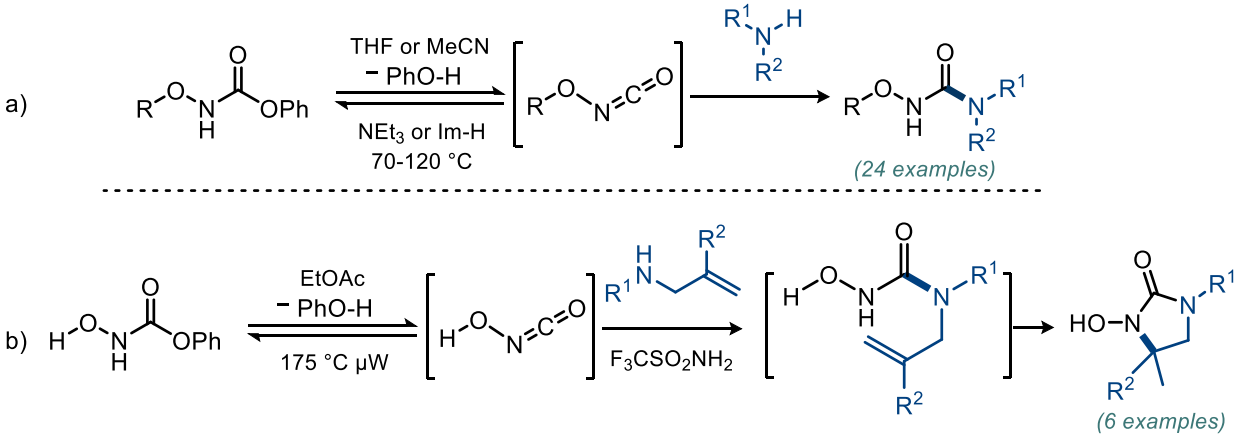

In an effort to understand the reactivity of *O*-isocyanate precursors, Beauchemin *et al.* initially investigated the potential of various oxy-carbamates and a single oxyurea to form *O*-isocyanates under conditions similar to those employed for *N*-isocyanates.[113] The experimental outcome demonstrated that

the conditions necessary for the deblocking equilibrium to release of reactive free *O*-isocyanates are dictated by the nature of the masking (leaving) group of the isocyanate precursor, as is the case with both carbon and nitrogen-substituted isocyanates. The screening study of various blocking groups (PhO, *p*-$NO_2C_6H_4O$, BnO, *t*-BuO, EtO, *i*-Pr_2N, and CF_3CH_2O) on various oxy-carbamate precursors (hydroxy-, alkoxy-, and acyloxy-substituted carbamates) revealed couple significant conclusions. Regarding the substituted oxy-carbamates, it was observed that hydroxy-carbamate precursors (R = H) were significantly less efficient at undergoing substitution compared to alkoxy and acyloxy carbamates. These findings are particularly significant given the lack of Lossen rearrangement under the reaction conditions and the considerable interest in OBz hydroxylamine derivatives as amination agents. Presumably, the susceptibility of hydroxycarbamates to oxidation and difficulties in their isolation accounted for the lower yields linked to their use.

Secondly, regarding the blocking groups, phenol emerged as the optimal leaving group for the substitution on hydroxy carbamates and was also found to be the most effective leaving group for alkyl and acyl-substituted examples. The conditions required when *p*-nitrophenol leaving group was found to be too mild, necessitating the addition of a stoichiometric base to mitigate the competing oligomerization reaction, and the corresponding precursors (with the nitrophenyl BG) were too unstable for routine use. Alternatively, phenol-derived masked isocyanates demonstrated stability over extended storage periods and exhibited high reactivity under the conditions.

1.5.3 Previous Efforts on Carbon-Based Nucleophilic Addition to Blocked *O*-Isocyanates

Inspired by their previous closely related study on blocked *N*-isocyanates, the Beauchemin group reported that amphoteric free *O*-isocyanates could be formed *in situ*, and engaged in high yielding oxy-carbonylative cycloadditions, wherein they serve as a non-charged 1,3-dipole equivalents in the concerted reaction with alkenes or pendant alkenes to access *aza*-oxonium ylides (Scheme 1.37).[114] These reactive ylide intermediates were involved in subsequent reactivities, such as C-H amination to generate six-membered oxazinones, [1,2]-shift to yield five-membered oxazolidinones, or ring opening followed by a ring closure to form four-membered lactam products (Scheme 1.37).

Scheme 1.37. Phenol-blocked O-isocyanates serve as a non-charged 1,3-dipole equivalents for the synthesis of aza-oxonium ylide via [3+2] cycloaddition.

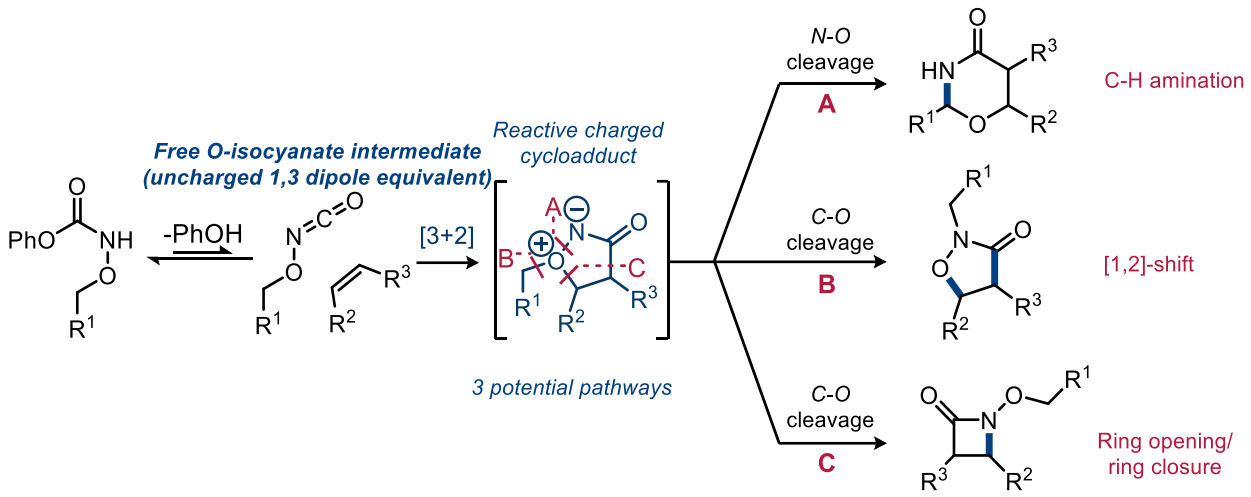

In their attempts to access hydroxamic acid-based metal chelating hosts with potential biological activity, Gopalan and coworkers developed an approach which is based on the use of bench stable *N*-benzyloxy carbamic acid ethyl ester, which is essentially a benzyloxy carbonyl building block with a leaving group, as an electrophilic platform for their reaction.[115] They aimed to use stoichiometric strong carbon nucleophiles, formed by deprotonation using LiHMDS, as reaction partners. However, prior to this substitution step, they had to initially modify the precursor carbamate by performing *N*-alkylation to the isocyanate nitrogen, a step which made the substitution reaction more feasible, considering the strong basic characteristics of the lithium reagent (Scheme 1.38). This strategy of protecting or functionalizing the isocyanate nitrogen presumably omitted the generation of the free isocyanate form as an intermediate of the reaction. Additionally, their postulate about the use of nucleophiles carrying electron-withdrawing sulfone groups was successful in suppressing the side reactions and promoting the pathway leading to the formation of the desired hydroxamate products.

Scheme 1.38. Gopalan's synthesis of hydroxamate derivatives.

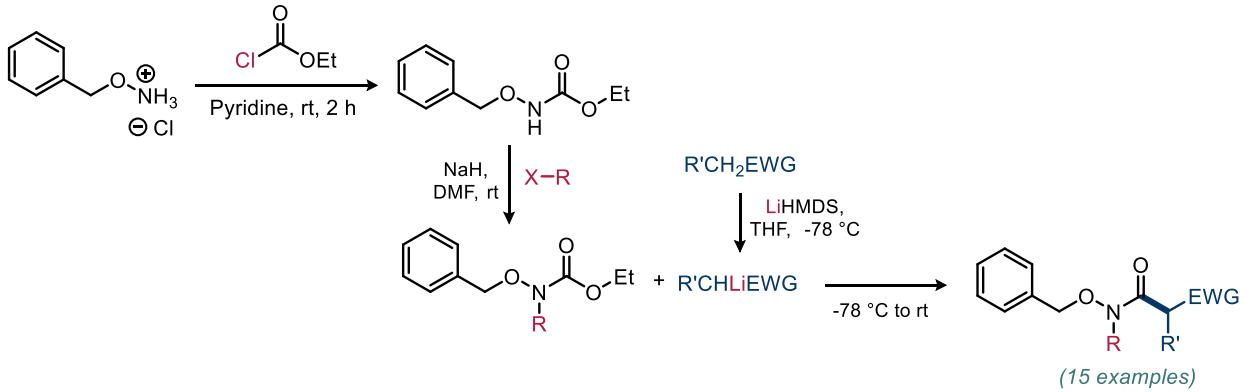

Following advances in studying blocked *O*-isocyanates applications in substitution and cycloaddition reactions, which provided access to several heterocycles, the Beauchemin group was enthusiastic about the reactivity of blocked *O*-isocyanates toward carbon centered nucleophiles to access hydroxamic acid/hydroxamates based molecules.[116] These are useful synthetic intermediates and powerful chiral ligand backbone which bind efficiently with metals like iron and zinc in biological systems. Hydroxamates exhibit potent biological activity ranging from antibacterial, anti-inflammatory, to anticancer agents. Inspired by the previous work of employing carboxylic acid nucleophiles to access amides from blocked *C*-isocyanates,[65–67] this isocyanate amidation approach attracted the attention to be probed on the blocked *O*-isocyanates, given the successful reactivity of masked *O*-isocyanates toward various heteroatom nucleophiles. The reaction of carboxylic acids on isocyanates eventually involves amide bond formation, this reaction takes place through the attack of the carboxylate nucleophile through its protic oxygen on the isocyanate electrophile (Scheme 1.39). Thus, it remains, to an extent, related to the protic nucleophilic substitution reactions. The bigger concern was the natural tendency of *O*-isocyanates to oligomerize in the absence of strong bases. Nevertheless, investigations proceeded by probing the ability of blocked *O*-isocyanates to serve as a backbone for this reaction. Extensive optimization study was conducted to provide knowledge about the reactivity of these species and the optimal conditions to promote the desired reaction pathway. Superstoichiometric carboxylic acid (at least 2.0 equivalents, preferably 3.0 equivalents) was necessary to circumvent the side reactions including hydrolysis which generated urea side products, and trimerization, which generated cyclic isocyanurate. The optimization of the amount of the base, to 0.2 equivalents, was also crucial for the reactivity. The optimal conditions included employing heat with temperatures as high as 120 °C for overnight reaction, polar aprotic solvent (MeCN), and a tertiary amine base such as Et_3N. Limitations included the relatively harsh conditions of the reaction and the incompatibility of the synthetic method with a number of substrates such as substrates bearing protic

motifs, benzoic acid derivates bearing a free phenolic OH, or electron poor aromatic rings with halide substituents. This methodology of amide synthesis provided the first official carbon centered nucleophilic substitution on masked *O*-isocyanates, where the free form of isocyanates is a potential *in situ* released intermediate. The success of this approach paves the way for successive investigations of substitution reactions of masked *O*-isocyanates with carbon-based nucleophiles.

Scheme 1.39. Synthesis of hydroxamate derivatives via amide bond formation reaction of carboxylic acids with blocked O-isocyanates.

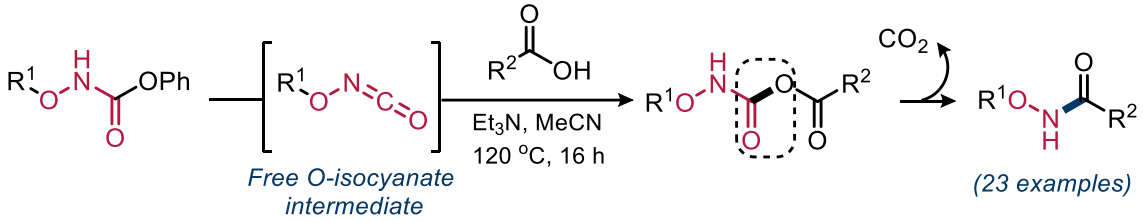

1.6 Research Hypothesis and Goals

The significance of nitrogen containing compounds in organic synthesis, the strategic application of a blocking group approach to heteroatom-substituted isocyanates, and our research group's interests in the synthesis of hydroxamates, hydrazides, and NNCO containing heterocycles such as pyrazolones, serve to provide context for the research contributions included within this thesis. Despite that the use of isocyanates as a platform for amide synthesis has been extensively studied, this field is still underdeveloped when it comes to heteroatom-substituted isocyanates. The central working hypothesis being that the employment of a blocking group strategy with these rare heteroatomic isocyanates could allow for the development of suitable precursors for controlled addition of carbon nucleophiles to masked *O*- and *N*- isocyanates and overcome the limitations that hinder the widespread adoption of these reagents. By optimizing the reactivity of the stoichiometric organometallic addition to masked *O*- and *N*-isocyanates, C-C bond forming reactions could be feasible. Efforts to mitigate the competing side reactions such as rearrangement and oligomerization reactions, could provide high yields of the desired products (hydoxamates or hydrazides for *O*- and *N*- isocyanates, respectively).

Inspired by the previous efforts on the organometallic addition on isocyanates by Bode, Pace, Kerr, and Kim (for free *C*-isocyanate precursors, Section 1.1.2), and by Bode, González, Maes, and Kambe (for masked *C*-isocyanate precursors, Section 1.2.5), this reactivity could be first investigated on the rare amphoteric *O*-isocyanates by applying blocking group strategy. This strategy is particularly attractive to address issues such as unwanted oligomerization and functional group limitations. The goal was to study the behavior of masked *O*-isocyanate reagents to identify the differences between these heteroatomic

isocyanates and the *C*-substituted counterparts, study the possibility of additional chelation of these substrates with the metal, and the effects of this additional chelation (if any) on the reactivity. The success of this approach would lead to the development of high yielding, intermolecular, stoichiometric organometallic substitution reactions with *O*-isocyanate reagents. Efforts toward this goal are presented in Chapter 2.

If successful, this goal would be extended to involve masked *N*-isocyanates as well. While potentially a straightforward extension, the reports of dimerization side reactions occurring at very low temperatures made this a more ambitious goal that could benefit from prior knowledge gained with *O*-isocyanate precursors. Importantly, this could allow for the expansion of research on the coordination with the metals by employing different types of nitrogen atoms with different geometric properties, Lewis basicity, and coordination abilities. The intermolecular addition organometallic to masked *N*-isocyanates would give access to different products, hydrazides, by using these precursors. Efforts toward this goal are presented in Chapter 2, and unexpected reactivity that resulted in the formation of pyrazolones, is presented in Chapter 3.

Then, this chemistry would be explored using intramolecular variants for the purpose of the synthesis of heterocyclic compounds. This is a more ambitious objective, as this requires controlled reactivity for the formation of the organometallic reagent and generation of the transient isocyanate, to provide access to the target heterocyclic product. Efforts toward this goal are presented in Chapter 4.

Chapter 2 Stoichiometric Addition of Organometallic Reagents to Masked Heteroatom-Substituted Isocyanates

2.1 Syntheses of Hydroxamic Acid and Derivatives

Given the importance of hydroxamic acid derivatives in synthetic organic and medicinal chemistry,[94–96,117–119] we elected to first revisit their formation from masked *O*-isocyanates. Recent advancements have centered on oxidative strategies, transforming alcohols,[120] aldehydes,[121] and oximes[122] into the corresponding hydroxamates/hydroxamic acids (Figure 2.1). Despite being innovative, these strategies are characterized by limited functional group tolerance. The direct conversion of inactivated esters to hydroxamates/hydroxamic acids has also been investigated, but it generally requires either strong bases, protic conditions, or a large excess of the hydroxylamine nucleophile, which typically limits functional group tolerance.[123,124] As a result, the most prevalent method for accessing hydroxamates/hydroxamic acids continues to be the stoichiometric activation of carboxylic acids (Figure 2.1).[96,119]

Figure 2.1. Previous efforts in synthesis of hydroxamates/hydroxamic acids.

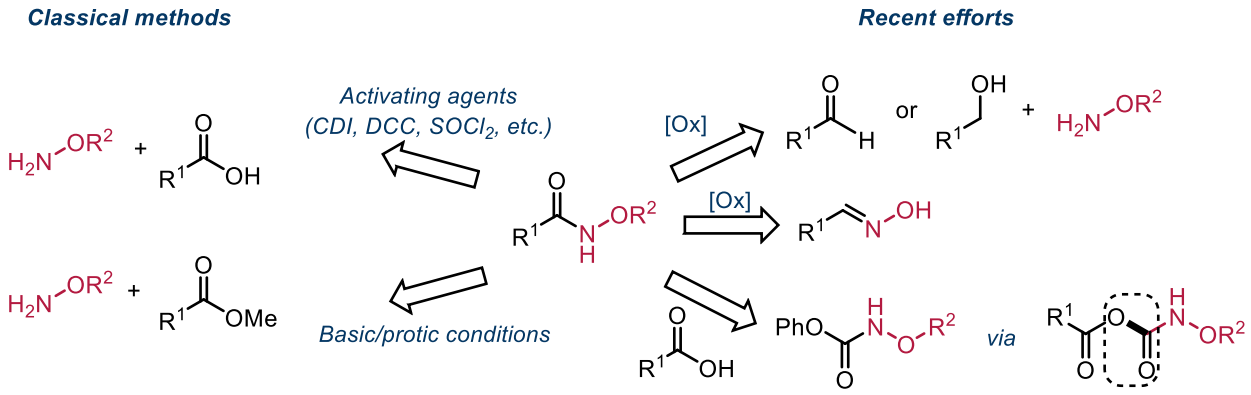

Related to this strategy, we have recently demonstrated that carboxylates can add to *O*-isocyanates (Figure 2.1 & Scheme 2.1, a),[116] however this required temperatures above 100 °C and faced limitations that could potentially be overcome through direct C-C bond formation using an organometallic reagent, such as Grignard reagent. With the intention to explore this chemistry on masked *O*-isocyanates, a concern arose of the effect of the basicity of the organometallic reagents on the outcomes of this reaction. While a catalytic amount of base is needed to cleave the blocking group of masked *O*-isocyanates, achieving C-C bond formation using Grignard reagents would necessitate superstoichiometric amounts of such bases to attain a full deprotonation of the masked substrate, which poses a risk of losing the control over the reactivity, potentially leading to oligomerization problems.

2.2 Optimization of Masked *O*-Isocyanates Reaction with Grignard Reagents

To test the reactivity of *O*-isocyanates towards Grignard reagents, the first attempt was intended as a control reaction with *C*-substituted isocyanate (Scheme 2.1, b). Treating this substrate with 4.0 equivalents of isopropylmagnesium chloride (*i*-PrMgCl) afforded the desired amide product after stirring the reaction mixture for two hours at room temperature with facile deblocking of the masked isocyanate. This result suggested that super-stoichiometric amounts of Grignard reagent are not detrimental to the C-C bond formation reactivity, and the conditions were ready to be tested on the masked *O*-isocyanates.

Initially, reagent **2a** (*O*-benzyl phenylcarbamate) was selected as an *O*-isocyanate precursor, due to its balance between stability and reactivity. Indeed, this substance is a solid stable for months at room temperature, but this precursor also conveniently forms an *O*-isocyanate upon heating above 70 °C, or in the presence of catalytic base (ejecting PhOH as a byproduct). Thus, the potential C-C forming reaction was explored with masked *O*-isocyanate **2a**, and *i*-PrMgCl. Applying the conditions developed for Grignard addition to *C*-isocyanates to substrate **2a** did not reveal the formation of the addition product; the NMR analysis revealed mostly unreacted starting material. Given this result, it was hypothesized that the generation of the reactive free isocyanate species from the *O*-isocyanate precursor is fundamentally different from its *C*-substituted counterpart (Scheme 2.1, b and c), possibly due to the formation of a relatively stable five-membered chelate complex upon deprotonation, making it reluctant to generate the reactive isocyanate species (Scheme 2.1, c).[125] Noteworthy, this kind of chelation with organometallics including Grignard reagents was previously described in literature.[125–128]

Pleasingly, after reflux with 4.0 equivalents of turbo Grignard (*i*-PrMgCl•LiCl), the desired product was formed in 85% NMR yield. Upon scaling up the reaction, the product was isolated in 66% yield (Scheme 2.1, c). Optimization of this reaction was carried out afterwards to further understand the behavior of this system. It included examining various reaction conditions, solvents, and additives (see selected examples in Table 2.1). This project was initiated by Dr. Joshua Derasp (a senior PhD candidate who graduated in 2019). The optimization of the reaction of Turbo Grignard with **2a** was done by both Dr. Derasp and Mr. Kwame Agyei **(**an undergraduate (Honours) student during 2018-2019).

*Scheme 2.1. a) Reactivity of masked O-isocyanates toward carboxylic acids. b) A control reaction of masked C-isocyanate precursor with i-PrMgCl. c) Reactivity of **2a** towards i-PrMgCl showing the formation of five-membered chelate.*

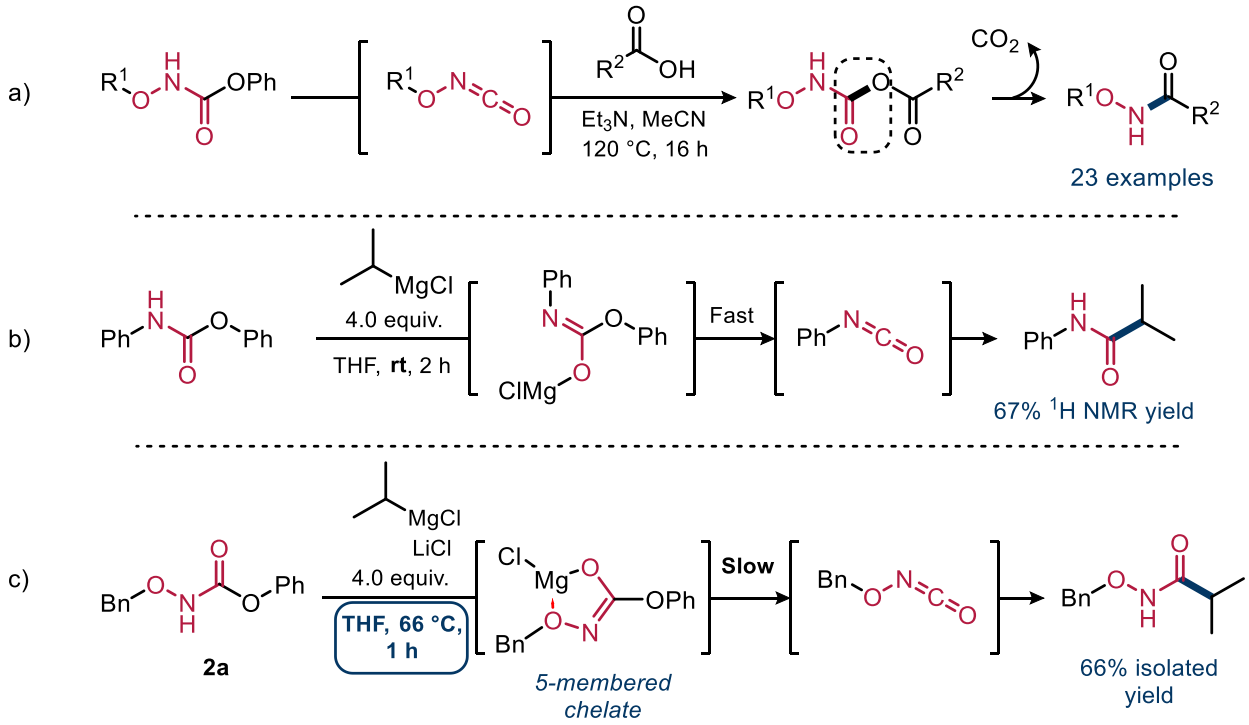

*Table 2.1. Preliminary optimization of **2a** with i-PrMgCl•LiCl.*

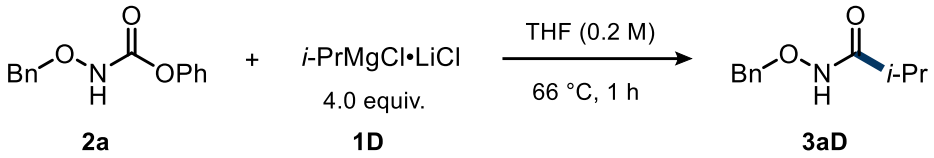

Entry	Deviation from above conditions[a]	Product yield (%)[b]	BnOH yield (%)[b]
1	rt	<2	<2
2	None	85 (66)[c]	10
3	2.5 equiv.	77	21
4	2 h	78	20
5	16 h	42	15
6	CH_2Cl_2	15	85
7	Toluene	84	15
8	$CuBr_2$ (0.1 equiv.)	72	28
9	$ZnCl_2$ (1.0 equiv.)	50	18

[a] Conditions: **2a** (0.2 mmol), **1D** (0.8 mmol), THF (0.2 M), at 66 °C in a sealed µW vial unless otherwise noted. [b] ^{1}H NMR yield determined by using 1,3,5-trimethoxybenzene as internal standard. [c] Yields in parenthesis indicate isolated yield from 0.6 mmol reaction scale.

The optimization with *i*-PrMgCl•LiCl revealed the formation of benzyl alcohol as a side product of this reaction, which was confirmed spectroscopically by spiking the NMR sample with benzyl alcohol. The benzyl alcohol formation suggested N-O bond cleavage as a competing degradation pathway under these conditions. Extending the reaction time to 2 hours resulted in a minor reduction in yield (entry 4), while a significant decrease in product formation was noted when the reaction was heated at reflux overnight (entry 5). These findings strongly indicate that the product degrades under the reaction conditions. Interestingly, the increased degradation was also associated with a reduced production of benzyl alcohol (entries 4 and 5). This unexpected outcome implied that the production of benzyl alcohol under these conditions is not benign and could potentially undergo additional nucleophilic reactions. However, no such side products were identified during the optimization process.

2.3 Mechanistic Insights via Optimization of Substrate 2a

2.3.1 The Hypothesized Mechanism of a Competitive Degradation Pathway

The hypothesized mechanism of the degradation pathway could be explained through the formation of a (benzyloxy carbamate conjugate base) dianion **A** (Figure 2.2) upon deprotonation with Grignard reagent, followed by spontaneous rearrangement and cleavage of the weak N-O bond to form benzyl alcohol after aqueous workup. Another potential mechanism could be the Lossen rearrangement pathway,[129,130] by the formation of hydroxamate conjugate base upon deprotonation with Grignard reagent and cleavage of the leaving group (-OPh), followed by rearrangement to cleave the N-O bond and form C-N bond with the generation of the free isocyanate species and cleavage of benzyloxy anion which reveals benzyl alcohol upon acidic quench (Figure 2.2). Given the results of Grignard addition to *C*-isocyanate precursor (control reaction; facile deblocking at room temperature) versus the *O*-isocyanate precursor **2a** (requiring high temperature), the pathway for the formation of the desired hydroxamate product is postulated to proceed through the formation of five-membered *O,N*-magnesium chelate upon deprotonation by a Grignard reagent. This chelation would afford certain stability to this transient species (**X**), which would result in a controlled release of the free reactive *O*-isocyanate *in situ*.[71,90,111] This would ensure the slow increase in the concentration of the free *O*-isocyanate intermediate in the reaction medium, which would provide good control over the reactivity. Subsequently, a nucleophilic addition of the Grignard reagent to the electrophilic isocyanate species would give rise to the C-C bond formation and the desired reactivity.

Figure 2.2. Hypothesized pathways for the formation of benzyl alcohol degradation product.

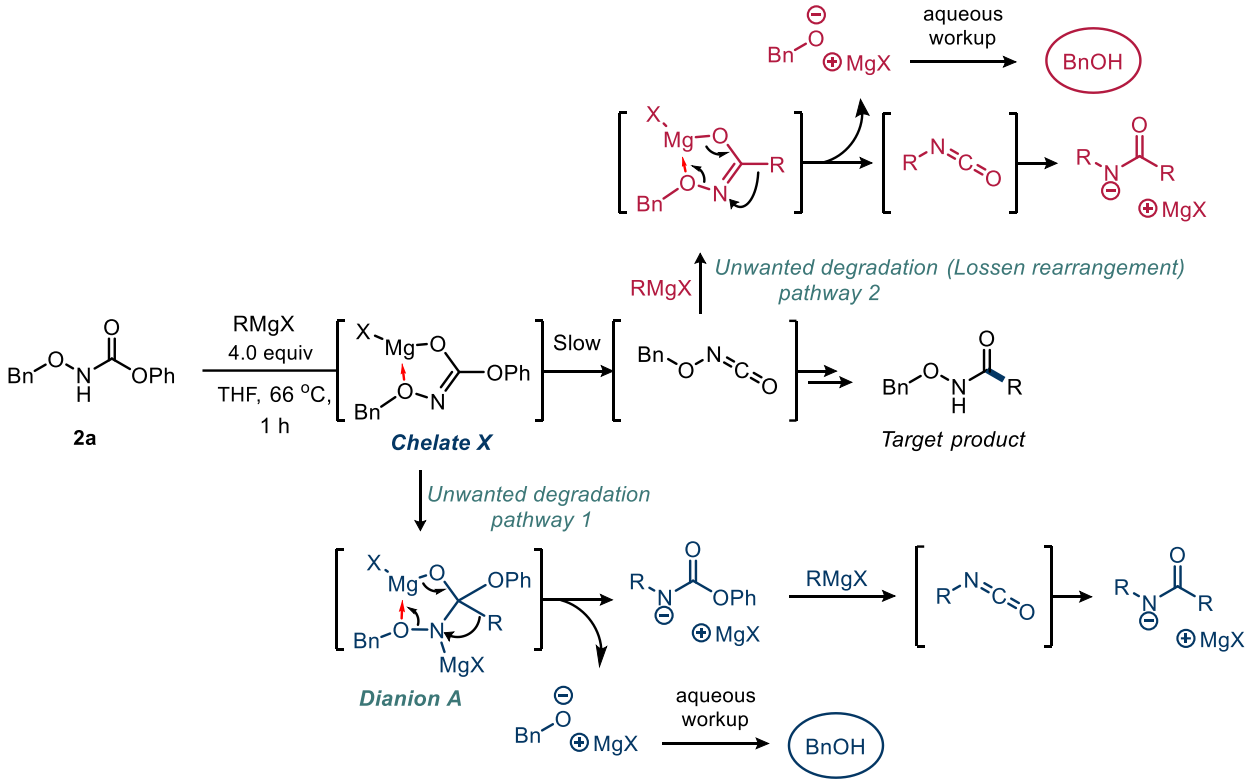

2.3.2 Optimization of **2a** with Ethylmagnesium Bromide

After the preliminary optimization performed on **2a** using *i*-PrMgCl•LiCl, ethylmagnesium bromide (EtMgBr) was introduced as a candidate for the reaction on the same substrate **2a**. Applying the optimized conditions from the reaction with Turbo Grignard revealed the addition product in 44%, while observing significant amounts of benzyl alcohol side product (46%, Table 2.2, entry 1). This unpleasant result suggested that further optimization would be necessary for different Grignard reagents.

*Table 2.2. Optimization of **2a** with EtMgBr.*

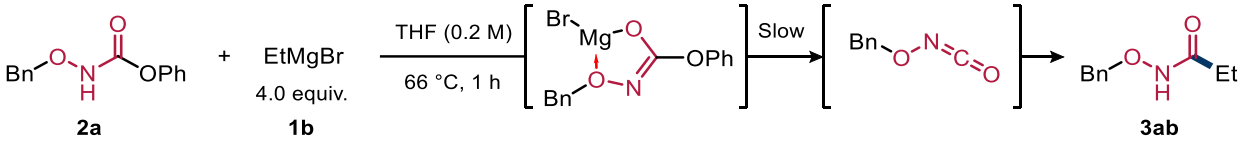

Entry	Deviation from above conditions [a]	Product yield (%)[c]	BnOH yield (%)[c]
1	None	44	46
2	rt	0	0
3	40 °C	20	66
4	2.0 equiv.	25	70
5	0.075 M	57	23
6	LiCl	10	21
7	Dioxane[b]	57	10
8	Dioxane[b] (to Grignard), 0.075 M, LiCl	85	15
9	Dioxane[b] (to Grignard), 0.075 M	80	15
10	**Dioxane[b] (to rxn mix.), 0.075 M**	**87 (80)[d]**	**10**

[a] Conditions: **2a** (0.2 mmol), **1b** (0.8 mmol), THF (0.2 M), at 66 °C in a sealed μW vial unless otherwise noted. [b] 1,4-Dioxane was added as a co-solvent with THF. [c] ^{1}H NMR yield determined by using 1,3,5-trimethoxybenzene as internal standard. [d] Yields in parenthesis indicate isolated yield from 0.6 mmol reaction scale.

In the efforts to improve the yield and suppress the N-O bond cleavage, extensive optimization was performed on EtMgBr, together with three more Grignard systems, to explore the reactivity trends. Different conditions have been submitted to the test, including lowering the temperature, using different number of equivalents of the Grignard reagent, changing the concentration, changing the reaction time, and using additives.

For ethylmagnesium bromide, performing the reaction at reflux proved necessary, both to minimize the formation of benzyl alcohol side product observed at lower temperatures (e.g., 40 °C, entry 3, Table 2.2), and to overcome the lack of reactivity observed at room temperature (entry 2). The use of excess Grignard reagent was ascertained to improve that ratio toward the formation of the desired product, as observed after lowering to 2.0 equivalents of Grignard reagent (entry 4). The outcome of the reaction also proved sensitive to changes in reaction concentration (entry 5) and additives (entries 6-7), such as lithium chloride, which was added to mimic the turbo Grignard (*i*-PrMgCl•LiCl) medium, and to reduce the precipitation of magnesium salts. When added alone, LiCl was found to be detrimental to the efficiency of the reaction. The presence of 1,4-dioxane, however, significantly promoted the formation of the desired product (entry 8). 1,4-Dioxane is commonly used to form diorganomagnesium reagents (R_2Mg) from organomagnesium halide reagents (RMgX).[131,132] Performing the reaction with dioxane as a co-solvent

proved both practical, as common Grignard reagents are typically commercially available in Et_2O or THF, and efficient to minimize the formation of side products arising from N-O bond cleavage. Interestingly, the reactivity proved quite similar if dioxane was added to the Grignard reagent (entry 8) or to substrate **2a** before Grignard addition (entry 9), with the latter providing somewhat better results and being more practical from a reaction setup standpoint.

2.3.3 Reactivity Towards RMgX vs R_2Mg (Effect of Dioxane Addition)

Dioxane favors the formation of diorganomagnesium species by shifting the Schlenk equilibrium between organomagnesium halides and diorganomagnesium species towards the formation of the latter (Scheme 2.2).[131] This switch is achieved by precipitation of a dioxane bridged MgX_2 adduct. In this case, when diorganomagnesium species is a predominant nucleophile in the reaction medium, it is hypothesized that the stability of the five-membered chelate is reduced, due to the lower Lewis acidity of the metal center, making the departure of the blocking group (-OPh) and the formation of the free isocyanate more favorable, which enables efficient addition of the Grignard to the transient isocyanate. In addition, the decreased Lewis acidity of the metal center likely results in reduced polarization of the N-O bond, which could help minimize side reactions associated with a N-O bond cleavage event.

Scheme 2.2. Effect of dioxane addition and the formation of diorganomagnesium species.

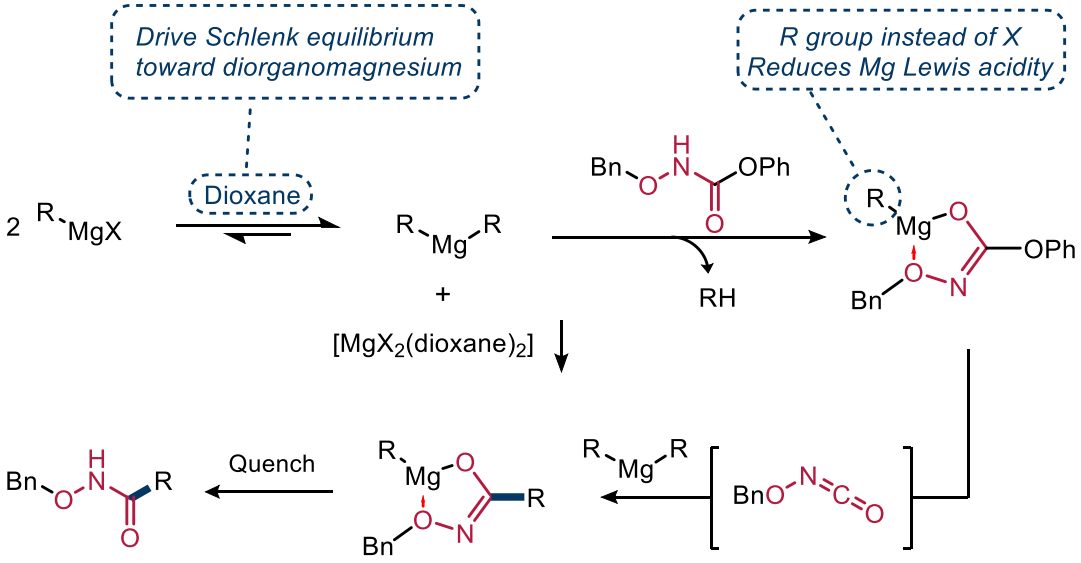

*Table 2.3. Optimization of **2a** with three Grignard reagents.*

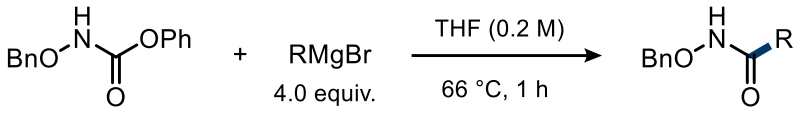

2a

Entry	Deviation from above conditions [a]	R = *i*-Pr [e]		R = *n*-Hex		R = Ph	
		Product yield (%)[c]	BnOH yield (%)[c]	Product yield (%)[c]	BnOH yield (%)[c]	Product yield (%)[c]	BnOH yield (%)[c]
1	None	72	10	62	25	65	25
2	LiCl	85	10	30	65	< 5	80
3	2.0 equiv.	76	21	-	-	58	14
4	0.075 M	72	10	72	25	67	22
5	Dioxane[b] (to Grignard), 0.075 M	85	10	82	12	85	7
6	Dioxane [b] (to rxn mix.), 0.075 M	85 (79)[d]	7	85 (75) [d]	8	90 (82) [d]	2

[a] Conditions: **2a** (0.2 mmol), Grignard reagent (0.8 mmol), THF (0.2 M), at 66 °C in a sealed μW vial unless otherwise noted. [b] 1,4-Dioxane was added as a co-solvent with THF. [c] ^{1}H NMR yield determined by using 1,3,5-trimethoxybenzene as internal standard. [d] Yields in parenthesis indicate isolated yield from 0.6 mmol reaction scale. [e] Using *i*-PrMgCl not *i*-PrMgBr.

Simultaneously, related optimization data was obtained for *i*-PrMgCl, PhMgBr, and *n*-HexMgBr demonstrated comparable reactivity trends, with some variability (Table 2.3). These trends include slightly better yields with more diluted reactions except for *i*-Pr (entry 4), dire effect of adding LiCl alone except for *i*-Pr (entry 2), and the beneficial effect of dioxane (entry 5 and 6), which supports the hypothesis that tuning the Lewis acidity of the metal center of the five-membered chelate intermediate (by manipulating the reactive Grignard species) is necessary for promoting the desired reactivity of the masked *O*-isocyanate system.

Noteworthy was the isolation of an anilide side product from phenylmagnesium bromide reaction with substrate **2a** in 3% yield. This finding lends support to the proposed competitive degradation pathway with two potential mechanisms as described above. (Scheme 2.3)

*Scheme 2.3. The formation of anilide side product from the reaction of PhMgBr with substrate **2a**.*

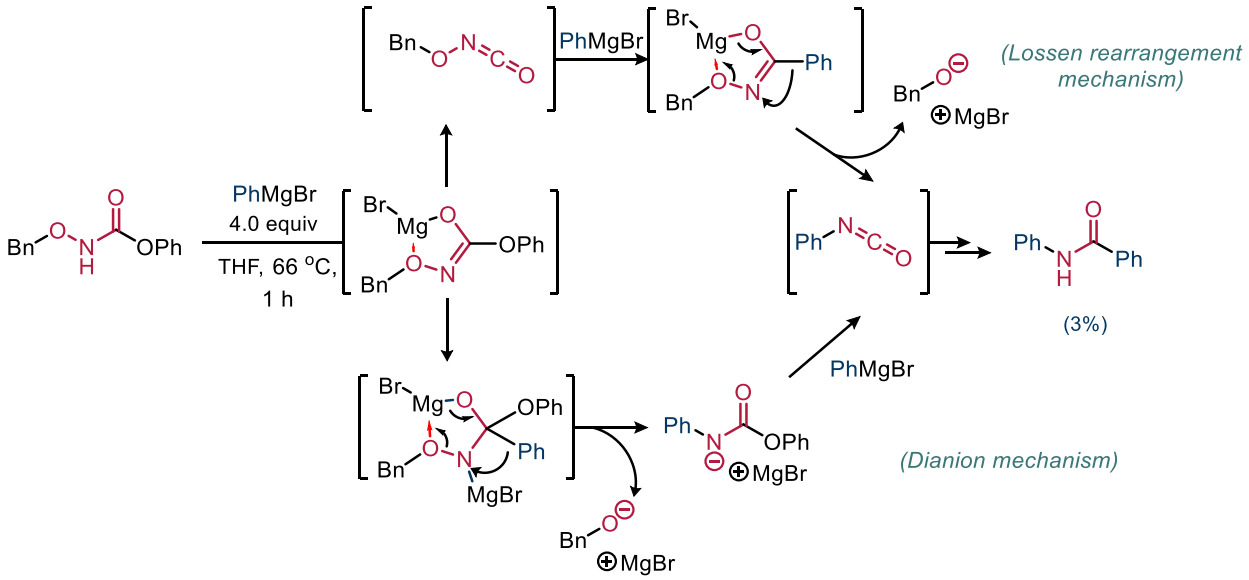

2.4 Scope of Stoichiometric Grignard Addition to Masked *O*-Isocyanates

2.4.1 Scope of Grignard Partner

Having these optimized conditions in hand, the attention was focused on the scope of this reaction with various Grignard reagents and masked *O*-isocyanate substrates.

Scheme 2.4. Stoichiometric Grignard addition to masked O-isocyanates: (Grignard scope).

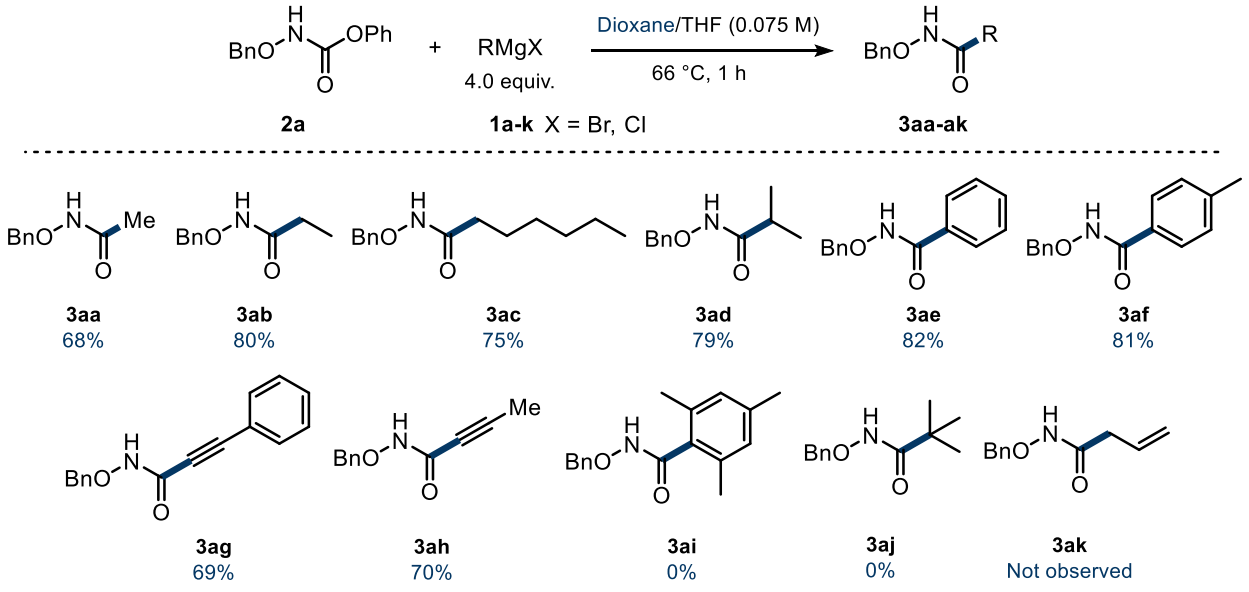

[a] Conditions: **2a** (0.6 mmol), Grignard **1a-k** (2.4 mmol), Dioxane/THF (0.075 M), at 66 °C in a sealed µW vial. Yields shown are isolated yields from 0.6 mmol reaction scale.

Upon reaction with compound **2a**, some alkyl and aryl Grignard reagents were competent reaction partners (Scheme 2.4), while other bulky groups like mesityl and *tert*-butyl were not amenable to this reaction, suggesting a deactivating effect of sterically demanding Grignard reagents. Allylmagnesium bromide, on the other hand, did not form the desired addition product, although the starting material was fully consumed.

2.4.2 Scope of *O*-Isocyanate Partner

The scope of *O*-isocyanate partner was then probed, using two selected Grignard reagents for this purpose; the use of an aromatic nucleophile was achieved by employing phenylmagnesium bromide, and isopropylmagnesium chloride was introduced to represent a bulky nucleophilic partner (Scheme 2.5).

Scheme 2.5. Stoichiometric Grignard addition to masked O-isocyanates: (isocyanate scope).

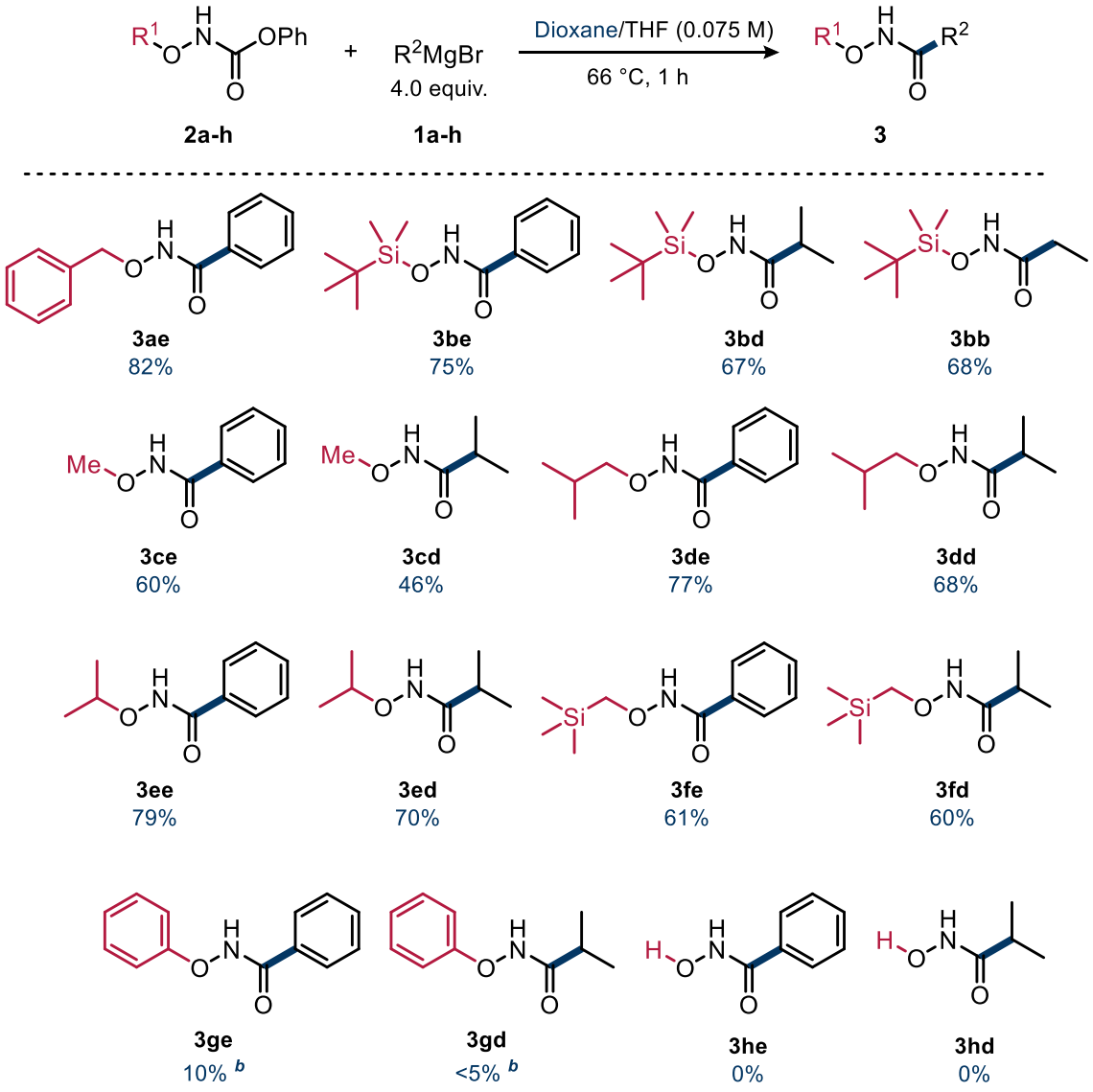

[a] Conditions: **2a-h** (0.6 mmol), Grignard reagent (2.4 mmol), Dioxane/THF (0.075 M), at 66 °C in a sealed μW vial. Yields shown are isolated yields from 0.6 mmol reaction scale. [b] After further optimization and the use of TMEDA (1.1 equiv.) **3ge** was isolated in 80% and **3gd** was isolated in 30%.

Benzyl, methyl, isopropyl, isobutyl, TBS, as well as TMS-CH_2 derived *O*-isocyanates were competent reaction partners giving yields ranging from moderate to good. They all showed similar reactivity trend in that they were more reactive toward PhMgBr than *i*-PrMgCl (Scheme 2.5). Unsurprisingly, blocked derivative bearing a free OH proved an unsuccessful candidate under a variety of reaction conditions and additives. This can be justified in light of the hypothesized pathway, by the formation of a dianion upon deprotonation, which forms a more stable five-membered chelate (Scheme 2.6).

*Scheme 2.6. Mechanistic justification of the unsuccessful formation of **3he**.*

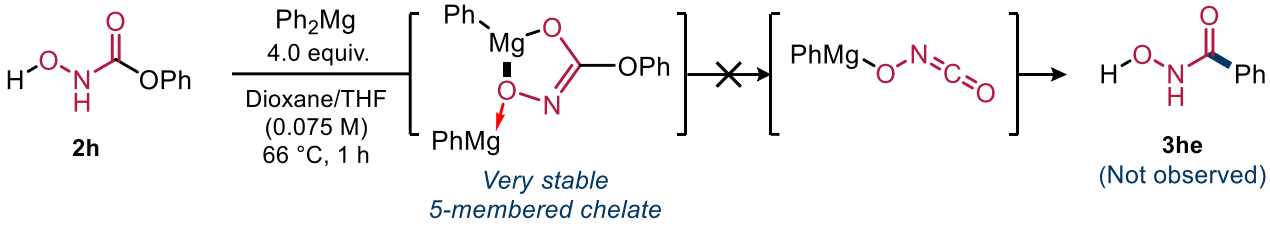

2.5 Optimizing the C-C Bond Forming Step for a Potential *O*-Isocyanate Amide Linchpin

In the Beauchemin group, there is a long-standing project envisioning the possible development of new biselectrophilic amide linchpin reagent in order to functionalize on both sides of amide group. This requires two functionalization methodologies, one for each side of the linchpin reagent. While many linchpin reagents have been developed for common functional groups,[133–138] to our knowledge an amide linchpin reagent has not been developed. Typically, the use of linchpin reagents requires perfect chemoselectivity for each bond-forming step to form the target bond without affecting the other side of the molecule. The first thing to consider is to determine the optimal LG^1 and LG^2 surrounding the amide functionality to achieve the balance between selectivity and reactivity. This goal can be approached through two different pathways to furnish the secondary amides. The first pathway (pathway A) is achieving a C-C bond formation reaction to functionalize on the carbonyl part of the compound, followed by a C-N bond formation reaction to decorate the other side of the compound (Scheme 2.7). The second pathway (pathway B), however, starts through the C-N bond formation, followed by C-C bond formation on the product of the first step. Masked *O*-isocyanates were proposed as potential candidates for this purpose, motivated by the promising results of stoichiometric Grignard addition to the blocked *O*-isocyanates, where the reaction was optimized to cleave the blocking group of the *O*-isocyanate (OPh in this case) to successfully achieve C-C bond. Consequently, pathway A was selected to be explored initially (Scheme 2.7).

Scheme 2.7. Pathways to the development biselectrophilic amide linchpin reagent showing ***2g*** *as a potential candidate.*

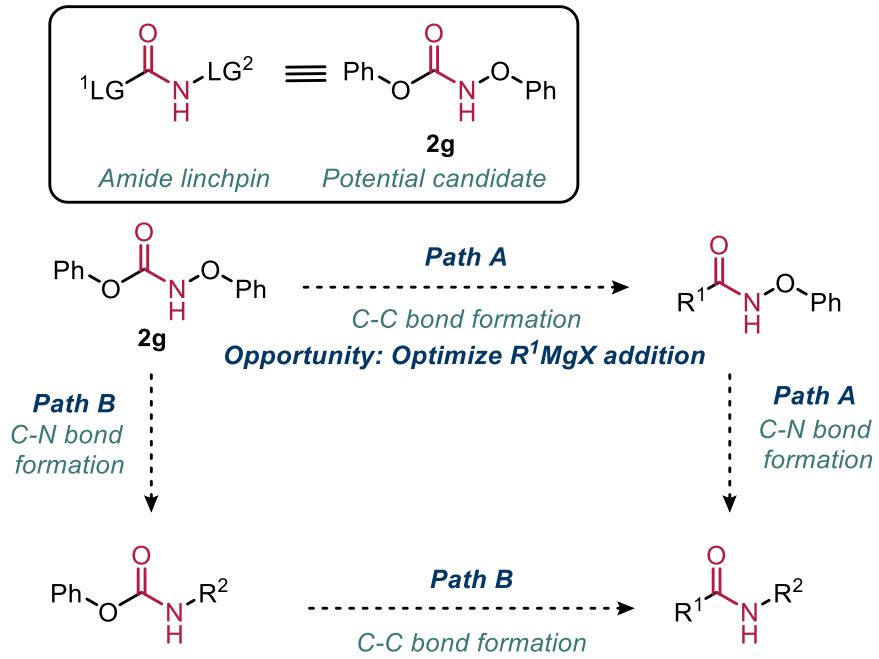

Compound **2g** (in which LG^1 = OPh and LG^2 = OPh) was proposed as a potential substrate for testing pathway A. Should the C-C bond forming stoichiometric Grignard addition be successful (cleavage of LG^1 is selectively achievable with the survival of LG^2), it will be conceivable that the product of this reaction could be used in a metal catalyzed cross coupling across the N-O bond to install different functional groups on the nitrogen side of the amide functionality giving access to secondary amides (Scheme 2.7). With the discouraging low yields with both Grignard reagents PhMgBr and *i*-PrMgCl on compound **2g**, it rapidly became apparent that further optimization was required with this substrate **2g**. This reactivity trend with **2g** was likely due to the electron-withdrawing effect of *O*-phenyl group, which appeared to promote the N-O bond cleavage/degradation pathway, as if this substituent had cancelled the beneficial effect of dioxane addition (Scheme 2.8). An alternative hypothesis is that it may have led to further weakening the coordination between the heteroatom and the metal center, to a degree that resulted in uncontrolled release of free isocyanate species, hence, uncontrolled reactivity. Thus, several changes in reaction conditions were investigated with both *i*-PrMgCl and PhMgBr (Table 2.4).

*Scheme 2.8. Possible rationale for the unsuccessful Grignard addition to **2g**.*

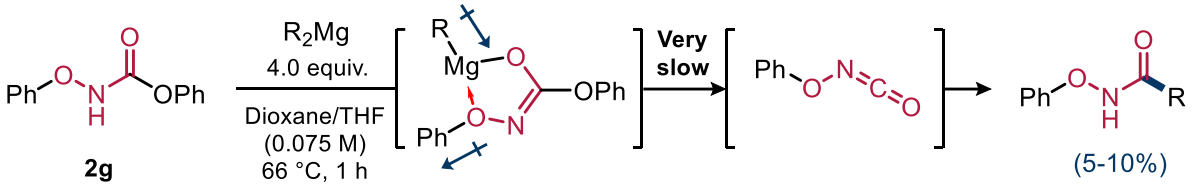

*Table 2.4. Optimizing Grignard addition to compound **2g**.*

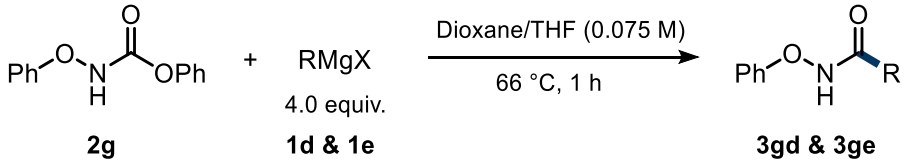

Entry	Deviation from above conditions [a]	PhMgBr	*i*-PrMgCl
		Product yield (%)[b]	Product yield (%)[b]
1	None	10	< 5
2	No Dioxane (only THF)	13	10
3	rt	0	0
4	2.5 equiv.	5	< 5
5	4 h	35	15
6	ON	39	15
7	3.3 equiv., 4 h	36	16
8	3.3 equiv., 4 h, 1,1-phenanthroline	< 5	-
9	**3.3 equiv., 4 h, TMEDA (1.1 equiv.)**	70	**33 (30)**[c]
10	3.3 equiv., 4 h, TMEDA (3.3 equiv.)	49	-
11	3.3 equiv., 4 h, RMgX•LiCl	70	< 5
12	**3.3 equiv., 4 h, TMEDA (1.1 equiv.), RMgX•LiCl**	**85 (80)**[c]	25

[a] Conditions: **2g** (0.2 mmol), Grignard reagent (0.8 mmol), THF (0.075 M), at 66 °C in a sealed µW vial unless otherwise noted. [b] ^{1}H NMR yield determined by using 1,3,5-trimethoxybenzene as internal standard. [c] Yields in parenthesis indicate isolated yield from 0.6 mmol reaction scale.

Interestingly, the reactivity of substrate **2g** varied significantly for the two Grignard reagents investigated. Poor activity was observed upon running the reaction at room temperature (entry 3). Excess Grignard reagent proved essential for the reactivity as reflected by the detrimental effect of lowering the Grignard load to 2.5 equivalents (entry 4). Running the reaction over a longer period of time improved the yields slightly of both products (**3gd** and **3ge**) with more improvement shown by the phenyl Grignard product (entries 5 & 6). The use of a smaller excess (3.3 equivalents) of Grignard reagents gave yields close to the original 4.0 equivalents (entry 7). While 1,1-phenanthroline addition proved unsuccessful for yield improvement (entry 8), adding TMEDA (at 1.1 equivalent) led to very good results for the phenyl product

(70%) and moderate improvement in isopropyl product yield (33%) with long reaction time (entry 9). The presence of lithium chloride in the reaction mixture, although being beneficial in the case of the phenyl product (70%), demonstrated dire effect on the isopropyl product (<5%) (entry 11). Combining both TMEDA and lithium chloride in a four-hour reaction generated the phenyl product in 80% isolated yield but did not help in the case of the isopropyl product (entry 12). As concluded from the aforementioned data, both products showed similar reactivity trends toward different conditions, with some exceptions. The isopropyl product, however, was much reluctant in its response to the optimization changes.

2.6 Reactivity of Masked *O*-Isocyanates Towards Other Organometallic Reagents

2.6.1 Reactivity Towards *n*-Butyllithium

The hypothesis of the importance of fine-tuning the Lewis acidity of the metal center of the five-membered complex to conquer the reactivity of the *O*-isocyanate system was further explored by changing the metal itself. Instead of manipulating the Grignard reagents (by switching the predominant form in the reaction mixture from RMgX to R_2Mg via dioxane addition), the use of different metals arose as a potential solution for the scope expansion issue. Consequently, parallel investigations with other organometallic reagents were performed using organolithium[139] and organozinc reagents.[140] *n*-Butyllithium did not demonstrate the desired reactivity toward the masked *O*-isocyanate system. Although the C-C addition product was not generated, N-O bond cleavage was observed even at lower temperatures, with the formation of significant amount of benzyl alcohol when the starting material **2a** was the reaction partner, therefore, *n*-butyllithium has received less attention as organometallic nucleophile with this system (Table 2.5).

*Table 2.5. n-BuLi addition to compound **2a***

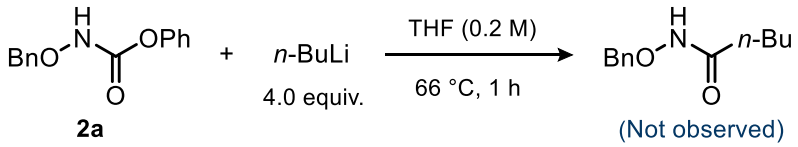

Entry	Deviation from above conditions[a]	Product yield (%)[b]	BnOH yield (%)[b]
1	None	0	60
2	rt	0	50
3	Et_2O, rt	0	50
4	2.0 equiv.	0	30

[a] Conditions: **2a** (0.2 mmol), *n*-BuLi (0.8 mmol), THF (0.2 M), at 66 °C in a sealed μW vial unless otherwise noted. [b] ^1H NMR yield determined by using 1,3,5-trimethoxybenzene as internal standard.

2.6.2 Reactivity Towards Organozinc Reagents.

Milder organozinc reagents were then evaluated as candidates for this reaction.[140,141] A variety of conditions were tested for their ability to promote the formation of the desired product (Table 2.6).

*Table 2.6. Optimization of **2a** with organozinc reagents.*

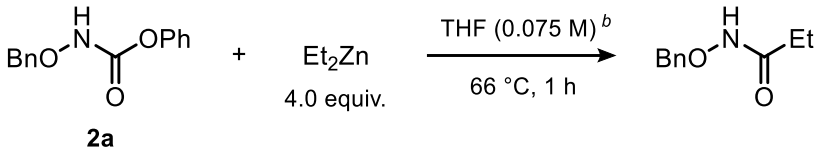

Entry	Deviation from above conditions [a]	Product yield (%) [c]
1	None	56
2	Dioxane	48
3	Change order of addition	44
4	**2 h**	**64 (59)** [d]
5	ON	64
6	0.2 M, 2 h	56
7	90 °C	50
8	EtZnI	20
9	EtZnI/ 2 h	21

[a] Conditions: **2a** (0.2 mmol), Et_2Zn (0.8 mmol), THF (0.075 M), at 66 °C in a sealed μW vial unless otherwise noted. [b] Hexanes was always a co-solvent; Et_2Zn was in hexanes. [c] ^1H NMR yield determined by using 1,3,5-trimethoxybenzene as internal standard. [d] Yields in parenthesis indicate isolated yield from 0.6 mmol reaction scale.

Employing the optimized conditions from organomagnesium reactions, but without the addition of dioxane (being no longer needed as the reacting species in this case is already the diorganozinc), achieved the addition product in 56% (entry 1). Addition of dioxane to the reaction slightly decreased the yield of the target product (entry 2), as did reversing the order of addition by adding the reagent **2a** to the diethylzinc in the sealed reaction vial (entry 3). Running the reaction for 2 hours moderately improved the product formation, while no dramatic change was observed upon allowing the reaction to reflux overnight (entries 4 and 5). A slight drop in yield was noted with increasing the reaction concentration (entry 6) or increasing the reaction temperature (entry 7). As expected, when the organozinc reagent was switched to ethylzinc iodide, a significant decline in reactivity was observed, revealing that Et_2Zn is superior to EtZnI. This result was consistent with the prior reactivity trend with organomagnesium reagent, presumably due to the same justification. This reactivity trend thus lends additional support to the postulate that precise adjustment of the Lewis acidity of the metal center is required to optimize the reactivity of the relatively stable five-membered complex, thus allowing for more facile release of the isocyanate and help minimize other degradation pathways (Scheme 2.9).

Scheme 2.9. Reactivity towards EtZnI vs Et_2Zn.

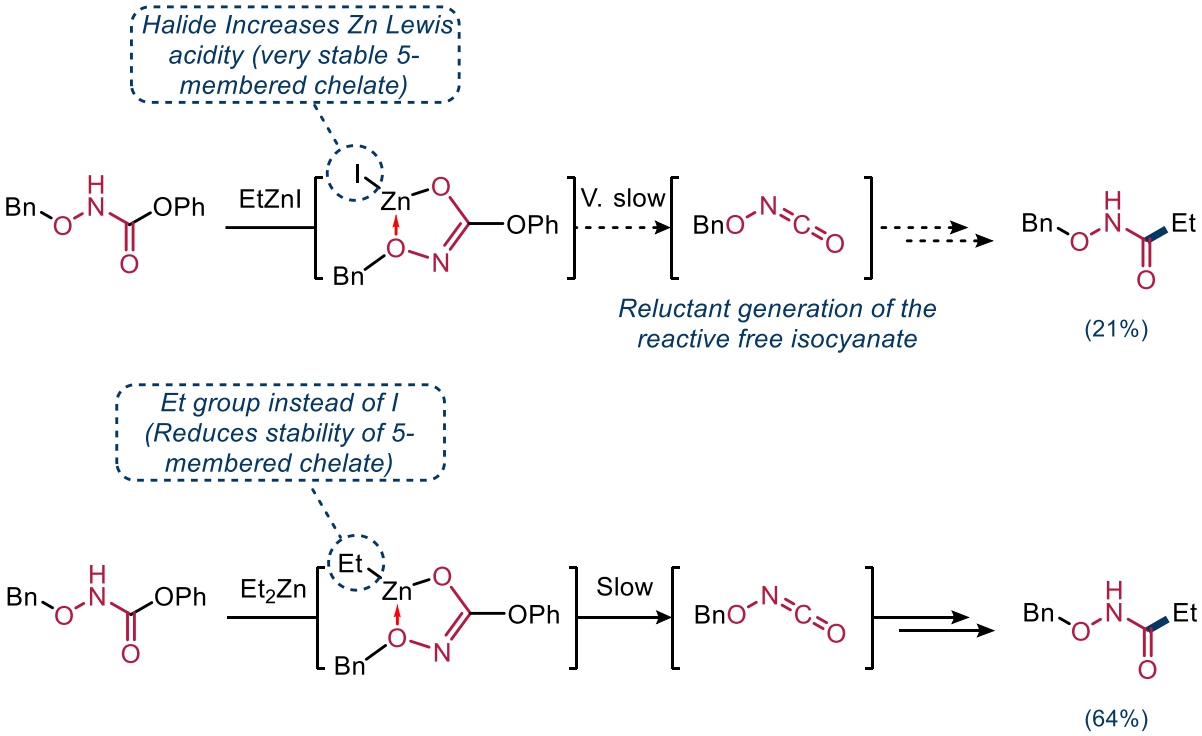

For the purpose of improving the reaction outcomes, various solvents were scanned for their ability to facilitate the desired transformation (Table 2.7). Running the reaction using dioxane as a co-solvent with THF did not seem beneficial, while removing THF altogether while keeping dioxane was found to have no substantial effect on the reaction outcome from using a mixture of both solvents (entries 2 and 3).

Table 2.7. Solvent scan for diethylzinc addition to masked O-isocyanates.

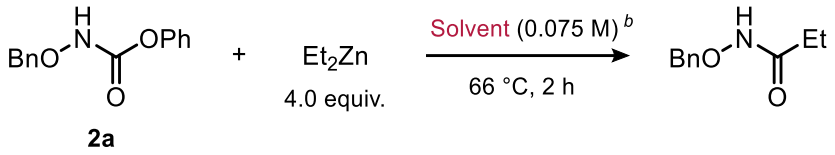

Entry	Solvent [b]	Product yield (%) [c]
1	**THF**	**64 (59) [d]**
2	THF/Dioxane	48
3	Dioxane	44
4	CH_2Cl_2	20
5	Et_2O	32
6	Toluene	37
7	DMA	25
8	NMP	14

[a] Conditions: **2a** (0.2 mmol), Et_2Zn (0.8 mmol), THF (0.075 M), at 66 °C in a sealed μW vial unless otherwise noted. [b] Hexanes was always a co-solvent; Et_2Zn was in hexanes. [c] ^1H NMR yield determined by using 1,3,5-trimethoxybenzene as internal standard. [d] Yields in parenthesis indicate isolated yield from 0.6 mmol reaction scale.

Various solvents including diethyl ether, dichloromethane, as well as toluene were found to have a dire effect on the reaction outcome (entries 4-6). Similar low yields were observed with the use of polar aprotic solvents such as *N*-methyl-2-pyrrolidone (NMP), and the more stable analogue of DMF, dimethylacetamide (DMA). It is worth noting that unreacted starting material was seen with most of the solvents under the reaction conditions.

Table 2.8. Additive scan for diethylzinc addition to masked O-isocyanates.

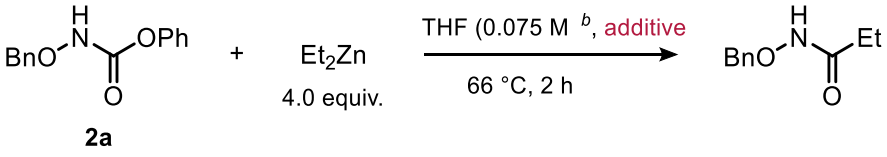

Entry	Additive/different conditions [a]	Product yield (%) [c]
1	LiCl/ 1 h	8
2	$MgCl_2$	< 5
3	$MgCl_2$/Dioxane	43
4	CuCN	20
5	CuCN/ON	35
6	CuCN/Toluene/ ON	50
7	2,2'-Bipyridyl	22
8	TMEDA	< 2

[a] Conditions: **2a** (0.2 mmol), Et_2Zn (0.8 mmol), THF (0.075 M), at 66 °C in a sealed μW vial unless otherwise noted. [b] Hexanes was always a co-solvent; Et_2Zn was in hexanes. [c] ^1H NMR yield determined by using 1,3,5-trimethoxybenzene as internal standard.

Finally, a variety of additives were employed to probe their potential toward this transformation (Table 2.8). The endeavors toward improving the nucleophilicity by incorporating copper[142–144] or magnesium[145] to the organozinc reagent did not prove a useful strategy (entries 2-6) and the yields ranged from very low to moderate, depending on other reaction conditions. Using chelating additives such as 2,2'-bipyridyl, or TMEDA resulted in low yielding reactions. The low reactivity of organozinc reagents reflected in their modest yields, under various reaction conditions, has discouraged further investigation with other organometallic reagents.

2.7 Previous Efforts Toward the Synthesis of Hydrazides

Hydrazides are valuable building blocks in organic synthesis. They have garnered significant interest in both organic and medicinal chemistry fields due to their versatile applications.[146,147] Their broad spectrum of biological activities, including anti-inflammatory, antihypertensive, and analgesic properties made them increasingly attractive compounds for synthetic investigations.[148] Various synthetic strategies have been reported including the reaction of hydrazine with different acyl derivatives[149,150] (acyl halides, esters, ketones, and cyclic anhydrides[151]) (Figure 2.3). Nitrene mediated intermolecular N-N cross-coupling have been reported for the synthesis of hydrazides (Figure 2.3, i), starting from benzoylated hydroxamates or cyclic 1,4,2-dioxazol-5-one with a broad range aromatic and aliphatic amines using transition metal catalysis like Ni,[152] Fe,[153] and Ir.[154] Iridium has been also employed for the synthesis of hydrazides via deoxygenative coupling of carboxylic acids with azobenzenes (Figure 2.3, k).[155] Metal-free conditions have been reported to access hydrazides from *N*-tosylhydrazones in the presence of *N*-chlorosuccinimide (Figure 2.3, j).[156] The synthetic methodologies involving C(sp^2)-N formation from arenes, aryl halide, arylboronic acids, olefins, alkynes, and alkynyl halides have been reported (Figure 2.3, h).[157] *N*-isocyanates have been employed in the synthesis of hydrazides via [3+2] cycloaddition reactions. This is achievable by *N*-isocyanates *in situ* formation either by *aza*-Curtius rearrangement (Lwowski work, Figure 2.3, f),[80] or via blocking group strategy (Beauchemin work, Figure 2.3, g).[85,90] Hydrazides were also accessible via stoichiometric carboxylic acid addition to oxadiazolones (which are considered as blocked *N*-isocyanate precursors) where the reaction proceeds through the generation of free *N*-isocyanate intermediate (Figure 2.3, e).[93]

Figure 2.3. Previous efforts towards the synthesis of hydrazides.

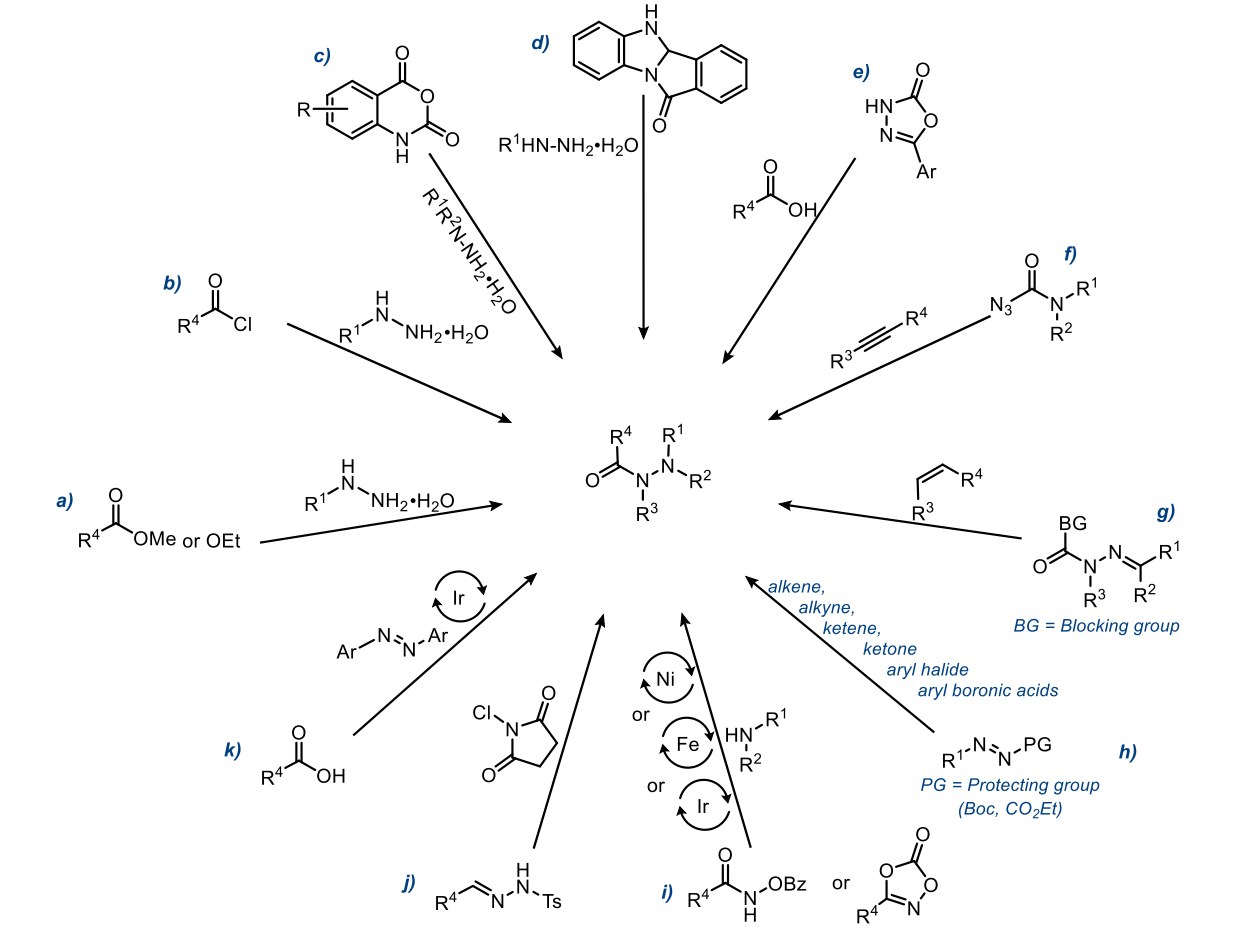

2.8 Masked *N*-Isocyanates Reaction with Grignard Reagents to Access Hydrazides

2.8.1 Mechanistic Insights Through *N*-Isocyanates Reactivity

The synthesis of hydrazides from masked *N*-isocyanate precursors was then investigated via carbon based nucleophilic addition to masked *N*-isocyanates. The successful addition of carboxylic acids to masked *O*-isocyanates motivated the exploration of this approach with masked *N*-isocyanates. Two masked amino- and imino-substituted isocyanate derivatives were probed, and carboxylic acids were attempted as nucleophiles to achieve this goal (Scheme 2.10, a). Unlike masked *O*-isocyanates, this strategy was met with failure with *N*-isocyanates, presumably due to competing oligomerization reaction that predominates in the absence of strong nucleophiles. Noteworthy, using oxadiazolones as a platform to access hydrazides instead of regular masked *N*-isocyanates was successful, resulting in the formation of the desired addition product (Scheme 2.10, b).[93] Such reactivity of oxadiazolones may be justified by the hypothesis that these precursors are actually heterocyclic precursors of blocked *N*-isocyanate. However, unlike their non-heterocyclic equivalents, these derivatives are highly resistant to oligomerization due to their aromatic, cyclic nature.

Scheme 2.10. a) Initial attempts to amidate amino- and imino-substituted isocyanate derivatives. b) Successful application of oxadiazolone precursor in N-isocyanate amidation.

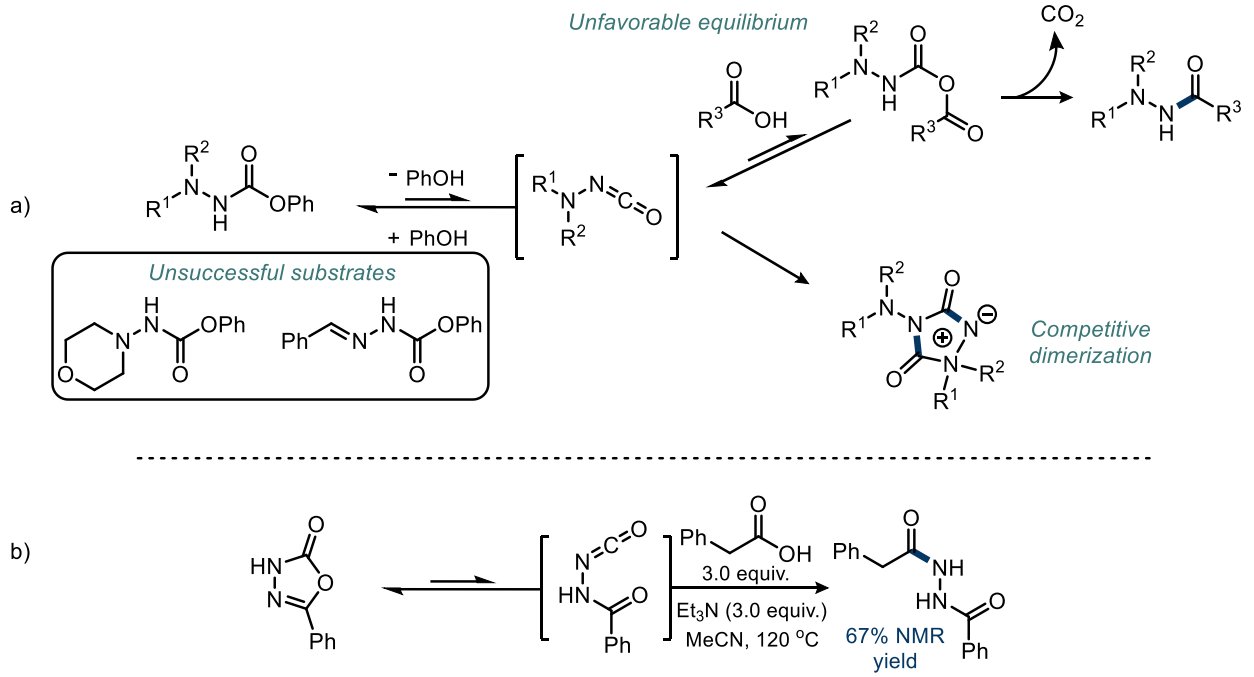

Alternatively, stoichiometric addition of Grignard reagents to provide access to hydrazides via C-C bond forming reaction with masked *N*-isocyanates was investigated, inspired by the success of this strategy with masked *O*-isocyanates which suggested the potential for achieving this goal. Initially, reagent **4a** (*N*-

(Phenoxycarbonylamino)morpholine) was selected as an *N*-isocyanate precursor for preliminary reaction optimization (Table 2.9). This precursor was not amenable to the carboxylic acid addition reaction.

*Table 2.9. Optimization of **4a** with i-PrMgCl and PhMgBr.*

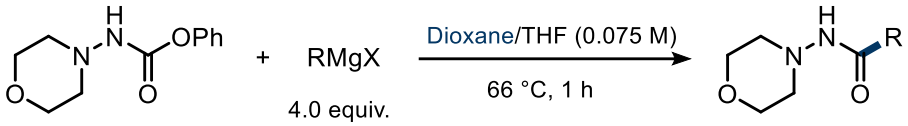

4a **1d-e** **5ad-ae**

Entry	R, X	Deviation from above conditions[a]	Product yield (%)[b]
1	*i*-Pr, Cl	None	42
2	*i*-Pr, Cl	Reverse addition of Grignard reagent	42
3	Ph, Br	None	45
4	*i*-Pr, Cl	1.1 equiv. TMEDA	95 (92)[c]
5	Ph, Br	1.1 equiv. TMEDA	99 (98)[c]

[a] Conditions: **4a** (0.2 mmol), **1d-e** (0.8 mmol), Dioxane/THF (0.075 M), at 66 °C in a sealed µW vial unless otherwise noted. [b] ^{1}H NMR yield determined by using 1,3,5-trimethoxybenzene as internal standard. [c] Yields in parenthesis indicate isolated yield from 0.6 mmol reaction scale.

Applying the optimized conditions (from *O*-isocyanate precursors) on this substrate gave 42% NMR yield when *i*-PrMgCl was the Grignard reaction partner, and 45% with PhMgBr (Table 2.9 entries 1-3). When it became apparent that further optimization was required to improve the reactivity, adopting TMEDA as an additive (1.1 equivalents) afforded the target product in 92% isolated yield with *i*-PrMgCl and 98% with PhMgBr (entries 4 and 5).

2.8.2 Different sp^3 Nitrogen Types

Motivated by the promising results provided by the reaction of **4a** with two Grignard reagents, the scope of this reaction was explored with the purpose of carefully studying the *N*-isocyanate system, addressing the differences between the behavior of the two masked heteroatom-substituted isocyanate systems, and testing the hypothesis that has been developed throughout the study of the reactivity of masked *O*-isocyanates. Noteworthy, the generation of the free form of *N*-isocyanate as a part of the substitution reaction pathway received supporting evidence, as the free isocyanate was observed by FTIR as a reaction intermediate in a previous study conducted by Beauchemin group.[90] However, the formation of the relatively stable five-membered chelate which is distinctive for the heteroatom-substituted isocyanate systems, and the beneficial effect of dioxane addition are two aspects of the hypothesis that required validation. Furthermore, exploring the effects of having different substituents (with different electronic and steric environments) on the β-nitrogen atom was another motif to evaluate. Throughout the exploration of the reactivity of masked *O*-isocyanates, we postulated the formation of a five-membered

chelate upon deprotonation. The stability of this complex required precise adjustment to optimize the release of the reactive free isocyanate species. This could be achieved by adjusting the coordination between the metal and the heteroatom (Scheme 2.11). By doing a solvent scan and using dioxane, which promotes the formation of diorganomagnesium species, it became apparent that fine-tuning the Lewis acidity of the metal by manipulating the predominant Grignard species greatly influenced the stability of the chelate and, consequently, the reactivity. Additionally, the initial outcomes of the *N*-isocyanate precursor **4a** with the optimized reaction conditions for *O*-isocyanate substrates yielding 42-45%, supported the hypothesis that the Lewis basicity of the beta nitrogen atom forming the chelate could impact the reactivity. With *N*-isocyanates, we got the chance to explore this aspect in depth. The scope of this reaction was targeted to assess the impact of varying the electronic environment surrounding the nitrogen atom, which would, in turn, influence the coordination strength between the magnesium and nitrogen atom. This alteration would influence the stability of the proposed five-membered chelate, thereby modifying its propensity to release the free reactive isocyanate species. In order to adjust the coordination from the heteroatom's perspective, an experiment was conducted to evaluate the influence of different substituents on the nitrogen atom's electronegativity, thus affecting its ability to donate a lone pair to the metal center. Four substrates were submitted to the Grignard addition applying the conditions optimized for the *O*-isocyanate system (Scheme 2.11). This experimentation was performed while maintaining the other factors affecting the coordination constant: therefore, dioxane was employed with all four precursors to ensure consistent reaction conditions.

Scheme 2.11. Stoichiometric addition of i-PrMgCl to masked N-isocyanates, five-membered complexes are demonstrated, different substituents on the sp^3 nitrogen revealed different yields.

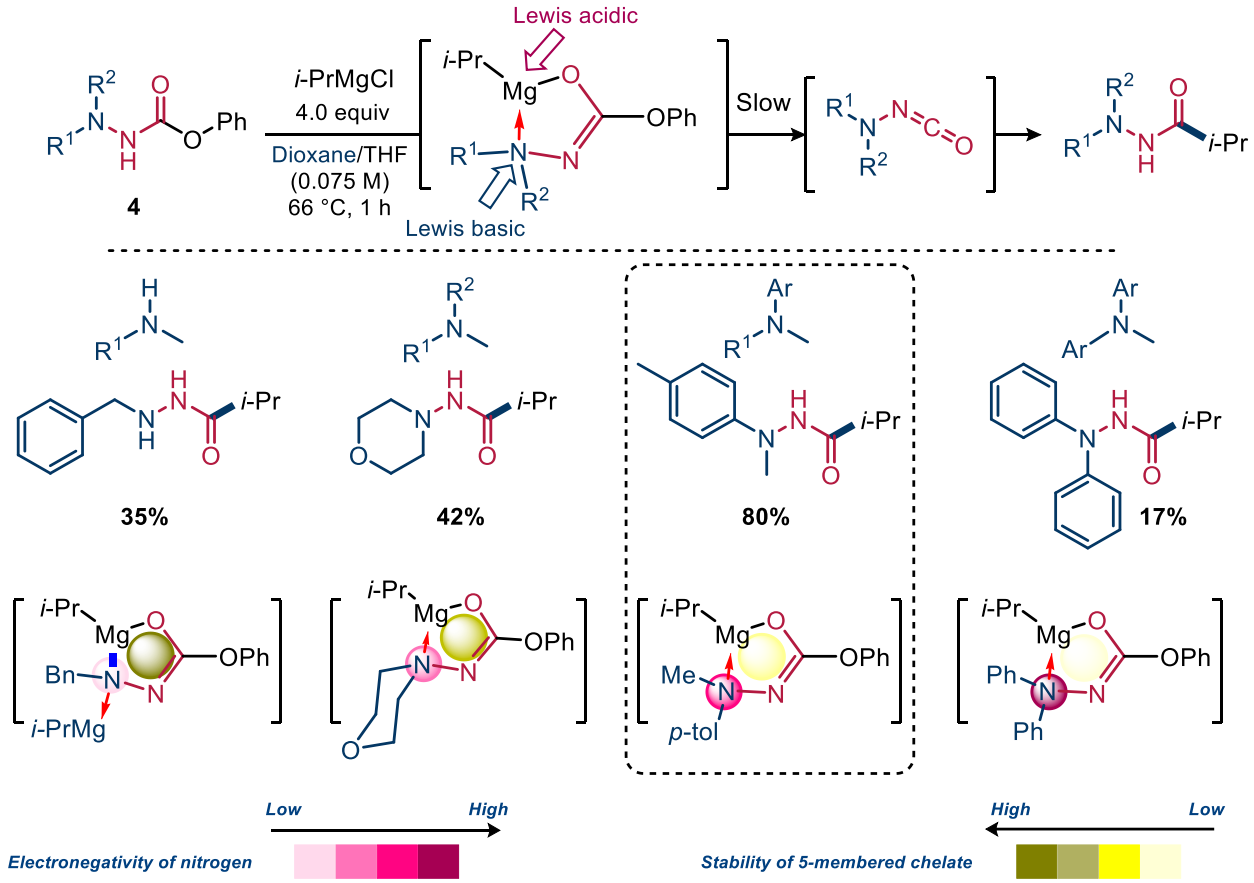

The variation in the yields indicated that the Lewis basicity of nitrogen is a significant aspect to consider in the process of tuning the stability of the five-membered complex. While the precursor featuring dialkyl-substituted nitrogen **4a** achieved moderate yield (42% NMR yield), increasing the electronegativity of the nitrogen atom by employing a nitrogen with one phenyl and one alkyl group revealed significant improvement of the reactivity, with 80% unoptimized NMR yield. Contrarily, a precursor with two phenyl groups on the nitrogen exhibited diminished reactivity towards Grignard addition (17% of the desired product) (Scheme 2.11 and Figure 2.4). It was interesting to notice that further increasing the electronegativity of the nitrogen beyond one aryl group seemed detrimental to the reactivity. This finding could be justified by postulating that the weakened interaction between the nitrogen and the metal resulted in an excessively unstable five-membered chelate, leading to a surplus of free reactive isocyanate species in the reaction medium. This excess, in turn, could lead to uncontrolled reactivity, despite the complete consumption of the starting material as indicated by TLC.

Figure 2.4. Crude ^{1}H NMR spectrum showing a precursor with two phenyl groups on the nitrogen exhibited diminished reactivity towards i-PrMgCl addition.

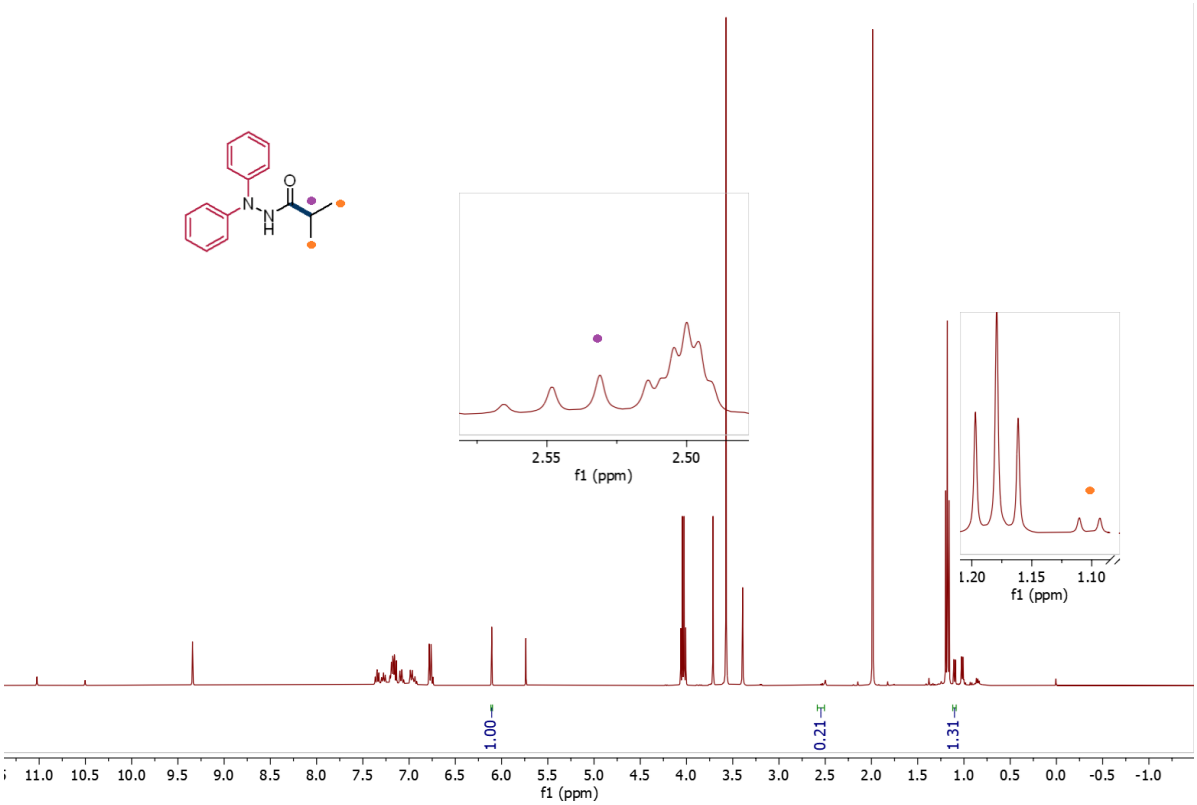

However, a precursor with monosubstituted nitrogen afforded, as anticipated, a lower yield (35%) due to the formation of a full covalent bond with the metal post-deprotonation, which revealed an extra stable five-membered chelate (Scheme 2.11). In conclusion, these reactivity trends with different sp^3 nitrogen types supported the mechanistic hypothesis previously described. The introduction of electron-withdrawing aryl groups as a nitrogen substituent appears to be more beneficial for the release of the isocyanate intermediate than the electron donating alkyl groups. This can be justified by withdrawing electron density from the nitrogen leading to a weaker dative bond between nitrogen and magnesium, resulting in less stable five-membered complex, hence more facile deblocking. Moreover, the use of the diaryl-substituted and the monosubstituted precursors provided another evidence that fine-tuning the stability of the five-membered chelate by making it neither overly stable (as in case of monosubstituted precursor) nor overly unstable (as in case of diaryl-substituted precursor) was crucial for the reactivity of this system (Scheme 2.11).

2.8.3 Reactivity Towards RMgX vs R_2Mg

At this stage, evaluating the effect of dioxane on the reactivity of the *N*-isocyanate system was probed. The aim was to explore the behavior of *N*-isocyanates toward the presence or absence of dioxane as a co-

solvent in the reaction medium, to determine whether *N*-isocyanates would behave like the *O*-isocyanates and benefit from dioxane addition, or they would prefer omitting dioxane from the reaction medium. Throughout the study of masked *O*-isocyanates, it was proposed that dioxane, by promoting the formation of diorganomagnesium species in the reaction medium, would lead to modulation of the structure of the relatively stable five-membered chelate, in the way that would lower the Lewis acidity of the magnesium atom. This structural modification would result in weakening the coordination between the heteroatom and the metal center, so that it would make this chelate less stable, and thus facilitate the release of free reactive isocyanate species and promote the formation of the desired product. To evaluate if the reactivity of the masked *N*-isocyanate would support this hypothesis, a control test was conducted (Scheme 2.12). For this purpose, compound **4c** was subjected to the same reaction with *i*-PrMgCl but with the absence of dioxane as a co-solvent. The ^{1}H NMR yield of the desired product was 21%, which is significantly lower than the yield of the product in the presence of dioxane (80% NMR yield). This result was consistent with the hypothesized mechanism where dioxane favors the formation of diorganomagnesium species which yield a less stable five-membered chelate, overall facilitating the desired reaction.

Scheme 2.12. The effect of dioxane addition on the reaction of masked N-isocyanates.

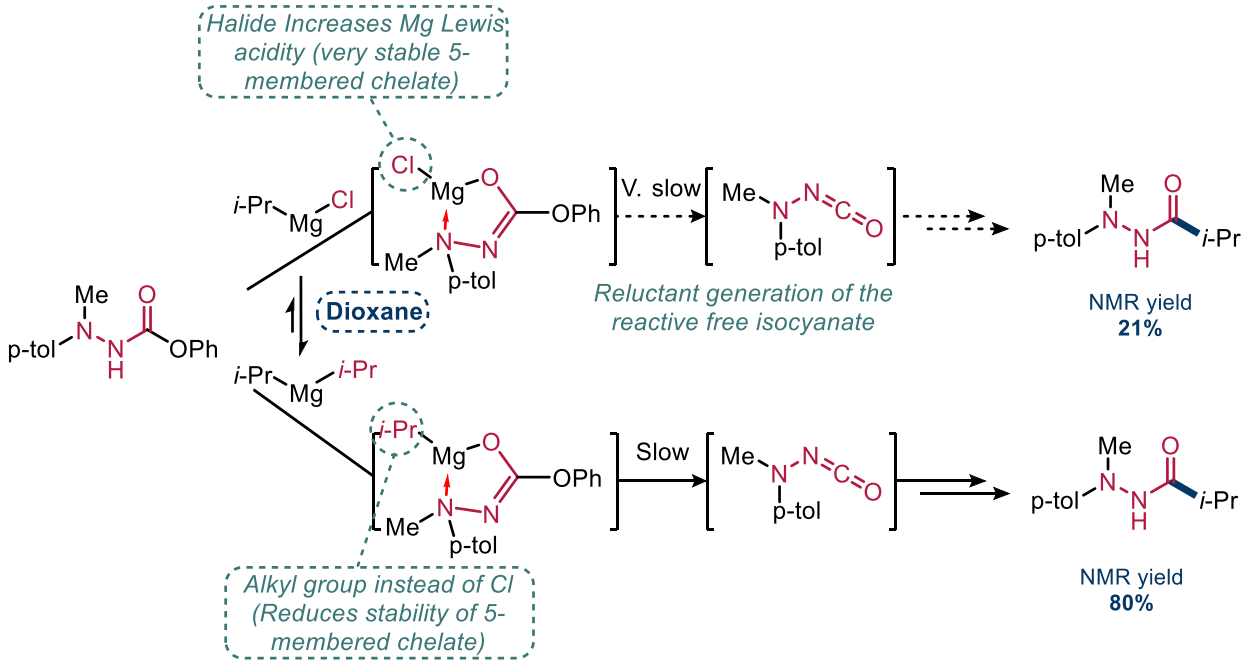

2.9 Scope of Grignard Addition to Masked *N*-Isocyanates

The scope of *N*-isocyanate partner was then probed, using two Grignard reagents *i*-PrMgCl and PhMgBr. TMEDA was adopted as an additive in 1.1 equivalents to optimize the products formation for substrates with different substituents on the nitrogen atom. It was expected that TMEDA could act as a chelating

ligand for magnesium,[158,159] which seemed to help tune the reactivity of the five-membered complex. This was represented in higher yields associated with its use especially with dialkyl-substituted *N*-isocyanates. The tested *N*-isocyanate substrates demonstrated similar reactivity trend toward the Grignard partners as observed for *O*-isocyanate system, in that for reactions with PhMgBr proved higher yielding than reactions with *i*-PrMgCl (Scheme 2.13).

Scheme 2.13. Scope of stoichiometric Grignard addition to masked N-isocyanates.

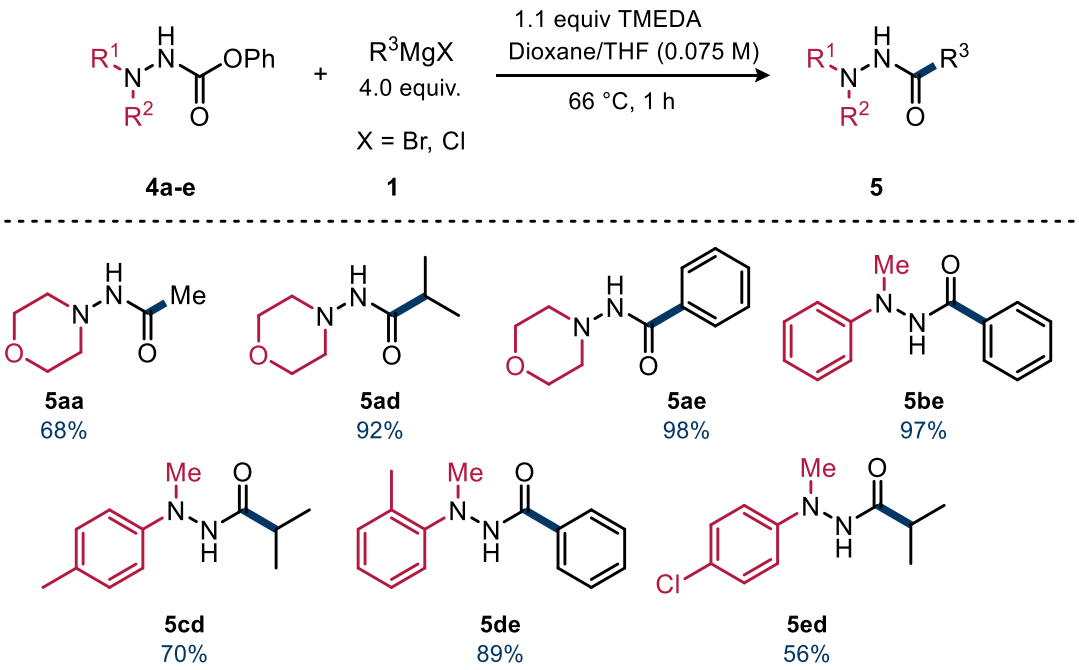

[a] Conditions: **4a-e** (0.6 mmol), Grignard **1** (2.4 mmol), Dioxane/THF (0.075 M), TMEDA (99 µL) at 66 °C in a sealed µW vial. Yields shown are isolated yields from 0.6 mmol reaction scale.

In addition, precursor **5b** was allowed to react with diethylzinc under the reaction conditions optimized for the addition of diethylzinc to the *O*-isocyanates, and a 30% ^{1}H NMR yield of the addition product was achieved, however, no further investigation of this route was carried out, given the challenges observed with varying organometallic reagents in the previous section (Scheme 2.14).

*Scheme 2.14. The reaction of **5b** with diethylzinc.*

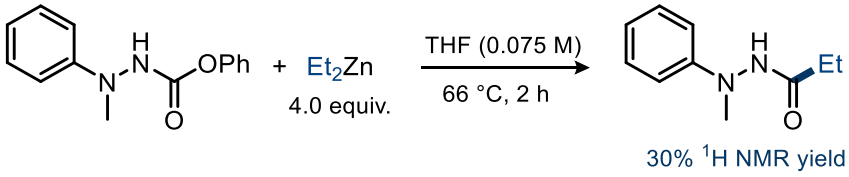

2.10 Summary of the Key Findings

This chapter centered on the study of masked *O*-isocyanates and their behavior toward the stoichiometric addition of Grignard reagents to achieve C-C bond formation to access hydroxamates. Preliminary studies comparing the masked *O*-isocyanate system with a masked *C*-isocyanate control reaction provided significant insights. The facile deblocking and ambient temperature reactivity observed with *C*-isocyanates, as opposed to the slow deblocking and thermal requirements for blocked *O*-isocyanates, led to the **first postulate** regarding *O*-isocyanates reactivity, that there is a fundamental difference between the generation of free reactive isocyanates species in phenol blocked *O*-isocyanates and their *C*-counterparts. This variance may be attributed to the additional coordination of the oxygen in these substrates with the metal, facilitating the formation of a relatively stable five-membered chelate upon Grignard-mediated deprotonation, a phenomenon absent in *C*-isocyanates analogues (Scheme 2.15, a and b). Although this chelate formation slows the reaction, it may be essential for the reactivity of the *O*-isocyanate system, given the high tendency of free *O*-isocyanates to trimerize when generated *in situ* at high concentrations. Consequently, the **second hypothesis** posits that the five-membered chelate, by moderating the release of the free *O*-isocyanate, maintains a low concentration of this reactive intermediate in the reaction medium, potentially reducing oligomerization (Scheme 2.15, b).

Scheme 2.15. a) Difference between masked O-isocyanate and C-substituted analogue in metal chelation affects the reactivity. b) The proposed mechanism of product formation of O-isocyanate, showing the benefits of forming five-membered chelate.

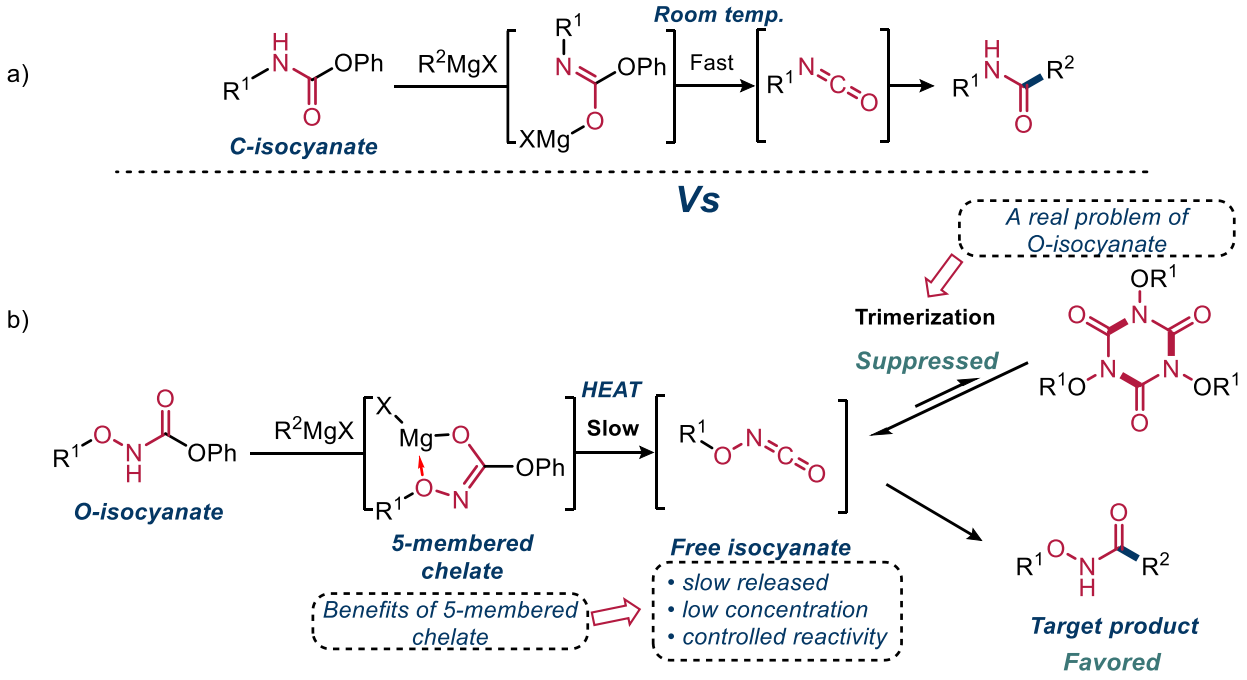

Subsequent research indicated the need for further optimization of the chelate structure to tune reactivity. Observations of benzyl alcohol as a common side product, along with reduced yields of the target addition product, pointed to a competitive N-O bond cleavage degradation mechanism. This could be rationalized by the high Lewis acidity of the metal, which may lead to increased polarization of the oxygen-metal dative bond, thereby further weakening the N-O bond and leading to its cleavage. At this juncture, a **proposed mechanism** for target product formation included deprotonation, five-membered chelate formation, deblocking, *in situ* release of free *O*-isocyanate, nucleophilic addition of Grignard reagents to the electrophilic isocyanate leading to C-C bond formation, and product furnishing following aqueous workup (Scheme 2.15, b). Additionally, two degradation mechanisms involving N-O bond cleavage were postulated: the dianion mechanism (via addition/elimination or double addition pathways) and Lossen rearrangement, as supported by the isolation of traces of a symmetric anilide product alongside benzyl alcohol (Scheme 2.16).

Scheme 2.16. Proposed mechanisms for degradation pathways showing common side products formation.

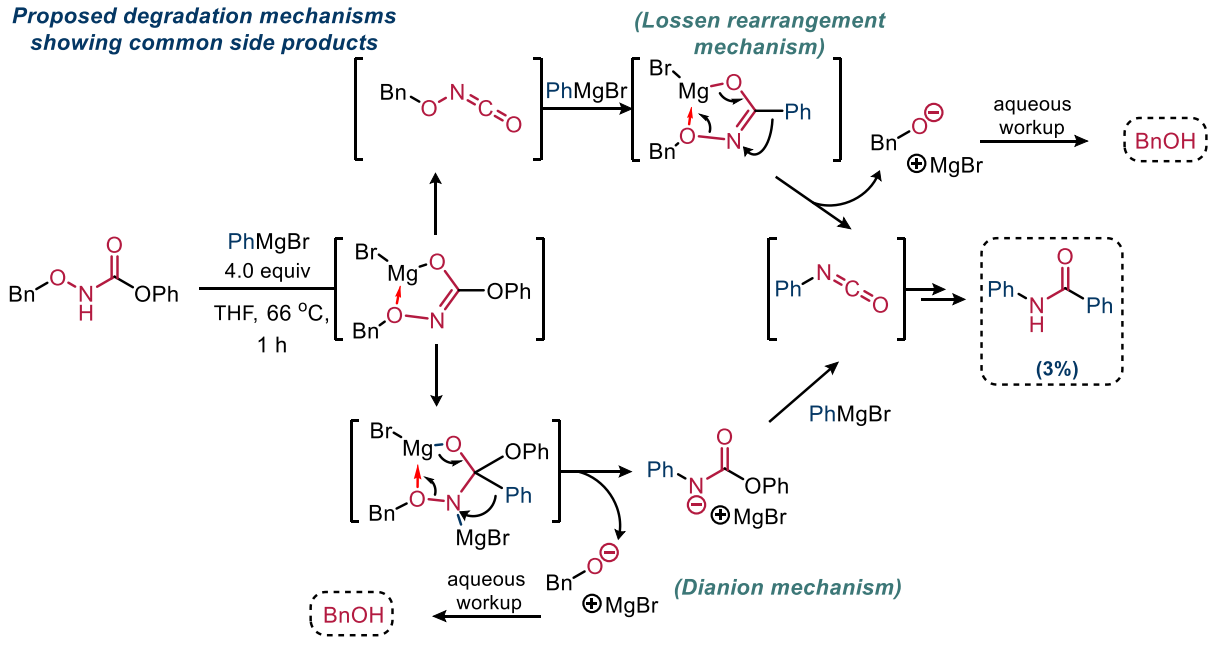

To address the competing degradation pathways, dioxane was introduced as a co-solvent in the reaction mixture which, gratifyingly, enhanced the yield. Dioxane promotes shifting the Schlenk equilibrium toward the formation of diorganomagnesium species, which became the predominant nucleophile in the reaction medium, thereby, led to the **fourth hypothesis**: the addition of dioxane presumably altered the five-membered chelate structure by substituting the metal-bound halogen with a less electronegative R group, reducing the Lewis acidity of the magnesium, resulting in a less polarized coordinate bond and a less labile N-O bond, thus mitigating degradation (Figure 2.5).

Figure 2.5. Effect of dioxane addition on the structure and the stability of the five-membered chelate.

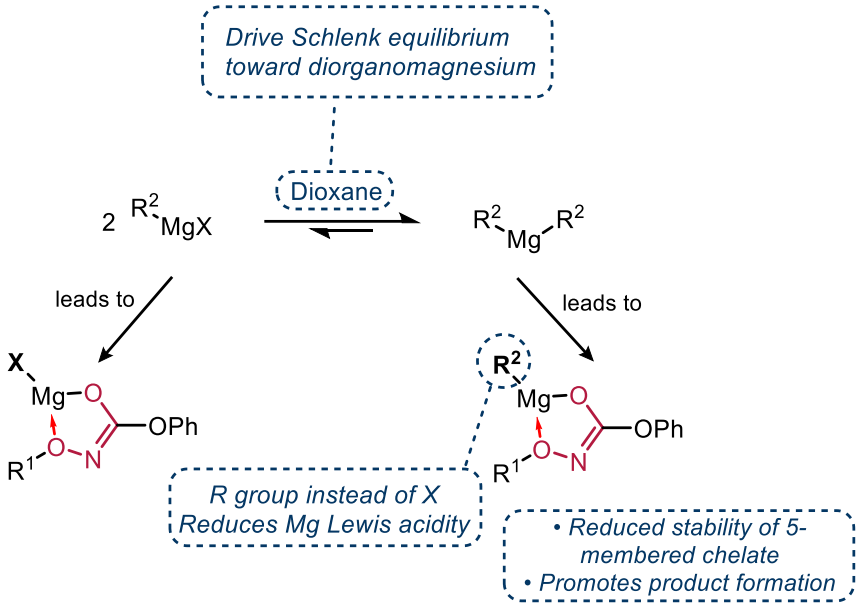

Subsequent investigations employed organozinc reagents, for the purpose of evaluating reactivity differences when the metal is changed. While organozinc reagents failed to yield high reactivity with the blocked *O*-isocyanate system, the differential reactivity towards diethylzinc in comparison to ethylzinc iodide lent additional support to our postulate that manipulating the R group on the metal could optimize the chelate structure, allowing for fine-tuning of the system's reactivity. Leveraging knowledge gained from *O*-isocyanate precursors, the stoichiometric addition of Grignard reagents was extended to include masked *N*-isocyanates. The reactivity trends of the masked *N*-isocyanate system supported the previously described mechanistic hypotheses, including the influence of the five-membered chelate and dioxane. However, it also highlighted the need to optimize another factor: the Lewis basicity of the sp^3 nitrogen adjacent to the isocyanate group, by varying the nitrogen substituents. Notably, electron-withdrawing groups enhanced product formation by diminishing the metal-nitrogen coordination, thereby weakening the chelate to a degree conducive to product synthesis. The exploration of using sp^2 nitrogen atom in place of sp^3 nitrogen atom will be detailed in the next chapter.

2.11 Conclusion and Future Work

The chapter investigates the formation of a relatively stable five-membered chelate as a key aspect in the stoichiometric addition of Grignard reagents to masked heteroatom-substituted isocyanates. This chelate controls the release of the reactive isocyanate, hence mitigating uncontrolled reactivity including oligomerization of free *O*- or *N*- isocyanates and/or rearrangement.

Future work will be geared towards exploration of the heteroatom-substituted isocyanates reactivity towards transition-metal catalysed addition of carbon nucleophiles using rhodium or ruthenium mediated catalysis, guided by the previous efforts on masked *C*-isocyanates.[69] Stoichiometric organometallic addition to heteroatom-substituted isocyanates should be revisited, benefiting from the recent advancements in organozinc,[140,160,161] organolithium,[139,162] cuperates,[142,163] and organomagnesium[164,165] chemistry.[166]

Chapter 3 Formation of Pyrazolones via Cyclization

Pyrazolones are considered key structural motifs in many biologically active heterocyclic compounds. They are known for their commercial use in pharmaceuticals, agrochemicals and dyes (Figure 3.1). In terms of biological applications, pyrazolones are among the oldest synthetic pharmaceuticals,[167,168] with antipyrine (phenazone) being the first introduced in the 1880s.[169] These compounds generally act as analgesics and include a variety of drugs such as dipyrone (Metamizole), aminophenazone, and propyphenazone. Other biological activities include antipyretic, antitumor, antibacterial, antidepressant, and several other medicinal applications.[170–175] Due to their widespread biological activities, pyrazolone derivatives are a very attractive class of heterocycles for chemists.

Figure 3.1. Selected pharmaceuticals and agrochemicals containing pyrazolone ring.

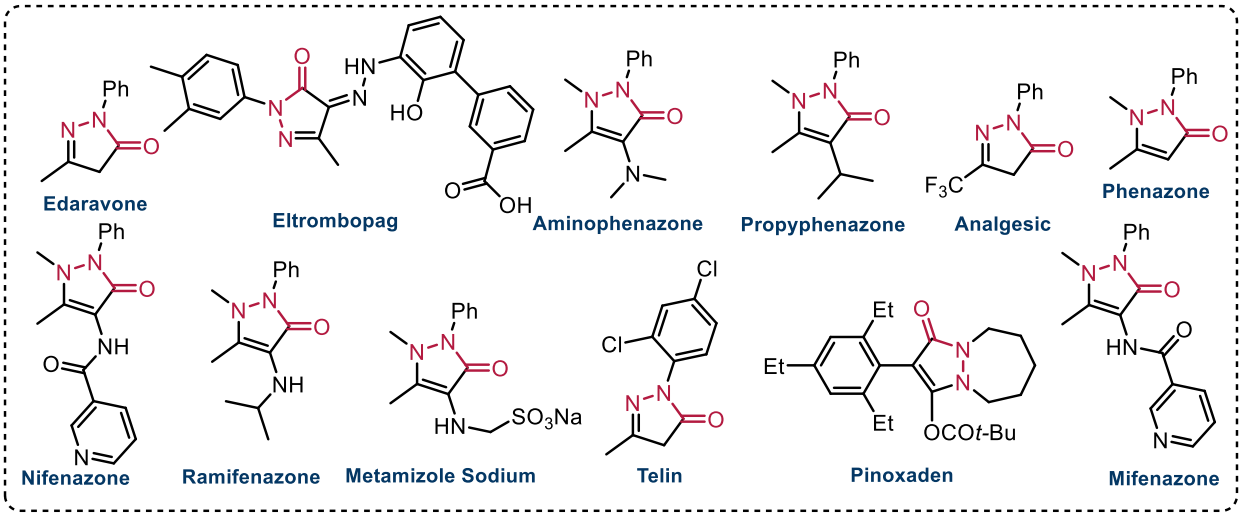

In 1883, Ludwig Knorr achieved the first successful synthesis of pyrazolones, marking a significant milestone in the field of heterocyclic chemistry, when he accessed 1-phenyl-3-methyl-2-pyrazolin-5-one (currently known as edaravone) via a condensation reaction between ethyl acetoacetate and phenylhydrazine.[176] Thereafter, conventional approaches to synthesizing pyrazolones predominantly utilize the Knorr synthesis approach, which involves the condensation of β-ketoesters with substituted hydrazines (Figure 3.2, a).[177] This process often requires the use of additives, elevated temperatures, or the application of microwave irradiation.[178–180] Different precursors were employed in such reactions included β-(carbonylhydrazono)esters (Figure 3.2, b)[181] or derivatives of propiolate esters (Figure 3.2, c).[182] Other coupling methods include palladium-catalyzed carbonylation of 1,2-diaza-1,3-butadies with carbon monoxide (Figure 3.2, d),[183] as well as α-chloroketones, with carbon monoxide in the presence of hydrazines (Figure 3.2, f).[184] Gold catalysis has also been reported in a cascade reaction for the synthesis

of pyrazolones (Figure 3.2, e).[185] Moreover, the Murarka group recently disclosed *N'*-arylidene-*N*-acryloyltosylhydrazides as novel frameworks for the generation of pyrazolones via a photoinduced radical cascade reaction involving *N*-(acyloxy)phthalimides (Figure 3.2, g).[186] Furthermore, *N*-isocyanates were employed in the synthesis of pyrazolones via [3+2] cycloaddition reactions. This is achievable by *in situ* formation *of N*-isocyanates either by an *aza*-Curtius rearrangement (Lwowski work, Figure 3.2, h)[80] or via a blocking group strategy, by Beauchemin group who reported aminocarbonylation of alkenes via inter- and intramolecular [3+2]-cycloadditions on masked *N*-isocyanates with the intermediary of *N,N'*-cyclic azomethine imines (Figure 3.2, i-k).[187–189]

Figure 3.2. Selected previous efforts towards the synthesis of pyrazolones.

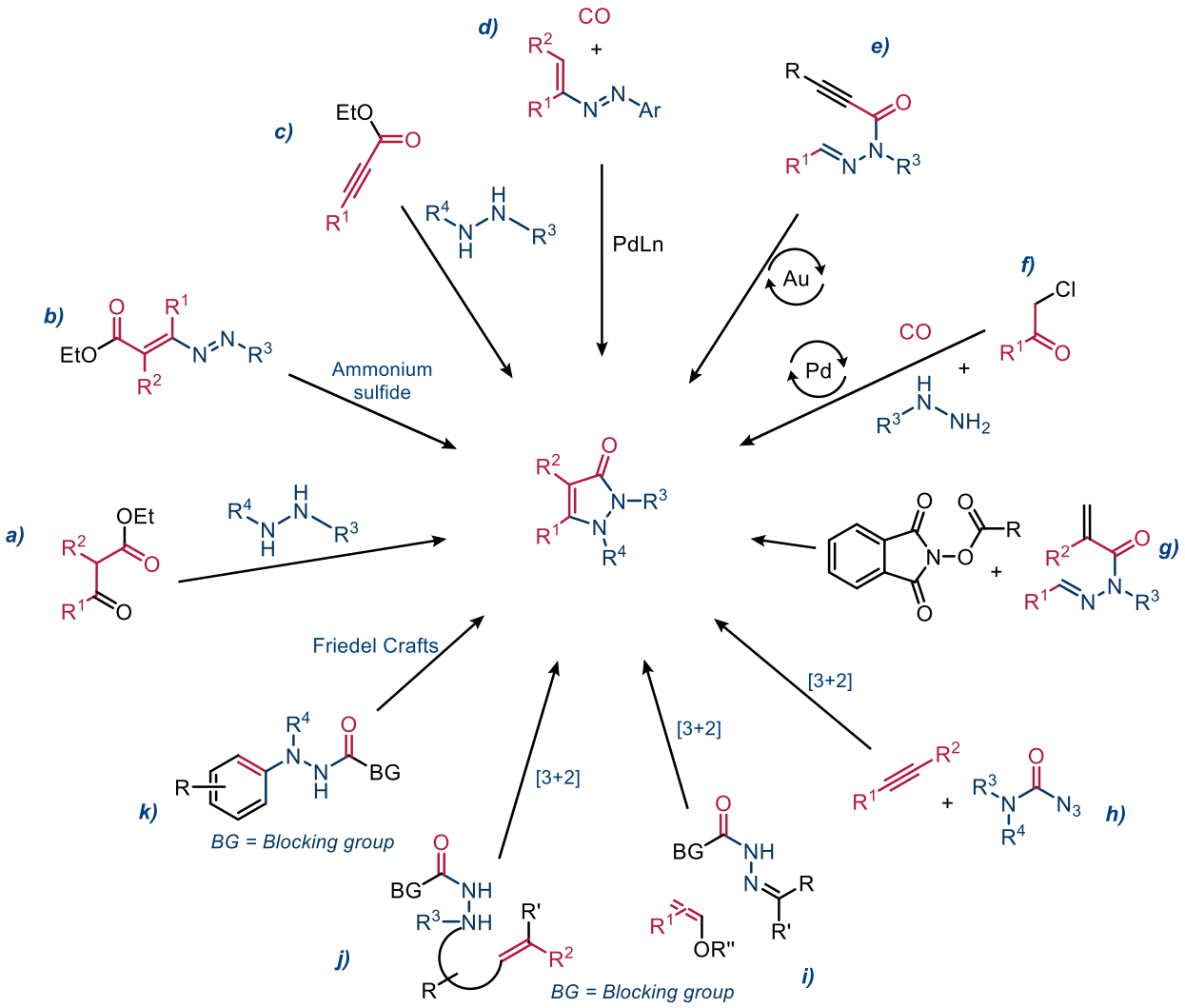

3.1 Different Nitrogen Type: Reactivity of sp^2 Nitrogen

In Chapter 2, to fully understand the behavior of nitrogen-substituted isocyanate precursors with Grignard reagents, it was required to study different types of sp^3 nitrogen atom, but one aspect that was not discussed in that chapter was the possible consequences of employing the more electronegative sp^2 nitrogen (Scheme 3.1). It was unclear if the sp^2 nitrogen with different geometry and electronics would change the coordination with the metal in such a way that would favor the formation of the addition product. The strength of coordination of the sp^2 nitrogen to the magnesium would control the equilibrium leading to the generation of the free reactive *N*-isocyanate species. Consequently, the yields of the addition products (if any) would be expected to reflect whether the stability of the five-membered chelate was sufficiently tuned to give the expected reactivity.

Scheme 3.1. Expected outcome of initial reaction of sp^2 nitrogen-substituted isocyanates.

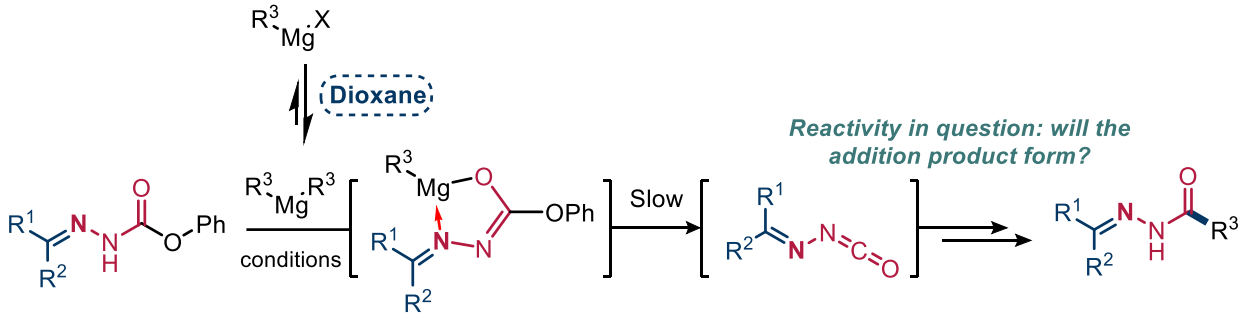

Initially, the masked N-isocyanate **6a** was selected as sp^2 nitrogen substrate to explore its reactivity toward *i*-PrMgCl. Unexpectedly, when **6a** was submitted to the reaction conditions optimized for *O*-isocyanates, the corresponding cyclic pyrazolone compound **7a** was observed in 56% NMR yield instead of the addition product (Scheme 3.2). Compound **6a** has 2 methylene hydrogens α to the imino group, and as such, it was inferred that the cyclic product was the outcome of a reaction sequence that included the deprotonation of one α hydrogen followed by intramolecular nucleophilic attack on the electrophilic *N*-isocyanate which led to cyclization. The conjugation was attained via the abstraction of the other α hydrogen using a base, which in this case was *i*-PrMgCl. The ^{1}H NMR analysis confirmed the structure of product **7a** by cleavage of phenoxy group (4 aromatic Hs in the product versus 9 aromatic Hs in the starting material), no signals for isopropyl addition, and the disappearance of a multiplet signal corresponding to two hydrogens in the product (Figure 3.3).

*Scheme 3.2. The reactivity of compound **6a** toward i-PrMgCl (formation of pyrazolones).*

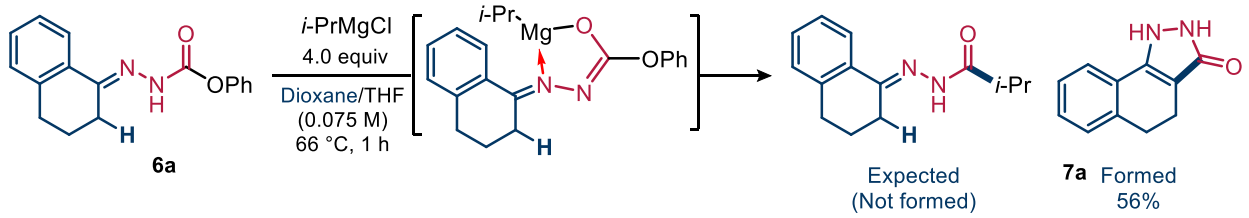

*Figure 3.3. Comparing the ^{1}H NMR spectra for the product **7a** and the precursor **6a**.*

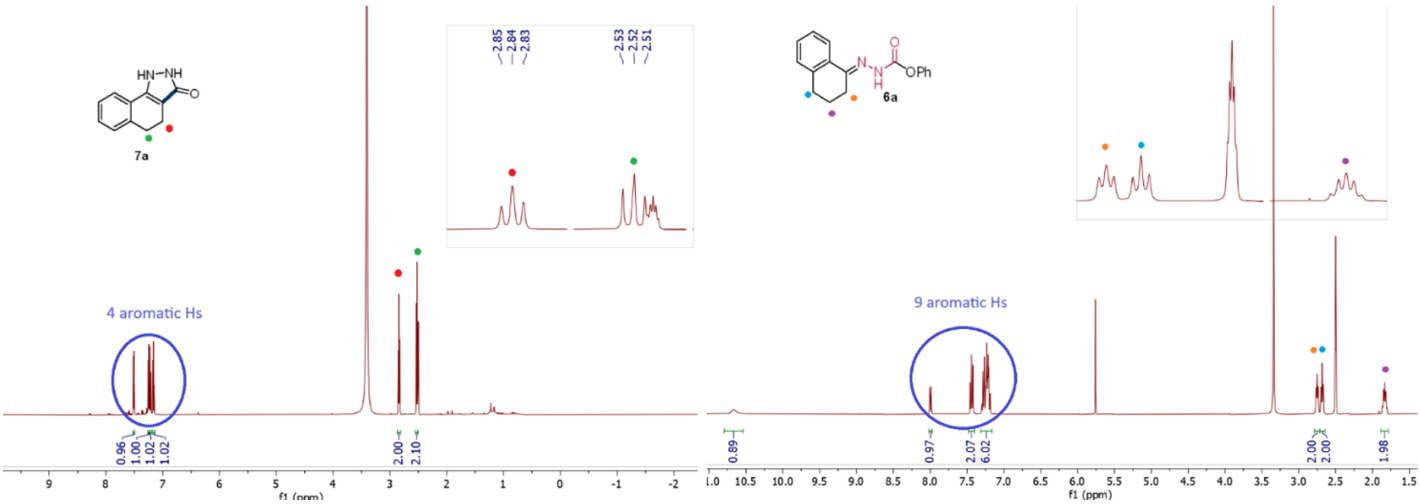

3.2 Mechanistic Hypothesis and Discussion

This unexpected formation of a cyclic pyrazolone instead of a non-cyclic addition product was a pleasant surprise, as the Beauchemin group had long been interested in the formation of pyrazolones from hydrazones, via *N*-isocyanates. Several students had attempted the reactivity with a variety of substrates, blocking groups, and strategies (including simple thermolysis), and most recently Mr. Frédéric Vuillermet (a current PhD candidate) had explored this reactivity using several basic conditions combined with several Lewis acids, some of which are illustrated below (Table 3.1 and Table 3.2).

Table 3.1. Previous unsuccessful reaction conditions to access pyrazolone from hydrazone carboxylate precursors.

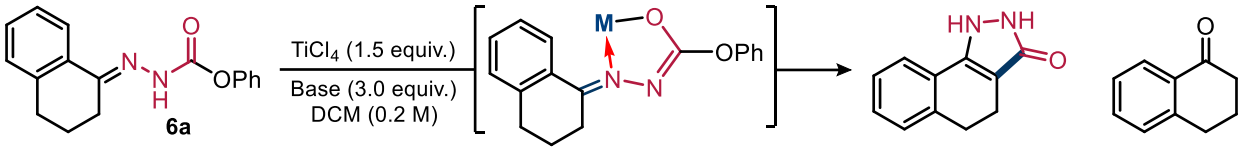

Base	Temperature °C	Time (hours)	NMR yield of ketone[a]
DBU	-78 to R.T.	1	40%
DIPEA	80	16	30%
Et_3N	80	16	30%

[a] ^1H NMR yield determined by using 1,3,5-trimethoxybenzene as internal standard.

Table 3.2. Previous unsuccessful reaction conditions to access pyrazolone from hydrazone carboxylate precursors (Continued).

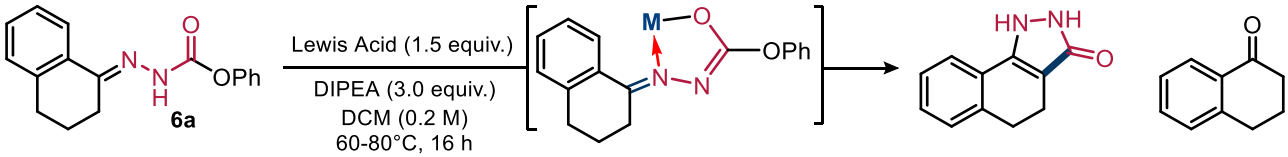

Lewis acid	NMR yield of ketone[a]	Lewis acid	NMR yield of ketone[a]
$AlCl_3$	S.M.	$Pb(OAc)_4$	S.M.
$Ba(OAc)_2$	50% hydrolysis	$RuCl_3•H_2O$	Degradation
$CuCl_2$	S.M. & degradation	$SnCl_2•2H_2O$	S.M.
$Cu(OAc)_2$	S.M. & degradation	$SnCl_4$	50% & 50% S.M.
$MgCl_2$	S.M.	$Ti(Cp)_2Cl_2$	10% & 50% S.M.
$MgBr_2•O(C_2H_5)_2$	9%	$Ti(O\textit{i}\text{-}Pr)_4$	99% *i*-Pr substituted product
$Mn(OAc)_3•3H_2O$	4% & S.M.	V_2O_5	S.M.
$Ni(OAc)_2•4H_2O$	S.M.	ZnX_2 (X = Cl, Br, I)	S.M.
$BF_3•Et_2O$	S.M.	$MgSO_4$	S.M.

[a] ^1H NMR yield determined by using 1,3,5-trimethoxybenzene as internal standard.

These failed attempts, together with the success of the cyclization of **6a** into pyrazolone **7a** using the stoichiometric Grignard conditions shed light on the importance of fine-tuning the equilibrium between the blocked and the free heteroatom isocyanates via manipulating the stability of the five-membered complex. It was crucial to control the concentration of the free reactive form of heteroatom isocyanate, and to only generate reasonably low amounts of this species at once in the reaction medium to mitigate oligomerization, so that the desired reactivity will have a chance to take place. In addition, it provided an

example of a successful strategy to form pyrazolones, and how a direct metalation could be achieved, thereby allowing a subsequent intramolecular reaction.

Based on what has been learned from studying masked *O*- and *N*- isocyanates, it was hypothesized that the mechanism starts through the deprotonation of N-H of **6a** by the Grignard base, leading to the formation of the five-membered chelate. This increases the acidity of the proton α to the imino group by electron-withdrawing effects. The five-membered chelate enables the coordination of a 2nd equivalent of Grignard to the nitrogen atom, possibly facilitating the deprotonation of the α-proton via a six-membered transition state (i.e., a directed metalation event).[190–193] This is followed by the slow generation of the electrophilic free isocyanate species,[90] which is then attacked by the olefinic nucleophile to allow pyrazolone ring formation. This hypothesis may provide further evidence of controlled or reluctant free isocyanate release by formation of the five-membered chelate (Figure 3.4).

Figure 3.4. Potential mechanism for the Grignard reaction with sp^2 nitrogen-substituted isocyanates.

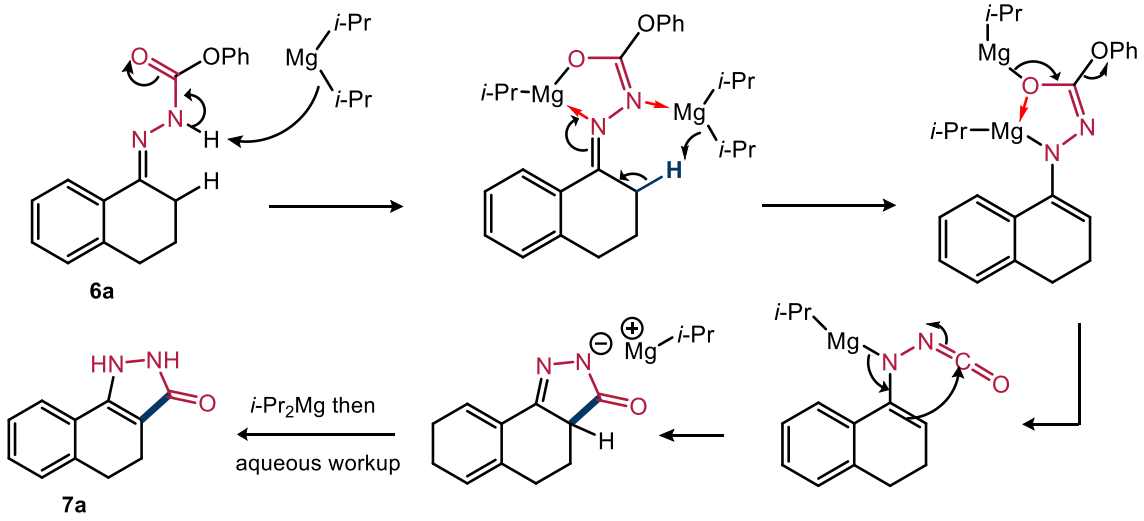

Similar approaches are adopted by research groups who have made modifications to SAMP/RAMP auxiliaries for asymmetric alkylation of ketones (Scheme 3.3, a)[194,195]. The primary design feature of these modified auxiliaries is the strategic placement of a carbonyl group adjacent to the hydrazone moiety.[196] Upon deprotonation and the formation of an *aza*-enolate, the metal forms a five-membered chelate with both the carbon-bound nitrogen of the hydrazone and the carbonyl of the auxiliary. This five-membered chelate enhances the acidity of the proton through tight chelation and electron-withdrawing effects, thereby facilitating deprotonation (Scheme 3.3, b).

Scheme 3.3. a) Enders SAMP/RAMP hydrazone for asymmetric alkylation reactions. b) Asymmetric alkylation of ketones by using chiral N-amino cyclic carbamate (ACC) hydrazones.

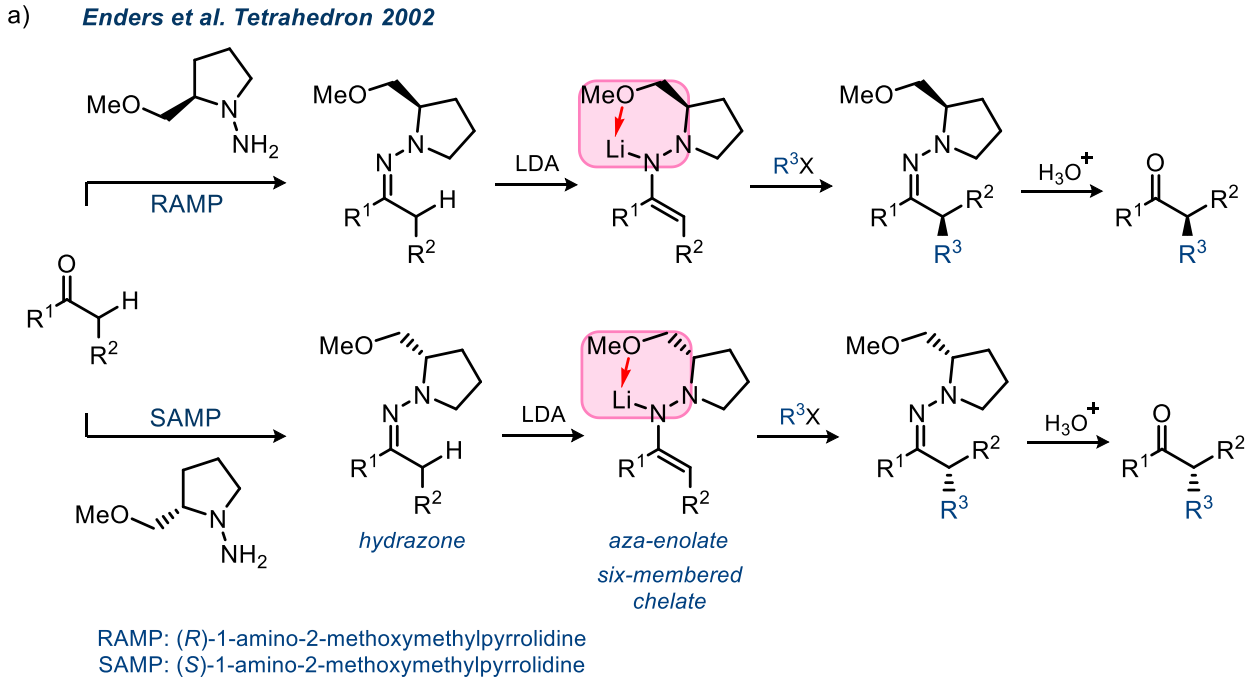

A related approach uses hydrazones to direct a deprotonation Using LDA at the opposite side of the molecule via complex-induced *syn*-deprotonation (CIS-D). Here, the carbonyl influences the regiochemistry of the deprotonation by chelating with the Lewis acidic metal of the base, guiding the base to remove a proton on the same side of the C=N bond as the heteroatom.[197,198] This process occurs in a configurationally controlled manner with respect to the hydrazone C=N bond geometry and is considered a directed metalation event (Scheme 3.4).

Scheme 3.4. Using chiral auxiliary to induce syn-deprotonation (directed deprotonation).

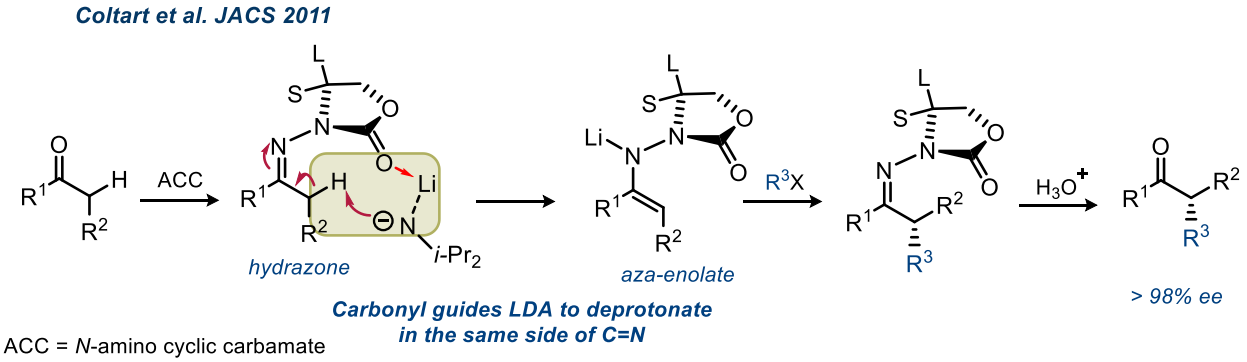

Mechanistically, it was hypothesized that both approaches take place in the case of the formation of pyrazolones from masked *N*-isocyanates, exploiting the relatively stable five-membered chelate. Upon deprotonation of the isocyanate nitrogen, the oxygen of the masked isocyanate forms a five-membered chelate with magnesium, enhancing the acidity of the proton through tight chelation and electron-withdrawing effects. Simultaneously, the nitrogen of the masked isocyanate chelates a second Grignard molecule, leading to directed deprotonation of the α-proton via a six-membered transition state (Scheme 3.5).

Scheme 3.5. Our hypothesis: both heteroatoms of isocyanate enable five-membered chelate electron withdrawing effect and directed metalation simultaneously.

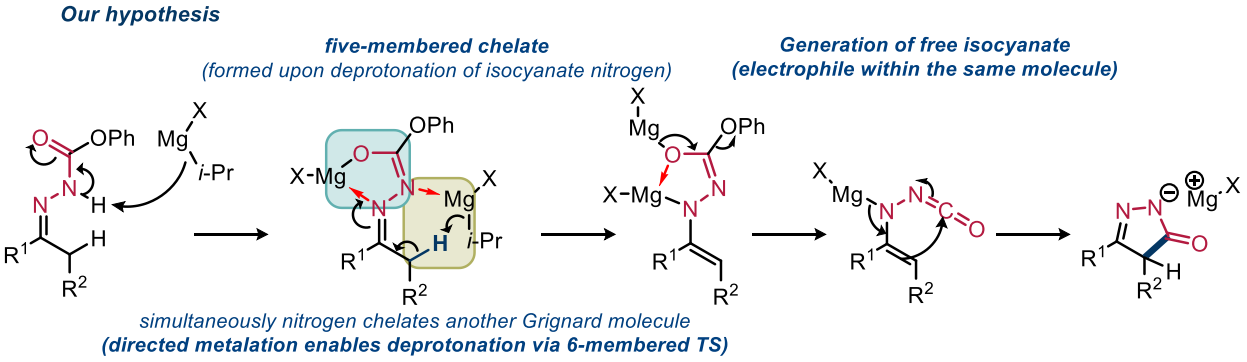

3.3 Optimization of The Reactivity of Compound 6a

Extensive optimization was conducted on compound **6a** to further investigate this reactivity and improve the yield of the cyclic product **7a**. Initially, different Grignard reagents were employed to compare their reactivities and assign the best base among them to access the pyrazolone product (Table 3.3). Performing the reaction in the absence of dioxane as a co-solvent was also probed with each of the tested Grignard reagents. The best reactivity was observed with *i*-PrMgCl amongst the attempted Grignard reagents. It

afforded the pyrazolone in 58% NMR yield and 55% isolated yield when the reaction was performed in the presence of dioxane, while it gave a better yield (78% NMR yield) in its absence. (Table 3.3, entry 1). Moderate cyclization capability was demonstrated by EtMgBr as it provided the cyclic pyrazolone product in 53% NMR yield, but unlike *i*-PrMgCl, running the reaction in the absence of dioxane seems to have dire effect on the product yield, as it formed in 38% (entry 2). The use of PhMgBr as a base appeared to result in an uncontrolled reaction where neither a good yield of the cyclized nor the addition product were obtained (entry 3). Employing MeMgBr in this reaction may have led to the formation of the addition product in a moderate yield (entry 4), but this has not been further investigated (Figure 3.5). This preliminary scan of the Grignard reagents led to the validation of *i*-PrMgCl as a platform for performing the remaining optimization process. (shown in Table 3.4), with results suggesting that both Lewis acidity, steric hindrance and basicity are important to favor the pyrazolone product.

*Figure 3.5. A crude ^{1}H NMR spectrum showing the proposed formation of the addition product from the reaction of **6a** with MeMgBr.*

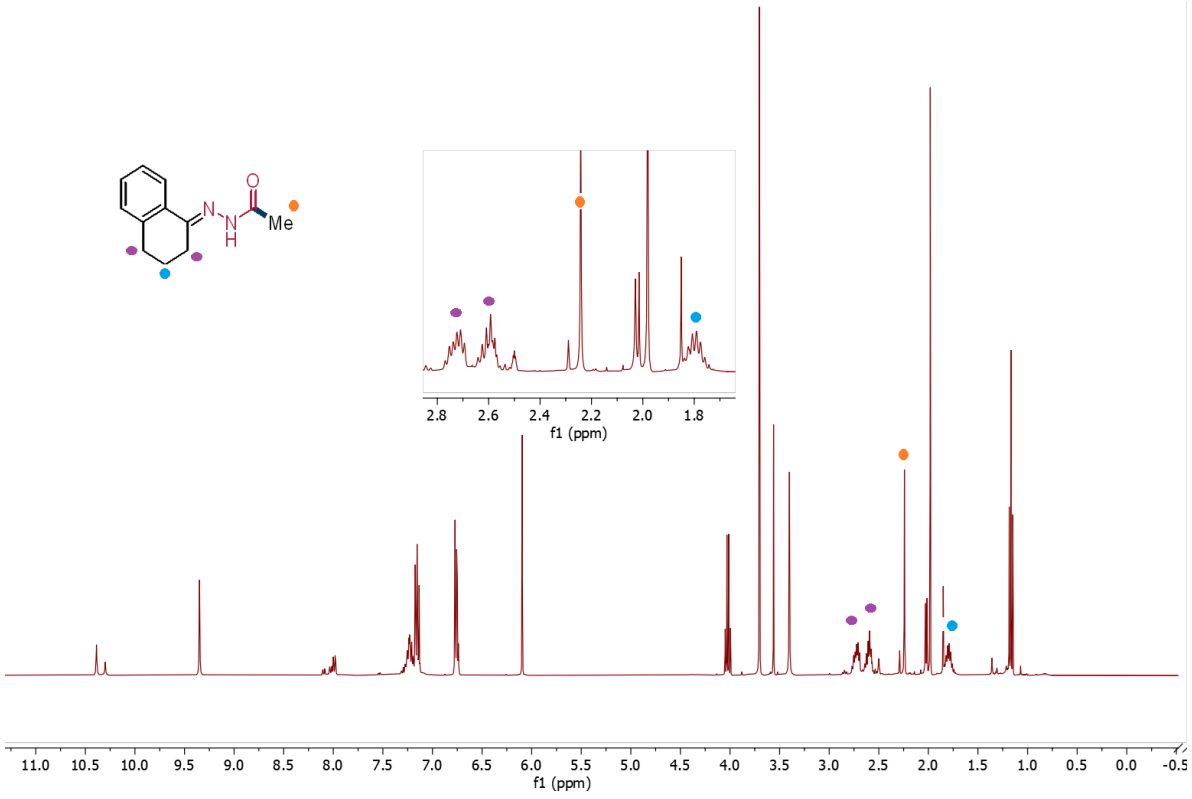

Table 3.3. Grignard screening for the synthesis of pyrazolone product.

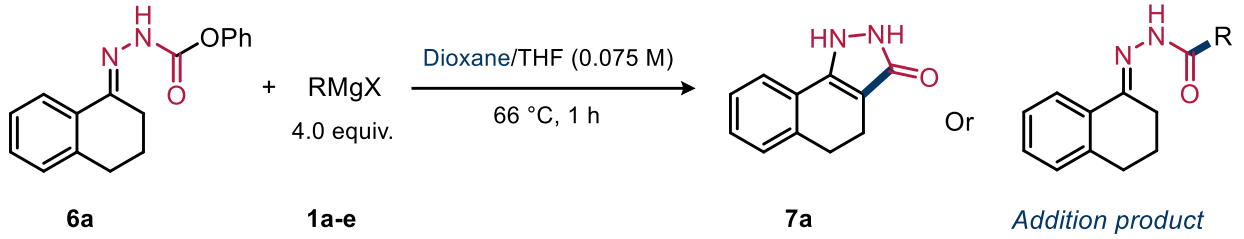

6a **1a-e** **7a** *Addition product*

Entry	R	X	Pyrazolone Product yield (%)[a]	
			With dioxane	**Without dioxane**
1	*i*-Pr	Cl	58 (55)[b]	78
2	Et	Br	53	38
3	Ph	Br	15	<2 Traces of addition product may have formed
4	Me	Br	Addition product may have formed	Addition product may have formed

[a] ^{1}H NMR yield determined by using 1,3,5-trimethoxybenzene as internal standard. [b] Yields in parenthesis indicate isolated yield from 0.6 mmol reaction scale.

*Table 3.4. Optimizing pyrazolone formation from the reaction of compound **6a** with i-PrMgCl.*

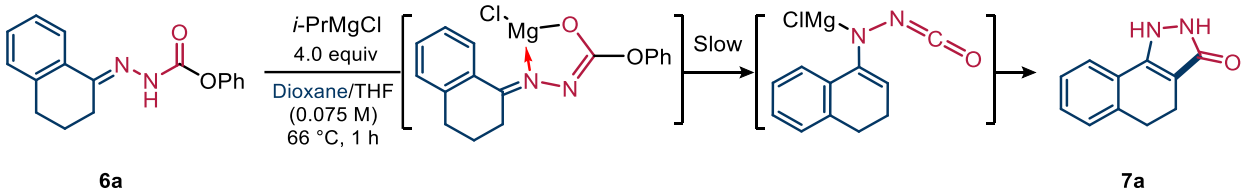

6a **7a**

Entry	Deviation from above conditions[a]	Pyrazolone yield (%)[c]
1	None	58 (55)[d]
2	rt	8
3	rt, ON	44
4	No dioxane (only THF)	78
5	Dioxane[b]	58
6	CH_2Cl_2[b]	56
7	Et_2O[b]	40
8	Toluene[b]	38
9	*i*-PrMgBr (not Cl)	40
10	2.5 equiv.	50
11	No dioxane (only THF), new Grignard bottle	52
12	0.1 M, only THF, new Grignard bottle	43
13	Only THF, new Grignard bottle, 1.0 equiv. LiCl (solid)	52
14	Only THF, *i*-PrMgCl•LiCl (turbo Grignard bottle)	30
15	None, old Grignard bottle	60
16	0.5 equiv. TMEDA, only THF, new Grignard bottle	68
17	**1.1 equiv. TMEDA, No dioxane (only THF), new Grignard bottle**	**82 (76)[d]**
18	1.1 equiv. TMEDA, No dioxane (only THF), old Grignard bottle	82
19	-15 °C to 5 °C, 1.1 equiv. TMEDA, only THF, 3 h, new Grignard bottle	52

[a] Conditions: **6a** (0.2 mmol), dioxane/THF (0.075 M), *i*-PrMgCl (0.8 mmol), at 66 °C in a sealed μW vial unless otherwise noted. [b] THF was always a co-solvent; *i*-PrMgCl was in THF. [c] ^{1}H NMR yield determined by using 1,3,5-trimethoxybenzene as internal standard. [d] Yields in parenthesis indicate isolated yield from 0.6 mmol reaction scale.

The reaction was initially attempted using the optimized conditions for *O*-isocyanates, which gave access to the cyclic pyrazolone in 58% NMR yield and 55% isolated yield (Table 3.4, entry 1). Performing the reaction at room temperature for 1 hour yielded traces of product, however, when the reaction was left to stir overnight at room temperature, 44% NMR yield of the cyclic product was obtained (entry 3). Removing dioxane from the reaction mixture resulted in an increased yield of 78% (entry 4). Solvent screening was conducted to reveal the best solvent for this reaction. Various solvents were evaluated

including dioxane, diethyl ether, dichloromethane, as well as toluene. While dioxane and CH_2Cl_2 did not enhance the pyrazolone formation, diethyl ether and toluene were found to have a detrimental effect on the reaction outcome (entries 5-8). A lower 40% yield was observed with the use of *i*-PrMgBr instead of chloride (entry 9), further supporting that increased Lewis acidity favors the cyclization pathway. Lowering the Grignard load to 2.5 equivalents afforded 50% of the product versus 78% using excess (4.0 equiv.) of Grignard (entry 10). At this stage of the optimization, a new batch of *i*-PrMgCl bottles arrived in the lab and yields started to drop with the use of these new bottles (53% yield, entry 11). Further optimization was required to tackle this issue. Increasing the concentration of the reaction was unfavorable and the NMR yield was 43% (entry 12). Adding 1.0 equivalent of dry LiCl solid to the reaction mixture did not affect the reaction outcome (entry 13), while switching to Turbo Grignard[165] appeared to have negative effect, giving 30% NMR yield (entry 14). The use of 0.5 equivalents of TMEDA as an additive was beneficial, affording the cyclic pyrazolone product in 68% yield (entry 16). Motivated by this result, TMEDA loading was increased to 1.1 equivalents and pleasingly, an 82% NMR yield was obtained along with 76% isolated yield (entry 17). Importantly, this result was reproducible even when switching between different *i*-PrMgCl bottles (entry 18). Eventually, TMEDA was able to mitigate the variation in the results that arose from the use of different reagent batches. An attempt to run the reaction at a lower temperature for longer time (3 h) resulted in the formation of the cyclized product in 52% yield, indicating that deblocking is possible at lower temperatures in this system. Noteworthy, *n*-butyllithium was employed as the basic reaction partner with compound **6a**, instead of the Grignard, to perform the cyclization reaction. The reaction was carried out at room temperature for 3 hours, after which the starting material was fully consumed and the corresponding cyclic pyrazolone product was achieved in 40% ^{1}H NMR yield (Scheme 3.6). This discovery that lithium intermediates can afford the desired cyclization constituted the basis upon which Mr. Frédéric Vuillermet successfully developed milder, second-generation conditions for the cyclization that will not be further discussed in this thesis.

*Scheme 3.6. Reactivity of **6a** towards n-butyllithium.*

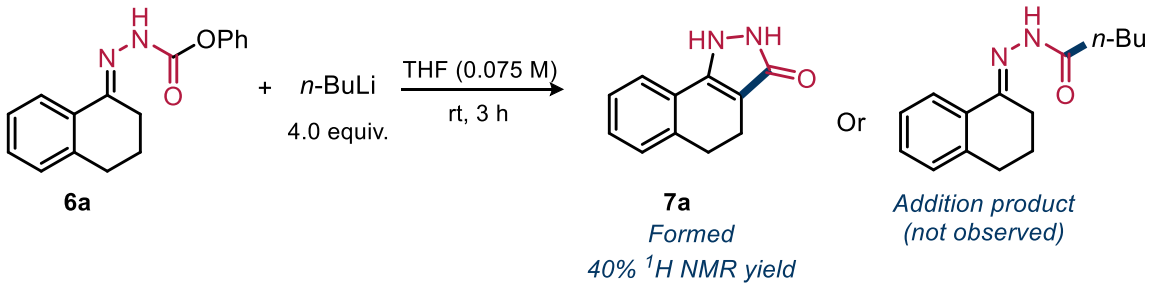

3.4 Scope and Different Substrate Reactivities

Following the optimization of cyclization conditions for **6a**, the attention was focused on the scope of the reaction. The first goal was to secure the production of sufficient hydrazone carboxylate precursors for scope purpose, a goal that was shared equally between Mr. Fred Vuillermet and myself. Condensation of phenyl carbazate with common ketones was carried out to synthesize the required starting materials following a literature procedure (Scheme 3.7).[86] Some products were successfully formed at lower temperatures and in shorter reaction times such as **6a** and **6c** (0 °C for 1 h), while others required stirring overnight at reflux.

Scheme 3.7. Scope of starting materials (hydrazone carboxylates) formation.

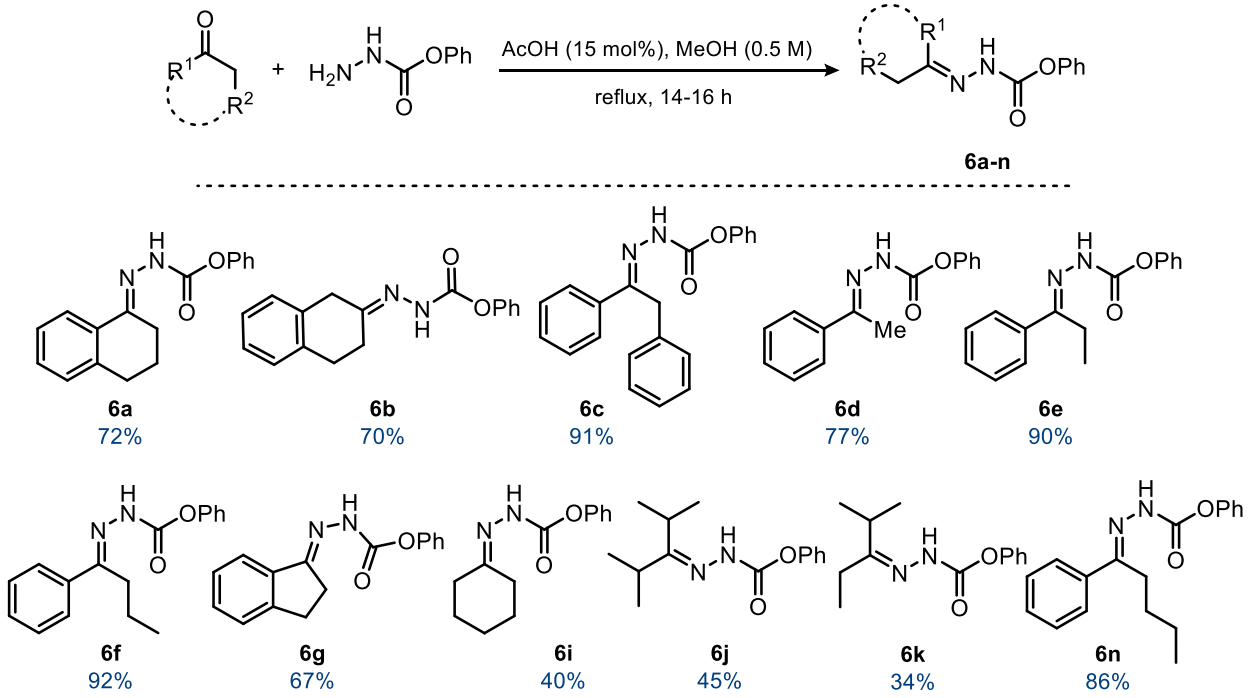

[a] Conditions: **Ketones** (10.0 – 20.0 mmol), phenylcarbazate (5.0 – 10.0 mmol), methanol (0.5 M), at reflux for 16 hours unless otherwise noted. Yields shown are isolated yields from 10.0 to 20.0 mmol reaction scale.

Several hydrazone carboxylate precursors (with α-hydrogens) were then submitted to the optimized reaction conditions and gave access to the cyclic pyrazolone products in moderate to good yields (Scheme 3.8). Addition products were observed as side reaction outcomes with some precursors like **6e** and **6f**, where R^2 is larger. Performing the reaction at lower temperatures (0 °C to rt) helped diminish the production of the addition side products for the precursors that suffered from this issue. Some products

were obtained in higher yields when the reaction was performed at lower temperatures such as **7d** (0 °C) and **7g** (rt) (Table 3.5). These results suggest that the control between the cyclization pathway and the addition pathway is quite sensitive to substrate structure and reaction conditions.

Scheme 3.8. Scope of pyrazolone formation.

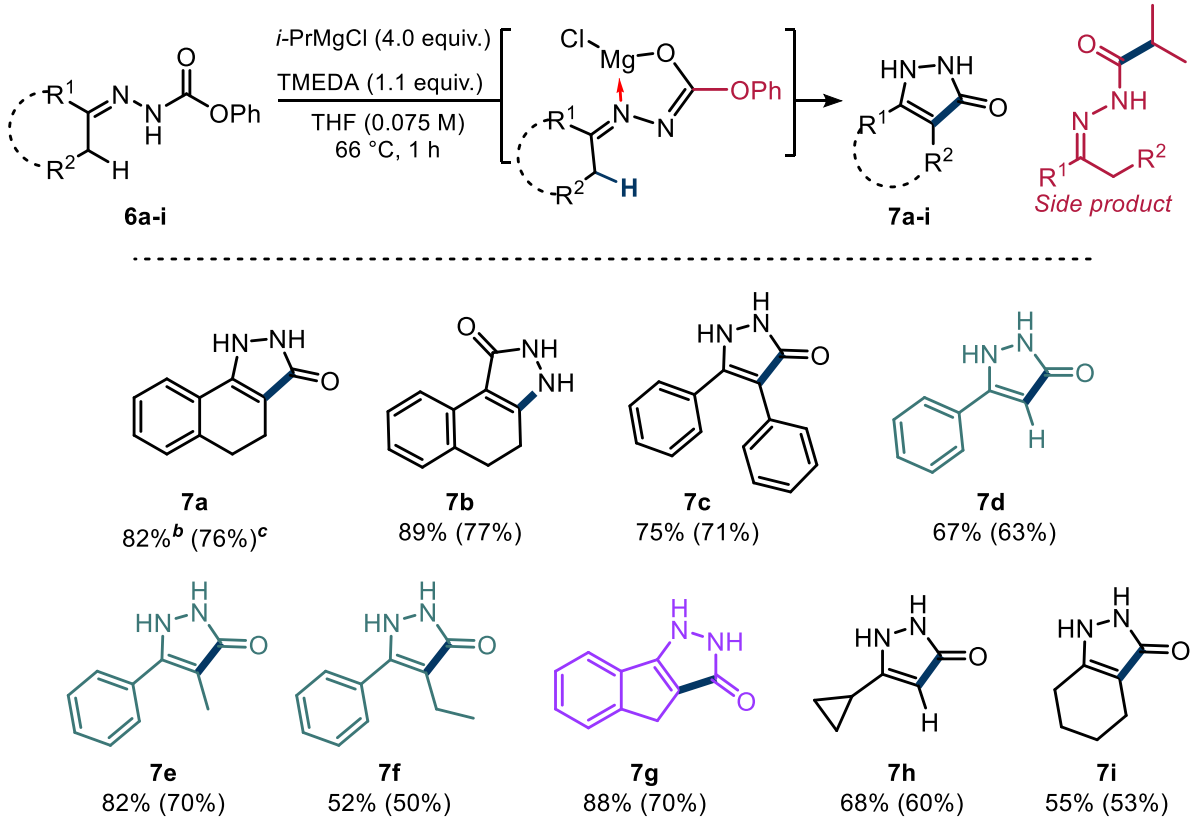

Higher yields of the products afforded at **0 °C** for **3 h**. Higher yield of the product afforded at **rt** for **2 h**.

[a] Conditions: **6a-i** (0.6 mmol), *i*-PrMgCl (2.4 mmol), THF (0.075 M), TMEDA (99 µL) at 66 °C in a sealed µW vial. [b] ^{1}H NMR yield determined by using 1,3,5-trimethoxybenzene as internal standard. [c] Yields in parenthesis indicate isolated yield from 0.6 mmol reaction scale.

Table 3.5. Lower temperature conditions allowed for better yields of some pyrazolone products.

Pyrazolone product	Pyrazolone product structure	Product yield (%) at 66 °C [a]	Lower temperature conditions	Product yield (%) at lower temperature conditions [a]
7d	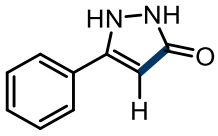	50	0 °C for 3 h	67
7e	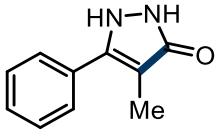	**54** with 17% addition product	0 °C for 3 h	82
7f	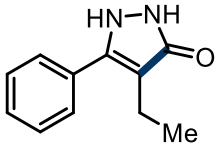	**45** with 25% addition product	0 °C for 3 h	52
7g	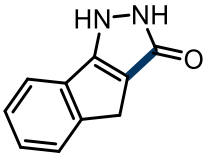	72	Rt for 2 h	88

[a] ^{1}H NMR yield determined by using 1,3,5-trimethoxybenzene as internal standard.

Some precursors have demonstrated poor or no cyclization reactivity when the optimized conditions were applied (Scheme 3.9). Compounds **6j** and **6k** lack one α hydrogen which upon abstraction, provides extra stability to the pyrazolone product via conjugation with the carbonyl group and the adjacent aromatic substituent (if any), making it thermodynamically favored (Scheme 3.9, a and b). The cyclized product **7j** was believed to be generated (by heating overnight) under the reaction conditions. Reaction progress was followed by TLC, and the consumption of the starting material was observed, as well as the formation of a new spot at the same R_f range at which other pyrazolones appear. However, it is hypothesized that the product decomposed rapidly after isolation attempts (Scheme 3.9, a) as the spot previously observed by TLC was no longer found. Compound **6k** was an unsuccessful candidate for this reaction and did not reveal the formation of either of the two possible pyrazolone products, presumably due to the difficulty of abstracting the more acidic proton (on the isopropyl group) under the reaction conditions due to steric hinderance (Scheme 3.9, b). While compound **6l** gave the cyclic product **7l** in 33% NMR yield, it demonstrated high water solubility which made the standard workup process not suitable for its isolation and purification (Scheme 3.9, c). Compound **6m** (the bromo version of the precursor **6d**) was submitted to the reaction condition in order to afford the corresponding cyclic product. Unfortunately, only traces of

the cyclic pyrazolone **7m** (which is the same as **7d**) was observed (<5%) as determined from the crude NMR analysis (Scheme 3.9, d).

Scheme 3.9. Unsuccessful cyclization precursors to access pyrazolones.

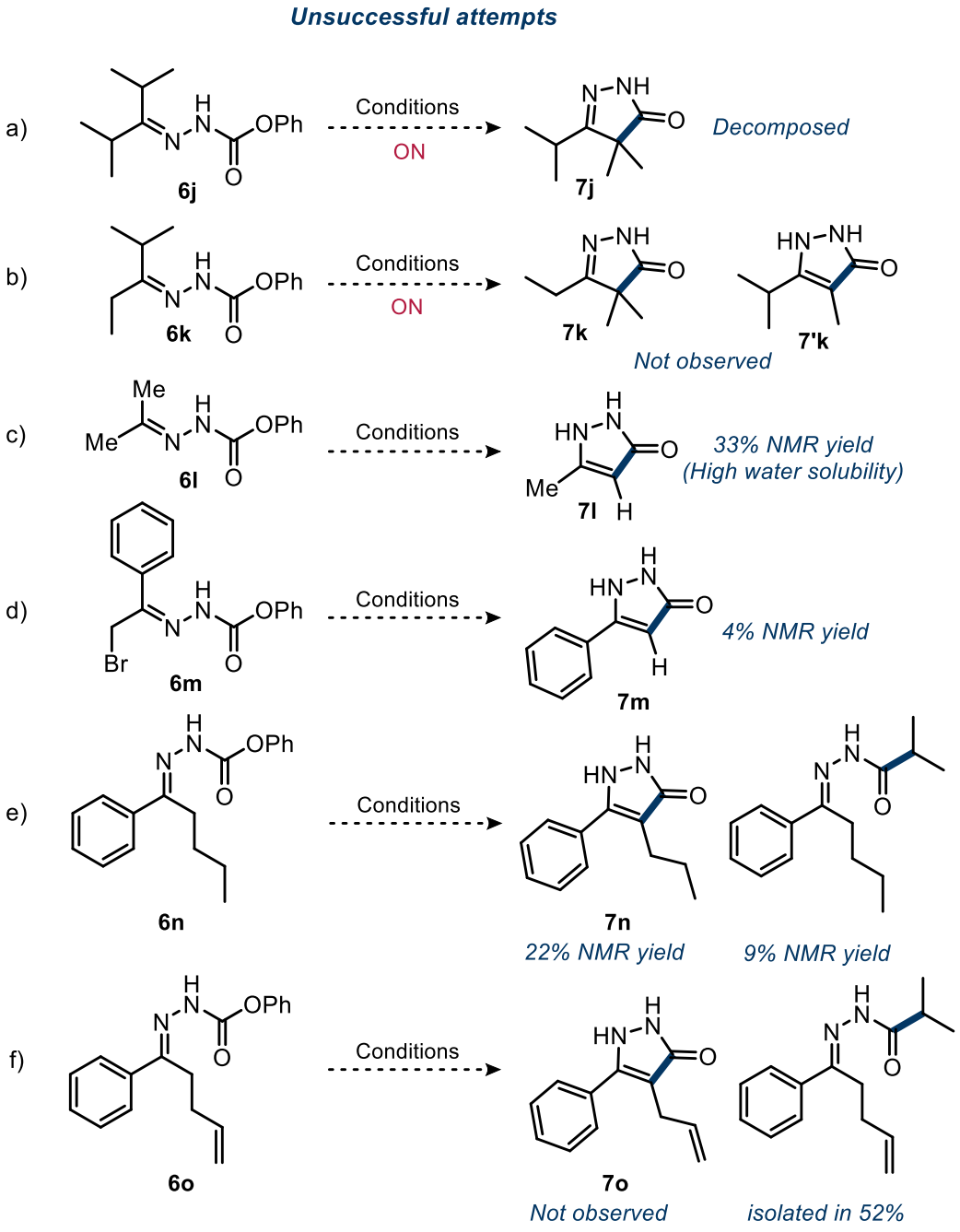

Conditions: *i*-PrMgCl (4.0 equiv.), TMEDA (1.1 equiv.), THF (0.075 M), 66 °C, 1 h

Hydrazone carboxylate precursors with longer linear alkyl groups **6n** and **6o** were also unsuccessful candidates for the cyclization reaction. Under the reaction conditions, **6n** with an *n*-butyl group formed the cyclized pyrazolone product in 22% NMR yield, while the addition product was observed in 9% NMR yield (Scheme 3.9, e). Interestingly, when the reaction was performed using **6o** precursor (differing in structure from **6n** only slightly), no cyclization product was observed, while the isopropyl addition product was isolated in 52% yield (Scheme 3.9, f). Comparing these results with the outcomes of the precursors with shorter linear R group such as **6e** and **6f**, which demonstrated higher yields especially with lower temperatures, it was suggested that the conformational flexibility and the degrees of freedom of these groups could be affecting the reactivity of the hydrazone carboxylate precursors towards cyclization (Table 3.6).

Table 3.6. Comparing the reactivity trends of hydrazone carboxylate precursors with different linear R groups.

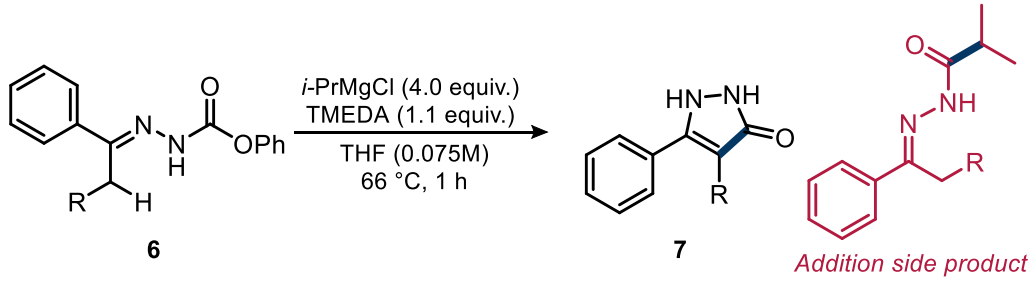

6 **7**

Hydrazone precursor	R	Cyclized pyrazolone product yield (%)[a]	Addition product yield (%)[a]
6d	H	50	0
6e	Me	54	17
6f	Et	52	25
6n	Propyl	22	9
6o	propenyl	0	(52)[b]

[a] ^{1}H NMR yield determined by using 1,3,5-trimethoxybenzene as internal standard. [b] Yields in parenthesis indicate isolated yield from 0.6 mmol reaction scale.

The reactivity trends of different precursors may suggest that cyclic precursors such as **6a**, **6b**, or **6g** with the restricted conformation on the R group attached to imine carbon due to ring closure, experienced lower steric hinderance and hence, could adopt a conformation that support deprotonation (by directed metalation) and subsequent cyclization (Scheme 3.10). This could be justified by the formation of *E*-enamine as the only possible intermediate upon deprotonation. This *E*-enamine may support facile cyclization to access pyrazolone products (Scheme 3.10). However, in the acyclic substrates, the R group, especially if larger, can adopt two conformations, leading to both metallo-enamine *E* and *Z* after

deprotonation. It is suggested that the conformer that could form the *Z*-enamine would be more stable than the other, due to the lack of the destabilizing interaction with the aromatic ring (Scheme 3.10). It is proposed that forming the *Z*-enamine would be more difficult, due to destabilization of the directed metalation transition state, resulting in a much more difficult deprotonation step. This could explain why these precursors do not work well. These findings highlight that cyclic substates could facilitate complex formation (if a directed deprotonation is indeed happening), and the deprotonation and cyclization steps. However, having linear R group with conformational flexibility could hinder the reactivity toward the formation of pyrazolone cyclic products and make the molecule conformationally unfavorable for the cyclization to take place.

Scheme 3.10. A proposed justification for the reactivity trends of hydrazone carboxylate precursors with cyclic versus linear R groups.

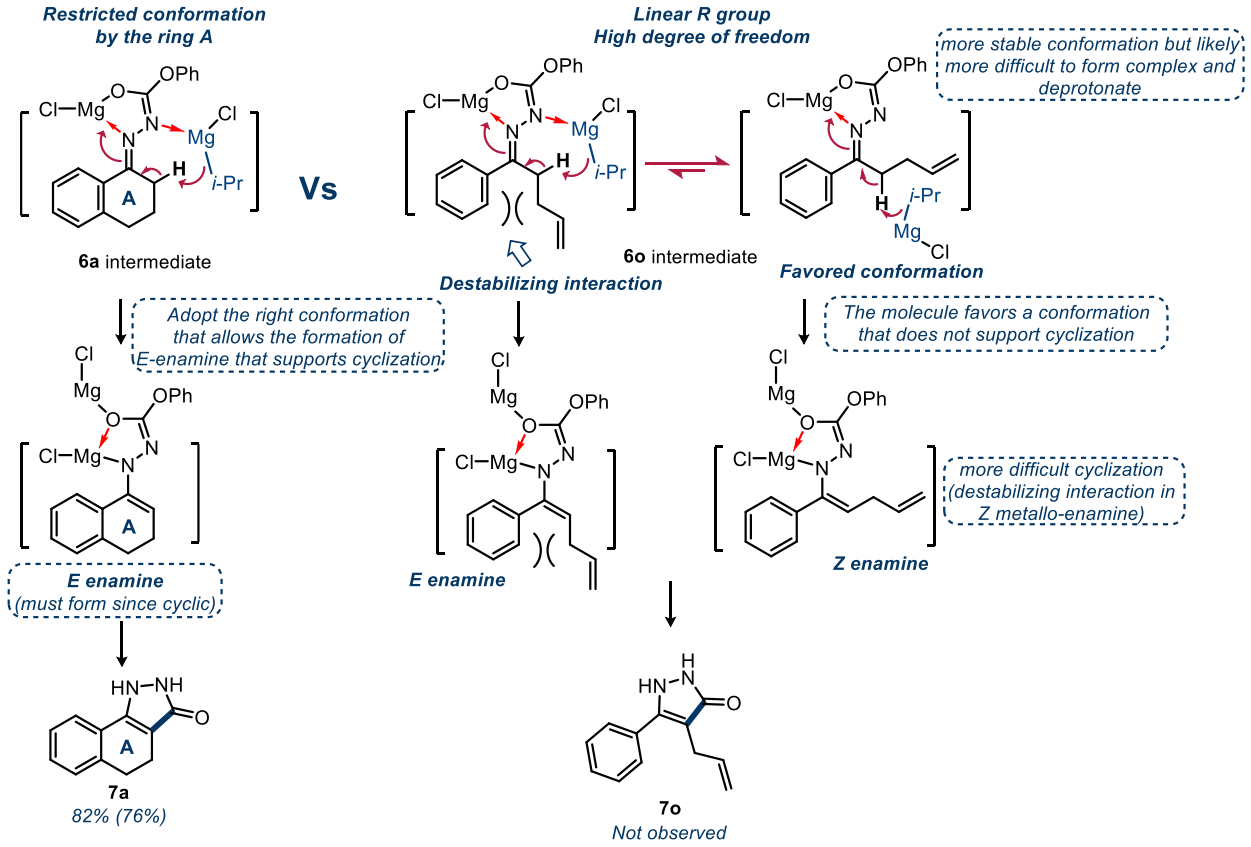

3.5 Conclusion

The study of nitrogen-substituted isocyanate precursors with Grignard reagents necessitated an examination of both sp^3 and sp^2 nitrogen atoms. The coordination of the sp^2 nitrogen to the magnesium, which could potentially favor the formation of the addition product, was of particular interest. In this chapter, unexpected reactivity was discovered with the masked sp^2 *N*-isocyanate precursors bearing α-hydrogens. This new reactivity was the cyclization to form five-membered pyrazolone derivatives. These unexpected outcomes not only highlighted the importance of fine-tuning the equilibrium between the blocked and free heteroatom-substituted isocyanates by manipulating the stability of the five-membered complex, and the need to control the concentration of the free reactive form of heteroatom isocyanate to prevent oligomerization and allow the desired reactivity to occur (the two concepts developed in Chapter 2), but these findings also underscored that the five-membered chelate facilitated unlocking of new reactivity which captured the attention of the group for a long period of time. This was achieved by allowing the coordination of a 2^{nd} equivalent of Grignard to the nitrogen atom, possibly facilitating the deprotonation of the α-proton via a six-membered transition state (i.e., a directed metalation event). This allows a direct synthesis of pyrazolones could be accessed from hydrazone precursors. Other findings observed during optimizing and scoping this reaction, included: the possible deblocking at lower temperatures in this system, the formation of the *i*-Pr addition competing side products with the sterically demanding precursors which could adopt a conformation that does not favor the deprotonation and cyclization, and that lithium intermediates can afford the desired cyclization. These findings constituted the basis for the development of second-generation conditions by Mr. Frédéric Vuillermet, benefitting from the Grignard addition approach, which suggested that the use of milder bases would be a strong asset to overcome limitations and to achieve broader functionality tolerance.

Chapter 4 Additional Cyclizations

4.1 Previous Cyclizations Using Masked *O*- and *N*-Isocyanates in Beauchemin Group

The Beauchemin Group has exploited masked heteroatom-substituted isocyanates in several heterocyclic cyclization reactions. *N*-isocyanates, with more than 20 publications, has gained the most attention. C-C bond formation was achieved by aminocarbonylation of alkenes via an inter- or intramolecular concerted [3+2]-cycloaddition mechanism, to achieve five-membered azomethine imines, pyrazolones, or pyrazolidinones (Figure 4.1, a and b).[84,86,90,187,188,199–201] Additionally, access of 5-aminopyridazinone provided C-C bond formation via the formation of enamine which acts as a carbon nucleophile (Figure 4.1, c).[202] Furthermore, Friedel-Crafts cyclization was employed with blocked amino-isocyanates bearing *N*-aromatic substituents to afford C-C bond formation to access indazolones (Figure 4.1, d).[89] Alternatively, other cyclization reactions included substitution reactions with various protic nucleophiles featured in cascade reactions to access 1,2,4-triazinones (Figure 4.1, e),[202–204] imidazolones,[205] thiazolidines (Figure 4.1, f),[205] *aza*-diketopiperazines (Figure 4.1, g),[92] aminobenzimidazolones (Figure 4.1, h),[206] aminohydantoins (Figure 4.1, i),[91] and oxadiazinones (Figure 4.1, j).[101]

Figure 4.1. Previous cyclizations using blocked N-isocyanates in Beauchemin group.

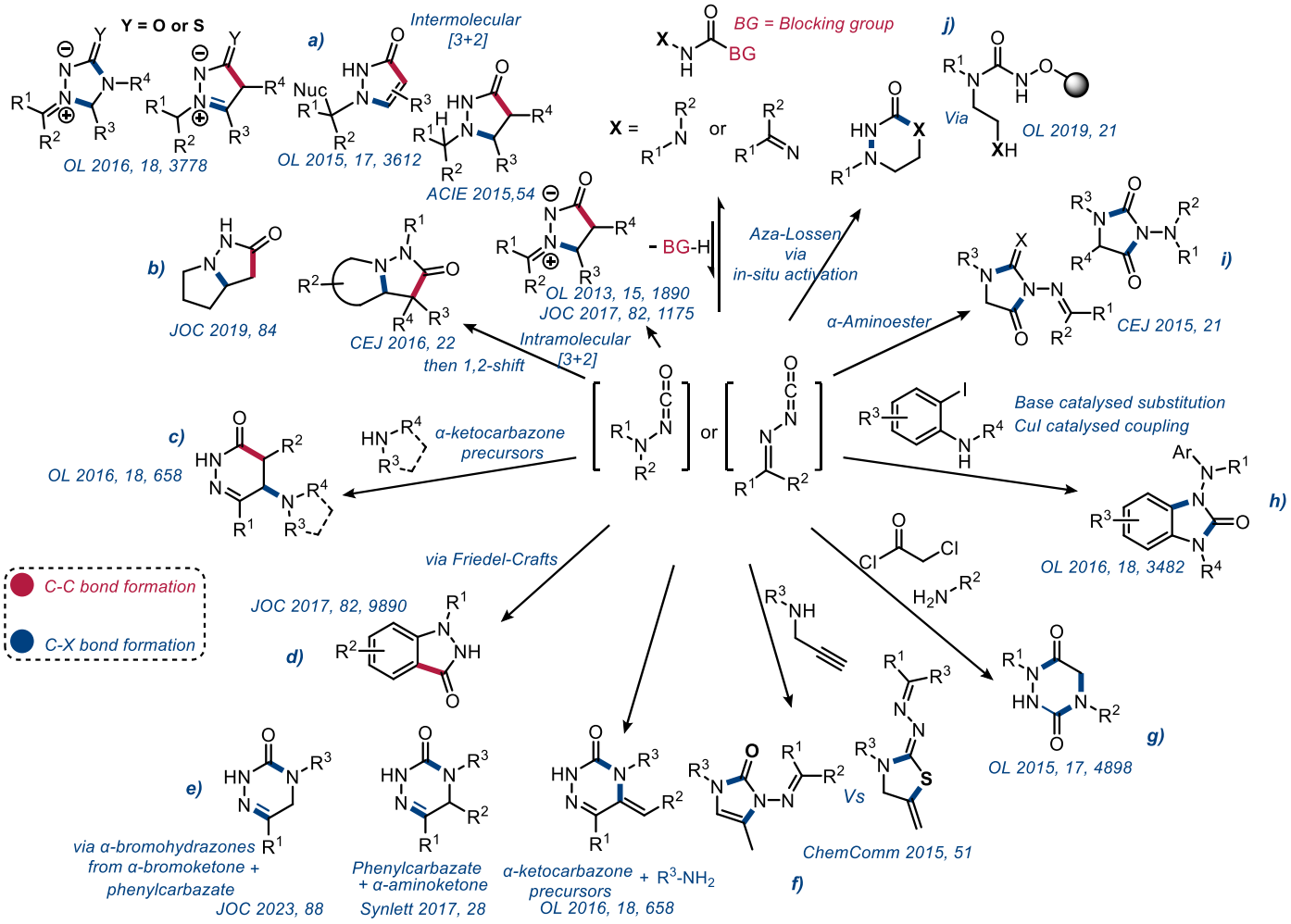

Masked *O*-isocyanates were employed in cyclization reactions exploiting the blocking group strategy that allowed controlled reactivity. Several heterocyclic products were accessible via substitution and cascade reactions such as hydantoins, dihydrouracils (Figure 4.2, a),[111] imidazolidinones (Figure 4.2, b),[113] benzimidazolones, 3,4-dihydroquinazolin-2(1*H*)-ones (Figure 4.2, c),[112] and the zwitterionic cycloadduct *aza*-oxonium ylide via oxycarbonylation which allowed C-C bond formation (Figure 4.2, d).[114]

Figure 4.2. Previous cyclizations using blocked O-isocyanates in Beauchemin group.

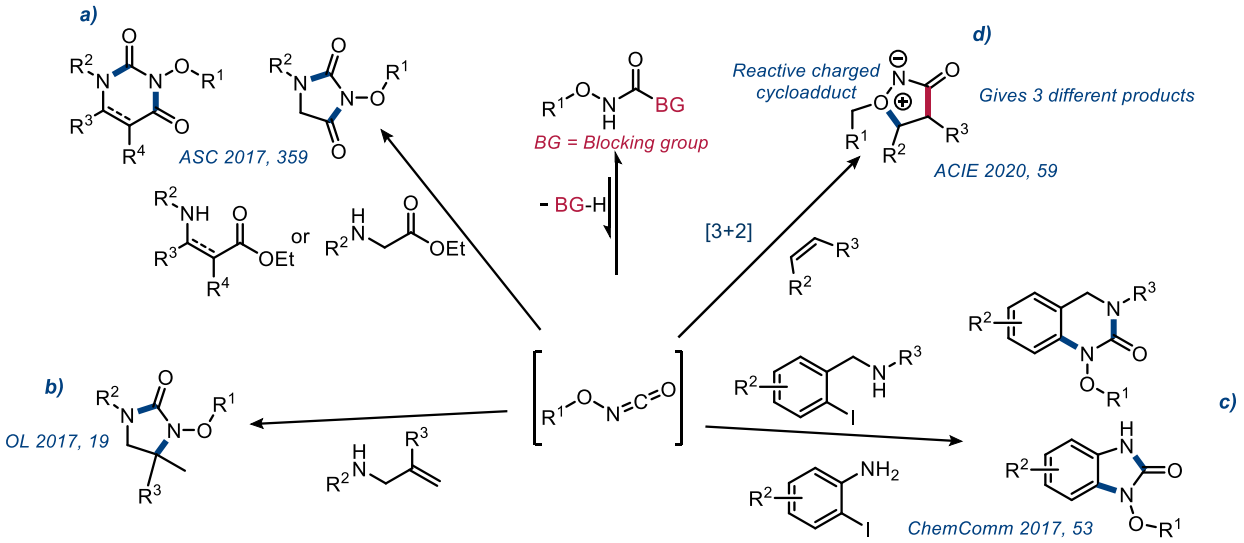

4.2 Efforts Towards Expansion of Application of New Reactivity

The research outlined in Chapter 2 demonstrated that Grignard reagents can effectively generate free *O*- and *N*- isocyanates *in situ* from blocked precursors, facilitating high-yielding addition reactions. The process requires heating to overcome the stability of the chelate formed upon deprotonation. Precise adjustment of the coordination environment of the isocyanate/metal complex controls the release of the reactive isocyanate, minimizing side reactions (rearrangement and/or oligomerization of the isocyanate) and enhancing the desired reactivity. A superstoichiometric amount of Grignard reagent is necessary to achieve high yields of the addition products. The Grignard reagent plays multiple roles, including deprotonation, coordination with the heteroatoms via its Lewis acidic metal center, and nucleophilic addition to the electrophilic center of the isocyanate, leading to C-C bond formation.

The formation of organometallic intermediates at low temperature, in the presence of functional groups, has long been a useful strategy in organometallic chemistry. For example, halogen-metal exchange and directed metalation reactions allow conversion of halides and substrates with acidic C-H bonds into a variety of organometallic intermediates.[165,207,208] While some functional groups are compatible with the reaction conditions, others must be protected to avoid undesired reactions. Importantly, to our knowledge, there are no reports of organometallic intermediates formed in the presence of an isocyanate, or a masked isocyanate intermediate. Given our group's longstanding interest in amphoteric molecules, including amphoteric isocyanates, we wondered if the controlled reactivity developed in the previous chapters could be used to form such rare intermediates, and use them in heterocyclic synthesis (Figure 4.3).

Figure 4.3. Hypothetical organometallic intermediate formed and cyclized in the presence of an isocyanate.

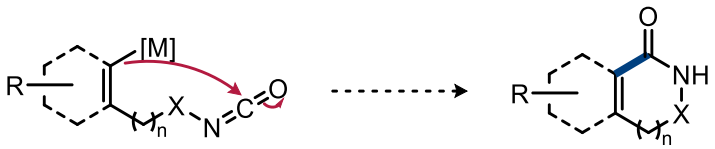

X = O or NR, n = 0 or 1

More specifically, the halogen-metal exchange ability of specific Grignard reagents has been optimized to provide access to various Grignard reagents. Knochel's Turbo Grignard (*i*-PrMgCl•LiCl) method has emerged as a broadly applicable procedure for this purpose, forming the desired organomagnesium intermediate in short time (10 minutes), at temperatures as low as -78 °C (Scheme 4.1).[132,165,209–212]

Scheme 4.1. Halogen-magnesium exchange using Turbo Grignard.

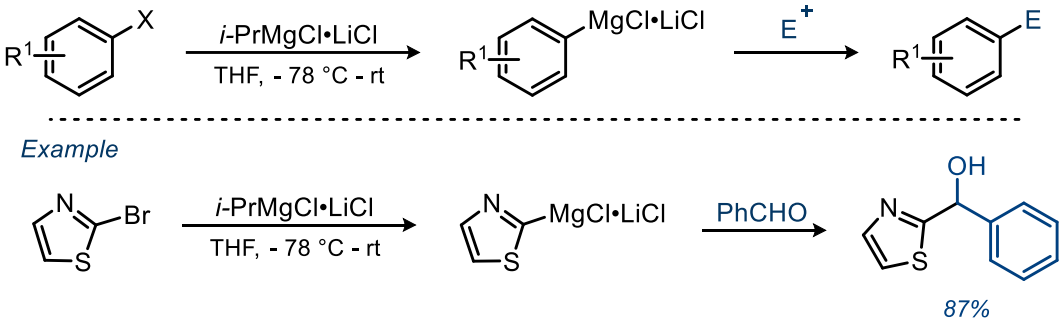

This seemed an ideal starting point to explore the strategy described above, resulting in intramolecular variants for the purpose of the synthesis of heterocyclic compounds (Scheme 4.2). The efforts towards validating this strategy were initially begun by designing the starting materials that could, in principle, cyclize to form five and six-membered rings. This exploratory work was anticipated to provide insight into the optimal reaction conditions to form these heterocyclic products, help to identify possible unproductive pathways, and demonstrate the potential of the strategy developed in Chapter 3, and in this Chapter, for future development.

Scheme 4.2. Intramolecular variants of masked heteroatom-substituted isocyanates as potential precursors for the purpose of the synthesis of heterocyclic compounds.

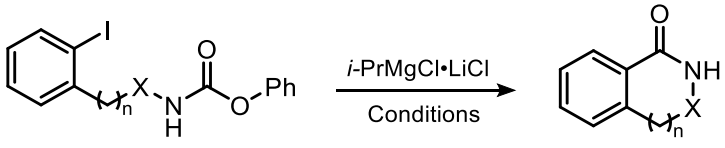

X = O or NR, n = 0 or 1

4.3 Mechanistic Blueprint

The optimal reaction pathway that would promote the formation of the cyclic products would proceed through the deprotonation of the N-H by the Turbo Grignard at low temperature. This deprotonation would lead to the formation of a five-membered chelate, which would be expected to survive at low temperature. This would be followed by the halogen-metal exchange at low temperature to form a transient arylmagnesium reagent on the aromatic ring. When the temperature rose, the deprotonated masked isocyanate would be expected to undergo cleavage of the blocking group to generate the free reactive isocyanate. Then, the nucleophilic Grignard formed via metal-halogen exchange would cyclize onto the isocyanate, thus providing the heterocycle using a C-C bond forming reaction (Scheme 4.3).

Scheme 4.3. A potential mechanism of cyclization products formation from intramolecular Grignard addition to masked heteroatom-substituted isocyanates.

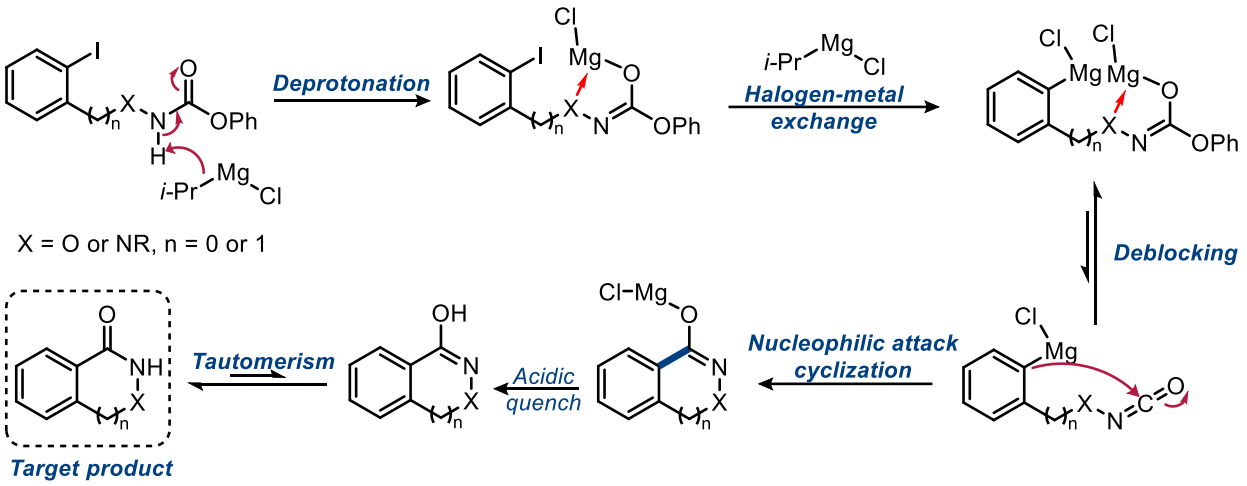

An unproductive pathway, however, could proceed through the halogen-metal exchange at low temperature, followed by the deprotonation at low temperature by this newly formed organomagnesium species, which would lead to the formation of C-H bond at the aromatic ring, effectively preventing the reaction (Scheme 4.4).

Scheme 4.4. A potential unproductive pathway preventing cyclization.

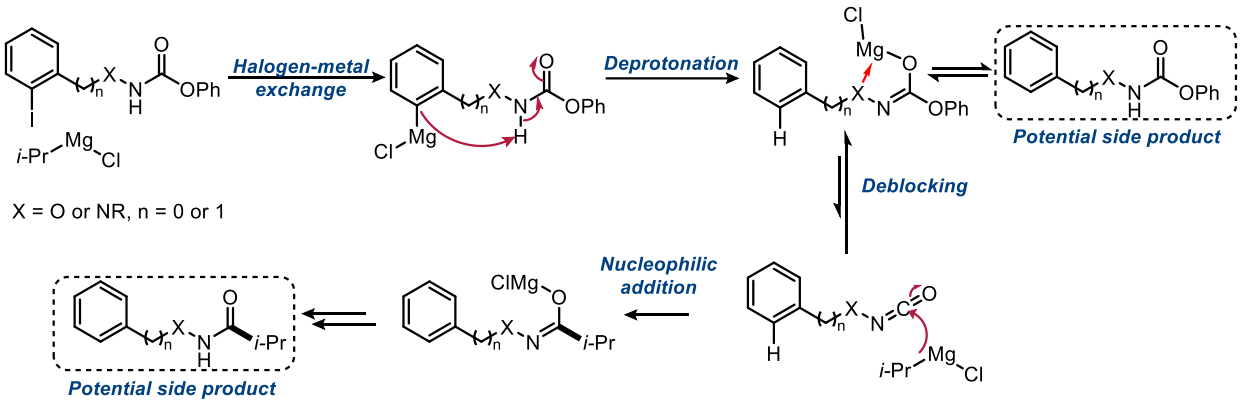

This concern about whether the protonation would take place before the halogen-metal exchange or the reverse appeared avoidable by modifying the approach, the reagents and/or reaction conditions. This may give an opportunity for deprotonation to take place prior to halogen-metal exchange. Furthermore, allowing the reaction to initially proceed at low temperature (-78 °C) for a period of time then gradually raising the temperature may provide an opportunity for better control over the reactivity. More options for condition modification could be fruitful if required, to give opportunity for developing the optimal conditions, such as the initial addition of a base to mediate deprotonation, and the ability to modify the blocking group.

4.4 Synthesis of Cyclization Precursors

The synthesis of suitable cyclization precursors was an important part of this approach. Four precursors were designed to investigate this reactivity. These two masked *O*-isocyanate precursors and two masked *N*-isocyanate precursors could conceivably give access to five- and six-membered ring products (Figure 4.4).

Figure 4.4. Design of cyclization precursors.

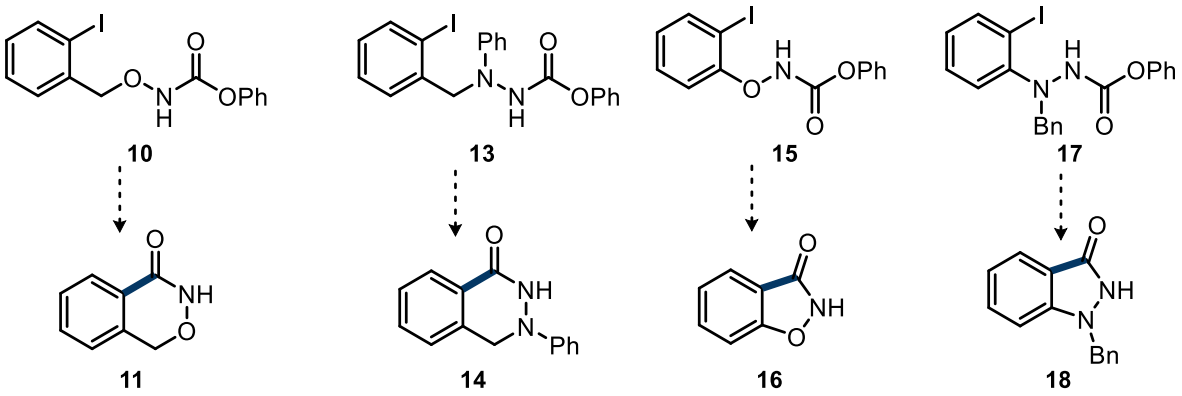

The synthetic pathway for the synthesis of substrate **10** was designed according to literature procedure.[112,213] *N*-Hydroxyphthalimide **A** was reacted overnight with 2-iodobenzyl bromide in the presence of triethylamine to give access to *O*-(2-iodobenzyl)-*N*-hydroxyphthalimide. This derivative was engaged in the second step by the reaction with hydrazine monohydrate to produce the primary hydroxylamine derivative, *O*-(2-iodobenzyl)hydroxylamine. This intermediate was used for the subsequent step without further purification. Reaction with phenylchloroformate in the presence of pyridine to afford the precursor **10** (*O*-(*o*-iodobenzyl) phenylcarbamate) in 80% yield (Scheme 4.5).

*Scheme 4.5. The synthetic pathway for the formation of precursor **10**.*

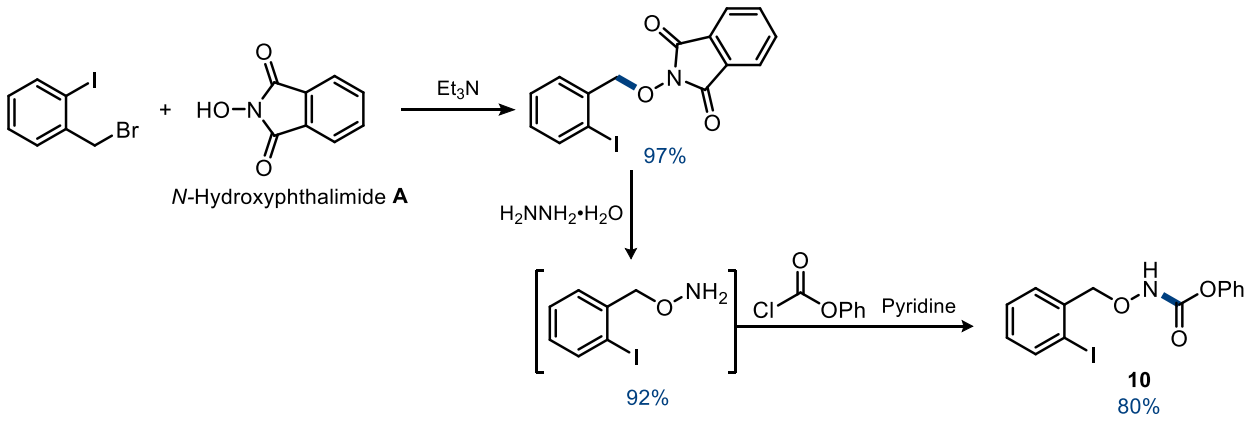

Compound **13** was successfully synthesized according to the literature procedure.[214,215] The synthesis included a two-step reaction pathway starting from 2-iodobenzyl bromide to yield *N*-(2-iodobenzyl)-*N*-phenylhydrazine **12** by the nucleophilic substitution reaction with phenylhydrazine in aqueous medium in 68%. After purification, this phenylhydrazine derivative underwent a nucleophilic substitution with

phenylchloroformate to access precursor **13** (phenyl 2-(*o*-iodobenzyl)-2-phenyl hydrazinecarboxylate) in 65% yield (Scheme 4.6).

*Scheme 4.6. The synthetic pathway for the formation of precursor **13**.*

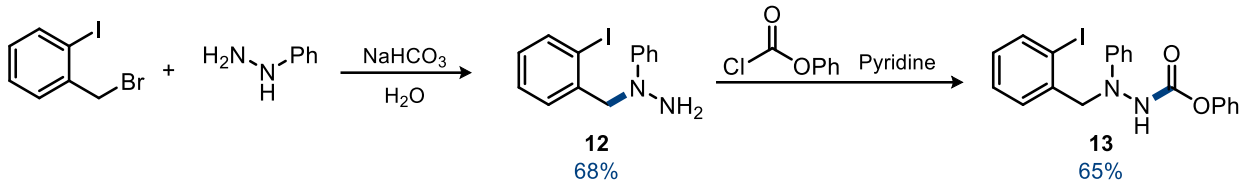

The synthesis of precursor **15** proceeded through a four-step synthetic pathway starting from the reaction of 1,2-diiodobenzene with Turbo Grignard and timethylborate to produce 2-iodophenylboronic acid. [216] Treatment of boronic acid **X** with *N*-hydroxyphthalimide gave access to the protected hydroxylamine **14** in 75% yield.[217] Subsequently, an overnight reaction with hydrazine hydrate yielded the corresponding primary hydroxylamine derivative, which was used without further purification in the last step for the formation of phenyl (*o*-iodophenoxy)carbamate **15**, using phenylchloroformate (Scheme 4.7).

*Scheme 4.7. The synthetic pathway for the formation of precursor **15**.*

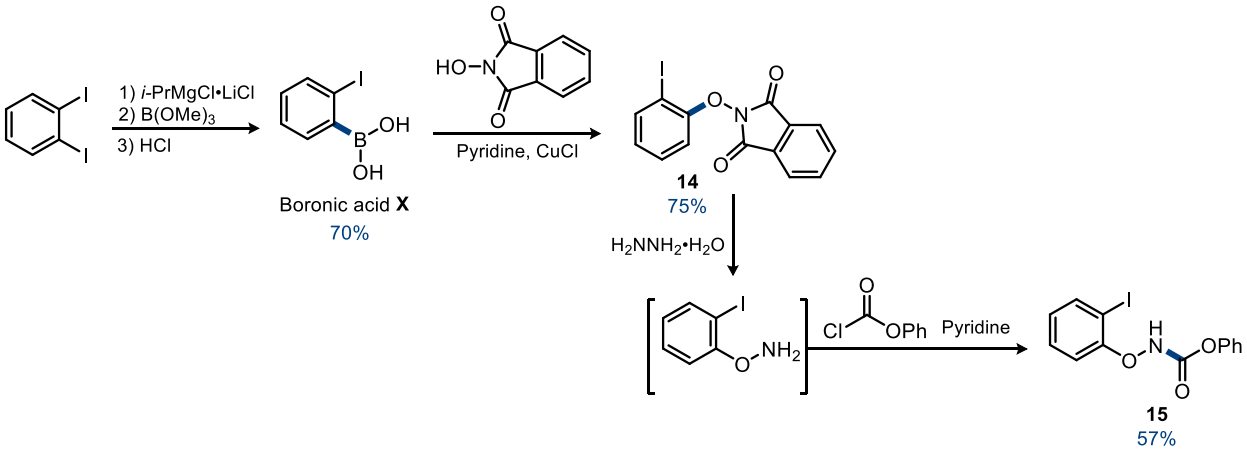

4.5 Successful Cyclization of *O*-Isocyanate Substrate 10

A preliminary designed procedure has been carried out on precursor **10,** starting with stirring **10** with *i*-PrMgCl•LiCl for 2 hours at -78 °C in a 0.075 M reaction in THF. The reaction progress was monitored by TLC. The persistence of the spot corresponding to the starting material after two hours at -78 °C suggested that a higher temperature might be necessary for the formation of the desired product. Therefore, the temperature was gradually raised to ambient temperature, then the reaction mixture was allowed to stir for 1 hour at 66 °C. An acidic quench was carried out after the TLC analysis indicated the reaction

completion, as gauged by consumption of the starting material **10**. Gratifyingly, the heterocyclic benzoxazinone product **11** was isolated in 65% yield as indicated by the NMR analysis (Scheme 4.8).

*Scheme 4.8. The formation of benzoxazinone **11** showing the proposed species exist in low versus high temperature.*

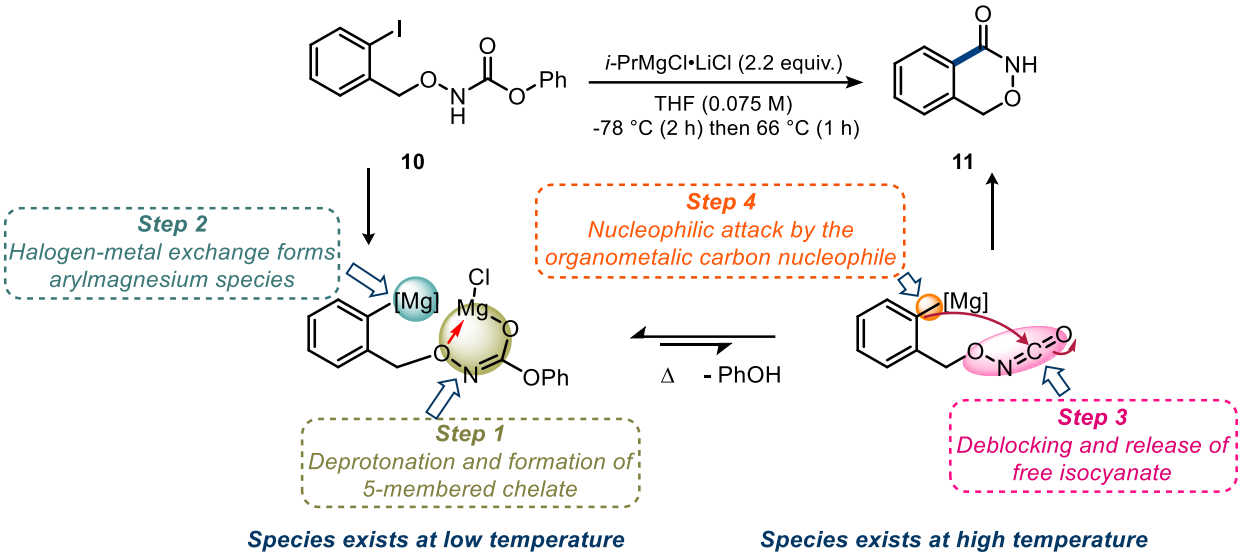

The observation of the cyclization supported that the deprotonation step preceded the halogen metal exchange. This allowed the formation of the five-membered chelate which demonstrated reasonable stability at low temperature (cyclization was possible at elevated temperatures). This resulted in the formation of organometallic intermediate formed in the presence of a masked *O*-isocyanate (in the form of five-membered magnesium chelate) at low temperature (Scheme 4.8). At elevated temperatures, a new transient species was formed by cleavage of the phenol blocking group, which is an organometallic intermediate formed in the presence of a free *O*-isocyanate. This species underwent an intramolecular cyclization via nucleophilic addition to give a six-membered heterocyclic compound through the formation of C-C bond (Scheme 4.8). This result implies that the process requires heating to overcome the stability of the chelate formed upon deprotonation. Furthermore, a slight excess of Turbo Grignard seemed sufficient to achieve the cyclization. These findings were consistent with the proposed mechanism based on the knowledge gained from studying masked *O*- and *N*- isocyanates in the previous Chapters 2 and 3. This successful cyclization supports our postulate that the formation of rare organometallic/heteroatom-isocyanate intermediates and employing controlled reactivity (developed in the previous chapters) is a valid strategy to access heterocyclic motifs.

Due to time constraints, it was not possible to evaluate the cyclization of the 2nd masked *O*-isocyanate substrate **15** that was anticipated to produce a fused 5,6-ring system; this will be addressed in future work.

4.6 Cyclization of *N*-Isocyanate Substrates

Due to time constraints, masked *N*-isocyanate substrates designed for intramolecular cyclization were not able to be investigated for their ability to cyclize. However, the promising result obtained from intramolecular cyclization of the corresponding *O*-isocyanate precursor suggests that this approach could be feasible with *N*-isocyanates as well. This will be discussed in the future work in the next section.

4.7 Conclusion and Future Work

This chapter has focused on the exploration of the formation of organometallic/heteroatom-isocyanate intermediates, and their ability to undergo intramolecular cyclization reactions to form heterocyclic compounds by C-C bond formation. To evaluate this strategy, model systems were designed that contained both masked heteroatom isocyanates and an aryl halide capable of undergoing metal-halogen exchange. It was hypothesized that the formation of the relatively stable five-membered chelate made this approach feasible, allowing the other abilities of the Grignard reagent namely, the halogen-metal exchange, to be exploited. Given the promising result obtained by the *O*-isocyanate precursor, it was suggested that optimal reaction conditions are possible for achieving this goal.

Future work includes the formation of the *N*-isocyanate precursor **17** anticipated to form five-membered indazolone derivative (upon successful cyclization). Its proposed synthetic strategy based on literature reports[214,215] begins with 2-iodoaniline, which would undergo diazotization and reduction to form the corresponding hydrazine hydrochloride salt **Y**, which would then react with benzyl bromide under inorganic alkaline medium to afford benzyl group addition to the internal (secondary) nitrogen atom of the hydrazine. A subsequent reaction with phenylchloroformate would afford the target substrate **17** (Scheme 4.9).

*Scheme 4.9. The proposed synthetic pathway for the formation of precursor **17**.*

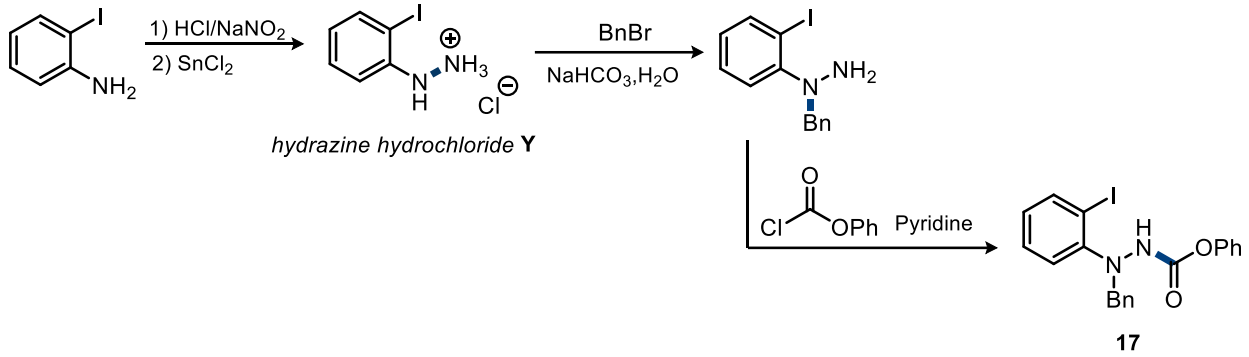

The cyclization approach for the other model substrates should then be evaluated to determine if desired products are formed in these instances as well. Exploring this cyclization approach fully on masked heteroatom isocyanate precursors is an important aspect of the future work to provide insight into the optimal reaction conditions to form these heterocyclic products and demonstrate the potential of the strategy developed throughout the study of the masked heteroatom-substituted isocyanates.

Chapter 5 Conclusion and Outlook

5.1 Conclusions

In this thesis, the reactivity of heteroatom-substituted isocyanates has been studied by stoichiometric addition of Grignard reagents to masked isocyanate precursors. A blocking group strategy was employed effectively with these rare heteroatomic isocyanates which allowed for the development of suitable procedures for controlled addition of Grignard nucleophiles to masked *O*- and *N*- isocyanates and to overcome the limitations that result from their amphoteric nature. Indeed, it was hypothesized that amphoteric free *O*- and *N*- isocyanates could be formed *in situ* from their masked precursors and engage in high yielding C-C bond forming reactions with Grignard reagents via controlled release of the reactive intermediate. Overall, the results obtained support that this controlled release was achieved through a relatively stable five-membered intermediate, a chelate formed upon deprotonation by the basic Grignard reagent. Interestingly, this type of coordination results in much more stable intermediates, which was shown to be a fundamental difference between heteroatom isocyanates and their *C*-analogues. Importantly, this allowed the synthesis of a variety of motifs possessing the NNCO and ONCO motifs, first by intermolecular reactions (Chapter 2), then by intramolecular reactions (Chapters 3 and 4).

In Chapter 2, this strategy enabled the synthesis of various hydroxamate derivatives from masked *O*-isocyanate precursors (21 examples) and hydrazide derivatives from masked *N*-isocyanate precursors (7 examples) (Scheme 5.1). Diorganomagnesium reagents were effectively employed to modify the structure of the five-membered chelate to reduce the Lewis acidity of the metal to a degree that favors optimal deblocking, hence, promoting the desired reactivity. This resulted in an optimal five-membered chelate, with the desired balance of stability and reactivity. Consequently, the competing side reactions (rearrangement and/or oligomerization of the isocyanate) were minimized, permitting the desired activity to predominate, enabling access to hydroxamate and hydrazide derivatives. Rearrangement side reactions caused by cleavage of the weak N-O or N-N bond were effectively suppressed by the use of diorganomagnesium reagents, formed *in situ* by Schlenk equilibrium with organomagnesium bromides, induced in the presence of dioxane. Importantly, the study of *N*-isocyanates allowed for the expansion of research on the heteroatom coordination with the metals by employing different types of nitrogen atoms with different geometric properties, Lewis basicity, and coordination abilities. This effect was represented in the higher yields obtained by the precursors with aromatic-substituted nitrogen compared to the ones with aliphatic substituted nitrogen, which required TMEDA addition to enhance the yield. The reactivity

trends of *N*-isocyanates and the beneficial influence of TMEDA as an additive supported the hypothesis of chelate formation and helped understand the significance of fine-tuning the coordination strength and the stability of the five-membered chelate on the reactivity.

Scheme 5.1. Summary of Chapter 2 Results.

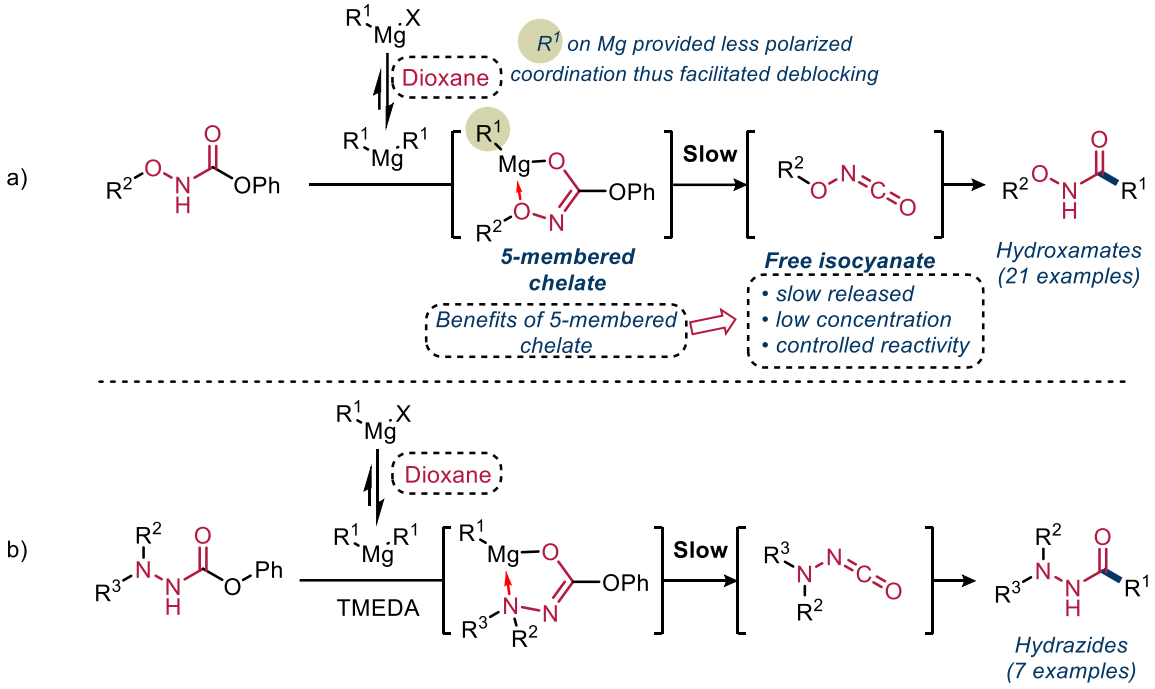

In Chapter 3, a new synthesis of pyrazolones has been optimized and studied, relying on hydrazones as *N*-isocyanate precursors, and using a Grignard reagent as base to allow an intramolecular reaction (Scheme 5.2). This unexpected reactivity was discovered from the masked sp^2 *N*-isocyanate precursors bearing α-hydrogens. Under optimized conditions, formation of pyrazolone derivatives by intramolecular cyclization was preferred over the intermolecular addition reactivity that was detailed in Chapter 2. It was hypothesized that this reactivity was feasible by effectively employing the five-membered chelate intermediate to facilitate deprotonation of the α-proton by increasing the acidity of the α-hydrogens, possibly by allowing the coordination of a 2nd equivalent of Grignard to the nitrogen atom, thus directing the deprotonation of the α-proton via a six-membered transition state (i.e., a directed metalation event). These hypotheses are supported by several experimental observations: that increased Lewis acidity of the Grignard reagent promotes the reaction, and that hydrazones derived from cyclic ketones cyclize more readily. Overall, this has enabled the access to a variety of pyrazolone products from simple starting materials, building on controlled reactivity of *N*-isocyanates.

Scheme 5.2. Summary of Chapter 3 Results.

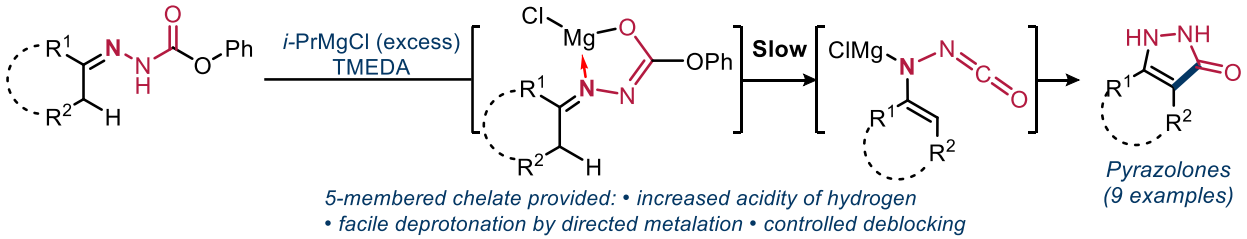

In Chapter 4, investigation was then focused on the formation of organometallic/heteroatom-isocyanate intermediates and their potential to participate in intramolecular cyclization reactions, leading to the synthesis of heterocyclic compounds via carbon-carbon bond formation (Scheme 5.3). This builds on the type of reactivity studied in Chapter 3 but was hypothesized to be potentially applicable to a variety of NNCO and ONCO heterocycles. Again, this process was facilitated through the use of a magnesium chelate formed upon deprotonation of the masked heteroatom isocyanate. The stability of the chelate at lower temperatures permitted a subsequent metal-halogen exchange reaction (yielding a Grignard reagent) to be performed within the same molecule. Upon heating, the isocyanate could be formed *in situ*, allowing cyclization. While only exploratory trials were performed, gratifyingly a sequence using a halogen-metal exchange reaction was unveiled, allowing the synthesis of a ONCO-containing heterocycle, a benzoxazinone. This result validates this strategy, suggesting that the findings in Chapter 2 can allow the generalization of this concept, and the development of intramolecular reactions forming ONCO and NNCO heterocycles. Conceptually, this is a new class of amphoteric molecule, the development of which was dependent entirely on the understanding of the stabilized chelate that can be formed from masked *O*- and *N*-isocyanates.

Scheme 5.3. Summary of Chapter 4 Results.

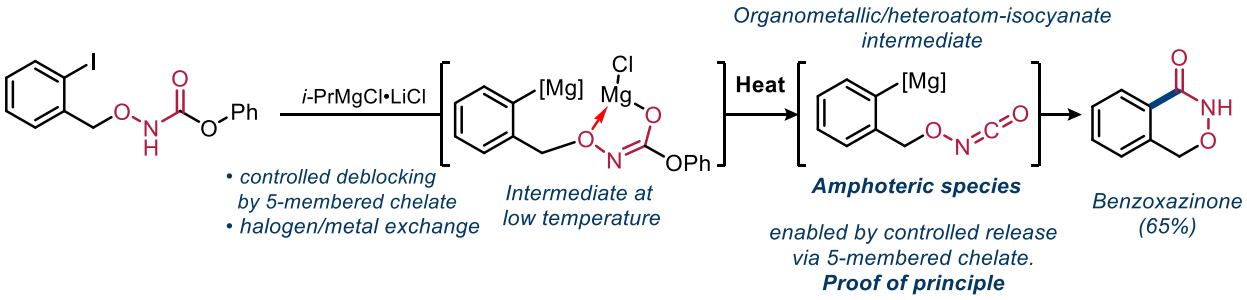

Overall, the findings in this thesis have resulted in broadly applicable procedures for the synthesis of ONCO and NNCO containing molecules, using both inter- and intramolecular C-C bond forming events.

As illustrated in Chapter 1, such reactions with masked isocyanates were rare prior to this work; the use of masked *O*- and *N*-isocyanates in C-C bond forming reactions were almost non-existent. This work has

found that the formation of stabilized chelate enables the use of masked *O*- and (sp^3) *N*-isocyanates in powerful C-C bond formation reactions. Further, this same stabilized chelate enables the formation of pyrazolones, an important class of heterocycles, by facilitating a more facile deprotonation of α-hydrogens on intermediates derived from masked sp^2 *N*-isocyanates. This research culminated in the successful proof of principle that the stability of the chelate can be exploited to perform a metal-halogen exchange within the same molecule. The resultant Grignard reagent can act as a nucleophile on the heteroatom isocyanate (released from chelate at higher temperatures) and cyclize to form heterocycles. This is a new class of amphoteric molecules that enables reactivity that was not previously possible.

5.2 Outlook

It will be important to continue the work started in Chapter 4 to further study this new class of amphoteric molecules (Scheme 5.4). The approach of intramolecular cyclization by applying halogen-metal exchange for the formation of organometallic/heteroatom-isocyanate intermediate has a great deal of potential to form interesting heterocycles in an efficient manner. Several substrates have already been prepared and work is on-going by Ms. Bhavana Uppalapati to complete the initial set of four model compounds that were described in Chapter 4. Further studies will evaluate the feasibility of this new amphoteric approach to a variety of NNCO and ONCO cyclic motifs.

Scheme 5.4. Future Work Exploring New Amphoteric Class of Molecules.

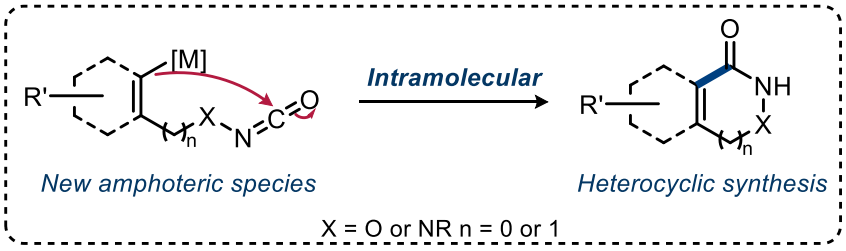

An additional opportunity is to extend the applicability of the intermediates formed in Chapters 2, 3 & 4, since nitrogen anions are present at the end of the reaction. Future work, some of which is already underway by Mr. Fred Vuillermet, will determine if these anions can be intercepted by other electrophiles (alkyl halides, for example), to form even more complex structures (Scheme 5.5). These studies will determine if this electrophilic interception can be made general.

Scheme 5.5. Future Work Exploring Electrophilic Interception of Anions.

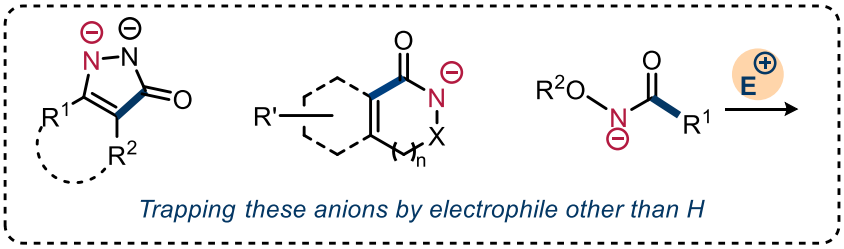

The masked *O*-isocyanate used as the starting material for Grignard addition in Chapter 2 can be considered as a bis-electrophilic synthon. Building on the results in this thesis, there is potential to access amides from the products shown in Chapter 2 if suitable conditions for the selective functionalization of the N-O bond to an N-R bond could be determined (Scheme 5.6).

Scheme 5.6. Future Work Exploring Potential Amide Synthesis from Chapter 2 Products.

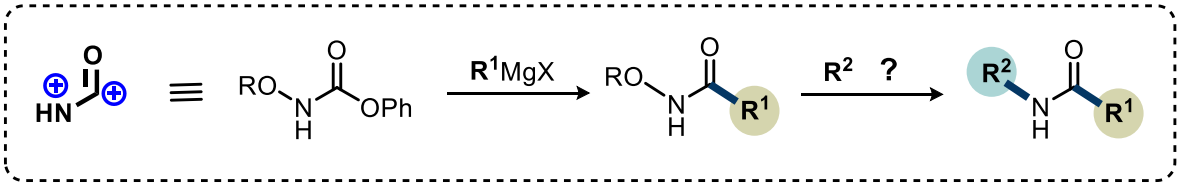

Chapter 6 Supporting Information

6.1 General Information

Purification of products was carried out by flash column chromatography using silica gel (40 – 63 µm), unless otherwise noted. Analytical thin layer chromatography (TLC) was performed on aluminum or glass plates, cut to size. Visualization was accomplished with UV light followed by staining with a potassium permanganate solution, cerium molybdate solution, ninhydrin, or anisaldehyde solution, and heating. Heating of reaction mixtures was accomplished using thermoprobe controlled oil bath. All air- and moisture-sensitive reactions were carried out in oven-dried 10 or 20 mL glass microwave vials with aluminum caps and septa as seals under an atmosphere of argon unless otherwise noted. ^{1}H NMR and ^{13}C NMR spectra were recorded on Bruker AVANCE 300 MHz, 400 MHz, 500 MHz, or 600 MHz spectrometers at ambient temperature, unless otherwise indicated. Spectral data is reported in ppm using residual protio-solvent as the reference (DMSO-d_6 at 2.50 ppm or $CDCl_3$ at 7.26 ppm for ^{1}H NMR and DMSO-d_6 at 39.52 ppm or $CDCl_3$ at 77.0 ppm for ^{13}C NMR). ^{1}H NMR data was reported as: multiplicity (ap = apparent, br = broad, s = singlet, d = doublet, t = triplet, q = quartet, quint = quintet, sext = sextuplet, sept = septuplet, m = multiplet), integration and coupling constant(s) in Hz. ^{13}C NMR is reported indicating information from distortionless enhancement by polarization transfer (DEPT) experiments. High-resolution mass spectroscopy (HRMS) was performed on a mass spectrometer with an electron beam of 70 eV (EI) or Micromass Q-TOF I - Time of flight Electrospray Ionisation mass spectrometer (ESI).

Unless otherwise noted, all materials were purchased from commercial sources and used without further purification. Tetrahydrofuran (THF) and dichloromethane (CH_2Cl_2) were passed through an activated alumina column embedded in a solvent purification system provided by LC Technology Solutions. 1,4-Dioxane was dried by reflux over calcium hydride then stored over 4 Å Molecular sieves.

6.2 Supporting Information for Stoichiometric Grignard Addition to Masked *O*-Isocyanates

6.2.1 General Procedure

6.2.1.1 General Procedure A: Synthesis of Hydroxamates

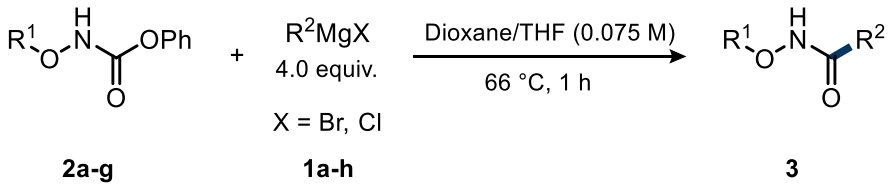

2a-g **1a-h** **3**

An oven dried and argon flushed 20 mL μW vial, equipped with a magnetic stir bar, was charged with *N*-alkoxycarbamates **2** (1.0 equiv) prepared following literature procedure,[215] and then was sealed. THF and 1,4-dioxane (0.075 M) were added sequentially via syringe. At 0 °C, the corresponding Grignard reagent (4.0 equiv), which was prepared as per literature procedure,[218] and titrated before use following the literature procedure,[219] was added by syringe, and the reaction mixture was stirred for 1 hour at 66 °C. The solution was then cooled in an ice bath and quenched using saturated $NH_4Cl_{(aq.)}$ and extracted three times with EtOAc. The combined organic phases were washed once with brine, dried over anhydrous Na_2SO_4, filtered, and concentrated under reduced pressure. Purification was achieved using silica gel flash column chromatography using EtOAc/Hexanes mixture.

6.2.2 Characterization Data

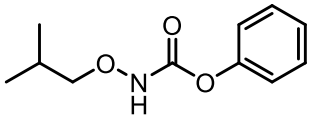

Phenyl *N*-(2-methylpropoxy)carbamate 2d

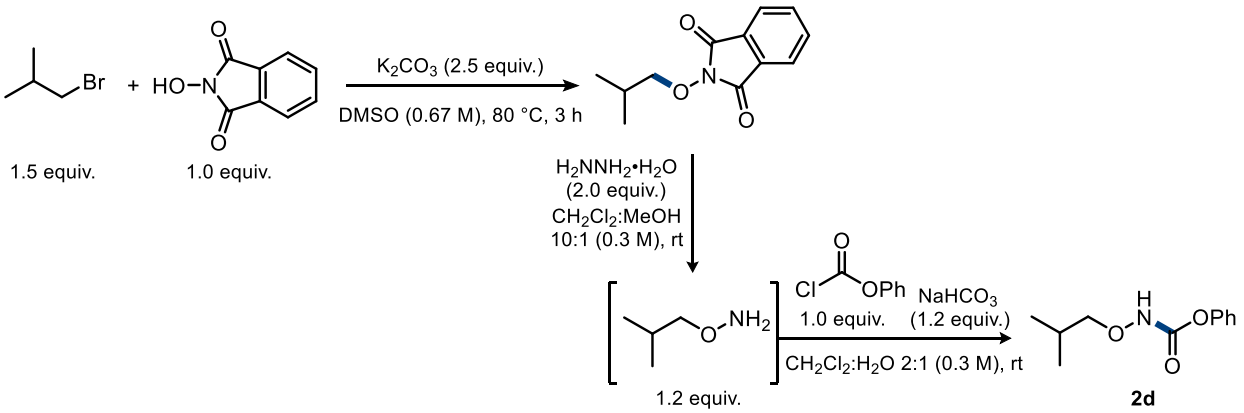

This substrate was synthesized by Dr Ryan Ivanovich. The title compound was synthesized according to a modified literature procedure.[112,213] To a 250 mL round bottom flask equipped with a stir bar *N*-hydroxyphthalimide (3.26 g, 20.0 mmol., 1.0 equiv) was dissolved in DMSO (30 mL, 0.67 M) at room temperature. Then K_2CO_3 (6.91 g, 50.0 mmol, 2.5 equiv) was added to the reaction flask, followed by isobutylbromide (5.52 g, 30.0 mmol, 1.5 equiv). The flask was sealed, and it was allowed to stir for 3 h at 80 °C. The reaction progress was monitored by TLC and stopped upon completion, as gauged by consumption of the *N*-hydroxyphthalimide. Most of the solvent was removed under reduced pressure, and the reaction mixture contents were transferred into a separatory funnel by rinsing the round bottom flask with CH_2Cl_2 and water. After the mixture contents separated, the organic layer was reserved, and the aqueous layer was extracted three times with CH_2Cl_2. The combined organic layers were then washed with

distilled water (x 3) and then brine (x 1). The organic layer was then dried over anhydrous Na_2SO_4 overnight. The final product was obtained by filtration and rotary evaporation and high vacuum to yield a white solid, with a yield of 63%. The **second step** of the reaction: To a 250 round bottom flask equipped with a stir bar was added *O*-1-(2-methyl)propyl-*N*-hydroxyphthalimide (2.78 g, 12.7 mmol, 1.0 equiv) followed by dilution in CH_2Cl_2:MeOH (55 mL : 5.5 mL, 10:1) (0.3 M) and cooled to 0 °C. To this vigorously stirred solution was added hydrazine hydrate (1.63 mL, 25.4 mmol, 2.0 equiv). The reaction was allowed to stir at room temperature, and the reaction progress was monitored by TLC and stopped upon completion, as gauged by consumption of the *O*-1-(2-methyl)propyl-*N*-hydroxyphthalimide. Upon completion, the solution was filtered over a fritted funnel and the filtrate was collected (the white precipitate was discarded). The filtrate was washed with sat. $NaHCO_3$ (x 2) and then brine (x 1). The organic phase was dried over anhydrous Na_2SO_4 and filtered over a fritted funnel. The filtrate was concentrated via rotary evaporation and used in the subsequent step without further purification. The **third step** of the reaction: To a 250 mL round bottom flask equipped with a stir bar was added the crude *O*-isobutylhydroxylamine from the previous step (1.13 g, 12.7 mmol, 1.2 equiv) followed by dilution with CH_2Cl_2:H_2O (30 mL : 15 mL, 2:1) (0.3 M) and cooled to 0 °C. To this vigorously stirred solution was added $NaHCO_3$ (1.06 g, 12.7 mmol, 1.2 equiv). After addition of $NaHCO_3$, the solution was allowed to stir at 0 °C for 0.5 h. Phenylchloroformate was then added dropwise (1.63 mL, 10.58 mmol, 1.0 equiv), and the reaction was allowed to stir at room temperature. The reaction progress was monitored by TLC and stopped upon completion, as gauged by consumption of the phenylchloroformate. Upon completion, the reaction was extracted using sat. $NaHCO_3$ (x 2) and then brine (x 1). The organic phase was dried over anhydrous Na_2SO_4 and filtered over a fritted funnel. The filtrate was concentrated via rotary evaporation and the crude was purified using silica-gel flash column chromatography using CH_2Cl_2 to afford the pure product as white solid (1.48 g, 67%).

TLC R_f : 0.40 in CH_2Cl_2.

^{1}H NMR (400 MHz, DMSO-d_6) δ 10.97 (s, 1H), 7.42 – 7.37 (m, 2H), 7.26 – 7.21 (m, 1H), 7.15 – 7.12 (m, 2H), 3.60 (d, *J* = 6.7 Hz, 2H), 1.90 (sept, *J* = 6.7 Hz, 1H), 0.91 (d, *J* = 6.7 Hz, 6H).

^{13}C NMR (101 MHz, DMSO-d_6) δ 154.6 (C), 150.4 (C), 129.4 (CH), 125.4 (CH), 121.7 (CH), 82.2 (CH_2), 26.7 (CH), 19.0 (CH_3).

HRMS (ESI): Exact mass calcd for $C_{11}H_{15}NO_3Na$ $[M+Na]^+$ 232.0950. Found: 232.0952.

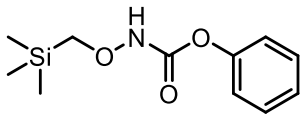

Phenyl *N*-(trimethylsilyl)methoxycarbamate 2f

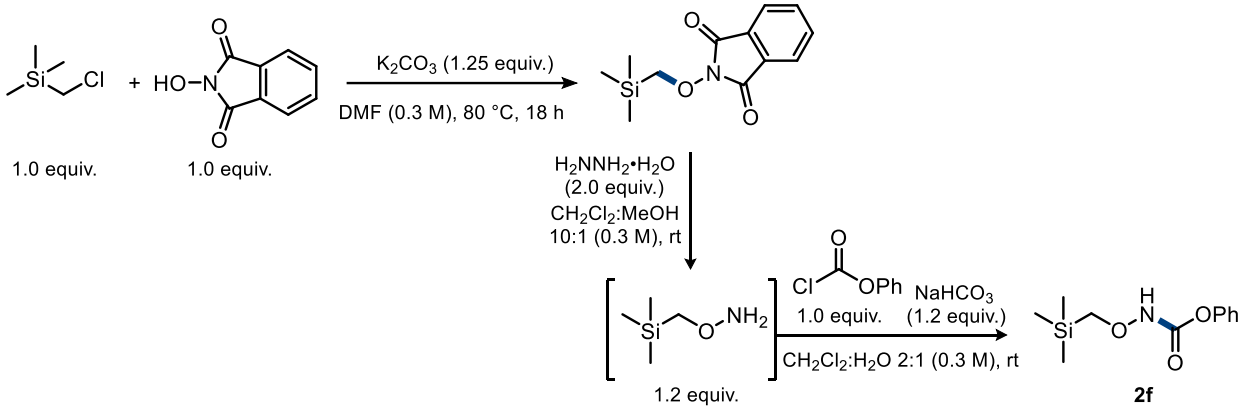

This substrate was synthesized by Dr Ryan Ivanovich. The title compound was synthesized according to a modified literature procedure[112,213] To a 250 mL round bottom flask equipped with a stir bar *N*-hydroxyphthalimide (3.26 g, 20.0 mmol., 1.0 equiv) was dissolved in DMF (66.7 mL, 0.3 M) at room temperature. Then K_2CO_3 (3.45 g, 25.0 mmol, 1.25 equiv) was added to the reaction flask, followed by chloromethyltrimethylsilane (2.45 g, 20.0 mmol, 1.0 equiv). The flask was sealed, and it was allowed to stir for overnight (18 h) at 80 °C. The reaction progress was monitored by TLC and stopped upon completion, as gauged by consumption of the *N*-hydroxyphthalimide. The solvent was removed under reduced pressure, the reaction mixture contents were transferred into a separatory funnel by rinsing of the round bottom flask with CH_2Cl_2 and water. After the mixture contents separated, the organic layer was reserved, and the aqueous layer was extracted three times with CH_2Cl_2. Then the combined organic layers were washed with distilled water (x 3) and then brine (x 1). The organic layer was then dried over anhydrous Na_2SO_4 overnight. The final product was obtained by filtration and rotary evaporation and high vacuum and used in the subsequent step without further purification (3.71 g, 73%). The **second step** of the reaction: To a 250 mL round bottom flask equipped with a stir bar was added *O*-(trimethylsilyl)methyl-*N*-hydroxyphthalimide from the previous step (3.71 g, 14.7 mmol, 1.0 equiv) followed by dilution in CH_2Cl_2:MeOH (50 mL : 5.0 mL, 10:1) (0.3 M) and cooled to 0 °C. To this vigorously stirred solution was added hydrazine hydrate (1.92 mL, 30.0 mmol, 2.0 equiv). The reaction was allowed to stir at room temperature, and the reaction progress was monitored by TLC and stopped upon completion, as gauged by consumption of the *O*-(trimethylsilyl)methyl-*N*-hydroxyphthalimide. Upon completion, the solution

was filtered over a fritted funnel and the filtrate was collected (the white precipitate was discarded). The filtrate was washed with sat. $NaHCO_3$ (x 2) and then brine (x 1). The organic phase was dried over anhydrous Na_2SO_4 and filtered over a fritted funnel. The filtrate was concentrated via rotary evaporation and used in the subsequent step without further purification (1.51 g, 86%). The **third step** of the reaction: To a 250 mL round bottom flask equipped with a stir bar was added the crude *O*-((trimethylsilyl)methyl)hydroxylamine from the previous step (1.51 g, 12.7 mmol, 1.2 equiv) followed by dilution with CH_2Cl_2:H_2O (30 mL : 15 mL, 2:1) (0.3 M) and cooled to 0 °C. To this vigorously stirred solution was added $NaHCO_3$ (1.06 g, 12.7 mmol, 1.2 equiv). After addition of $NaHCO_3$, the solution was allowed to stir at 0 °C for 0.5 h. Phenylchloroformate was then added dropwise (1.63 mL, 10.58 mmol, 1.0 equiv). The reaction progress was monitored by TLC and stopped upon completion, as gauged by consumption of the phenylchloroformate. Upon completion, the reaction was extracted using sat. $NaHCO_3$ (x 2) and then brine (x 1). The organic phase was dried over anhydrous Na_2SO_4 and filtered over a fritted funnel. The filtrate was concentrated via rotary evaporation and isolated using silica-gel flash column chromatography using CH_2Cl_2 to afford the pure product as white solid (1.82 g, 72%).

TLC R_f : 0.63 in 25% EtOAc/Hexanes.

^{1}H NMR (400 MHz, DMSO-d_6) δ 11.03 (s, 1H), 7.45 – 7.38 (m, 2H), 7.25 – 7.21 (m, 1H), 7.14 – 7.11 (m, 2H), 3.71 (s, 2H), 0.06 (s, 9H).

^{13}C NMR (101 MHz, DMSO-d_6) δ 150.5 (C), 129.4 (C), 125.4 (CH), 121.6 (CH), 121.5 (CH), 71.1 (CH_2), -3.0 (CH_3).

HRMS (ESI): Exact mass calcd for $C_{11}H_{17}NO_3SiNa$ $[M+Na]^+$ 262.0875. Found: 262.0860.

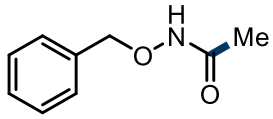

***N*-Benzyloxy acetamide 3aa**

The title compound was synthesized following General Procedure A using *O*-benzyl phenylcarbamate **2a** (0.122 g, 0.50 mmol. 1.0 equiv), methylmagnesium bromide **1a** (2.2 mL, 0.90 M in THF, 4.0 equiv), THF (3.0 mL) and 1,4-dioxane (1.5 mL) (0.075 M). The crude product was purified by flash column chromatography (50% EtOAc/Hexanes) to afford the pure compound as an off-white solid (0.056 g, 68%).

TLC R_f = 0.028 in 25% EtOAc/Hexanes.

^{1}H NMR (400 MHz, DMSO-*d*$_6$) δ 10.95 (s, 1H), 7.41 – 7.31 (m, 5H), 4.78 (s, 2H), 1.72 (s, 3H).

^{13}C NMR (101 MHz, DMSO-*d*$_6$) δ 166.5 (C), 136.1 (C), 128.7 (CH), 128.3 (CH), 128.2 (CH), 76.8 (CH_2), 19.6 (CH_3). Spectral data (using $CDCl_3$) was found consistent with literature reports.[220]

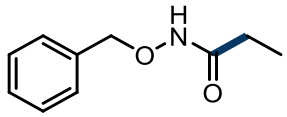

***N*-Benzyloxy propionamide 3ab**

The title compound was synthesized following General Procedure A using *O*-benzyl phenylcarbamate **2a** (0.146 g, 0.60 mmol, 1.0 equiv), ethylmagnesium bromide **1b** (2.5 mL, 0.95 M in THF, 4.0 equiv), THF (4.0 mL) and 1,4-dioxane (1.5 mL) (0.075 M). The crude product was purified by flash column chromatography (40% EtOAc/Hexanes) to afford the pure compound as an off-white solid (0.086 g, 80%).

TLC R_f = 0.10 in 25% EtOAc/Hexanes.

^{1}H NMR (400 MHz, DMSO-*d*$_6$) δ 10.92 (s, 1H), 7.39 – 7.34 (m, 5H), 4.77 (s, 2H), 1.96 (q, *J* = 7.6 Hz, 2H), 0.99 (t, *J* = 7.6 Hz, 3H).

^{13}C NMR (101 MHz, DMSO-*d*$_6$) δ 170.3 (C), 136.1 (C), 128.8 (CH), 128.3 (CH), 128.2 (CH), 76.7 (CH_2), 25.6 (CH_2), 9.7 (CH_3). Spectral data (using $CDCl_3$) was found consistent with literature reports.[221]

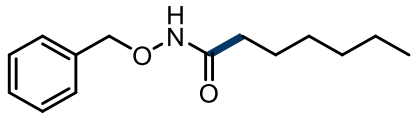

***N*-Benzyloxy heptanamide 3ac**

The title compound was synthesized following General Procedure A using *O*-benzyl phenylcarbamate **2a** (0.146 g, 0.60 mmol, 1.0 equiv), *n*-hexylmagnesium bromide **1c** (2.7 mL, 0.90 M in THF, 4.0 equiv), THF (3.8 mL) and 1,4-dioxane (1.5 mL) (0.075 M). The crude product was purified by flash column chromatography (25% EtOAc/Hexanes) to afford the pure compound as an off-white solid (0.106 g, 75%).

TLC R_f = 0.20 in 25% EtOAc/Hexanes.

^{1}H NMR (400 MHz, DMSO-*d*$_6$) δ 10.93 (s, 1H), 7.39 – 7.32 (m, 5H), 4.77 (s, 2H), 1.93 (t, *J* = 7.3 Hz, 2H), 1.47 (m, 2H), 1.28 – 1.21 (m, 6H), 0.85 (t, *J* = 7.0 Hz, 3H).

^{13}C NMR (101 MHz, DMSO-*d*$_6$) δ 169.4 (C), 136.1 (C), 128.7 (CH), 128.3 (CH), 128.2 (CH), 76.7 (CH_2), 32.2 (CH_2), 30.9 (CH_2), 28.1 (CH_2), 24.9 (CH_2), 22.0 (CH_2), 13.9 (CH_3) ppm. Spectral data (using $CDCl_3$) was found consistent with literature reports.[222]

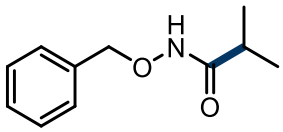

***N*-Benzyloxy isobutyramide 3ad**

The title compound was synthesized following General Procedure A using *O*-benzyl phenylcarbamate **2a** (0.146 g, 0.60 mmol, 1.0 equiv), isopropylmagnesium chloride **1d** (2.5 mL, 0.95 M in THF, 4.0 equiv), THF (4.0 mL) and 1,4-dioxane (1.5 mL) (0.075 M). The crude product was purified by flash column chromatography (30% EtOAc/Hexanes) to afford the pure compound as an off-white solid (0.091 g, 79%).

TLC R_f = 0.16 in 25% EtOAc/Hexanes.

^{1}H NMR (400 MHz, DMSO-*d*$_6$) δ 10.96 (s, 1H), 7.39 – 7.32 (m, 5H), 4.77 (s, 2H), 2.20 (sept, *J* = 6.9 Hz, 1H), 0.98 (d, *J* = 6.9 Hz, 6H).

^{13}C NMR (101 MHz, DMSO-*d*$_6$) δ 173.2 (C), 136.1 (C), 128.8 (CH), 128.3 (CH), 128.2 (CH), 76.6 (CH_2), 31.2 (CH), 19.2 (CH_3) ppm. Spectral data (using $CDCl_3$) was found consistent with literature reports.[221]

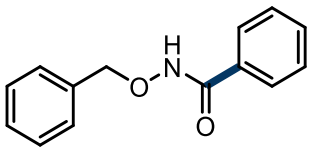

***N*-Benzyloxy benzamide 3ae**

The title compound was synthesized according to General Procedure A using *O*-benzyl phenylcarbamate **2a** (0.146 g, 0.60 mmol, 1.0 equiv), phenylmagnesium bromide **1e** (2.7 mL, 0.90 M in THF, 4.0 equiv), THF (3.8 mL) and 1,4-dioxane (1.5 mL) (0.075 M). The crude product was purified by flash column chromatography (25% EtOAc/Hexanes) to afford the pure compound as an off-white solid (0.112 g, 82%).

TLC R_f = 0.26 in 25% EtOAc/Hexanes.

^{1}H NMR (400 MHz, DMSO-*d*$_6$) δ 11.78 (s, 1H), 7.76 – 7.73 (m, 2H), 7.57 – 7.34 (m, 8H), 4.93 (s, 2H).

^{13}C NMR (101 MHz, DMSO-*d*$_6$) δ 169.8 (C), 136.0 (C), 132.3 (C), 131.6 (CH), 128.9 (CH), 128.5 (CH), 128.4 (CH), 128.3 (CH), 127.1 (CH), 76.9 (CH_2) ppm. Spectral data was consistent with literature reports.[223]

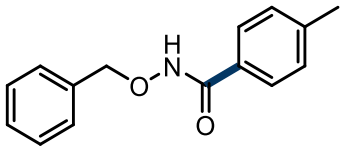

***N*-Benzyloxy 4-methylbenzamide 3af**

The title compound was synthesized following a modified General Procedure A using *O*-benzyl phenylcarbamate **2a** (0.146 g, 0.60 mmol, 1.0 equiv), tolylmagnesium bromide **1f** (2.5 mL, 0.95 M in THF, 4.0 equiv) and THF (0.5 mL, 0.20 M). The crude product was purified by flash column chromatography (20% EtOAc/Hexanes) to afford the pure compound as a white solid (0.117 g, 81%).

TLC R_f = 0.20 in 20% EtOAc/Hexanes.

^{1}H NMR (400 MHz, DMSO-*d*$_6$) δ 11.71 (s, 1H), 7.68 – 7.64 (m, 2H), 7.47 – 7.36 (m, 5H), 7.29 – 7.25 (m, 2H), 4.92 (s, 2H), 2.34 (s, 3H).

^{13}C NMR (101 MHz, DMSO-*d*$_6$) δ 164.4 (C), 141.6 (C), 136.0 (C), 129.5 (C), 129.0 (CH), 128.9 (CH), 128.3 (CH), 128.3 (CH), 127.1 (CH), 77.0 (CH_2), 21.0 (CH_3). Spectral data was consistent with literature reports.[224]

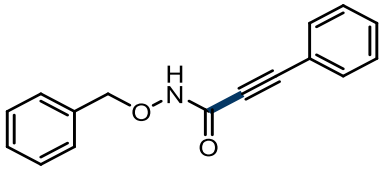

***N*-Benzyloxy-3-phenylpropiolamide 3ag**

The title compound was synthesized following a modified General Procedure A using *O*-benzyl phenylcarbamate **2a** (0.146 g, 0.60 mmol, 1.0 equiv), 2-phenylethynylmagnesium chloride lithium chloride **1g** (3.0 mL, 0.8 M in THF, 4.0 equiv), which was synthesized following the literature procedure,[209] and THF (5.0 mL, 0.075 M). The crude product was purified by flash column chromatography (25% EtOAc/Hexanes) to afford the pure compound as an off-white solid (0.104 g, 69%).

TLC R_f = 0.29 in 25% EtOAc/Hexanes.

^{1}H NMR (400 MHz, DMSO-*d*$_6$) δ 11.93 (br s, 1H), 7.59 – 7.36 (m, 10H), 4.87 (s, 2H).

^{13}C NMR (101 MHz, DMSO-*d*$_6$) δ 150.1 (C), 135.6 (C), 132.2 (CH), 130.6 (CH), 129.0 (CH), 128.8 (CH), 128.4 (CH), 128.4 (CH), 119.3 (C), 85.4 (C), 81.2 (C), 77.2 (CH_2). Spectral data (using $CDCl_3$) was consistent with literature reports.[225]

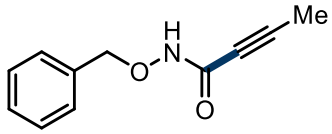

***N*-Benzyloxybut-2-ynamide 3ah**

The title compound was synthesized following General Procedure A using *O*-benzyl phenylcarbamate **2a** (0.146 g, 0.60 mmol, 1.0 equiv), 1-propynylmagnesium bromide solution **1h** (6.7 mL, 0.36 M in THF, 4.0 equiv) and 1,4-dioxane (1.4 mL, 0.075 M). The crude product was purified by flash column chromatography (30% EtOAc/Hexanes) to afford the pure compound as a white solid (0.079 g, 70%).

TLC R$_f$ = 0.15 in 25% EtOAc/Hexanes.

^{1}H NMR (400 MHz, DMSO-*d*$_6$) δ 11.61 (br s, 1H), 7.40 – 7.34 (m, 5H), 4.79 (s, 2H), 1.96 (s, 3H).

^{13}C NMR (101 MHz, DMSO-*d*$_6$) δ 150.4 (C), 135.6 (C), 129.4 (CH), 128.8 (CH), 128.3 (CH), 85.3 (C), 77.0 (CH_2), 72.7 (C), 3.1 (CH_3).

HRMS (ESI): Exact mass calcd for $C_{11}H_{11}NO_2Na$ $[M+Na]^+$ 212.0687. Found: 212.0695.

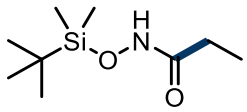

***N*-((*Tert*-butyldimethylsilyl)oxy)propionamide 3bb**

The title compound was synthesized following General Procedure A using phenyl (*tert*-butyldimethylsilyl)oxycarbamate **2b** (0.160 g, 0.60 mmol, 1.0 equiv), ethylmagnesium bromide **1b** (2.7 mL, 0.90 M in THF, 4.0 equiv), THF (3.6 mL) and 1,4-dioxane (1.7 mL) (0.075 M). The crude product was purified by flash column chromatography (25% EtOAc/Hexanes) to afford the pure compound as a white solid (0.083 g, 68%).

TLC R$_f$ = 0.25 in 25% EtOAc/Hexanes.

^{1}H NMR (300 MHz, DMSO-*d*$_6$) δ 10.52 (s, 1H), 1.96 (q, *J* = 7.6 Hz, 2H), 0.99 (t, *J* = 7.6 Hz, 3H), 0.90 (s, 9H), 0.09 (s, 6H).

^{13}C NMR (75 MHz, DMSO-*d*$_6$) δ 170.7 (C), 25.7 (CH_2), 25.6 (C), 17.9 (CH_3), 10.0 (CH_3), -5.6 (CH_3).

HRMS (ESI): Exact mass calcd for $C_9H_{21}SiNO_2Na$ $[M+Na]^+$ 226.1239. Not found.*

*Detailed analysis of the HRMS data obtained using TOF MS ES+ shows similar peaks being present for five molecules with different molecular weights, and three different types of structures. Thus, it is not possible to retrieve LRMS data, and further analysis will be carried out by Mr. Frederic Vuillermet.

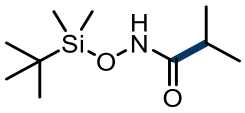

***N*-((*Tert*-butyldimethylsilyl)oxy) isobutyramide 3bd**

The title compound was synthesized following General Procedure A using phenyl (*tert*-butyldimethylsilyl)oxycarbamate **2b** (0.160 g, 0.60 mmol, 1.0 equiv), isopropylmagnesium chloride **1d** (1.3 mL, 1.80 M in THF, 4.0 equiv), THF (4.5 mL) and 1,4-dioxane (2.2 mL) (0.075 M). The crude product was purified by flash column chromatography (20% EtOAc/Hexanes) to afford the pure compound as a white solid (0.087 g, 67%).

TLC R_f = 0.32 in 20% EtOAc/Hexanes.

^{1}H NMR (300 MHz, DMSO-*d*$_6$) δ 10.57 (s, 1H), 2.25 (sept, *J* = 6.8 Hz, 1H), 0.98 (d, *J* = 6.8 Hz, 6H), 0.90 (s, 9H), 0.08 (s, 6H).

^{13}C NMR (75 MHz, DMSO-*d*$_6$) δ 173.7 (C), 31.2 (CH), 25.7 (CH_3), 19.4 (CH_3), 17.9 (C), -5.6 (CH_3).

HRMS (ESI): Exact mass calcd for $C_{10}H_{23}SiNO_2Na$ $[M+Na]^+$ 240.1396. Not found.*

*Detailed analysis of the HRMS data obtained using TOF MS ES+ shows similar peaks being present for five molecules with different molecular weights, and three different types of structures. Thus, it is not possible to retrieve LRMS data, and further analysis will be carried out by Mr. Frederic Vuillermet.

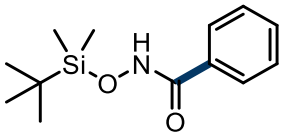

***N*-((*Tert*-butyldimethylsilyl)oxy)benzamide 3be**

The title compound was synthesized following General Procedure A using phenyl (*tert*-butyldimethylsilyl)oxycarbamate **2b** (0.160 g, 0.60 mmol, 1.0 equiv), phenyllmagnesium bromide **1e** (3.0

mL, 0.80 M in THF, 4.0 equiv), THF (3.4 mL) and 1,4-dioxane (1.6 mL) (0.075 M). The crude product was purified by flash column chromatography (10% EtOAc/Hexanes) to afford the pure compound as a white solid (0.113 g, 75%).

TLC R_f = 0.32 in 10% EtOAc/Hexanes.

^{1}H NMR (400 MHz, DMSO-*d*$_6$) δ 11.33 (s, 1H), 7.76 – 7.70 (m, 2H), 7.53 – 7.52 (m, 1H), 7.48 – 7.46 (m, 2H), 0.96 (s, 9H), 0.17 (s, 6H).

^{13}C NMR (101 MHz, DMSO-*d*$_6$) δ 165.4 (C), 131.4 (C), 128.4 (CH), 127.1 (CH), 115.2 (CH), 25.8 (CH_3), 18.0 (C), -5.4 (CH_3). Spectral data was consistent with literature reports.[226]

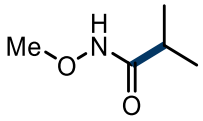

***N*-Methoxyisobutyramide 3cd**

The title compound was synthesized following General Procedure A using phenyl *N*-methoxycarbamate **2c** (0.100 g, 0.60 mmol, 1.0 equiv), isopropylmagnesium chloride **1d** (1.3 mL, 1.80 M in THF, 4.0 equiv), THF (4.5 mL) and 1,4-dioxane (2.2 mL) (0.075 M). The crude product was purified by flash column chromatography (50% EtOAc/Hexanes) to afford the pure compound as a white solid (0.032 g, 46%).

TLC R_f = 0.18 in 50% EtOAc/Hexanes.

^{1}H NMR (600 MHz, DMSO-*d*$_6$) δ 10.94 (s, 1H), 3.55 (s, 3H), 2.17 (sept, *J* = 6.9 Hz, 1H), 0.98 (d, *J* = 6.9 Hz, 6H).

^{13}C NMR (151 MHz, DMSO-*d*$_6$) δ 173.1 (C), 63.0 (CH_3), 31.2 (CH), 19.2 (CH_3). Spectral data (using $CDCl_3$) was consistent with literature reports.[227]

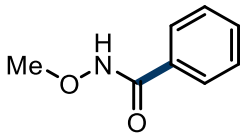

***N*-Methoxybenzamide 3ce**

The title compound was synthesized following General Procedure A using phenyl *N*-methoxycarbamate **2c** (0.100 g, 0.60 mmol, 1.0 equiv), phenylmagnesium bromide **1e** (3.0 mL, 0.80 M in THF, 4.0 equiv), THF (3.4

mL) and 1,4-dioxane (1.6 mL) (0.075 M). The crude product was purified by flash column chromatography (30% EtOAc/Hexanes) to afford the pure compound as a white solid (0.054 g, 60%).

TLC R_f = 0.1 in 25% EtOAc/Hexanes.

^{1}H NMR (300 MHz, DMSO-*d*$_6$) δ 11.76 (s, 1H), 7.79 – 7.75 (m, 2H), 7.57 – 7.43 (m, 3H), 3.72 (s, 3H).

^{13}C NMR (75 MHz, DMSO-*d*$_6$) δ 164.2 (C), 132.3 (C), 131.6 (CH), 128.5 (CH), 127.1 (CH), 63.3 (CH_3). Spectral data was consistent with literature reports.[228]

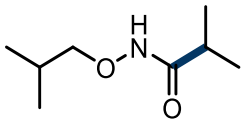

2-Methyl-*N*-(2-methylpropoxy)propanamide 3dd

The title compound was synthesized following General Procedure A using phenyl *N*-(2-methylpropoxy)carbamate **2d** (0.125 g, 0.60 mmol, 1.0 equiv), isopropylmagnesium chloride **1d** (1.3 mL, 1.80 M in THF, 4.0 equiv), THF (4.5 mL) and 1,4-dioxane (2.2 mL) (0.075 M). The crude product was purified by flash column chromatography (25% EtOAc/Hexanes) to afford the pure compound as a white solid (0.065 g, 68%).

TLC R_f = 0.26 in 25% EtOAc/Hexanes.

^{1}H NMR (300 MHz, DMSO-*d*$_6$) δ 10.84 (s, 1H), 3.50 (d, *J* = 6.7 Hz, 2H), 2.18 (sept, *J* = 6.8 Hz, 1H), 1.83 (dh, *J* = 13.2, 6.5 Hz, 1H), 0.98 (d, *J* = 6.8 Hz, 6H), 0.88 (d, *J* = 6.7 Hz, 6H).

^{13}C NMR (75 MHz, DMSO-*d*$_6$) δ 173.0 (C), 81.4 (CH_2), 31.2 (CH), 26.7 (CH), 19.2 (CH_3), 19.1 (CH_3).

HRMS (ESI): Exact mass calcd for $C_8H_{17}NO_2Na$ $[M+Na]^+$ 182.1157. Found: 182.1154.

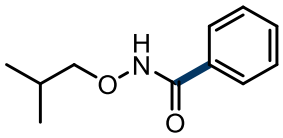

***N*-Isobutoxybenzamide 3de**

The title compound was synthesized following General Procedure A using phenyl *N*-(2-methylpropoxy)carbamate **2d** (0.125 g, 0.60 mmol, 1.0 equiv), phenylmagnesium bromide **1e** (3.0 mL, 0.80 M in THF, 4.0 equiv), THF (3.4 mL) and 1,4-dioxane (1.6 mL) (0.075 M). The crude product was purified by

flash column chromatography (20% EtOAc/Hexanes) to afford the pure compound as a white solid (0.089 g, 77%).

TLC R_f = 0.29 in 20% EtOAc/Hexanes.

^{1}H NMR (400 MHz, DMSO-*d*$_6$) δ 11.64 (s, 1H), 7.76 – 7.74 (m, 2H), 7.56 – 7.51 (m, 1H), 7.48 – 7.44 (m, 2H), 3.66 (d, *J* = 6.6 Hz, 2H), 1.92 (dh, *J* = 13.4, 6.7 Hz, 1H), 0.94 (d, *J* = 6.7 Hz, 6H).

^{13}C NMR (101 MHz, DMSO-*d*$_6$) δ 164.2 (C), 132.5 (C), 131.5 (CH), 128.4 (CH), 127.1 (CH), 81.7 (CH_2), 26.9 (CH), 19.6 (CH_3). Spectral data (using $CDCl_3$) was found consistent with literature reports.[229]

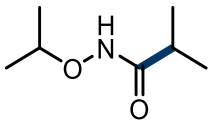

2-Methyl-*N*-propan-2-yloxypropanamide 3ed

The title compound was synthesized following General Procedure A using phenyl isopropoxycarbamate **2e** (0.117 g, 0.60 mmol, 1.0 equiv), isopropylmagnesium chloride **1d** (1.3 mL, 1.80 M in THF, 4.0 equiv), THF (4.5 mL) and 1,4-dioxane (2.2 mL) (0.075 M). The crude product was purified by flash column chromatography (33% EtOAc/Hexanes) to afford the pure compound as an off-white solid (0.061 g, 70%).

TLC R_f = 0.27 in 33% EtOAc/Hexanes.

^{1}H NMR (400 MHz, DMSO-*d*$_6$) δ 10.67 (s, 1H), 3.94 (sept, *J* = 6.2 Hz, 1H), 2.23 (sept, *J* = 6.8 Hz, 1H), 1.10 (d, *J* = 6.2 Hz, 6H), 0.98 (d, *J* = 6.8 Hz, 6H).

^{13}C NMR (101 MHz, DMSO-*d*$_6$) δ 173.2 (C), 76.0 (CH), 31.2 (CH), 20.5 (CH_3), 19.4 (CH_3).

HRMS (ESI): Exact mass calcd for $C_7H_{15}NNaO_2$ $[M+Na]^+$ 168.0995. Found: 168.1000.

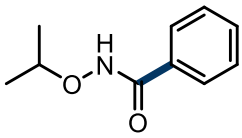

***N*-Isopropoxybenzamide 3ee**

The title compound was synthesized following General Procedure A using phenyl isopropoxycarbamate **2e** (0.117 g, 0.60 mmol, 1.0 equiv), phenylmagnesium bromide **1e** (3.0 mL, 0.80 M in THF, 4.0 equiv), THF (3.4

mL) and 1,4-dioxane (1.6 mL) (0.075 M). The crude product was purified by flash column chromatography (25% EtOAc/Hexanes) to afford the pure compound as an off-white solid (0.085 g, 79%).

TLC R_f = 0.24 in 25% EtOAc/Hexanes.

^{1}H NMR (300 MHz, DMSO-*d*$_6$) δ 11.44 (s, 1H), 7.78 – 7.74 (m, 2H), 7.57 – 7.43 (m, 3H), 4.13 (sept, *J* = 6.2 Hz, 1H), 1.20 (d, *J* = 6.2 Hz, 6H).

^{13}C NMR (75 MHz, DMSO-*d*$_6$) δ 164.5 (C), 132.6 (C), 131.4 (CH), 128.4 (CH), 127.1 (CH), 76.5 (CH), 20.7 (CH_3). Spectral data was consistent with literature reports.[230]

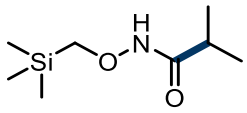

2-Methyl-*N*-(trimethylsilyl)methoxypropanamide 3fd

The title compound was synthesized following General Procedure A using phenyl *N*-(trimethylsilyl)methoxycarbamate **2f** (0.143 g, 0.60 mmol, 1.0 equiv), isopropylmagnesium chloride **1d** (1.3 mL, 1.80 M in THF, 4.0 equiv), THF (4.5 mL) and 1,4-dioxane (2.2 mL) (0.075 M). The crude product was purified by flash column chromatography (20% EtOAc/Hexanes) to afford the pure compound as a white solid (0.068 g, 60%).

TLC R_f = 0.25 in 20% EtOAc/Hexanes.

^{1}H NMR (300 MHz, DMSO-*d*$_6$) δ 10.94 (s, 1H), 3.61 (s, 2H), 2.11 (sept, *J* = 6.8 Hz, 1H), 0.97 (d, *J* = 6.8 Hz, 6H), 0.05 (s, 9H).

^{13}C NMR (76 MHz, DMSO-*d*$_6$) δ 172.5 (C), 70.4 (CH_2), 31.3 (CH), 19.2 (CH_3), -3.0 (CH_3).

HRMS (ESI): Exact mass calcd for $C_8H_{19}SiNO_2Na$ $[M+Na]^+$ 212.1083. Found: 212.1081.

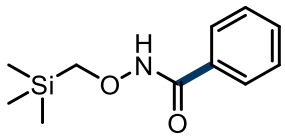

***N*-(Trimethylsilyl)methoxybenzamide 3fe**

The title compound was synthesized following General Procedure A using phenyl *N*-(trimethylsilyl)methoxycarbamate **2f** (0.143 g, 0.60 mmol, 1.0 equiv) phenylmagnesium bromide **1e** (3.0 mL, 0.80 M in THF, 4.0 equiv), THF (3.4 mL) and 1,4-dioxane (1.6 mL) (0.075 M). The crude product was

purified by flash column chromatography (25% EtOAc/Hexanes) to afford the pure compound as a white solid (0.081 g, 61%).

TLC R_f = 0.32 in 25% EtOAc/Hexanes.

^{1}H NMR (400 MHz, DMSO-*d*$_6$) δ 11.75 (s, 1H), 7.74-7.72 (m, 2H), 7.57 – 7.44 (m, 3H), 3.78 (s, 2H), 0.10 (s, 9H).

^{13}C NMR (101 MHz, DMSO-*d*$_6$) δ 163.7 (C), 132.7 (C), 131.4 (CH), 128.4 (CH), 126.9 (CH), 70.6 (CH_2), -2.9 (CH_3).

HRMS (ESI): Exact mass calcd for $C_{11}H_{17}SiNO_2Na$ $[M+Na]^+$ 246.0926. Found: 246.0923.

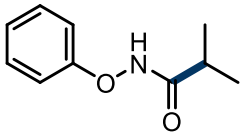

***N*-Phenoxyisobutyramide 3gd**

The title compound was synthesized following a modified General Procedure A using phenyl phenoxycarbamate **2g** (0.137 g, 0.60 mmol, 1.0 equiv), isopropylmagnesium chloride **1d** (1.1 mL, 1.80 M in THF, 3.3 equiv), **TMEDA** (0.099 mL, 0.66 mmol, 1.1 equiv), THF (4.6 mL) and 1,4-dioxane (2.3 mL) (0.075 M). The crude product was purified by flash column chromatography (25% EtOAc/Hexanes) to afford the pure compound as an off-white solid (0.032 g, 30%).

TLC R_f = 0.31 in 25% EtOAc/Hexanes.

^{1}H NMR (400 MHz, DMSO-*d*$_6$) δ 11.69 (s, 1H), 7.35 – 7.29 (m, 2H), 7.03 – 6.96 (m, 3H), 2.43 (sept, *J* = 6.8 Hz, 1H), 1.10 (d, *J* = 6.8 Hz, 6H).

^{13}C NMR (101 MHz, DMSO-*d*$_6$) δ 173.9 (C), 159.6 (C), 129.5 (CH), 122.2 (CH), 112.7 (CH), 31.3 (CH), 19.2 (CH_3). Spectral data (using $CDCl_3$) was found consistent with literature reports.[231]

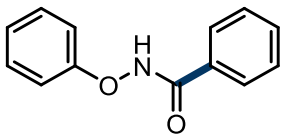

***N*-Phenoxybenzamide 3ge**

The title compound was synthesized following a modified General Procedure A using phenyl phenoxycarbamate **2g** (0.137 g, 0.60 mmol, 1.0 equiv), phenylmagnesium bromide **1e** (2.5 mL, 0.80 M in THF, 3.3 equiv), **TMEDA** (0.099 mL, 0.66 mmol, 1.1 equiv), THF (3.7 mL) and 1,4-dioxane (1.8 mL) (0.075 M). The crude product was purified by flash column chromatography (20% EtOAc/Hexanes) to afford the pure compound as an off-white solid (0.102 g, 80%).

TLC R_f = 0.29 in 20% EtOAc/Hexanes.

^{1}H NMR (400 MHz, DMSO-*d*$_6$) δ 12.49 (br s, 1H), 7.94 – 7.87 (m, 2H), 7.64 – 7.51 (m, 3H), 7.37 – 7.32 (m, 2H), 7.11 – 7.02 (m, 3H).

^{13}C NMR (101 MHz, DMSO-*d*$_6$) δ 164.9 (C), 159.6 (C), 132.1 (C), 131.5 (CH), 129.5 (CH), 128.7 (CH), 127.3 (CH), 122.4 (CH), 113.0 (CH). Spectral data was consistent with literature reports. [232]

6.3 Supporting Information for Stoichiometric Grignard Addition to Masked *N*-Isocyanates

6.3.1 General Procedure

6.3.1.1 General Procedure B: Synthesis of N-Substituted Hydrazides

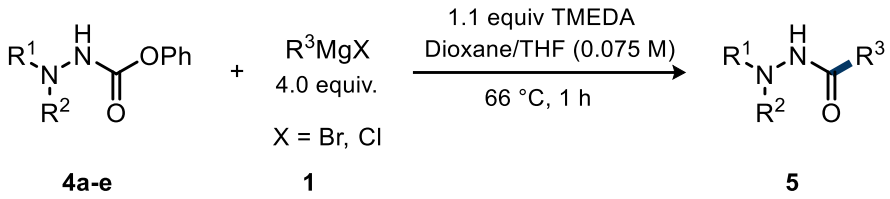

4a-e **1** **5**

An oven dried and argon flushed 20 mL µW vial, equipped with a magnetic stir bar, was charged with hydrazinecarboxylates **4** (1.0 equiv) prepared following literature procedure,[233] and then was sealed. THF and 1,4-dioxane (0.075 M) were added sequentially via syringe. At 0 °C, TMEDA (1.1 equiv) was added via micro-syringe. The corresponding Grignard reagent **1** (4.0 equiv), which was prepared as per literature procedure,[218] and titrated before use following the literature procedure,[219] was then added by syringe at 0 °C, and the reaction mixture was stirred for 1 hour at 66 °C. The solution was then cooled in an ice bath and quenched using saturated $NH_4Cl_{(aq.)}$ and extracted three times with EtOAc. The combined organic phases were washed once with brine, dried over anhydrous Na_2SO_4, filtered, and concentrated under reduced pressure. Purification was achieved using silica gel flash column chromatography.

6.3.2 Characterization Data

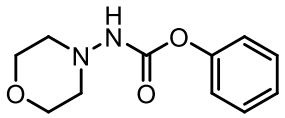

***N*-(Phenoxycarbonylamino)morpholine 4a**

The title compound was synthesized according to a modified literature procedure.[233] An oven dried, and argon flushed 250 mL RBF, equipped with a magnetic stir bar, was charged with *N*-aminomorpholine (1.2 mL, 12.0 mmol, 1.0 equiv). The flask was sealed and purged with argon, then CH_2Cl_2 (26 mL) was added, followed by pyridine (1.0 mL, 12.0 mmol, 1.0 equiv). At 0 °C, phenyl chloroformate (1.5 mL, 12.0 mmol, 1.0 equiv) was added, and the reaction mixture was stirred overnight at room temperature. The reaction mixture was then diluted with more CH_2Cl_2 (10 mL), and was extracted once with water, once with brine, dried over anhydrous Na_2SO_4, filtered, and concentrated under reduced pressure. Purification was achieved via crystallization from CH_2Cl_2/hexanes to yield off-white solid (2.11 g, 79%).

TLC R_f : 0.37 in 5% MeOH/ CH_2Cl_2.

^{1}H NMR (400 MHz, DMSO-*d*$_6$) δ 9.08 (s, 1H), 7.38 – 7.36 (m, 2H), 7.23 – 7.18 (m, 1H), 7.11 – 7.09 (m, 2H), 3.63 (t, *J* = 4.7 Hz, 4H), 2.81 (t, *J* = 4.7 Hz, 4H).

^{13}C NMR (101 MHz, DMSO-*d*$_6$) δ 152.9 (C), 150.8 (C), 129.3 (CH), 125.1 (CH), 121.7 (CH), 65.9 (CH_2), 55.0 (CH_2).

HRMS (ESI): Exact mass calcd for $C_{11}H_{14}N_2O_3Na$ $[M+Na]^+$ 245.0902. Found: 245.0900.

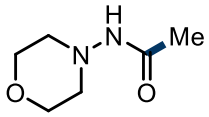

***N*-Acetylaminomorpholine 5aa**

The title compound was synthesized following General Procedure B, using *N*-(phenoxycarbonylamino) morpholine **4a** (0.133 g, 0.60 mmol, 1.0 equiv), methylmagnesium bromide **1a** (2.4 mL, 1.00 M in THF, 4.0 equiv), TMEDA (0.099 mL, 0.66 mmol, 1.1 equiv), THF (3.8 mL) and 1,4-dioxane (1.8 mL) (0.075 M). The

crude product was purified by flash column chromatography (6% MeOH/ CH_2Cl_2) to afford the pure compound as a white solid (0.058 g, 68%).

TLC R_f : 0.20 in 6% MeOH/ CH_2Cl_2.

^{1}H NMR (600 MHz, DMSO-*d*$_6$) for two conformers δ 8.86 (s, 1H), 8.39 (s, 1H), 3.60 – 3.58 (m, 8H), 2.72 – 2.70 (m, 8H), 1.93 (s, 3H), 1.71 (s, 3H).

^{13}C NMR (151 MHz, DMSO-*d*$_6$) for two conformers δ 172.2 (C), 166.3 (C), 66.0 (CH_2), 65.9 (CH_2), 55.8 (CH_2), 54.7 (CH_2), 21.3 (CH_3), 19.8 (CH_3). Spectral data (using $CDCl_3$) was found consistent with literature reports.[234]

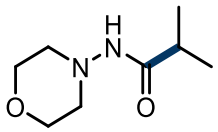

***N*-Morpholin-4-yl-isobutyramide 5ad**

The title compound was synthesized following General Procedure B, using *N*-(phenoxycarbonylamino) morpholine **4a** (0.133 g, 0.60 mmol, 1.0 equiv), isopropylmagnesium chloride **1d** (1.5 mL, 1.62 M in THF, 4.0 equiv), TMEDA (0.099 mL, 0.66 mmol, 1.1 equiv), THF (4.4 mL) and 1,4-dioxane (2.1 mL) (0.075 M). The crude product was purified by flash column chromatography (5.5% MeOH/ CH_2Cl_2) to afford the pure compound as a white solid (0.095 g, 92%).

TLC R_f : 0.28 in 5.5% MeOH/ CH_2Cl_2.

^{1}H NMR (600 MHz, DMSO-*d*$_6$) for two conformers δ 8.79 (s, 1H), 8.30 (s, 0.3H), 3.59 (t, *J* = 4.7 Hz, 4H), 3.06 (sept, *J* = 6.9 Hz, 0.3H), 2.71 (t, *J* = 4.7 Hz, 4H), 2.22 (sept, *J* = 6.8 Hz, 1H), 0.97 (dd, *J* = 6.9, 6.8 Hz, 9H).

^{13}C NMR (151 MHz, DMSO-*d*$_6$) for two conformers δ 178.3 (C), 173.4 (C), 66.0 (CH_2), 65.9 (CH_2), 56.2 (CH_2), 54.6 (CH_2), 32.4 (CH), 28.7 (CH), 19.4 (CH_3), 19.1 (CH_3).

HRMS (ESI): Exact mass calcd for $C_8H_{16}N_2O_2Na$ $[M+Na]^+$ 195.1109. Found: 195.1109.

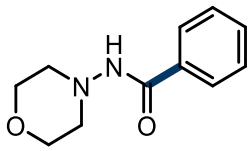

***N*-Morpholinobenzamide 5ae**

The title compound was synthesized following General Procedure B, using *N*-(phenoxycarbonylamino) morpholine **4a** (0.133 g, 0.60 mmol, 1.0 equiv), phenylmagnesium bromide **1e** (2.6 mL, 0.90 M in THF, 4.0 equiv), TMEDA (0.099 mL, 0.66 mmol), THF (3.6 mL) and 1,4-dioxane (1.8 mL) (0.075 M). The crude product was purified by flash column chromatography (5.5% MeOH/ CH_2Cl_2) to afford the pure compound as a white solid (0.122 g, 98%).

TLC R_f : 0.31 in 5.5% MeOH/ CH_2Cl_2.

^{1}H NMR (600 MHz, DMSO-d_6) δ 9.49 (s, 1H), 7.78 – 7.76 (m, 2H), 7.54 – 7.51 (m, 1H), 7.46 – 7.44 (m, 2H), 3.66 (t, *J* = 4.6 Hz, 4H), 2.88 (t, *J* = 4.6 Hz, 4H).

^{13}C NMR (151 MHz, DMSO-d_6) δ 164.2 (C), 134.0 (C), 131.2 (CH), 128.3 (CH), 127.3 (CH), 66.0 (CH_2), 54.4 (CH_2). Spectral data (using $CDCl_3$) was found consistent with literature reports. [152]

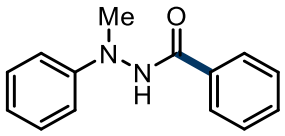

***N'*-Methyl-*N'*-phenylbenzohydrazide 5be**

The title compound was synthesized following a modified General Procedure B (TMEDA omitted), using phenyl 2-methyl-2-phenylhydrazinecarboxylate **4b** (0.097 g, 0.40 mmol, 1.0 equiv), phenylmagnesium bromide **1e** (1.8 mL, 0.90 M in THF, 4.0 equiv), THF (2.4 mL) and 1,4-dioxane (1.1 mL) (0.075 M). The crude product was purified by flash column chromatography (25% EtOAc/Hexanes) to afford the pure compound as a white solid (0.088 g, 97%).

TLC R_f: 0.27 in 25% EtOAc/Hexanes.

^{1}H NMR (600 MHz, DMSO-d_6) δ 10.64 (s, 1H), 7.92 – 7.90 (m, 2H), 7.60 – 7.57 (m, 1H), 7.53 – 7.49 (m, 2H), 7.23 – 7.19 (m, 2H), 6.83 – 6.81 (m, 2H), 6.77 – 6.74 (m, 1H), 3.20 (s, 3H).

^{13}C NMR (151 MHz, DMSO-*d*$_6$) δ 165.5 (C), 149.9 (C), 132.9 (C), 131.8 (CH), 128.9 (CH), 128.5 (CH), 127.3 (CH), 118.2 (CH), 112.3 (CH), 40.2 (CH_3). Spectral data (using $CDCl_3$) was found consistent with literature reports. [235]

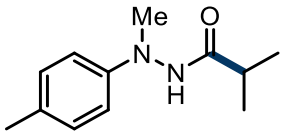

***N'*-Methyl-*N'*-(4-tolyl)-isobutyrohydrazide 5cd**

The title compound was synthesized following General Procedure B, using phenyl 2-methyl-2-(4'-tolyl)hydrazinecarboxylate **4c** (0.076 g, 0.30 mmol, 1.0 equiv), isopropylmagnesium chloride **1d** (0.75 mL, 1.60 M in THF, 4.0 equiv), TMEDA (0.050 mL, 0.33 mmol, 1.1 equiv), THF (2.2 mL) and 1,4-dioxane (1.0 mL) (0.075 M). The crude product was purified by flash column chromatography (40% EtOAc/Hexanes) to afford the pure compound as a white solid (0.043 g, 70%).

TLC R_f : 0.29 in 40% EtOAc/Hexanes.

^{1}H NMR (600 MHz, DMSO-*d*$_6$) δ 9.81 (s, 1H), 6.99 (d, *J* = 8.6 Hz, 2H), 6.64 (d, *J* = 8.6 Hz, 2H), 3.02 (s, 3H), 2.40 (sept, *J* = 6.9 Hz, 1H), 2.19 (s, 3H), 1.05 (d, *J* = 6.9 Hz, 6H).

^{13}C NMR (151 MHz, DMSO-*d*$_6$) δ 175.1 (C), 148.0 (C), 129.3 (CH), 126.7 (C), 112.4 (CH), 40.4 (CH_3), 32.2 (CH), 20.0 (CH_3), 19.3 (CH_3).

HRMS (ESI): Exact mass calcd for $C_{12}H_{18}N_2ONa$ $[M+Na]^+$ 229.1317. Found: 229.1339.

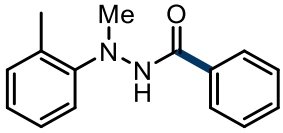

***N'*-Methyl-*N'*-(2-tolyl)benzohydrazide 5de**

The title compound was synthesized following General Procedure B, using phenyl 2-methyl-2-(2'-tolyl)hydrazinecarboxylate **4d** (0.076 g, 0.30 mmol, 1.0 equiv), phenylmagnesium bromide **1e** (1.3 mL, 0.90 M in THF, 4.0 equiv), TMEDA (0.050 mL, 0.33 mmol, 1.1 equiv), THF (1.8 mL) and 1,4-dioxane (0.9 mL)

(0.075 M). The crude product was purified by flash column chromatography (33% EtOAc/Hexanes) to afford the pure compound as a white solid (0.065 g, 89%).

TLC R_f : 0.34 in 33% EtOAc/Hexanes.

^{1}H NMR (600 MHz, DMSO-*d*$_6$) δ 10.23 (s, 1H), 7.83 – 7.81 (m, 2H), 7.55 – 7.52 (m, 1H), 7.47 – 7.44 (m, 2H), 7.20 – 7.11 (m, 3H), 6.95- 6.93 (m, 1H), 3.06 (s, 3H), 2.22 (s, 3H).

^{13}C NMR (151 MHz, DMSO-*d*$_6$) δ 164.5 (C), 149.0 (C), 133.3 (C), 131.4 (CH), 131.0 (CH), 130.4 (C), 128.4 (CH), 127.3 (CH), 126.1 (CH), 122.7 (CH), 117.8 (CH), 41.8 (CH_3), 18.6 (CH_3).

HRMS (ESI): Exact mass calcd for $C_{15}H_{16}N_2ONa$ $[M+Na]^+$ 263.1160. Found: 263.1152.

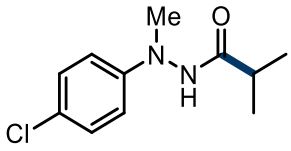

***N'*-(4-Chlorophenyl)-*N'*-methyl-isobutyrohydrazide 5ed**

The title compound was synthesized following General Procedure B, using phenyl 2-(4-chlorophenyl)-2-methylhydrazinecarboxylate **4e** (0.069 g, 0.25 mmol, 1.0 equiv), isopropylmagnesium chloride **1d** (0.6 mL, 1.60 M in THF, 4.0 equiv), TMEDA (0.041 mL, 0.27 mmol, 1.1 equiv), THF (1.8 mL) and 1,4-dioxane (0.9 mL) (0.075 M). The crude product was purified by flash column chromatography (33% EtOAc/Hexanes) to afford the pure compound as a pale-yellow solid (0.032 g, 56%).

TLC R_f : 0.20 in 33% EtOAc/Hexanes.

^{1}H NMR (600 MHz, DMSO-*d*$_6$) δ 9.97 (s, 1H), 7.21 (d, *J* = 9.2 Hz, 2H), 6.72 (d, *J* = 9.2 Hz, 2H), 3.06 (s, 3H), 2.42 (sept, *J* = 6.9 Hz, 1H), 1.06 (d, *J* = 6.9 Hz, 6H).

^{13}C NMR (151 MHz, DMSO-*d*$_6$) δ 175.0 (C), 148.9 (C), 128.5 (CH), 121.6(C), 113.6 (CH), 40.2 (CH_3), 32.1 (CH), 19.2 (CH_3).

HRMS (ESI): Exact mass calcd for $C_{11}H_{15}ClN_2ONa$ $[M+Na]^+$ 249.0771. Found: 249.0772.

6.4 Supporting Information for Chapter 3

6.4.1 General Procedure

6.4.1.1 General Procedure C: Synthesis of Hydrazonecarboxylates

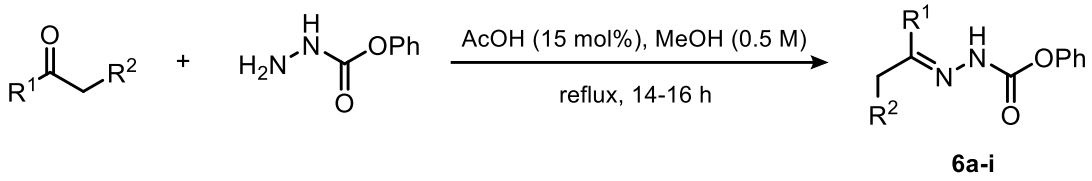

6a-i

Condensation of acyl hydrazines with ketones was conducted following literature procedure.[86] A round bottom flask 100 mL, equipped with a magnetic stir bar, was charged with phenyl hydrazinecarboxylate (1.0 equiv) which was prepared following literature procedure.[236] Methanol (0.5 M) was then added to the flask, followed by the ketone (2.0 equiv). A catalytic amount of AcOH (15 mol%) was added and the reaction mixture was stirred at reflux for overnight (14 – 16 h). The reaction mixture was then cooled to ambient temperature, concentrated under reduced pressure, and purified by silica gel flash column chromatography or crystallization to afford the corresponding hydrazone.

6.4.1.2 General Procedure D: Synthesis of Pyrazolones:

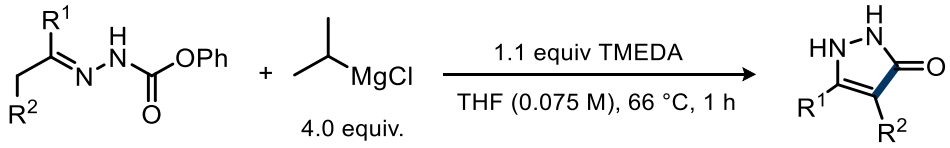

6a-i **1d** **7a-i**

An oven dried and argon flushed 20 mL µW vial, equipped with a magnetic stir bar, was charged with (phenoxycarbonyl)hydrazones **6** (1.0 equiv) prepared following General Procedure C,[237] and then was sealed. THF (0.075 M) was added via syringe. At 0 °C, TMEDA (1.1 equiv) was added via micro-syringe. Isopropylmagnesium chloride **1d** (4.0 equiv), which was titrated before use following the literature procedure,[219] was then added by syringe at 0 °C, and the reaction mixture was stirred for 1 hour at 66 °C. The solution was then cooled in an ice bath and quenched using saturated $NH_4Cl_{(aq.)}$ and extracted three times with EtOAc. The combined organic phases were washed once with brine, dried over anhydrous Na_2SO_4, filtered, and concentrated under reduced pressure. Purification was achieved using silica gel flash column chromatography using MeOH/CH_2Cl_2 mixture.

6.4.2 Characterization Data

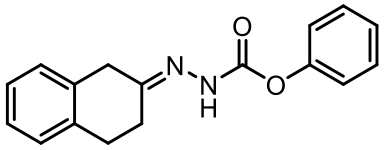

Phenyl 2-(3,4-dihydronaphthalen-2(1H)-ylidene)hydrazinecarboxylate 6b

The title compound was synthesized following General Procedure C, using phenyl hydrazinecarboxylate (1.5 g, 10.0 mmol, 1.0 equiv), β-tetralone (2.60 mL, 20.0 mmol, 2.0 equiv), methanol (20.0 mL, 0.5 M) and AcOH (15 mol%). The crude product was purified by crystallization from Et_2O to afford the pure compound as a pale-yellow solid (1.96 g, 70%).

TLC R_f : 0.34 in 50% EtOAc/Hexanes.

^{1}H NMR (300 MHz, DMSO-*d*$_6$) δ 10.48 (s, 1H), 7.46 – 7.38 (m, 2H), 7.28 – 7.13 (m, 8H), 3.77 (s, 2H), 2.86 (t, *J* = 6.5 Hz, 2H), 2.54 (t, *J* = 6.5 Hz, 2H).

^{13}C NMR (151 MHz, DMSO-*d*$_6$) δ 150.7 (C), 137.2 (C), 133.2 (CH), 129.5 (CH), 128.6 (CH), 128.1 (CH), 127.3 (C), 127.1 (C), 126.5 (CH), 126.2 (CH), 125.4 (C), 121.9 (CH), 31.8 (CH_2), 31.1 (CH_2), 28.6 (CH_2).

HRMS (ESI): Exact mass calcd for $C_{17}H_{16}N_2O_2Na$ $[M+Na]^+$ 303.1109. Found: 303.1099.

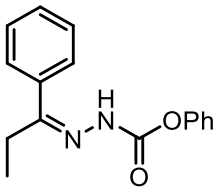

Phenyl 2-(1-phenylpropylidene)hydrazinecarboxylate 6e

The title compound was synthesized following a modified General Procedure C, using phenyl hydrazinecarboxylate (1.5 g, 10.0 mmol, **1.0 equiv**), 1-phenyl-propan-1-one (1.32 mL, 10.0 mmol, 1.0 equiv), methanol (20.0 mL, 0.5 M) and AcOH (15 mol%). The crude product was purified by crystallization from minimal amount of MeOH to afford the pure compound as a white solid (2.41 g, 90%).

TLC R_f : 0.33 in 50% EtOAc/Hexanes.

^{1}H NMR (300 MHz, DMSO-*d*$_6$) δ 10.84 (s, 1H), 7.79 – 7.75 (m, 2H), 7.47 – 7.38 (m, 5H), 7.30 – 7.22 (m, 3H), 2.85 (q, *J* = 7.6 Hz, 2H), 1.06 (t, *J* = 7.6 Hz, 3H).

^{13}C NMR (126 MHz, DMSO-*d*$_6$) δ 150.7 (C), 136.9 (C), 129.5 (CH), 129.0 (C), 128.4 (CH), 126.3 (CH), 125.4 (CH), 121.9 (CH), 19.6 (CH_2), 10.8 (CH_3).

HRMS (ESI): Exact mass calcd for $C_{16}H_{16}N_2O_2Na$ $[M+Na]^+$ 291.1110. Not found.*

*Detailed analysis of the HRMS data obtained using TOF MS ES+ shows similar peaks being present for five molecules with different molecular weights, and three different types of structures. Thus, it is not possible to retrieve LRMS data, and further analysis will be carried out by Mr. Frederic Vuillermet.

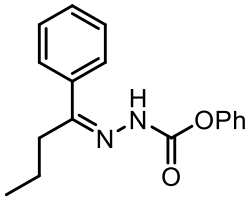

Phenyl 2-(1-phenylbutylidene)hydrazinecarboxylate 6f

The title compound was synthesized following a modified General Procedure C, using phenyl hydrazinecarboxylate (1.5 g, 10.0 mmol, **1.0 equiv**), butyrophenone (1.45 mL, 10.0 mmol, 1.0 equiv), methanol (20.0 mL, 0.5 M) and AcOH (15 mol%). The crude product was purified by crystallization from Et_2O to afford the pure compound as a white solid (2.59 g, 92%).

TLC R_f : 0.30 in 50% EtOAc/Hexanes.

^{1}H NMR (600 MHz, DMSO-*d*$_6$) δ 10.88 (s, 1H), 7.77 – 7.75 (m, 2H), 7.45 – 7.38 (m, 5H), 7.28 – 7.23 (m, 3H), 2.82 (t, *J* = 7.3 Hz, 2H), 1.47 (m, 2H), 0.97 (t, *J* = 7.3 Hz, 3H).

^{13}C NMR (151 MHz, DMSO-*d*$_6$) δ 150.7 (C), 137.3 (C), 129.5 (CH), 129.0 (CH), 128.4 (CH), 128.2 (C), 126.3 (CH), 125.4 (CH), 121.9 (CH), 121.4 (C), 28.0 (CH_2), 19.5 (CH_2), 13.7 (CH_3).

HRMS (ESI): Exact mass calcd for $C_{17}H_{18}N_2O_2Na$ $[M+Na]^+$ 305.1266. Not found.*

*Detailed analysis of the HRMS data obtained using TOF MS ES+ shows similar peaks being present for five molecules with different molecular weights, and three different types of structures. Thus, it is not possible to retrieve LRMS data, and further analysis will be carried out by Mr. Frederic Vuillermet.

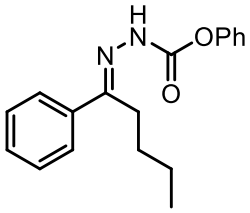

Phenyl 2-(1-phenylpentylidene)hydrazinecarboxylate 6n

The title compound was synthesized following a modified General Procedure C, using phenyl hydrazinecarboxylate (0.520 g, 3.60 mmol, **1.2 equiv**), valerophenone (0.49 mL, 3.00 mmol, 1.0 equiv), methanol (10.0 mL, 0.3 M) and AcOH (15 mol%). The crude product was purified by crystallization from MeOH to afford the pure compound as a white solid (0.764 g, 86%).

TLC R_f : 0.24 in 50% EtOAc/Hexanes.

^{1}H NMR (400 MHz, $CDCl_3$) δ 8.22 (s, 1H), 7.82 – 7.79 (m, 2H), 7.43 – 7.37 (m, 5H), 7.27 – 7.23 (m, 3H), 2.69 (t, *J* = 7.3 Hz, 2H), 1.63 – 1.58 (m, 2H), 1.56 – 1.44 (m, 2H), 0.98 (t, *J* = 7.2 Hz, 3H).

^{13}C NMR (151 MHz, $CDCl_3$) δ 137.1 (C), 129.7 (C), 129.5 (CH), 128.6 (CH), 126.6 (CH), 125.9 (CH), 121.7(CH), 120.5 (C), 115.5 (CH), 105.2 (C), 28.2 (CH_2), 26.5 (CH_2), 23.1 (CH_2), 13.9 (CH_3).

HRMS (ESI): Exact mass calcd for $C_{18}H_{20}N_2O_2Na$ $[M+Na]^+$ 319.1412. Found: 319.1422.

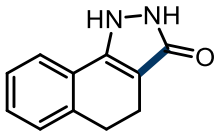

1,2,4,5-Tetrahydro-benz[g]indazol-3-one 7a

The title compound was synthesized following General Procedure D, using phenyl 2-(3,4-dihydronaphthalen-1(2*H*)-ylidene)hydrazinecarboxylate **6a** (0.168 g, 0.60 mmol, 1.0 equiv),

isopropylmagnesium chloride **1d** (1.3 mL, 1.80 M in THF, 4.0 equiv), TMEDA (0.099 mL, 0.66 mmol, 1.1 equiv), THF (6.7 mL, 0.075 M). The crude product was purified by flash column chromatography (6% MeOH/ CH_2Cl_2) to afford the pure compound as a pale-yellow solid (0.085 g, 76%).

TLC R_f : 0.15 in 6% MeOH/ CH_2Cl_2.

^{1}H NMR (600 MHz, DMSO-d_6) δ 7.52 - 7.51 (m, 1H), 7.26 – 7.21 (m, 2H), 7.17 – 7.15 (m, 1H), 2.84 (t, *J* = 7.6 Hz, 2H), 2.52 (t, *J* = 7.6 Hz, 2H).

^{13}C NMR (151 MHz, DMSO-d_6) δ 155.2 (C), 141.2 (C), 136.9 (C), 129.0 (CH), 128.7 (CH), 126.8 (CH), 125.4 (C), 122.2 (CH), 98.8 (C), 28.6 (CH_2), 16.9 (CH_2).

HRMS (ESI): Exact mass calcd for $C_{11}H_{10}N_2ONa$ $[M+Na]^+$ 209.0691. Found: 209.0690.

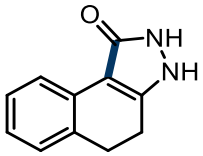

2,3,4,5-Tetrahydro-benz[e]indazol-1-one 7b

The title compound was synthesized following General Procedure D, using phenyl 2-(3,4-dihydronaphthalen-2(1H)-ylidene)hydrazinecarboxylate **6b** (0.168 g, 0.60 mmol, 1.0 equiv), isopropylmagnesium chloride **1d** (1.3 mL, 1.80 M in THF, 4.0 equiv), TMEDA (0.099 mL, 0.66 mmol, 1.1 equiv), THF (6.7 mL, 0.075 M). The crude product was purified by flash column chromatography (7.5% MeOH/ CH_2Cl_2) to afford the pure compound as a pale-yellow solid (0.086 g, 77%).

TLC R_f : 0.27 in 7.5% MeOH/ CH_2Cl_2.

^{1}H NMR (600 MHz, DMSO-d_6) δ 7.55 – 7.53 (m, 1H), 7.15 – 7.12 (m, 2H), 6.97 – 6.94 (m, 1H), 2.88 (t, *J* = 7.7 Hz, 2H), 2.70 (t, *J* = 7.7 Hz, 2H).

^{13}C NMR (151 MHz, DMSO-d_6) δ 157.7 (C), 141.3 (C), 132.2 (C), 131.5 (C), 127.8 (CH), 126.5 (CH), 123.9 (CH), 121.7 (CH), 100.0 (C), 28.9 (CH_2), 20.4 (CH_2).

HRMS (ESI): Exact mass calcd for $C_{11}H_{10}N_2ONa$ $[M+Na]^+$ 209.0691. Found: 209.0692.

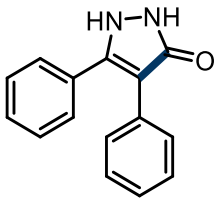

4,5-Diphenyl-1,2-dihydro-3*H*-pyrazol-3-one 7c

The title compound was synthesized following General Procedure D, using phenyl 2-(1,2-diphenylethylidene)hydrazinecarboxylate **6c** (0.198 g, 0.60 mmol, 1.0 equiv), isopropylmagnesium chloride **1d** (1.3 mL, 1.80 M in THF, 4.0 equiv), TMEDA (0.099 mL, 0.66 mmol, 1.1 equiv), THF (6.7 mL, 0.075 M). The crude product was purified by flash column chromatography (5% MeOH/ CH_2Cl_2) to afford the pure compound as a yellowish white solid (0.100 g, 71%).

TLC R_f : 0.24 in 5% MeOH/ CH_2Cl_2.

^{1}H NMR (600 MHz, DMSO-d_6) δ 7.38 – 7.33 (m, 5H), 7.28 – 7.23 (m, 4H), 7.17 – 7.15 (m, 1H).

^{13}C NMR (151 MHz, DMSO-d_6) δ 159.0 (C), 139.8 (C), 132.7 (C), 130.6 (C), 128.9 (CH), 128.6 (CH), 128.2 (CH), 128.1 (CH), 127.5 (CH), 125.6 (CH), 102.7 (C). Spectral data was consistent with literature reports.[238]

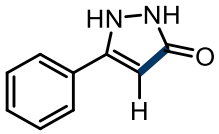

5-Phenyl-1,2-dihydro-3*H*-pyrazol-3-one 7d

The title compound was synthesized following a modified General Procedure D, using phenyl 2-(1-phenylethylidene)hydrazinecarboxylate **6d** (0.153 g, 0.60 mmol, 1.0 equiv), isopropylmagnesium chloride **1d** (1.3 mL, 1.80 M in THF, 4.0 equiv), TMEDA (0.099 mL, 0.66 mmol, 1.1 equiv), THF (6.7 mL, 0.075 M) and the reaction was **stirred at 0 °C for 3 h**. The crude product was purified by flash column chromatography (7.5% MeOH/ CH_2Cl_2) to afford the pure compound as a yellowish white solid (0.060 g, 63%).

TLC R_f : 0.30 in 7.5% MeOH/ CH_2Cl_2.

^{1}H NMR (600 MHz, DMSO-d_6) δ 7.67 – 7.65 (m, 2H), 7.41 - 7.38 (m, 2H), 7.30 – 7.27 (m, 1H), 5.89 (s, 1H).

^{13}C NMR (151 MHz, DMSO-*d*$_6$) δ 161.1 (C), 143.6 (C), 130.7 (C), 128.8 (CH), 127.8 (CH), 124.8 (CH), 86.8 (CH). Spectral data was consistent with literature reports.[238]

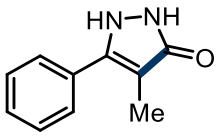

4-Methyl-5-phenyl-1,2-dihydro-3*H*-pyrazol-3-one 7e

The title compound was synthesized following a modified General Procedure D, using phenyl 2-(1-phenylpropylidene)hydrazinecarboxylate **6e** (0.161 g, 0.60 mmol, 1.0 equiv), isopropylmagnesium chloride **1d** (1.3 mL, 1.80 M in THF, 4.0 equiv), TMEDA (0.099 mL, 0.66 mmol, 1.1 equiv), THF (6.7 mL, 0.075 M) and the reaction was **stirred at 0 °C for 3 h**. The crude product was purified by flash column chromatography (7% MeOH/ CH_2Cl_2) to afford the pure compound as a yellowish white solid (0.073 g, 70%).

TLC R$_f$: 0.25 in 7% MeOH/ CH_2Cl_2.

^{1}H NMR (600 MHz, DMSO-*d*$_6$) δ 7.56 – 7.54 (m, 2H), 7.46 – 7.43 (m, 2H), 7.35 – 7.31 (m, 1H), 2.01 (s, 3H).

^{13}C NMR (151 MHz, DMSO-*d*$_6$) δ160.4 (C), 139.7 (C), 131.2 (C), 128.9 (CH), 127.6 (CH), 126.4 (CH), 96.1 (C), 7.7 (CH_3). Spectral data was consistent with literature reports.[239]

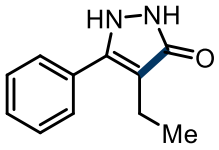

4-Ethyl-5-phenyl-1,2-dihydro-3*H*-pyrazol-3-one 7f

The title compound was synthesized following a modified General Procedure D, using phenyl 2-(1-phenylbutylidene)hydrazinecarboxylate **6f** (0.170 g, 0.60 mmol, 1.0 equiv), isopropylmagnesium chloride **1d** (1.3 mL, 1.80 M in THF, 4.0 equiv), TMEDA (0.099 mL, 0.66 mmol, 1.1 equiv), THF (6.7 mL, 0.075 M) and the reaction was **stirred at 0 °C for 3 h**. The crude product was purified by flash column chromatography (7% MeOH/ CH_2Cl_2) to afford the pure compound as a yellowish white solid (0.056 g, 50%).

TLC R_f : 0.33 in 7% MeOH/ CH_2Cl_2.

^{1}H NMR (600 MHz, DMSO-d_6) δ 7.50 – 7.44 (m, 3H), 7.36 – 7.33 (m, 1H), 2.44 (q, *J* = 7.5 Hz, 2H), 1.06 (t, *J* = 7.5 Hz, 3H).

^{13}C NMR (151 MHz, DMSO-d_6) δ160.1 (C), 139.3 (C), 131.2 (C), 128.8 (CH), 127.6 (CH), 126.6 (CH), 102.8 (C), 15.3 (CH_2), 15.0 (CH_3).

HRMS (ESI): Exact mass calcd for $C_{11}H_{12}N_2ONa$ $[M+Na]^+$ 211.0847. Found: 211.0846.

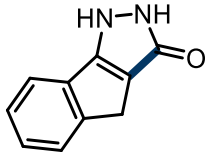

2,4-Dihydro-1*H*-indeno[1,2-c]pyrazol-3(3*H*)-one 7g

The title compound was synthesized following a modified General Procedure D, using phenyl 2-(2,3-dihydro-inden-1-ylidene)hydrazinecarboxylate **6g** (0.160 g, 0.60 mmol, 1.0 equiv), isopropylmagnesium chloride **1d** (1.3 mL, 1.80 M in THF, 4.0 equiv), TMEDA (0.099 mL, 0.66 mmol, 1.1 equiv), THF (6.7 mL, 0.075 M) and the reaction was **stirred at room temperature for 2 h**. The crude product was purified by flash column chromatography (9% MeOH/ CH_2Cl_2) to afford the pure compound as a yellowish white solid (0.072 g, 70%).

TLC R_f : 0.26 in 9% MeOH/ CH_2Cl_2.

^{1}H NMR (600 MHz, DMSO-d_6) δ 7.49 – 7.47 (m, 2H), 7.31 – 7.29 (m, 1H), 7.23 – 7.20 (m, 1H), 3.43 (s, 2H).

^{13}C NMR (151 MHz, DMSO-d_6) δ 175.1 (C), 148.5 (C), 130.4 (C), 129.6 (C), 126.7 (CH), 126.2 (CH), 126.0 (CH), 118.7 (CH), 82.9 (C), 28.1 (CH_2).

HRMS (ESI): Exact mass calcd for $C_{10}H_8N_2ONa$ $[M+Na]^+$ 195.0534. Found: 195.0537.

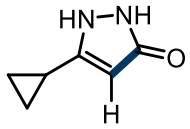

5-Cyclopropyl-2,4-dihydro-3*H*-pyrazol-3-one 7h

The title compound was synthesized following General Procedure D, using phenyl 2-(1-cyclopropylethylidene)hydrazinecarboxylate **6h** (0.131 g, 0.60 mmol, 1.0 equiv), isopropylmagnesium chloride **1d** (1.3 mL, 1.80 M, 4.0 equiv), TMEDA (0.099 mL, 0.66 mmol, 1.1 equiv), THF (6.7 mL, 0.075 M). The crude product was purified by flash column chromatography (9% MeOH/ CH_2Cl_2) to afford the pure compound as a yellowish white solid (0.045 g, 60%).

TLC R_f : 0.24 in 9% MeOH/ CH_2Cl_2.

^{1}H NMR (600 MHz, DMSO-d_6) δ 5.33 (s, 1H), 1.82 (tt, *J* = 8.5, 5.0 Hz, 1H), 0.96 – 0.91 (m, 2H), 0.73 – 0.69 (m, 2H).

^{13}C NMR (151 MHz, DMSO-d_6) δ 159.2 (C), 149.6 (C), 86.0 (CH), 8.2 (CH_2), 7.3 (CH). Spectral data was consistent with literature reports.[240]

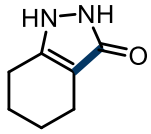

4,5,6,7-Tetrahydro-1*H*-indazol-3(2*H*)-one 7i

The title compound was synthesized following General Procedure D, using phenyl *N*-(cyclohexylideneamino)carbamate **6i** (0.139 g, 0.60 mmol, 1.0 equiv), isopropylmagnesium chloride **1d** (1.3 mL, 1.80 M, 4.0 equiv), TMEDA (0.099 mL, 0.66 mmol, 1.1 equiv), THF (6.7 mL, 0.075 M). The crude product was purified by flash column chromatography (9% MeOH/ CH_2Cl_2) to afford the pure compound as a yellowish white solid (0.044 g, 53%).

TLC R_f : 0.32 in 9% MeOH/ CH_2Cl_2.

^{1}H NMR (600 MHz, DMSO-d_6) δ 2.42 (t, *J* = 6.2 Hz, 2H), 2.21 (t, *J* = 6.2 Hz, 2H), 1.67 – 1.58 (m, 4H).

^{13}C NMR (151 MHz, DMSO-d_6) δ 158.5 (C), 139.8 (C), 98.5 (C), 22.9 (CH_2), 22.3 (CH_2), 21.3 (CH_2), 18.9 (CH_2).

HRMS (ESI): Exact mass calcd for $C_7H_{10}N_2ONa$ $[M+Na]^+$ 161.0691. Found: 161.0691.

6.5 Supporting Information for Chapter 4

6.5.1 General Procedure

6.5.1.1 General Procedure E: Intramolecular Cyclization

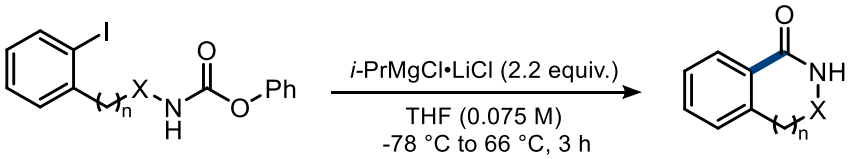

X = O or NR, n = 0 or 1

An oven dried and argon flushed 20 mL µW vial, equipped with a magnetic stir bar, was charged with the corresponding iodo-substituted carbamate (1.0 equiv) prepared following specific procedure for each substrate (see following section), and then was sealed. THF (0.075 M) was added via syringe and the reaction mixture was allowed to stir at -78 °C for 10 minutes. At -78 °C, isopropylmagnesium chloride lithium chloride **1D** (2.2 equiv), which was titrated before use following the literature procedure,[219] was then added by syringe, and the reaction mixture was allowed to stir for 2 hours at -78 °C. The temperature was gradually raised to ambient temperature, then the reaction mixture was allowed to stir for 1 hours at 66 °C. The solution was then cooled in an ice bath and quenched using saturated $NH_4Cl_{(aq.)}$ and extracted three times with EtOAc. The combined organic phases were washed once with brine, dried over anhydrous Na_2SO_4, filtered, and concentrated under reduced pressure. Purification was achieved using silica gel flash column chromatography.

6.5.2 Characterization Data

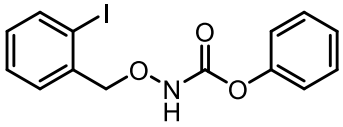

***O*-(*o*-Iodobenzyl) phenylcarbamate 10**

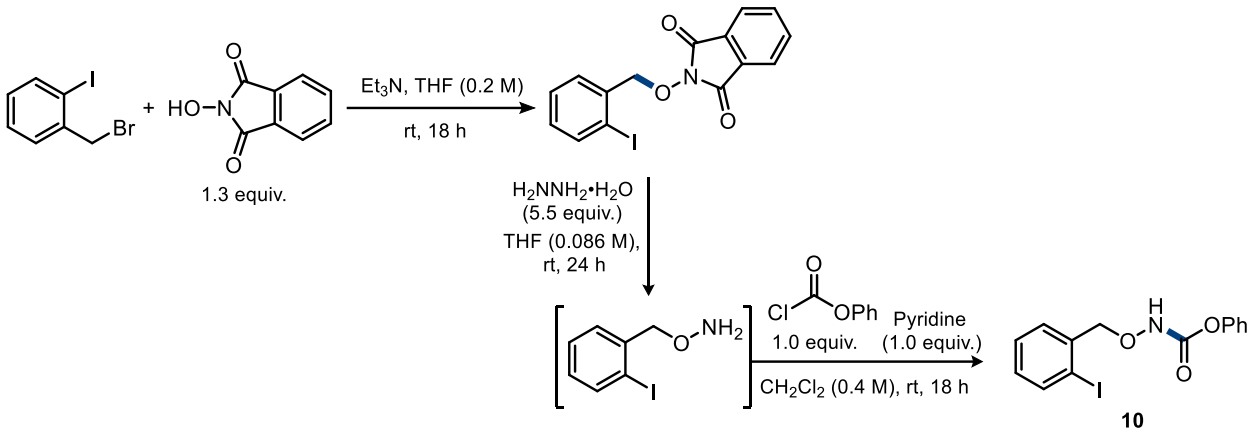

The title compound was synthesized following literature procedure.[112,213] To a 500 mL round bottom flask equipped with a stir bar *N*-hydroxyphthalimide (2.86 g, 17.53 mmol., 1.3 equiv) was dissolved in THF (45 mL) at room temperature. Triethylamine (2.8 mL, 20.1 mmol, 1.5 equiv) was added to the reaction flask using a syringe and a red color was immediately appeared upon addition while the drop hits the solution. A stock solution of 2-iodobenzyl bromide (3.97 g, 13.4 mmol, 1.0 equiv) in THF (15 mL) (0.2 M) was added dropwise (in three aliquots of 5 mL) to the reaction flask over 10 min. The flask was sealed, and it was allowed to stir for 18 h at room temperature. The mixture was characterized by TLC with 40% EtOAc/Hexanes eluent. After the THF solvent was removed under reduced pressure, the reaction mixture contents were transferred into a separatory funnel by rinsing the round bottom flask with CH_2Cl_2 (165 mL) and water (165 mL). After the mixture contents separated, the organic layer was reserved, and the aqueous layer was extracted with CH_2Cl_2 (x 3). Then the combined organic layers were washed three times using 100 mL distilled water and once with 100 mL brine. The organic layer was then dried over anhydrous Na_2SO_4 overnight. The final product was obtained by filtration and rotary evaporation and high vacuum to yield an off-white powdery solid (4.93 g, 97%, without further purification). The **second step** of the reaction was to obtain the *O*-(2-iodobenzyl)hydroxylamine. *O*-(2-iodobenzyl)-*N*-hydroxyphthalimide (4.93 g, 13.0 mmol, 1.0 equiv) was added into a 500 mL round bottom flask with 150 mL THF (0.086 M) and the mixture was kept stir for 10 min to fully dissolve. Hydrazine monohydrate (3.5 mL, 71.5 mmol, 5.5 equiv) was added through a syringe to the vigorously stirred solution and the color was changed to a light-yellow. The reaction was allowed to stir for 24 h at room temperature during which time, the reaction mixture turned murky white. The solvent was evaporated under reduced pressure, then CH_2Cl_2 (100 mL) was added to the reaction mixture, layers were separated, and the combined organic layer was then washed with water (x 2) and brine (x 1). The organic layer was then dried over anhydrous Na_2SO_4, and solvent was evaporated to yield the product as an off-white oil which was used for the subsequent step without

further purification (3.00 g, 92%,). The **third step** of the reaction: To a 250 mL round bottom flask equipped with a stir bar was added *O*-(2-iodobenzyl)hydroxylamine from the previous step (3.0 g, 12.0 mmol, 1.0 equiv) followed by dilution with CH_2Cl_2 (26 mL, 0.4 M) and cooled to 0 °C. To this stirred solution was added pyridine (1 mL, 12 mmol, 1.0 equiv). After addition of pyridine, the solution was allowed to stir at 0 °C for 0.5 h. Then phenylchloroformate (1.5 mL, 12.0 mmol, 1.0 equiv) was added dropwise at 0 °C, and the reaction mixture was allowed to stir for overnight (18 h) at room temperature. The mixture was characterized by TLC with 40% EtOAc/Hexanes eluent. Upon completion, the reaction was extracted using sat. $NaHCO_3$ (x 2) and then brine (x 1). The organic phase was dried over anhydrous Na_2SO_4 and filtered over a fritted funnel. The filtrate was concentrated via rotary evaporation and purified using silica-gel flash column chromatography using 20% EtOAc/Hexanes to afford the pure compound as white solid (3.54 g, 80%).

TLC R_f : 0.30 in 20% EtOAc/Hexanes.

^{1}H NMR (600 MHz, DMSO-*d*$_6$) δ 7.89 (dd, *J* = 7.9, 1.2 Hz, 1H), 7.52 (dd, *J* = 7.6, 1.7 Hz, 1H), 7.45 (ddd, *J* = 7.6, 1.7, 1.2 Hz, 1H), 7.43 – 7.38 (m, 2H), 7.24 (ddd, *J* = 7.9, 1.7, 1.2 Hz, 1H), 7.14 – 7.11 (m, 3H), 4.92 (s, 2H).

^{13}C NMR (151 MHz, DMSO-*d*$_6$) δ 154.8 (C), 150.4 (C), 139.2 (CH), 138.2 (CH), 130.7 (C), 130.4 (CH), 129.5 (CH), 128.5 (CH), 125.5 (CH), 121.7 (CH), 99.8 (C), 80.8 (CH_2).

HRMS (ESI): Exact mass calcd for $C_{14}H_{12}INO_3Na$ $[M+Na]^+$ 391.9766. Found: 391.9760.

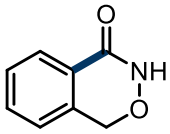

1*H*-2,3-Benzoxazin-4(3*H*)-one 11

The title compound was synthesized following General Procedure E, using *O*-(*o*-iodobenzyl) phenylcarbamate **10** (0.369 g, 1.00 mmol, 1.0 equiv), isopropylmagnesium chloride lithium chloride **1D** (2.0 mL, 1.10 M, 2.2 equiv), and THF (11.0 mL, 0.075 M). The crude product was purified by flash column chromatography (28% EtOAc/Hexanes) to afford the pure compound as a yellowish white solid (0.097 g, 65%).

TLC R_f : 0.21 in 28% EtOAc/Hexanes.

^{1}H NMR (600 MHz, DMSO-*d*$_6$) δ 11.26 (s, 1H), 7.88 (dd, *J* = 7.7, 1.6 Hz, 1H), 7.60 (ddd, *J* = 7.5, 1.6, 1.4 Hz, 1H), 7.48 (ddd, *J* = 7.7, 1.6, 1.4 Hz, 1H), 7.35 (dd, *J* = 7.5, 1.4 Hz, 1H), 5.07 (s, 2H).

^{13}C NMR (101 MHz, DMSO-*d*$_6$) δ 165.3 (C), 137.9 (C), 132.9 (CH), 128.1 (CH), 126.3 (CH), 125.8 (C), 124.1 (CH), 70.1 (CH_2).

HRMS (ESI): Exact mass calcd for $C_8H_7NO_2Na$ $[M+Na]^+$ 172.0374. Not found.*

*Detailed analysis of the HRMS data obtained using TOF MS ES+ shows similar peaks being present for five molecules with different molecular weights, and three different types of structures. Thus, it is not possible to retrieve LRMS data, and further analysis will be carried out by Mr. Frederic Vuillermet.

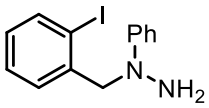

***N*-(2-Iodobenzyl)-*N*-phenylhydrazine 12**

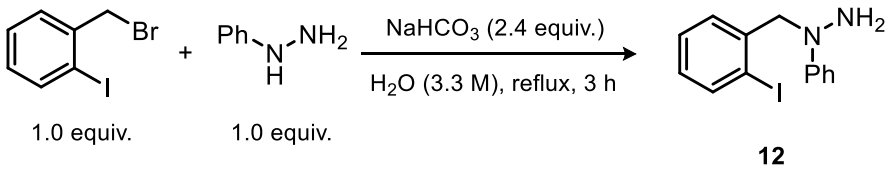

The title compound was synthesized following a modified literature procedure.[214] In a 100 mL round bottom flask equipped with a stir bar phenylhydrazine (0.49 mL, 5.0 mmol., 1.0 equiv) was dissolved in distilled water (1.5 mL, 3.3 M) at room temperature. Then $NaHCO_3$ (1.01 g, 12.0 mmol, 2.4 equiv) was added to the reaction flask, followed by 2-iodobenzyl bromide (1.48 g, 5.0 mmol, 1.0 equiv), then the reaction was allowed to stir at reflux for 3 h. The reaction progress was monitored by TLC and stopped upon completion, as gauged by consumption of the 2-iodobenzyl bromide. The reaction mixture contents were transferred into a separatory funnel by rinsing the round bottom flask with Et_2O. After the mixture contents separated, the organic layer was reserved, and the aqueous layer was extracted with Et_2O (x 3), then the combined organic layers were washed with brine (x 1). The organic layer was then dried over anhydrous Na_2SO_4, filtered, and concentrated under reduced pressure. The crude product was purified using silica-gel flash column chromatography using 10% EtOAc/Hexanes, to yield the purified product as yellow oil (1.1 g, 68%).

TLC R_f : 0.42 in 20% EtOAc/Hexanes.

^{1}H NMR (600 MHz, DMSO-d_6) δ 7.87 – 7.85 (m, 1H), 7.30 (dd, *J* = 7.5, 1.3 Hz, 1H), 7.16 – 7.11 (m, 3H), 7.02 – 7.00 (m, 1H), 6.85 – 6.83 (m, 2H), 6.63 (dd, *J* = 7.5, 1.5 Hz, 1H), 4.50 (s, 2H).

^{13}C NMR (151 MHz, DMSO-d_6) δ 151.5 (C), 139.8 (C), 139.5 (C), 129.3 (CH), 129.0 (CH), 128.5 (CH), 128.5 (CH), 117.2 (CH), 112.3 (CH), 98.7 (CH), 64.6 (CH_2).

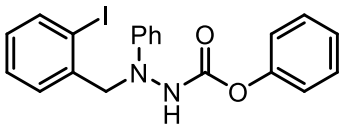

Phenyl 2-(*o*-iodobenzyl)-2-phenyl hydrazinecarboxylate 13

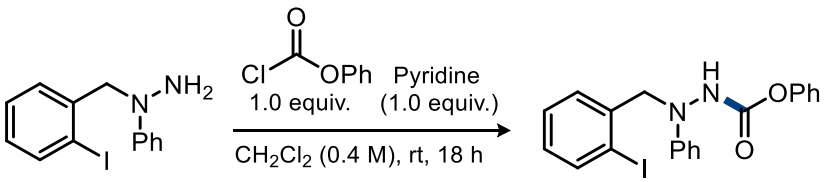

12 **13**

The title compound was synthesized following a modified literature procedure.[112] To a 250 mL round bottom flask equipped with a stir bar was added *N*-(2-Iodobenzyl)-*N*-phenylhydrazine **12** (1.1 g, 3.4 mmol, 1.0 equiv) followed by dilution with CH_2Cl_2 (8.5 mL, 0.4 M) and cooled to 0 °C. To this stirred solution was added pyridine (0.32 mL, 4.0 mmol, 1.2 equiv). After addition of pyridine, the solution was allowed to stir at 0 °C for 10 minutes. Then phenylchloroformate (0.5 mL, 3.4 mmol, 1.0 equiv) was added dropwise at 0 °C, and the reaction mixture was allowed to stir for overnight (18 h) at room temperature. The mixture was characterized by TLC with 17% EtOAc/Hexanes eluent. Upon completion, the reaction was extracted using sat. $NaHCO_3$ (x 2) and then brine (x 1). The organic phase was dried over anhydrous Na_2SO_4 and filtered over a fritted funnel. The filtrate was concentrated via rotary evaporation and purified using silica-gel flash column chromatography using 14% EtOAc/Hexanes to afford the pure compound as a yellowish white solid (0.98 g, 65%).

TLC R_f : 0.35 in 17% EtOAc/Hexanes.

^{1}H NMR (600 MHz, DMSO-d_6) δ 10.15 (s, 1H), 7.91 (dd, *J* = 7.9, 1.1 Hz, 1H), 7.51 (dd, *J* = 7.7, 1.2 Hz, 1H), 7.41 – 7.38 (m, 3H), 7.26 -7.22 (m, 3H), 7.14 – 7.13 (m, 2H), 7.09 – 7.06 (m, 1H), 6.83 – 6.80 (m, 3H), 4.67 (s, 2H).

^{13}C NMR (151 MHz, DMSO-d_6) δ 154.3 (C), 150.6 (C), 148.7 (C), 139.2 (CH), 139.1 (C), 129.5 (CH), 129.3 (CH), 129.2 (CH), 128.4 (CH), 125.5 (CH), 121.8 (CH), 119.2 (CH), 113.1 (C), 112.6 (CH), 99.0 (CH), 61.9 (CH_2).

HRMS (ESI): Exact mass calcd for $C_{20}H_{17}IN_2O_2Na$ $[M+Na]^+$ 467.0232. Found: 467.0237.

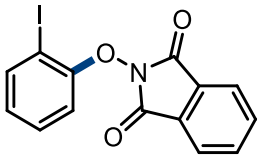

2-(2-Iodophenoxy)isoindole-1,3-dione 14

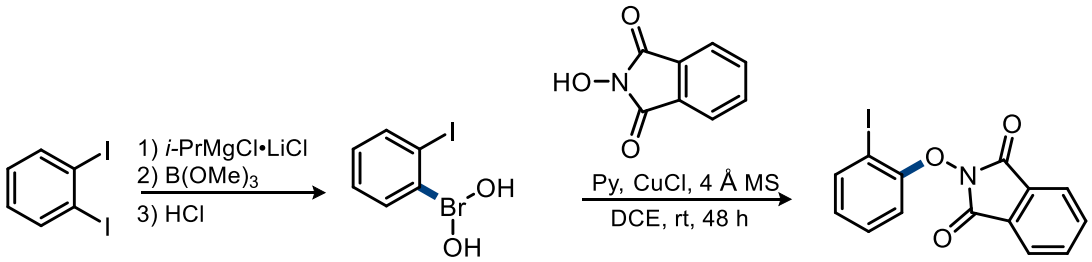

The title compound was synthesized following literature procedure.[216] An oven dried, and argon flushed 250 mL RBF, equipped with a magnetic stir bar, was charged with 1,2-diiodobenzene (3.3 g, 10.0 mmol, 1.0 equiv), and then was sealed. THF (50 mL) and Et_2O (50 mL) (0.10 M) were added sequentially via syringe. The reaction mixture was cooled in dry ice/acetone bath for 10 minutes, then isopropylmagnesium chloride lithium chloride **1D** (9.1 mL, 1.10 M, 1.0 equiv) was added dropwise via a syringe. At -78 °C, trimethyl borate (3.4 mL, 30.0 mmol, 3.0 equiv) was added to the reaction mixture, and the temperature was gradually raised to room temperature, then the reaction mixture was allowed to stir at room temperature for overnight. Hydrochloric acid (100 mL, 10% v/v) was added, and the reaction mixture was stirred for 30 minutes, then the content of the flask was transferred to a 1 L separatory funnel and the two layers were separated. The aqueous layer was extracted with Et_2O (x 3), then the combined organic layer was washed with brine (x 1), dried over anhydrous Na_2SO_4 and filtered over a fritted funnel. The filtrate was concentrated via rotary evaporation and the crude was purified using silica-gel flash column chromatography using 25% EtOAc/Hexanes to yield the boronic acid **X** as white solid (1.75 g, 70%). The **second step** of the reaction: A 100 mL RBF equipped with a magnetic stir bar was charged with *N*-hydroxyphthalimide (0.365 g, 2.0 mmol, 1.0 equiv) and dissolved in 1,2-dichloroethane (10 mL, 0.2 M) and was allowed to stir at room temperature. Boronic acid **X** from the previous step (1.00 g, 4.0 mmol, 2.0

equiv) was added to the reaction mixture followed by CuCl (0.198 g, 2.0 mmol, 1.0 equiv). Activated 4 Å molecular sieves were added followed by pyridine (0.17 mL, 2.2 mmol, 1.1 equiv), then the reaction mixture was allowed to stir at room temperature for 48 hours. The reaction mixture was diluted with CH_2Cl_2, filtered over a fritted funnel, washed with CH_2Cl_2 (x 3), concentrated via rotary evaporation and the crude was purified by crystallization from CH_2Cl_2/hexanes mixture to yield compound **14** as white solid (0.547 g, 75%).

TLC R_f : 0.57 in 40% EtOAc/Hexanes.

^{1}H NMR (400 MHz, DMSO-d_6) δ 7.97 – 7.88 (m, 5H), 7.36 – 7.29 (m, 2H), 6.97 – 6.93 (m, 1H).

^{13}C NMR (101 MHz, DMSO-d_6) δ 162.6 (C), 157.1 (C), 139.6 (C), 135.2 (C), 130.1 (CH), 128.8 (CH), 126.0 (CH), 123.8 (CH), 112.7 (CH), 81.0 (CH).

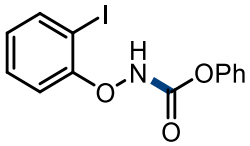

Phenyl (2-iodophenoxy)carbamate 15

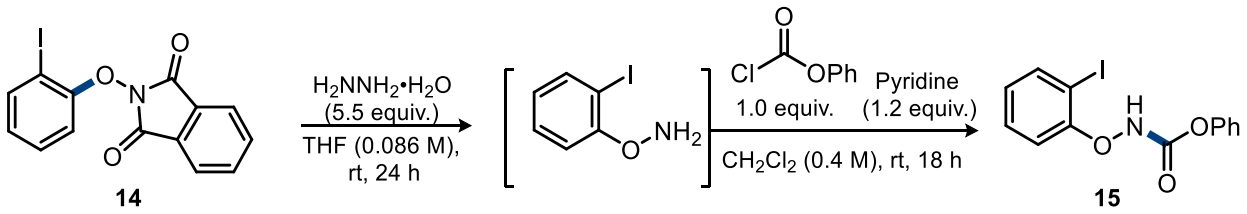

The title compound was synthesized following the literature procedure. A 100 mL RBF equipped with a magnetic stir bar was charged with2-(2-Iodophenoxy)isoindole-1,3-dione **14** (0.530 g, 1.45 mmol, 1.0 equiv) and dissolved in THF (16.9 mL, 0.086 M). The mixture was kept to stir for 10 min to fully dissolve then hydrazine monohydrate (0.39 mL, 7.97 mmol, 5.5 equiv) was added through a syringe to the vigorously stirred solution and the color was changed to a light-yellow. The reaction was allowed to stir for 24 h at room temperature. The solvent was evaporated under reduced pressure, then CH_2Cl_2 (10 mL) was added to the reaction mixture, layers were separated, and the combined organic layer was then washed with water (x 2) and brine (x 1). The organic layer was then dried over anhydrous Na_2SO_4, and solvent was evaporated to yield the product as an off-white oil in 90%, which was used for the subsequent step without further purification. The second step of the reaction: To a 50 mL round bottom flask equipped with a stir bar was added *O*-(2-iodophenyl)hydroxylamine from the previous step (0.306 g, 1.3 mmol, 1.0 equiv)

followed by dilution with CH_2Cl_2 (3.2 mL, 0.4 M) and cooled to 0 °C. To this stirred solution was added pyridine (0.12 mL, 1.56 mmol, 1.2 equiv). After addition of pyridine, the solution was allowed to stir at 0 °C for 0.5 h. Then phenylchloroformate (0.19 mL, 1.3 mmol, 1.0 equiv) was added dropwise at 0 °C, and the reaction mixture was allowed to stir for overnight (18 h) at room temperature. The mixture was characterized by TLC with 25% EtOAc/Hexanes eluent. Upon completion, the reaction was extracted using sat. $NaHCO_3$ (x 2) and then brine (x 1). The organic phase was dried over anhydrous Na_2SO_4 and filtered over a fritted funnel. The filtrate was concentrated via rotary evaporation and purified using silica-gel flash column chromatography using 25% EtOAc/Hexanes to give the pure compound as off-white solid (0.263 g, 57%).

TLC R_f : 0.16 in 25% EtOAc/Hexanes.

^{1}H NMR (300 MHz, DMSO-d_6) δ 10.89 (s, 1H), 8.02 – 7.4 (m, 4H), 7.47 – 7.42 (m, 2H), 7.31 – 7.26 (m, 1H), 7.23 – 7.20 (m, 2H).

^{13}C NMR (151 MHz, DMSO-d_6) δ 165.2 (C), 153.6 (C), 150.3 (C), 135.6 (CH), 129.8 (CH), 129.5 (C), 129.3 (CH), 126.1 (CH), 124.1 (CH), 121.5 (CH), 115.3 (CH).

Claims to Original Research

1) The first C-C bond forming stoichiometric organometallic addition to masked *O*- and *N*-isocyanates has been described.
2) A relatively stable five-membered chelate is suggested as a key reactivity controlling factor for stoichiometric organometallic addition to masked heteroatom-substituted isocyanates.
3) A novel synthesis of pyrazolones from intramolecular cyclization of hydrazone carboxylate precursors mediated by Grignard reagents is reported.
4) The synthesis of iodinated masked heteroatom-substituted isocyanates to serve as precursors for intramolecular cyclizations is reported.
5) The development of a novel heterocyclic synthesis via intramolecular cyclization of iodinated masked heteroatom-substituted isocyanates enabled by amphoteric metalated *O*-isocyanate intermediate is reported.

Publications from this Work

1) **Synthesis of Hydroxamic Acid Derivatives Using Masked *O*-Isocyanates and Organomagnesium Reagents.** Manuscript in preparation.
2) **A Direct Synthesis of Pyrazolones from Hydrazones Enabled by an Amphoteric Metalated *N*-Isocyanate Intermediate.** Manuscript in preparation.

Presentations from this Work

Oral Presentations (* indicates presenter)

1) **New Reactions of Masked Isocyanates with Organometallic Reagents.** Mohamed, A. M.*; Vuillermet, F.; Gill, M.; Beauchemin, A. M. Ottawa-Carleton Chemistry Institute Day. May 31, 2023.
2) **New Reactions of Masked Isocyanates with Organometallic Reagents.** Mohamed, A. M.*; Vuillermet, F.; Gill, M.; Beauchemin, A. M. QOMSBOC. November 10-12, 2023.

Poster Presentations (* indicates presenter)

1) **Development of a New Linchpin Reagent Towards the Modular Synthesis of Amides.** Uppalapati, B*; Mohamed, A. M.; Aubry, M.; Beauchemin, A. M. QOMSBOC. October 14-16, 2022.
2) **Synthesis of Pyrazolones by Cyclisation of *N*-Isocyanate Precursors.** Vuillermet, F.*; Mohamed, A. M.; Gill, M.; Beauchemin, A. M. QOMSBOC. November 10-12, 2023.
3) **Synthesis of Pyrazolones by Cyclisation of *N*-Isocyanate Precursors.** Vuillermet, F.*; Mohamed, A. M.; Gill, M.; Beauchemin, A. M. Paraza, 2023.

References

[1] Von Wurtz, A. Ueber Die Verbindungen Der Cyanursäure Und Cyansäure Mit Aethyloxyd, Methyloxyd, Amyloxyd Und Die Daraus Entstehenden Producte; Acetyl- Und Metacetylharnstoff, Methylamin, Aethylamin, Valeramin. *Liebigs Ann.* **1849**, *71*, 326–342.

[2] Bayer, O. Das Di-Isocyanat-Polyadditionsverfahren (Polyurethane). *Angew. Chem.* **1947**, *59*, 257–272.

[3] Sardon, H.; Engler, A. C.; Chan, J. M. W.; García, J. M.; Coady, D. J.; Pascual, A.; Mecerreyes, D.; Jones, G. O.; Rice, J. E.; Horn, H. W.; Hedrick, J. L. Organic Acid-Catalyzed Polyurethane Formation via a Dual-Activated Mechanism: Unexpected Preference of *N*-Activation over *O*-Activation of Isocyanates. *J. Am. Chem. Soc.* **2013**, *135*, 16235–16241.

[4] C. Six, F. Richter "Isocyanates, Organic", Ullmann's Encyclopedia of Industrial Chemistry, Electronic Release, vol. 20, Wiley-VCH, Weinheim 2003.

[5] Richter, R.; Ulrich, H. Syntheses and Preparative Applications of Isocyanates. In *Cyanates and Their Thio Derivatives*, Patai, S., Ed.; PATAI'S Chemistry of Functional Groups, Vol. 2; Wiley: United Kingdom, 1977; 619-818.

[6] Muranaka, R.; Liu, Y.; Okada, I.; Okazoe, T.; Tsuda, A. Photo-on-Demand Phosgenation Reactions with Chloroform for Selective Syntheses of *N*-Substituted Ureas and Isocyanates. *ACS Omega*. **2022**, *7*, 5584–5594.

[7] Guo, Z.; Ding, X.; Wang, Y. How To Get Isocyanate? *ACS Omega*. **2024**, *9*, 11168–11180.

[8] Boros, R. Z.; Koós, T.; Wafaa, C.; Nehéz, K.; Farkas, L.; Viskolcz, B.; Szőri, M. A Theoretical Study on the Phosgenation of Methylene Diphenyl Diamine (MDA). *Chem. Phys. Lett.* **2018**, *706*, 568–576.

[9] Mattke, T.; Olbert, G.; Knoesche, C.; Schelling, H. Method for Producing Diisocyanates by Gas-Phase Phosgenation. US8716517B2, August 10, 2010.

[10] Ferretti, F.; Ragaini, F.; Lariccia, R.; Gallo, E.; Cenini, S. New Nonsymmetric Phenanthrolines as Very Effective Ligands in the Palladium-Catalyzed Carbonylation of Nitrobenzene. *Organometallics*. **2010**, *29*, 1465–1471.

[11] Mooibroek, T. J.; Schoon, L.; Bouwman, E.; Drent, E. Carbonylation of Nitrobenzene in Methanol with Palladium Bidentate Phosphane Complexes: An Unexpectedly Complex Network of Catalytic Reactions, Centred around a Pd–Imido Intermediate. *Chem. Eur. J.* **2011**, *17*, 13318–13333.

[12] Nguyen, T. T.; Tran, A. V.; Lee, H. J.; Baek, J.; Kim, Y. J. Palladium-Catalyzed Reductive Carbonylation of Nitrobenzene for Producing Phenyl Isocyanate. *Tetrahedron Lett.* **2019**, *60*, 151310.

[13] Cao, Y.; He, L. Synthesis of Carbonyl Compounds by Gold-Catalyzed Carbonylation Reactions. *Synlett*. **2022**, *33*, 1003–1010.

[14] Knölker, H. -J; Braxmeier, T.; Schlechtingen, G. A Novel Method for the Synthesis of Isocyanates Under Mild Conditions. *Angew. Chem. Int. Ed.* **1995**, *34*, 2497–2500.

[15] Kreye, O.; Mutlu, H.; Meier, M. A. R. Sustainable Routes to Polyurethane Precursors. *Green Chem.* **2013**, *15*, 1431–1455.

[16] Li, Z.; Mayer, R. J.; Ofial, A. R.; Mayr, H. From Carbodiimides to Carbon Dioxide: Quantification of the Electrophilic Reactivities of Heteroallenes. *J. Am. Chem. Soc.* **2020**, *142*, 8383–8402.

[17] Diirr, H.; Pauly, K.; Quast, H.; Ross, K.; Spiegel, E.; Peters, K.; uon, H. G.; Gerhard Hofle, B.; Steglich, W. 4-Dialkylaminopyridines as Highly Active Acylation Catalysts. *Angew. Chem., Int. Ed.* **1978**, *17*, 569–583.

[18] Sasaki, K.; Crich, D. Facile Amide Bond Formation from Carboxylic Acids and Isocyanates. *Org. Lett.* **2011**, *13*, 2256–2259.

[19] Peixoto, P. A.; Boulangé, A.; Ball, M.; Naudin, B.; Alle, T.; Cosette, P.; Karuso, P.; Franck, X. Design and Synthesis of Epicocconone Analogues with Improved Fluorescence Properties. *J. Am. Chem. Soc.* **2014**, *136*, 15248–15256.

[20] Yoshimitsu, T.; Matsuda, K.; Nagaoka, H.; Tsukamoto, K.; Tanaka, T. Radical Fixation of Functionalized Carbon Resources: α-sp^3 C-H Carbamoylation of Tertiary Amines with Aryl Isocyanates. *Org. Lett.* **2007**, *9*, 5115–5118.

[21] Blaise, E. Nouvelles Réactions de Dérivés Organométalliques. *Compt. Rend.* **1901**, *132*, 478–480.

[22] Gilman, H.; Furry, M. The Identification of Organomagnesium Halides by Crystalline Derivatives Prepared from α-Naphthyl Isocyanate. *J. Am. Chem. Soc.* **1928**, *50*, 1214–1216.

[23] Gilman, H.; Kinney, C. R. The Mechanism of the Reaction of Isocyanates and Isothiocyanates with the Grignard Reagent. *J. Am. Chem. Soc.* **1924**, *46*, 493–497.

[24] Gilman, H.; Marple, K. E. Relative Reactivities of Organometallic Compounds VI. Boron. *Recl. Trav. Chim. Pays-Bas.* **1936**, *55*, 76–79.

[25] Gilman, H.; Hofferth, B.; Melvin, H. W. The Preparation and Some Properties of Triphenylsilyl Isocyanate and Triphenylsilyl Isothiocyanate. *J. Am. Chem. Soc.* **1950**, *72*, 3045–3047.

[26] Field, L.; Lawson, J. E.; McFarland, J. W. Grignard Reagents of Sulfones. IV. Reactions with Nitriles, Esters and an Isocyanate. *J. Am. Chem. Soc.* **1956**, *78*, 4389–4394.

[27] Parker, K. A.; Gibbons, E. G. A Direct Synthesis of Primary Amides from Grignard Reagents. *Tetrahedron Lett.* **1975**, *16*, 981–984.

[28] Padwa, A.; Crawford, K. R.; Rashatasakhon, P.; Rose, M. Several Convenient Methods for the Synthesis of 2-Amido Substituted Furans. *J. Org. Chem.* **2003**, *68*, 2609–2617.

[29] Chorell, E.; Das, P.; Almqvist, F. Diverse Functionalization of Thiazolo Ring-Fused 2-Pyridones. *J. Org. Chem.* **2007**, *72*, 4917–4924.

[30] Lygin, A. V.; De Meijere, A. Ortho-Lithiophenyl Isocyanide: A Versatile Precursor for 3H-Quinazolin-4-Ones and 3H-Quinazolin-4-Thiones. *Org. Lett.* **2009**, *11*, 389–392.

[31] Schade, M. A.; Manolikakes, G.; Knochel, P. Preparation of Primary Amides from Functionalized Organozinc Halides. *Org. Lett.* **2010**, *12*, 3648–3650.

[32] Hill, M. S.; Liptrot, D. J.; Mahon, M. F. A Magnesium-Mediated Cascade Assembly for the Atom-Economical Synthesis of Bis(Imidazolidine-2,4-Dione)s. *Angew. Chem. Int. Ed.* **2013**, *125*, 5472–5475.

[33] Geri, J. B.; Wade Wolfe, M. M.; Szymczak, N. K. Borazine-CF_3– Adducts for Rapid, Room Temperature, and Broad Scope Trifluoromethylation. *Angew. Chem. Int. Ed.* **2018**, *130*, 1395–1399.

[34] Pace, V.; Monticelli, S.; De La Vega-Hernández, K.; Castoldi, L. Isocyanates and Isothiocyanates as Versatile Platforms for Accessing (Thio)Amide-Type Compounds. *Org. Biomol. Chem.* **2016**, *14*, 7848–7854.

[35] Schäfer, G.; Matthey, C.; Bode, J. W. Facile Synthesis of Sterically Hindered and Electron-Deficient Secondary Amides from Isocyanates. *Angew. Chem. Int. Ed.* **2012**, *51*, 9173–9175.

[36] Antczak, M. I.; Ready, J. M. Two-, Three- and Four-Component Coupling to Form Isoquinolones Based on Directed Metalation. *Chem. Sci.* **2012**, *3*, 1450–1454.

[37] Pace, V.; Castoldi, L.; Holzer, W. Addition of Lithium Carbenoids to Isocyanates: A Direct Access to Synthetically Useful *N*-Substituted 2-Haloacetamides. *Chem. Commun.* **2013**, *49*, 8383–8385.

[38] Pace, V.; Castoldi, L.; Mamuye, A. D.; Holzer, W. Homologation of Isocyanates with Lithium Carbenoids: A Straightforward Access to α-Halomethyl- and α,α-Dihalomethylamides. *Synthesis* **2014**, *46*, 2897–2909.

[39] Pace, V.; Castoldi, L.; Monticelli, S.; Safranek, S.; Roller, A.; Langer, T.; Holzer, W. A Robust, Eco-Friendly Access to Secondary Thioamides through the Addition of Organolithium Reagents to Isothiocyanates in Cyclopentyl Methyl Ether (CPME). *Chem. Eur. J.* **2015**, *21*, 18966–18970.

[40] Pulis, A. P.; Varela, A.; Citti, C.; Songara, P.; Leonori, D.; Aggarwal, V. K. Asymmetric Synthesis of Tertiary Alcohols and Thiols via Nonstabilized Tertiary α-Oxy- and α-Thio-Substituted Organolithium Species. *Angew. Chem. Int. Ed*. **2017**, *56*, 10835–10839.

[41] Pace, V.; De La Vega-Hernández, K.; Urban, E.; Langer, T. Chemoselective Schwartz Reagent Mediated Reduction of Isocyanates to Formamides. *Org. Lett.* **2016**, *18*, 2750–2753.

[42] Williams, J. D.; Kerr, W. J.; Leach, S. G.; Lindsay, D. M. A Practical and General Amidation Method from Isocyanates Enabled by Flow Technology. *Angew. Chem. Int. Ed.* **2018**, *57*, 12126–12130.

[43] Kim, H.; Lee, H. J.; Kim, D. P. Integrated One-Flow Synthesis of Heterocyclic Thioquinazolinones through Serial Microreactions with Two Organolithium Intermediates. *Angew. Chem. Int. Ed.* **2015**, *54*, 1877–1880.

[44] Wicks, Z. W. Blocked Isocyanates. *Prog. Org. Coat.* **1975**, *3*, 73–99.

[45] Wicks, D. A.; Wicks, Z. W. Blocked Isocyanates III: Part B: Uses and Applications of Blocked Isocyanates. *Prog. Org. Coat.* **2001**, *41*, 1–83.

[46] Rolph, M. S.; Markowska, A. L. J.; Warriner, C. N.; O'Reilly, R. K. Blocked Isocyanates: From Analytical and Experimental Considerations to Non-Polyurethane Applications. *Polym. Chem.* **2016**, *7*, 7351–7364.

[47] Wicks, D. A.; Wicks, Z. W. Blocked Isocyanates III: Part A. Mechanisms and Chemistry. *Prog. Org. Coat.* **1999**, *36*, 148–172.

[48] Wicks, D. A.; Wicks, Z. W. Multistep Chemistry in Thin Films; the Challenges of Blocked Isocyanates. *Prog. Org. Coat.* **2001**, *43*, 131–140.

[49] Delebecq, E.; Pascault, J. P.; Boutevin, B.; Ganachaud, F. On the Versatility of Urethane/Urea Bonds: Reversibility, Blocked Isocyanate, and Non-Isocyanate Polyurethane. *Chem. Rev.* **2013**, *113*, 80–118.

[50] Nasar, A. S.; Kalaimani, S. Synthesis and Studies on Forward and Reverse Reactions of Phenol-Blocked Polyisocyanates: An Insight into Blocked Isocyanates. *RSC Adv.* **2016**, *6*, 76802–76812.

[51] Kothandaraman, H.; Nasar, A. S. The Thermal Dissociation of Phenol-Blocked Toluene Diisocyanate Crosslinkers. *Polymer* **1993**, *34*, 610–615.

[52] Jana, S.; Samanta, D.; Fahad, M.; Jaisankar, S. N.; Kim, H. Blocking and Deblocking of Diisocyanate to Synthesize Polyurethanes. *Polymers* **2021**, *13*, 2875.

[53] Knospe, P.; Reichmann, R.; Gutmann, J. S.; Dornbusch, M. Vanillin as Low-Temperature Isocyanate-Blocking Agent and Its Use in One-Component Aqueous Coatings. *J. Coat. Technol. Res.* **2023**, *20*, 501–520.

[54] Bajji, A. C.; Sundaram, M.; Myszka, D. G.; Davis, D. R. An RNA Complex of the HIV-1 A-Loop and TRNALys,3 Is Stabilized by Nucleoside Modifications. *J. Am. Chem. Soc.* **2002**, *124,* 14302–14303.

[55] Wang, W.; Xu, S.; Duan, Y.; Liu, X.; Li, X.; Wang, C.; Zhao, B.; Zheng, P.; Zhu, W. Synthesis and Bioevaluation and Doking Study of 1H-Pyrrolo[2,3-b]Pyridine Derivatives Bearing Aromatic Hydrazone Moiety as c-Met Inhibitors. *Eur. J. Med. Chem.* **2018**, *145*, 315–327.

[56] Qi, B.; Yang, Y.; Gong, G.; He, H.; Yue, X.; Xu, X.; Hu, Y.; Li, J.; Chen, T.; Wan, X.; Zhang, A.; Zhou, G. Discovery of N^1-(4-((7-(3-(4-Ethylpiperazin-1-Yl)Propoxy)-6-Methoxyquinolin-4-Yl)Oxy)-3,5-Difluorophenyl)-N^3-(2-(2,6-Difluorophenyl)-4-Oxothiazolidin-3-Yl)Urea as a Multi-Tyrosine Kinase Inhibitor for Drug-Sensitive and Drug-Resistant Cancers Treatment. *Eur. J. Med. Chem.* **2019**, *163*, 10–27.

[57] Wang, C.; Xu, S.; Peng, L.; Zhang, B.; Zhang, H.; Hu, Y.; Zheng, P.; Zhu, W. Design, Synthesis and Biological Evaluation of Novel 4-Anlinoquinazoline Derivatives as EGFR Inhibitors with the Potential to Inhibit the Gefitinib-Resistant Nonsmall Cell Lung Cancers. *J. Enzyme Inhib. Med. Chem.* **2019**, *34*, 204–218.

[58] Vinogradova, E. V.; Fors, B. P.; Buchwald, S. L. Palladium-Catalyzed Cross-Coupling of Aryl Chlorides and Triflates with Sodium Cyanate: A Practical Synthesis of Unsymmetrical Ureas. *J. Am. Chem. Soc.* **2012**, *134*, 11132–11135.

[59] Vinogradova, E. V.; Park, N. H.; Fors, B. P.; Buchwald, S. L. Palladium-Catalyzed Synthesis of *N*-Aryl Carbamates. *Org. Lett.* **2013**, *15*, 1394–1397.

[60] Kubota, K.; Dai, P.; Pentelute, B. L.; Buchwald, S. L. Palladium Oxidative Addition Complexes for Peptide and Protein Cross-Linking. *J. Am. Chem. Soc.* **2018**, *140*, 3128–3133.

[61] Raspoet, G.; Nguyen, M. T.; McGarraghy, M.; Hegarty, A. F. The Alcoholysis Reaction of Isocyanates Giving Urethanes: Evidence for a Multimolecular Mechanism. *J. Org. Chem.* **1998**, *63*, 6878–6885.

[62] Rawling, T.; McDonagh, A. M.; Tattam, B.; Murray, M. Synthesis of Unsymmetrical Biaryl Ureas from *N*-Carbamoylimidazoles: Kinetics and Application. *Tetrahedro*n **2012**, *68*, 6065–6070.

[63] Duspara, P. A.; Islam, M. S.; Lough, A. J.; Batey, R. A. Synthesis and Reactivity of *N* -Alkyl Carbamoylimidazoles: Development of *N*-Methyl Carbamoylimidazole as a Methyl Isocyanate Equivalent. *J. Org. Chem.* **2012**, *77*, 10362–10368.

[64] Duspara, P. A.; Batey, R. A. A Short Total Synthesis of the Marine Sponge Pyrrole-2-Aminoimidazole Alkaloid (±)-Agelastatin A. *Angew. Chem. Int. Ed.* **2013**, *52*, 10862–10866.

[65] Gante, J. Peptid- Und Azapeptid-Synthesen Mittels Neuer *N*-Aktivierter Aminosäure-Derivat. *Chem Ber.* **1966**, *99*, 1576–1579.

[66] Gertzmann, R.; Gürtler, C. A Catalyst System for the Formation of Amides by Reaction of Carboxylic Acids with Blocked Isocyanates. *Tetrahedron Lett.* **2005**, *46*, 6659–6662.

[67] Suppo, J.-S.; Subra, G.; Bergès, M.; Marcia De Figueiredo, R.; Campagne, J.-M. Inverse Peptide Synthesis via Activated α-Aminoesters. *Angew. Chem. Int. Ed.* **2014**, *53*, 5389–5393.

[68] Lim, D. S. W.; Lew, T. T. S.; Zhang, Y. Direct Amidation of *N*-Boc- and *N*-Cbz-Protected Amines via Rhodium-Catalyzed Coupling of Arylboroxines and Carbamates. *Org. Lett.* **2015**, *17*, 6054–6057.

[69] Derasp, J. S.; Beauchemin, A. M. Rhodium-Catalyzed Synthesis of Amides from Functionalized Blocked Isocyanates. *ACS Catal*. **2019**, *9*, 8104–8109.

[70] Latorre, A.; Rodríguez, S.; Izquierdo, J.; González, F. V. Amidation through Carbamates. *Tetrahedron Lett*. **2009**, *50*, 2653–2655.

[71] Schäfer, G.; Bode, J. W. Synthesis of Sterically Hindered *N*-Acylated Amino Acids from *N*-Carboxyanhydrides. *Org. Lett.* **2014**, *16*, 1526–1529.

[72] Smith, S. N.; Connon, S. J. *N*-Carboxyanhydrides (NCAs): Unorthodox and Useful Reagents for Amide Synthesis. *Eur. J. Org. Chem.* **2024**, *27*, e202301032.

[73] Mampuys, P.; Ruijter, E.; Orru, R. V. A.; Maes, B. U. W. Synthesis of Secondary Amides from Thiocarbamates. *Org. Lett.* **2018**, *20*, 4235–4239.

[74] Zhu, L.; Le, L.; Yan, M.; Au, C. T.; Qiu, R.; Kambe, N. Carbon-Carbon Bond Formation of Trifluoroacetyl Amides with Grignard Reagents via C(O)-CF_3 Bond Cleavage. *J. Org. Chem.* **2019**, *84*, 5635–5644.

[75] Wentrup, C.; J. Finnerty, J.; Koch, R. Amino-, Alkoxy-, and Alkylthio-Isocyanates and -Isothiocyanates, RX-NCY, Their Isomers RX-YCN and RX-CNY, and Their Rearrangements. *Curr. Org. Chem.* **2012**, *15*, 1745–1759.

[76] Reichen, W. Oxygen-, Nitrogen-, and Sulfur-Substituted Heteroallenes. *Chem. Rev.* **1978**, *78*, 569–588.

[77] Stollé, R. Über Die Curtius'sche Umlagerung Bei Carbaminsäureaziden: Bildung von Indazolonen Und Dimolekularen Carbonylhydrazinen. *J. Prakt. Chem.* **1927**, *116*, 192–204.

[78] Lwowski, W.; DeMauriac, R.; Mattingly, T. W.; Scheiffele, E. Curtius-Rearrangement of "Rigid" Azides. *Tetrahedron Lett.* **1964**, *5*, 3285–3288.

[79] Stollé, R.; Merkle, M. 191. Über Die Curtius'sche Umlagerung Bei Carbaminsäureaziden: Bildung von Indazolonen Und Dimolekularen Carbonylhydrazinen. *J. Prakt. Chem.* **1928**, *119*, 275–278.

[80] Lockley, W. J. S.; Lwowski, W. Cyclic Aminimides Containing the Pyrazolone Skeleton. *Tetrahedron Lett.* **1974**, *15*, 4263–4266.

[81] Lwowski, W.; Kanemasa, S.; Murray, R. A.; Ramakrishnan, V. T.; Thiruvengadam, T. K.; Yoshida, K.; Subbaraj, A. The Photolysis of Carbamoyl Azides in the Presence of Carbodiimides. *J. Org. Chem.* **1986**, *51*, 1719–1723.

[82] Gibson, H. H.; Weissinger, K.; Abashawl, A.; Hall, G.; Lawshae, T.; LeBlanc, K.; Moody, J.; Lwowski, W. Photolysis of Dimethylcarbamoyl Azide in the Presence of a Cyclic Aminimide. *J. Org. Chem.* **1986**, *51*, 3858–3861.

[83] Jones, D. W. Generation of an *N*-Isocyanatoimine and Its Cycloadditions Leading to Sterically Stabilised Zwitterions. *J. Chem. Soc. Chem. Commun.* **1982**, 766–768.

[84] Roveda, J. G.; Clavette, C.; Hunt, A. D.; Gorelsky, S. I.; Whipp, C. J.; Beauchemin, A. M. Hydrazides as Tunable Reagents for Alkene Hydroamination and Aminocarbonylation. *J. Am. Chem. Soc.* **2009**, *131*, 8740–8741.

[85] Clavette, C.; Gan, W.; Bongers, A.; Markiewicz, T.; Toderian, A. B.; Gorelsky, S. I.; Beauchemin, A. M. A Tunable Route for the Synthesis of Azomethine Imines and β-Aminocarbonyl Compounds from Alkenes. *J. Am. Chem. Soc.* **2012**, *134*, 16111–16114.

[86] Gan, W.; Moon, P. J.; Clavette, C.; Das Neves, N.; Markiewicz, T.; Toderian, A. B.; Beauchemin, A. M. Synthesis and Reactivity of Unsymmetrical Azomethine Imines Formed Using Alkene Aminocarbonylation. *Org. Lett.* **2013**, *15*, 1890–1893.

[87] Garland, K.; Gan, W.; Depatie-Sicard, C.; Beauchemin, A. M. A Practical Approach to Semicarbazone and Hydrazone Derivatives via Imino-Isocyanates. *Org. Lett.* **2013**, *15*, 4074–4077.

[88] Clavette, C.; Rocan, J.-F. V.; Beauchemin, A. M. Diversity-Oriented Synthesis of Hydrazine-Derived Compounds from Amino Isocyanates Generated *In Situ*. *Angew. Chem. Int. Ed.* **2013**, *52*, 12705–12708.

[89] Elkaeed, E. B.; An, J.; Beauchemin, A. M. Synthesis of Indazolones via Friedel-Crafts Cyclization of Blocked (Masked) *N*-Isocyanates. *J. Org. Chem.* **2017**, *82*, 9890–9897.

[90] Bongers, A.; Clavette, C.; Gan, W.; Gorelsky, S. I.; Betit, L.; Lavergne, K.; Markiewicz, T.; Moon, P. J.; Neves, N. Das; Obhi, N. K.; Toderian, A. B.; Beauchemin, A. M. Intermolecular Aminocarbonylation of Alkenes Using Concerted Cycloadditions of Iminoisocyanates. *J. Org. Chem.* **2017**, *82*, 1175–1194.

[91] Vincent-Rocan, J.-F.; Clavette, C.; Leckett, K.; Beauchemin, A. M.; Vincent-Rocan, J.-F.; Clavette, C.; Leckett, K.; Beauchemin, A. M. A Cascade Synthesis of Aminohydantoins Using *In Situ*-Generated *N*-Substituted Isocyanates. *Chem. Eur. J.* **2015**, *21*, 3886–3890.

[92] Ivanovich, R. A.; Vincent-Rocan, J. F.; Elkaeed, E. B.; Beauchemin, A. M. One-Pot Synthesis of *Aza*-Diketopiperazines Enabled by Controlled Reactivity of *N*-Isocyanate Precursors. *Org. Lett.* **2015**, *17*, 4898–4901.

[93] Gagné-Monfette, W.; Vincent-Rocan, J. F.; Lutes, O. C.; O'Keefe, G. F.; Jeanneret, A. D. M.; Blanger, C.; Ivanovich, R. A.; Beauchemin, A. M. Investigation of Masked *N*-Acyl-*N*-Isocyanates: Support for Oxadiazolones as Blocked *N*-Isocyanate Precursors. *Chem. Eur. J*. **2021**, *27*, 14051–14056.

[94] Boissavy, T.; Rotili, D.; Mouveaux, T.; Roger, E.; Aliouat, E. M.; Pierrot, C.; Valente, S.; Mai, A.; Gissot, M. Hydroxamate-Based Compounds Are Potent Inhibitors of Toxoplasma Gondii HDAC Biological Activity. *Antimicrob. Agents Chemother.* **2023**, 67.

[95] Bertrand, S.; Hélesbeux, J.-J.; Larcher, G.; Duval, O. Hydroxamate, a Key Pharmacophore Exhibiting a Wide Range of Biological Activities. *Mini Rev. Med. Chem.* **2013**, *13*, 1311–1326.

[96] Citarella, A.; Moi, D.; Pinzi, L.; Bonanni, D.; Rastelli, G. Hydroxamic Acid Derivatives: From Synthetic Strategies to Medicinal Chemistry Applications. *ACS Omeg*a **2021**, *6*, 21843–21849.

[97] Bantscheff, M.; Hopf, C.; Savitski, M. M.; Dittmann, A.; Grandi, P.; Michon, A. M.; Schlegl, J.; Abraham, Y.; Becher, I.; Bergamini, G.; Boesche, M.; Delling, M.; Dümpelfeld, B.; Eberhard, D.; Huthmacher, C.; Mathieson, T.; Poeckel, D.; Reader, V.; Strunk, K.; Sweetman, G.; Kruse, U.; Neubauer, G.; Ramsden, N. G.; Drewes, G. Chemoproteomics Profiling of HDAC Inhibitors Reveals Selective Targeting of HDAC Complexes. *Nat. Biotechnol.* **2011**, *29*, 255–265.

[98] Lossen, W. Ueber Amidartige Derivate Des Hydroxylamins. 18. Ueber Das Auftreten Polymorpher Modificationen Bei Hydroxylaminderivaten. *Liebigs Ann.* **1894**, *281*, 169–305.

[99] Lossen, W. Ueber Die Structurformel Des Hydroxylamins Und Seiner Amidartigen Derivate. *Liebigs Ann.***1877**, *186*, 1–74.

[100] Lossen, W. Methode, Die Carboxylgruppe Aromatischer Säuren Durch Die Amidgruppe Zu Ersetzen. *Liebigs Ann.* **1875**, *175*, 271–304.

[101] Polat, D. E.; Brzezinski, D. D.; Beauchemin, A. M. Formation of Complex Hydrazine Derivatives via Aza-Lossen Rearrangement. *Org. Lett.* **2019**, *21*, 4849–4852.

[102] Hanessian, S.; Johnstone, S. Synthesis of Hydroxamic Esters via Alkoxyaminocarbonylation of β-Dicarbonyl Compounds. *J. Org. Chem.* **1999**, *64*, 5896–5903.

[103] Fioravanti, S.; Marchetti, F.; Morreale, A.; Pellacani, L.; Tardella, P. A. One-Pot Synthesis of Polyfunctionalized Cyclic Urea Derivatives. *Org. Lett.* **2003**, *5*, 1019–1021.

[104] Krause, J. G.; Leskiw, B. D.; Emery, M. L.; McGahan, M. E.; McCourt, M. P.; Priefer, R. Synthesis of Substituted *N*-Hydroxyureas via the *in Situ* Generation of *t*-Butoxy Isocyanate. *Tetrahedron Lett.* **2010**, *51*, 3568–3570.

[105] Baburaj, T.; Thambidurai, S. *N*-Boc-*O*-Tosyl Hydroxylamine as a Safe and Efficient Nitrogen Source for the *N*-Amination of Aryl and Alkyl Amines: Electrophilic Amination. *Synlett* **2011**, *22*, 1993–1996.

[106] Baburaj, T.; Thambidurai, S. *N*-Amination of Amino Acids and Its Derivatives Using *N*-Boc-*O*-Tosyl Hydroxylamine as an Efficient NH-Boc Transfer Reagent: Electrophilic Amination. *Tetrahedron Lett.* **2012**, *53*, 2292–2294.

[107] Baburaj, T.; Thambidurai, S. Corrigendum to '*N*-Amination of Amino Acids and Its Derivatives Using *N*-Boc-*O*-Tosyl Hydroxylamine as an Efficient NH-Boc Transfer Reagent: Electrophilic Amination' [*Tetrahedron Lett*. **2012**, *53*, 2292–2294]. *Tetrahedron Lett.* **2014**, *55*, 561–563.

[108] Baburaj, T.; Thambidurai, S. Erratum: *N*-Boc-*O*-Tosyl Hydroxylamine as a Safe and Efficient Nitrogen Source for the *N*-Amination of Aryl and Alkyl Amines: Electrophilic Amination [*Synlett* **2011**, *22*,1993-1996]. *Synlett* **2015**, *26*, 1137.

[109] Romine, J. L.; Martin, S. W.; Meanwell, N. A.; Epperson, J. R. Synthesis of 3-Hydroxypyrimidine-2,4-Diones. Addition of Anilines to Benzyloxy Isocyanate Synthons to Give *N*-Hydroxyureas. *Synthesis* **1994**, *1994*, 846–850.

[110] Berry, J. F.; Ferraris, D. V.; Duvall, B.; Hin, N.; Rais, R.; Alt, J.; Thomas, A. G.; Rojas, C.; Hashimoto, K.; Slusher, B. S.; Tsukamoto, T. Synthesis and SAR of 1-Hydroxy-1 *H* -Benzo[d]Imidazol-2(3 *H*)-Ones as Inhibitors of d -Amino Acid Oxidase. *ACS Med. Chem. Lett.* **2012**, *3*, 839–843.

[111] Ivanovich, R. A.; Polat, D. E.; Beauchemin, A. M. Oxygen-Substituted Isocyanates: Blocked (Masked) Isocyanates Enable Controlled Reactivity. *Adv. Synth. Catal.* **2017**, *359*, 4289–4293.

[112] Wang, Q.; An, J.; Alper, H.; Xiao, W. J.; Beauchemin, A. M. Catalytic Substitution/Cyclization Sequences of O-Substituted Isocyanates: Synthesis of 1-Alkoxybenzimidazolones and 1-Alkoxy-3,4-Dihydroquinazolin-2(1*H*)-Ones. *Chem. Commun.* **2017**, *53*, 13055–13058.

[113] Allen, M. A.; Ivanovich, R. A.; Polat, D. E.; Beauchemin, A. M. Synthesis of *N*-Oxyureas by Substitution and Cope-Type Hydroamination Reactions Using *O*-Isocyanate Precursors. *Org. Lett.* **2017**, *19*, 6574–6577.

[114] Allen, M. A.; Ivanovich, R. A.; Beauchemin, A. M. *O*-Isocyanates as Uncharged 1,3-Dipole Equivalents in [3+2] Cycloadditions. *Angew. Chem. Int. Ed.* **2020**, *59*, 23188–23197.

[115] Liu, Y.; Jacobs, H. K.; Gopalan, A. S. Reactions of *N*-Benzyloxycarbamate Derivatives with Stabilized Carbon Nucleophiles: A New Synthetic Approach to Polyhydroxamic Acids and Other Hydroxamate-Containing Mixed Ligand Systems. *J. Org. Chem.* **2009**, *74*, 782–788.

[116] Derasp, J. S.; Barbera, E. A.; Séguin, N. R.; Brzezinski, D. D.; Beauchemin, A. M. Synthesis of Hydroxamic Acid Derivatives Using Blocked (Masked) *O*-Isocyanate Precursors. *Org. Lett.* **2020**, *22*, 7403–7407.

[117] Zhu, R. Y.; Farmer, M. E.; Chen, Y. Q.; Yu, J. Q. A Simple and Versatile Amide Directing Group for C−H Functionalizations. *Angew. Chem. Int. Ed.* **2016**, *55*, 10578–10599.

[118] Pirnot, M. T.; Wang, Y. M.; Buchwald, S. L. Copper Hydride Catalyzed Hydroamination of Alkenes and Alkynes. *Angew. Chem. Int. Ed.* **2016**, *55*, 48–57.

[119] Ganeshpurkar, A.; Kumar, D.; Singh, S. K. Strategies for the Synthesis of Hydroxamic Acids. *Curr. Org. Synth.* **2018**, *15*, 154–165.

[120] Dettori, G.; Gaspa, S.; Porcheddu, A.; De Luca, L. A Two-Step Tandem Reaction to Prepare Hydroxamic Acids Directly from Alcohols. *Org. Biomol. Chem.* **2014**, *12*, 4582–4585.

[121] Dettori, G.; Gaspa, S.; Porcheddu, A.; De Luca, L. One-Pot Synthesis of Hydroxamic Acids from Aldehydes and Hydroxylamine. *Adv. Synth. Catal.* **2014**, *356*, 2709–2713.

[122] Ghosh, H.; Patel, B. K. Hypervalent Iodine(III)-Mediated Oxidation of Aldoximes to *N*-Acetoxy or *N*-Hydroxy Amides. *Org. Biomol. Chem.* **2009**, *8*, 384–390.

[123] Beillard, A.; Bhurruth-Alcor, Y.; Bouix-Peter, C.; Bouquet, K.; Chambon, S.; Clary, L.; Harris, C. S.; Millois, C.; Mouis, G.; Ouvry, G.; Pierre, R.; Reitz, A.; Tomas, L. A Facile and Rapid Preparation of Hydroxamic Acids by Hydroxylaminolysis Using DBU as Base. *Tetrahedron Lett.* **2016**, *57*, 2165–2170.

[124] Gissot, A.; Volonterio, A.; Zanda, M. One-Step Synthesis of *O*-Benzyl Hydroxamates from Unactivated Aliphatic and Aromatic Esters. *J. Org. Chem.* **2005**, *70*, 6925–6928.

[125] Charette, A. B.; Mellon, C. Enantioselective Synthesis of α,α-Disubstituted-α-Amino Acids by a Sequential Nucleophilic Addition to Nitriles. *Tetrahedro*n **1998**, *54*, 10525–10535.

[126] Chen, X.; Hortelano, E. R.; Eliel, L.; Frye, S. V. Chelates as Intermediates in Nucleophilic Additions to Alkoxy Ketones According to Cram's Rule (Cyclic Model)1″. *J. Am. Chem. Soc.* **1992**, *14*, 1778–1784.

[127] Reetz, M. T. Chelation or Non-Chelation Control in Addition Reactions of Chiral α- and β- Alkoxy Carbonyl Compounds [New Synthetic Methods (44)]. *Angew. Chem. Int. Ed.* **1984**, *23*, 556–569.

[128] Reetz, M. T. Structural, Mechanistic, and Theoretical Aspects of Chelation-Controlled Carbonyl Addition Reactions. *Acc. Chem. Res.* **1993**, *26*, 462–468.

[129] AbdelHafez, E. S. M. N.; Aly, O. M.; Abuo-Rahma, G. E. D. A. A.; King, S. B. Lossen Rearrangements under Heck Reaction Conditions. *Adv. Synth. Catal.* **2014**, *356*, 3456–3464.

[130] Kreye, O.; Wald, S.; Meier, M. A. R. Introducing Catalytic Lossen Rearrangements: Sustainable Access to Carbamates and Amines. *Adv. Synth. Catal.* **2013**, *355*, 81–86.

[131] Krasovskiy, A.; Malakhov, V.; Gavryushin, A.; Knochel, P. Efficient Synthesis of Functionalized Organozinc Compounds by the Direct Insertion of Zinc into Organic Iodides and Bromides. *Angew. Chem. Int. Ed.* **2006**, *45*, 6040–6044.

[132] Klatt, T.; Markiewicz, J. T.; Sämann, C.; Knochel, P. Strategies to Prepare and Use Functionalized Organometallic Reagents. *J. Org. Chem.* **2014**, *79*, 4253–4269.

[133] Smith, A. B.; Boldi, A. M. Multicomponent Linchpin Couplings of Silyl Dithianes via Solvent- Controlled Brook Rearrangement. *J. Am. Chem. Soc.* **1997**, *119*, 6925–6926.

[134] Heller, S. T.; Newton, J. N.; Fu, T.; Sarpong, R. One-Pot Unsymmetrical Ketone Synthesis Employing a Pyrrole-Bearing Formal Carbonyl Dication Linchpin Reagent. *Angew. Chem. Int. Ed.* **2015**, *54*, 9839–9843.

[135] Barbero, A.; Cuadrado, P.; Fleming, I.; González, A. M.; Pulido, F. J. The Stannyl–Cupration of Acetylenes and the Reaction of the Intermediate Cuprates with Electrophiles as a Synthesis of Substituted Vinylstannanes. *Chem. Commun.* **1992**, 351–353.

[136] Rivas, A.; Areal, A.; Mora, P.; Álvarez, R.; de Lera, A. R. Synthesis of Symmetrical and Nonsymmetrical Polyenes by Iterative and Bidirectional Palladium-Catalyzed Cross-Coupling Reactions. *Chem. Eur. J.* **2020**, *26*, 13543–13567.

[137] Matsumoto, A.; Maeda, N.; Maruoka, K. Bidirectional Elongation Strategy Using Ambiphilic Radical Linchpin for Modular Access to 1,4-Dicarbonyls via Sequential Photocatalysis. *J. Am. Chem. Soc.* **2023**, *145*, 20344–20354.

[138] Liu, T.; Qiao, J. X.; Poss, M. A.; Yu, J. Q. Palladium(II)-Catalyzed Site-Selective C(Sp^3)−H Alkynylation of Oligopeptides: A Linchpin Approach for Oligopeptide–Drug Conjugation. *Angew. Chem. Int. Ed.* **2017**, *56*, 10924–10927.

[139] Skotnitzki, J.; Kremsmair, A.; Knochel, P. Stereoselective Preparation and Reactions of Chiral Secondary Alkyllithiums. *Synthesis*. **2020**, *52*, 189–196.

[140] Skotnitzki, J.; Kremsmair, A.; Keefer, D.; Gong, Y.; de Vivie-Riedle, R.; Knochel, P. Stereoselective Csp^3–Csp^2 Cross-Couplings of Chiral Secondary Alkylzinc Reagents with Alkenyl and Aryl Halides. *Angew. Chem. Int. Ed.* **2020**, *59*, 320–324.

[141] Piller, F. M.; Metzger, A.; Schade, M. A.; Haag, B. A.; Gavryushin, A.; Knochel, P. Preparation of Polyfunctional Arylmagnesium, Arylzinc, and Benzylic Zinc Reagents by Using Magnesium in the Presence of LiCl. *Chem. Eur. J.* **2009**, *15*, 7192–7202.

[142] Skotnitzki, J.; Spessert, L.; Knochel, P. Regio- and Stereoselective Allylic Substitutions of Chiral Secondary Alkylcopper Reagents: Total Synthesis of (+)-Lasiol, (+)-13-Norfaranal, and (+)-Faranal. *Angew. Chem. Int. Ed.* **2019**, *58*, 1509–1514.

[143] Leuser, H.; Perrone, S.; Liron, F.; Kneisel, F. F.; Knochel, P. Highly Enantioselective Preparation of Tertiary Alcohols and Amines by Copper-Mediated Diastereoselective Allylic SN2' Substitutions. *Angew. Chem. Int. Ed.* **2005**, *44*, 4627–4631.

[144] Harrington-Frost, N.; Leuser, H.; Calaza, M. I.; Kneisel, F. F.; Knochel, P. Highly Stereoselective Anti SN2' Substitutions of (*Z*)-Allylic Pentafluorobenzoates with Polyfunctionalized Zinc-Copper Reagents. *Org. Lett.* **2003**, *5*, 2111–2114.

[145] Klier, L.; Aranzamendi, E.; Ziegler, D.; Nickel, J.; Karaghiosoff, K.; Carell, T.; Knochel, P. Lewis Acid Triggered Regioselective Magnesiation and Zincation of Uracils, Uridines, and Cytidines. *Org. Lett*. **2016**, *18*, 1068–1071.

[146] Waldman, A. J.; Ng, T. L.; Wang, P.; Balskus, E. P. Heteroatom-Heteroatom Bond Formation in Natural Product Biosynthesis. *Chem. Rev.* **2017**, *117*, 5784–5863.

[147] Popiołek, Ł. Hydrazide–Hydrazones as Potential Antimicrobial Agents: Overview of the Literature since 2010. *Med. Chem. Res.* **2017**, *26*, 287–301.

[148] Mali, S. N.; Thorat, B. R.; Gupta, D. R.; Pandey, A. Mini-Review of the Importance of Hydrazides and Their Derivatives—Synthesis and Biological Activity. *Eng. Proc.* **2021**, *11*, 21.

[149] Gorobets, N. Y.; Yousefi, B. H.; Belaj, F.; Kappe, C. O. Rapid Microwave-Assisted Solution Phase Synthesis of Substituted 2-Pyridone Libraries. *Tetrahedron* **2004**, *60*, 8633–8644.

[150] Majumdar, P.; Pati, A.; Patra, M.; Behera, R. K.; Behera, A. K. Acid Hydrazides, Potent Reagents for Synthesis of Oxygen-, Nitrogen-, and/or Sulfur-Containing Heterocyclic Rings. *Chem. Rev.* **2014**, *114*, 2942–2977.

[151] Kornet, M. J.; Varia, T.; Beaven, W. Synthesis and Anticonvulsant Activity of 3-amino-4(3H)-quinazolinones. *J. Heterocycl. Chem.* **1983**, *20*, 1553–1555.

[152] Barbor, J. P.; Nair, V. N.; Sharp, K. R.; Lohrey, T. D.; Dibrell, S. E.; Shah, T. K.; Walsh, M. J.; Reisman, S. E.; Stoltz, B. M. Development of a Nickel-Catalyzed N-N Coupling for the Synthesis of Hydrazides. *J. Am. Chem. Soc.* **2023**, *145*, 15071–15077.

[153] Zhu, S. Y.; He, W. J.; Shen, G. C.; Bai, Z. Q.; Song, F. F.; He, G.; Wang, H.; Chen, G. Ligand-Promoted Iron-Catalyzed Nitrene Transfer for the Synthesis of Hydrazines and Triazanes through *N*-Amidation of Arylamines. *Angew. Chem. Int. Ed.* **2024**, *63*, e202312465.

[154] Wang, H.; Jung, H.; Song, F.; Zhu, S.; Bai, Z.; Chen, D.; He, G.; Chang, S.; Chen, G. Nitrene-Mediated Intermolecular N–N Coupling for Efficient Synthesis of Hydrazides. *Nat. Chem.* **2021**, *13*, 378–385.

[155] Li, Q.; Chen, J.; Luo, Y.; Xia, Y. Photoredox-Catalyzed Hydroacylation of Azobenzenes with Carboxylic Acids. *Org. Lett.* **2024**, *26*, 1517–1521.

[156] Zhang, S.; Zhang, Q.; Tang, M. Synthesis of Hydrazides from N-Tosylhydrazones and Its Application in the Preparation of Indazolones. *J. Org. Chem.* **2022**, *87*, 3845–3850.

[157] Lei, J.; Xie, W.; Li, J.; Wu, Y.; Xie, X. Synthesis of *N*-Aryl- and *N*-Alkenylhydrazides through C(Sp^2)−N Bond Construction. *Eur. J. Org. Chem.* **2021**, 4364–4387.

[158] Haynes, R. K.; Vonwiller, S. C.; Luderer, M. R. *N*,*N*,*N*′,*N*′-Tetramethylethylenediamine. In *Encyclopedia of Reagents for Organic Syntheis (EROS)*; Wiley, 2006.

[159] Huang, X. Z.; Gao, L. H.; Huang, P. Q. Enantioselective Total Syntheses of (+)-Stemofoline and Three Congeners Based on a Biogenetic Hypothesis. *Nat. Commun.* **2020**, *11*, 1–9.

[160] Mair, B. A.; Fouad, M. H.; Ismailani, U. S.; Munch, M.; Rotstein, B. H. Rhodium-Catalyzed Addition of Organozinc Iodides to Carbon-11 Isocyanates. *Org. Lett.* **2020**, *22*, 2746–2750.

[161] Sunagatullina, A. S.; Hess, A.; Kremsmair, A.; Li, Y.; Chen, Y. H.; Knochel, P. Transition-Metal Free Electrophilic Aminations of Polyfunctional *O*-2,4,6-Trimethylbenzoyl Hydroxylamines with Zinc and Magnesium Organometallics. *Angew. Chem. Int. Ed.* **2023**, *62*, e202304445.

[162] Kremsmair, A.; Wilke, H. R.; Harenberg, J. H.; Bissinger, B. R. G.; Simon, M. M.; Alandini, N.; Knochel, P. In Situ Quench Reactions of Enantioenriched Secondary Alkyllithium Reagents in Batch and Continuous Flow Using an I/Li-Exchange. *Angew. Chem. Int. Ed.* **2023**, *62*, e202214377.

[163] Liang, B.; Cai, X.; Liu, J. Y.; Huang, J.; Chen, Y.; Deng, H.; Zhou, Q.; Chen, T.; Chen, X.; Zhu, Z. Syntheses of 3H-1,2,4-Triazol-3-Ones by Copper-Promoted Oxidative N–N Bond Formation of Amidines with Isocyanates. *Org. Chem. Front.* **2024**, *11*, 343–347.

[164] Pietrasiak, E.; Ha, S.; Jeon, S.; Jeong, J.; Lee, J.; Seo, J.; Lee, E. Cobalt-Catalyzed Formation of Grignard Reagents via C-O or C-S Bond Activation. *J. Org. Chem.* **2022**, *87*, 8380–8389.

[165] Ziegler, D. S.; Wei, B.; Knochel, P. Improving the Halogen–Magnesium Exchange by Using New Turbo-Grignard Reagents. *Chem. Eur. J.* **2019**, *25*, 2695–2703.

[166] Spennacchio, M.; Natho, P.; Andresini, M.; Colella, M. Continuous Flow Generation of Highly Reactive Organometallic Intermediates: A Recent Update. *J. Flow Chem.* **2023**, *14*, 43–83.

[167] Brogden, R. N. Pyrazolone Derivatives. *Drugs* **1986**, *32*, 60–70.

[168] Zhao, Z.; Dai, X.; Li, C.; Wang, X.; Tian, J.; Feng, Y.; Xie, J.; Ma, C.; Nie, Z.; Fan, P.; Qian, M.; He, X.; Wu, S.; Zhang, Y.; Zheng, X. Pyrazolone Structural Motif in Medicinal Chemistry: Retrospect and Prospect. *Eur. J. Med. Chem.* **2020**, *186*, 111893.

[169] Brune, K. The Early History of Non-Opioid Analgesics. *Acute Pain* **1997**, *1*, 33–40.

[170] Naik, C. G.; Malik, G. M. Synthesis of Pyrazolone Derivatives and Their Biological Activities. *Orient. J Chem.* **2010**, *26*, 113–116.

[171] Polkam, N.; Ramaswamy, V. R.; Rayam, P.; Allaka, T. R.; Anantaraju, H. S.; Dharmarajan, S.; Perumal, Y.; Gandamalla, D.; Yellu, N. R.; Balasubramanian, S.; Anireddy, J. S. Synthesis, Molecular Properties Prediction and Anticancer, Antioxidant Evaluation of New Edaravone Derivatives. *Bioorg. Med. Chem. Lett.* **2016**, *26*, 2562–2568.

[172] Zhang, J.; Yang, Y.; Qian, X. K.; Song, P. F.; Zhao, Y. S.; Guan, X. Q.; Zou, L. W.; Bao, X.; Wang, H. Design, Synthesis, and Structure-Activity Relationship Study of Pyrazolones as Potent Inhibitors of Pancreatic Lipase. *ChemMedChem* **2021**, *16*, 1600–1604.

[173] Sheng, X.; Hua, K.; Yang, C.; Wang, X.; Ji, H.; Xu, J.; Huang, Z.; Zhang, Y. Novel Hybrids of 3-n-Butylphthalide and Edaravone: Design, Synthesis and Evaluations as Potential Anti-Ischemic Stroke Agents. *Bioorg. Med. Chem. Lett*. **2015**, *25*, 3535–3540.

[174] Hadi, V.; Koh, Y. H.; Sanchez, T. W.; Barrios, D.; Neamati, N.; Jung, K. W. Development of the next Generation of HIV-1 Integrase Inhibitors: Pyrazolone as a Novel Inhibitor Scaffold. *Bioorg. Med. Chem. Lett.* **2010**, *20*, 6854–6857.

[175] Polkam, N.; Ramaswamy, V. R.; Rayam, P.; Allaka, T. R.; Anantaraju, H. S.; Dharmarajan, S.; Perumal, Y.; Gandamalla, D.; Yellu, N. R.; Balasubramanian, S.; Anireddy, J. S. Synthesis, Molecular Properties Prediction

and Anticancer, Antioxidant Evaluation of New Edaravone Derivatives. *Bioorg. Med. Chem. Lett.* **2016**, *26*, 2562–2568.

[176] Knorr, L. Einwirkung von Acetessigester Auf Phenylhydrazin. *Ber. Dtsch. Chem. Ges.* **1883**, *16*, 2597–2599.

[177] Nef, J. U. Zur Kenntniss Des Acetessigäthers. *Liebigs Ann.* **1891**, *266*, 52–138.

[178] Mojtahedi, M. M.; Jalali, M. R.; Saeed Abaee, M.; Bolourtchian, M. Microwave-Assisted Synthesis of Substituted Pyrazolones under Solvent-Free Conditions. *Heterocycl. Commun.* **2006**, *12*, 225–228.

[179] Mojtahedi, M. M.; Javadpour, M.; Abaee, M. S. Convenient Ultrasound Mediated Synthesis of Substituted Pyrazolones under Solvent-Free Conditions. *Ultrason. Sonochem.* **2008**, *15*, 828–832.

[180] Desroses, M.; Jacques-Cordonnier, M. C.; Llona-Minguez, S.; Jacques, S.; Koolmeister, T.; Helleday, T.; Scobie, M. A Convenient Microwave-Assisted Propylphosphonic Anhydride (T3P®) Mediated One-Pot Pyrazolone Synthesis. *Eur. J. Org. Chem.* **2013**, 5879–5885.

[181] Tabei, K.; Kawashima, E.; Kato, T. Reaction of N-Hydroxyacetoacetanilide with Carbonyl Reagents. *Chem. Pharm. Bull.* **1981**, *29*, 244–249.

[182] Feist, F. Ein Kondensationsprodukt Aus Vier Acetessigester-Molekülen, α-(1,3 Dimethyl-2-Carboxy-Phenyl)-β-Methyl-Glutaconsäure. *Liebigs Ann.* **1923**, *433*, 51–64.

[183] Boeckman, R. K.; Reed, J. E.; Ge, P. A Novel Route to 2,3-Pyrazol-1(5*H*)-Ones via Palladium-Catalyzed Carbonylation of 1,2-Diaza-1,3-Butadienes. *Org. Lett.* **2001**, *3*, 3651–3653.

[184] Capua, M.; Granito, C.; Perrone, S.; Salomone, A.; Troisi, L. Palladium-Catalyzed Carbonylative Coupling of α-Chloroketones with Hydrazines: A Simple Route to Pyrazolone Derivatives. *Tetrahedron Lett.* **2016**, *57*, 3363–3367.

[185] Ding, Z. C.; Tang, H. T.; Li, R. H.; Ju, L. C.; Zhan, Z. P. Synthesis of 4-Arylidenepyrazolones by a Gold-Catalyzed Cyclization/Arylidene Group Transfer Cascade of *N*-Propioloyl Hydrazones. *J. Org. Chem.* **2015**, *80*, 9307–9313.

[186] Panda, S. P.; Dash, R.; Hota, S. K.; Murarka, S. Photodecarboxylative Radical Cascade Involving *N*-(Acyloxy)Phthalimides for the Synthesis of Pyrazolones. *Org. Lett.* **2024**, *26*, 3667–3672.

[187] Lavergne, K.; Bongers, A.; Betit, L.; Beauchemin, A. M. Modular Synthesis of Pyrazolones Using an Alkene Aminocarbonylation Reaction. *Org. Lett.* **2015**, *17*, 3612–3615.

[188] Bongers, A.; Ranasinghe, I.; Lemire, P.; Perozzo, A.; Vincent-Rocan, J. F.; Beauchemin, A. M. Synthesis of Cyclic Azomethine Imines by Cycloaddition Reactions of *N*-Isocyanates and *N*-Isothiocyanates. *Org. Lett.* **2016**, *18*, 3778–3781.

[189] Ivanovich, R. A.; Clavette, C.; Vincent-Rocan, J. F.; Roveda, J. G.; Gorelsky, S. I.; Beauchemin, A. M. Intramolecular Alkene Aminocarbonylation Using Concerted Cycloadditions of Amino-Isocyanates. *Chem. Eur. J.* **2016**, *22*, 7906–7916.

[190] Beak, P.; Brown, R. A. The Tertiary Amide as an Effective Director of Ortho Lithiation. *J. Org. Chem.* **1982**, *47*, 34–46.

[191] Beak, P.; Tse, A.; Haawkins, J.; Chen, C. W.; Mills, S. A Comparison of Secondary and Tertiary Amides as Directors of Ortho and Adjacent Benzylic Lithiation and of Asymmetric Induction in Ortho Lithiated Benzamides. *Tetrahedron* **1983**, *39*, 1983–1989.

[192] de Silva, S. O.; Ahmad, I.; Snieckus, V. Directed Lithiation of *N*,*N*-Diethylbenzamides. A Short Route to Phthalideisoquinoline Alkaloids. *Tetrahedron Lett.* **1978**, *19*, 5107–5110.

[193] Knochel, P.; Cole, K. P. Directed Ortho Metalation in 2021: A Tribute to Victor Snieckus (August 1, 1937-December 18, 2020). *Org. Process Res. Dev.* **2021**, *25*, 2188–2191.

[194] Corey, E. J.; Enders, D. Applications of *N,N*-Dimethylhydrazones to Synthesis. Use in Efficient, Positionally and Stereochemically Selective C–C Bond Formation; Oxidative Hydrolysis to Carbonyl Compounds. *Tetrahedron Lett.* **1976**, *17*, 3–6.

[195] Job, A.; Janeck, C. F.; Bettray, W.; Peters, R.; Enders, D. The SAMP-/RAMP-Hydrazone Methodology in Asymmetric Synthesis. *Tetrahedron* **2002**, *58*, 2253–2329.

[196] Lim, D.; Coltart, D. M. Simple and Efficient Asymmetric α-Alkylation and α,α-Bisalkylation of Acyclic Ketones by Using Chiral *N*-Amino Cyclic Carbamate Hydrazones. *Angew. Chem. Int. Ed.* **2008**, *47*, 5207–5210.

[197] Dauben, W. G.; Rivers, G. T.; Zimmerman, W. T.; Yang, N. C.; Kim, B.; Yang, J. The Role of Tosylhydrazone Stereochemistry upon the Regiospecificity of Olefin Formation. *Tetrahedron Lett.* **1976**, *17*, 2951–2954.

[198] Wengryniuk, S. E.; Lim, D.; Coltart, D. M. Regioselective Asymmetric α,α-Bisalkylation of Ketones via Complex-Induced *Syn* -Deprotonation of Chiral *N* -Amino Cyclic Carbamate Hydrazones. *J. Am. Chem. Soc.* **2011**, *133*, 8714–8720.

[199] Ivanovich, R. A.; Quartus, J. A. M.; Das Neves, N.; Loiseau, F.; Raymond, M.; Beauchemin, A. M. Aminimide Synthesis Using Concerted Amination Reactions of Alkenes: Scope and Mechanistic Information. *J. Org. Chem.* **2019**, *84*, 9792–9800.

[200] Ivanovich, R. A.; Clavette, C.; Vincent-Rocan, J. F.; Roveda, J. G.; Gorelsky, S. I.; Beauchemin, A. M. Intramolecular Alkene Aminocarbonylation Using Concerted Cycloadditions of Amino-Isocyanates. *Chem. Eur. J.* **2016**, *22*, 7906–7916.

[201] Bongers, A.; Moon, P. J.; Beauchemin, A. M. Kinetic Resolution of Azomethine Imines by Brønsted Acid Catalyzed Enantioselective Reduction. *Angew. Chem. Int. Ed.* **2015**, *54*, 15516–15519.

[202] Derasp, J. S.; Vincent-Rocan, J. F.; Beauchemin, A. M. Divergent Reactivity of *N*-Isocyanates with Primary and Secondary Amines: Access to Pyridazinones and Triazinones. *Org. Lett.* **2016**, *18*, 658–661.

[203] Dahab, M. A.; Derasp, J. S.; Beauchemin, A. M. A Cascade Synthesis of 1,2,4-Triazin-3(2 *H*)-Ones Using Nitrogen-Substituted Isocyanates. *Synlett* **2017**, *28*, 456–460.

[204] Vuillermet, F.; Dahab, M. A.; Abdelhamid, D.; Polat, D. E.; Gill, M. A.; Beauchemin, A. M. Synthesis of 1,2,4-Triazinones Exploiting the Reactivity of Diazadiene and *N*-Isocyanate Intermediates. *J. Org. Chem.* **2023**, *88*, 2095–2102.

[205] Vincent-Rocan, J. F.; Derasp, J. S.; Beauchemin, A. M. Diversity-Oriented Heterocyclic Synthesis Using Divergent Reactivity of *N*-Substituted Iso(Thio)Cyanates. *Chem. Commun.* **2015**, *51*, 16405–16408.

[206] An, J.; Alper, H.; Beauchemin, A. M. Copper-Catalyzed Cascade Substitution/Cyclization of *N*-Isocyanates: A Synthesis of 1-Aminobenzimidazolones. *Org. Lett.* **2016**, *18*, 3482–3485.

[207] Feng, Y.; Yukioka, T.; Matsuyama, M.; Mori, A.; Okano, K. Deprotonative Generation and Trapping of Haloaryllithium in a Batch Reactor. *Org. Lett.* **2023**, *25*, 3013–3017.

[208] Kauch, M.; Hoppe, D. Efficient Two-Step Synthesis of Salicylaldehydes via Directed Ortho-Lithiation of in Situ *N*-Silylated *O*-Aryl *N*-Isopropylcarbamates. *Synthesis* **2006**, 1575–1577.

[209] Krasovskiy, A.; Knochel, P. A LiCl-Mediated Br/Mg Exchange Reaction for the Preparation of Functionalized Aryl- and Heteroarylmagnesium Compounds from Organic Bromides. *Angew. Chem. Int. Ed.* **2004**, *43*, 3333–3336.

[210] Ren, H.; Krasovskiy, A.; Knochel, P. Stereoselective Preparation of Functionalized Acyclic Alkenylmagnesium Reagents Using *i*-PrMgCl-LiCl. *Org. Lett.* **2004**, *6*, 4215–4217.

[211] Mulvey, R. E. Modern Ate Chemistry: Applications of Synergic Mixed Alkali-Metal - Magnesium or - Zinc Reagents in Synthesis and Structure Building. *Organometallics* **2006**, *25*, 1060–1075.

[212] Krasovskiy, A.; Straub, B. F.; Knochel, P. Highly Efficient Reagents for Br/Mg Exchange. *Angew. Chem. Int. Ed.* **2006**, *45*, 159–162.

[213] Wang, W.; Sang, L.; Kong, W.; Zhao, Y.; Wei, Z.; Li, Y. In-Chain Functionalization through the Combination of Ring Opening Copolymerization and Oxime “Click” Reaction towards X-Ray Opaque Polylactide Copolymers. *Chin. Chem. Lett.* **2020**, *31*, 551–553.

[214] Dierks, A.; Fliegel, L.; Schmidtmann, M.; Christoffers, J. Preparation of Hexahydrocarbazole Derivatives by Reductive Indolization. *Eur. J. Org. Chem.* **2020**, 7164–7175.

[215] Wang, Q.; An, J.; Alper, H.; Xiao, W. J.; Beauchemin, A. M. Catalytic Substitution/Cyclization Sequences of O-Substituted Isocyanates: Synthesis of 1-Alkoxybenzimidazolones and 1-Alkoxy-3,4-Dihydroquinazolin-2(1H)-Ones. *Chem. Commun.* **2017**, *53*, 13055–13058.

[216] Al-Zoubi, R. M.; Marion, O.; Hall, D. G. Direct and Waste-Free Amidations and Cycloadditions by Organocatalytic Activation of Carboxylic Acids at Room Temperature. *Angew. Chem. Int. Ed.* **2008**, *47*, 2876–2879.

[217] Johnson, S. M.; Petrassi, H. M.; Palaninathan, S. K.; Mohamedmohaideen, N. N.; Purkey, H. E.; Nichols, C.; Chiang, K. P.; Walkup, T.; Sacchettini, J. C.; Sharpless, K. B.; Kelly, J. W. Bisaryloxime Ethers as Potent Inhibitors of Transthyretin Amyloid Fibril Formation. *J. Med. Chem.* **2005**, *48*, 1576–1587.

[218] Yu, F.; Li, P.; Wang, B.; Han, K. Reversible Near-Infrared Fluorescent Probe Introducing Tellurium to Mimetic Glutathione Peroxidase for Monitoring the Redox Cycles between Peroxynitrite and Glutathione in Vivo. *J. Am. Chem. Soc.* **2013**, *135*, 7674–7680.

[219] Love, B. E.; Jones, E. G. The Use of Salicylaldehyde Phenylhydrazone as an Indicator for the Titration of Organometallic Reagents. *J. Org. Chem.* **1999**, *64*, 3755–3756.

[220] Janza, B.; Studer, A. Stereoselective Cyclization Reactions of IBX-Generated Alkoxyamidyl Radicals. *J. Org. Chem.* **2005**, *70*, 6991–6994.

[221] Ju, G.; Li, G.; Qian, G.; Zhang, J.; Zhao, Y. Rh(III)-Catalyzed C-H Amidation of Arenes with N-Methoxyamide as an Amidating Reagent. *Org. Lett.* **2019**, *21*, 7333–7336.

[222] Ludwig, B. J.; Dörsch, F.; Auerbach, M.; Tumeczek, K.; Berger, F. M. The Synthesis of Hydroxylamine Derivatives Possessing Hypocholesteremic Activity. *J. Med. Chem.* **1967**, *10*, 556–564.

[223] Mocci, R.; De Luca, L.; Delogu, F.; Porcheddu, A. An Environmentally Sustainable Mechanochemical Route to Hydroxamic Acid Derivatives. *Adv. Synth. Catal.* **2016**, *358*, 3135–3144.

[224] Kim, J. J.; Park, Y. D.; Kim, H. K.; Cho, S. D.; Kim, J. K.; Lee, S. G.; Yoon, Y. J. Convenient Preparation of *O*-Alkylhydroxamic Acids Using 2-Acylpyridazin-3(2*H*)-ones. *Synth. Commun.* **2005**, *35*, 731–738.

[225] Hu, L.; Xu, S.; Zhao, Z.; Yang, Y.; Peng, Z.; Yang, M.; Wang, C.; Zhao, J. Ynamides as Racemization-Free Coupling Reagents for Amide and Peptide Synthesis. *J. Am. Chem. Soc.* **2016**, *138*, 13135–13138.

[226] Majewski, M. W.; Cho, S.; Miller, P. A.; Franzblau, S. G.; Miller, M. J. Syntheses and Evaluation of Substituted Aromatic Hydroxamates and Hydroxamic Acids That Target Mycobacterium Tuberculosis. *Bioorg. Med. Chem. Lett.* **2015**, *25*, 4933–4936.

[227] Banjo, S.; Nakasuji, E.; Meguro, T.; Sato, T.; Chida, N. Copper-Catalyzed Electrophilic Amidation of Organotrifluoroborates with Use of *N*-Methoxyamides. *Chem. Eur. J.* **2019**, *25*, 7941–7947.

[228] Kukosha, T.; Trufilkina, N.; Belyakov, S.; Katkevics, M. Copper-Catalyzed Cross-Coupling of *O*-Alkyl Hydroxamates with Aryl Iodides. *Synthesis* **2012**, *44*, 2413–2423.

[229] Nasier, A.; Chang, X.; Guo, C. Electrodimerization Of *N*-Alkoxyamides for the Synthesis of Hydrazines. *J. Org. Chem.* **2021**, *86*, 16068–16076.

[230] Wrigglesworth, J. W.; Cox, B.; Lloyd-Jones, G. C.; Booker-Milburn, K. I. New Heteroannulation Reactions of *N*-Alkoxybenzamides by Pd(II) Catalyzed C-H Activation. *Org. Lett.* **2011**, *13*, 5326–5329.

[231] Ozols, K.; Onodera, S.; Woźniak, Ł.; Cramer, N. Cobalt(III)-Catalyzed Enantioselective Intermolecular Carboamination by C−H Functionalization. *Angew. Chem. Int. Ed.* **2021**, *60*, 655–659.

[232] Guimond, N.; Gorelsky, S. I.; Fagnou, K. Rhodium(III)-Catalyzed Heterocycle Synthesis Using an Internal Oxidant: Improved Reactivity and Mechanistic Studies. *J. Am. Chem. Soc.* **2011**, *133*, 6449–6457.

[233] An, J.; Alper, H.; Beauchemin, A. M. Copper-Catalyzed Cascade Substitution/Cyclization of *N*-Isocyanates: A Synthesis of 1-Aminobenzimidazolones. *Org. Lett.* **2016**, *18*, 3482–3485.

[234] Härter, H. P.; Neuenschwander, M.; Schindler, O. Eine Photochemisch Ausgelöste Reduktion von *N*-Nitrosomorpholin. *Helv. Chim. Acta.* **1971**, *54*, 649–653.

[235] Han, S.; Shin, Y.; Sharma, S.; Mishra, N. K.; Park, J.; Kim, M.; Kim, M.; Jang, J.; Kim, I. S. Rh(III)-Catalyzed Oxidative Coupling of 1,2-Disubstituted Arylhydrazines and Olefins: A New Strategy for 2,3-Dihydro-1H-Indazoles. *Org. Lett.* **2014**, *16*, 2494–2497.

[236] Gagné-Monfette, W.; Vincent-Rocan, J. F.; Lutes, O. C.; O'Keefe, G. F.; Jeanneret, A. D. M.; Blanger, C.; Ivanovich, R. A.; Beauchemin, A. M. Investigation of Masked *N*-Acyl-*N*-Isocyanates: Support for Oxadiazolones as Blocked *N*-Isocyanate Precursors. *Chem. Eur. J.* **2021**, *27*, 14051–14056.

[237] Gan, W.; Moon, P. J.; Clavette, C.; Das Neves, N.; Markiewicz, T.; Toderian, A. B.; Beauchemin, A. M. Synthesis and Reactivity of Unsymmetrical Azomethine Imines Formed Using Alkene Aminocarbonylation. *Org. Lett.* **2013**, *15*, 1890–1893.

[238] Burja, B.; Kočevar, M.; Polanc, S. A Simple Approach to Pyrazol-3-Ones via Diazenes. *Tetrahedron* **2009**, *65*, 8690–8696.

[239] Barcelos, R. C.; Zeoly, L. A.; Rodrigues, M. T.; Ferreira, B. R. V.; Eberlin, M. N.; Coelho, F. Morita-Baylis-Hillman Adducts as Building Blocks of Heterocycles: A Simple Approach to 4-Substituted Pyrazolones, and Mechanism Investigation via ESI-MS(/MS). *Monatsh. Chem.* **2015**, *146*, 1557–1570.

[240] Schwertz, G.; Witschel, M. C.; Rottmann, M.; Bonnert, R.; Leartsakulpanich, U.; Chitnumsub, P.; Jaruwat, A.; Ittarat, W.; Schäfer, A.; Aponte, R. A.; Charman, S. A.; White, K. L.; Kundu, A.; Sadhukhan, S.; Lloyd, M.; Freiberg, G. M.; Srikumaran, M.; Siggel, M.; Zwyssig, A.; Chaiyen, P.; Diederich, F. Antimalarial Inhibitors Targeting Serine Hydroxymethyltransferase (SHMT) with in Vivo Efficacy and Analysis of Their Binding Mode Based on X-Ray Cocrystal Structures. *J. Med. Chem.* **2017**, *60*, 4840–4860.

Spectra

AM-SM-iBu.1.fid — 1d_1H_16_scans DMSO D:\\ Beau 4

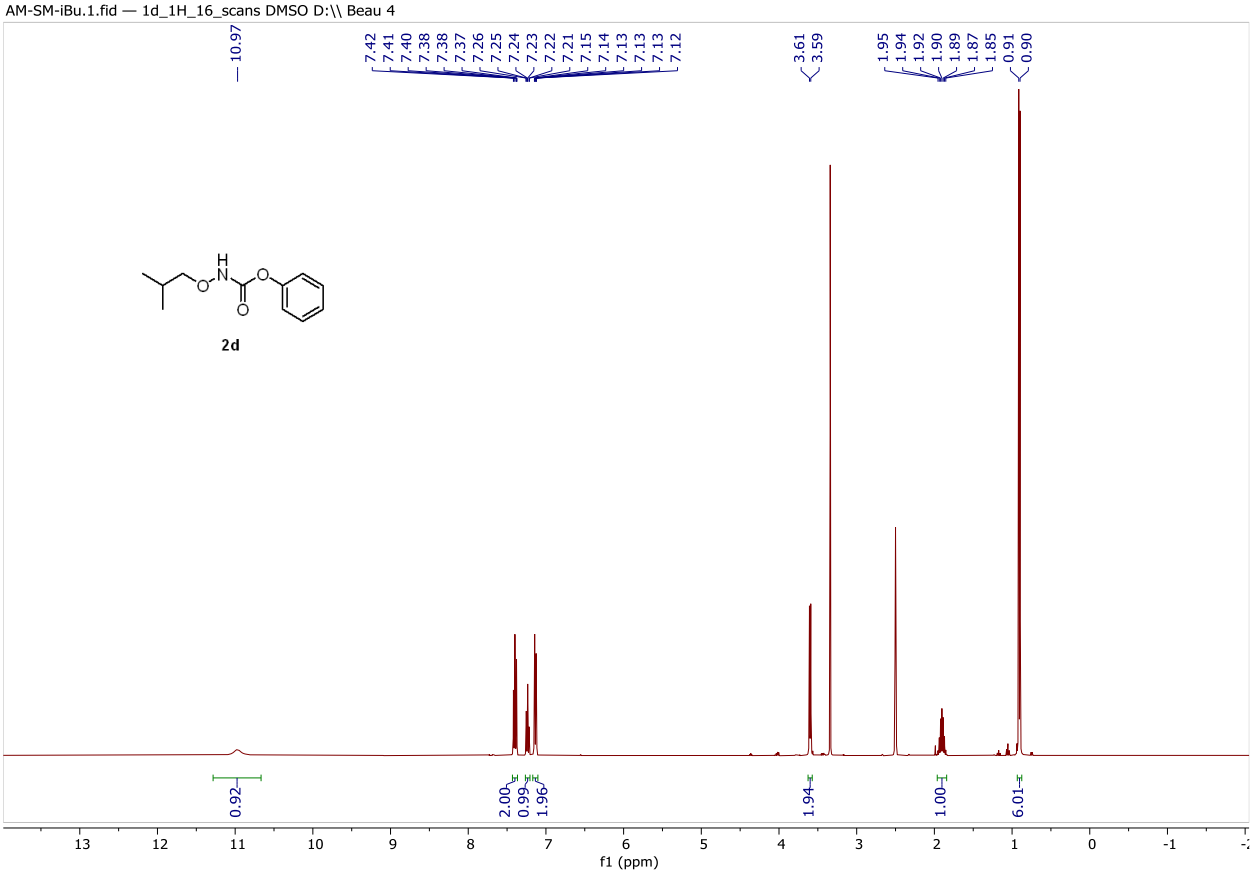

2d

AM-SM-iBu.2.fid — 1d_13C_20_minutes DMSO D:\\ Beau 4

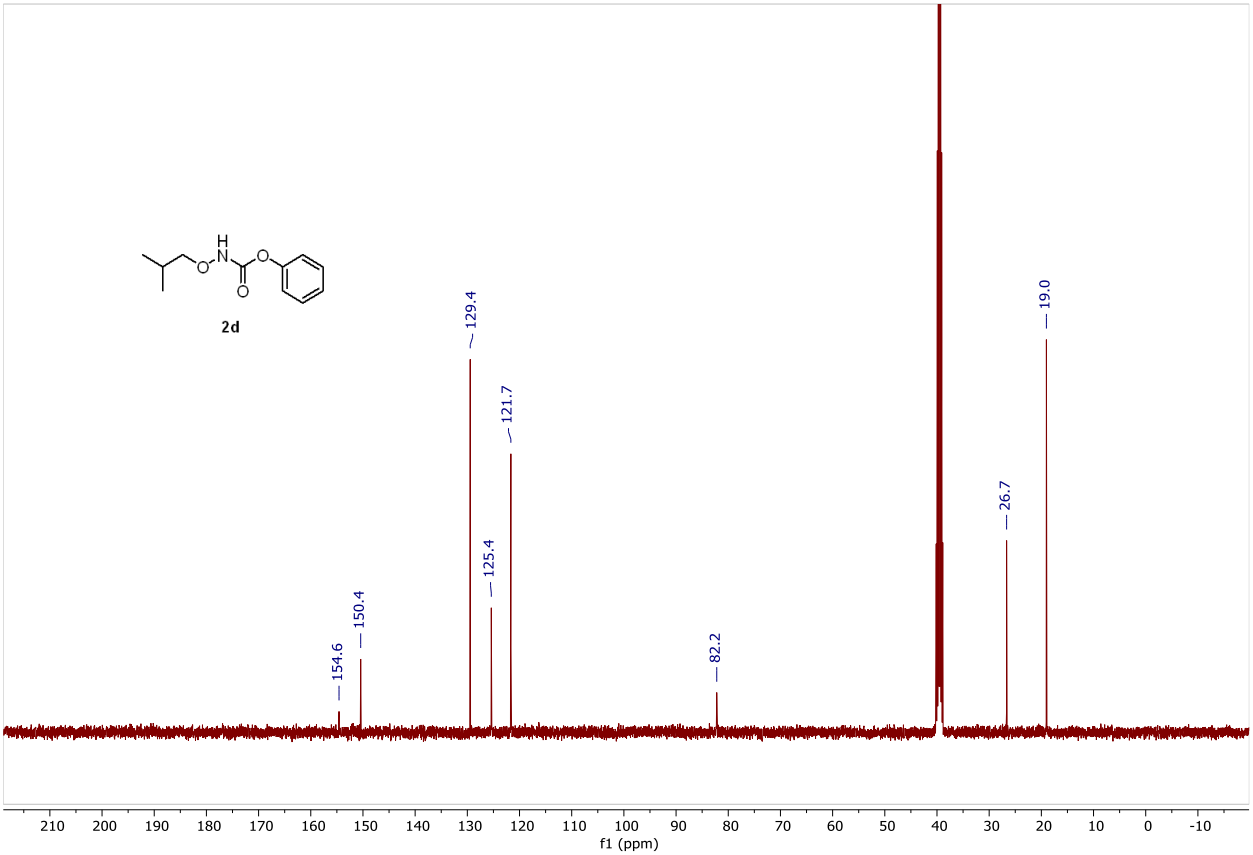

AM-SM-TMS-pure.1.fid — 1d_1H_16_scans DMSO D:\\ Beau 39

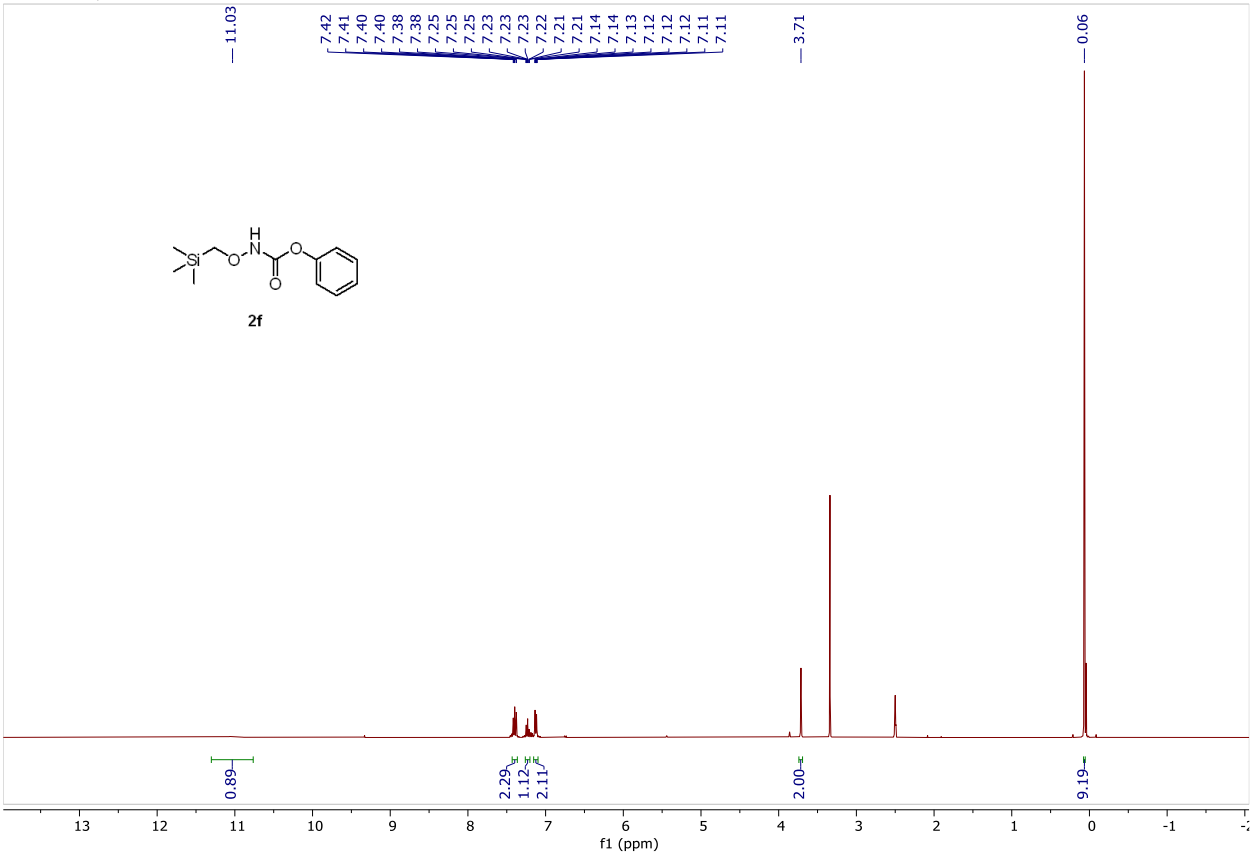

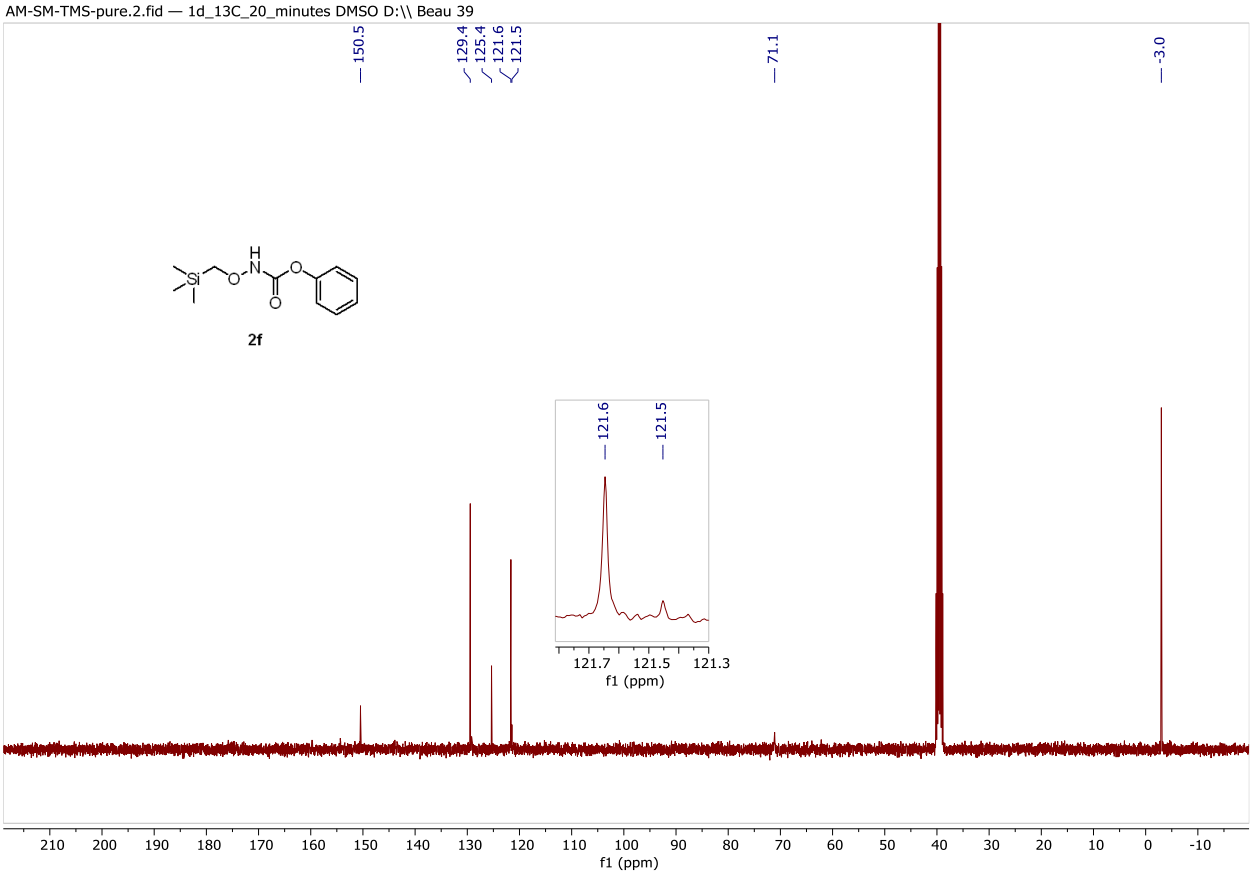
AM-SM-TMS-pure.2.fid — 1d_13C_20_minutes DMSO D:\\ Beau 39
150.5
129.4
125.4
121.6
121.5
71.1
-3.0
2f
121.6
121.5
121.7
121.5
121.3
f1 (ppm)
210 200 190 180 170 160 150 140 130 120 110 100 90 80 70 60 50 40 30 20 10 0 -10
f1 (ppm)

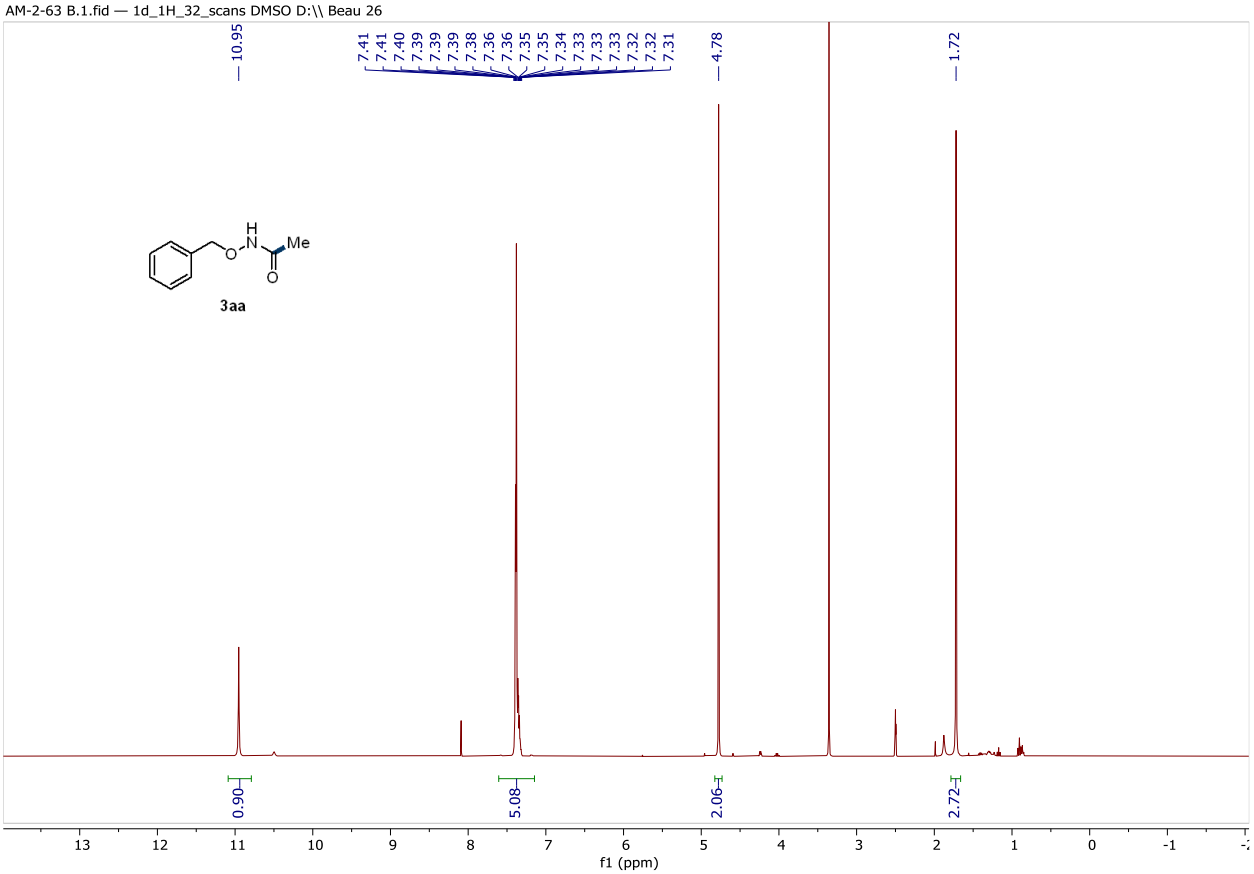
AM-2-63 B.1.fid — 1d_1H_32_scans DMSO D:\\ Beau 26
10.95
7.41
7.41
7.40
7.39
7.39
7.39
7.38
7.36
7.36
7.35
7.35
7.34
7.33
7.33
7.33
7.32
7.32
7.31
4.78
1.72
H
N
O
Me
O
3aa
0.90
5.08
2.06
2.72
13
12
11
10
9
8
7
6
5
4
3
2
1
0
-1
f1 (ppm)

AM-2-63 B.2.fid — 1d_13C_20_minutes DMSO D:\\ Beau 26

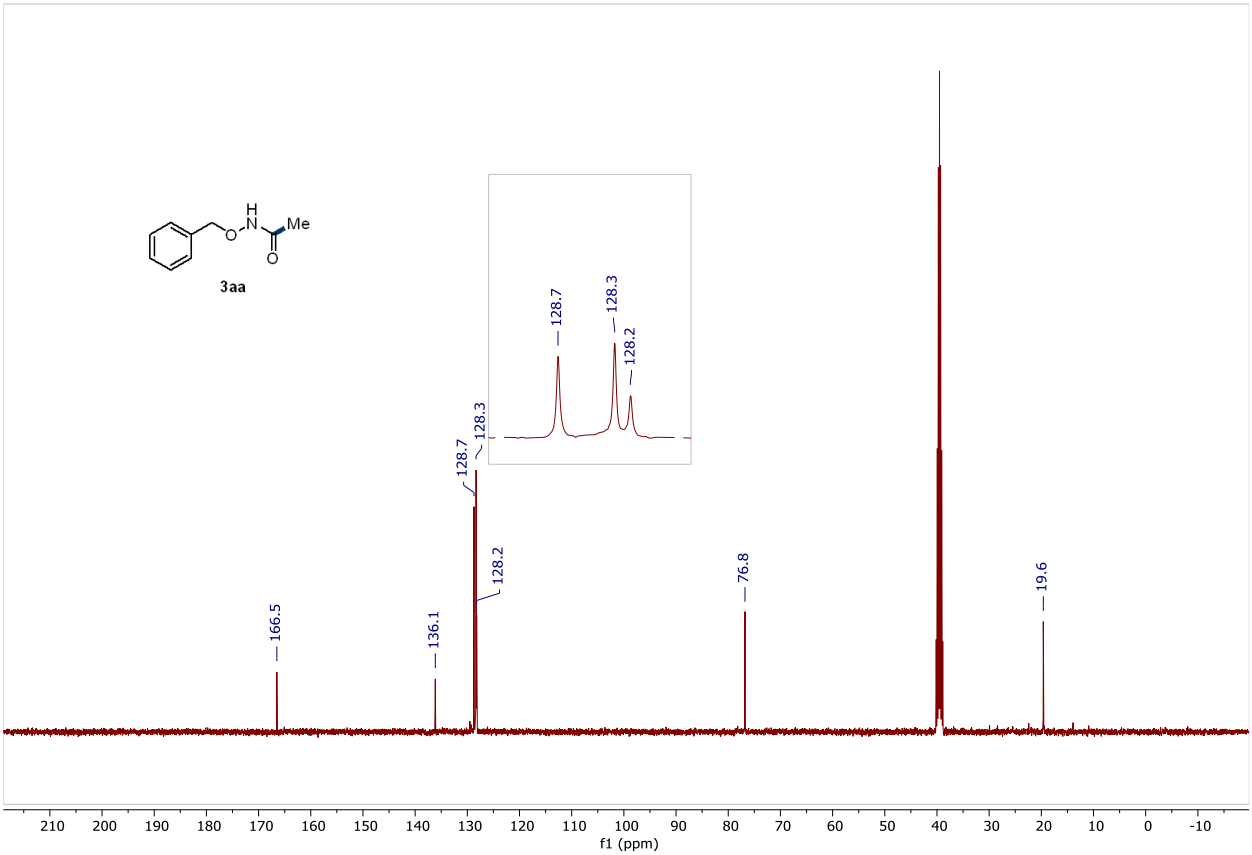

AM-89.1.fid — 1d_1H_16_scans DMSO D:\\ Beau 19

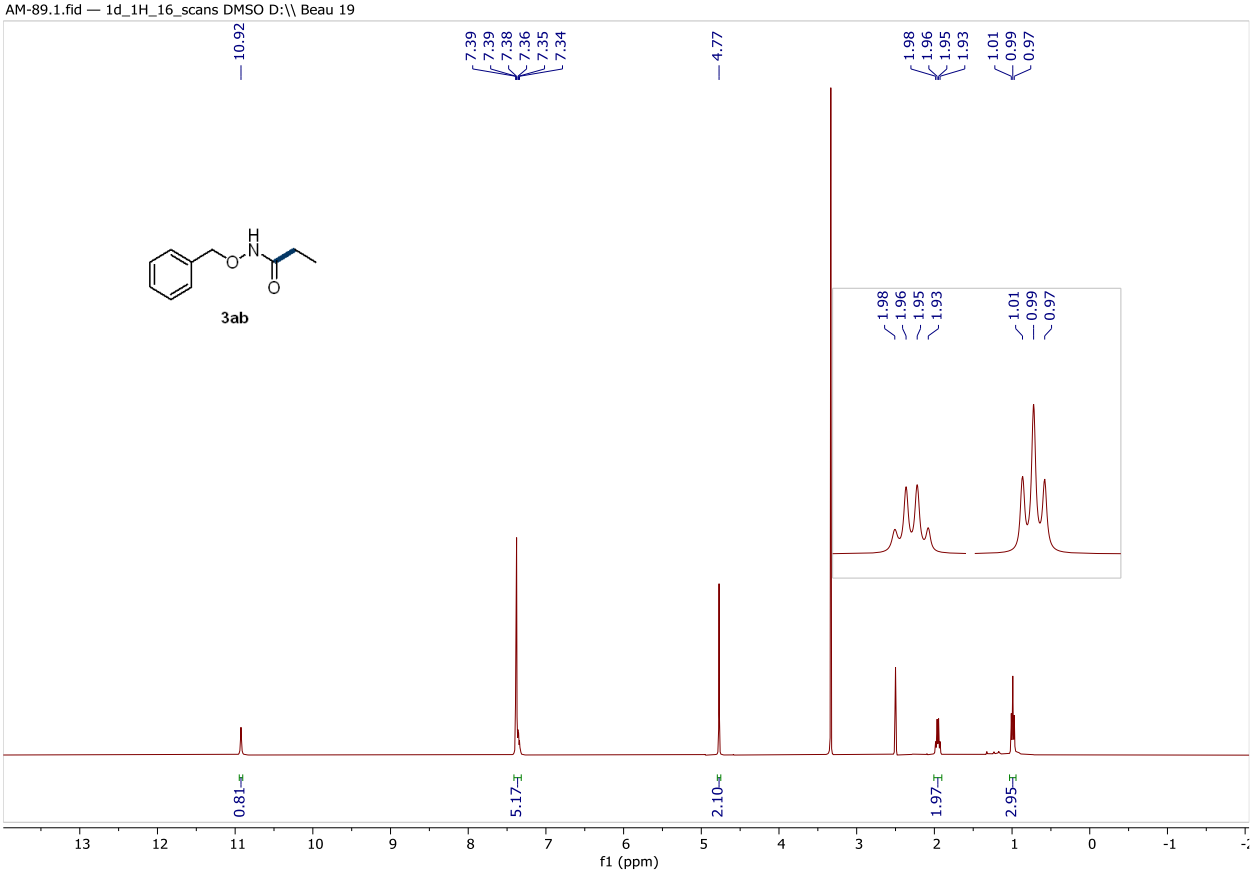

AM-2-15.2.fid — 1d_13C_20_minutes DMSO D:\\ Beau 18

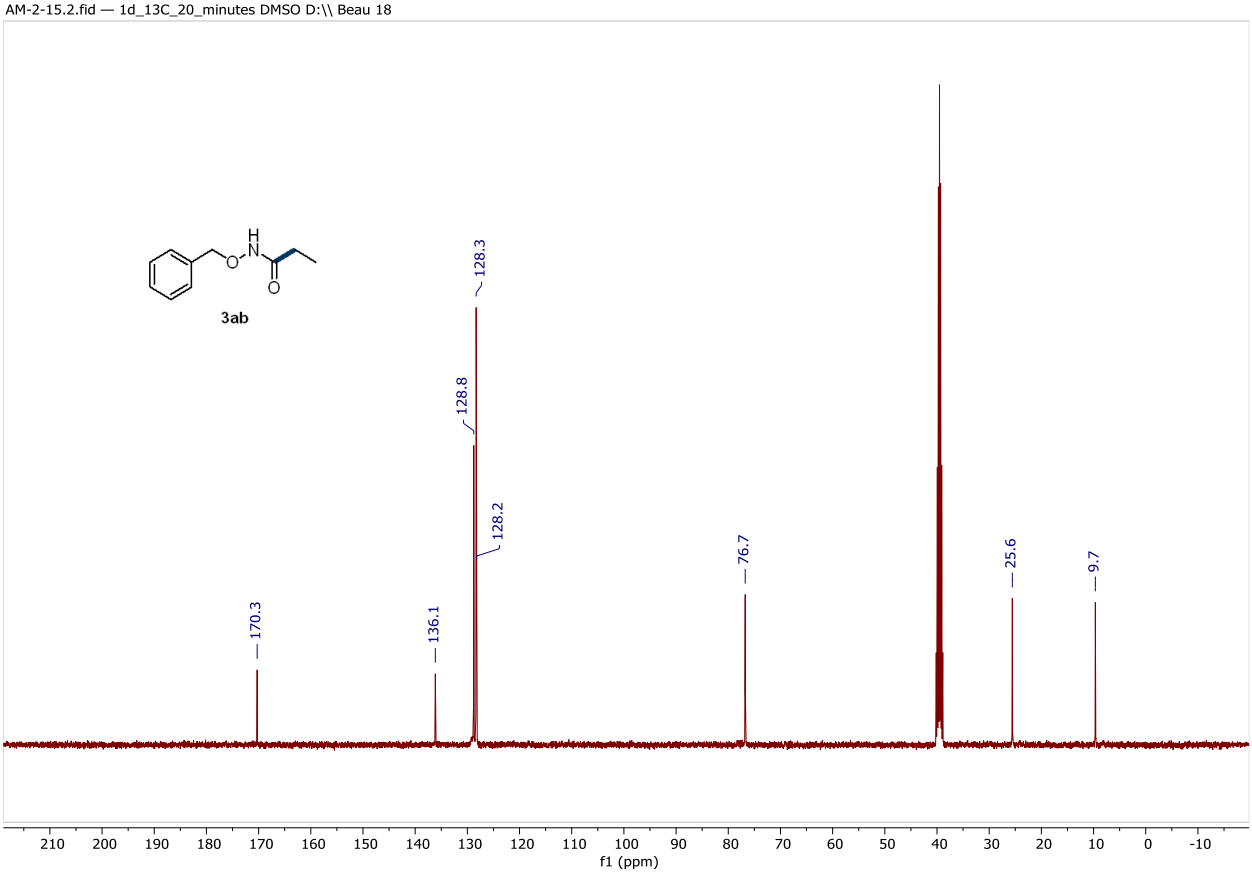

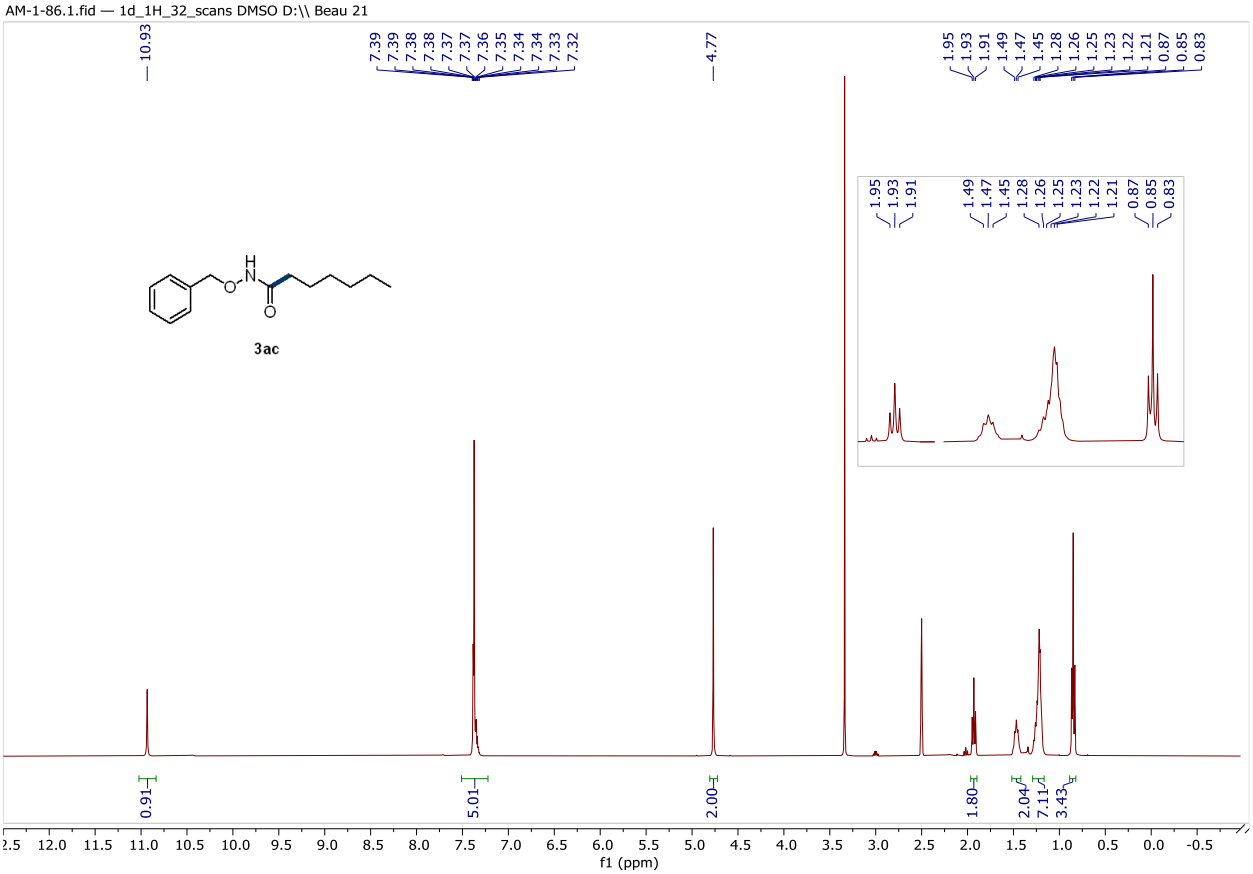
AM-1-86.1.fid — 1d_1H_32_scans DMSO D:\\ Beau 21
10.93
7.39
7.39
7.38
7.38
7.37
7.37
7.36
7.35
7.34
7.34
7.33
7.32
4.77
1.95
1.93
1.91
1.49
1.47
1.45
1.28
1.26
1.25
1.23
1.22
1.21
0.87
0.85
0.83
3ac
0.91
5.01
2.00
1.80
2.04
7.11
3.43
f1 (ppm)

AM-1-86.2.fid — 1d_13C_1_hour DMSO D:\\ Beau 21

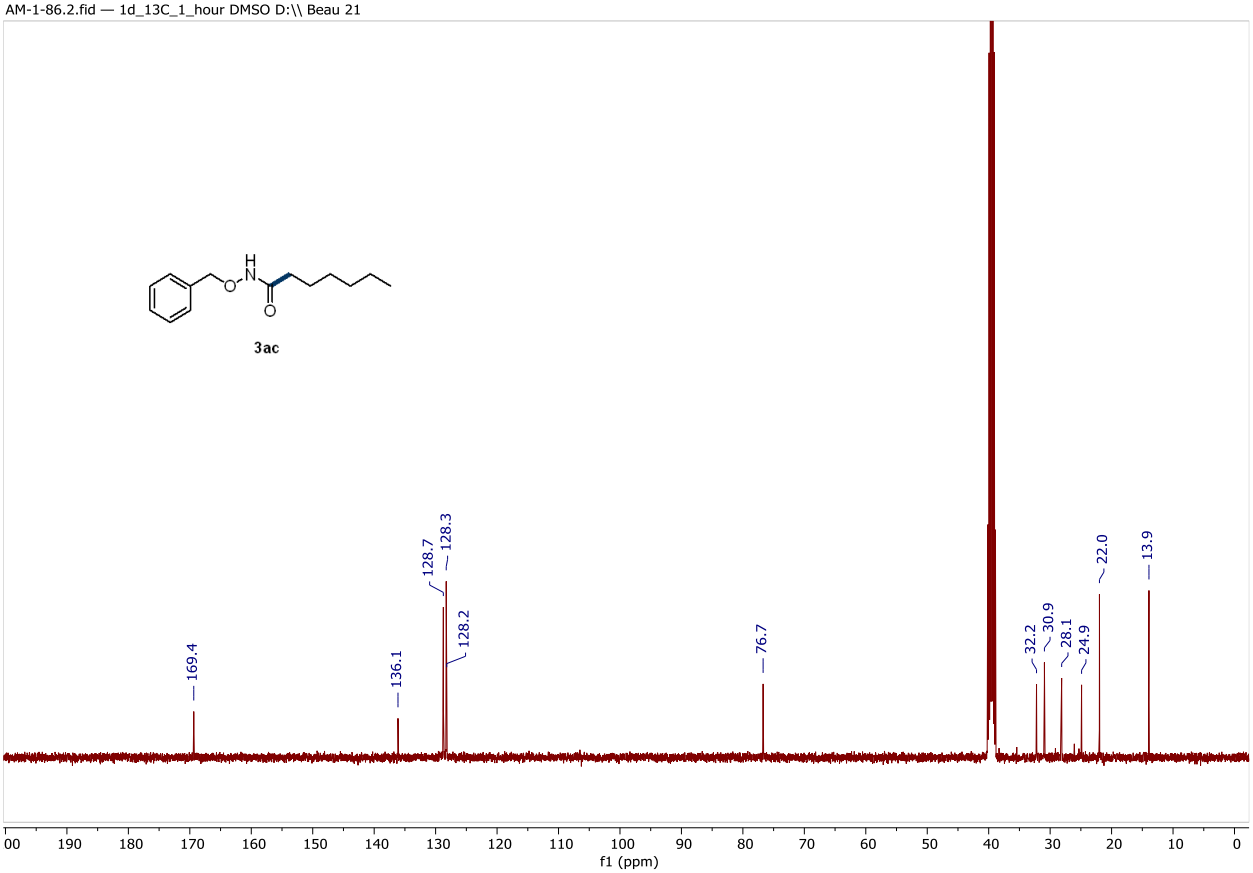

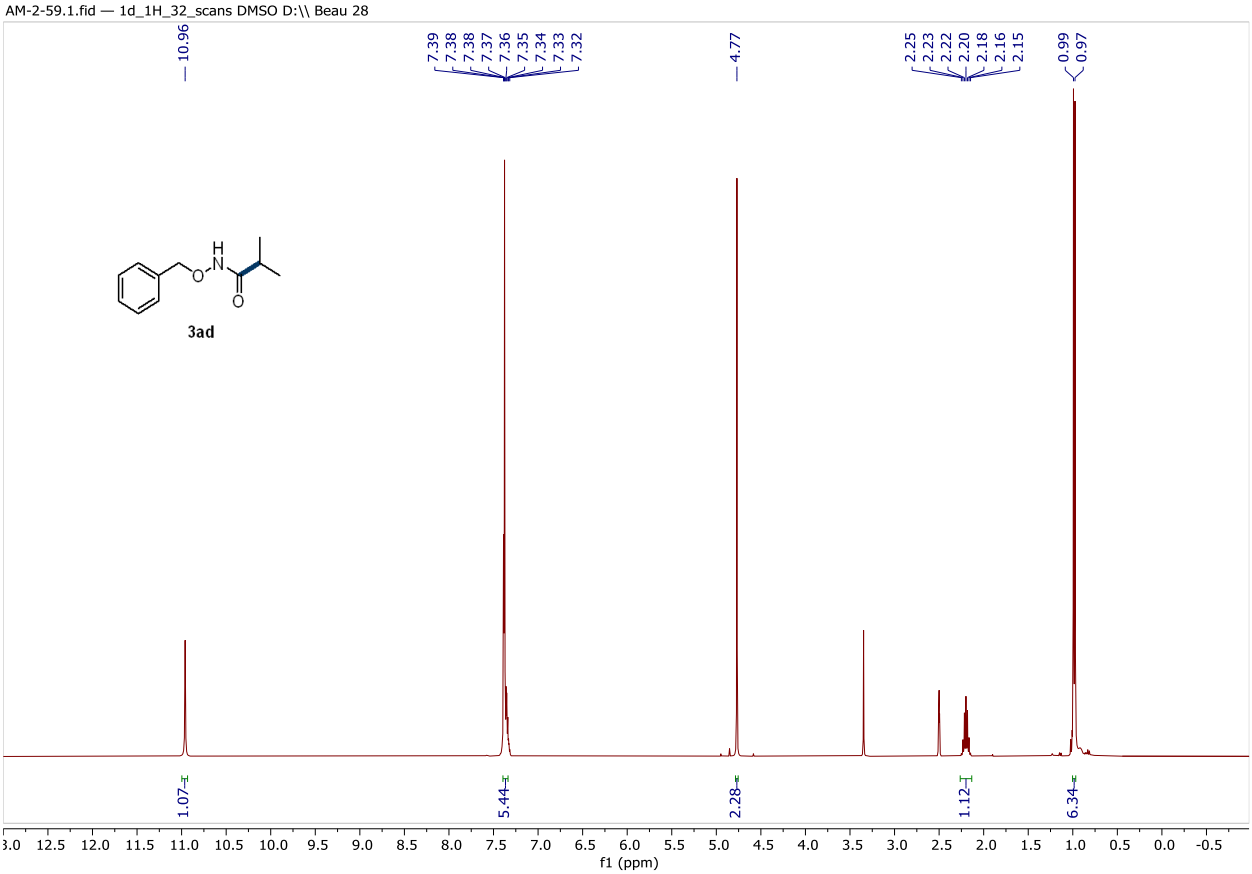
AM-2-59.1.fid — 1d_1H_32_scans DMSO D:\\ Beau 28
10.96
7.39
7.38
7.38
7.37
7.36
7.35
7.34
7.33
7.32
4.77
2.25
2.23
2.22
2.20
2.18
2.16
2.15
0.99
0.97
3ad
1.07
5.44
2.28
1.12
6.34
f1 (ppm)

AM-2-59.2.fid — 1d_13C_1_hour DMSO D:\\ Beau 28

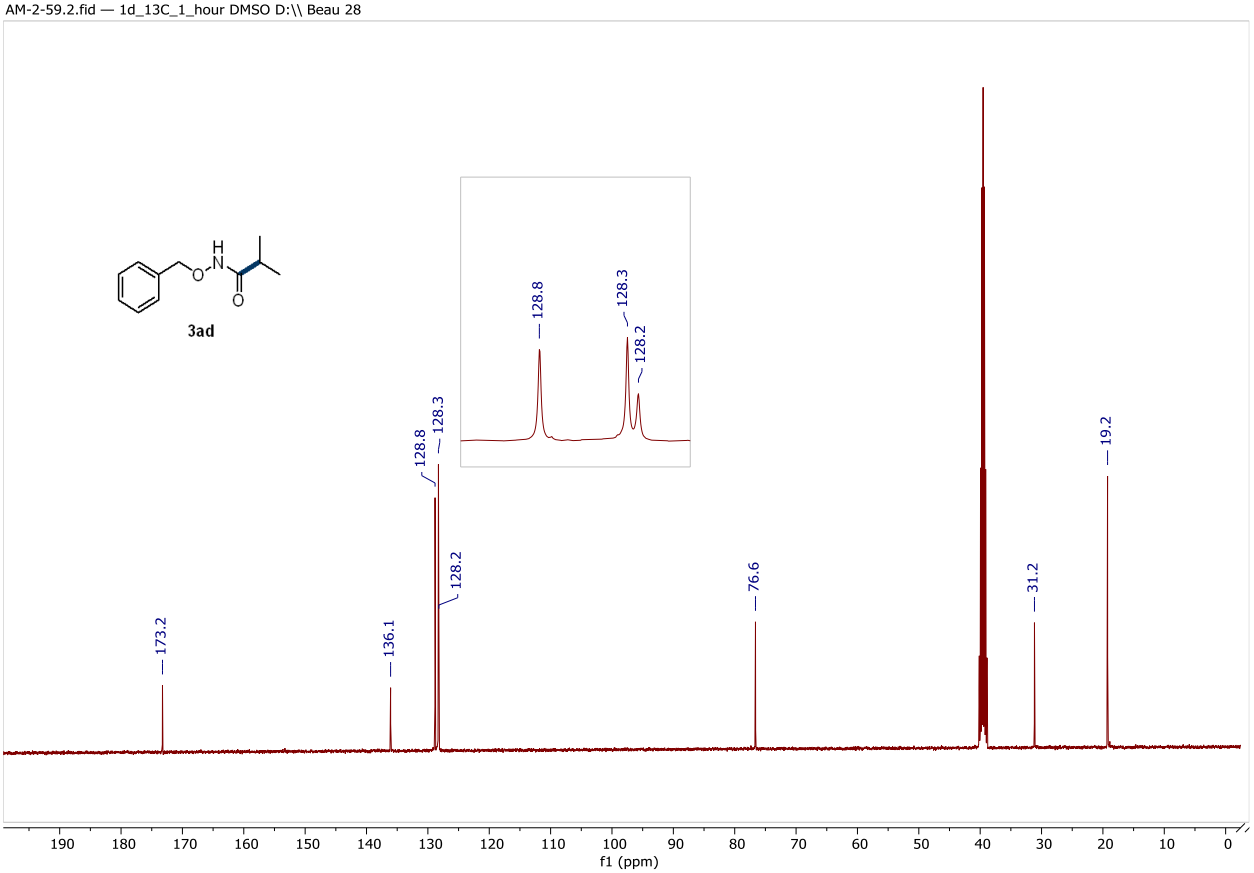

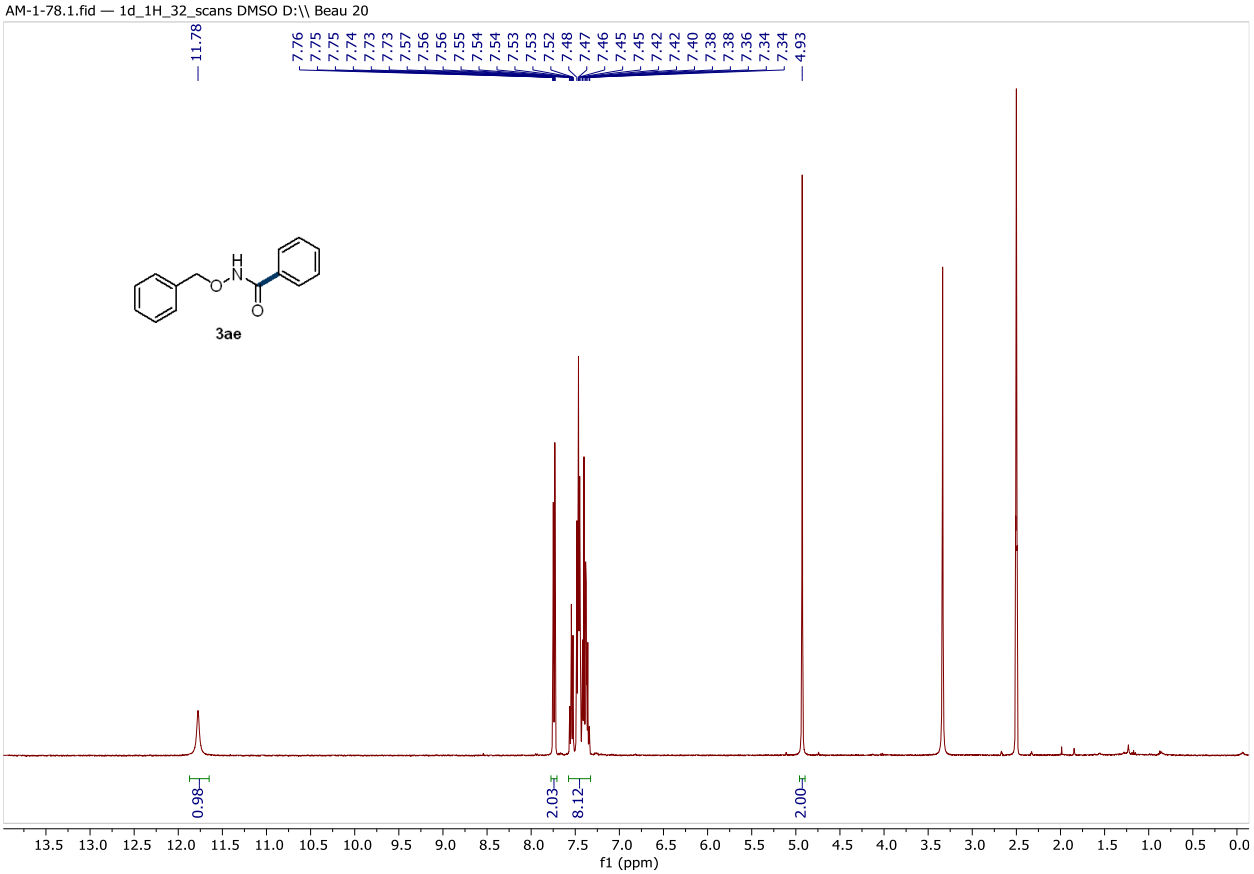
AM-1-78.1.fid — 1d_1H_32_scans DMSO D:\\ Beau 20
11.78
7.76
7.75
7.75
7.74
7.73
7.73
7.57
7.56
7.56
7.55
7.54
7.54
7.53
7.53
7.52
7.48
7.47
7.46
7.45
7.45
7.42
7.42
7.40
7.38
7.38
7.36
7.34
7.34
4.93
3ae
0.98
2.03
8.12
2.00
13.5 13.0 12.5 12.0 11.5 11.0 10.5 10.0 9.5 9.0 8.5 8.0 7.5 7.0 6.5 6.0 5.5 5.0 4.5 4.0 3.5 3.0 2.5 2.0 1.5 1.0 0.5 0.0
f1 (ppm)

AM-1-78.2.fid — 1d_13C_1_hour DMSO D:\\ Beau 20

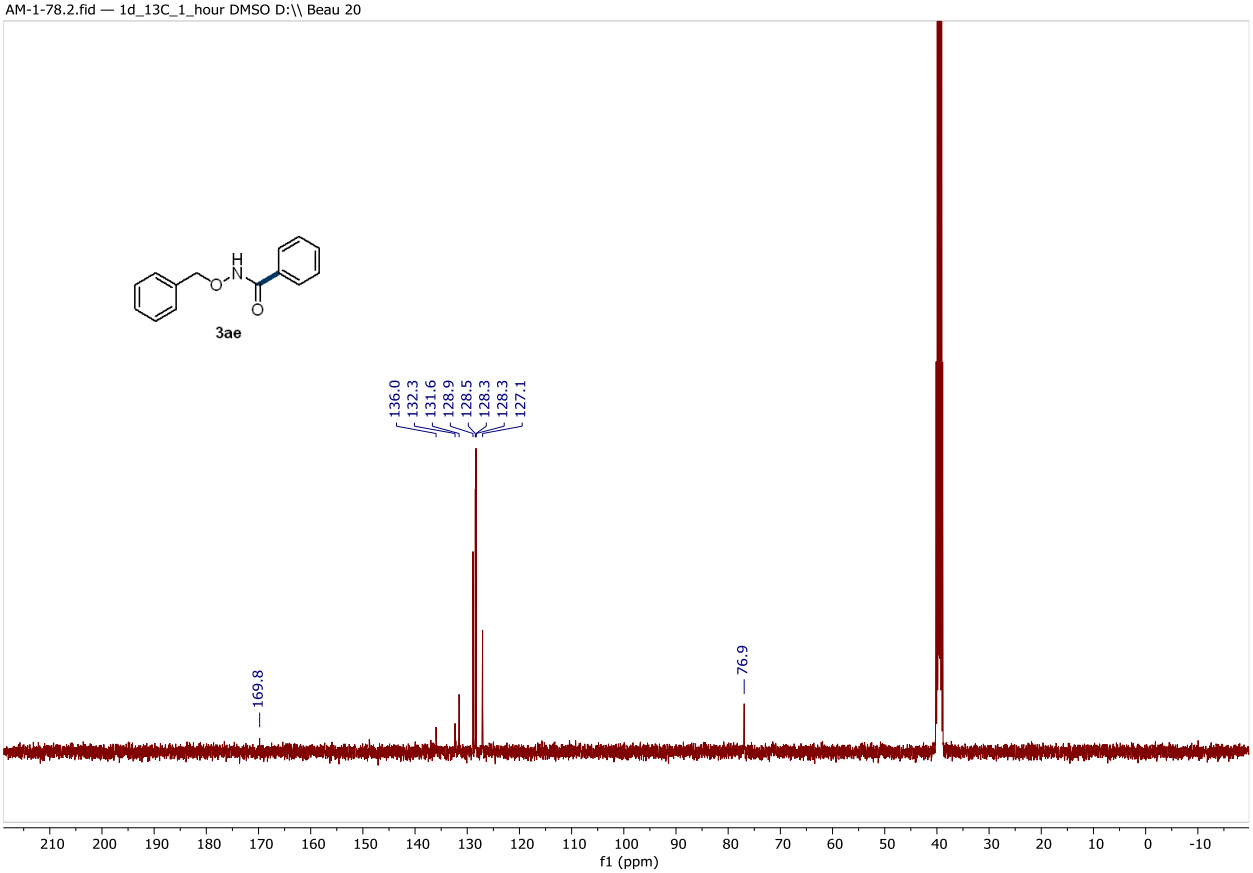

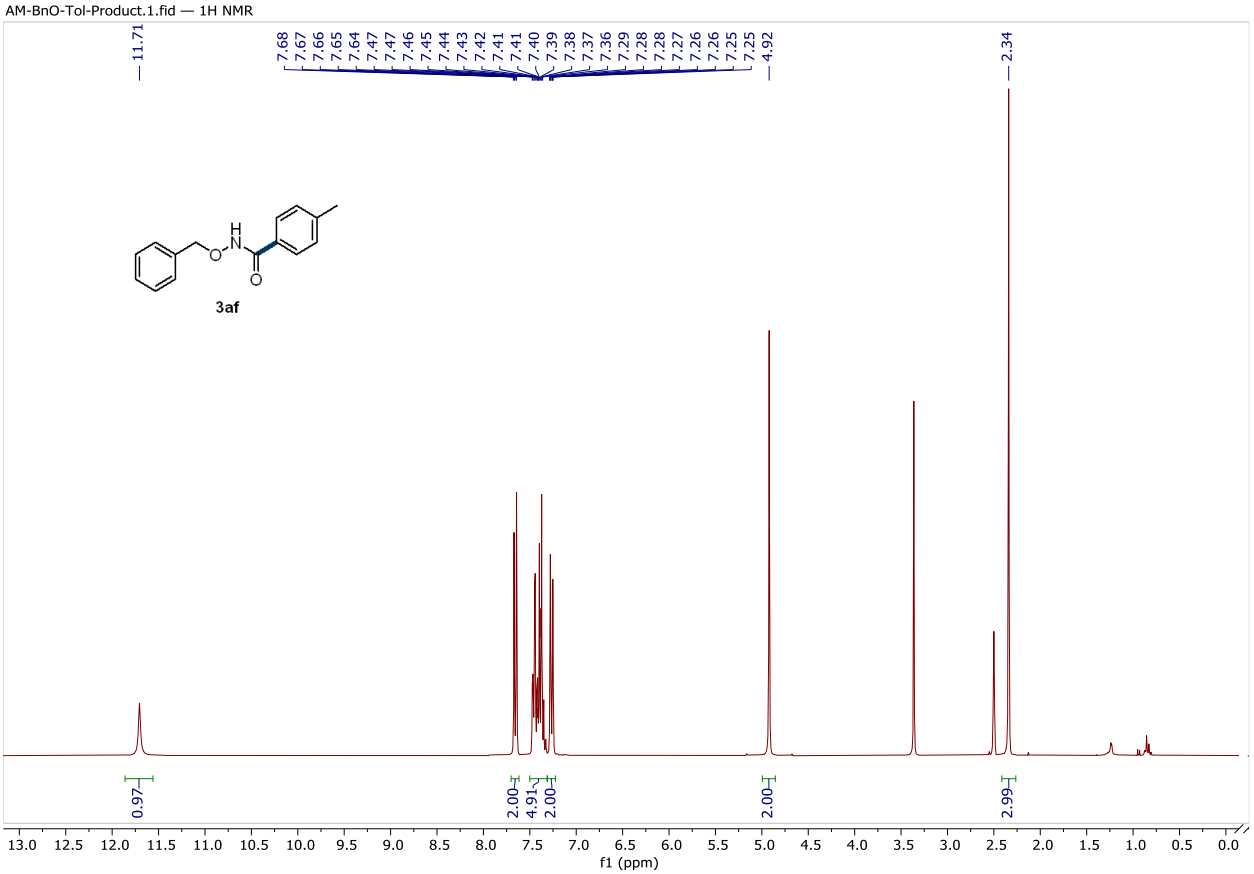
AM-BnO-Tol-Product.1.fid — 1H NMR
11.71
7.68
7.67
7.66
7.65
7.64
7.47
7.47
7.46
7.45
7.44
7.43
7.42
7.41
7.41
7.40
7.39
7.38
7.37
7.36
7.29
7.28
7.28
7.27
7.26
7.26
7.25
7.25
4.92
2.34
3af
0.97
2.00
4.91
2.00
2.00
2.99
f1 (ppm)

AM-BnO-Tol-Product.2.fid — 13C NMR with proton decoupling

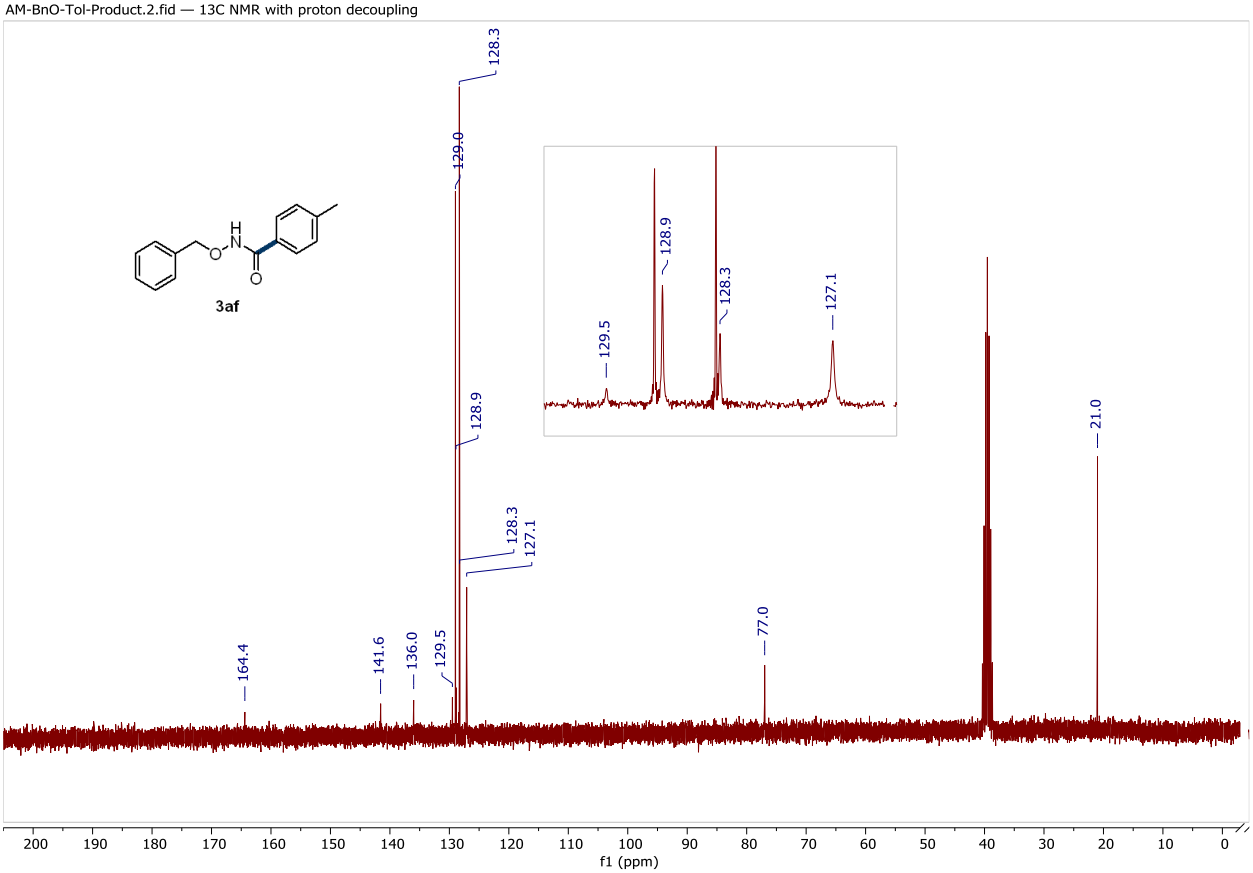

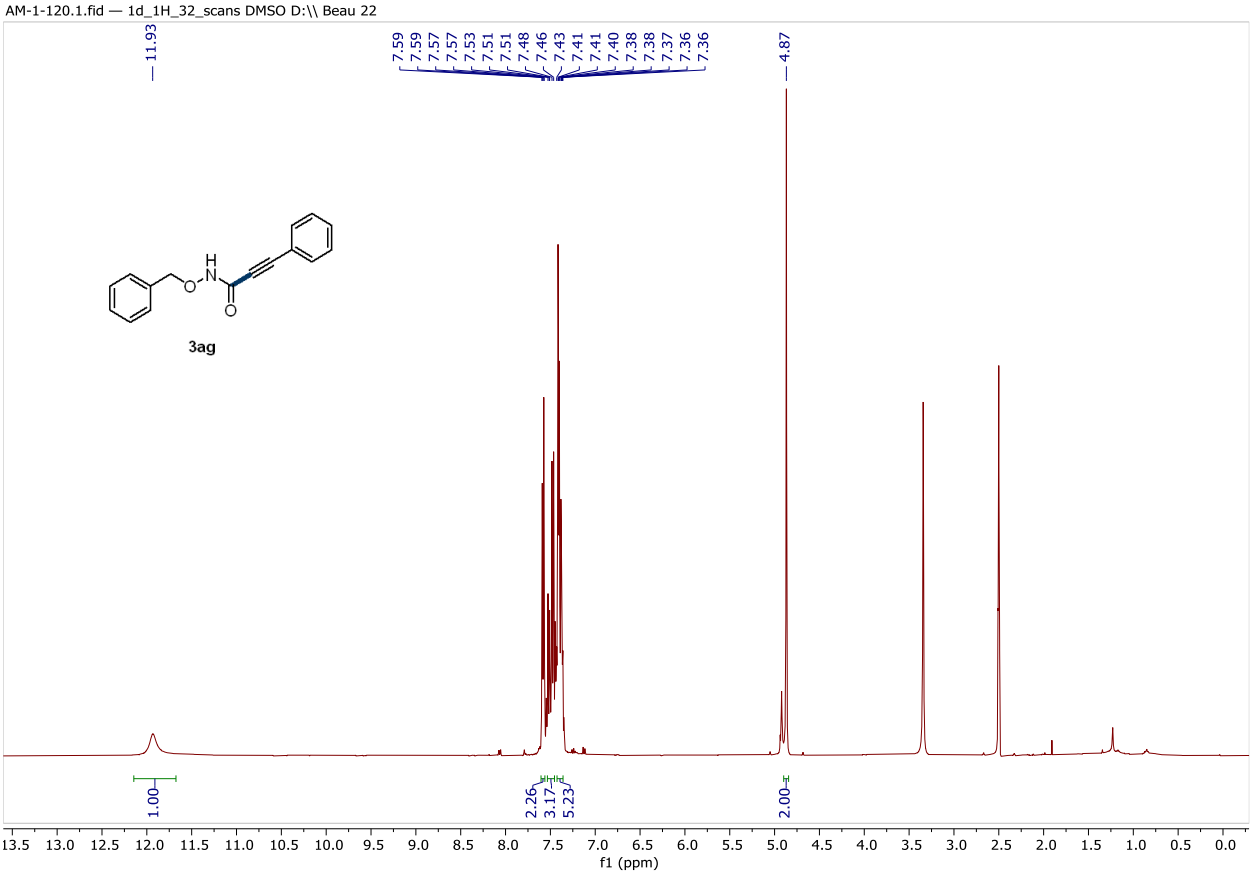
AM-1-120.1.fid — 1d_1H_32_scans DMSO D:\\ Beau 22
11.93
7.59
7.59
7.57
7.57
7.53
7.51
7.51
7.48
7.46
7.43
7.41
7.41
7.40
7.38
7.38
7.37
7.36
7.36
4.87
3ag
1.00
2.26
3.17
5.23
2.00
13.5 13.0 12.5 12.0 11.5 11.0 10.5 10.0 9.5 9.0 8.5 8.0 7.5 7.0 6.5 6.0 5.5 5.0 4.5 4.0 3.5 3.0 2.5 2.0 1.5 1.0 0.5 0.0
f1 (ppm)

AM-1-120.2.fid — 1d_13C_1_hour DMSO D:\\ Beau 22

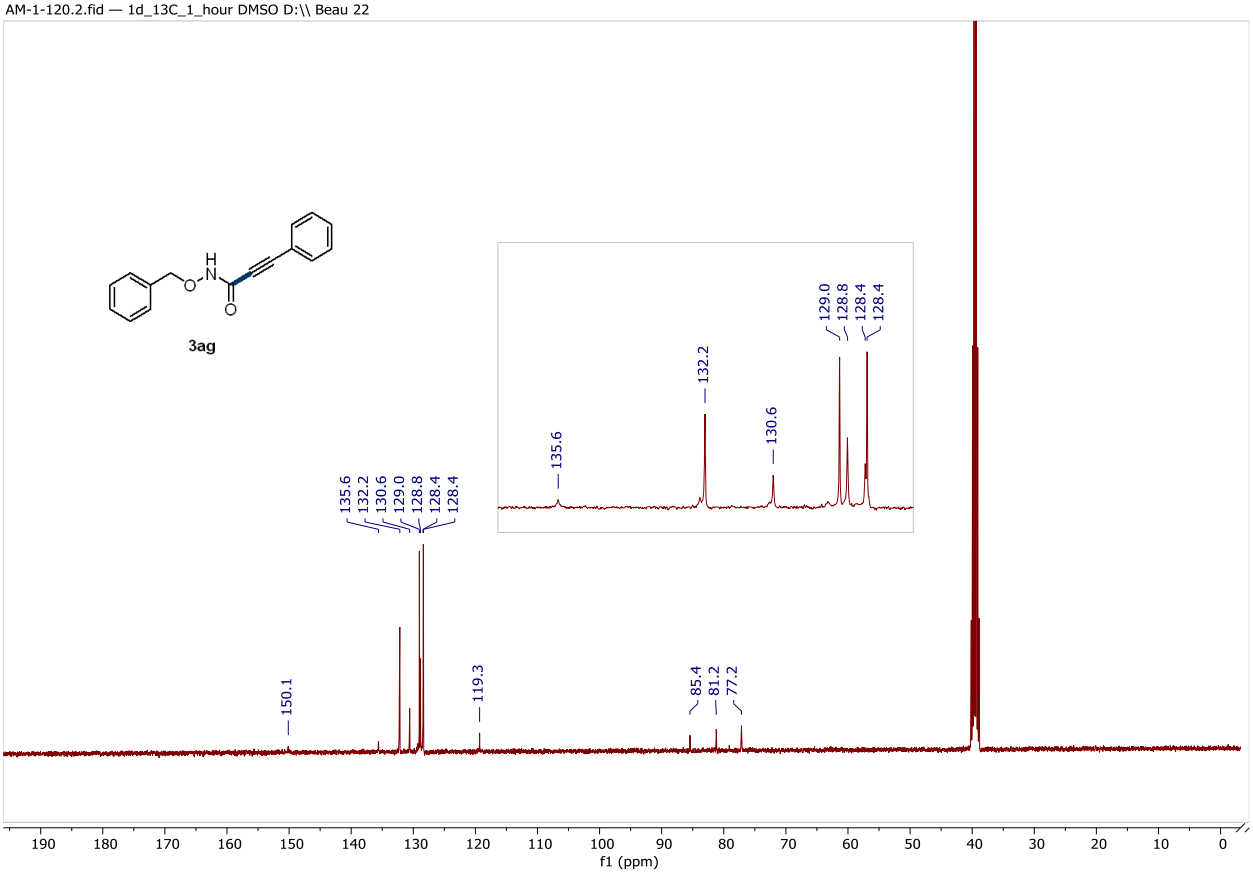

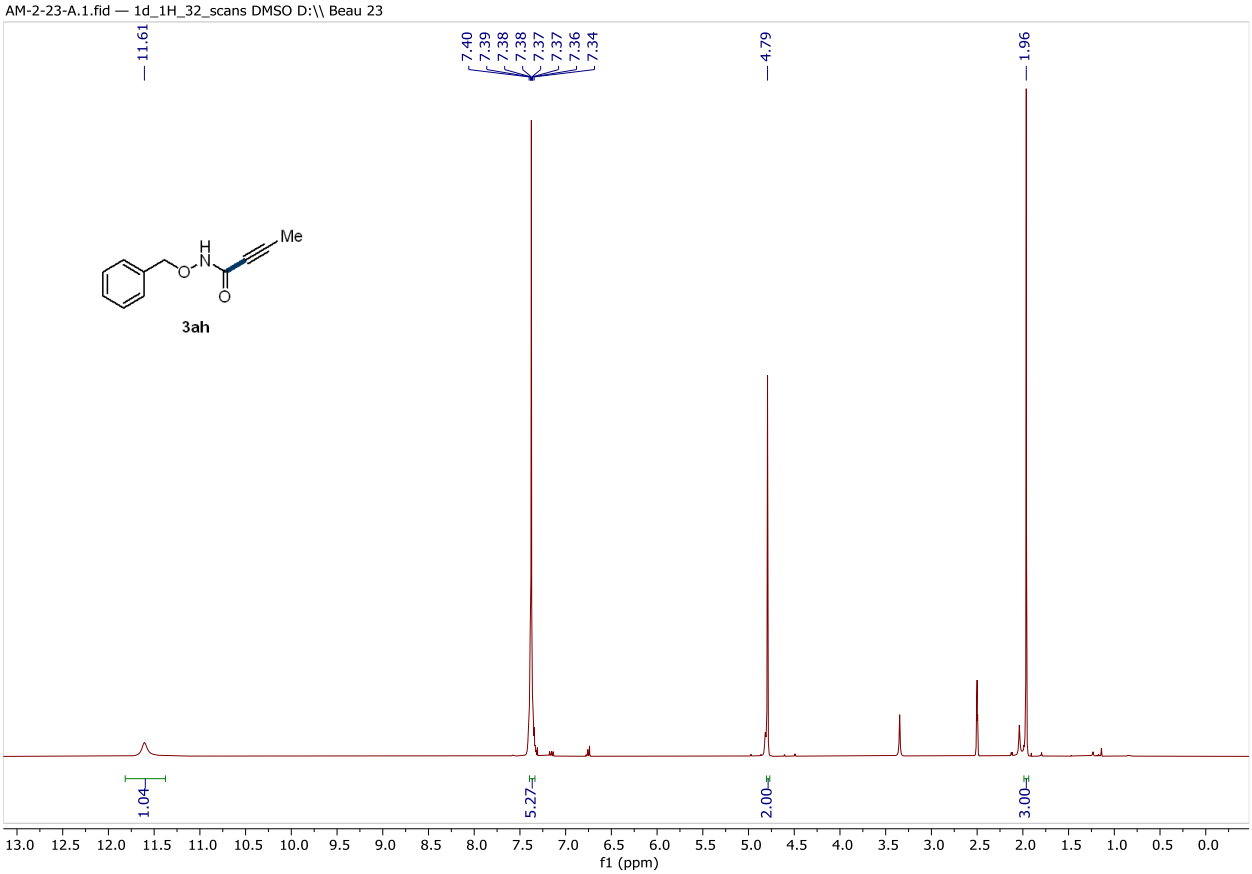
AM-2-23-A.1.fid — 1d_1H_32_scans DMSO D:\\ Beau 23
11.61
7.40
7.39
7.38
7.38
7.37
7.37
7.36
7.34
4.79
1.96
Me
H
N
O
O
3ah
1.04
5.27
2.00
3.00
13.0 12.5 12.0 11.5 11.0 10.5 10.0 9.5 9.0 8.5 8.0 7.5 7.0 6.5 6.0 5.5 5.0 4.5 4.0 3.5 3.0 2.5 2.0 1.5 1.0 0.5 0.0
f1 (ppm)

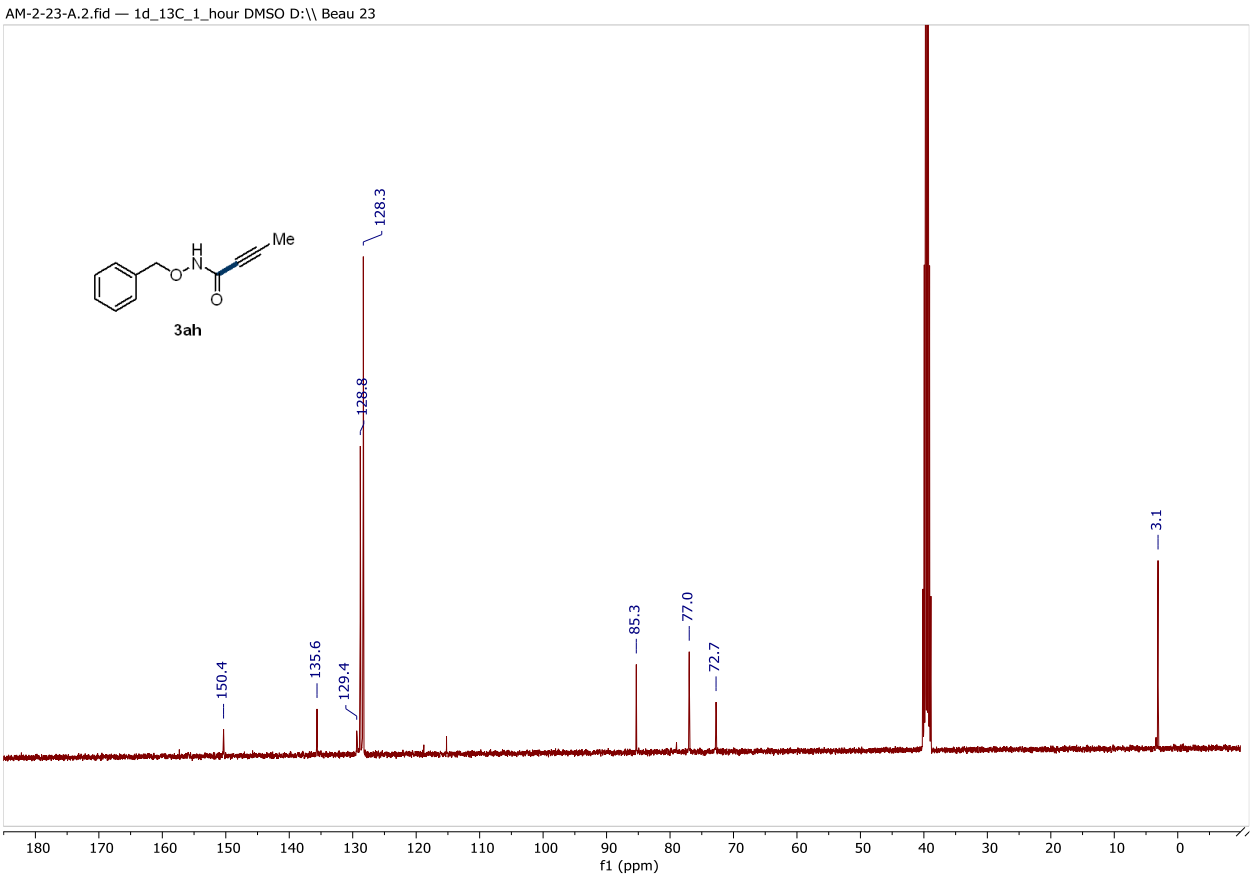
AM-2-23-A.2.fid — 1d_13C_1_hour DMSO D:\\ Beau 23
Me
H
N
O
O
3ah
128.3
128.8
150.4
135.6
129.4
85.3
77.0
72.7
3.1
180
170
160
150
140
130
120
110
100
90
80
70
60
50
40
30
20
10
0
f1 (ppm)

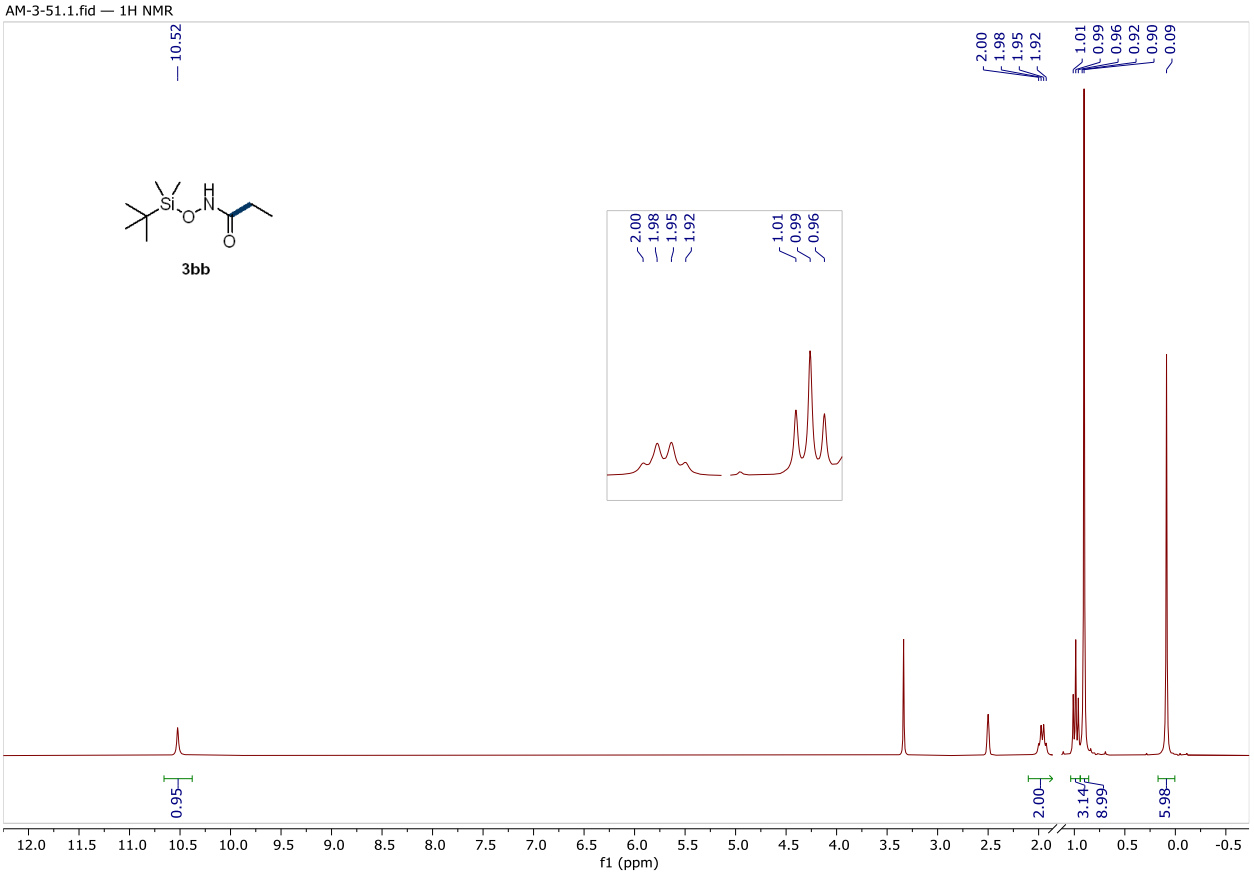
AM-3-51.1.fid — 1H NMR
10.52
2.00
1.98
1.95
1.92
1.01
0.99
0.96
0.92
0.90
0.09
3bb
0.95
2.00
3.14
8.99
5.98
f1 (ppm)

AM-3-51.2.fid — 13C NMR with proton decoupling

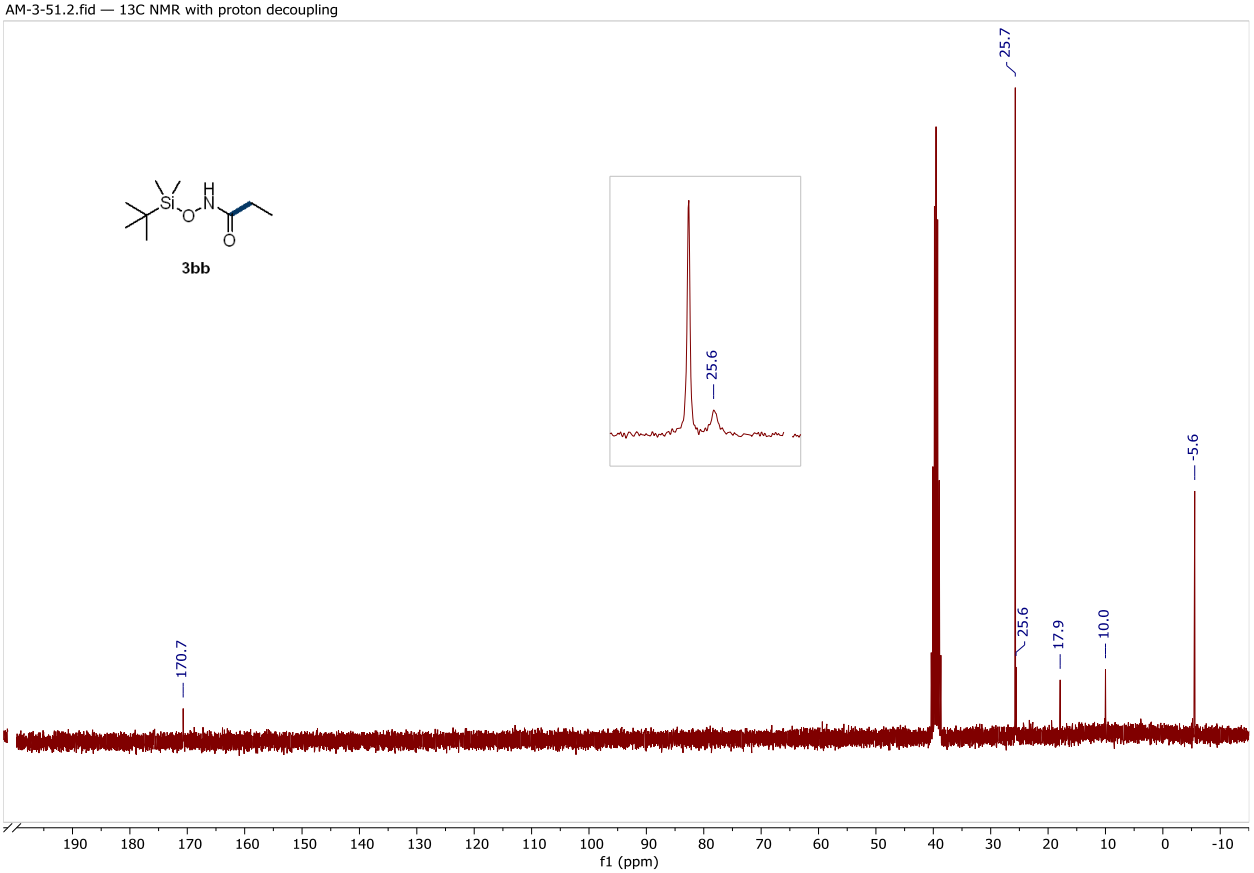

AM-3-51.3.fid — 13C DEPT 135

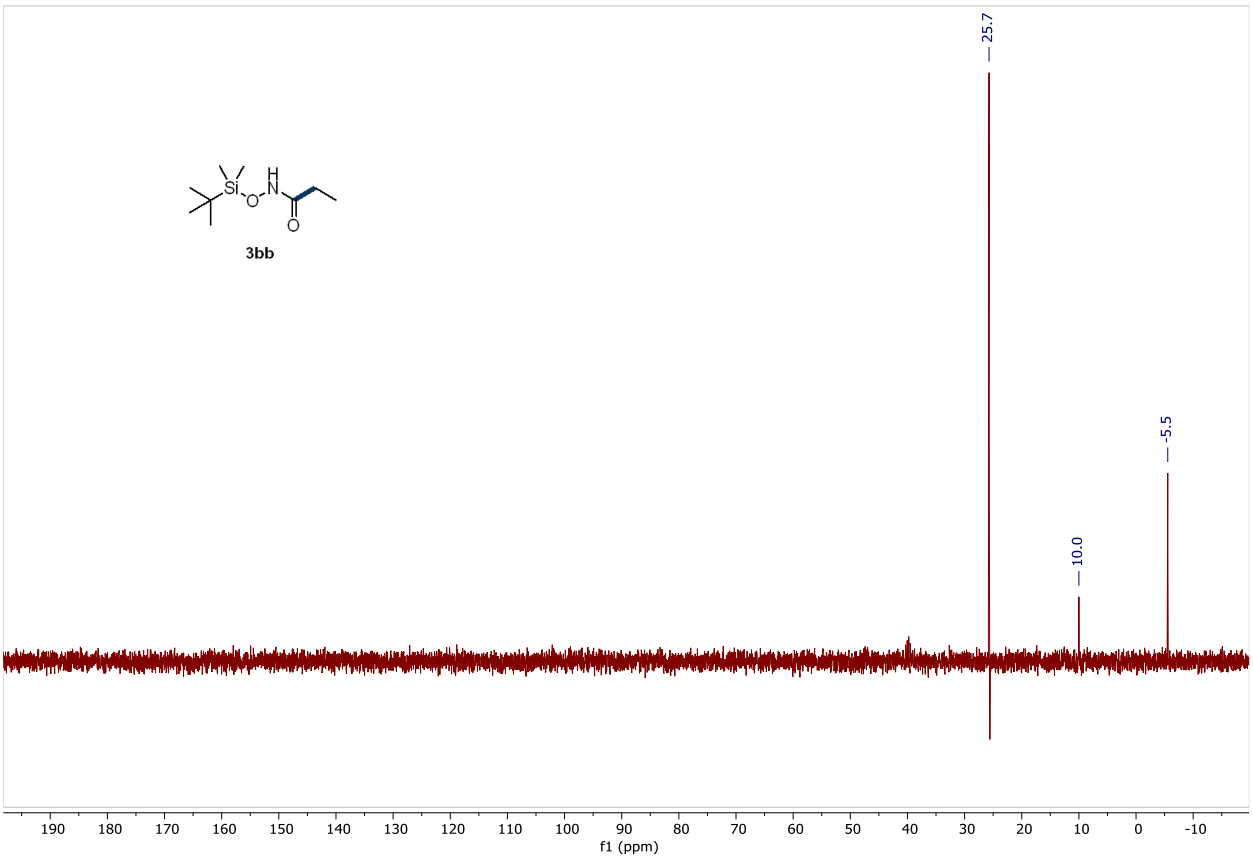

AM-3-52.1.fid — 1H NMR

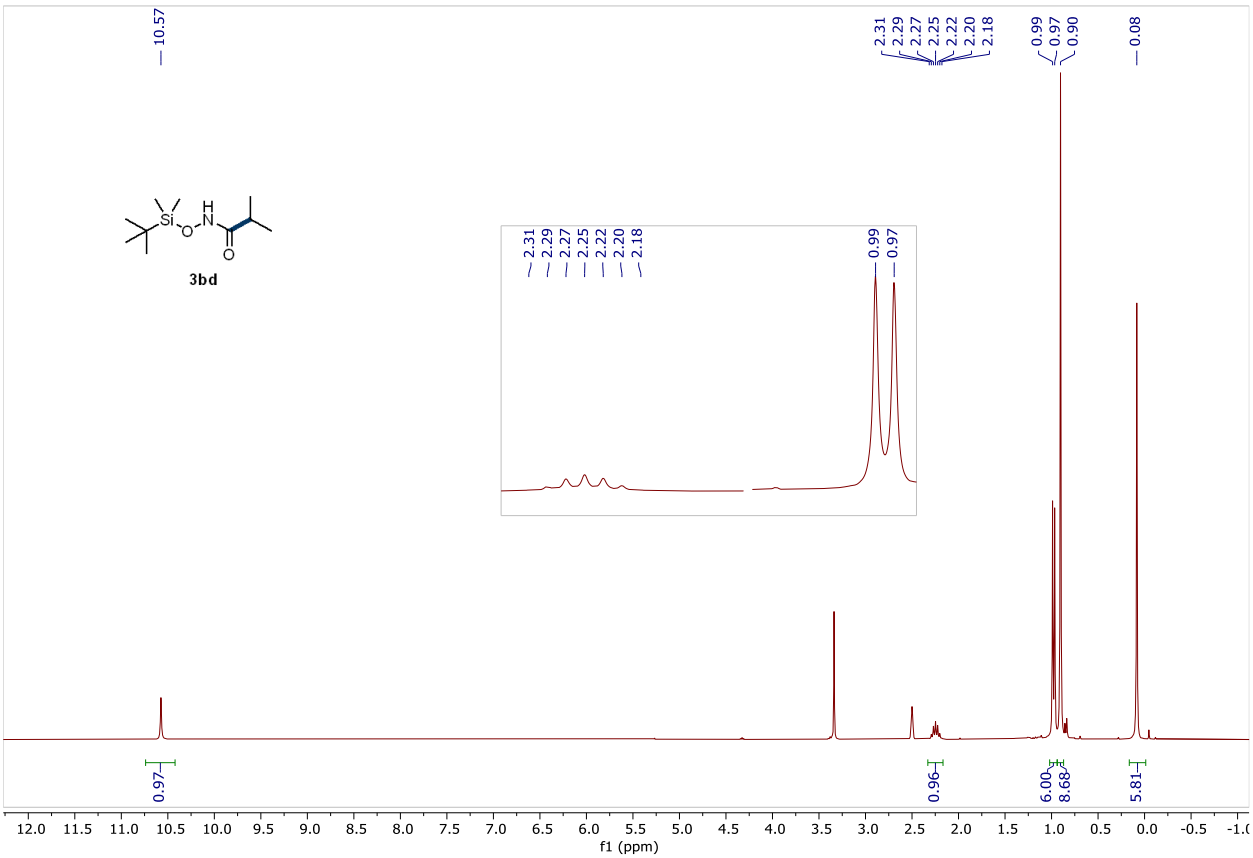

AM-3-52.2.fid — 13C NMR with proton decoupling

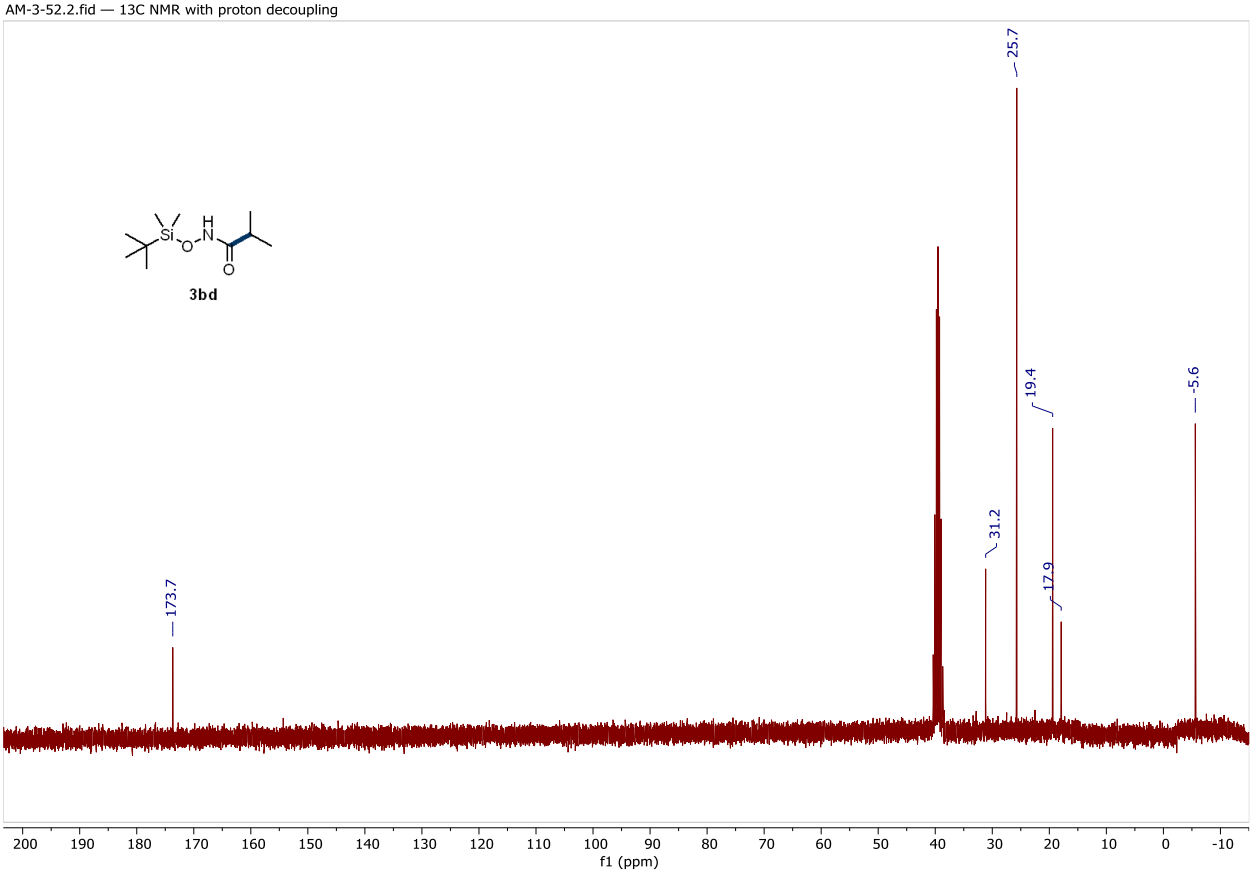

AM-3-53.1.fid — 1d_1H_16_scans DMSO D:\\ Beau 36

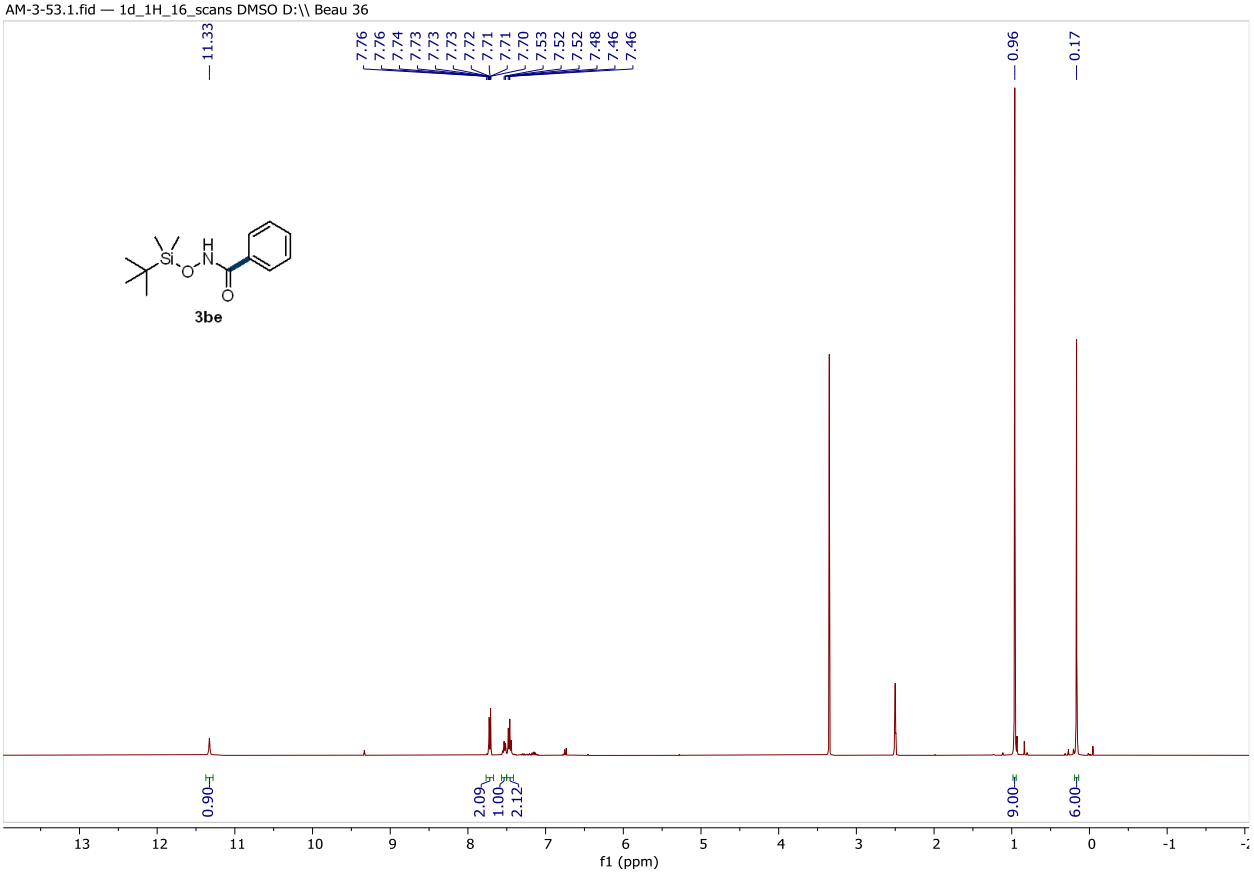

AM-3-53.2.fid — 1d_13C_20_minutes DMSO D:\\ Beau 36

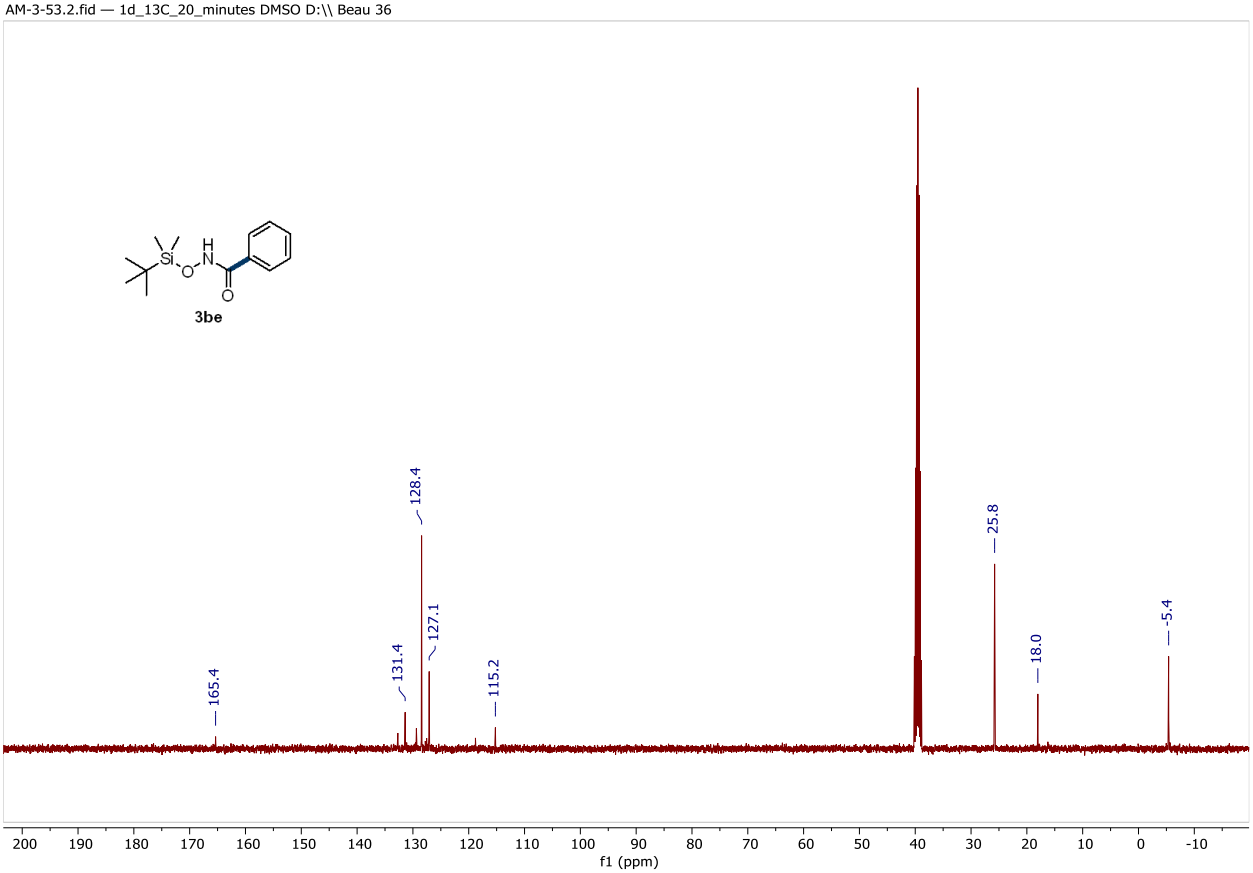

AM-3-60.10.fid — 1d_1H_4min DMSO {C:\data} Beau 14

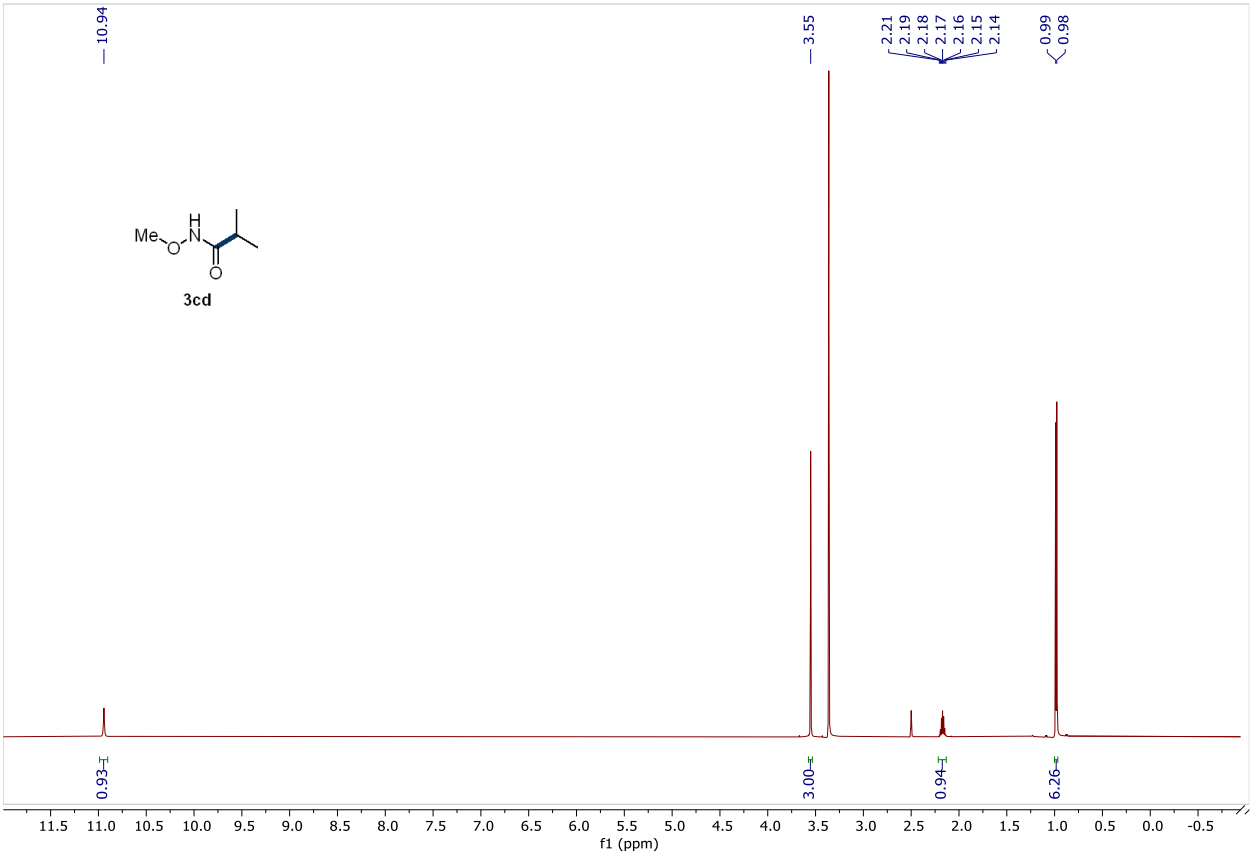

AM-3-60.11.fid — {1d_13C[1H]_35min} DMSO {C:\data} Beau 14

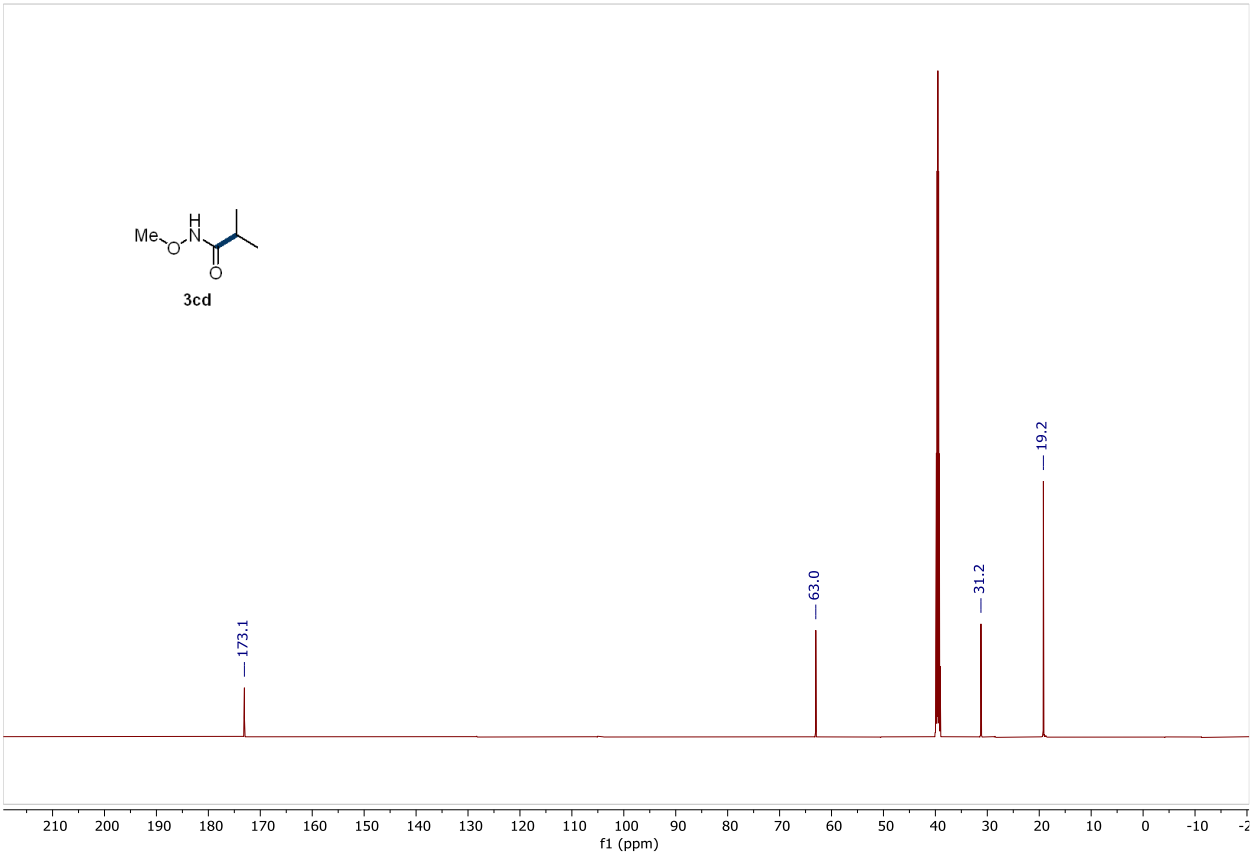

AM-OMe-Ph-product.1.fid — 1H NMR

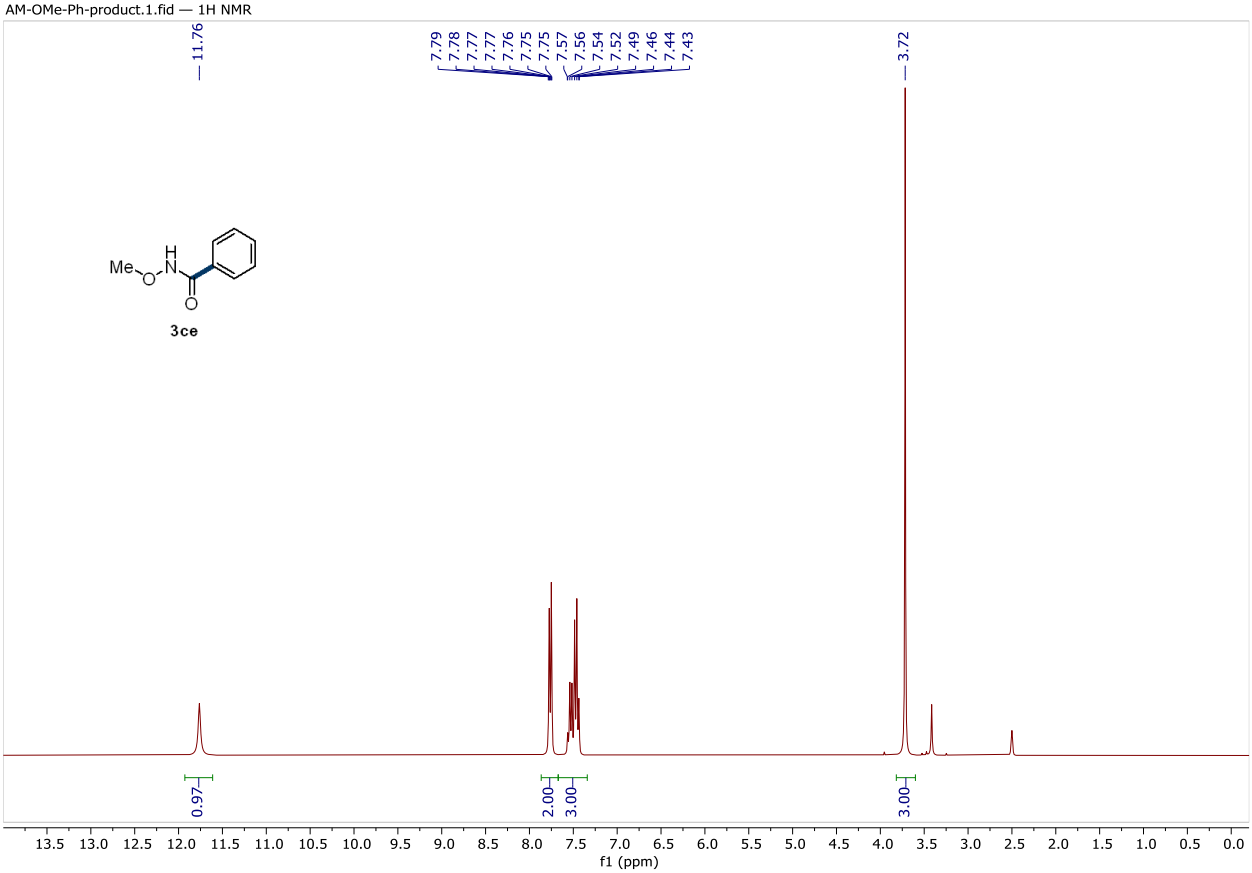

AM-OMe-Ph-product.2.fid — 13C NMR with 1H decoupling

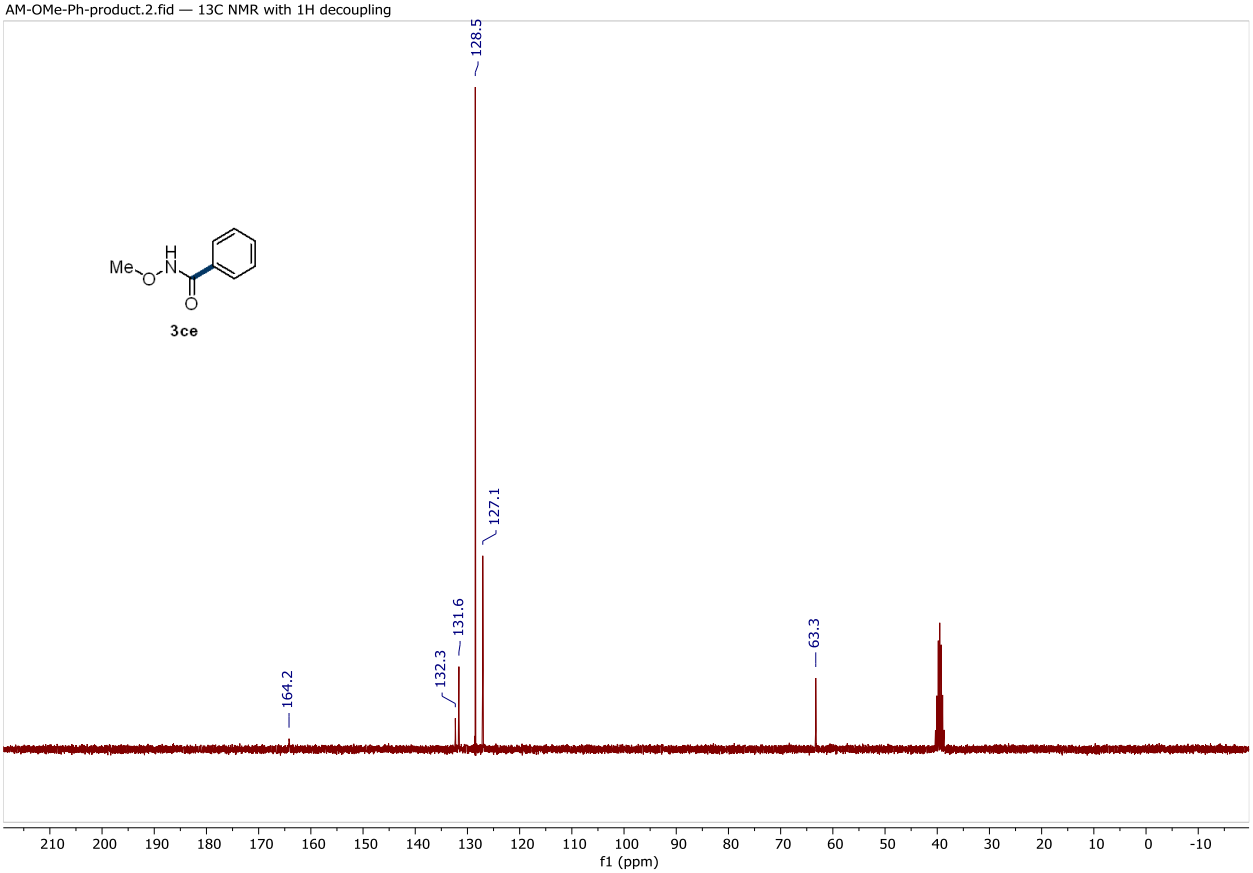

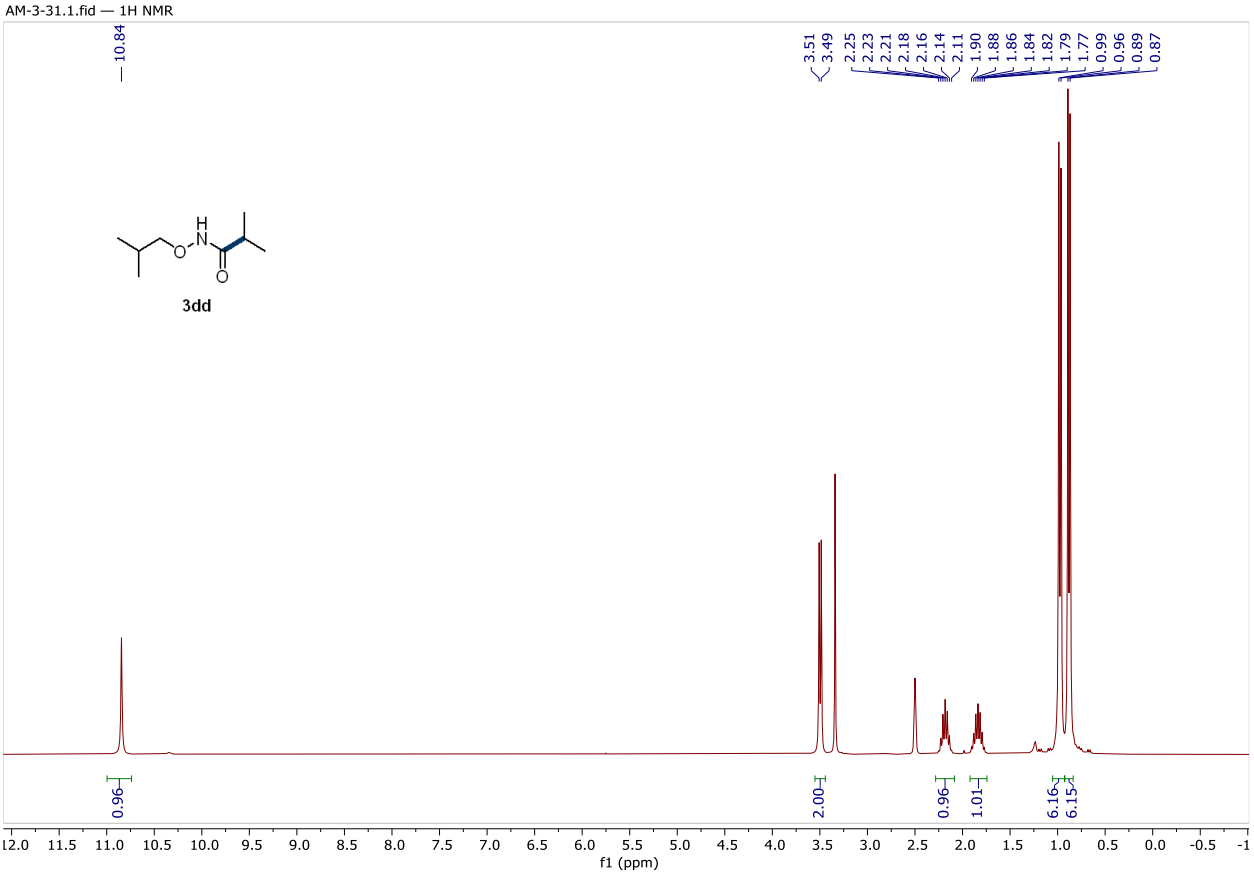
AM-3-31.1.fid — 1H NMR
10.84
3.51
3.49
2.25
2.23
2.21
2.18
2.16
2.14
2.11
1.90
1.88
1.86
1.84
1.82
1.79
1.77
0.99
0.96
0.89
0.87
H
N
O
O
3dd
0.96
2.00
0.96
1.01
6.16
6.15
12.0
11.5
11.0
10.5
10.0
9.5
9.0
8.5
8.0
7.5
7.0
6.5
6.0
5.5
5.0
4.5
4.0
3.5
3.0
2.5
2.0
1.5
1.0
0.5
0.0
-0.5
f1 (ppm)

AM-3-31.2.fid — 13C NMR with proton decoupling

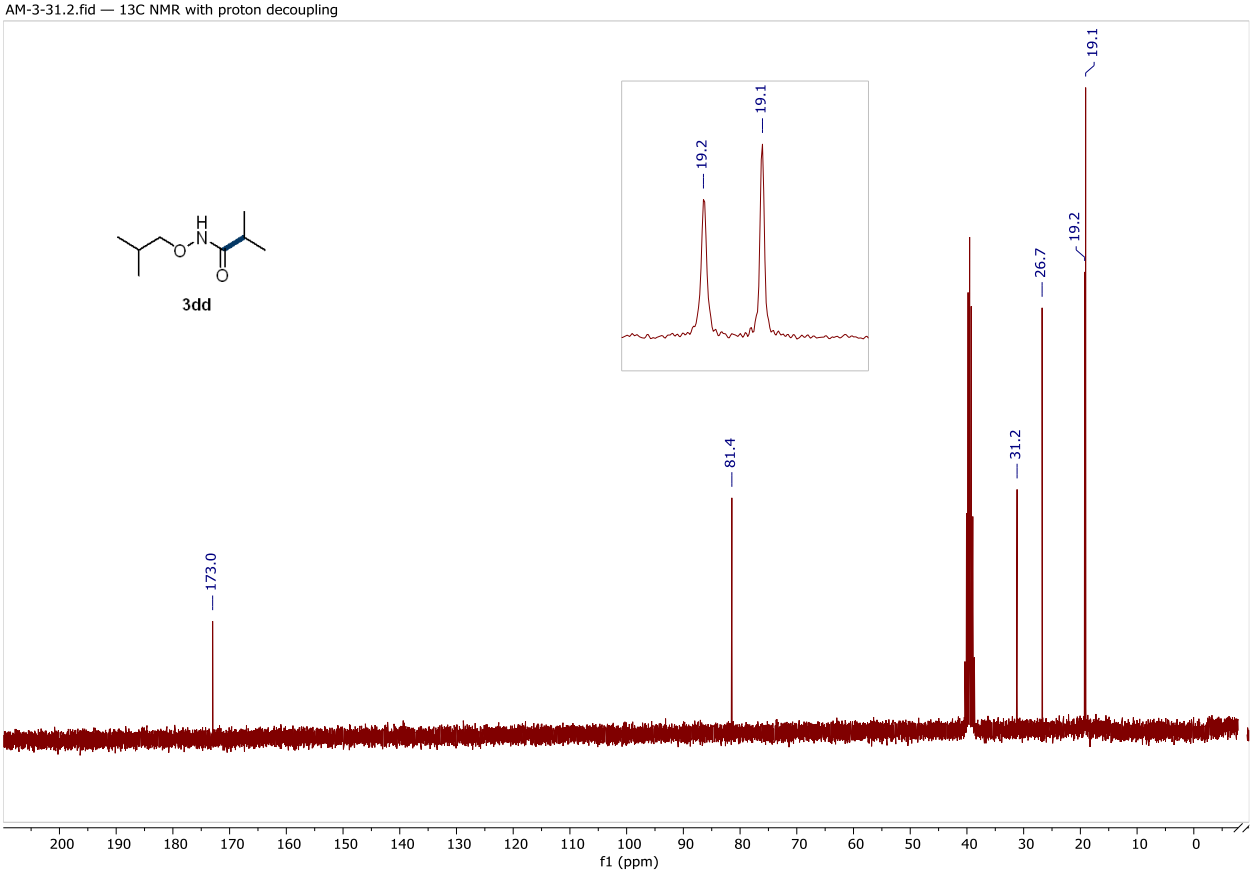

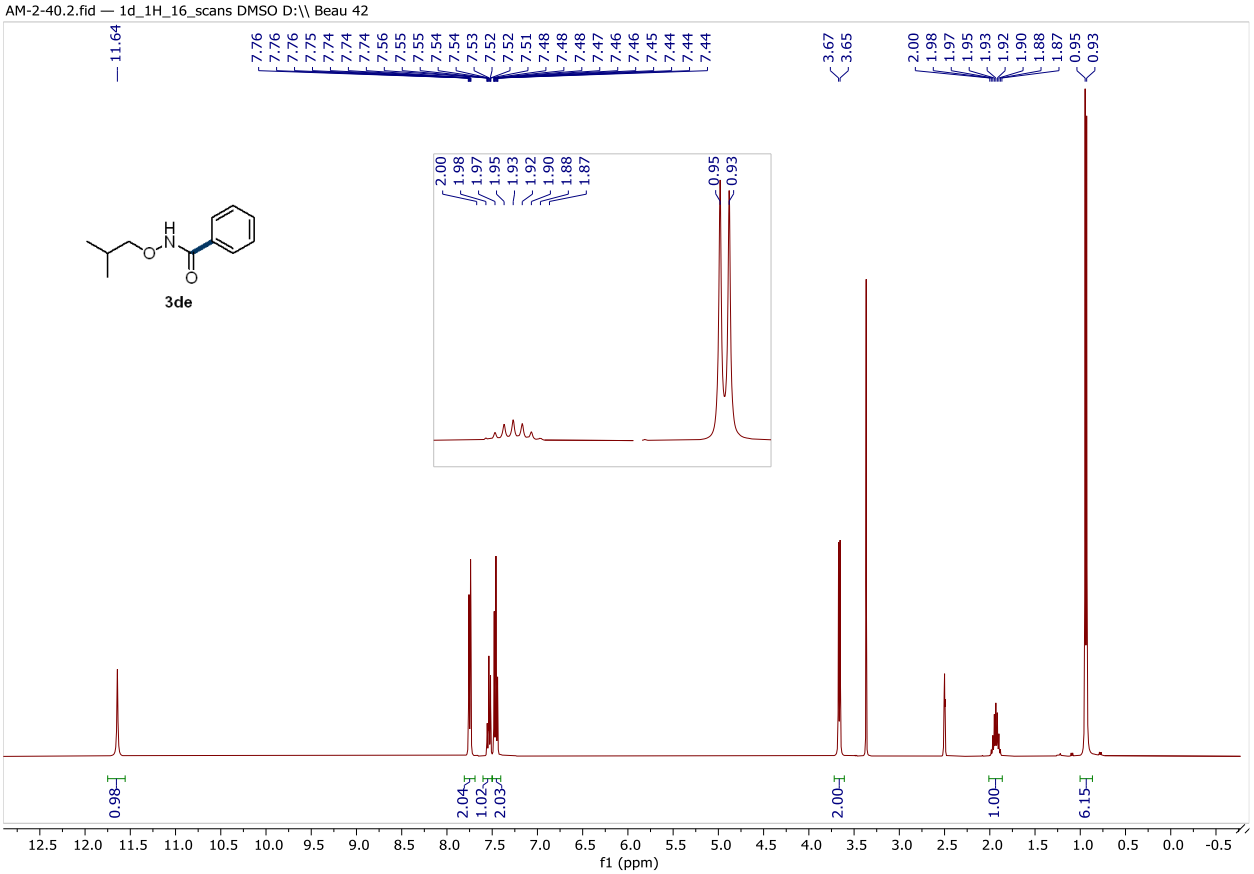
AM-2-40.2.fid — 1d_1H_16_scans DMSO D:\\ Beau 42
11.64
7.76 7.76 7.76 7.75 7.74 7.74 7.74 7.56 7.55 7.55 7.54 7.54 7.53 7.52 7.52 7.51 7.48 7.48 7.48 7.47 7.46 7.46 7.45 7.44 7.44 7.44
3.67 3.65
2.00 1.98 1.97 1.95 1.93 1.92 1.90 1.88 1.87 0.95 0.93
3de
0.98 2.04 1.02 2.03 2.00 1.00 6.15
f1 (ppm)

AM-2-40.3.fid — 1d_13C_20_minutes DMSO D:\\ Beau 42

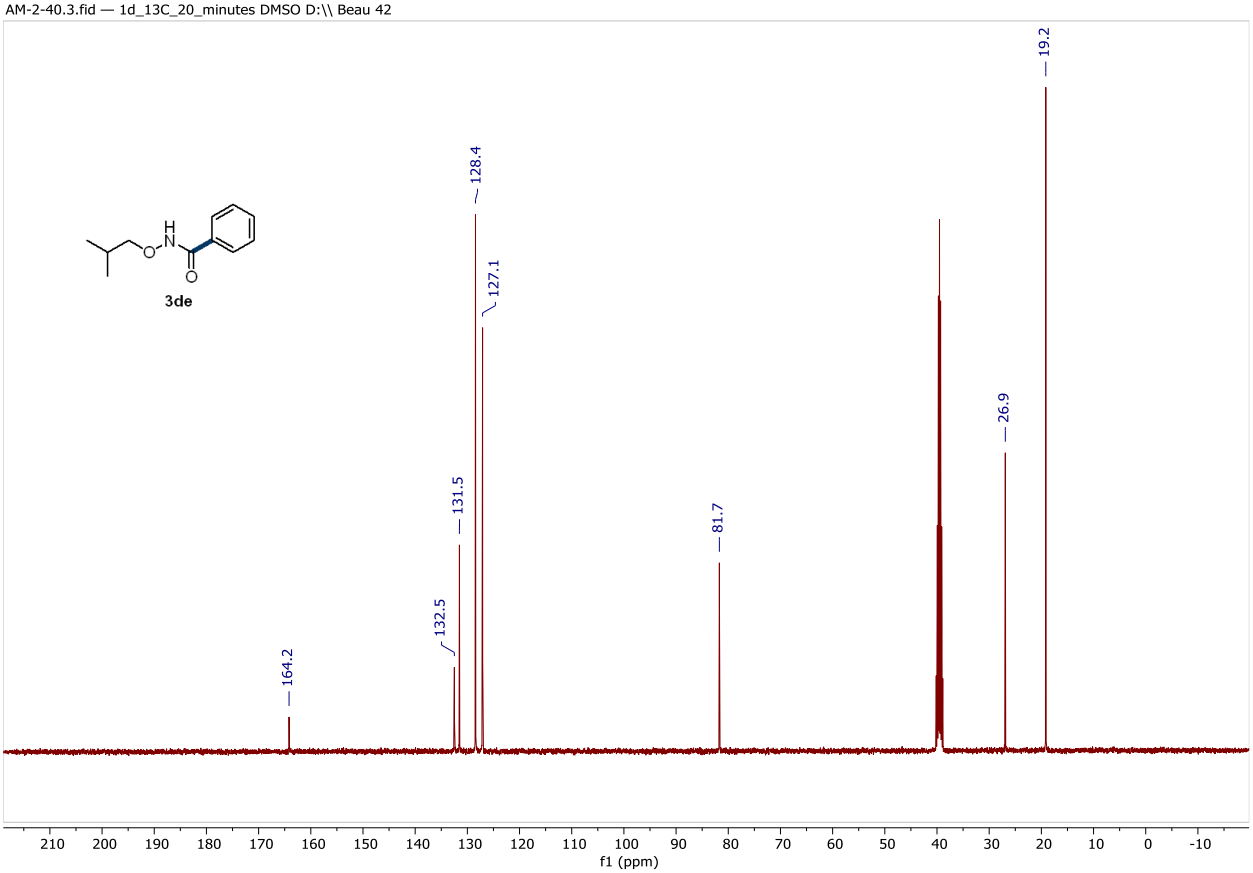

AM-3-32.1.fid — 1d_1H_16_scans DMSO D:\\ Beau 37

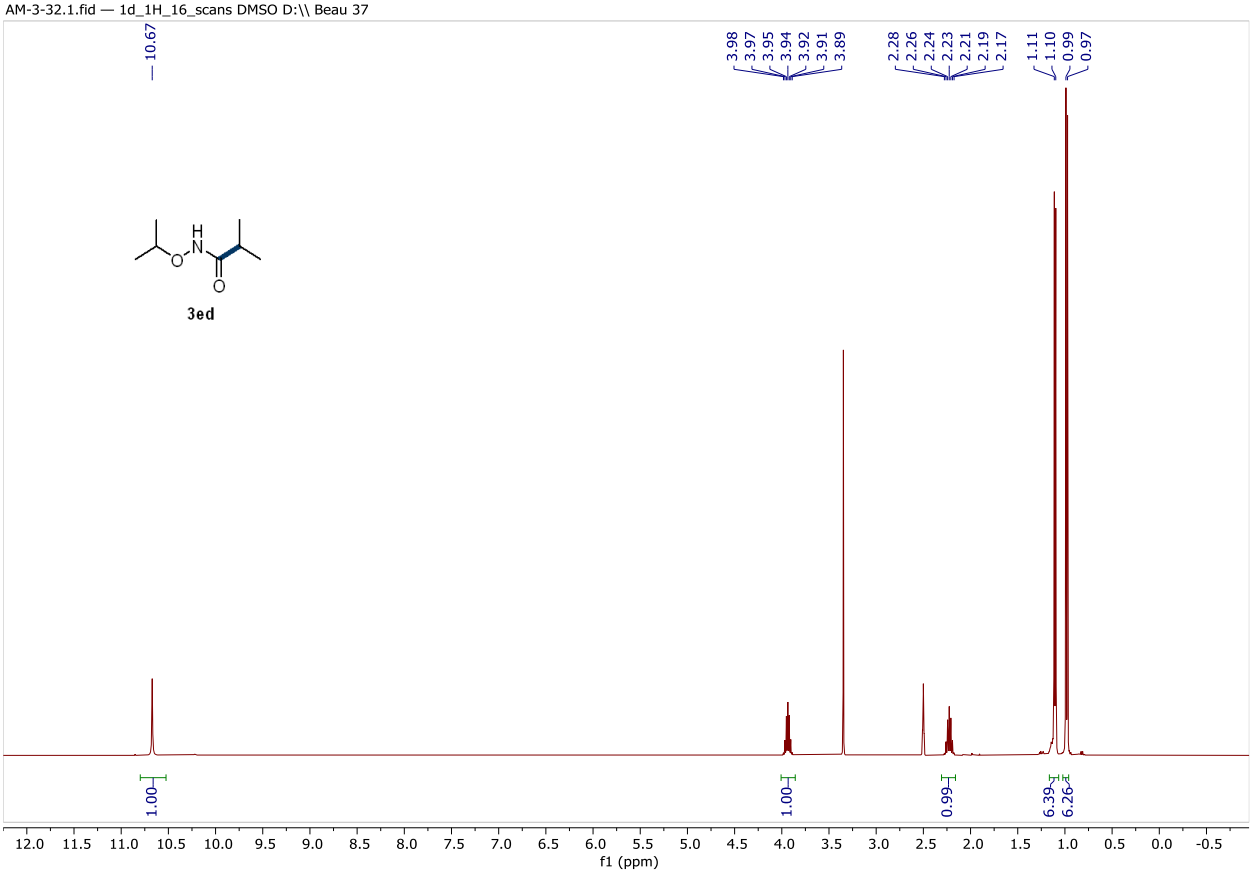

AM-3-32.2.fid — 1d_13C_20_minutes DMSO D:\\ Beau 37

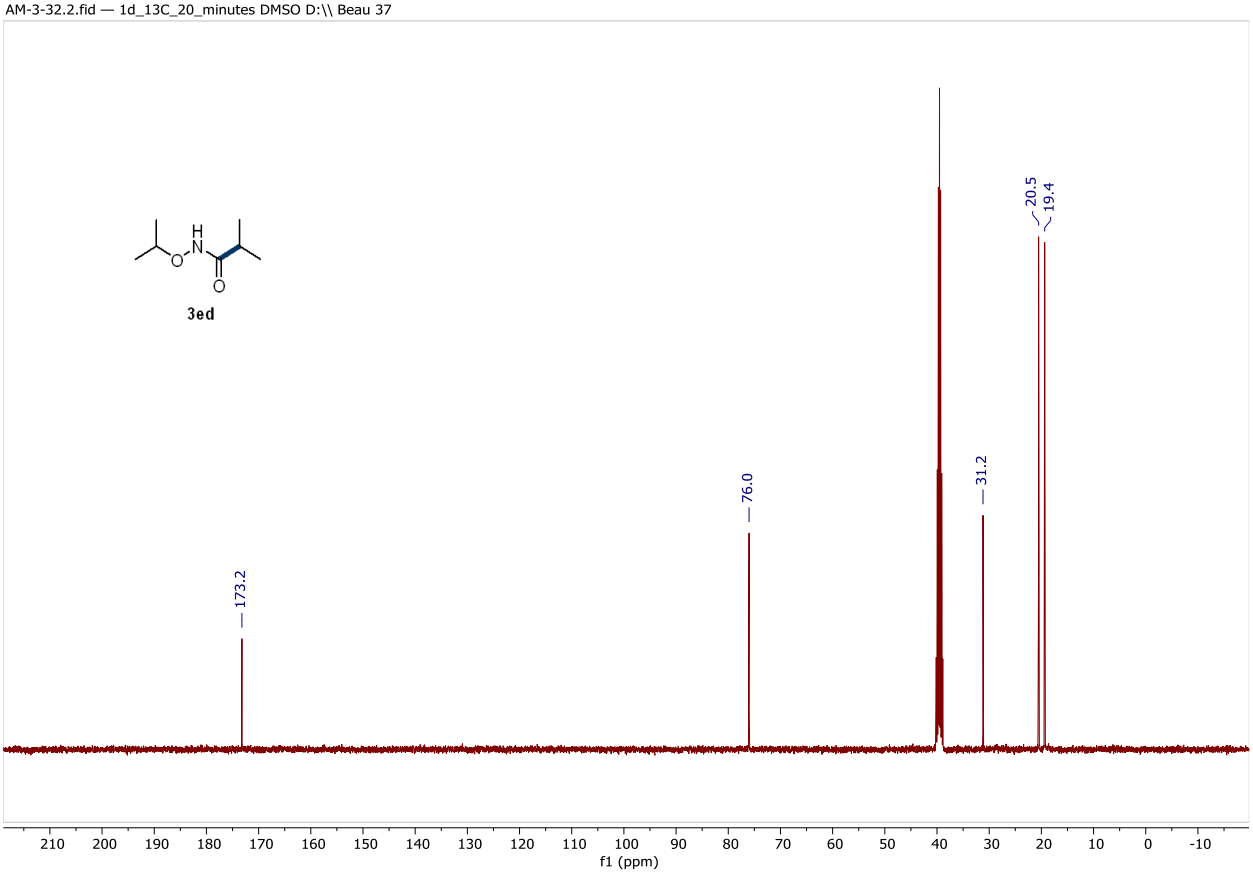

AM-3-42.1.fid — 1H NMR

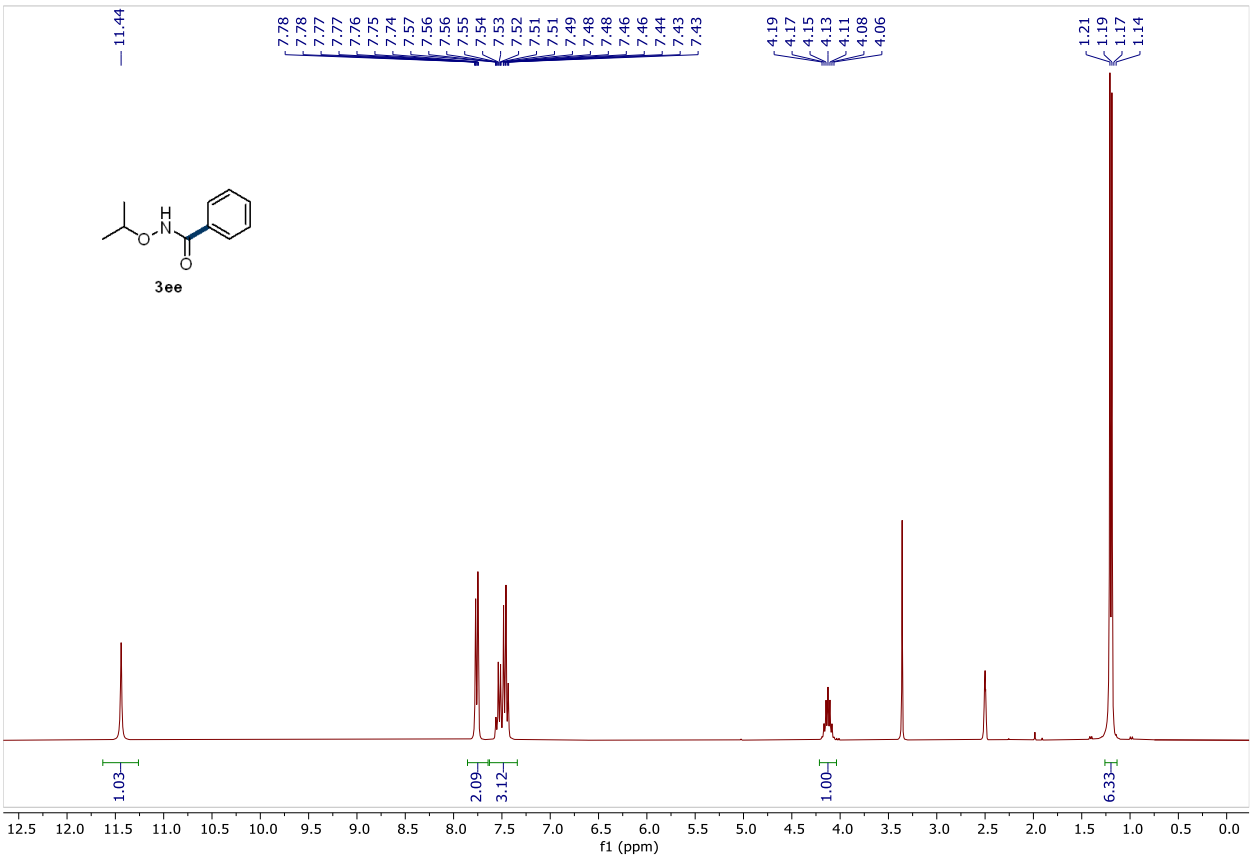

AM-3-42.2.fid — 13C NMR with 1H decoupling

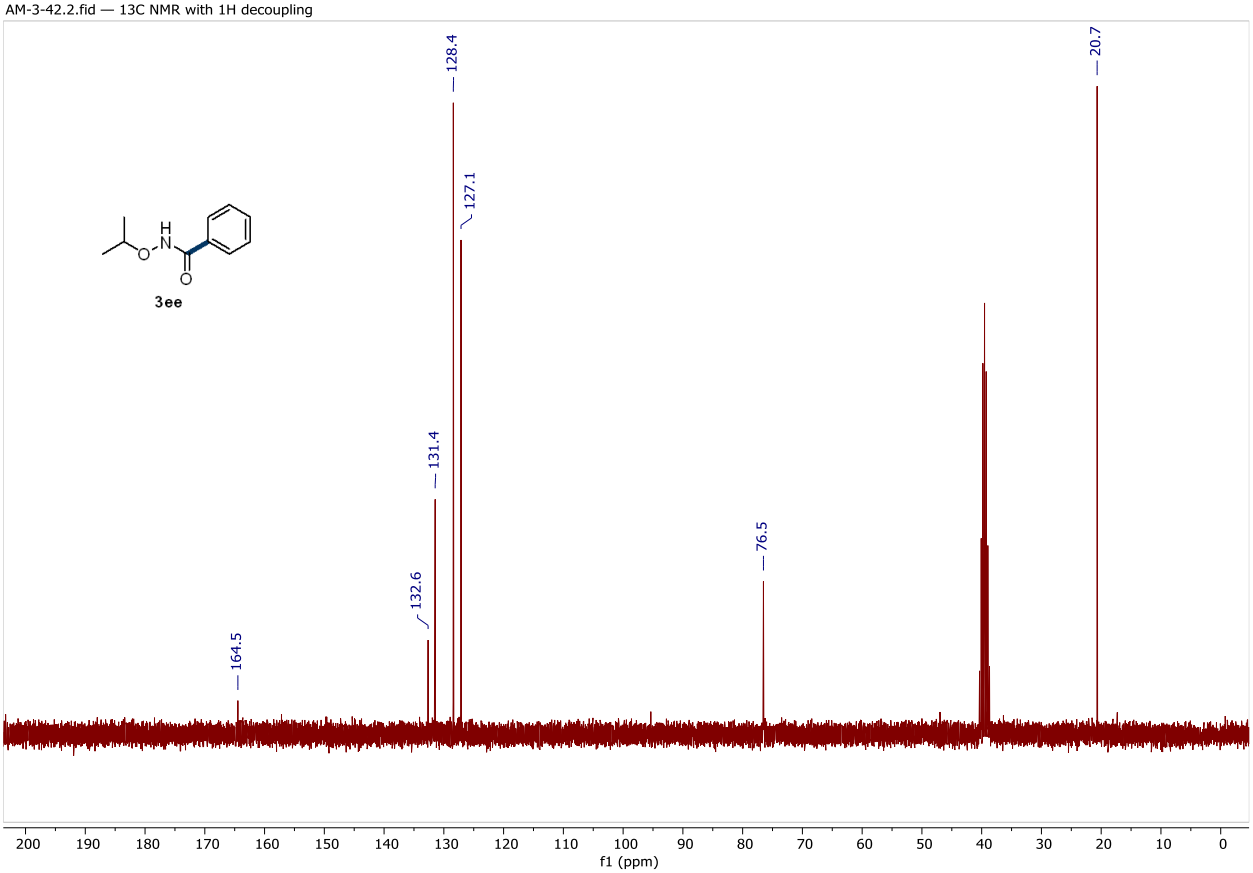

AM-3-34.1.fid — 1H NMR

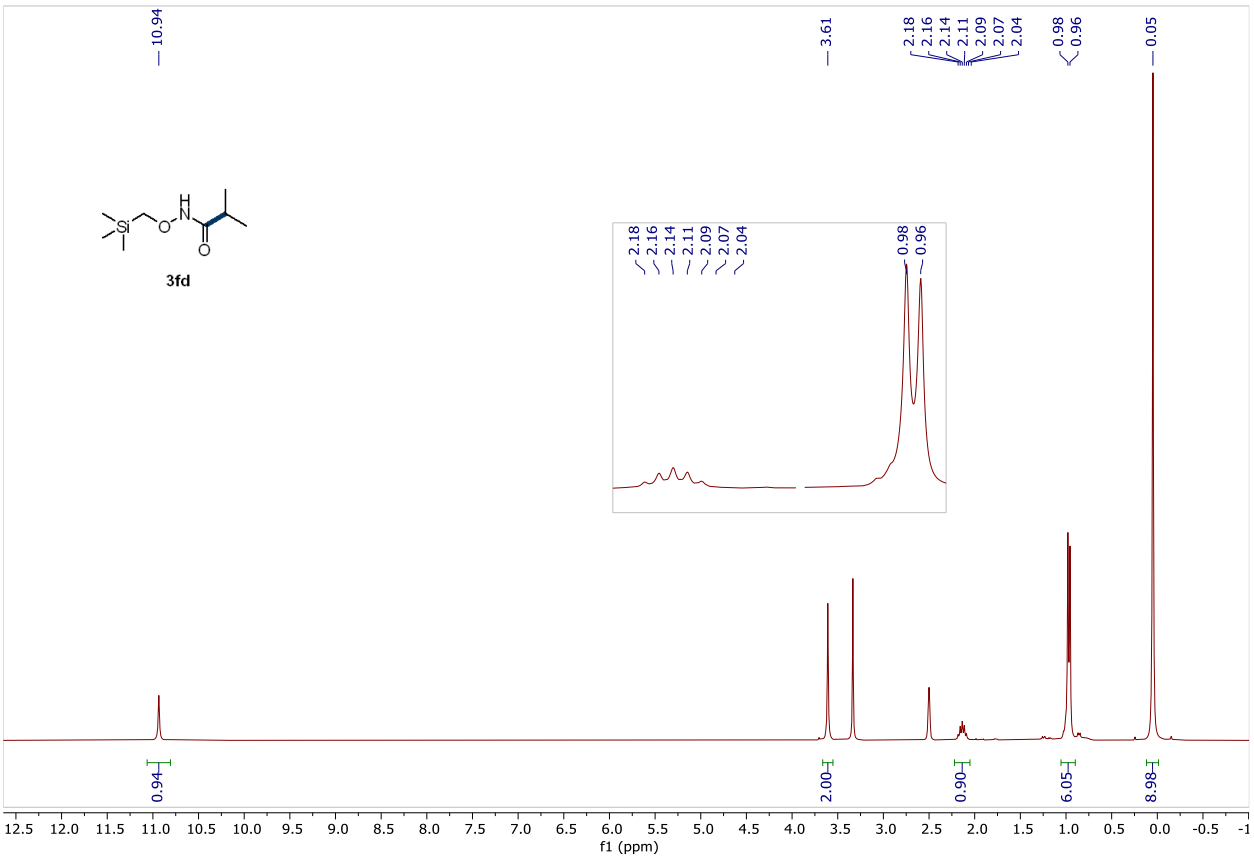

AM-3-34.2.fid — 13C NMR with 1H decoupling

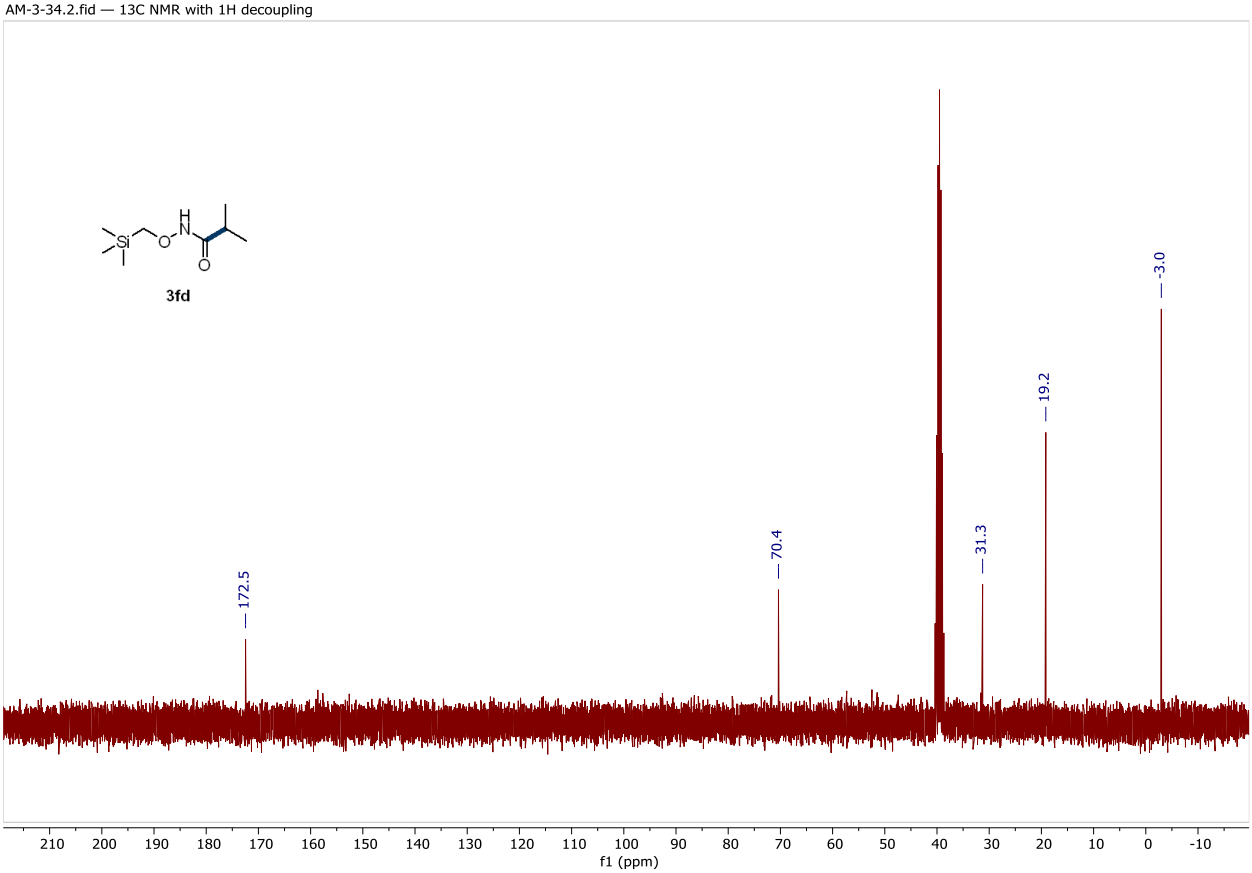

AM-3-43-run2.10.fid — 1d_1H_1min DMSO {C:\data} Beau 2

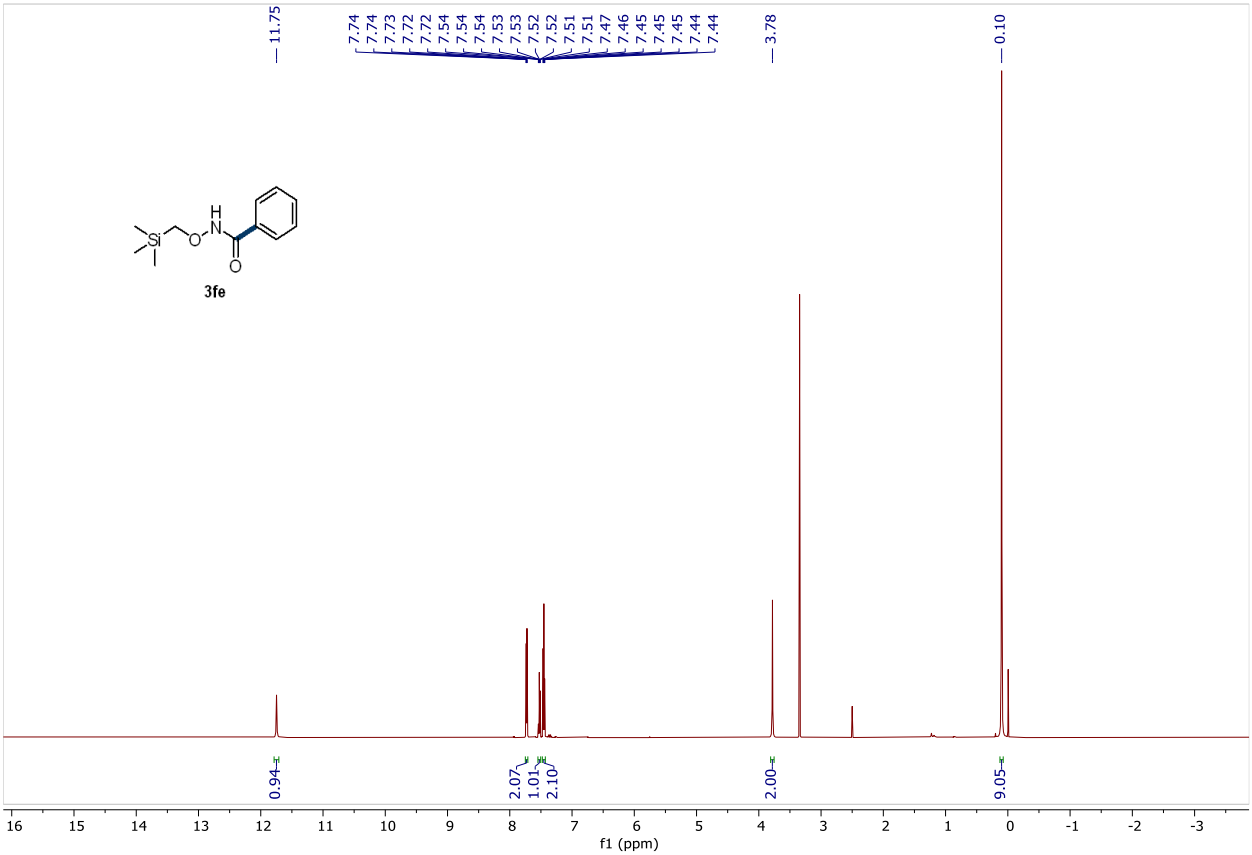

3fe

AM-3-43-run2.11.fid — {1d_13C[1H]_18min} DMSO {C:\data} Beau 2

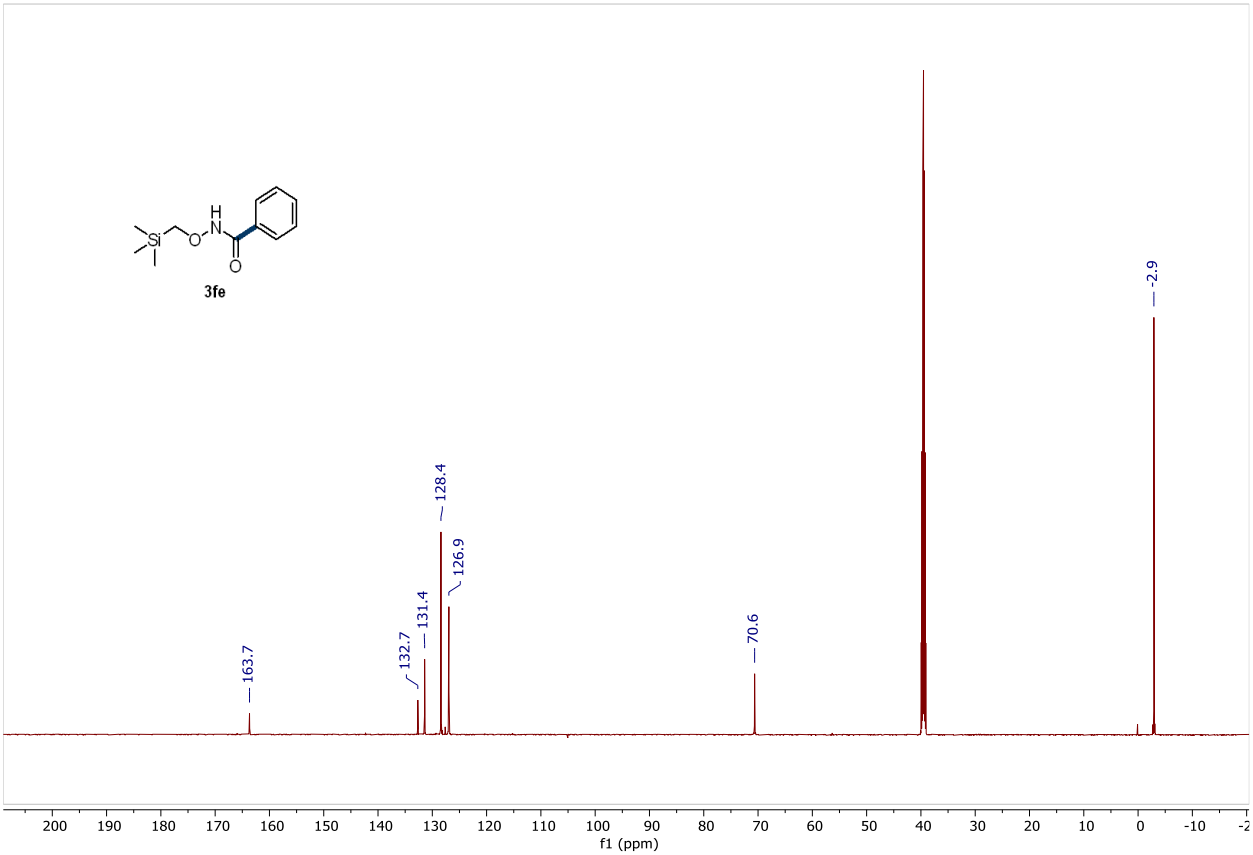

AM-3-43-run2.12.fid — 1d_13C_dept135 DMSO {C:\data} Beau 2

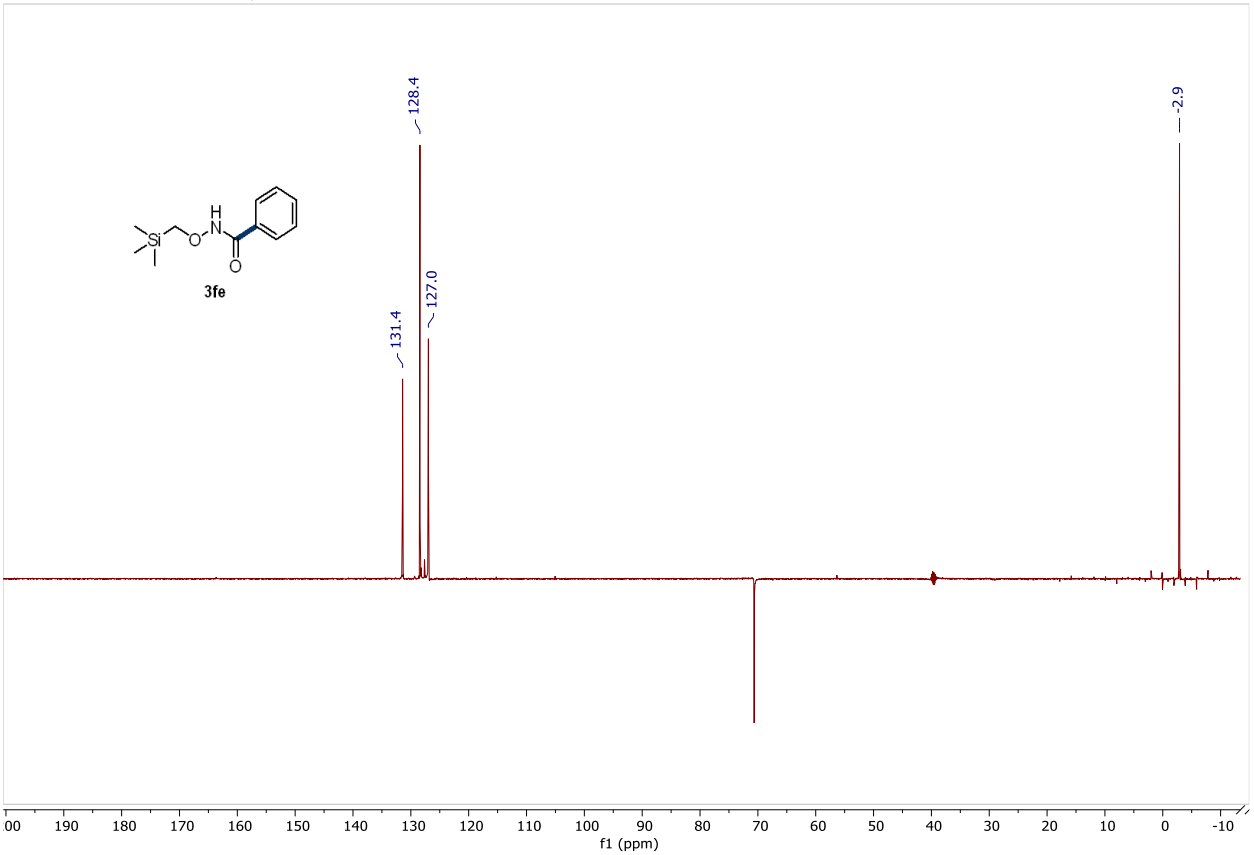

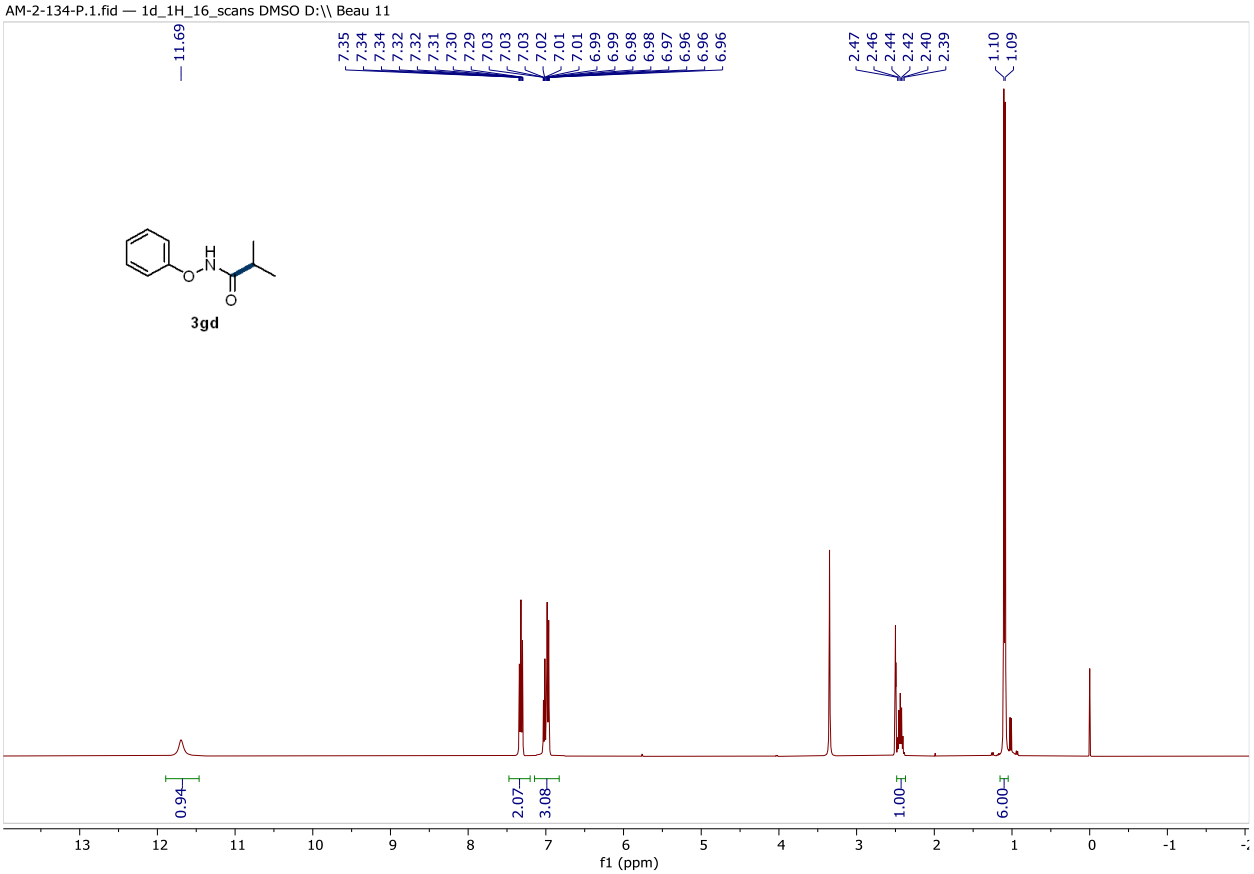
AM-2-134-P.1.fid — 1d_1H_16_scans DMSO D:\\ Beau 11
11.69
7.35
7.34
7.34
7.32
7.32
7.31
7.30
7.29
7.03
7.03
7.03
7.02
7.01
7.01
6.99
6.99
6.98
6.98
6.97
6.96
6.96
6.96
2.47
2.46
2.44
2.42
2.40
2.39
1.10
1.09
3gd
0.94
2.07
3.08
1.00
6.00
13
12
11
10
9
8
7
6
5
4
3
2
1
0
-1
f1 (ppm)

AM-2-134.11.fid — {1d_13C[1H]_8min} DMSO {C:\data} Beau 6

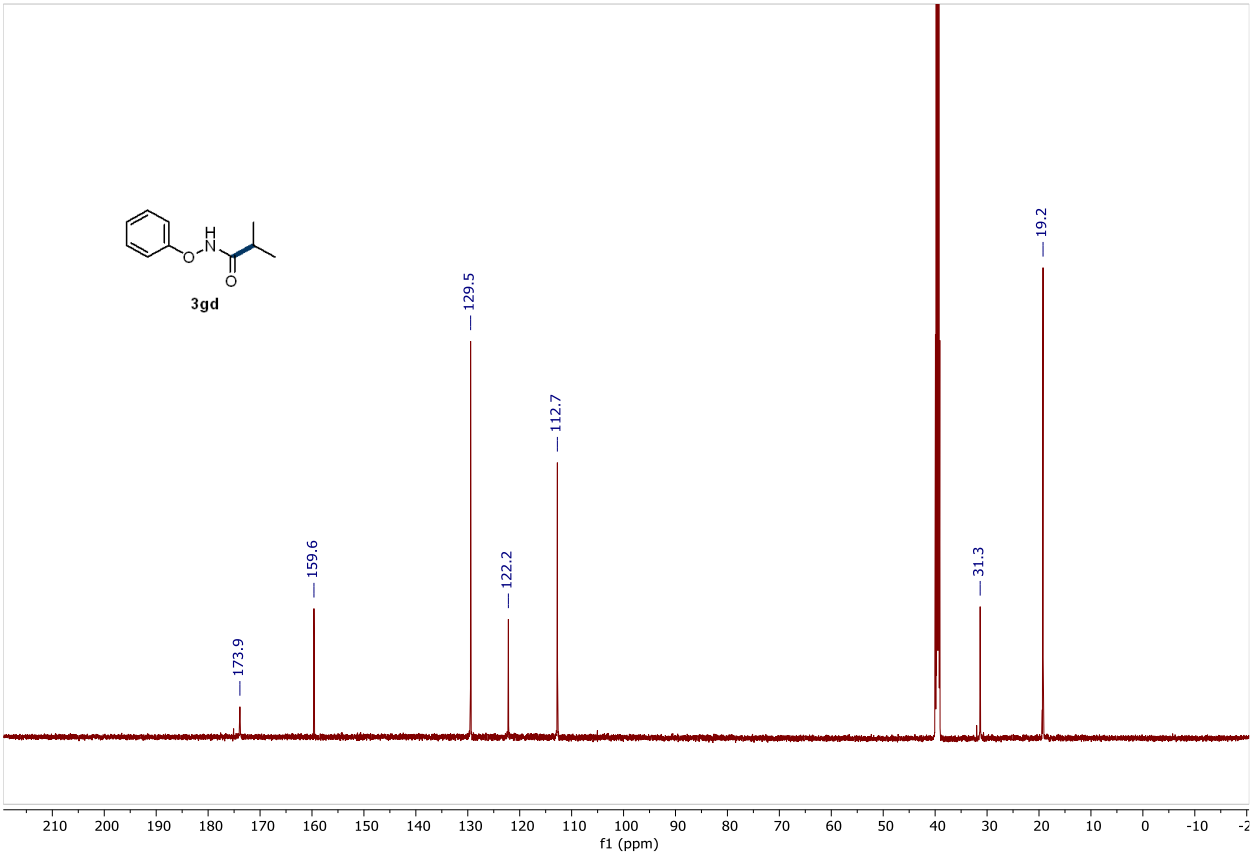

AM-2-106-P.1.fid — 1d_1H_16_scans DMSO D:\\ Beau 5

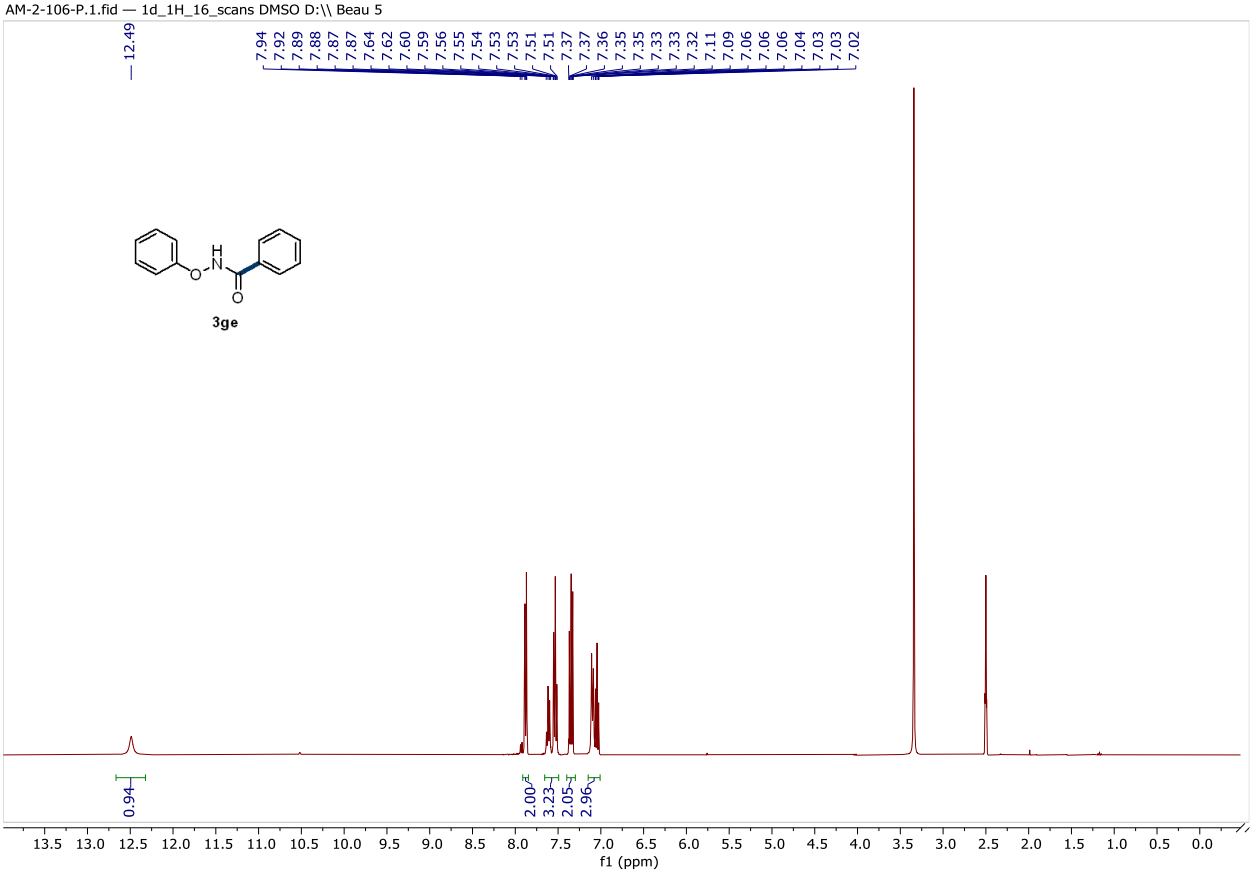

AM-2-158.11.fid — {1d_13C[1H]_8min} DMSO {C:\data} Beau 4

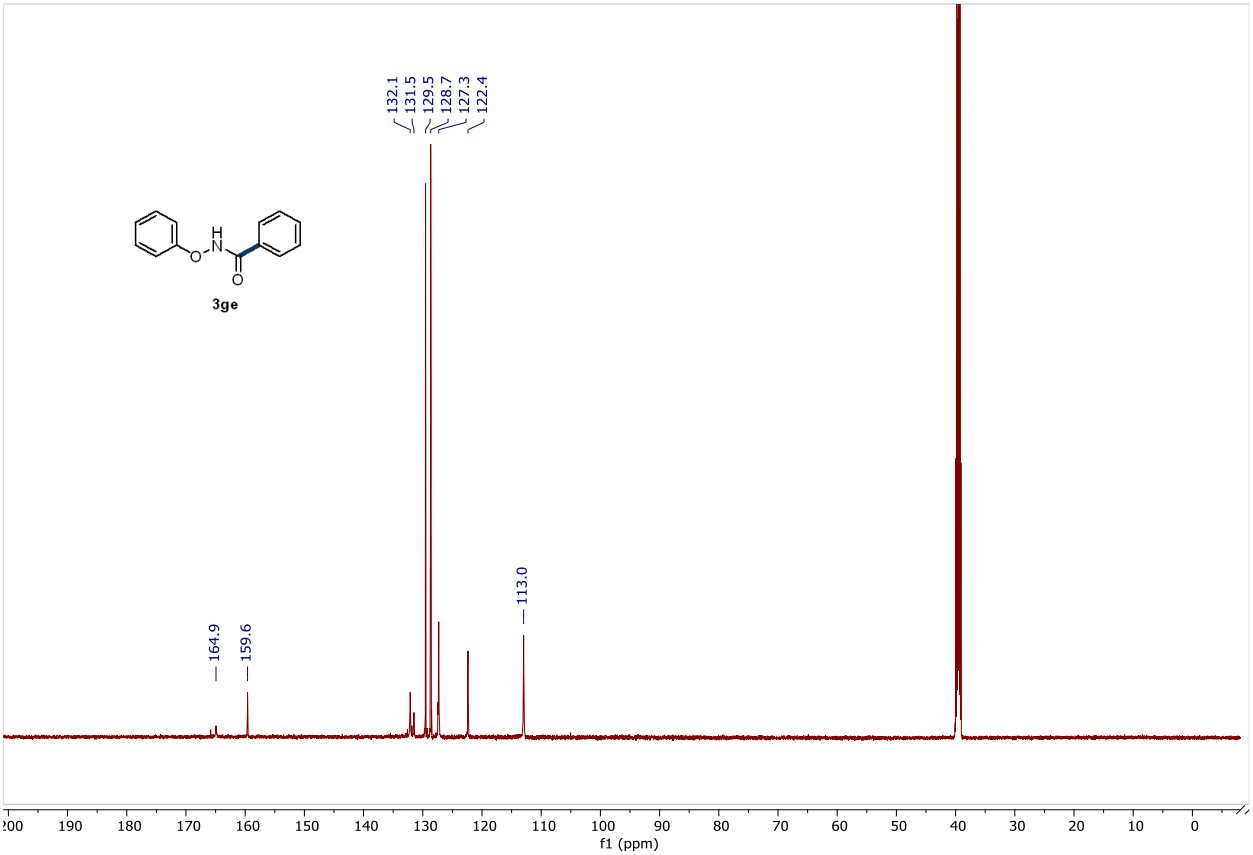

AM-2-102-Pure.1.fid — 1d_1H_16_scans DMSO D:\\ Beau 57

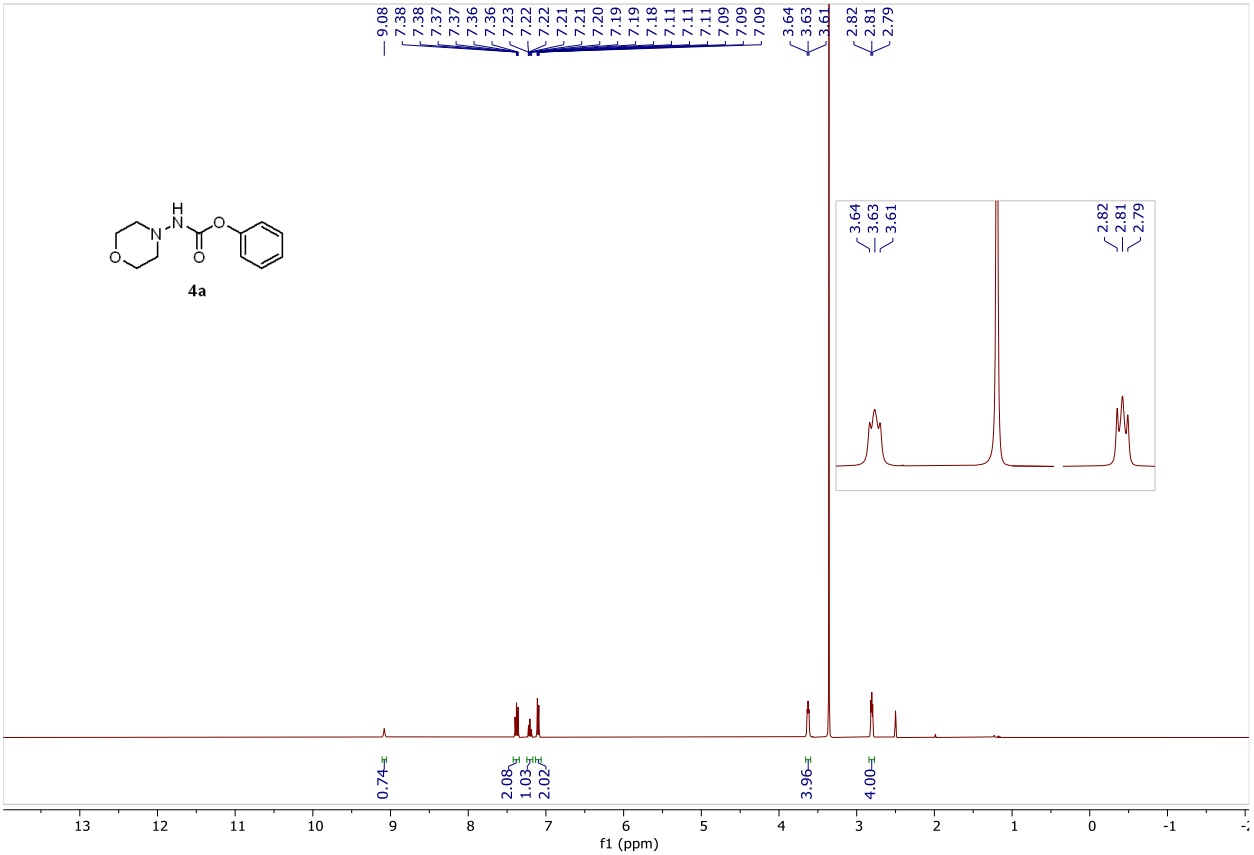

4a

AM-2-102-Pure.2.fid — 1d_13C_20_minutes DMSO D:\\ Beau 57

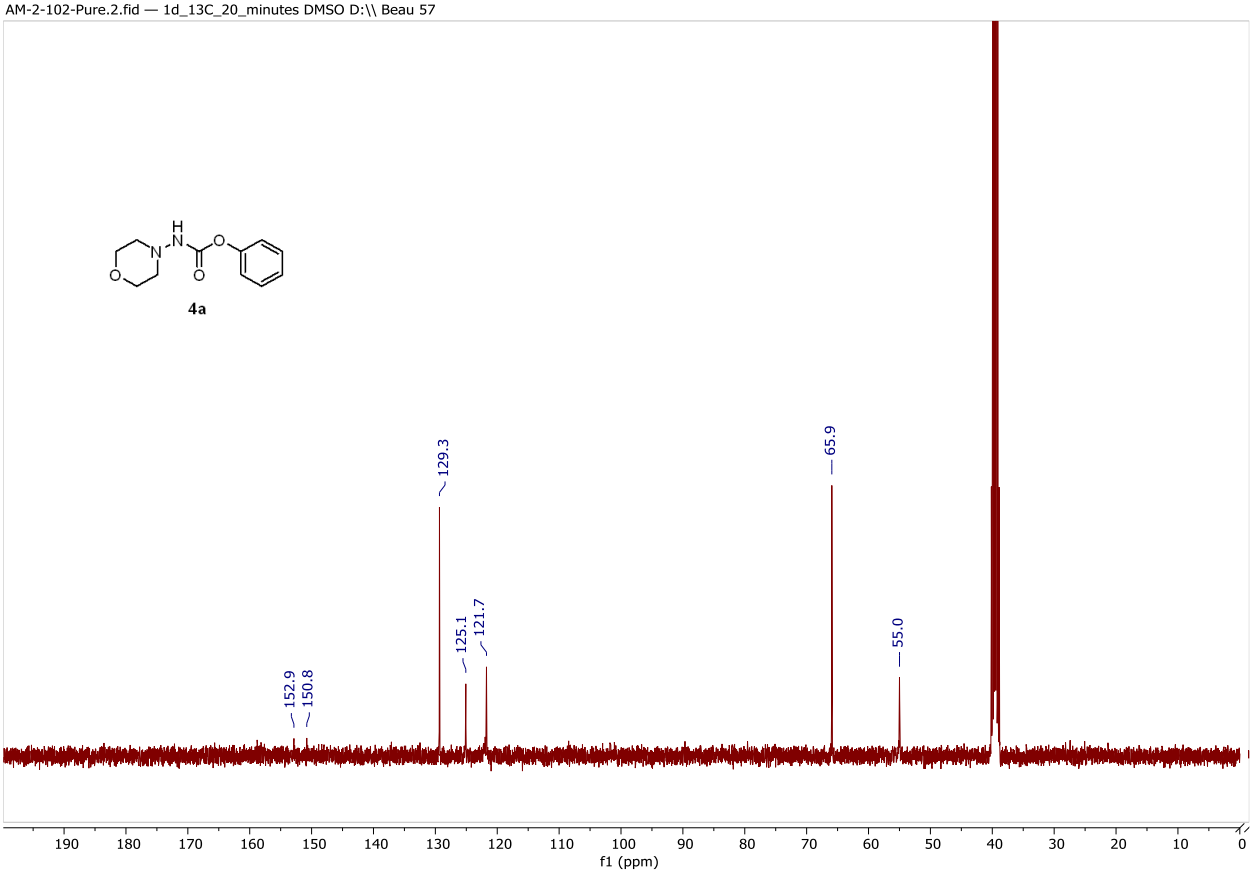

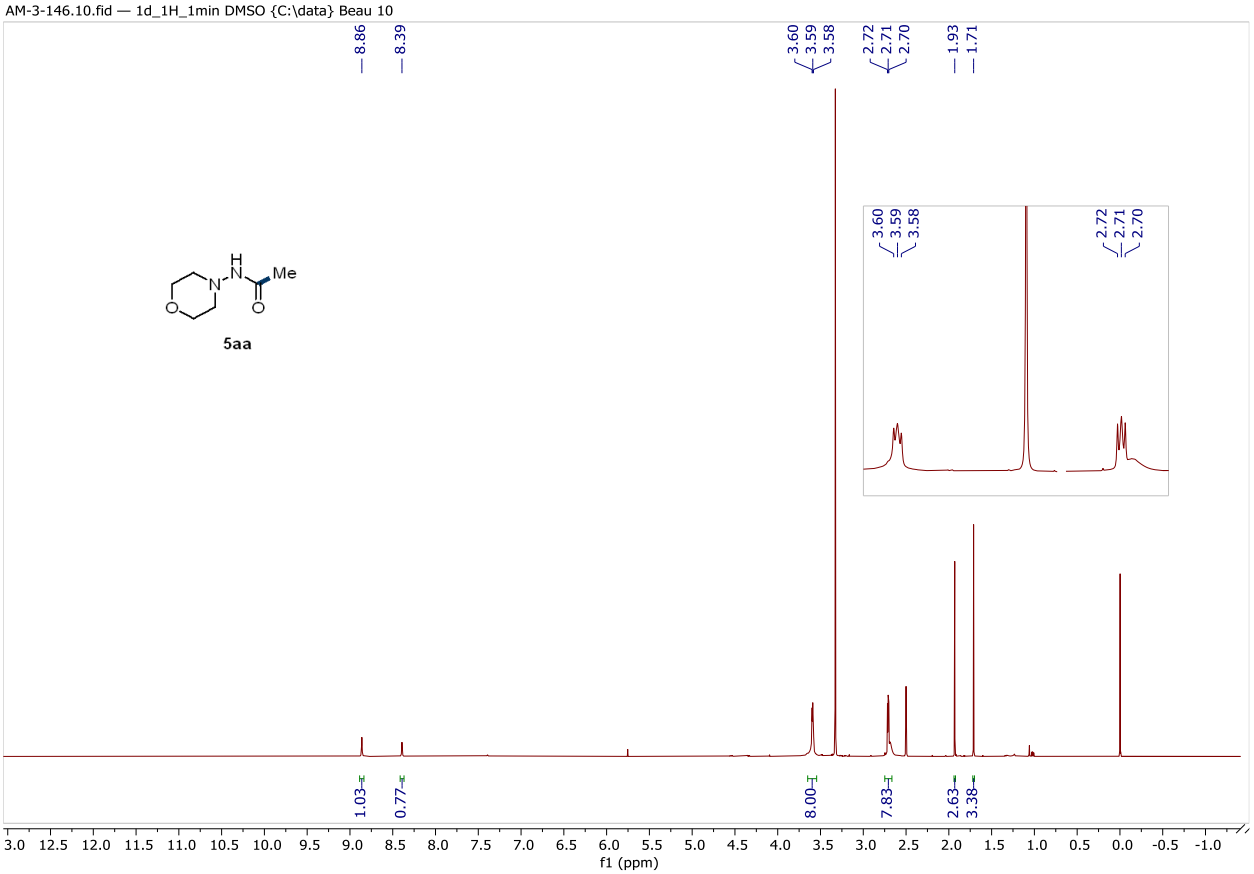
AM-3-146.10.fid — 1d_1H_1min DMSO {C:\data} Beau 10
8.86
8.39
3.60
3.59
3.58
2.72
2.71
2.70
1.93
1.71
Me
5aa
1.03
0.77
8.00
7.83
2.63
3.38
f1 (ppm)

AM-3-146.11.fid — {1d_13C[1H]_1h10min} DMSO {C:\data} Beau 10

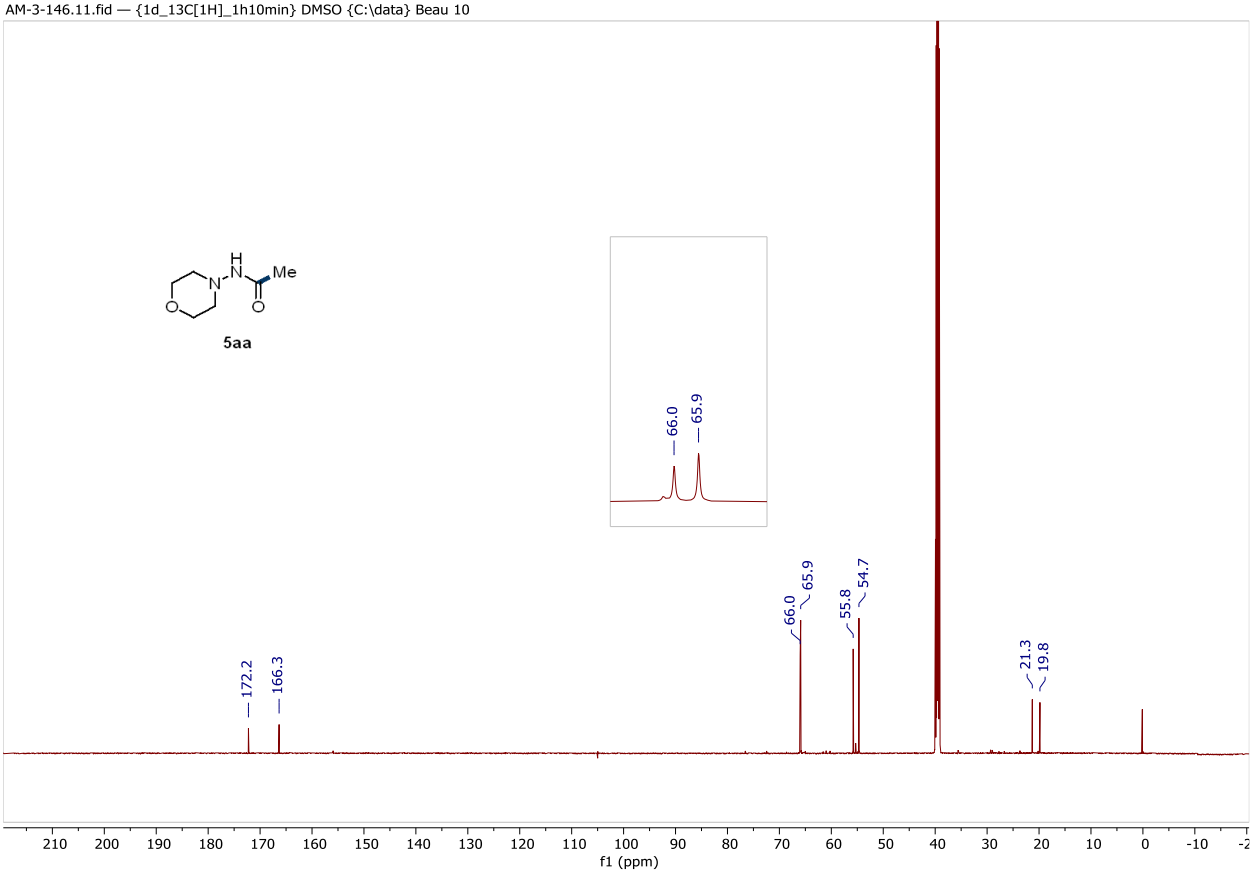

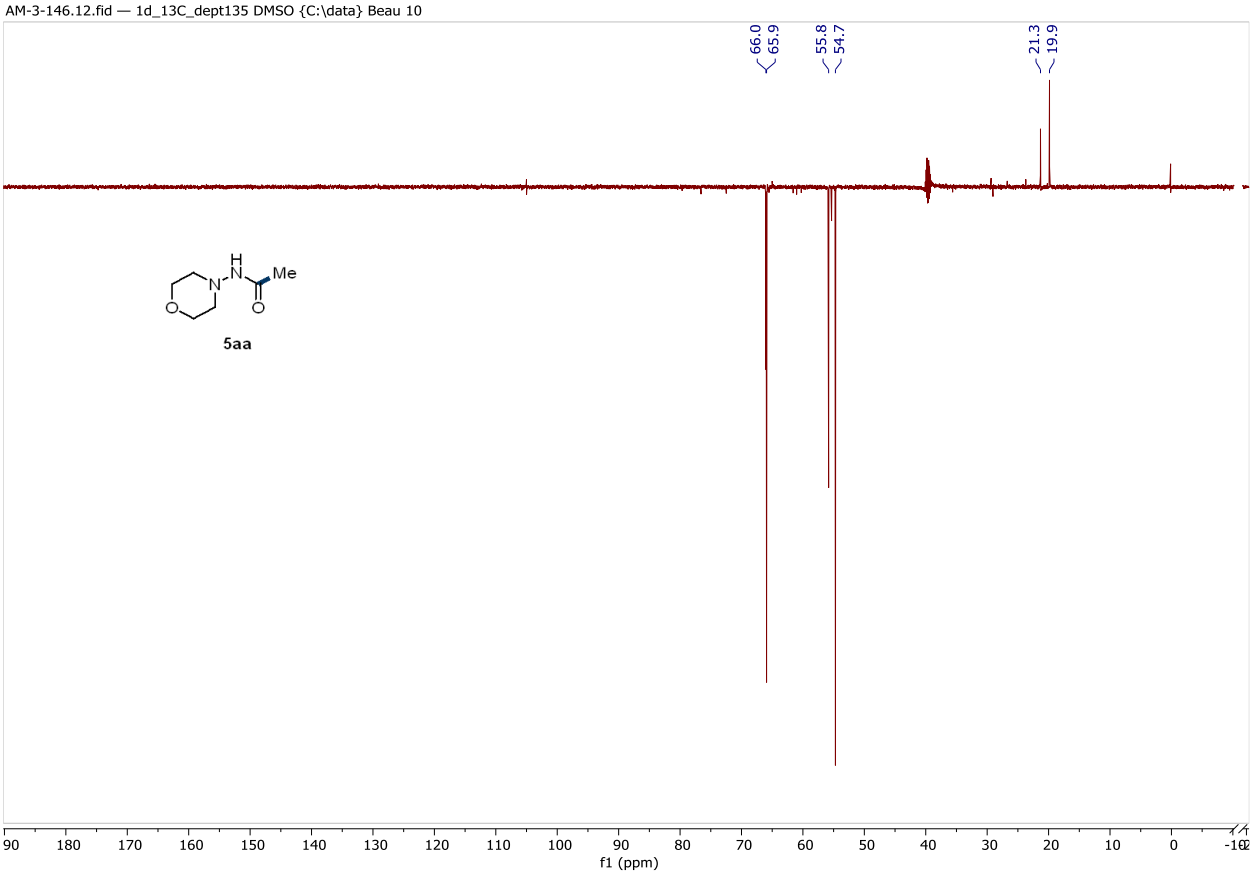
AM-3-146.12.fid — 1d_13C_dept135 DMSO {C:\data} Beau 10
66.0
65.9
55.8
54.7
21.3
19.9
Me
5aa
90 180 170 160 150 140 130 120 110 100 90 80 70 60 50 40 30 20 10 0
f1 (ppm)

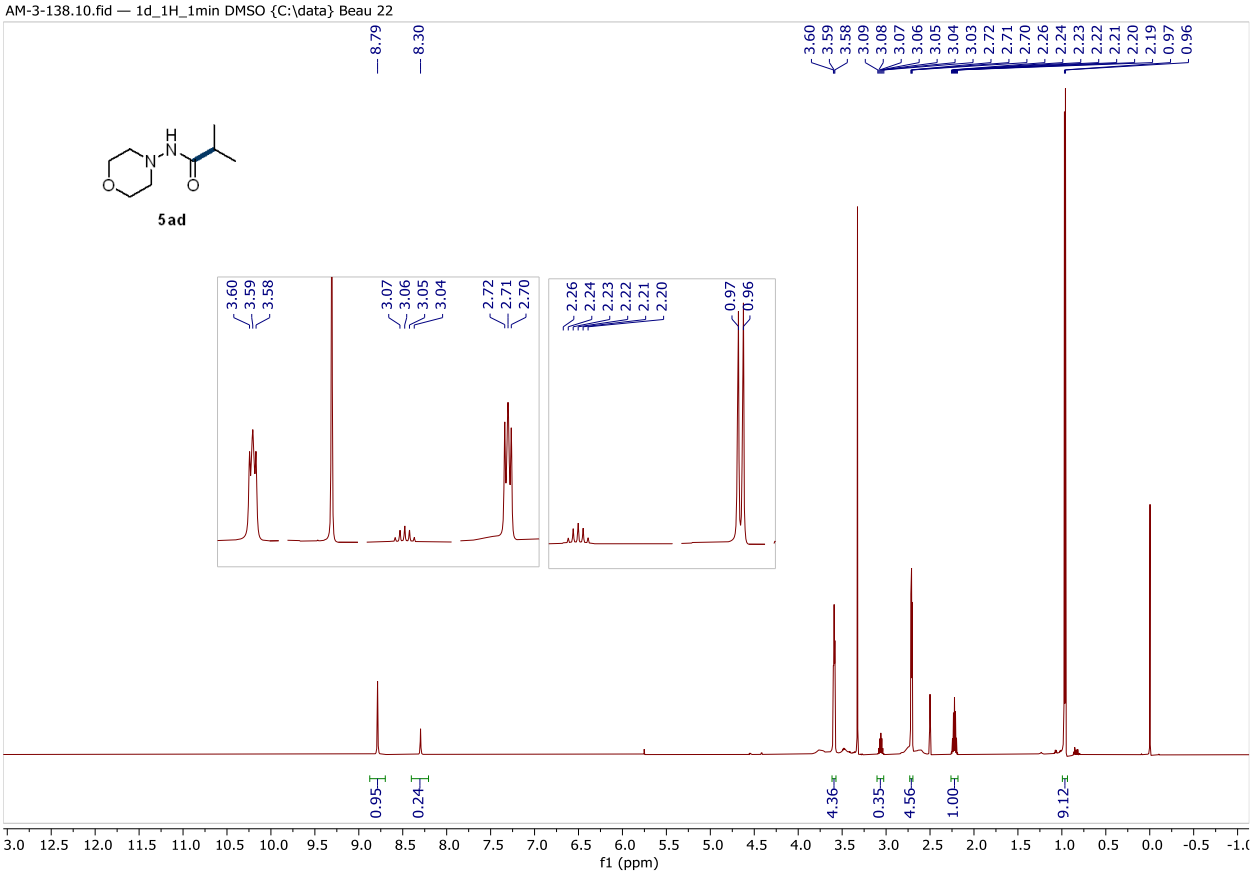
AM-3-138.10.fid — 1d_1H_1min DMSO {C:\data} Beau 22
8.79
8.30
3.60
3.59
3.58
3.09
3.08
3.07
3.06
3.05
3.04
3.03
2.72
2.71
2.70
2.26
2.24
2.23
2.22
2.21
2.20
2.19
0.97
0.96
5ad
0.95
0.24
4.36
0.35
4.56
1.00
9.12
f1 (ppm)

AM-3-138.11.fid — {1d_13C[1H]_1h10min} DMSO {C:\data} Beau 22

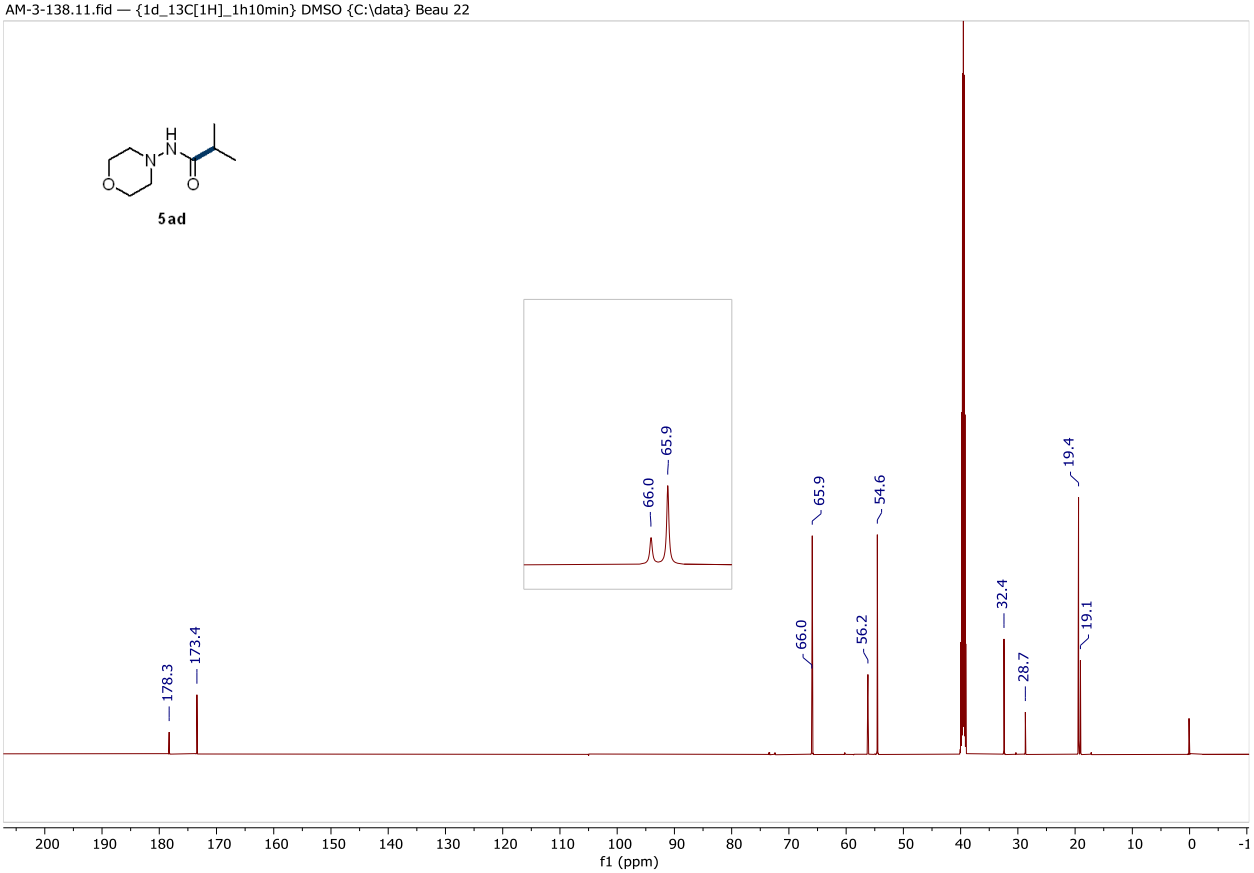

AM-3-138.12.fid — 1d_13C_dept135 DMSO {C:\data} Beau 22

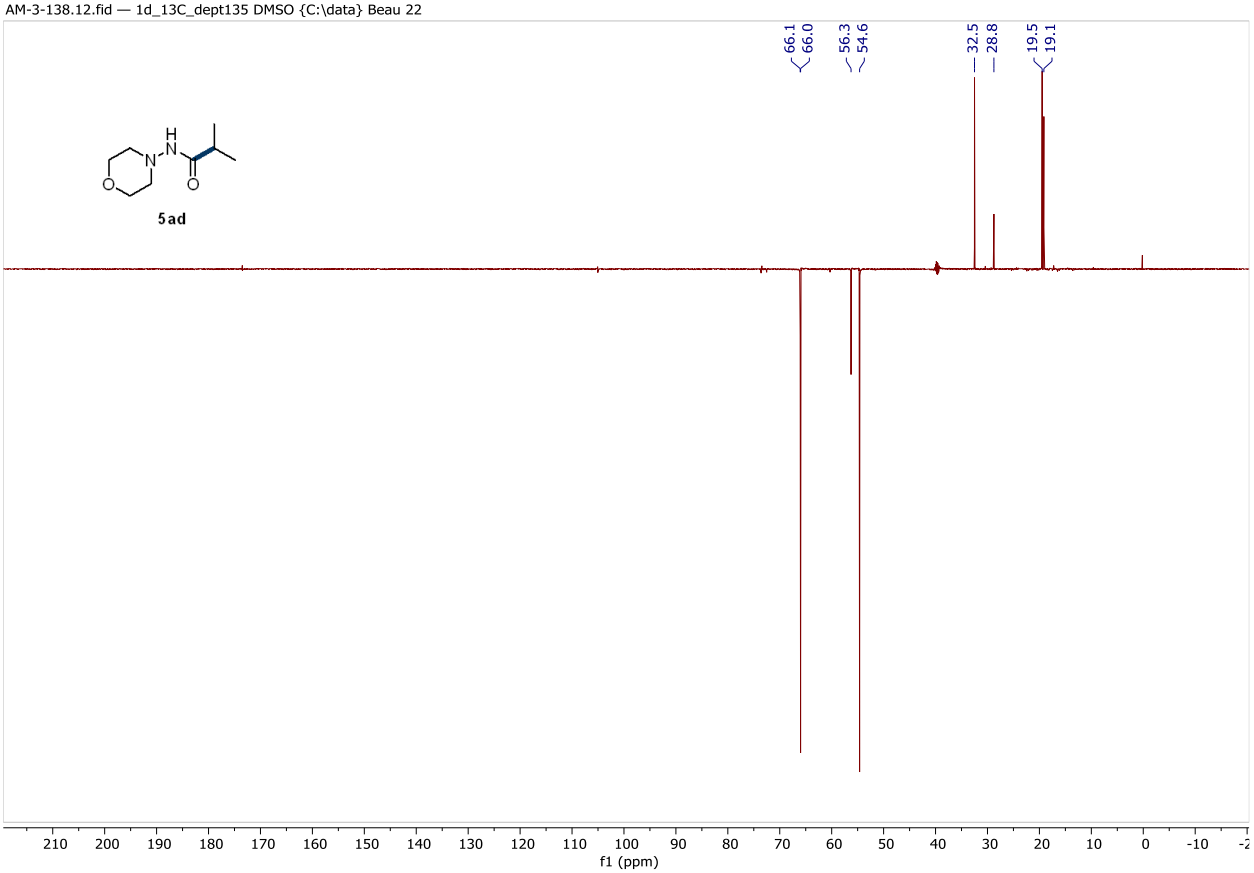

Am-3-139.10.fid — 1d_1H_1min DMSO {C:\data} Beau 16

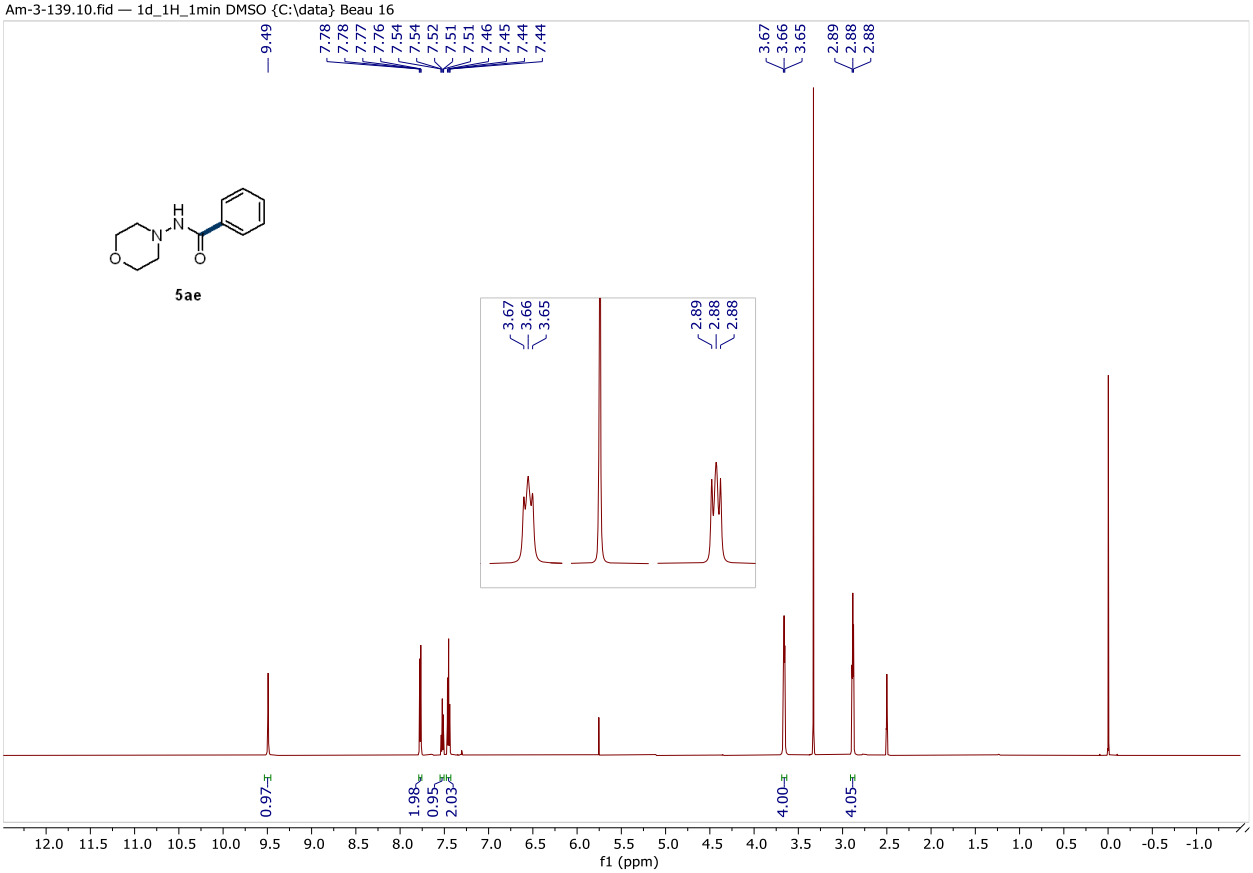

Am-3-139.11.fid — {1d_13C[1H]_1h10min} DMSO {C:\data} Beau 16

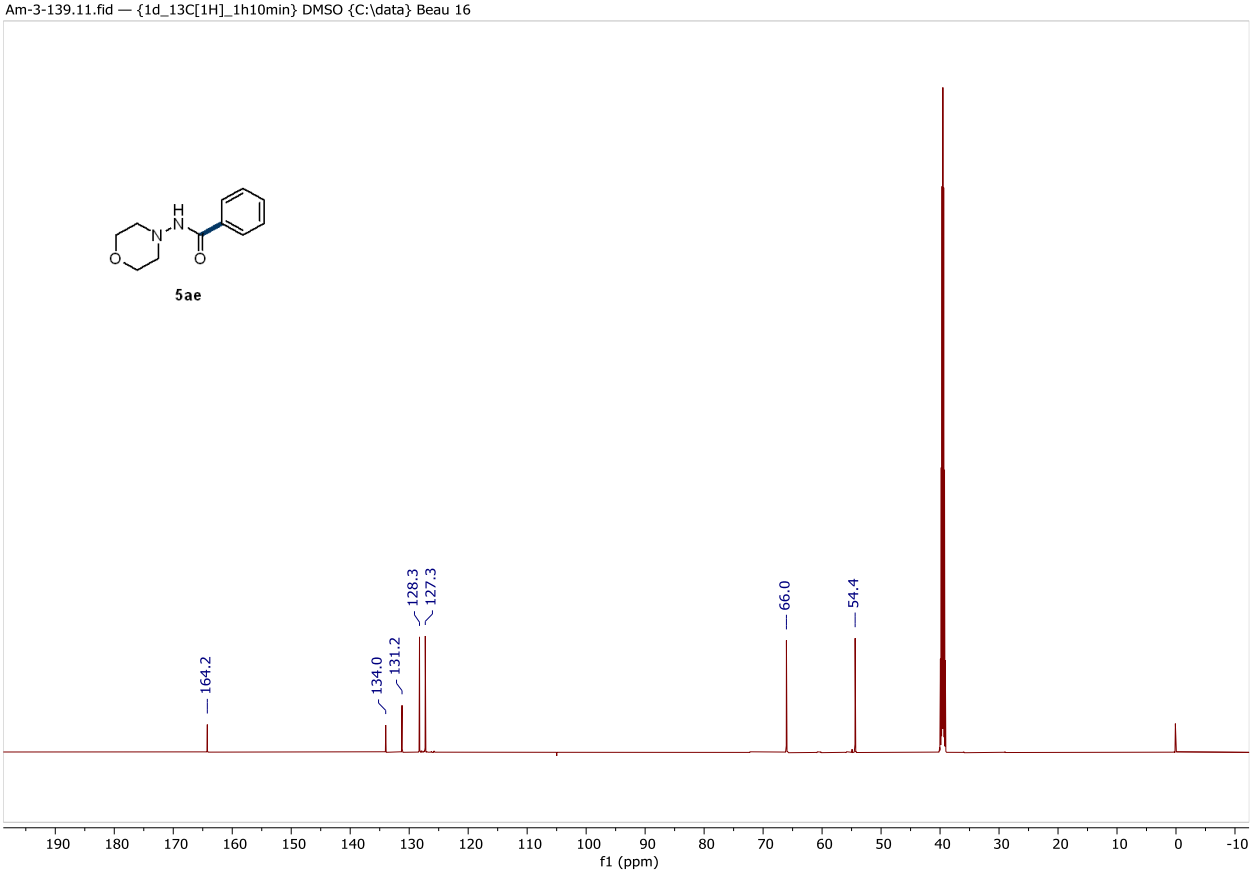

Am-3-139.12.fid — 1d_13C_dept135 DMSO {C:\data} Beau 16

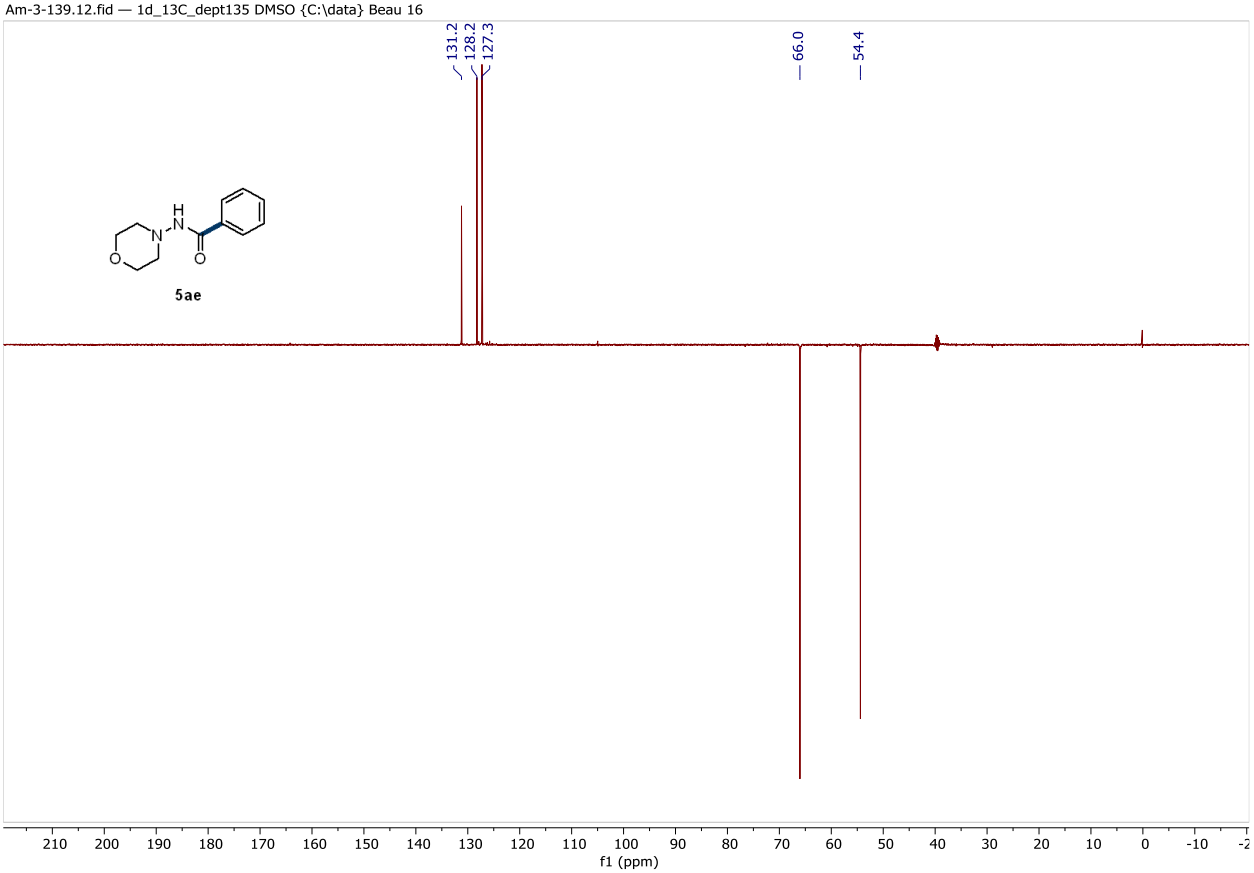

AM-3-141.10.fid — 1d_1H_1min DMSO {C:\data} Beau 23

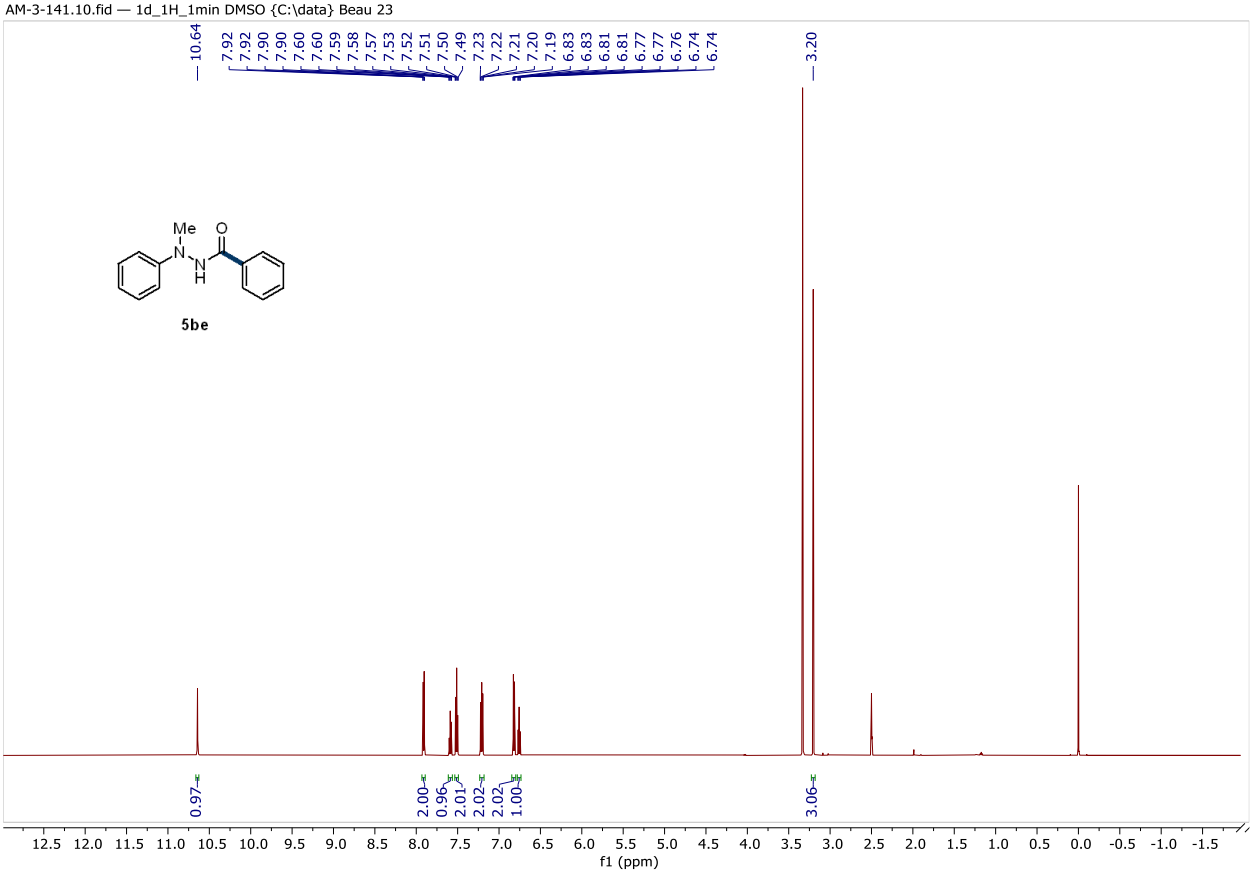

AM-3-141.11.fid — {1d_13C[1H]_1h10min} DMSO {C:\data} Beau 23

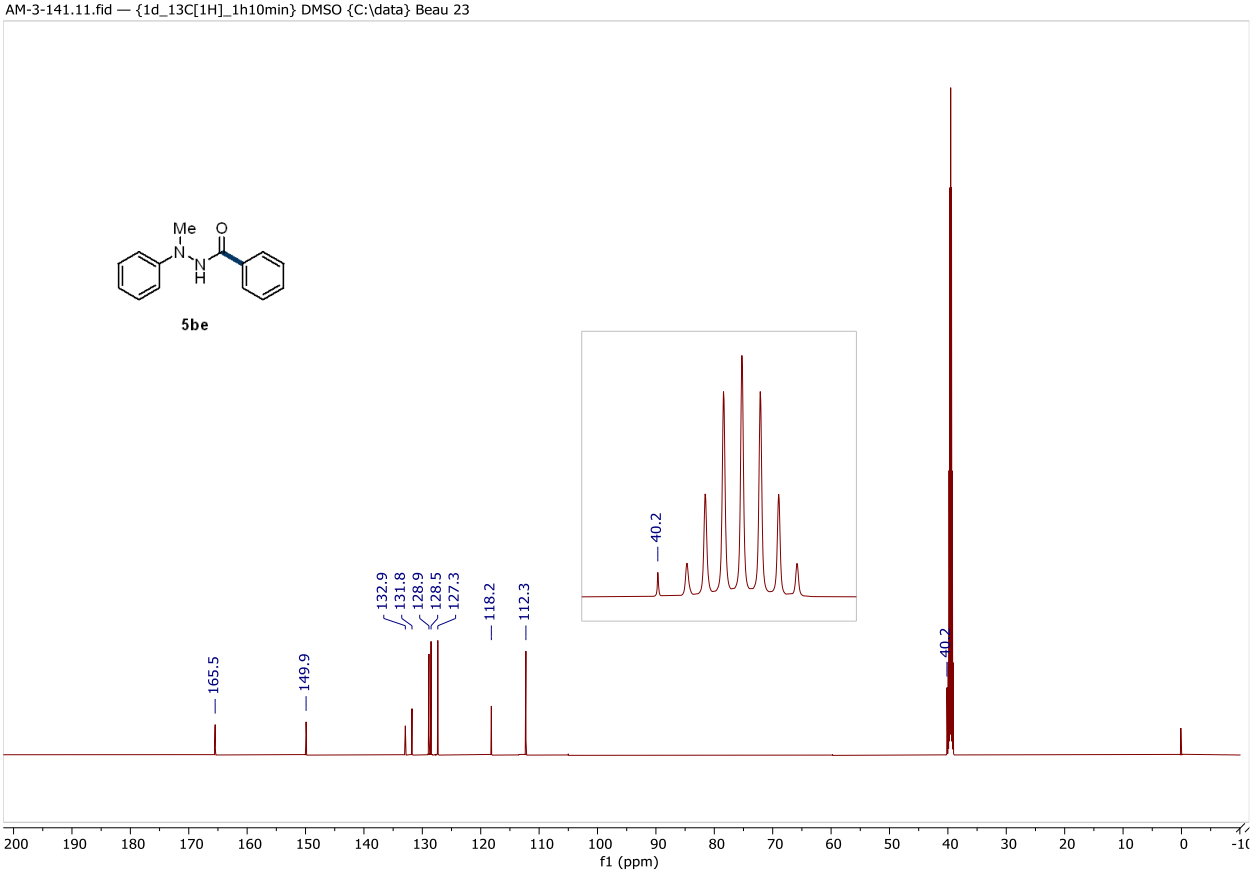

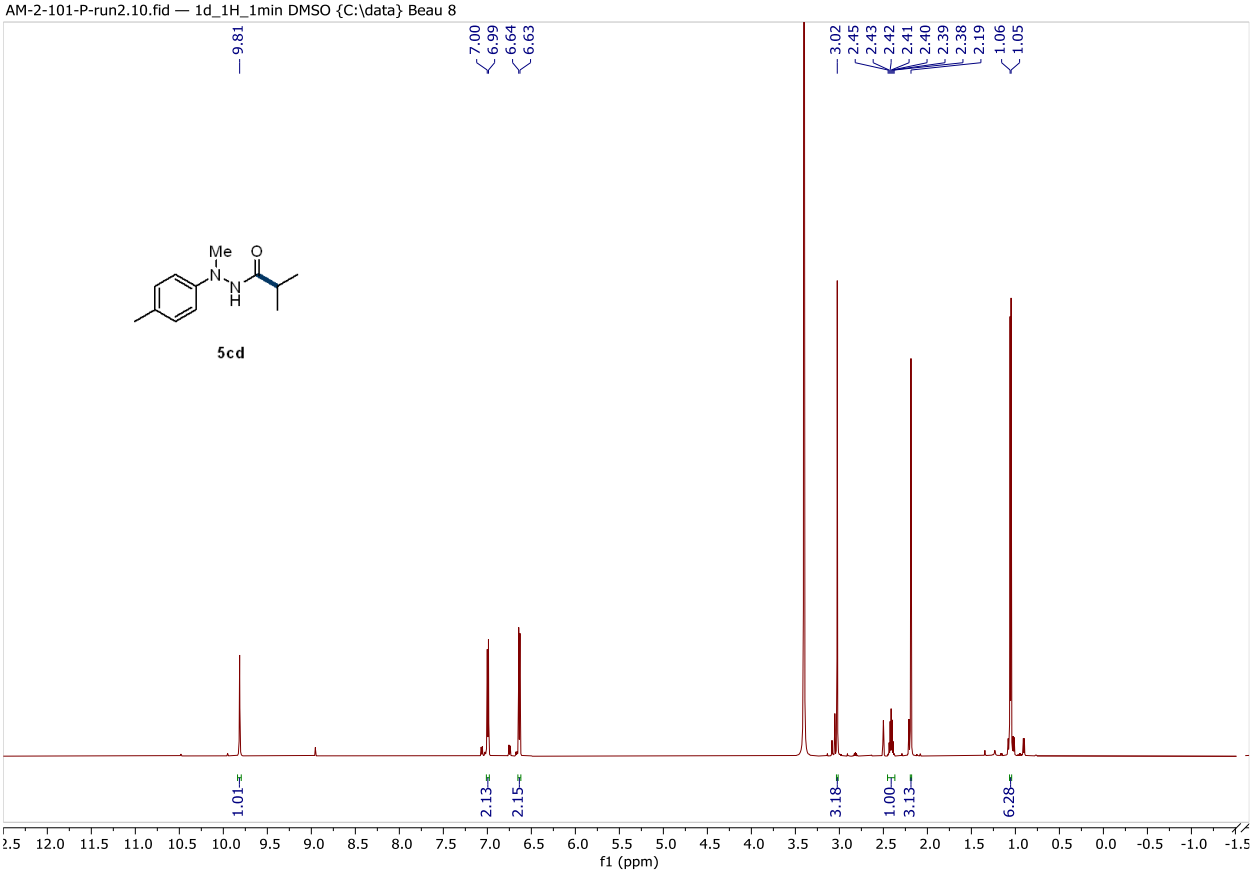
AM-2-101-P-run2.10.fid — 1d_1H_1min DMSO {C:\data} Beau 8
9.81
7.00
6.99
6.64
6.63
3.02
2.45
2.43
2.42
2.41
2.40
2.39
2.38
2.19
1.06
1.05
Me
O
N
N
H
5cd
1.01
2.13
2.15
3.18
1.00
3.13
6.28
f1 (ppm)

AM-2-101-P-run2.11.fid — {1d_13C[1H]_18min} DMSO {C:\data} Beau 8

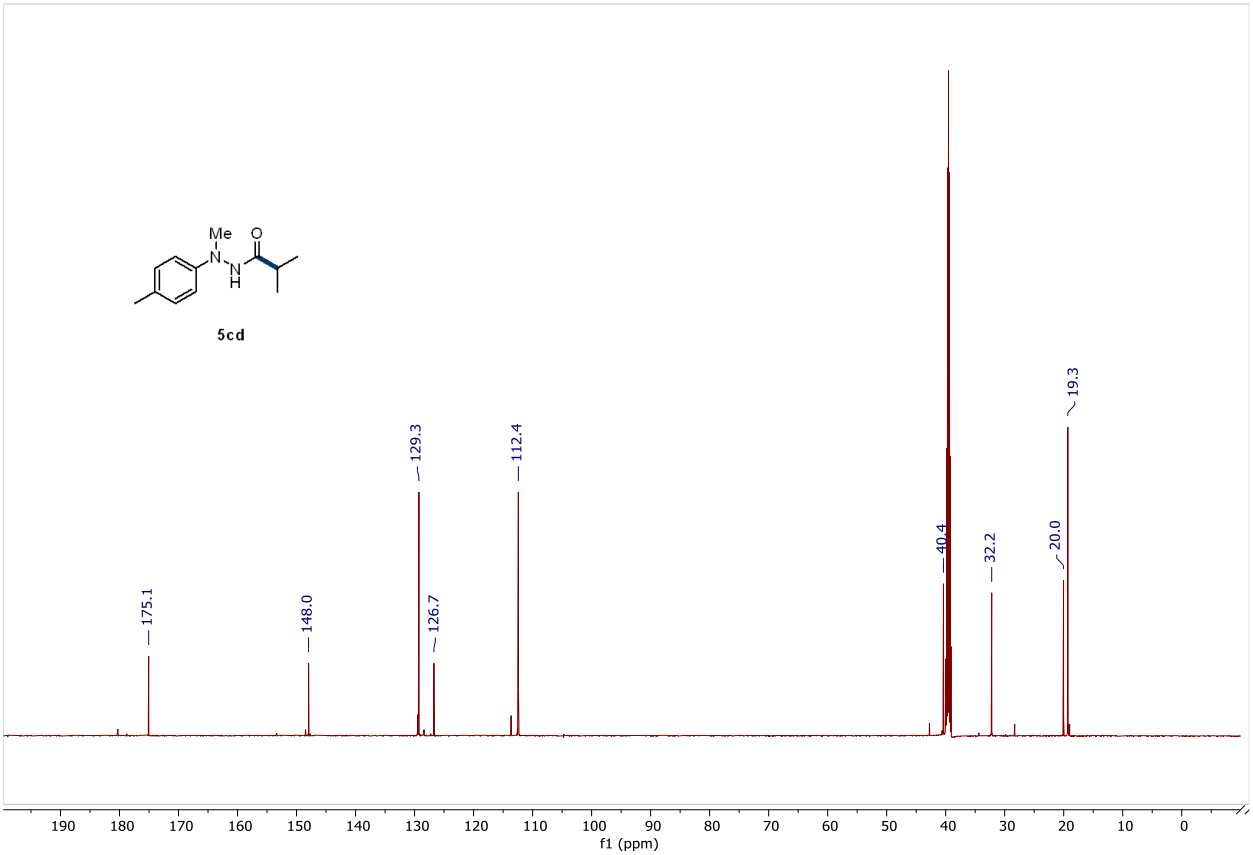

AM-3-144.10.fid — 1d_1H_1min DMSO {C:\data} Beau 19

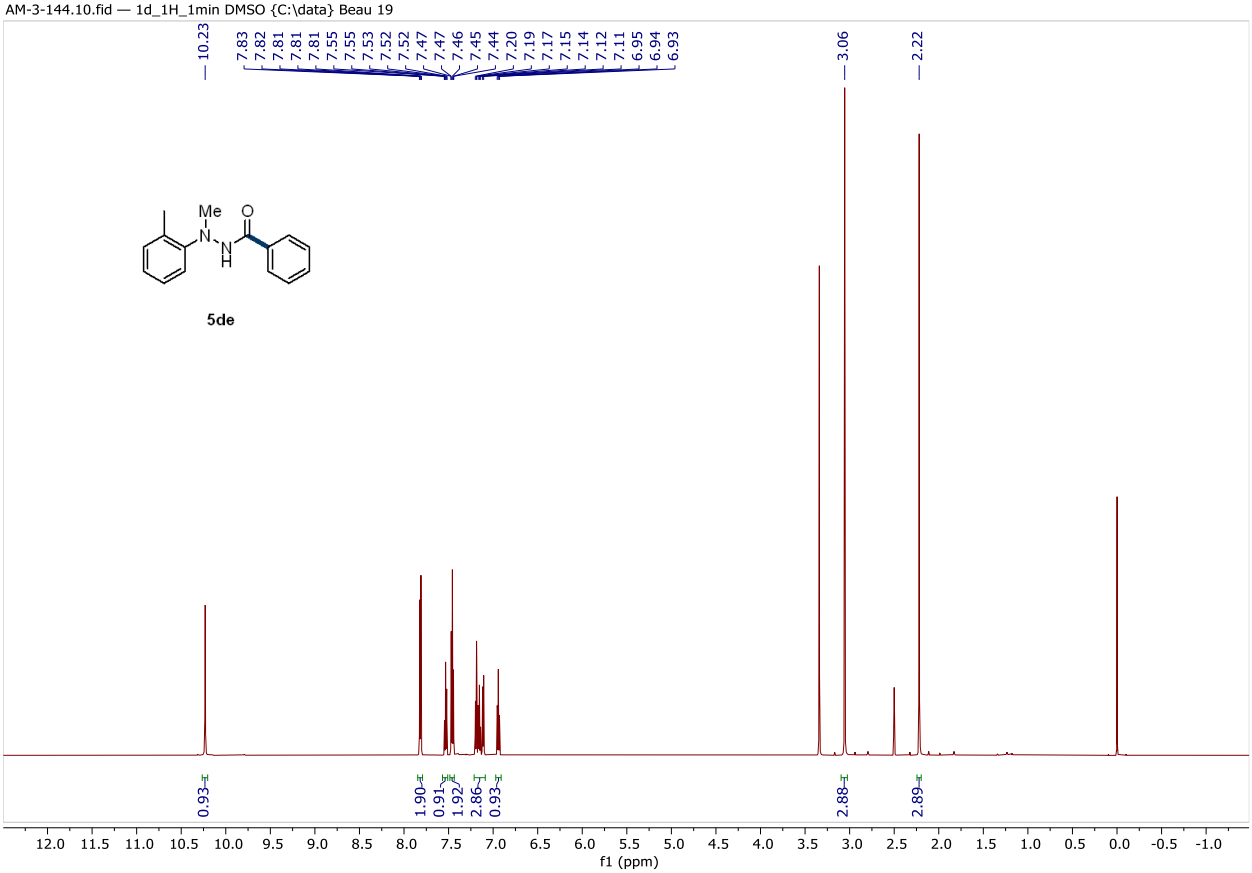

AM-3-144.11.fid — {1d_13C[1H]_1h10min} DMSO {C:\data} Beau 19

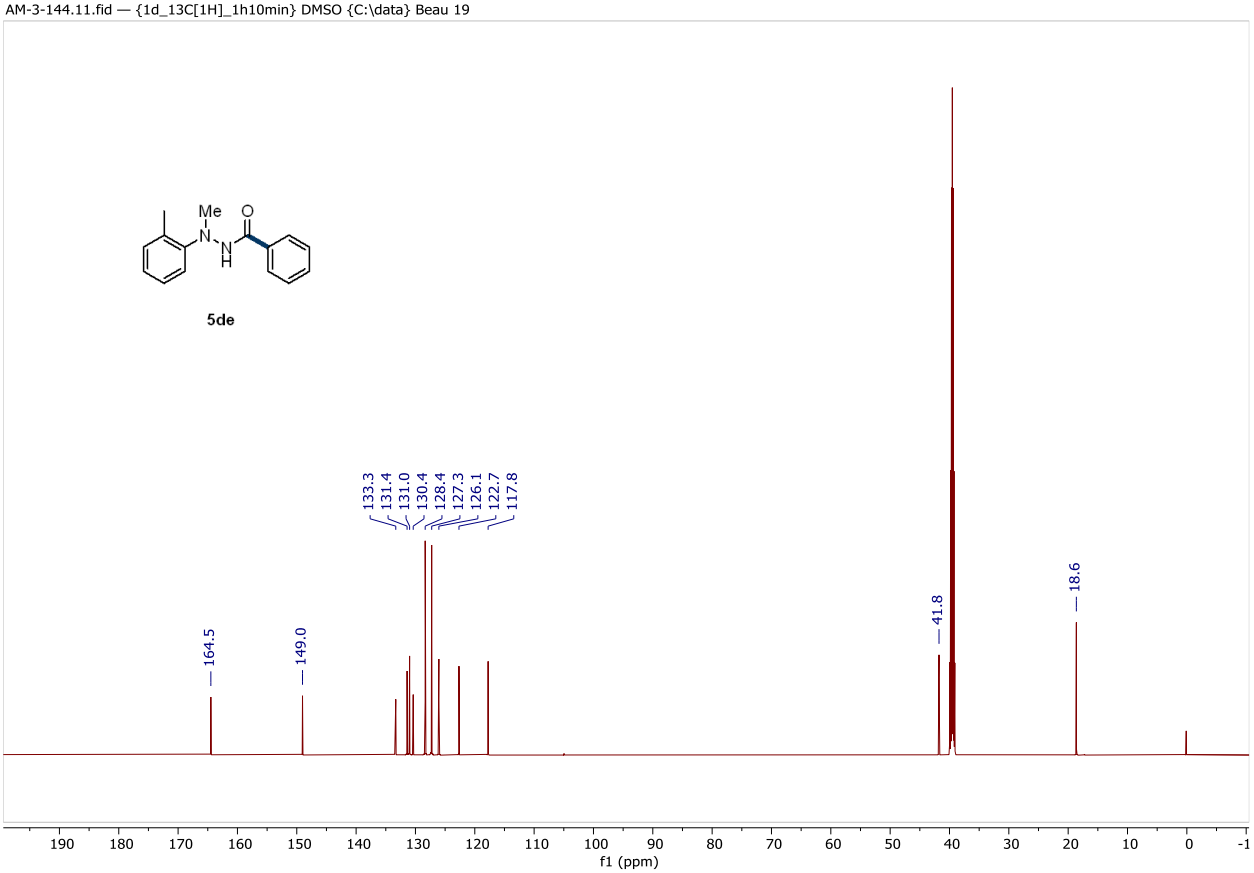

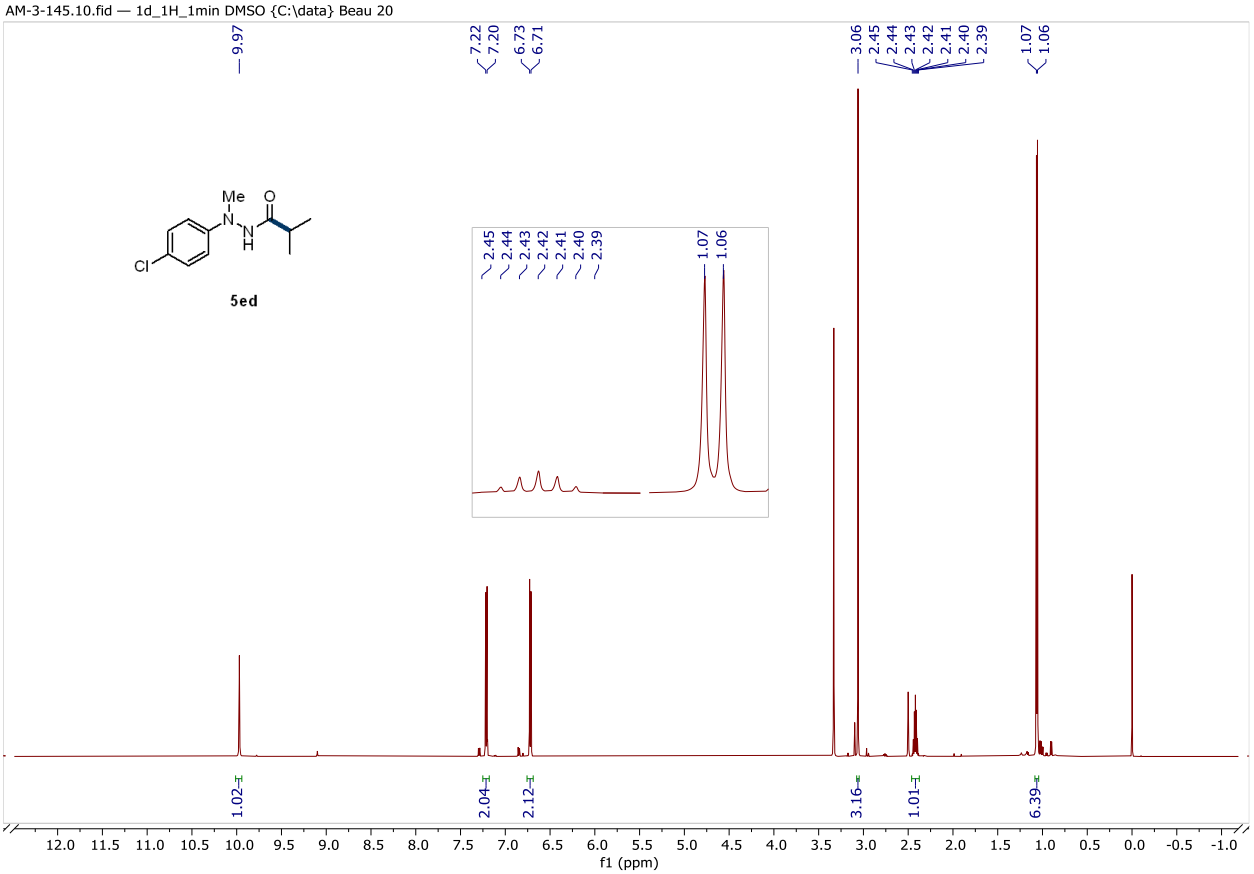
AM-3-145.10.fid — 1d_1H_1min DMSO {C:\data} Beau 20
9.97
7.22
7.20
6.73
6.71
3.06
2.45
2.44
2.43
2.42
2.41
2.40
2.39
1.07
1.06
Me
O
N
N
H
Cl
5ed
1.02
2.04
2.12
3.16
1.01
6.39
12.0 11.5 11.0 10.5 10.0 9.5 9.0 8.5 8.0 7.5 7.0 6.5 6.0 5.5 5.0 4.5 4.0 3.5 3.0 2.5 2.0 1.5 1.0 0.5 0.0 -0.5 -1.0
f1 (ppm)

AM-3-145.11.fid — {1d_13C[1H]_1h10min} DMSO {C:\data} Beau 20

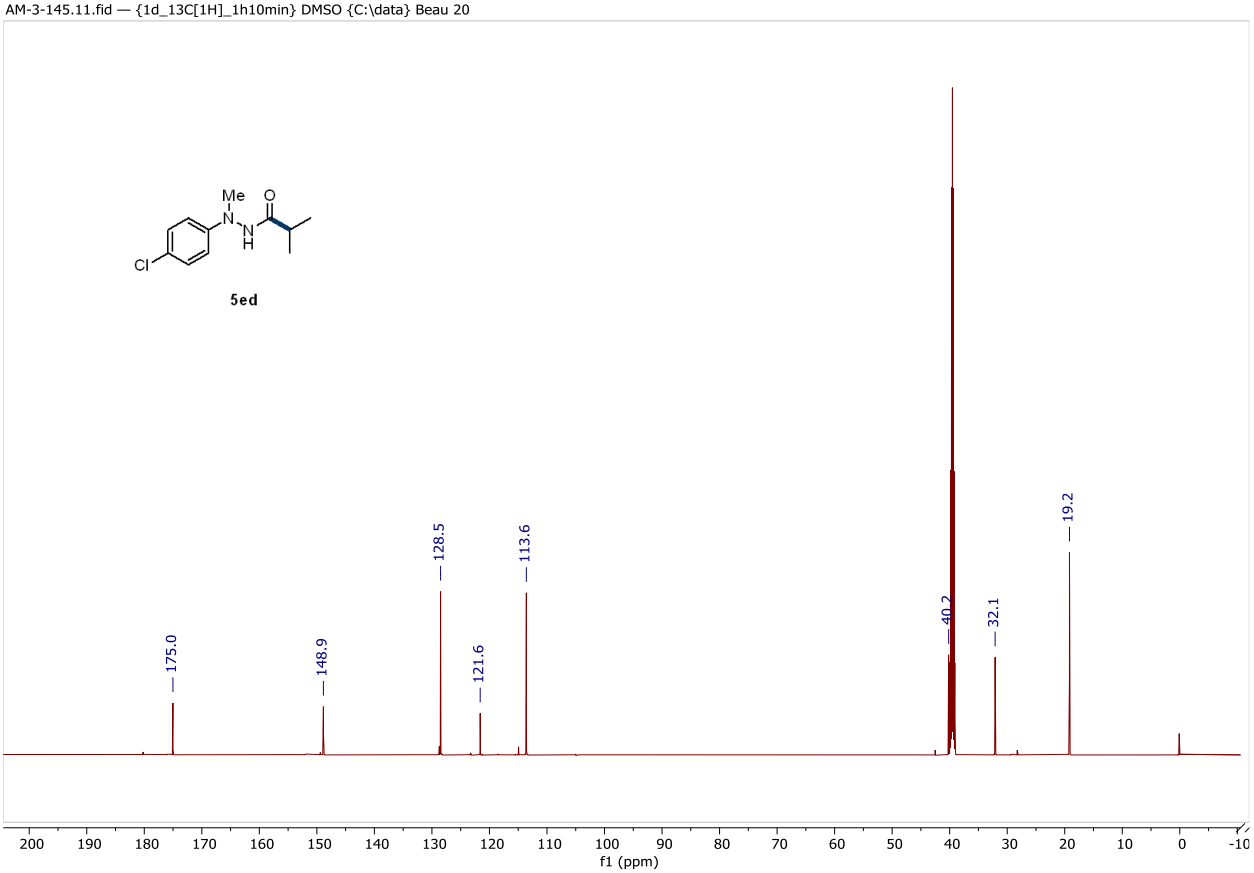

AM-3-81-cryst.1.fid — 1H NMR

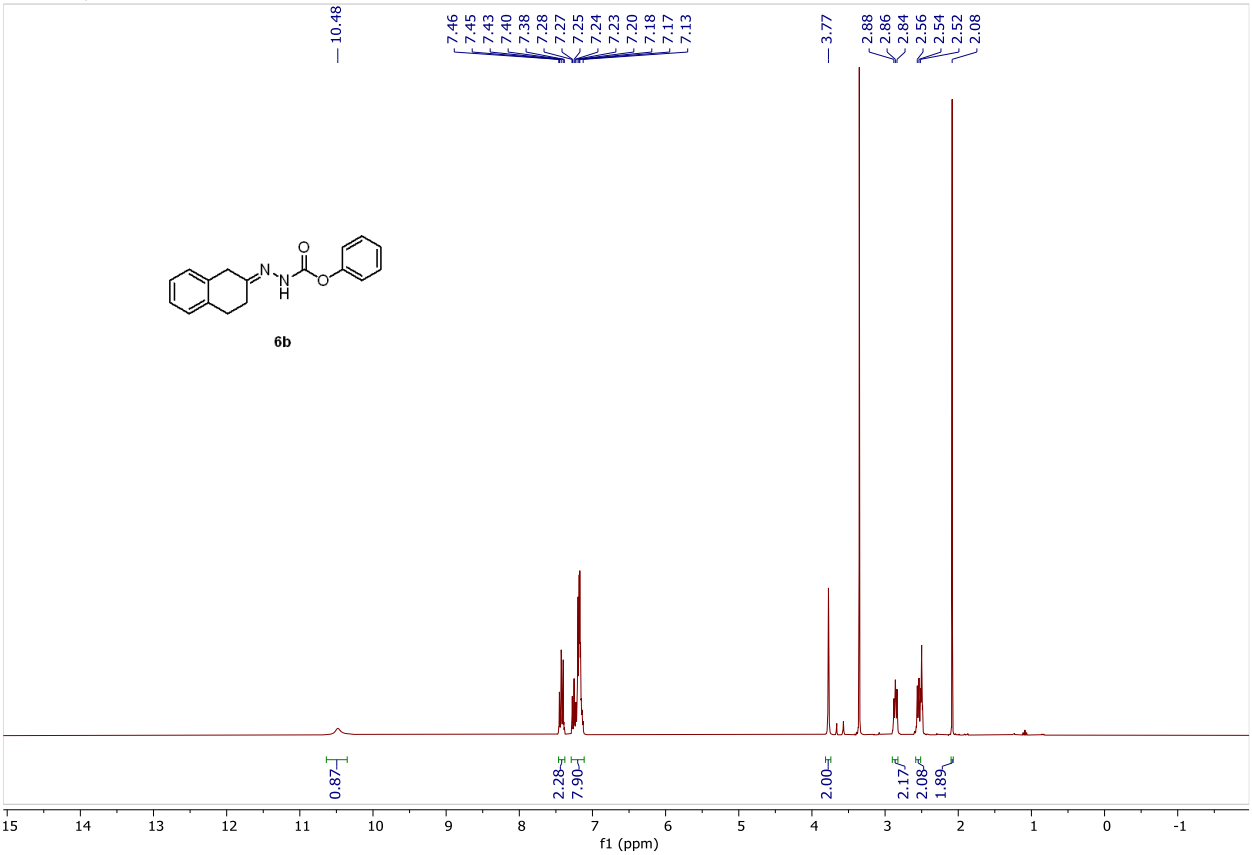

6b

AM-3-81-P-DMSO-May24.11.fid — {1d_13C[1H]_18min} DMSO {C:\data} Beau 21

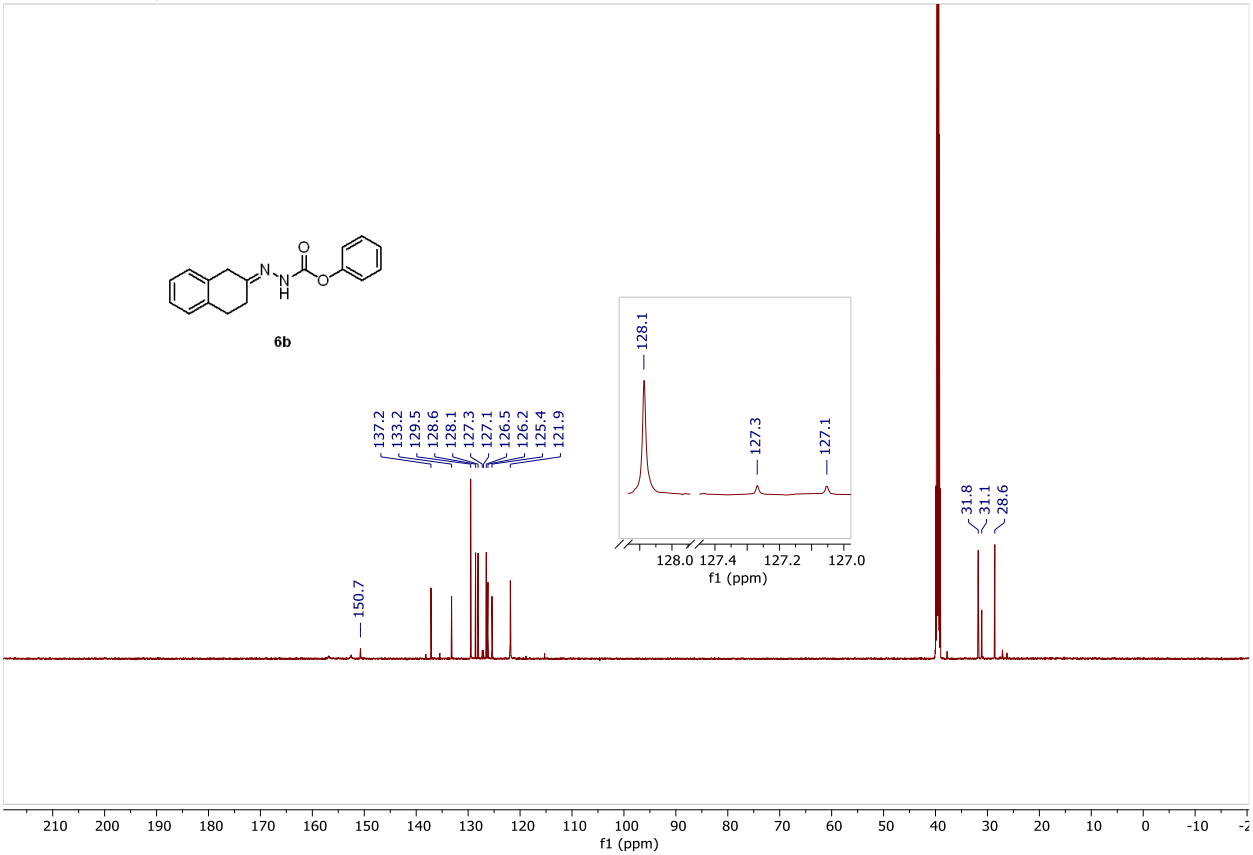

FV-SM-phenyl-ethyl.1.fid — 1H NMR

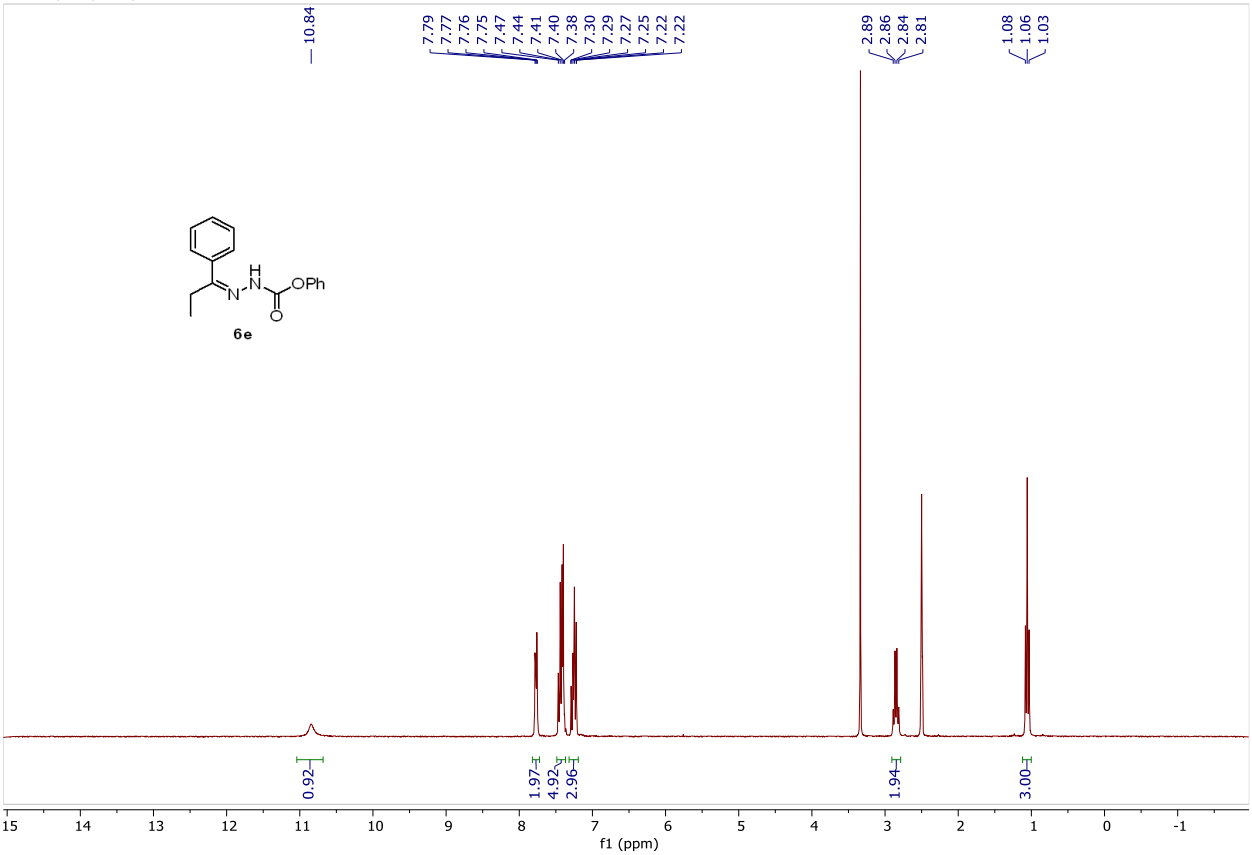

FV-SM-phenyl-ethyl.2.fid — 13C

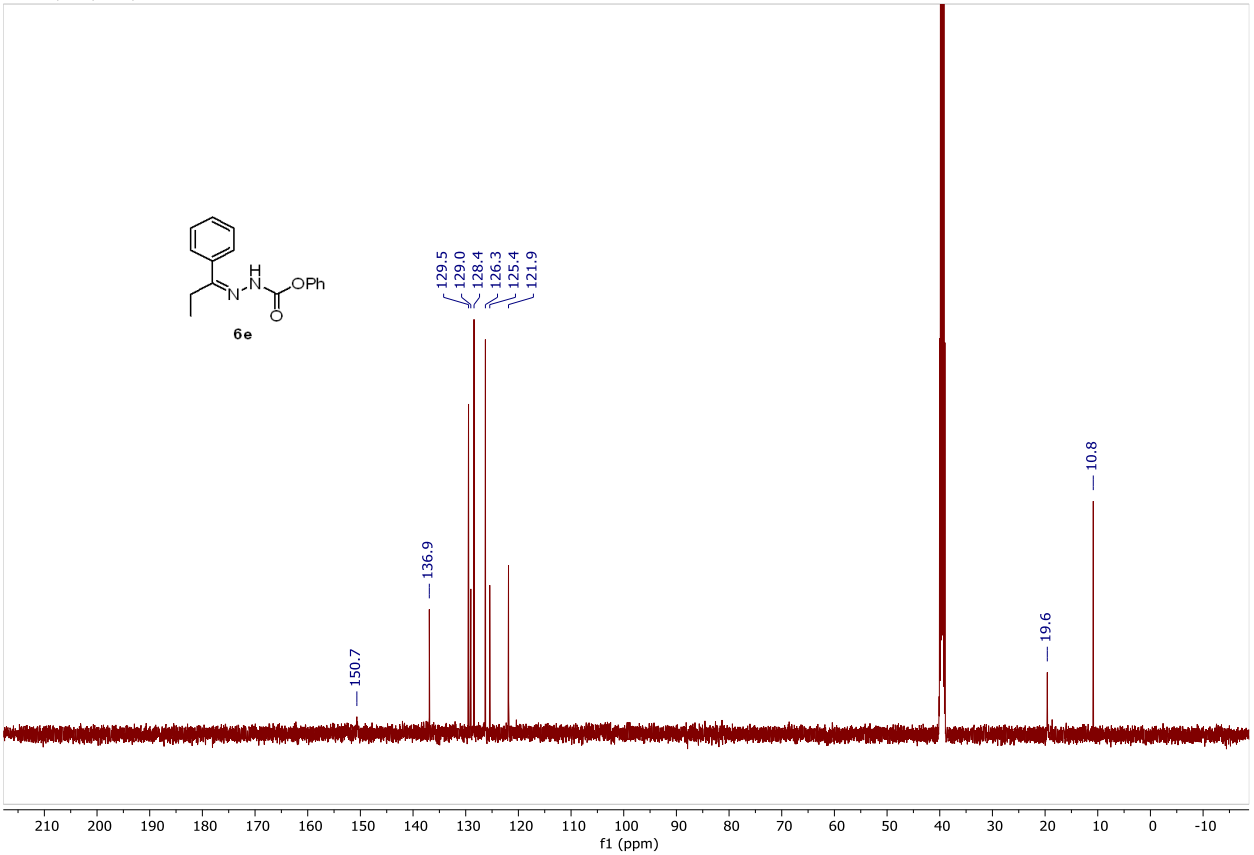

FV-sm-Phenyl-propyl.10.fid — 1d_1H_1min DMSO {C:\data} Beau 17

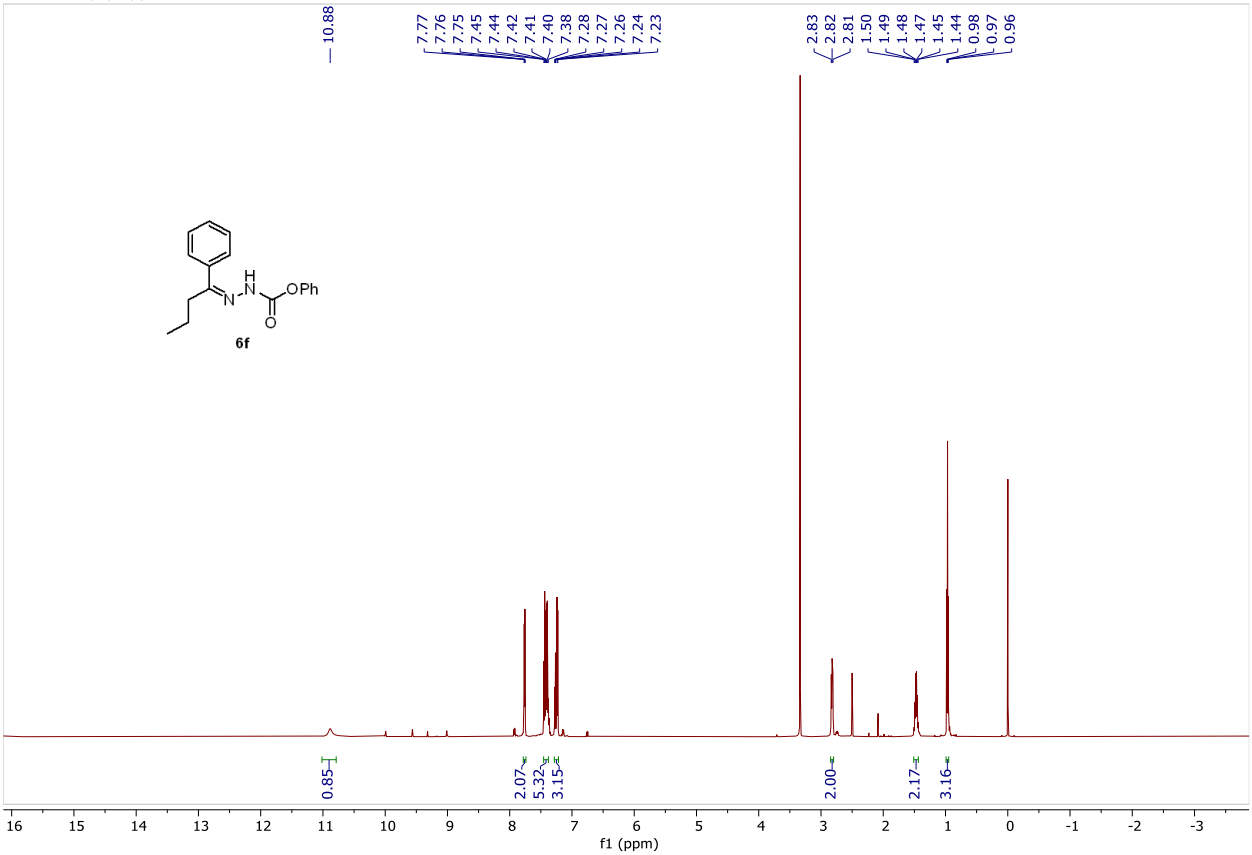

FV-sm-Phenyl-propyl.11.fid — {1d_13C[1H]_18min} DMSO {C:\data} Beau 17

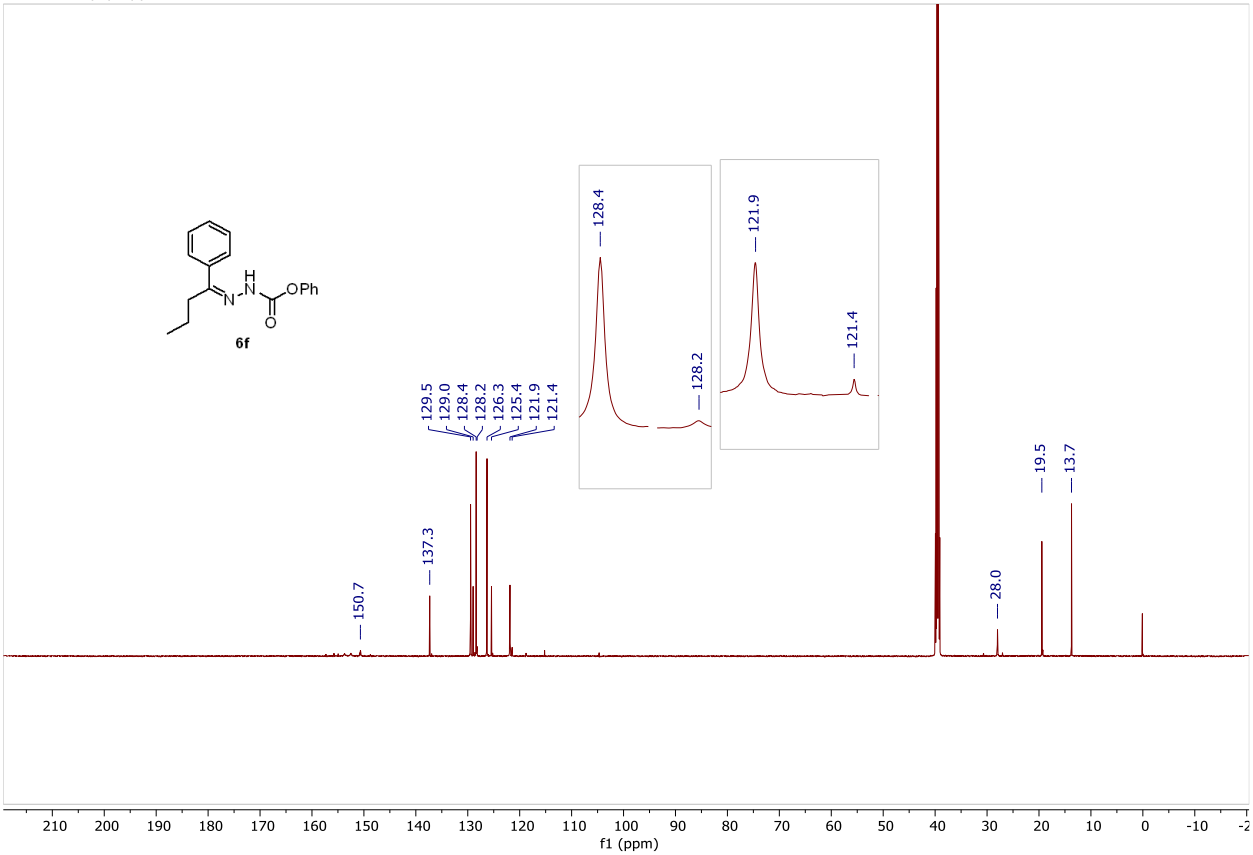

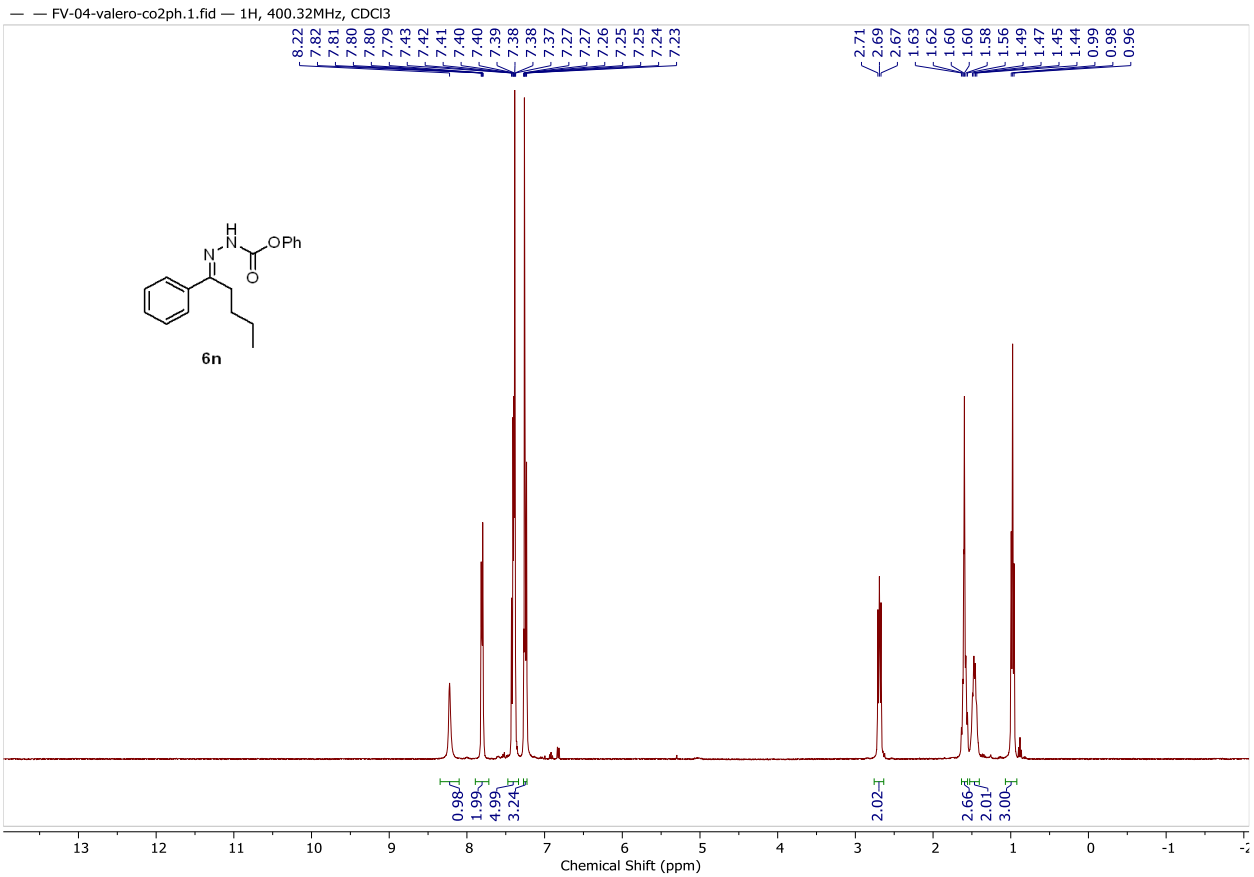
— — FV-04-valero-co2ph.1.fid — 1H, 400.32MHz, CDCl3
8.22
7.82
7.81
7.80
7.80
7.79
7.43
7.42
7.41
7.40
7.40
7.39
7.38
7.38
7.37
7.27
7.27
7.26
7.25
7.25
7.24
7.23
2.71
2.69
2.67
1.63
1.62
1.60
1.60
1.58
1.56
1.49
1.47
1.45
1.44
0.99
0.98
0.96
H
N
N
OPh
O
6n
0.98
1.99
4.99
3.24
2.02
2.66
2.01
3.00
13
12
11
10
9
8
7
6
5
4
3
2
1
0
-1
Chemical Shift (ppm)

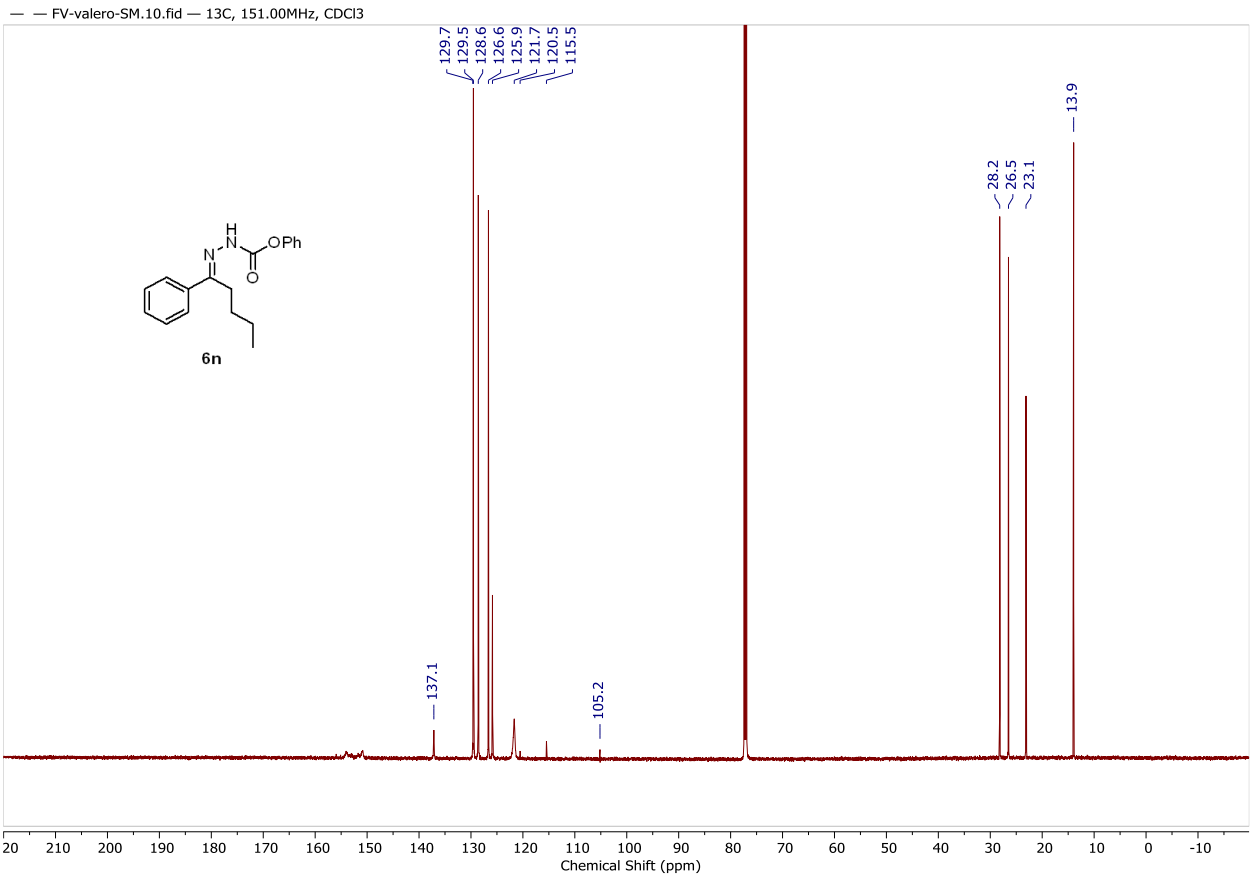
— — FV-valero-SM.10.fid — 13C, 151.00MHz, CDCl3
129.7
129.5
128.6
126.6
125.9
121.7
120.5
115.5
137.1
105.2
28.2
26.5
23.1
13.9
OPh
6n
20 210 200 190 180 170 160 150 140 130 120 110 100 90 80 70 60 50 40 30 20 10 0 -10
Chemical Shift (ppm)

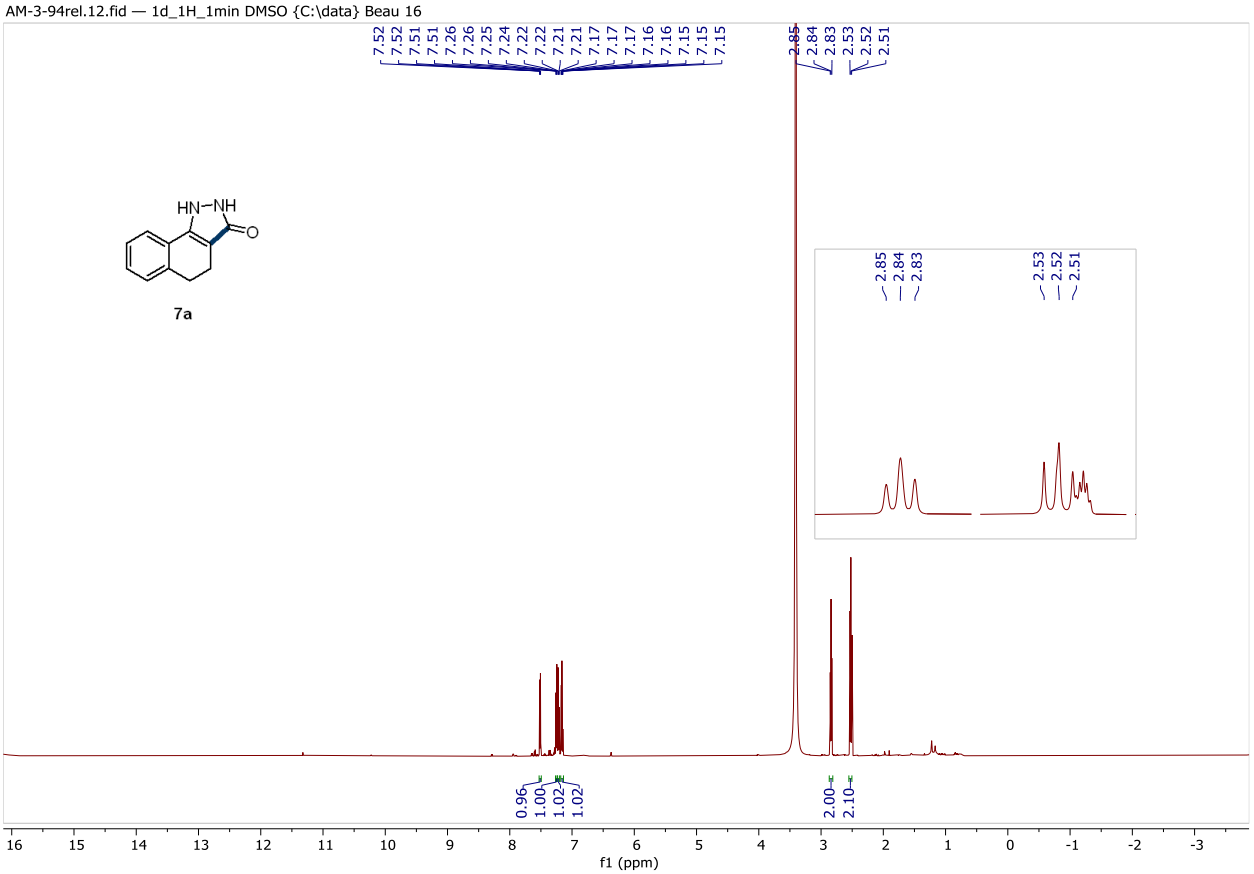
AM-3-94rel.12.fid — 1d_1H_1min DMSO {C:\data} Beau 16
7.52
7.52
7.51
7.51
7.26
7.26
7.25
7.24
7.22
7.22
7.21
7.21
7.17
7.17
7.17
7.16
7.16
7.15
7.15
7.15
2.85
2.84
2.83
2.53
2.52
2.51
HN–NH
O
7a
0.96
1.00
1.02
1.02
2.00
2.10
16
15
14
13
12
11
10
9
8
7
6
5
4
3
2
1
0
-1
-2
-3
f1 (ppm)

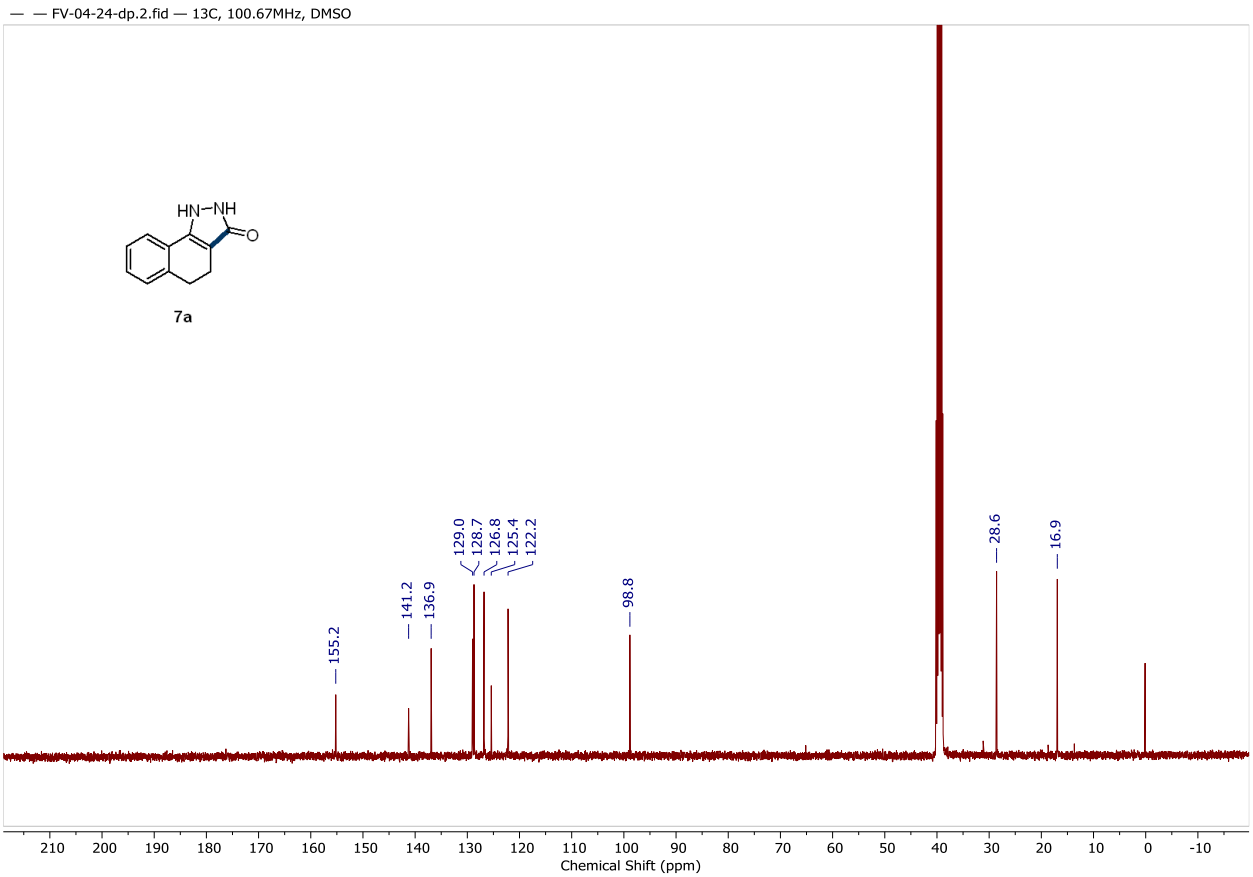
— — FV-04-24-dp.2.fid — 13C, 100.67MHz, DMSO
HN–NH
O
7a
155.2
141.2
136.9
129.0
128.7
126.8
125.4
122.2
98.8
28.6
16.9
210 200 190 180 170 160 150 140 130 120 110 100 90 80 70 60 50 40 30 20 10 0 -10
Chemical Shift (ppm)

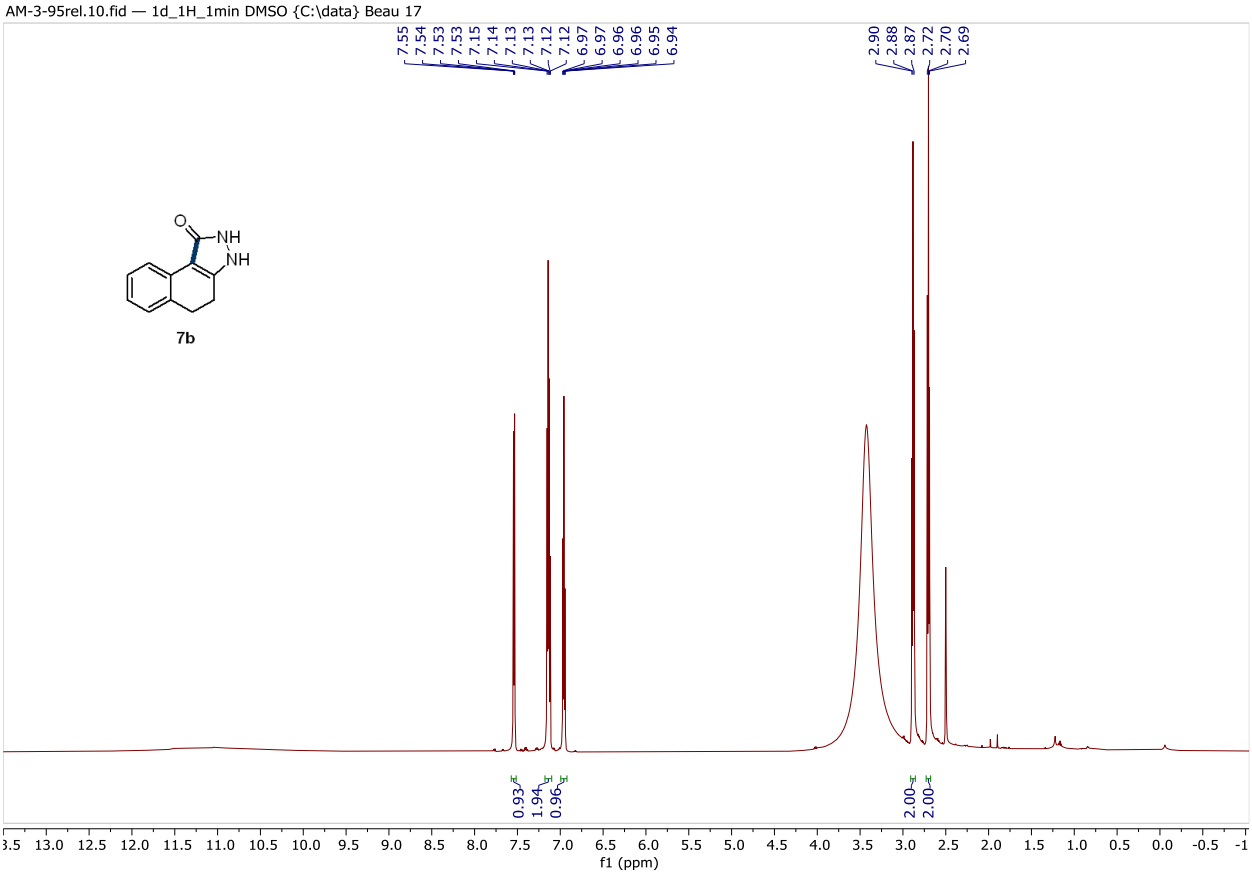
AM-3-95rel.10.fid — 1d_1H_1min DMSO {C:\data} Beau 17
7.55
7.54
7.53
7.53
7.15
7.14
7.13
7.13
7.12
7.12
6.97
6.97
6.96
6.96
6.95
6.94
2.90
2.88
2.87
2.72
2.70
2.69
O
NH
NH
7b
0.93
1.94
0.96
2.00
2.00
f1 (ppm)

AM-3-95-P.11.fid — {1d_13C[1H]_8min} DMSO {C:\data} Beau 15

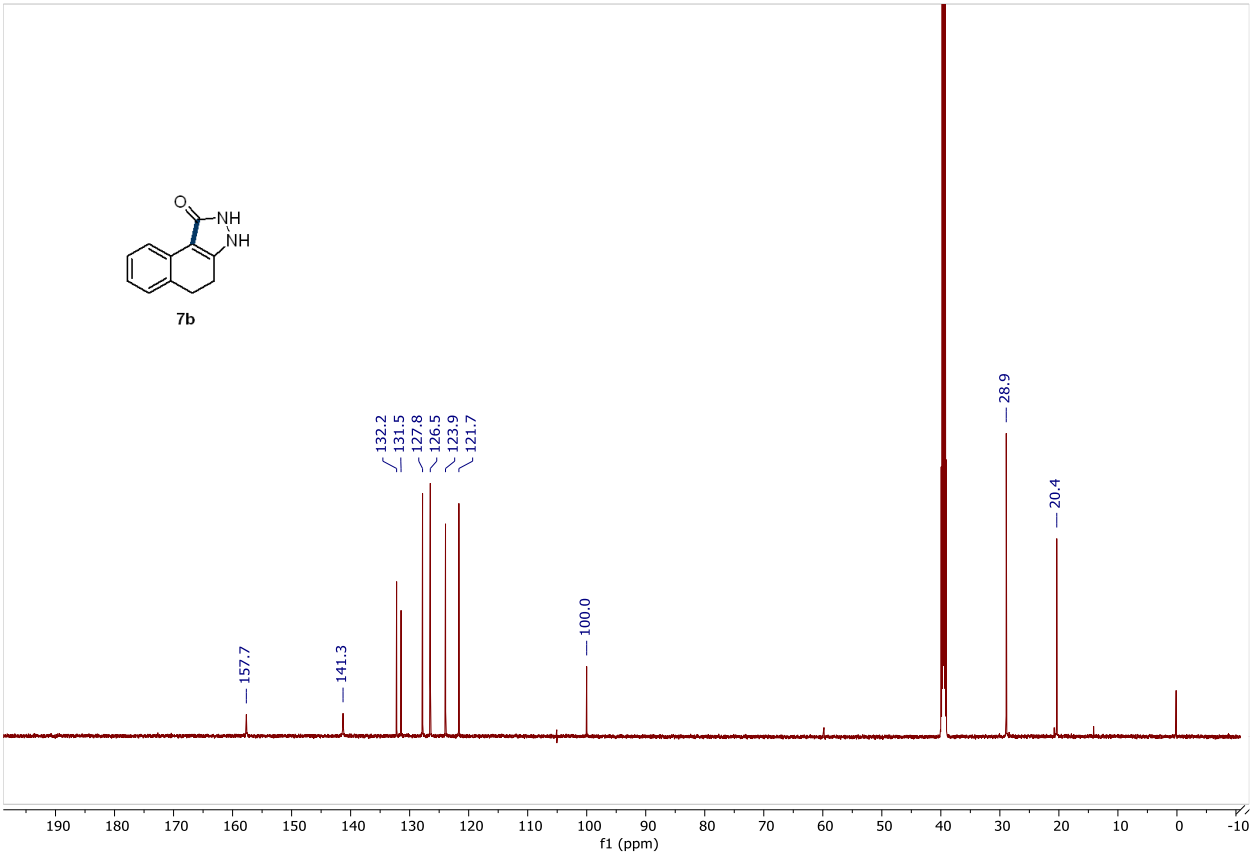

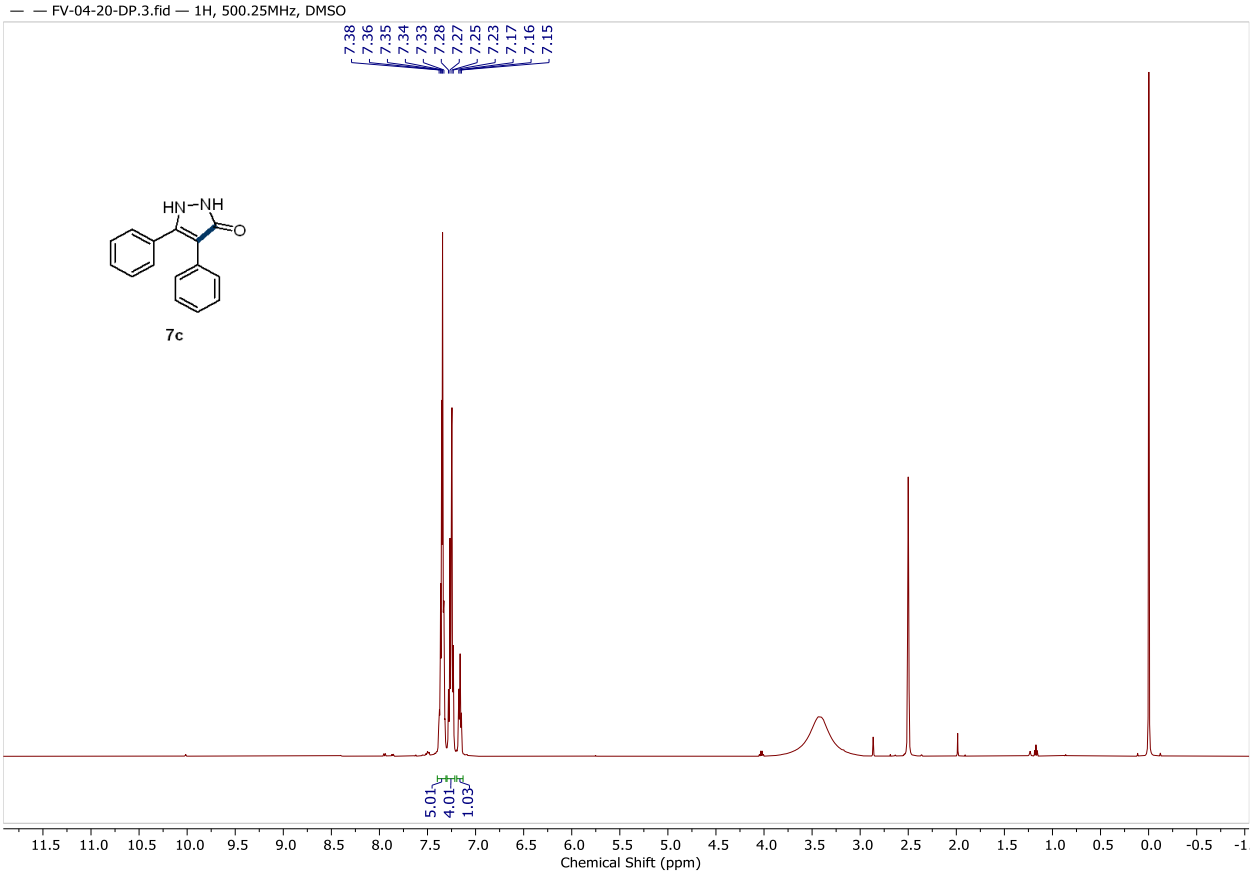
— — FV-04-20-DP.3.fid — 1H, 500.25MHz, DMSO
7.38
7.36
7.35
7.34
7.33
7.28
7.27
7.25
7.23
7.17
7.16
7.15
HN–NH
O
7c
5.01
4.01
1.03
11.5 11.0 10.5 10.0 9.5 9.0 8.5 8.0 7.5 7.0 6.5 6.0 5.5 5.0 4.5 4.0 3.5 3.0 2.5 2.0 1.5 1.0 0.5 0.0 -0.5 -1
Chemical Shift (ppm)

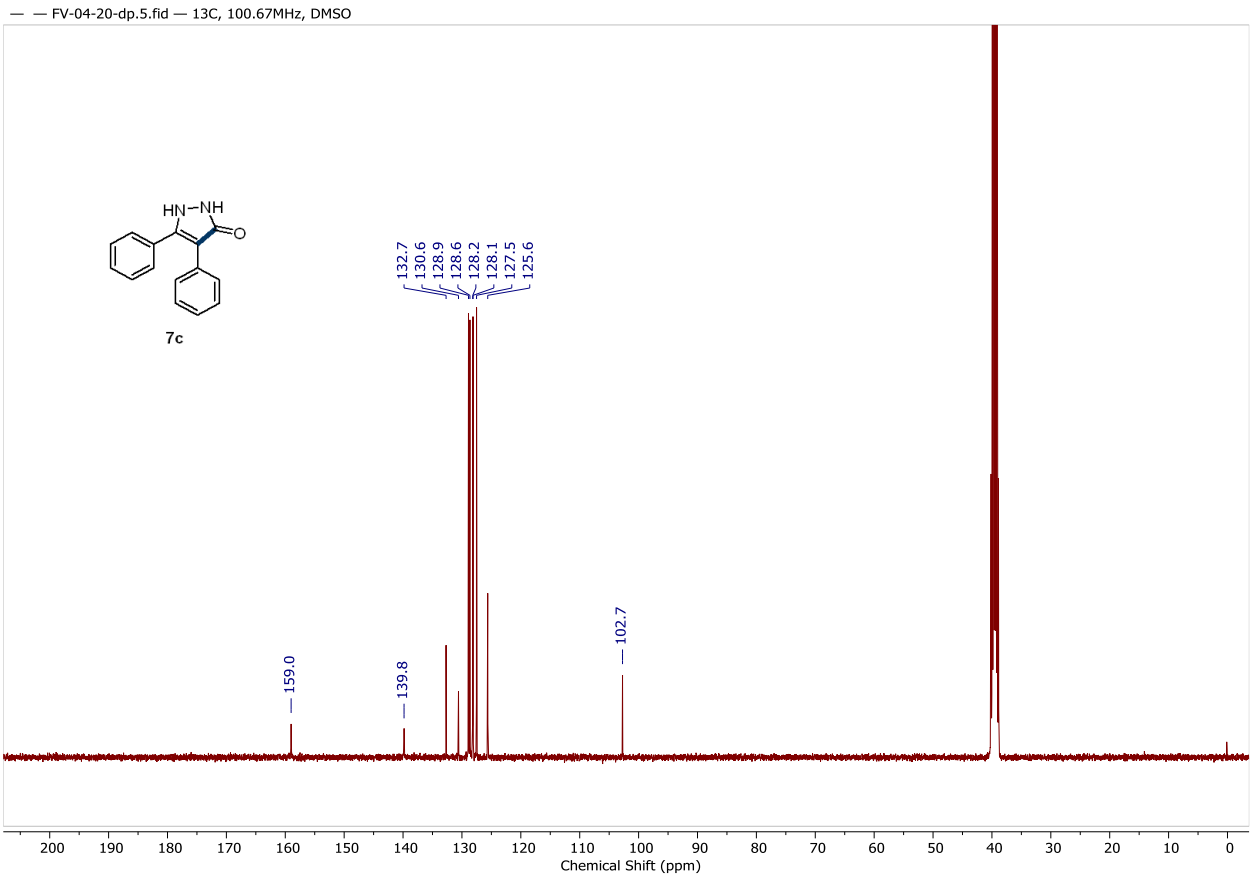
— — FV-04-20-dp.5.fid — 13C, 100.67MHz, DMSO
HN–NH
O
7c
132.7
130.6
128.9
128.6
128.2
128.1
127.5
125.6
159.0
139.8
102.7
200 190 180 170 160 150 140 130 120 110 100 90 80 70 60 50 40 30 20 10 0
Chemical Shift (ppm)

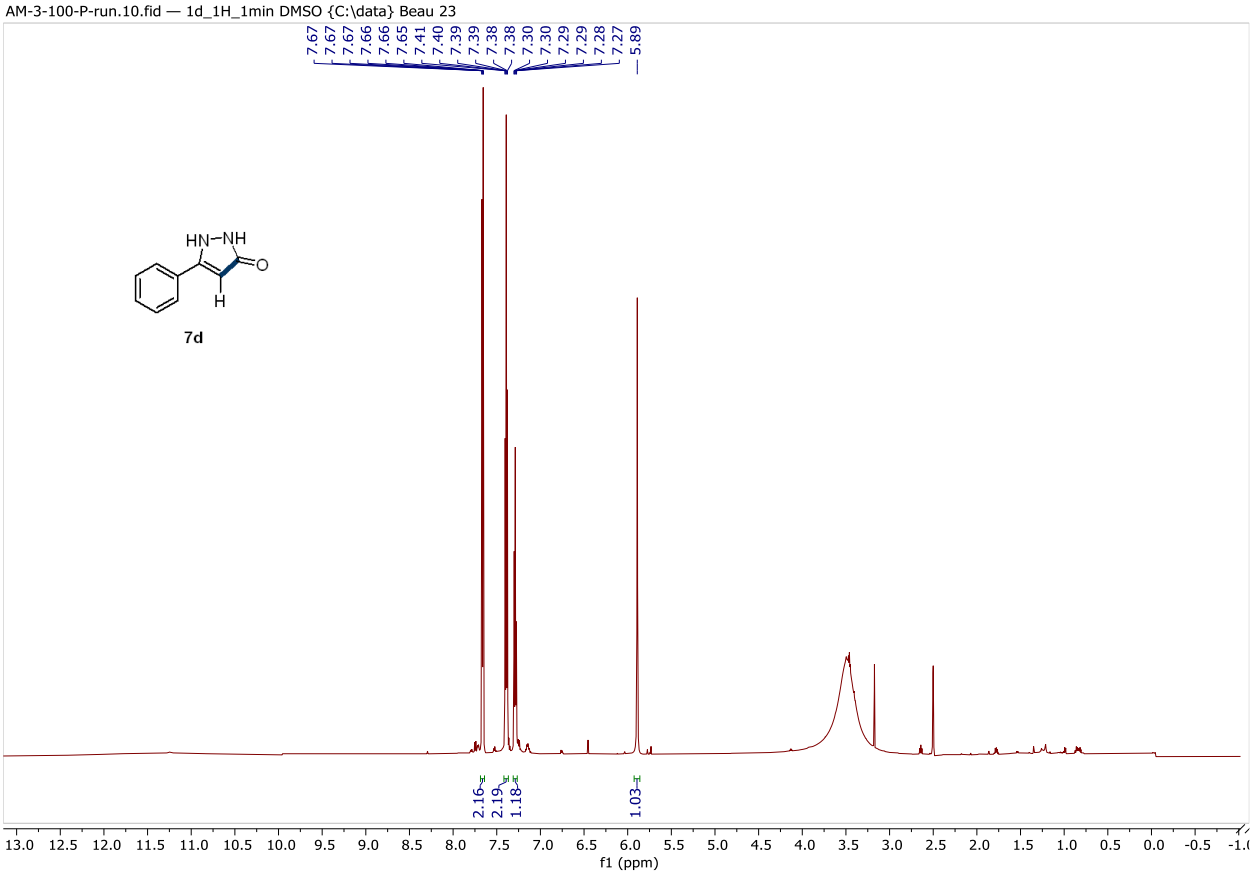
AM-3-100-P-run.10.fid — 1d_1H_1min DMSO {C:\data} Beau 23
7.67
7.67
7.67
7.66
7.66
7.65
7.41
7.40
7.39
7.39
7.38
7.38
7.30
7.30
7.29
7.29
7.28
7.27
5.89
HN
NH
O
H
7d
2.16
2.19
1.18
1.03
13.0 12.5 12.0 11.5 11.0 10.5 10.0 9.5 9.0 8.5 8.0 7.5 7.0 6.5 6.0 5.5 5.0 4.5 4.0 3.5 3.0 2.5 2.0 1.5 1.0 0.5 0.0 -0.5
f1 (ppm)

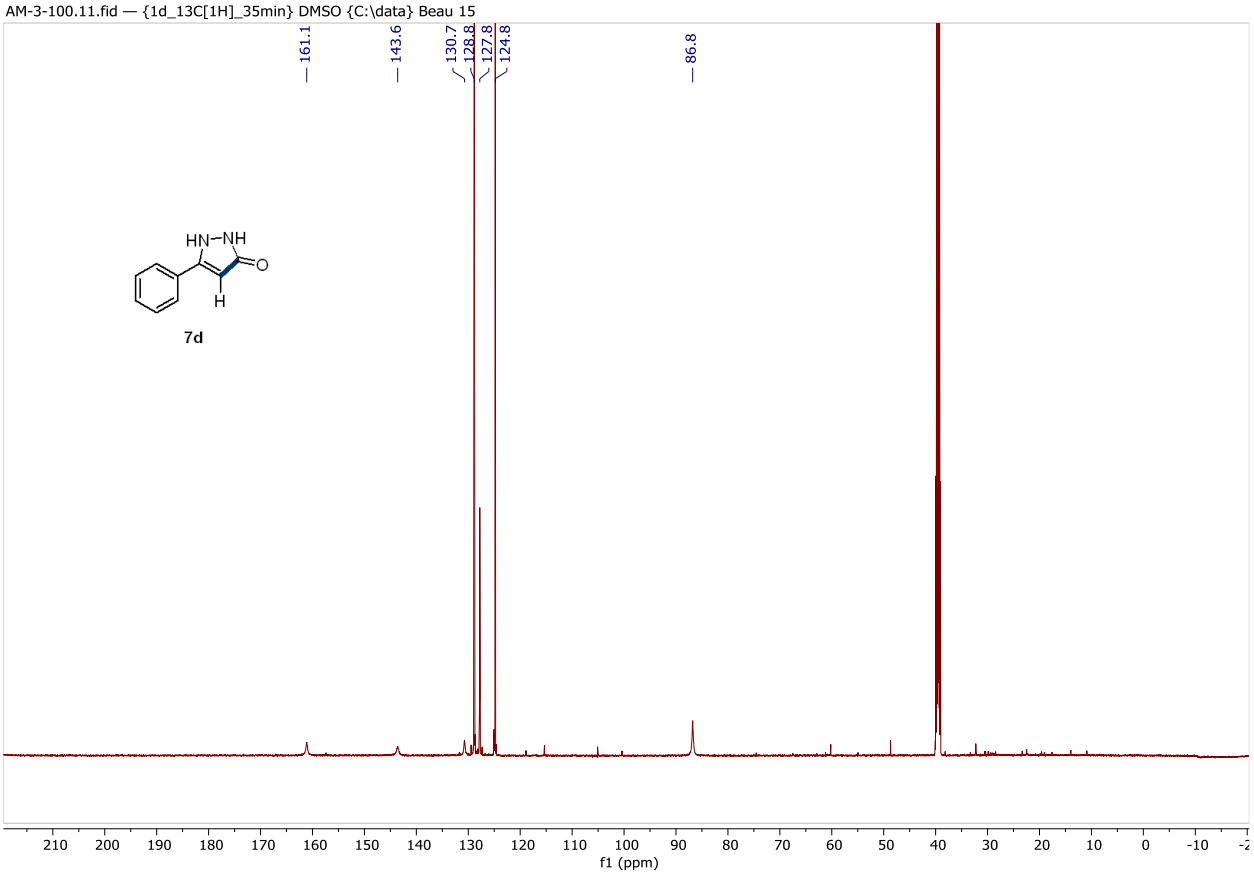
AM-3-100.11.fid — {1d_13C[1H]_35min} DMSO {C:\data} Beau 15
161.1
143.6
130.7
128.8
127.8
124.8
86.8
HN
NH
O
H
7d
210
200
190
180
170
160
150
140
130
120
110
100
90
80
70
60
50
40
30
20
10
0
-10
f1 (ppm)

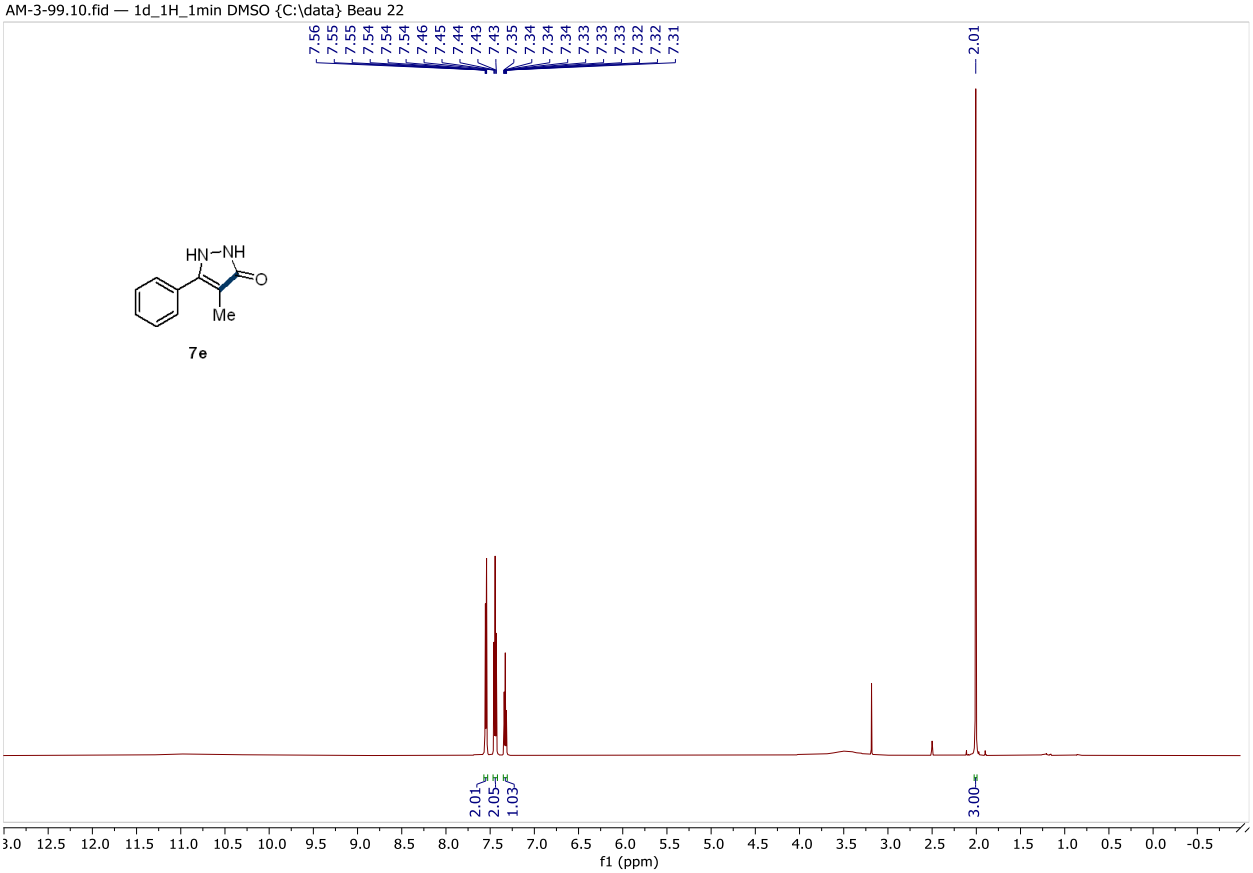
AM-3-99.10.fid — 1d_1H_1min DMSO {C:\data} Beau 22
7.56
7.55
7.55
7.54
7.54
7.54
7.46
7.45
7.44
7.43
7.43
7.35
7.34
7.34
7.34
7.33
7.33
7.33
7.32
7.32
7.31
2.01
HN
NH
O
Me
7e
2.01
2.05
1.03
3.00
f1 (ppm)

AM-3-99.11.fid — {1d_13C[1H]_18min} DMSO {C:\data} Beau 22

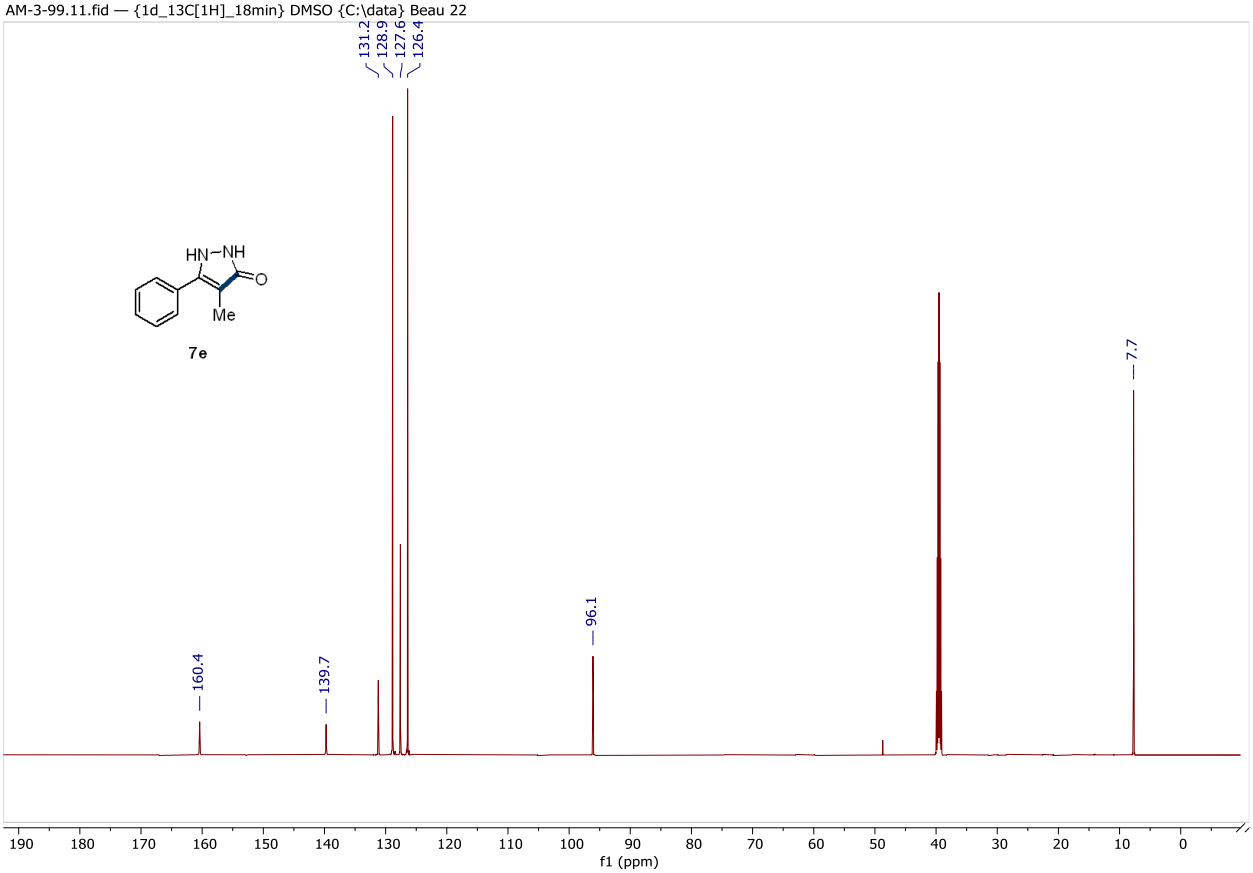

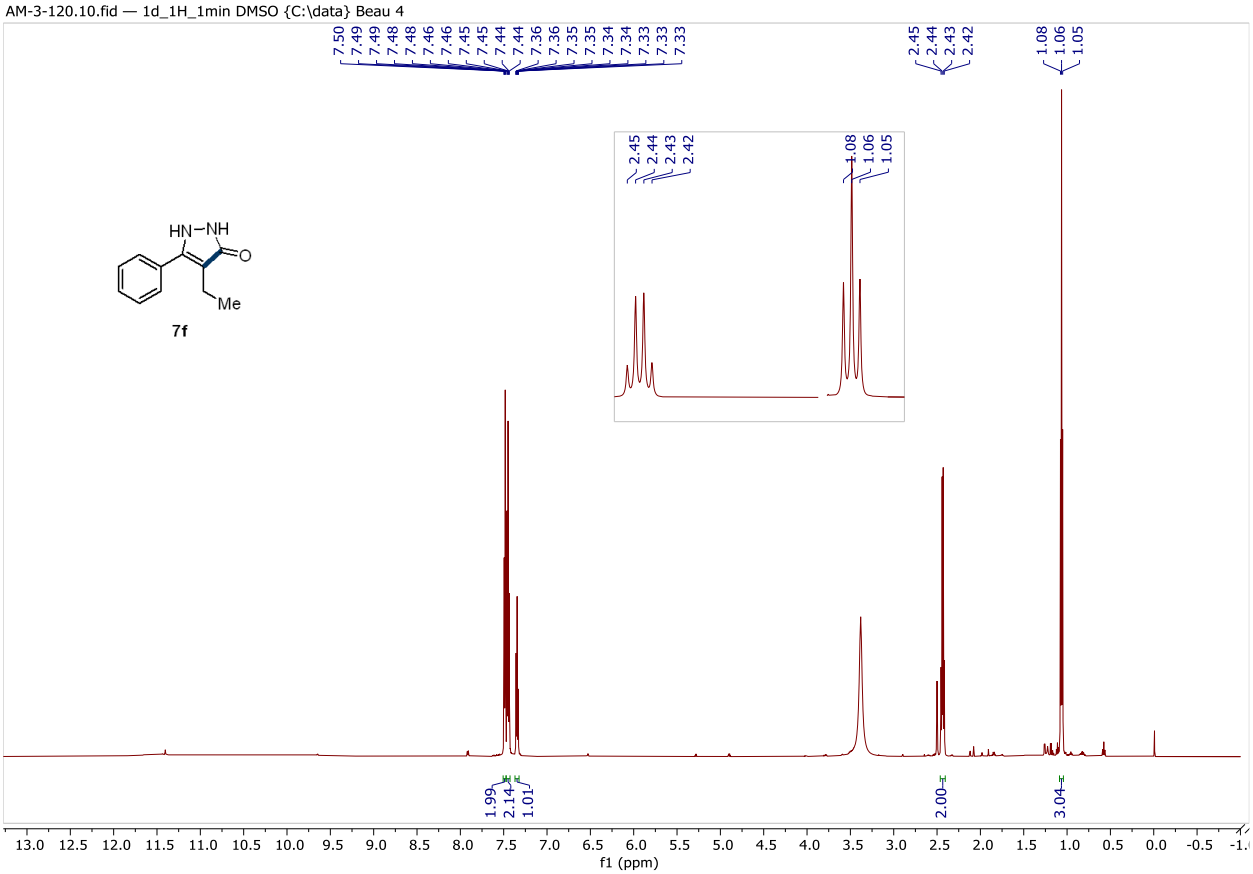
AM-3-120.10.fid — 1d_1H_1min DMSO {C:\data} Beau 4
7.50 7.49 7.49 7.48 7.48 7.46 7.46 7.45 7.45 7.44 7.44 7.36 7.36 7.35 7.35 7.34 7.34 7.33 7.33 7.33
2.45 2.44 2.43 2.42
1.08 1.06 1.05
HN–NH
O
Me
7f
1.99 2.14 1.01
2.00
3.04
13.0 12.5 12.0 11.5 11.0 10.5 10.0 9.5 9.0 8.5 8.0 7.5 7.0 6.5 6.0 5.5 5.0 4.5 4.0 3.5 3.0 2.5 2.0 1.5 1.0 0.5 0.0 -0.5
f1 (ppm)

AM-3-120.11.fid — {1d_13C[1H]_1h10min} DMSO {C:\data} Beau 4

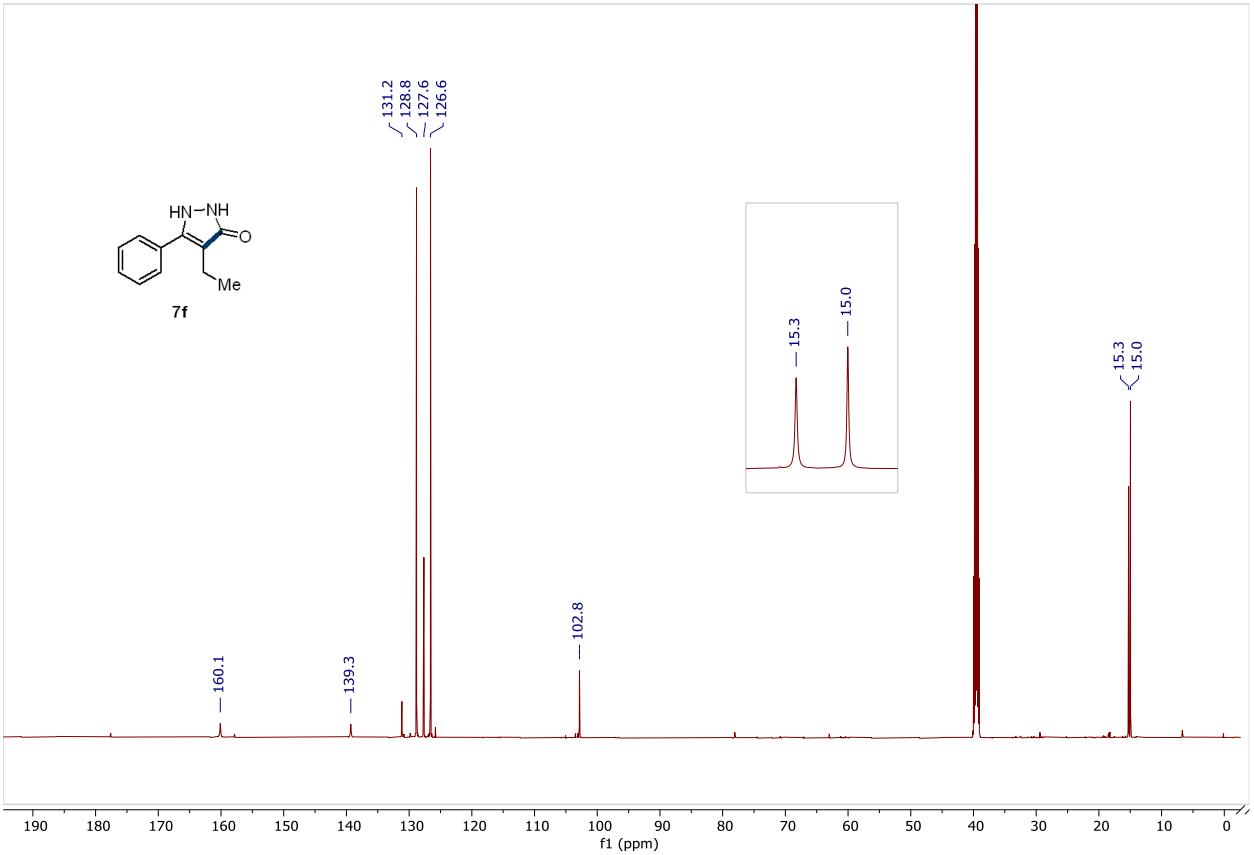

AM-3-97.10.fid — 1d_1H_1min DMSO {C:\data} Beau 2

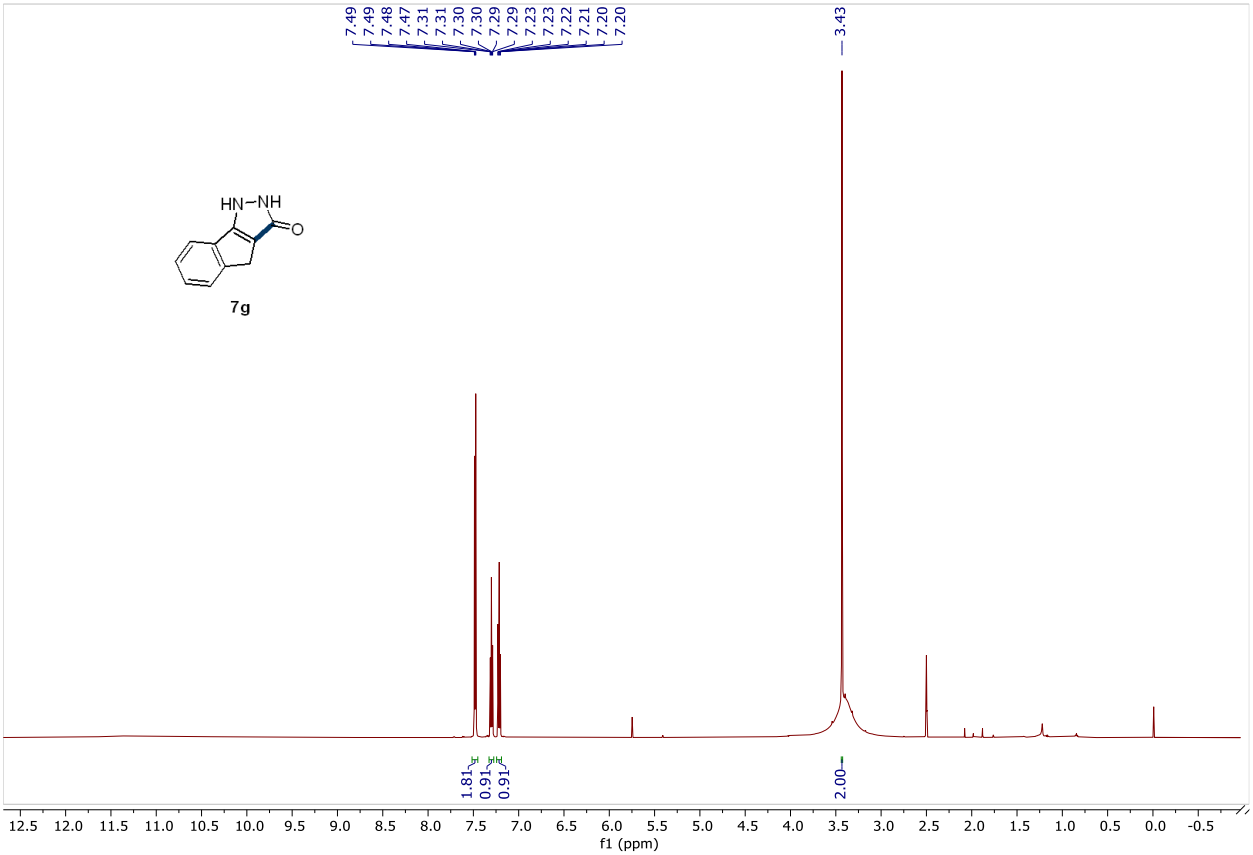

AM-3-97-run2-rel.11.fid — {1d_13C[1H]_1h10min} DMSO {C:\data} Beau 9

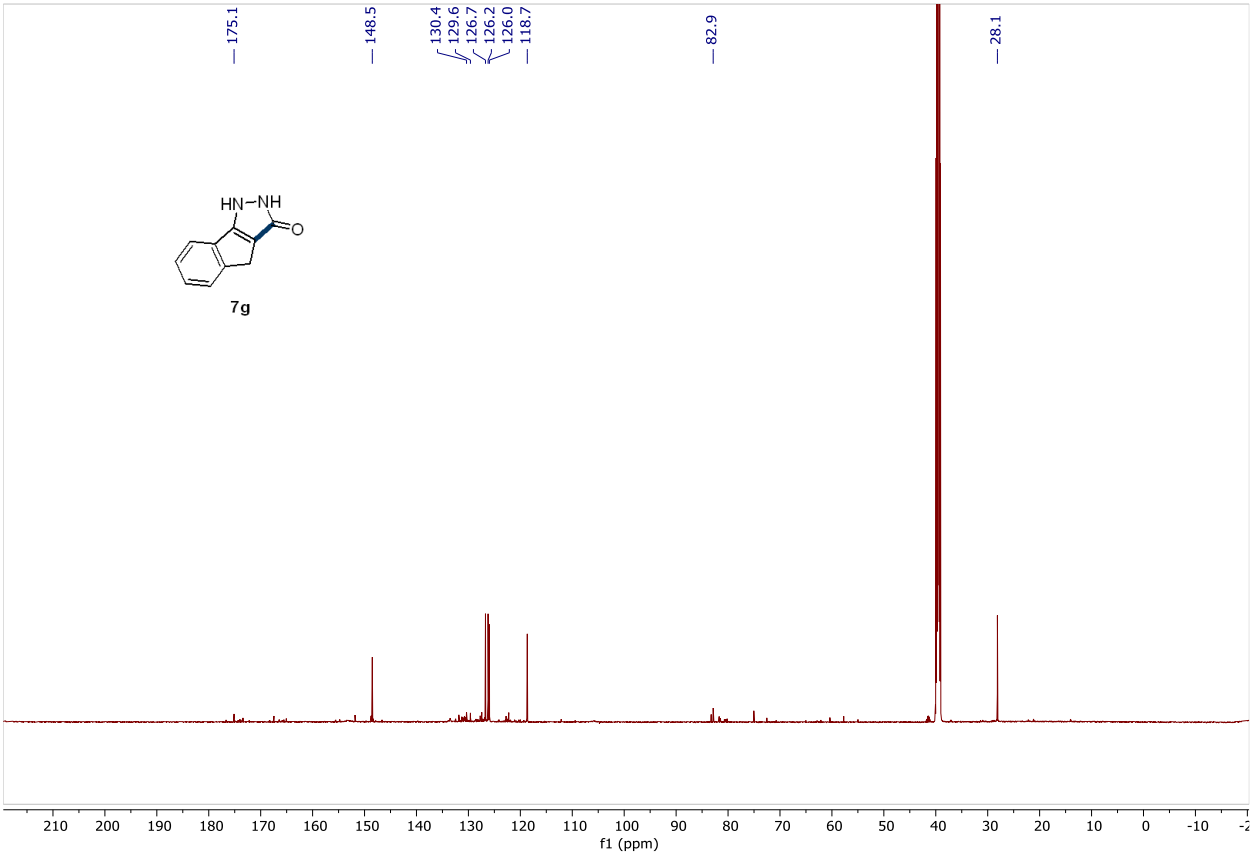

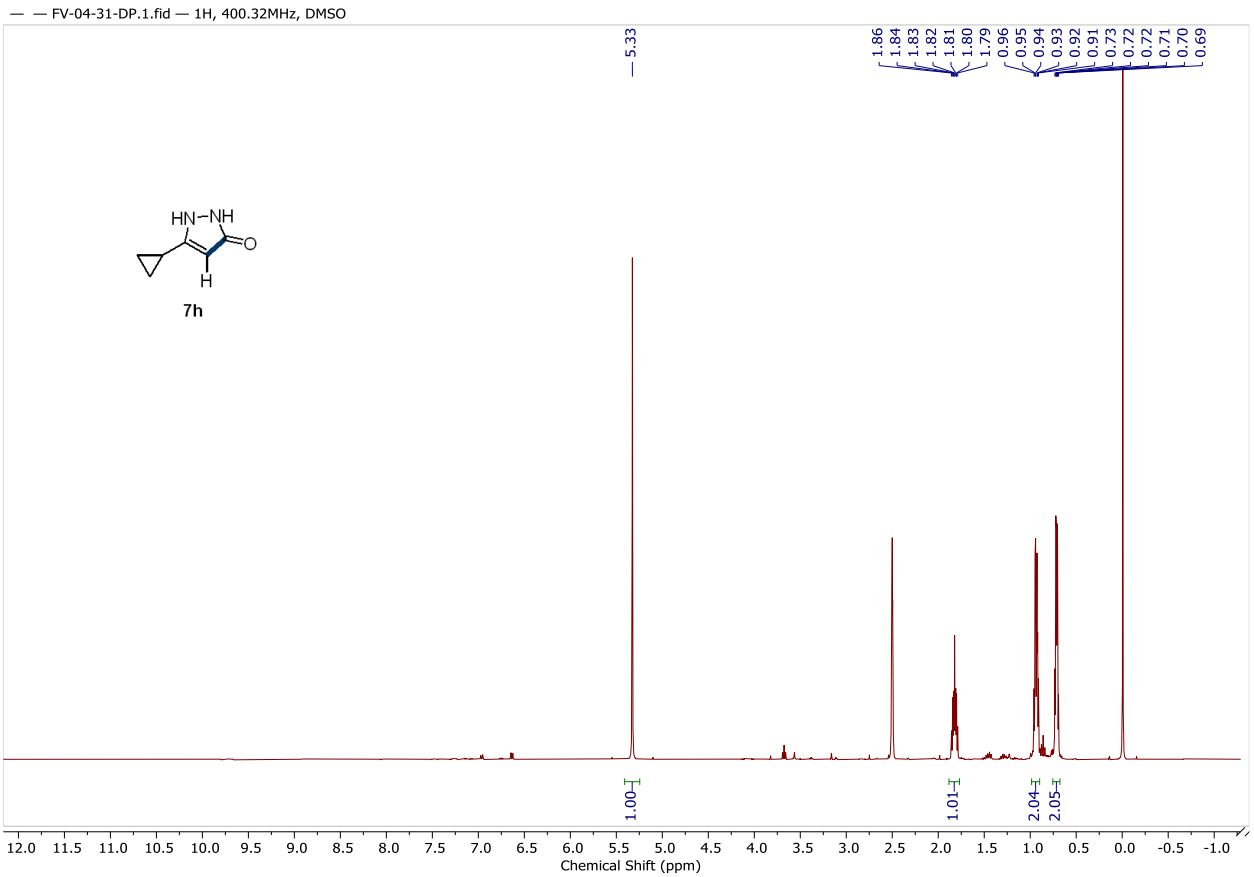
— — FV-04-31-DP.1.fid — 1H, 400.32MHz, DMSO
5.33
1.86
1.84
1.83
1.82
1.81
1.80
1.79
0.96
0.95
0.94
0.93
0.92
0.91
0.73
0.72
0.72
0.71
0.70
0.69
HN
NH
O
H
7h
1.00
1.01
2.04
2.05
12.0 11.5 11.0 10.5 10.0 9.5 9.0 8.5 8.0 7.5 7.0 6.5 6.0 5.5 5.0 4.5 4.0 3.5 3.0 2.5 2.0 1.5 1.0 0.5 0.0 -0.5 -1.0
Chemical Shift (ppm)

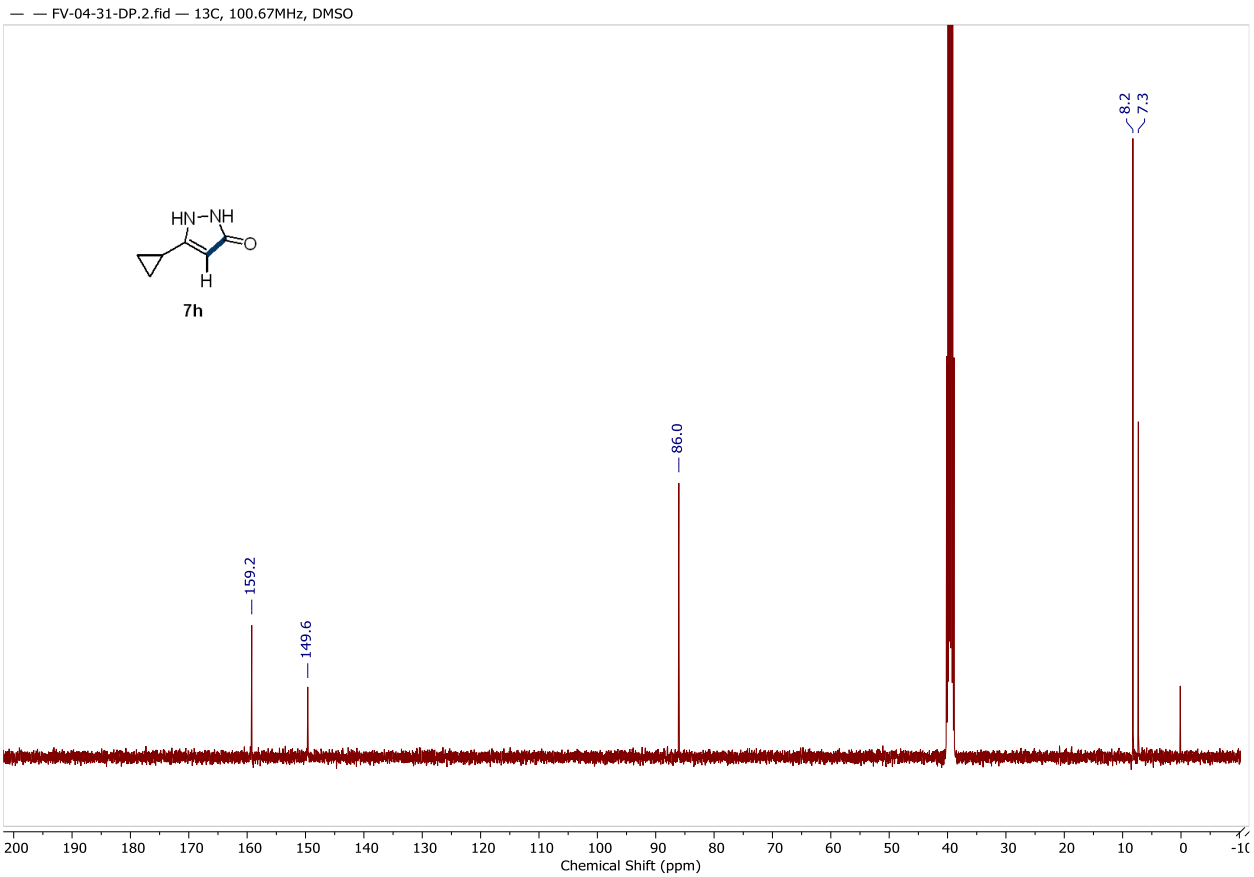
— — FV-04-31-DP.2.fid — 13C, 100.67MHz, DMSO
HN–NH
O
H
7h
159.2
149.6
86.0
8.2
7.3
200 190 180 170 160 150 140 130 120 110 100 90 80 70 60 50 40 30 20 10 0 -10
Chemical Shift (ppm)

AM-3-112.10.fid — 1d_1H_1min DMSO {C:\data} Beau 3

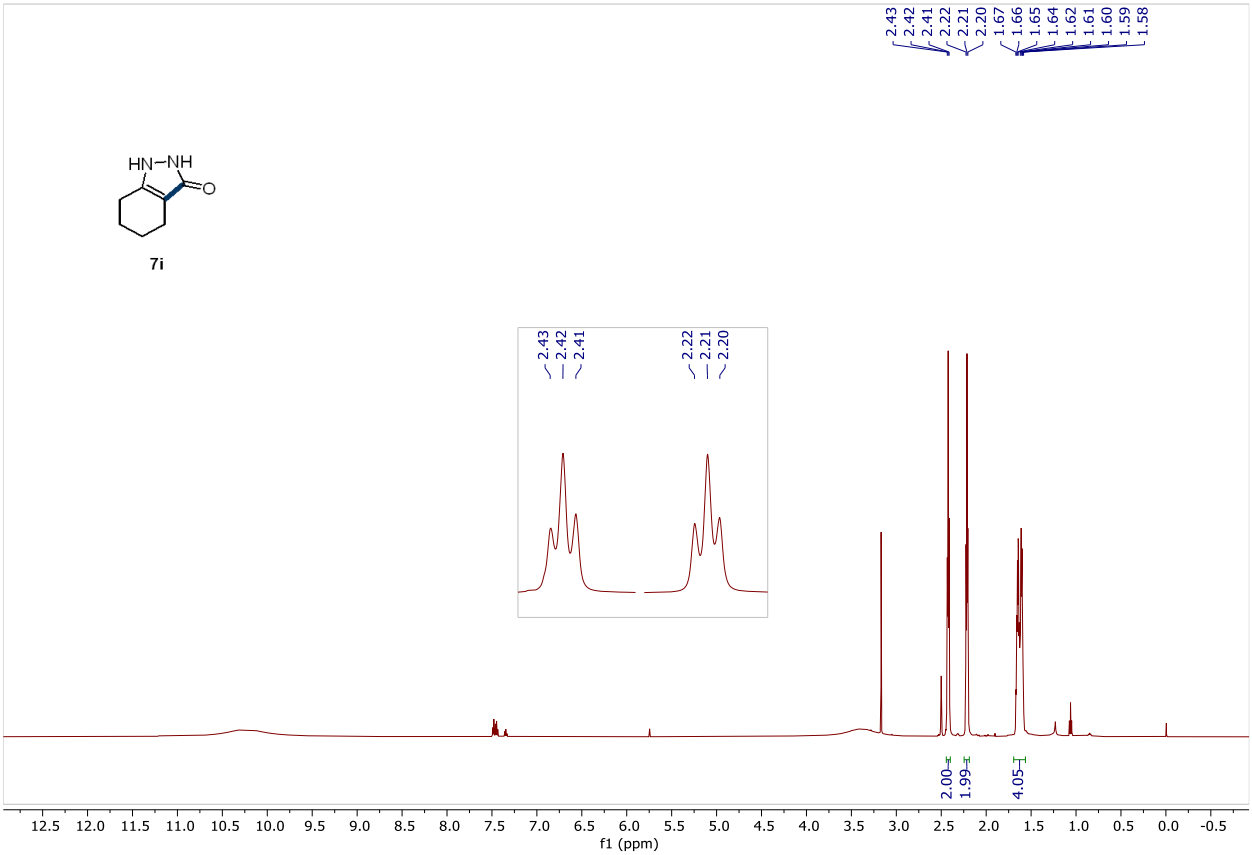

AM-3-112.11.fid — {1d_13C[1H]_1h10min} DMSO {C:\data} Beau 3

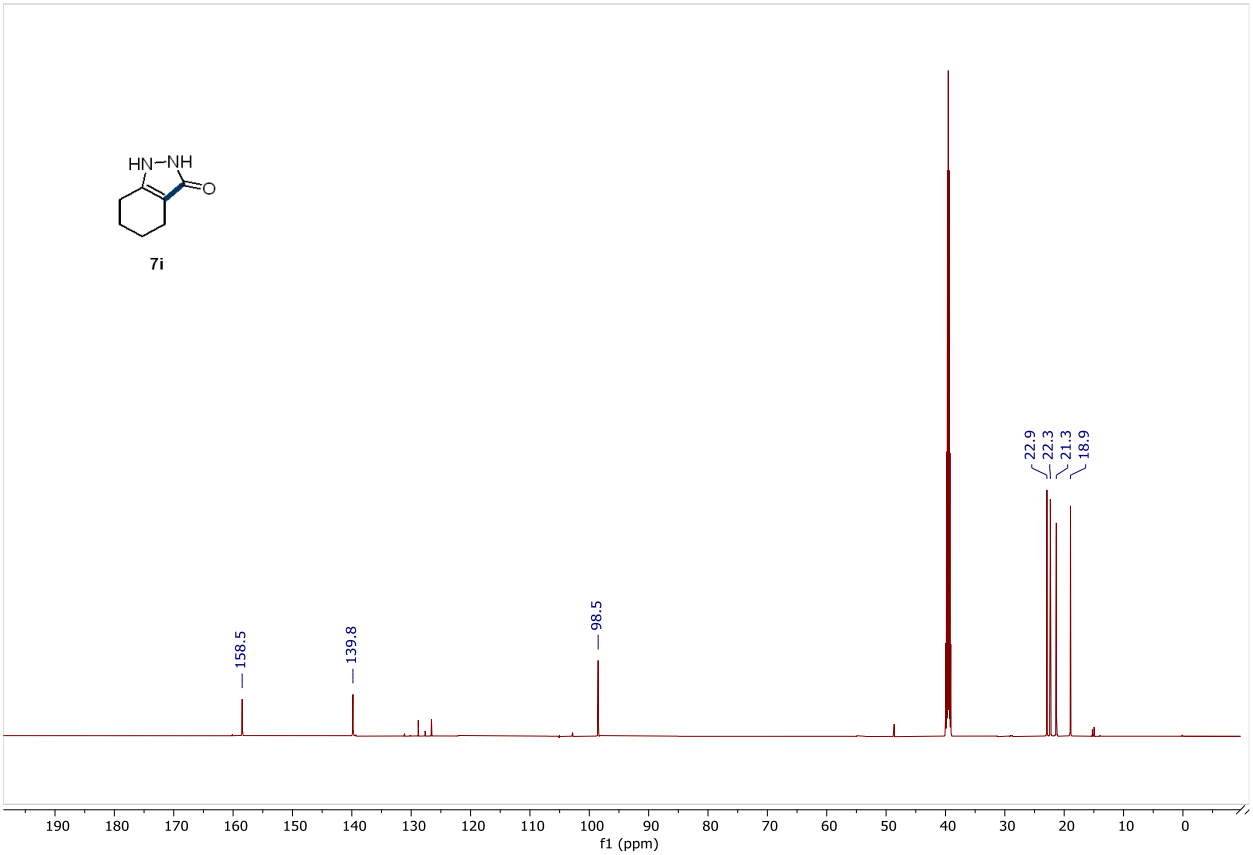

AM-3-115-P-May24.10.fid — 1d_1H_1min DMSO {C:\data} Beau 23

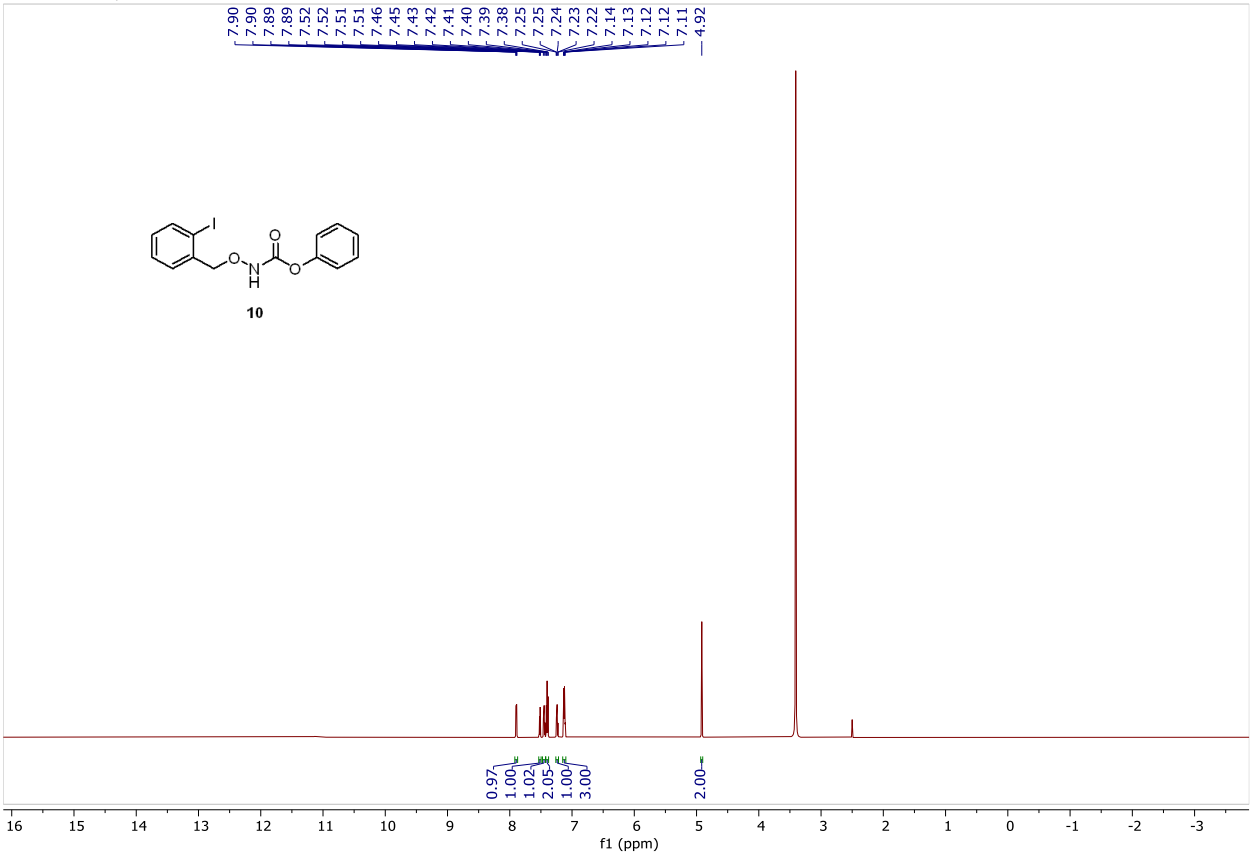

AM-3-115-P-May24.11.fid — {1d_13C[1H]_18min} DMSO {C:\data} Beau 23

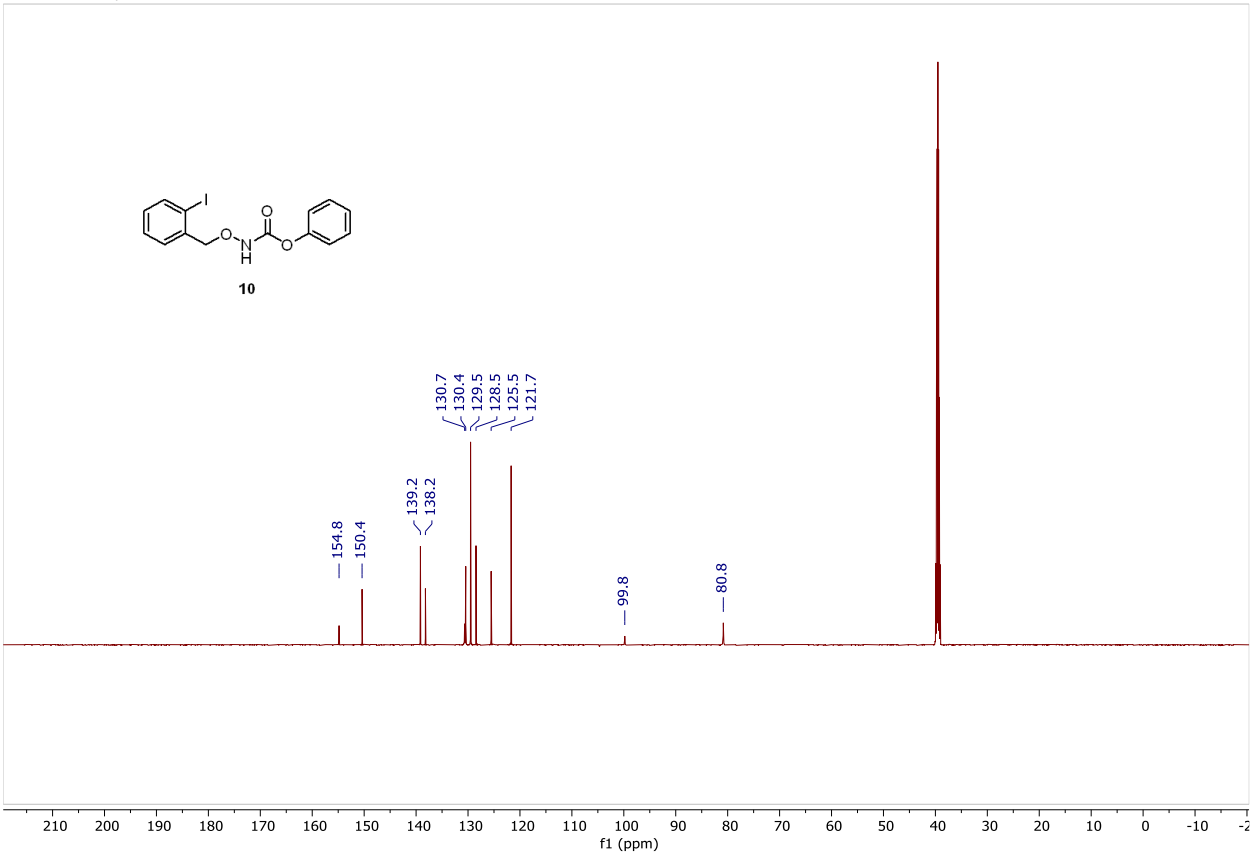

AM-3-131-May24.10.fid — 1d_1H_1min DMSO {C:\data} Beau 3

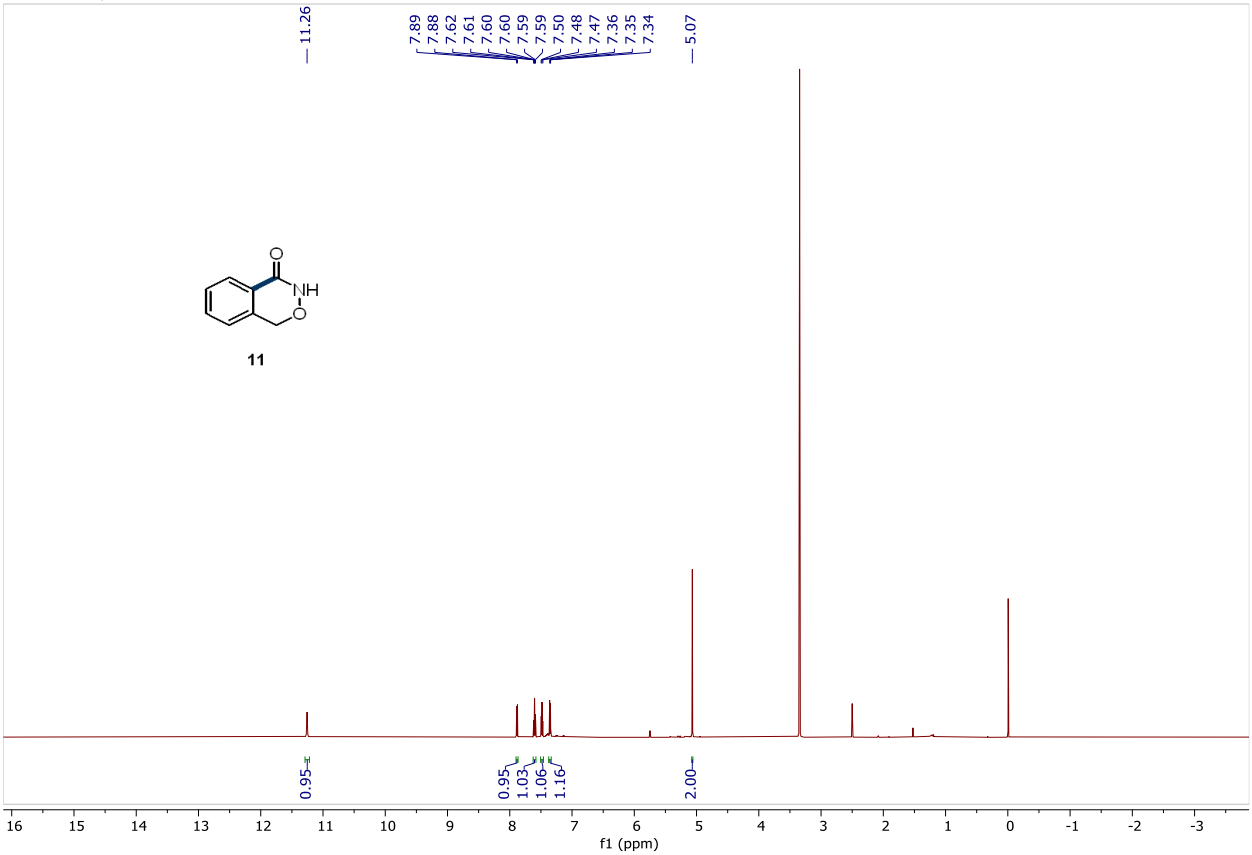

AM-3-131.2.fid — 1d_13C_1_hour DMSO C:\\ Beau 42

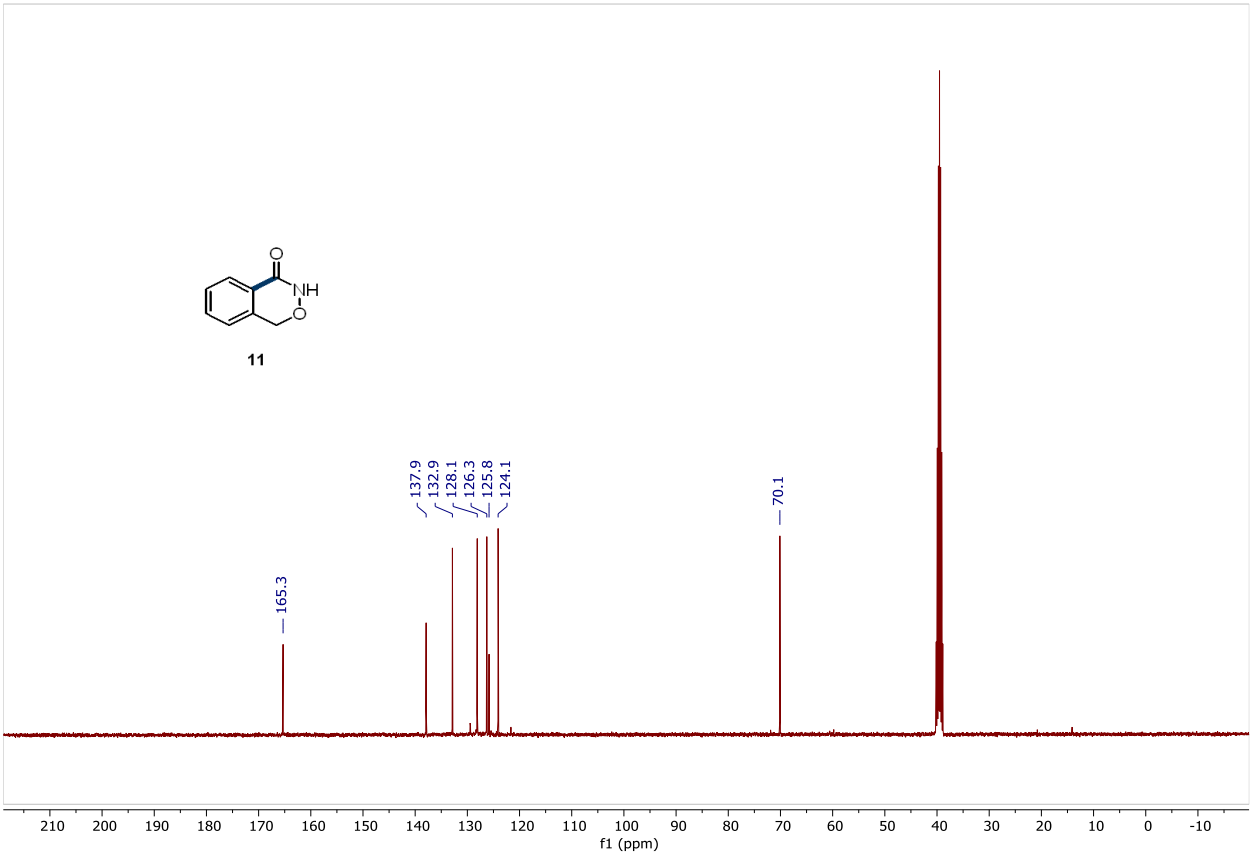

AM-3-131.3.fid — 1d_13C_DEPT_135_1_hour DMSO C:\\ Beau 42

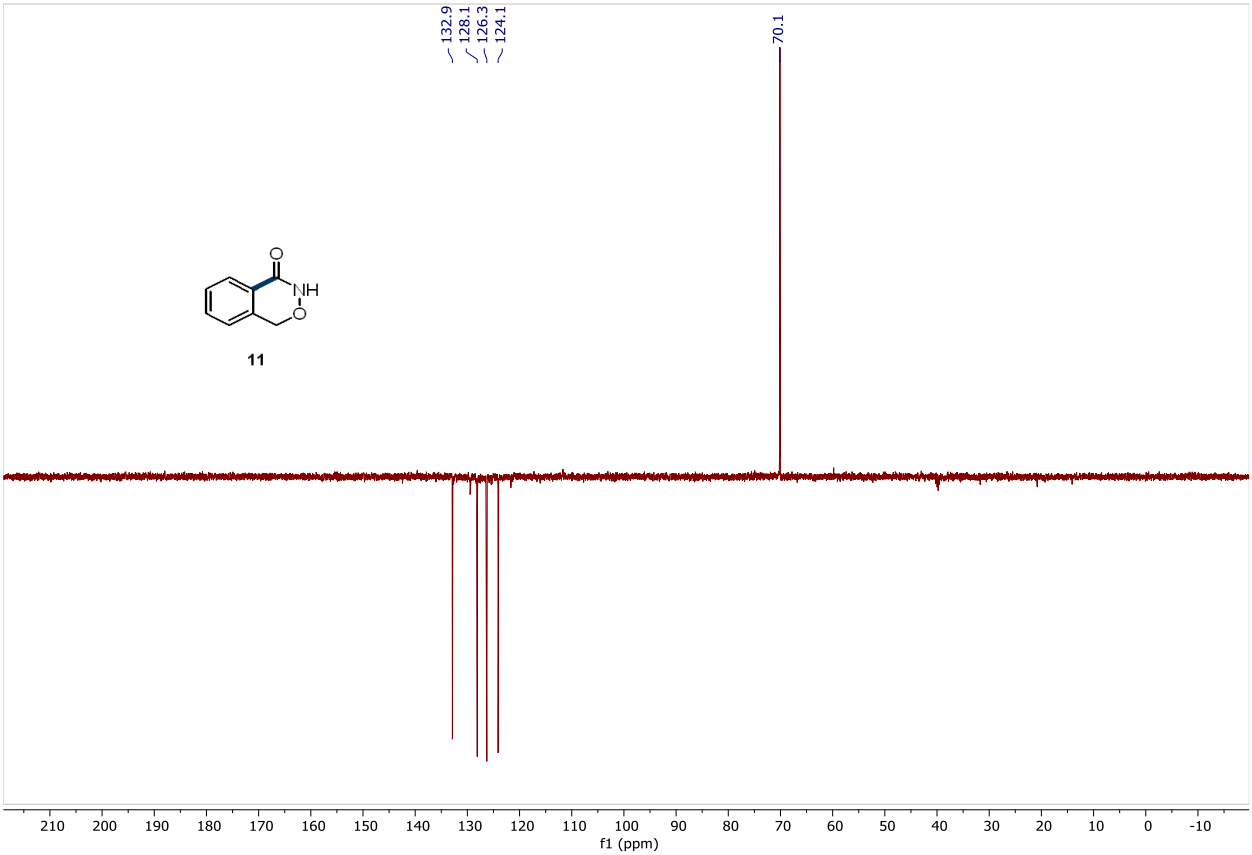

AM-3-154.10.fid — 1d_1H_1min DMSO {C:\data} Beau 8

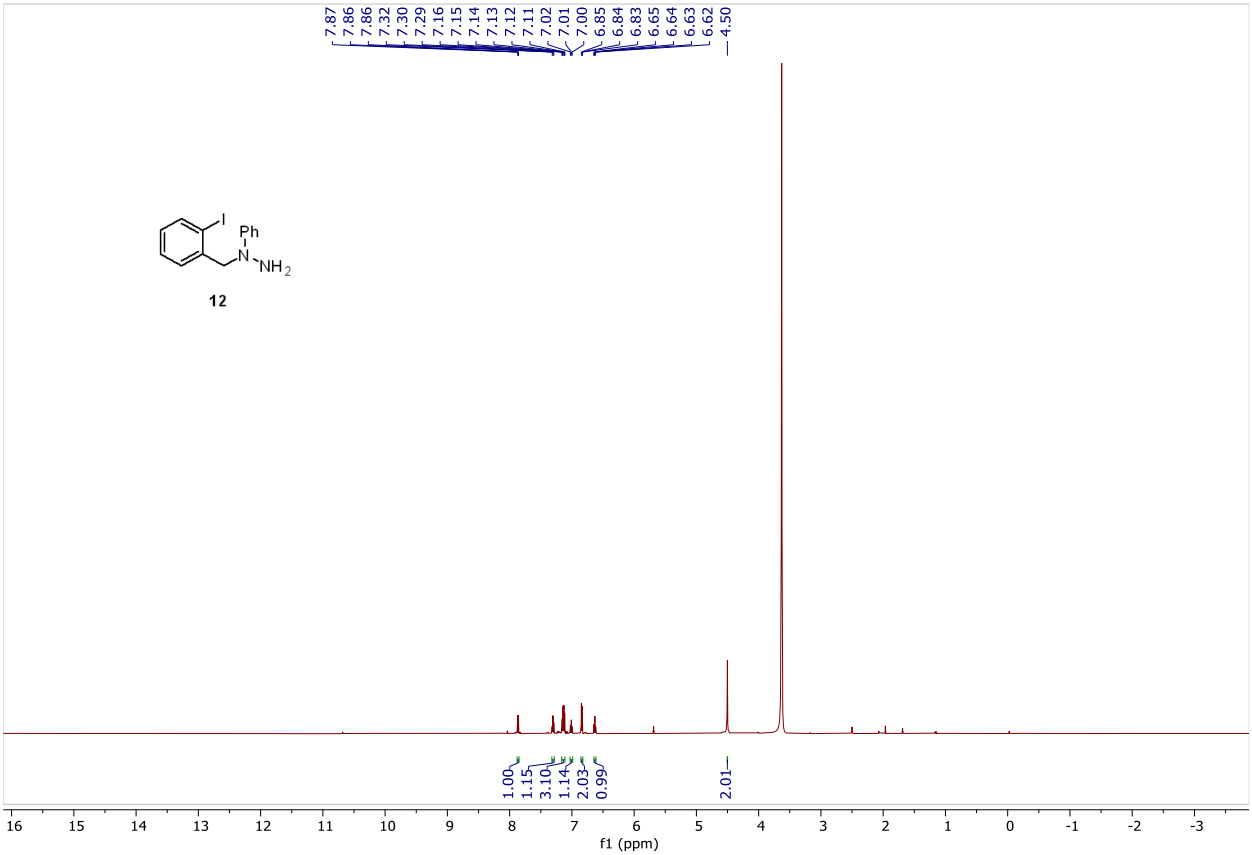

AM-3-154.11.fid — {1d_13C[1H]_1h10min} DMSO {C:\data} Beau 8

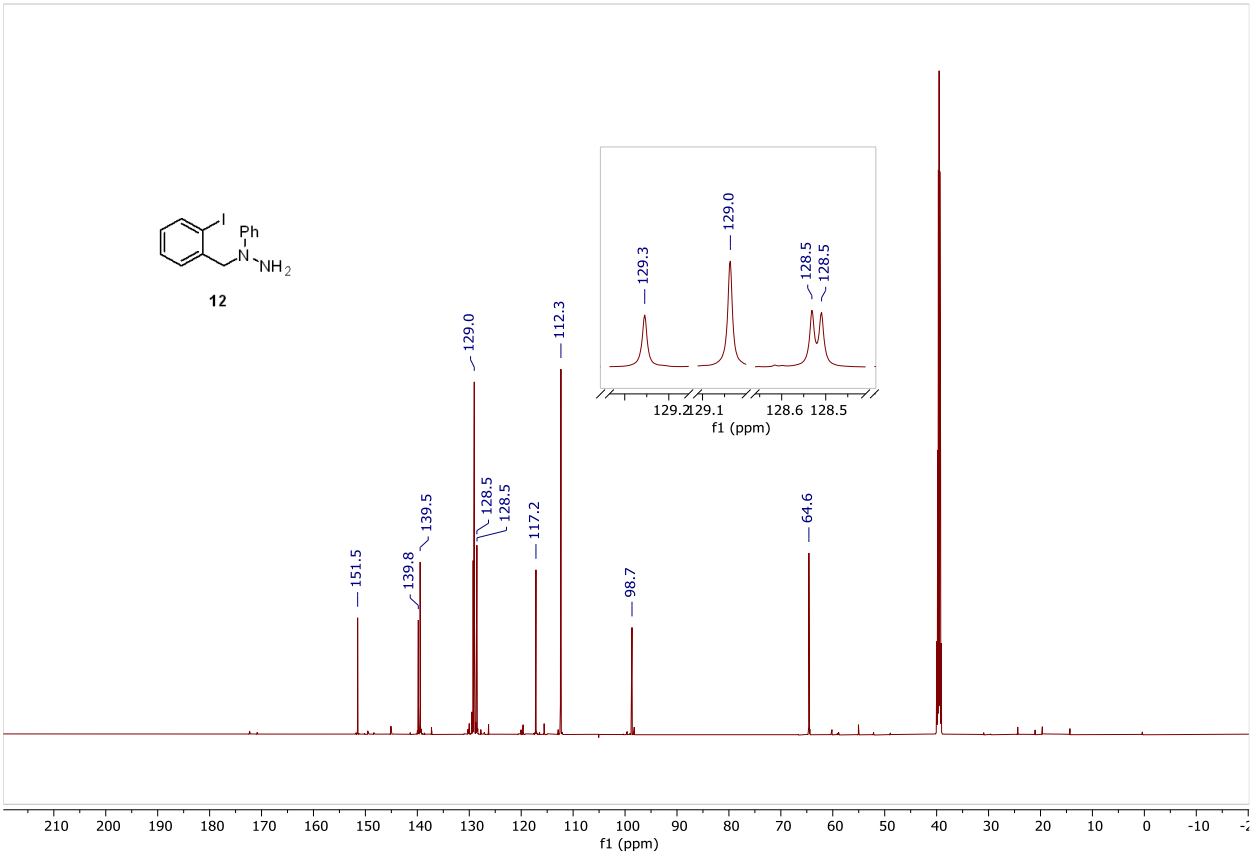

AM-3-157-2ndtry-May24.10.fid — 1d_1H_1min DMSO {C:\data} Beau 10

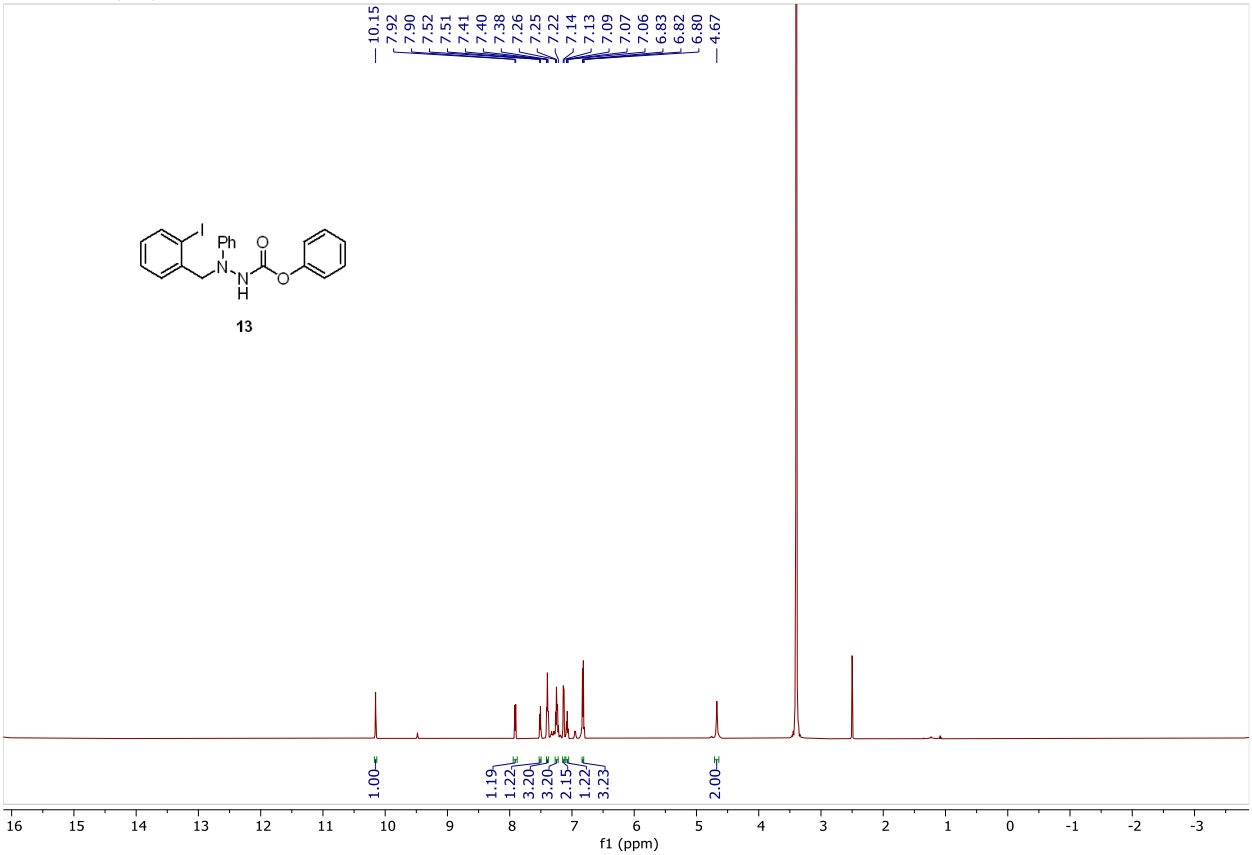

AM-3-157-2ndtry-May24.11.fid — {1d_13C[1H]_18min} DMSO {C:\data} Beau 10

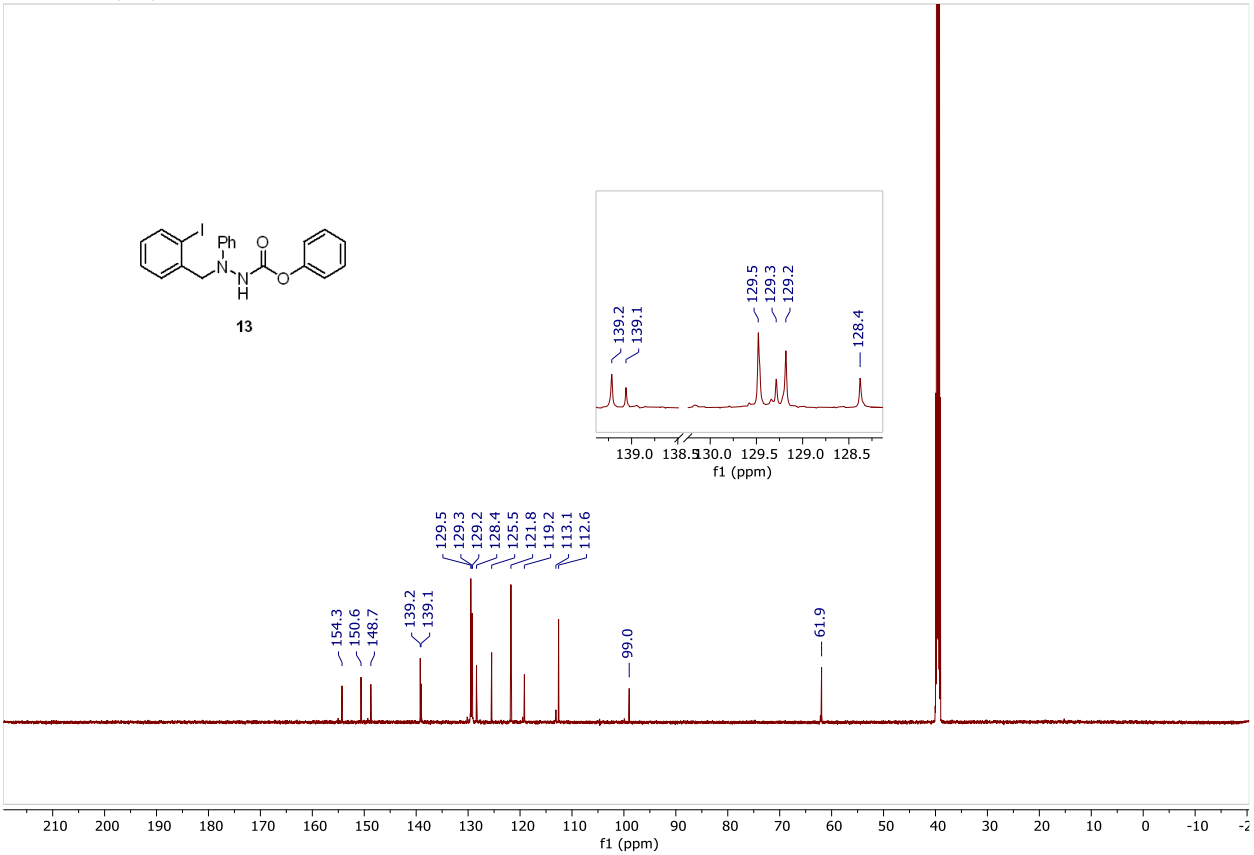

AM-3-136-P-May24.1.fid — 1d_1H_16_scans DMSO C:\\ Beau 17

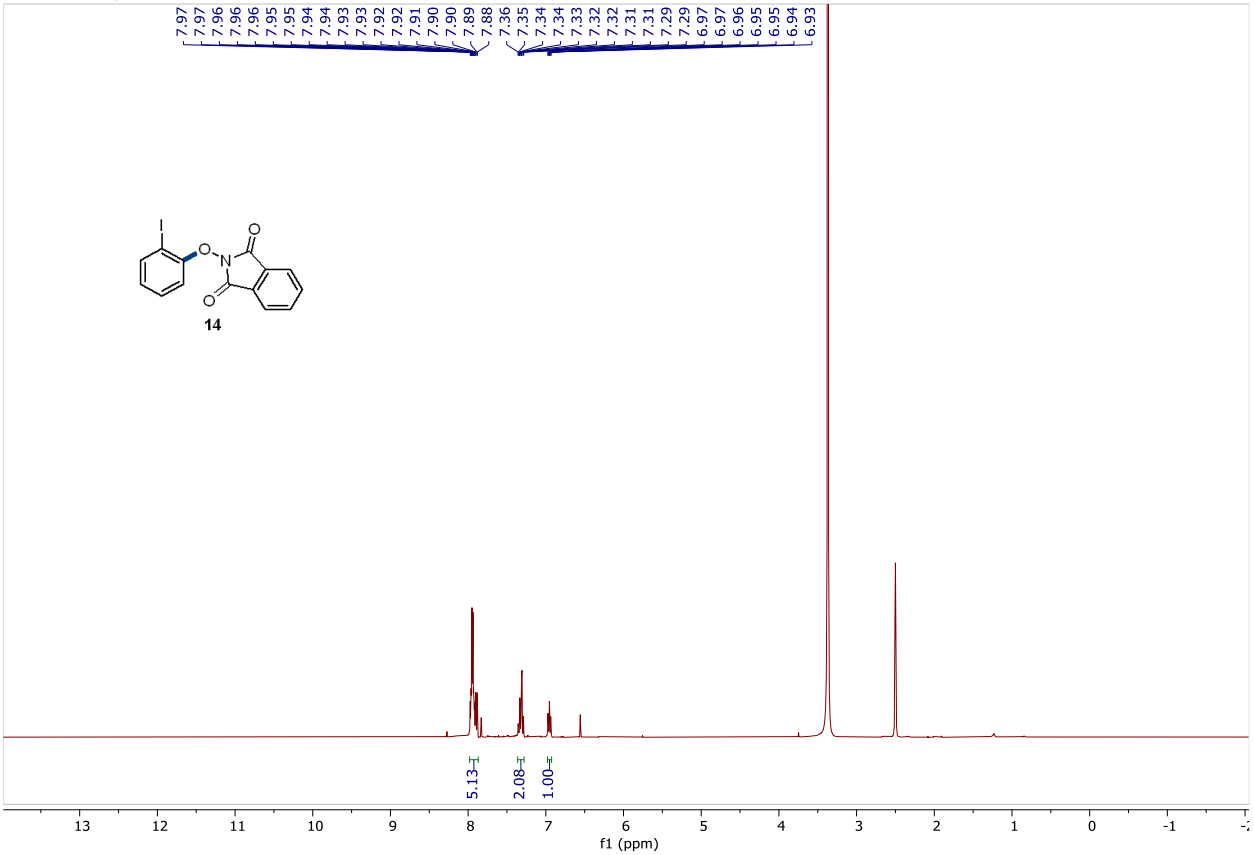

AM-3-136-P-May24.2.fid — 1d_13C_1_hour DMSO C:\\ Beau 17

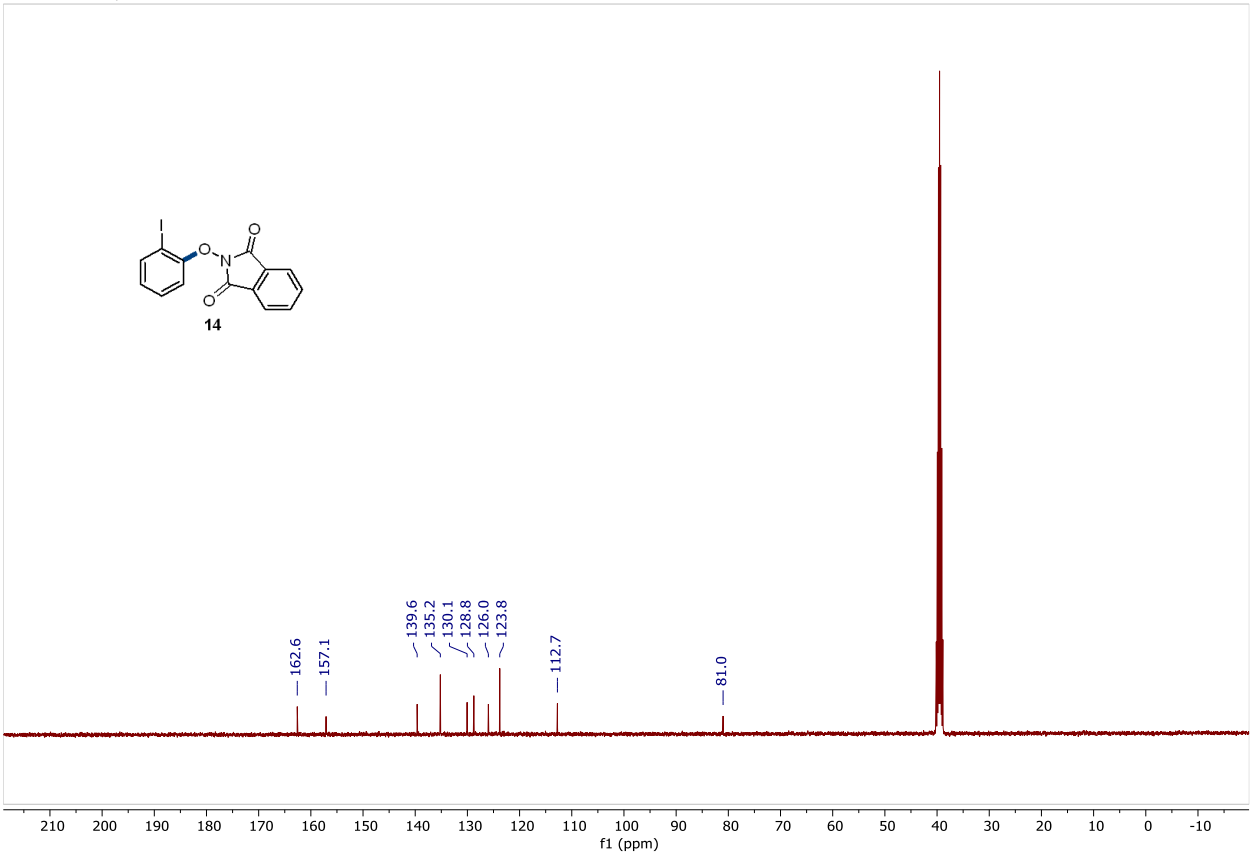

AM-3-164-lower-product.1.fid — 1H NMR

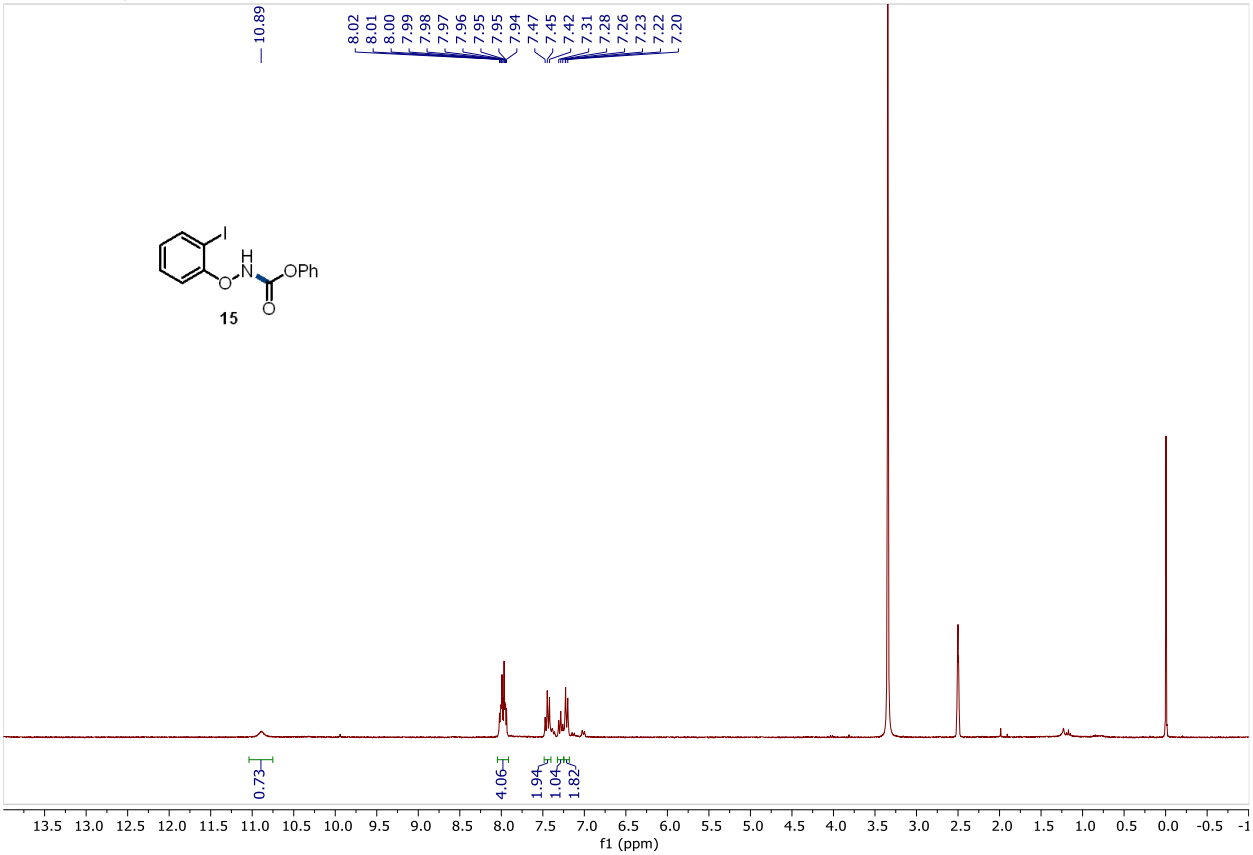

AM-3-164-lower-myproduct-May24.11.fid — {1d_13C[1H]_35min} DMSO {C:\data} Beau 14